THE FRIB SUPERCONDUCTING LINAC: STATUS AND PLANS*

J. Wei[#], H. Ao, S. Beher, N. Bultman, F. Casagrande, C. Compton, L. Dalesio, K. Davidson, A. Facco[1], F. Feyzi, V. Ganni, A. Ganshyn, P. Gibson, T. Glasmacher, W. Hartung, L. Hodges, L. Hoff, K. Holland, H.-C. Hseuh[2], A. Hussain, M. Ikegami, S. Jones, K. Kranz, R.E. Laxdal[3], S. Lidia, G. Machicoane, F. Marti, S. Miller, D. Morris, A.C. Morton, J. Nolen[4], P. Ostroumov, J. Popielarski, L. Popielarski, E. Pozdeyev, T. Russo, K. Saito, G. Shen, S. Stanley, H. Tatsumoto, T. Xu, Y. Yamazaki,

Facility for Rare Isotope Beams, Michigan State University, East Lansing, MI, USA

K. Dixon, M. Wiseman, Thomas Jefferson National Laboratory, Newport News, VA, USA

M. Kelly, Argonne National Laboratory, Argonne, IL, USA

K. Hosoyama, KEK, Tsukuba, Japan

[1] also at INFN - Laboratori Nazionali di Legnaro, Legnaro (Padova), Italy

[2] also at Brookhaven National Laboratory, Upton, NY, USA

[3] also at TRIUMF, Vancouver, Canada

[4] also at Argonne National Laboratory, Argonne, IL, USA

Abstract

With an average beam power two orders of magnitude higher than operating heavy-ion facilities, the Facility for Rare Isotope Beams (FRIB) stands at the power frontier of the accelerator family. This report summarizes the current design and construction status as well as plans for commissioning, operations, and upgrades.

INTRODUCTION

During the past decades, accelerator-based neutron-generating facilities, such as SNS [1], J-PARC [2], PSI [3], and LANSCE [4], advanced the frontier of proton beam power to the 1 MW level, as shown in Fig. 1; the beam-on-target power is the product of the average beam current and the beam kinetic energy [5]. FRIB is designed to advance the power frontier for heavy ions by more than two orders of magnitude, to 400 kW.

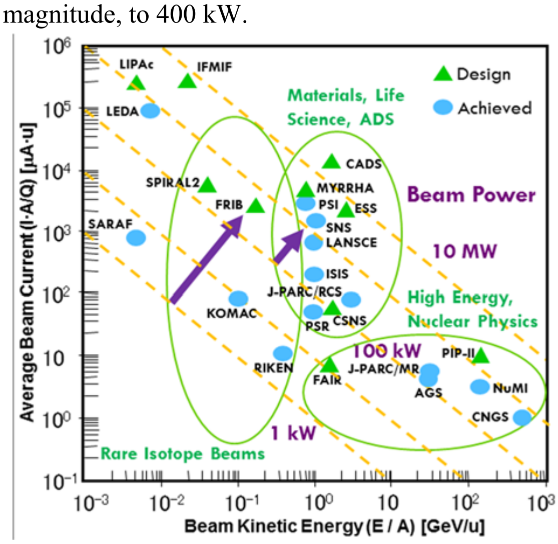

Figure 1: Hadron accelerator power frontier, showing the beam energy, current and average power on target.

*Work supported by the U.S. Department of Energy Office of Science under Cooperative Agreement DE-SC0000661 and the National Science Foundation under Cooperative Agreement PHY-1102511.

#wei@frib.msu.edu

In August 2014, the US Department of Energy's Office of Science (DOE-SC) approved Critical Decision-3b (Approve Start of Technical Construction) for the FRIB project (Fig. 2). The total project cost for FRIB is $730M, of which $635.5M is provided by DOE and $94.5M is provided by Michigan State University (MSU). The project will be completed by 2022. "When completed, FRIB will provide access to completely uncharted territory at the limits of nuclear stability, revolutionizing our understanding of the structure of nuclei as well as the origin of the elements and related astrophysical processes" [6].

In creating this new one-of-a-kind facility, FRIB builds upon the achievements of the National Superconducting Cyclotron Laboratory (NSCL), a National Science Foundation (NSF) user facility at MSU. Starting in 2014, the re-accelerator (ReA3), consisting of a radio-frequency quadrupole (RFQ) and a superconducting radio-frequency (SRF) linac, was constructed and commissioned to accelerate beams of rare isotopes. The FRIB project scope includes a high-power driver accelerator, a high-power target, and fragment separators.

The FRIB driver accelerator is designed to accelerate all stable ions to energies >200 MeV/u with a beam power on the target of up to 400 kW. The driver accelerator consists of a 47 m long Front End containing electron-cyclotron-resonance (ECR) ion sources and a room temperature RFQ followed by a 472 m long SRF linac with quarter-wave-resonators (QWR) of β_0=0.041 and 0.085 and half-wave-resonators (HWR) of β_0=0.29 and 0.53 in a folded layout to facilitate charge stripping and beam collimation and to accommodate the limited real estate footprint in the center of the MSU campus [7].

FRIB accelerator systems design and construction have been facilitated under work-for-others agreements with many DOE-SC national laboratories including ANL, BNL, FNAL, JLab, LANL, LBNL, ORNL, and SLAC, and in collaboration with institutes worldwide including BINP, KEK, IHEP, IMP, INFN, INR, RIKEN, TRIUMF, and

ISBN 978-3-95450-169-4

STATUS OF THE EUROPEAN XFEL*

H. Weise, Deutsches Elektronen-Synchrotron, Hamburg, Germany
on behalf of the European XFEL Accelerator Consortium

Abstract

The European XFEL under construction in Hamburg, Northern Germany, aims at producing X-rays in the range from 260 eV up to 24 keV out of three undulators that can be operated simultaneously with up to 27,000 pulses per second. The FEL is driven by a 17.5 GeV superconducting linac. Installation of this linac is now finished and commissioning is next. First lasing is expected for spring 2017. The paper summarizes the status of the project. First results of the injector commissioning are given.

INTRODUCTION

The accelerator complex of the European XFEL [1] is being constructed by an international consortium under the leadership of DESY. Seventeen European research institutes contribute to the accelerator complex and to the comprehensive infrastructure. DESY coordinates the European XFEL Accelerator Consortium but also contributes with many accelerator components, and the technical equipment of buildings, with its associated general infrastructure. With the finishing of the accelerator installation, the commissioning phase is now starting, with cool down of the main linac scheduled for October 2016.

LAYOUT OF THE EUROPEAN XFEL

In the following the overall layout of the European XFEL is given with emphasis on the different sections of the accelerator complex.

Introduction to the Accelerator

The European XFEL with its total facility length of 3.4 km follows the established layout of high performance single pass Self-Amplified Spontaneous Emission (SASE) FELs. A high bunch charge, low emittance electron gun is followed by some first acceleration to typically 100 MeV. In the following, magnetic chicanes help to compress the bunch and therefore increase the peak current. This happens at different energies to take care of beam dynamic effects which would deteriorate the bunch emittance in case of too early compression at too low energies. Thus the linac is separated by several of such chicanes. The European XFEL main linac accelerates the beam in three sections, following the first acceleration in the injector.

Injector

The injector design of the European XFEL is visibly affected by the need of long bunch trains which are required for the efficient use of superconducting linac technology. Like many other FELs it starts with a normal-conducting 1.6 cell radio frequency (RF) electron gun but here the source has to deliver 600 µs long trains i.e. the rf-on time is equivalently long, and not just some few µs. The produced 6 MeV electron beam is almost immediately injected into the first superconducting accelerator section which allows efficient acceleration of bunch trains. This first linac section consists of a standard eight cavity XFEL module, followed by a harmonic 3.9 GHz module. The latter is needed to manipulate the longitudinal beam profile together with the later bunch compression in magnetic chicanes. Beam diagnostics is used to verify the electron beam quality at energy of about 130 MeV. The in total 50 m long injector installation ends with a beam dump being able to take the full beam power.

The injector of the European XFEL was commissioned and operated during the installation period of the main linac sections. First beam was accelerated in 12/2015. At the end of the injector, 600 µs long electron bunch trains of typ. 500 pC bunches are available with measured projected emittances of 1 to 1.5 mm mrad. Most relevant for the FEL process is the slice emittance which was found to be of the order of 0.5 mm mrad for 500 pC.

The next section downstream of the injector is a warm beam line including a so-called dogleg and the first bunch compressor, for historical reasons named BC0. The dogleg takes care of the vertical offset between the injector tunnel and the main linac tunnel.

Compression in all bunch compressors is reached by creating different path lengths in a four dipole magnet chicane. Electrons with slightly lower beam energy are deflected stronger and thus pass the chicane on an 'outward curve'. The acceleration in the injector section is done slightly off-crest, i.e. the energy of the leading electrons in the bunch is intentionally lower. The above mentioned 3.9 GHz harmonic system helps to get the proper energy modulation along the bunch. Since all electrons have essentially the same speed, the leading ones travel slightly longer, and the bunch is compressed.

The XFEL bunch compressor BC0 does a first slight compression by roughly a factor 2. The bunches ready for further acceleration reach 1 mm length, approx. 100 A peak current, with an energy spread of 1.5% at 130 MeV beam energy.

At present the European XFEL uses the lower of two injector tunnels. The second one was originally built to install a copy of the first injector – availability depending on reliable injector operation was the issue. Meanwhile it seems to be more adequate to aim for a different injector favoring longer pulse or even continuous wave (CW) operation.

* Work supported by the respective funding agencies of the contributing institutes; for details please see http:www.xfel.eu

ISBN 978-3-95450-169-4

COMMISSIONING AND EARLY OPERATION OF THE ARIEL E-LINAC*

T. Planche†, M. Marchetto‡, M.M. Alcorta, F.A. Ames, R.A. Baartman, C.B. Barquest,
B. Humphries, D. Kaltchev, S.R. Koscielniak, R.E. Laxdal, Y. Ma,
E. Thoeng, S. Saminathan, TRIUMF, Vancouver, Canada
P.M. Jung, University of Waterloo, Canada

Abstract

The ARIEL electron linac has been added to the TRIUMF facility as a new driver for the production of radioactive isotopes through photo-fission to complement the existing 500 MeV, H^- TRIUMF cyclotron. The electron beam driver is specified as a 50 MeV, 10 mA cw superconducting electron linac at 1.3 GHz. The first 30 MeV stage of the e-linac consisting of two cryomodules is completed. The paper will describe the recent commissioning and early operation results.

INTRODUCTION

The ARIEL facility [1, 2] is expected to triple the availability of radioactive beams at TRIUMF. This facility complements the existing ISAC facility, adding to it two driver beams: an additional proton beam from the existing 500 MeV H^- TRIUMF cyclotron, and an electron beam from our new electron linac. The electron linac (e-linac) is designed to produce a 50 MeV, 10 mA cw beam using five 1.3 GHz nine-cell superconducting rf cavities distributed in three different cryomodules. In the present stage, only two cryomodules have been installed, limiting the achievable energy to around 30 MeV.

In this paper we report the progress made with machine commissioning since September 2014, when the first high-energy (22.9 MeV) low-power electron beam was demonstrated [2]. We have since put our beam dynamics models to the test; we now have available an accurate lightweight optics model of our entire linac (which includes 3-dimensional space-charge). We have encountered a variety of issues, ranging from beam optics to machine and personnel safety, that have been studied and addressed. Peak and average beam power are gradually being brought up; 1 kW of average beam power has recently been delivered to our very first users: our own target and ion-source development group.

TESTING OUR MODELS

Optics model

Different codes are used at TRIUMF to study different aspects of the electron beam dynamics: `GPT` for gun simulations, `ASTRA` from non-linear dynamics with space-charge, `G4beamline` for collimation studies, `COSY-∞` for non-linear optics, etc. But our main workhorse is the envelope code `TRANSOPTR` [3]. Rather than tracking a large number of macro-particles, this code keeps track of statistical quantities of the beam distribution: its 21 independent second moments. This is achieved by numerically integrating the envelope equation (in contrast with matrix codes like `TRANSPORT`); it includes 3-dimensional linear space-charge.

The gain in computation time compared to multi-particle space-charge codes is such that multi-parameter optimizations through our entire linac converge within seconds [4].

The code also estimates 2nd and 3rd order aberrations from dipoles, quadrupoles and solenoids. This allows the user to make sure that the simulation stays within the bounds of the model, i.e. linear optics. It can also be used to constrain the optimizer to converge to tunes with minimal non-linear aberration.

A comparison between the calculated envelope and measured beam size for a 9 MeV tune through the first accelerating cryomodule is shown in Fig. 1.

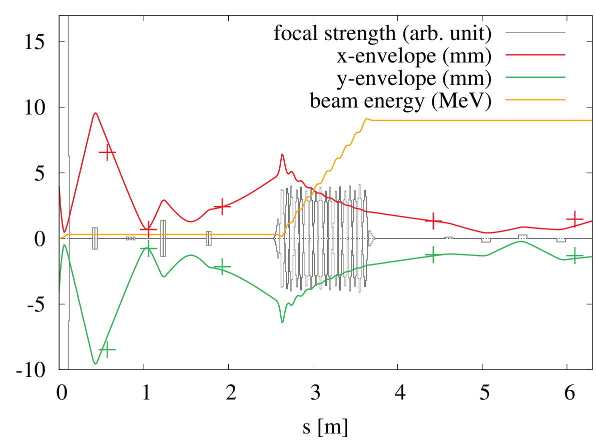

Figure 1: **Solid lines** present results of a `TRANSOPTR` simulation, which starts near rest on the e-gun grid, and goes through the injector cryomodule; **Crosses** present actual 2*rms beam size measured on view screens. The beam-energy curve (yellow) rises from 300 keV to 9 MeV; the 9-cell structure of the superconducting rf cavity is reflected in this curve.

A web-based graphical user interface (GUI) has been developed for this code (see Fig. 2). The choice of a browser based interface makes this tool reliable and platform-independent [5]. This GUI greatly facilitated commissioning, and is now used daily by operators.

* ARIEL is funded by the Canada Foundation for Innovation, the Provinces AB, BC, MA, ON, QC, and TRIUMF. TRIUMF receives funding via a contribution agreement with the National Research Council of Canada.
† tplanche@triumf.ca
‡ marco@triumf.ca

LOW EMITTANCE AND HIGH CURRENT ELECTRON LINAC DEVELOPMENT AT TSINGHUA UNIVERSITY

Chuanxiang Tang*, Zhen Zhang, Yingchao Du, Lianmin Zheng, Zhe Zhang, Zheng Zhou, Dong Wang, Qili Tian, Zhijun Chi, Wei Wang, Jiaru Shi, Lixin Yan, Wenhui Huang, Huaibi Chen
Tsinghua University, Beijing 100084, China

Abstract

A 50 MeV electron linac have been developed in Tsinghua University, which consists of a 1.6 cell photocathode rf gun, a 3-meter s-band SLAC type traveling wave (TW) accelerating structure an a s-band TW buncher. The photocathode rf gun is working at ~110 MV/m with very small dark current. The emittance of the electron beam is less than 1mm·mrad at 500 pC, and 0.5 mm.mrad at 200 pC. The linac is designed for Tsinghua Thomson scattering X-ray source (TTX). The total photon yield has been increased to ~2×10^7 photon/bunch at 50 keV after upgrade of the facility and the spectra have been reconstructed by two kinds of methods. Recent experiments have demonstrate that TTX can be applied in phase contrast imaging, computed tomography and X-ray polarization control. Electron bunch train has been produced to generate narrow-band THz radiation.

INTRODUCTION

Low emittance and high brightness electron beam has driven various applications, from radiation generation of different wavelength to direct probes of ultrafast process. As the development of state-of-the-art laser and RF technology, the laser-driven electron gun and linac made many electron-based facilities possible during the last decades, such as X-ray free-electron lasers, Thomson scattering sources and ultrafast electron diffraction and microscopy.

Tsinghua University (THU) has been devoted to producing high quality electron beam and promoting advanced applications. A 50 MeV electron linac has been developed for the Tsinghua Thomson scattering X-ray source (TTX) [1], which consists of a 1.6 cell photocathode RF gun, a 3-meter S-band traveling wave (TW) accelerating structure, a S-band TW buncher and a magnetic chicane. The facility was first proposed and operated as the first dedicated Thomson scattering source of China and have performed many photocathode studies and electron beam based experiments.

The RF gun was first developed based on the BNL/SLAC/UCLA gun at 2001. And since then three kinds of gun design have been fabricated, tested and operated in the beam line. The first two kinds of guns suffer from high dark current, RF breakdown and low acceleration gradient, which make obtaining small emittance challenging [2, 3]. The 3rd-type guns were developed at 2011 to address the problems above. Many improvements have been proposed and applied to the new gun based on the previous operation experiences.

Recently, a S-band TW buncher cavity and a magnetic chicane have been installed into the beam line with the purpose of beam compression. The buncher locates between the gun and the acceleration structure and the chicane is at the downstream of the acceleration structure. The combination of the ballistic bunching from the buncher and the magnetic compression enable us to generate < 100 fs kA-level electron beam, which can be used in the THz radiation generation and beam-driven plasma acceleration experiments. The detailed descriptions of the compression scheme will be discussed in the following sections.

PHOTOCATHODE RF GUN DEVELOPMENT AT THU

Improvements of the THU Gun

With the experiences of the first two types of gun design, we perform many improvements in the new gun design to addressing the problems of RF breakdown and low acceleration gradient. We adopted some beneficial modifications of other guns in the world, including LCLS [4], Eindhoven [5], KEK [6] and PAL [7] guns. The gun geometry was modified with disk iris changing from circular to elliptical to reduce surface electric field. Furthermore, the coupling between the full and half cells was enhanced by increasing the coupling iris radius and decreasing its thickness, and the mode separation was modified to about 15.3 MHz with the 0-mode excitation reduced by 80 %. The gun corner was curved to increase the quality factor of the gun cavity.

Another factor that we are paying attention to are the multipole field components in the RF gun. The dipole field kicks contribute greatly to the RF emittance increase. Our gun adopted the nonsymmmetric vacuum port design to eliminate the dipole field, and 4-port scheme was used to reduce the quadrupole components. In addition, the manufacturing process was improved and copper cathode plate was polished by polycrystalline, which is expected to reduce the breakdown rate, dark current and thermal emittance. To date seven new guns have been fabricated and cold tests have been completed. One of them has been installed on TTX and operated successfully for four years, showing a good performance at high gradient, low dark current, stable quantum efficiency and small emittance [8]. A simple summary of the cold testings for all guns developed at THU is presented in Fig. 1 with unloaded quality factor Q_0 and mode separations.

* tang.xuh@tsinghua.edu.cn

ISBN 978-3-95450-169-4

STATUS OF SwissFEL

F. Loehl for the SwissFEL team
Paul Scherrer Institut, Villigen PSI, Switzerland

Abstract

SwissFEL is a hard x-ray free-electron laser facility that is currently constructed at PSI. This paper gives an overview of the facility, describes the main sub-systems of the accelerator, and summarizes the installation and commissioning status.

INTRODUCTION

A schematic drawing of SwissFEL [1] is shown in Fig. 1. The accelerator is divided into an S-band injector, a C-band main linac (Linacs 1-3), and two undulator lines, Aramis and Athos. The Aramis line will provide hard x-ray radiation in the wavelength range from 0.1 – 0.7 nm and is part of the currently active first construction phase of SwissFEL. The soft x-ray undulator line Athos will cover the wavelength range from 0.6 – 4.9 nm and will be realized in a second phase from 2017 – 2020. The facility will operate at a repetition rate of 100 Hz.

The construction of the SwissFEL building started in spring 2013, and in summer 2015 the installation of first accelerator components begun. Today, October 2016, the vacuum line of the entire around 620 m long accelerator is close to being completed, and a first electron beam was generated and accelerated in the first 120 m of the facility.

INJECTOR

The electron source of the injector is an S-band gun [2] which was developed at PSI and first commissioned in the SwissFEL injector test facility [3]. This gun (for a picture see Fig. 2) combines design features of the LCLS gun and the CTF/PHIN gun. It has quadrupole-compensated symmetric couplers and is equipped with a load-lock system to allow for the exchange of cathodes. The gun is not equipped with tuning plungers and no tuning steps were applied during the manufacturing process. Instead, the gun is machined on frequency by using ultra-precision machining. While all the RF and mechanical design, as well as the brazing and most of the machining was performed at PSI, the ultra-precision machining took place at VDL-ETG. The nominal accelerating field at the cathode is 100 MV/m and the nominal energy gain is 7.1 MeV. As the cathode material, two options are available: copper or Cs_2Te. The baseline is Cs_2Te due to its higher quantum efficiency and its slower response time. The gun produced a first electron beam on August 24 of this year.

The electron beam from the gun is further accelerated in a total of six 4 m long S-band structures. The RF design of these structures was performed at PSI [4] and it includes dual-feed racetrack couplers and combines a constant gradient along the structure with a constant power loss. The structures were manufactured by Research Instruments. The first two structures are driven by an independent klystron, and the remaining four structures are grouped into two structures per klystron. After the first two structures, a laser heater is installed to circumvent the micro-bunch instability.

Two X-band structures follow the S-band section and are used to linearize the energy slope that the electron bunches obtain by being accelerated off-crest in the last four S-band structures. The X-band structures were designed and built in a collaboration between CERN, PSI, and Sincrotrone Trieste [5], and are followed by the first bunch compressor BC1 at a beam energy of 320 MeV. The injector ends with a diagnostics section that involves an S-band transverse deflecting structure that is used to setup the bunch compression.

C-BAND LINAC

The C-band Linac is divided into three segments: Linac 1, Linac 2, and Linac 3. After Linac 1, the electron bunches are further compressed in a second bunch compressor BC2 at an energy of 2.1 GeV. At the end of Linac 2, at 3.0 GeV of energy, a switch-yard [6] is installed with which electron bunches can be sent either straight into Linac 3 and consequently the hard x-ray Aramis line, or into the future soft x-ray line Athos. At the end of Linac 3, C-band transversely deflecting structures will be located that will allow for measurements of the longitudinal charge profile with a resolution of a few femtoseconds. These structures will arrive at PSI in February 2017 and are currently replaced by a vacuum pipe.

A total of 26 C-band modules are installed in the C-band Linac, and each module consists out of four C-band structures that are mounted onto two granite girders (see [7] for a schematic and [8] for further information). The C-band structures [9] are stacked and brazed at PSI [10] out of copper cells that were produced at VDL ETG (J-couplers) and VDL ETG Switzerland (regular cells) with micrometer precision using ultra-precision diamond milling and turning. This production process allows for avoiding any tuning steps while still achieving excellent field flatness and phase advance errors (for an example, see [7]). Furthermore, the achieved straightness of the structures is excellent: an example for a straightness measurement of a structure is shown in Fig. 3. The maximum measured deviations from a straight line are typically below 20 μm. In addition to the four structures, each Linac module also comprises a barrel open cavity (BOC) pulse compressor [11], and these were machined and brazed at PSI [12].

After the brazing, a vacuum leak test was performed for both the C-band structures and the BOC pulse compressors, and the RF properties were measured. Based on these RF measurements, a sorting of structures based on their resonance frequencies was performed with the goal of grouping four similar structures. This was necessary because all struc-

ACHIEVEMENT OF SMALL BEAM SIZE AT ATF2 BEAMLINE

T. Okugi†, KEK/SOKENDAI, Tsukuba, Ibaraki, Japan
ATF International Collaboration

Abstract

The purpose of ATF2 project is to develop and establish a new final focus method, called "Local Chromaticity Correction (LCC)", which will be used at International Linear Collider (ILC). ATF2 project has been performed by utilizing a small emittance beam of KEK Accelerator Test Facility (KEK-ATF). The beam optics of ATF2 is designed to be based on the same method as ILC, with the equivalent beam energy spread and natural chromaticity, the tolerances of magnetic field errors are also equivalent to the ILC final focus system. The vertical beam size was focused to less than 41 nm at the bunch population of 0.7×10^9 at ATF2 virtual IP. The achieved beam size is close to the ATF2 target value of 37 nm. The bunch population at the recent ATF2 beam operation is much smaller than ILC. The reason why the bunch population of ATF2 is smaller than ILC is strong intensity dependence of vertical beam size at the virtual IP. The candidate of the intensity dependence source is IP angle jitter via wakefield.

INTRODUCTION

The KEK-ATF [1, 2, 3, 4] has been built for accelerator R&D, especially for ILC [5]. Figure 1 shows a schematic view of the KEK-ATF accelerator complex. KEK-ATF consists of an injector linac, a damping ring, a beam extraction line and ATF2 beamline. The purpose of the damping ring is to supply a low emittance beam to the extraction line and ATF2 beamline for accelerator R&D. The vertical beam emittance produced by damping ring is less than 10 pm [6, 7] (smaller than 12 pm of the ATF2 requirement). The corresponding 30 nm normalized emittance is comparable with the requirement of the ILC beam delivery system. The ATF2 beamline was constructed to study the ILC final focus system, utilizing the small emittance beam generated by the damping ring.

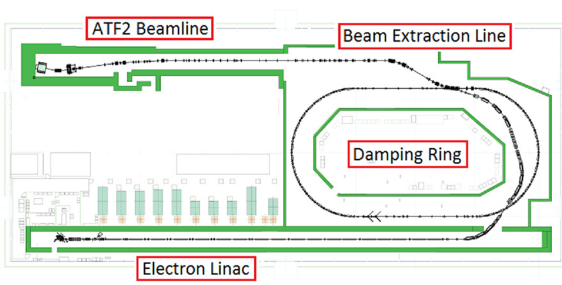

Figure 1: Accelerator complex of KEK-ATF, consisting of an electron linac, a damping ring, a beam extraction line and the ATF2 beamline.

Table 1: Beam and Optics Parameters for the ILC and ATF2 Final Focus Beamlines (10×1 Optics)

	ILC	ATF2
E [GeV]	250	1.28
L^* [m]	4.1	1.0
ε_x [nm] / ε_y [pm]	0.02 / 0.07	2 / 12
$\gamma\varepsilon_x$ [μm] / $\gamma\varepsilon_y$ [μm]	10 / 0.035	5 / 0.030
β_x^* [mm] / β_y^* [mm]	11 / 0.48	40 / 0.10
σ_x^* [μm] / σ_y^* [nm]	0.47 / 5.9	8.9 / 37
σ_z [mm]	0.3	7.0
σ_p/p	0.12 %	0.07%

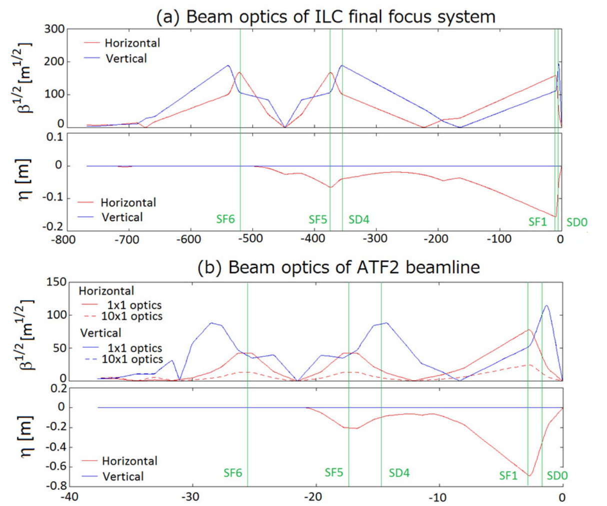

Figure 2: Beam optics of the ILC final focus beamline (a) and the ATF2 beamline (b). Both the 1×1 optics and the 10×1 optics are shown.

ATF2 BEAMLINE

Beam Optics of ATF2 Beamline

The ILC final focus system is designed based on the LCC technique [8]. The main purpose of the ATF2 beamline is to demonstrate beam focusing with the LCC method, and to establish a beam tuning method for ILC final focus systems. Therefore, the ATF2 beam optics was designed based on the LCC scheme. The IP horizontal and vertical beta-functions (β_x^*, β_y^*) of ATF2 were originally designed to generate the same horizontal and vertical chromaticities as ILC (1×1 optics). However, since the ATF2 beam energy is much smaller than ILC, the geometrical aberrations of ATF2 are much larger than ILC, and the effect of the multipole errors are larger than ILC. Therefore, in recent ATF2 beam operation, the ATF2 beamline was operated with a 10 times larger horizontal IP beta-function than that of original optics in order to reduce sensitivity to the multipole errors. We call the beam optics as "10×1 optics". The beam optics for ILC and ATF2 beamlines are shown in Fig. 2, and the main parameters are listed in Table 1. The

† toshiyuki.okugi@kek.jp

ISBN 978-3-95450-169-4

SPACEBORNE ELECTRON ACCELERATORS*

J.W. Lewellen†, C. Buechler, G. Dale, N.A. Moody, D.C. Nguyen
Los Alamos National Laboratory, Los Alamos, United States

Abstract

High-power electron beam generators in space will enable the studies of solar and space physics, specifically the interrogation of the magnetic connection between the magnetosphere and ionosphere. The CONNEX collaboration plans to map the magnetic connection between the magnetosphere and ionosphere, using a satellite equipped with an electron beam accelerator that can create a spot in the ionosphere – an artificial aurora – observable by optical and radar detectors on the ground.

To date, a number of spacecraft carrying low-power, <50 keV DC electron beam sources have been launched to study the upper ionosphere, however, reaching the average beam power required for future missions requires a switch to RF technology. We present the concept for a quasi-CW, C-band electron accelerator with 1-MeV beam energy, 10-mA beam current, and requiring 40 kW of prime power during operation. Our novel accelerator concept includes the following features: individually powered cavities driven by 5 GHz high-electron mobility transistors (HEMT), passively cooled accelerator structures, and active frequency control for operating over a range of temperatures.

INTRODUCTION

The earth's magnetosphere is the region surrounding the earth in which its magnetic field is the dominant influence on charged-particle dynamics. Near the surface, it can be approximated by a dipole field, but further out it becomes an increasingly structurally complex and time-varying phenomenon, as it is influenced by the solar wind as well as geodynamics. Existing models of the magnetosphere are mostly empirical, and measurements are obtained primarily by magnetometer data from spacecraft [1,2]. These provide the magnetic field at a particular location but little direct data elsewhere.

The CONNEX collaboration proposes using an electron beam to probe the coupling between the magnetosphere and ionosphere. The intent is to direct an electron beam into the "loss cone" [3], approximately parallel to the earth's field at the satellite's location, which will result in the beam being lost in the ionosphere. As the beam enters the atmosphere it generates ionization and auroral glow, which can be observed via ground-based camera and radar observation. Thus, knowing the location of the satellite and the beam's re-entry point, we obtain information about the magnetic connection between the satellite's location and the ionosphere.

The intensity of the optical signature depends more strongly on the total beam power and net energy deposited than on the beam voltage. Approximately 10 kJ – 1 kW average power over 10 s – is required to obtain sufficient signal-to-noise.

BASIC OPERATIONAL CONSTRAINTS

Beam Current

A satellite that can be approximated by a 2-m radius sphere has a capacitance C_{sat} of ~ 0.2 nF. Neglecting charge neutralization processes, the satellite can emit approximately 10 µC from a 50-kV beam source before the beam is emitted at zero voltage relative to infinity, or for approximately 50 µs if a 200-mA beam (10 kW at 50 kV) is being generated. In contrast, given a beam voltage of 1 MV, the satellite can emit approximately 200 µC, or a beam current of 10 mA for 20 ms.

Satellites are not isolated conductors; the orbital environment of most satellites is a neutral plasma, and charge neutralization will occur at some rate. That said, even without beam emission, spacecraft charging can be problematic from an operational standpoint [4,5]. There are several techniques for satellite charge neutralization, such as plasma contactors [6]; but in any case the satellite must eventually expel an equal but opposite charge as delivered by the electron beam. Thus, all else equal, for the same beam power a higher voltage beam provides an easier task for the neutralization system. This leads naturally to the selection of an RF-based accelerator.

High Voltage

The orbital environment of most satellites can be considered a neutral plasma. DC potentials will drive plasma currents and corresponding currents within the satellite [7,8]; high-voltage systems on satellites operating above approximately 30 kV have generally proven problematic and should be avoided if possible for the CONNEX mission [9]. This precludes very high-voltage DC guns, and also suggests that other systems requiring high voltages (such as most tube-based RF sources) are preferably avoided. HEMT RF amplifiers are typically driven with ~50 V power supplies, addressing this concern.

Size, Weight and Power

Terrestrial accelerators are typically optimized based around the total cost of the installation, which for machines such as X-FELs tends to scale with the overall size of the facility. The typical approach is to increase the real-estate

* Work supported by Los Alamos National Laboratory Pathfinder and Program Development. Approved for public release; distribution is unlimited: LA-UR-16-27164.
† jwlewellen@lanl.gov

THE SARAF-LINAC PROJECT STATUS

N. Pichoff, N. Bazin, L. Boudjaoui, P. Bredy, D. Chirpaz-Cerbat, R. Cubizolle, B. Dalena, G. Ferrand, B. Gastineau, P. Gastinel, P. Girardot, F. Gougnaud, P. Hardy, M. Jacquemet, F. Leseigneur, C. Madec, N. Misiara, P. Nghiem, F. Rossi, D. Uriot
CEA/IRFU, Gif-sur-Yvette, France
P. Bertrand, M. Di Giacomo, J-M. Lagniel, J-F Leyge, M. Michel, P. Toussaint
CEA/GANIL, Caen, France

Abstract

SNRC and CEA collaborate to the upgrade of the SARAF accelerator to 5 mA CW 40 MeV deuteron and proton beams (Phase 2). CEA is in charge of the design, construction and commissioning of the superconducting linac (SARAF-LINAC Project). This paper presents to the accelerator community the status at August 2016 of the SARAF-LINAC Project.

INTRODUCTION

The SARAF-LINAC project, managed by CEA (France), is integrated to the SARAF-Phase 2 project managed by SNRC (Israel) and has been already introduced in [1].

In 2014, a first System Design Report (on the base of which [1] was written) was presented and provided a basis for an agreement between CEA and SNRC.

The project can be simplified in 3 overlapping phases (Fig. 1) lasting less than 8 years:

- ~3 years of detailed design, including prototyping,
- ~4 years of construction, assembly and test at Saclay,
- ~2 years of installation and commissioning at Soreq.

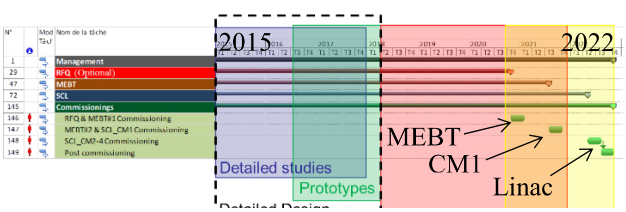

Figure 1 SARAF-LINAC major schedule.

During the first phase, two Preliminary Design Reviews and one Critical Design Review took place at Saclay:

- October 2015: major components PDR.
- January 2016: system PDR.
- June 2016: major components CDR.

In this paper, the status of these developments after the first year of detailed design phase is presented.

SYSTEM

The SARAF-LINAC System Preliminary Design Review (PDR) took place at Saclay on January 2016. Status on beam dynamics, vacuum design, beam diagnostics, local control systems was presented. The linac layout is given on Fig. 2.

Since then [2], the project decided to use a modified version (exiting with 1.3 MeV/u) of SNRC 4-rod RFQ (the 4-vane RFQ being optional). A first pole geometry (v1) has been established and implemented in the TraceWIN package code [3]. The calculated beam losses with errors are higher than those observed with the 4-vane RFQ, reaching those specified by the Top-Level Requirements by activation considerations (below 1 nA/m above 20 MeV) (TLR level = 1 on vertical on Fig. 3). A new pole design is in progress to reduce the losses in the linac (mainly due to particle exiting the RFQ in the longitudinal tails).

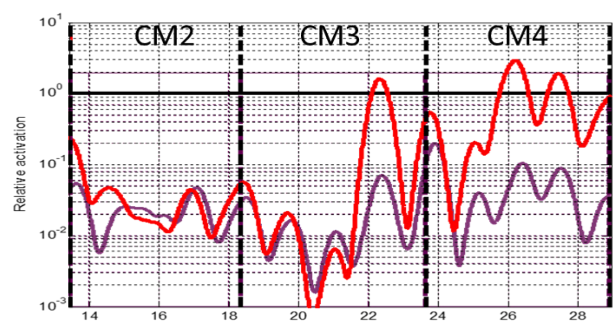

Figure 3 : Beam losses in the three last cryomodules (CM). Purple: with 4-vane RFQ; Red: with 4-rod v1 RFQ.

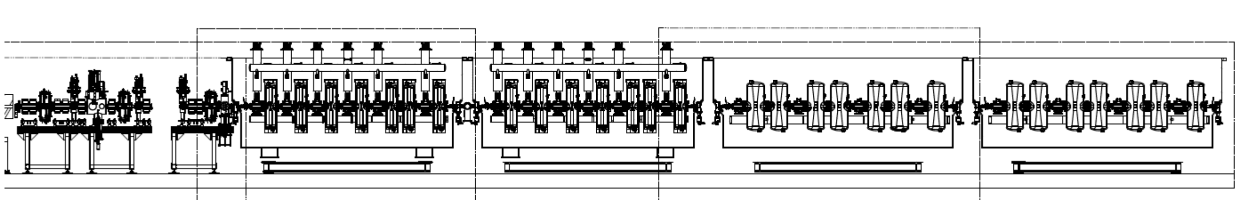

Figure 2: SARAF-LINAC layout.

CURRENT STATUS ON SUPERCONDUCTING LINAC FOR THE RARE ISOTOPE SCIENCE PROJECT

H. J. Kim*, W. K. Kim, Y. K. Kim, I. K. Shin, H. C. Jung, I. S. Hong, Y. H. Kim, B. S. Park
IBS, Daejeon, Korea

Abstract

The Rare Isotope Science Project(RISP) has been proposed as a multi-purpose accelerator facility for providing beams of exotic rare isotopes of various energies. It can deliver ions from hydrogen (proton) to uranium. Protons and uranium ions are accelerated up to 600 MeV and 200 MeV/u respectively. The facility consists of three superconducting linacs whose superconducting cavities are independently phased. The requirement for the linac design is especially high for the acceleration of multiple charge beams. In this paper, we present the design for the linac at the RISP and discuss the development of the electron cyclotron resonator, the radio-frequency quadrupole the superconducting cavity, and the cryomodule.

INTRODUCTION

The RISP accelerator has been planned to study a wide range of cutting edge science programs in atomic physics, material science, bio and medical science, nuclear astrophysics, nuclear science, and interdisciplinary science programs at the Institute for Basic Science (IBS). In order to meet the diverse demands, it can deliver various high intensity stable ions from protons to uranium atoms with a final beam energy, for example, 200 MeV/u for uranium and 600 MeV for protons, and with a beam current range from 8.3 pμA (uranium) to 660 pμA (protons) [1–3]. It can provide various rare isotope beams which are produced by isotope separator on-line (ISOL) system. The facility consists of three superconducting linacs of which superconducting cavities are independently phased and operating at three different frequencies, namely, 81.25, 162.5 and 325 MHz.

SUPERCONDUCTING LINAC

Lattice Design

The configuration of the accelerator facility within the RISP is shown in Fig. 1. An injector system accelerates a heavy ion beam to 500 keV/u and creates the desired bunch structure for injection into the superconducting linac. The injector system comprises an electron cyclotron resonance ion source, a low-energy beam transport, a radio-frequency quadrupole, and a medium-energy beam transport. The superconducting driver linac accelerates the beam to 200 MeV/u. The driver linac is divided into three different sections, as shown in Fig. 2: a low-energy superconducting linac (SCL1), a charge stripper section (CSS) and a high-energy superconducting linac (SCL2). The SCL1 accelerates the beam to 18.5 MeV/u. The SCL1 uses two different

* hjkim@ibs.re.kr

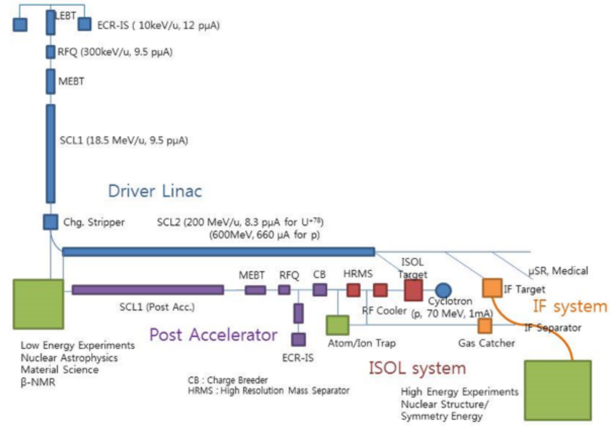

Figure 1: Layout of the RISP accelerator.

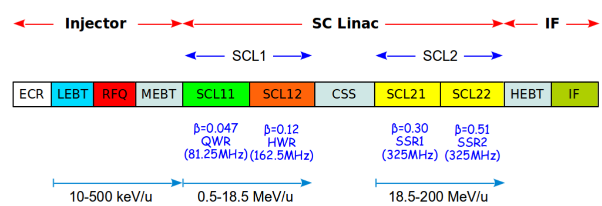

Figure 2: The RAON linear accelerator.

families of superconducting resonators, i.e., a quarter wave resonator (QWR) and a half wave resonator (HWR). The CSS accepts beams at 18.5 MeV/u. The charge stripper strips electrons from the heavy-ion beams to enhance the acceleration efficiency in the high-energy linac section. The SCL2 accepts a beam at 18.5 MeV/u and accelerates it to 200 MeV/u. The SCL2 uses two types of single spoke resonators, i.e., SSR1 and SSR2. The SCL2 provides a beam into the in-flight fragmentation (IF) system via a high-energy beam transport (HEBT).

The post accelerator (SCL3) is designed to accelerate the rare isotopes produced in the ISOL (Isotope Separation On-Line) system. The SCL3 is, in principle, a duplicate of the driver linac up to low energy linear accelerator. The accelerated rare isotope beams are reaccelerated in the SCL2. Hence, the RISP accelerator provides a large number of rare isotopes with high intensity and with various beam energies.

Injector System

The driver linac injector consists of a 28 GHz superconducting ECR ion source, the LEBT, the 500 keV/u RFQ and the MEBT. For the ECR ion source, superconducting magnets and dual high power RF sources of 28 GHz and

ISBN 978-3-95450-169-4

HIGH GRADIENT ACCELERATING STRUCTURES FOR CARBON THERAPY LINAC*

S.V. Kutsaev[1], R. Agustsson[1], L. Faillace[1], A. Goel[2], B. Mustapha[2], A. Nassiri[2], P. Ostroumov[2], A. Plastun[2], and E. Savin[1,3]

[1]RadiaBeam Systems, LLC, Santa Monica, CA, 90404, USA

[2]Argonne National Laboratory, Lemont, IL, 60439, USA

[3] National Research Nuclear University «MEPhI», Moscow, Russia

Abstract

Carbon therapy is the most promising among techniques for cancer treatment, as it has demonstrated significant improvements in clinical efficiency and reduced toxicity profiles in multiple types of cancer through much better localization of dose to the tumor volume. RadiaBeam Systems, in collaboration with Argonne National Laboratory, are developing a high-gradient linear accelerator, Advanced Compact Carbon Ion Linac (ACCIL), for the delivery of ion beams with end-energies up to 450 MeV/u for $^{12}C^{6+}$ ions and 250 MeV for protons. In this paper, we present a thorough comparison of standing and traveling wave designs for high gradient S-Band accelerating structures operating with ions at various velocities, relative to the speed of light, in the range 0.3-0.7. In this paper, we will compare these types of accelerating structures regarding RF, beam dynamics, and thermo-mechanical performance.

INTRODUCTION

ACCIL is designed for the full energy range from the ion source to 450 MeV/u for $^{12}C^{6+}$ and includes the following main sections: a radio-frequency quadrupole (RFQ) accelerator, a drift-tube linac (DTL), and a coupled-DTL sections operating at a sub-harmonic of the S-band frequency to accelerate carbon ions up to 45 MeV/m. For effective acceleration to higher energies, a high gradient S-band structure will be used. An overview of the linac is given in [1].

The compact footprint of ACCIL (8x45m) can be achieved if the accelerating structure capable of providing 50 MV/m for the particles with beta from 0.3 to 0.7 is developed. Such high accelerating gradients of the ACCIL linac will be feasible due to the operation at high frequency, 2856 MHz, at very low duty cycle <0.06% and very short <0.5 μs beam pulses. The known RF breakdown limit is much higher for high-frequency structures than for traditional low-β structures operating at lower frequencies.

There are several known criteria for RF breakdown limit that we have used for the EM design:

- Peak surface fields of 250 MV/m at 11-12 GHz, and ~160 MV/m for S-band have been demonstrated in RF guns and side-coupled linacs [2,3,4];
- Peak surface magnetic field that causes pulse heating, which can damage the structure if the peak temperature rise is higher than 50 ºC [5];
- There are also new theories of a unified criterion, such as a modified Poynting vector (<S>) [6] that may impact the gradients. However, there is not many experimental data for S-band structures;

In our design, we considered keeping all three parameters below known limits.

HIGH BETA STRUCTURE

Recently, A compact ultra-high gradient S-Band β=1 accelerating structure, operating in the π-mode at 2856 MHz, has been developed at RadiaBeam [7] (see Fig.1). The electromagnetic design and optimization of the cell shape to maximize RF efficiency and minimize surface fields at very high accelerating gradients included elliptical iris geometry to decrease surface electric field and "fat-lip" coupler to reduce surface RF pulsed heating. A 5-cell prototype HGS structure was fabricated with 4-6 μm surface finish, followed by SLAC prescription for cleaning and surface processing, and initially tested in 2013 at LLNL at 10Hz rep rate and max accelerating gradient of 50MV/m at 1.3 μs pulse duration [8].

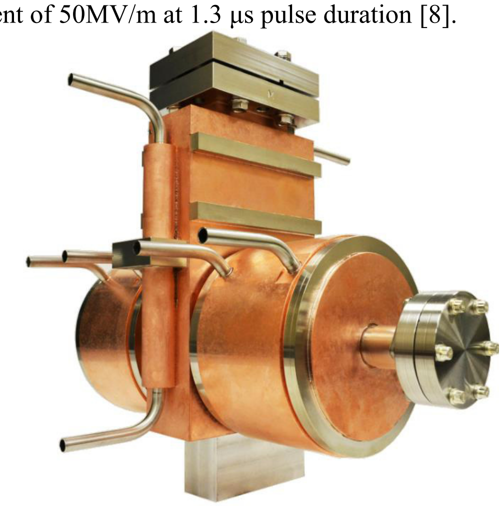

Figure 1: S-band 50 MV/m high-gradient structure (HGS) developed at RadiaBeam.

In February 2015, the structure was delivered to Argonne to perform high power tests and to check if the structure parameters deteriorated during the extended storage. Cavity conditioning was conducted with a 30 Hz pulse rep rate and varying pulse widths. With no bake, a

* This work was supported by the U.S. Department of Energy, Office of High Energy Physics, under Accelerator Stewardship Grant, Proposal No. 0000219678 and STTR grant DE-SC0015717

TRAVELING WAVE LINEAR ACCELERATOR WITH RF POWER FLOW OUTSIDE OF ACCELERATING CAVITIES*

Valery A. Dolgashev†, SLAC National Accelerator Laboratory, Menlo Park, CA, USA

Abstract

An accelerating structure is a critical component of particle accelerators for medical, security, industrial and scientific applications. Standing-wave side-coupled accelerating structures are used when available rf power is at a premium and average current and average power lost in the structure are large. These structures are expensive to manufacture and typically require a circulator; a device that diverts structure-reflected power away from rf source, klystron or magnetron. In this report a traveling wave accelerating structure is presented, which combines the high shunt impedance of the side-coupled standing wave structures with the advantages of traveling wave structures, such as simpler tuning and manufacturing. In addition, the traveling wave structure is matched to the rf source so no circulator is needed. This paper presents the motivation for this structure and shows a practical example.

INTRODUCTION AND MOTIVATION

Physics and technology of rf accelerating structures is a mature field with variety of existing geometries and methods. To distinguish a new approach from existing ones, first we will discuss accelerating structures used for the same applications. In this discussion we will emphasize the disadvantages to be improved upon using this new accelerating structure.

Side Coupled Standing Wave Accelerating Structure

In Fig. 1 a cell of a typical side-coupled standing wave (SW) accelerating structure is shown. This type of accelerator is widely used in medical, industrial and security applications because it offers very high shunt impedance and operational stability [1, 2]. For example, this high shunt impedance permits positioning of the complete accelerator on the arm of a robot for radio-surgery [3].

This accelerating structure is a bi-periodic system that works at the $\pi/2$ resonant mode. the structure made up of of accelerating and coupling cavities. In the working mode, most of the electro-magnetic fields are in the accelerating cells as seen in Fig. 1. The cavities are coupled magnetically with the coupling slots located near the outer diameter of the accelerating cavity.

Electron beam deflection The coupling slots in the side-coupled SW structure are located asymmetrically with respect to the axis where electrons or other charged particles are accelerated. This asymmetry, as well as power flow

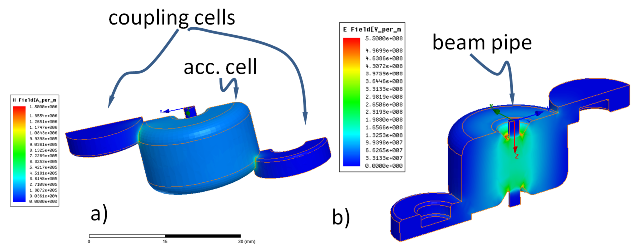

Figure 1: Finite element model of a half-cell of a side-coupled standing wave accelerating structure. Surface fields are normalized to 100 MV/m accelerating gradient: a) magnetic fields with peak magnitude of ~1.5 MA/m; b) electric fields with peak magnitude ~550 MV/m. This electromagnetic simulations were performed using a commercial finite-element code HFSS [4].

through the accelerating cell, creates electric and magnetic fields deflecting the beam off its axis. This deflection distorts the beam, especially during initial stages of acceleration, increasing beam losses and creating an uneven pattern on the x-ray target thus reducing the performance of the system.

Complexity of tuning and manufacturing The side-coupled SW structures are typically brazed in pieces, where each piece includes one half of accelerating cell and one half of coupling cell. When joined, two such pieces create the cavity shown in Fig. 1. The complexity of the joint's surface complicates the brazing so each cell has to be significantly tuned. The tuning is done to insure the desired field profile and make the frequencies of coupling and accelerating cells the same. The tuning is made difficult by the small fields in the coupling cell. This low field prevents tuning of this cell while in working configuration, so the cell typically has a hole to insert a measurement probe or perturb the cavity volume. This complexity both increases manufacturing and tuning cost and makes it difficult to evaluate the quality of the tuned structure.

Protection of RF source from reflected power By its nature of being a resonant cavity, a standing-wave structure absorbs rf signals in a narrow frequency band. For higher efficiency, the rf loss in the structure has to be as small as practical. The lower the rf losses, the narrower the frequency response of the structure. During initial transient, when such a narrow-band structure is filled with rf power, most of the power is reflected. If this reflected power does propagate back to the rf source, it will degrade its performance or may damage it. To protect the rf source, a waveguide isolator (typically a circulator) is installed between the SW accelerating structure and rf source. The isolator attenuates precious

* Work supported by the US DOE under contract DEAC02-76SF00515
† dolgash@slac.stanford.edu

DRY-ICE CLEANING OF RF-STRUCTURES AT DESY

A. Brinkmann[†], J.Ziegler, Deutsches Elektronen-Synchrotron DESY, Hamburg, Germany

Abstract

Dry-Ice cleaning is today a well-established cleaning method in matters of reducing harmful dark current and field emission in copper RF-structures like RF-Guns such as for the European XFEL, FLASH and REGAE. This led to the idea to clean longer RF-structures, in particular 3GHz transverse deflecting structures for the European XFEL. We developed a cleaning device with the capability to clean up to 2 m long structures in horizontal position with an inner diameter of not more than 40 mm. Furthermore this device allows cleaning 9-cell TESLA-type Nb-cavities as well. A report of the technical layout and results of RF-tests will be given.

INTRODUCTION

For the past ten years cleaning of copper RF-structures such as RF-photo Guns at FLASH and PITZ with carbon dioxide dry-ice snow cleaning became a well-established method to reduce harmful dark currents emitted from particles raised from the inner surface of the copper structure [1]. It could be shown that dry ice cleaning reduces dark currents by an order of magnitude. The present dark current of the Gun 3.1 at FLASH is about 5µA while running with operating parameters, whereat the limiting value is 20uA. Former cleaning methods, like High Pressure Water (HPWR) or alcohol rinsing led to dark currents in a range of hundreds µA. The very good achievements resulted in cleaning RF-Photo Guns for REGAE and the EXFEL as well. Since the 3 GHz Copper REGAE-Gun was never cleaned with liquids like water or alcohol, we do not have a direct comparison here. But the subsequent RF-conditioning was done very fast. It took no longer than 2 weeks to reach a gradient of 100MV/m [2]. Measurements at the EXFEL Gun, while running under operating parameters, led to dark currents in the range of 20µA.This altogether brought us to the idea, to clean more challenging structures from a cleaning point of view, such as Transverse Deflecting Structures (TDS) [3] for the EXFEL.

Originally the dry ice snow cleaning project was started to show if full equipped superconducting Niobium cavities could be cleaned in that way in addition and as a final step after a HPWR. With the original cavity cleaning device, it was only possible to clean 1-cell test cavities, whereas the new setup allows us to clean 9-cell 1.3 GHz Niobium cavities in horizontal position.

CARBON DIOXIDE DRY-ICE SNOW CLEANING

The functional principle and a detailed description of the cleaning mechanism are described in [4]. Liquid carbon dioxide flows at high pressure (50 bar) through a special formed nozzle, expands at the outlet and forms a dry-ice/gas mixture with a ratio of 45 % snow. This mixture is surrounded by a Nitrogen-gas stream, with 15 bar pressure, to ensure a proper acceleration of the jet. The cleaning takes place by thermal-mechanical and chemical forces: Breaking up the contaminations by shock-freezing, applying high shearing forces due to high momentum of the snow crystals and increasing of the volume by a factor of 500 after sublimation of the snow and acting as good chemical solvent for hydrocarbons and silicones.

CLEANING OF RF-PHOTO GUNS

The vertical cleaning device used for RF-photo Guns installed at FLASH, EXFEL and REGAE is shown in Fig.1.

Figure 1: Set-up for RF-photo Guns.

Here the Gun moves up and down while it rotates. The cleaning lance stays in a fixed position while the nozzle can be moved continuously from horizontal to vertical orientation to ensure that the overall inner surface of the Gun will be cleaned. A more detailed set of cleaning parameters can be found in [5].

CLEANING OF TRANSVERSE DEFLECTING STRUCTURES FOR EXFEL

The requirements for operating RF – structures under ultra-high vacuum conditions are i.a. particle free vacuum and a short conditioning time. Cleaning such components with fluids, implicates the difficulty to get rid of fluid residues after the cleaning process. In certain cases complex geometries inside the structures, like trapped volumes, prevent the draining of fluids. Anyway the draining can only be done in vertical orientation and moreover in a

† arne.brinkmann@desy.de

DEVELOPMENT OF ULTRACOLD NEUTRON ACCELERATOR FOR TIME FOCUSING OF PULSED NEUTRONS

S. Imajo, Department of Physics, Kyoto University, Kyoto, 606-8502, Japan
Y. Iwashita, ICR, Kyoto University, Uji, Kyoto, 611-0011, Japan
M. Kitaguchi, H. M. Shimizu, Department of Physics, Nagoya University, Chikusa, Nagoya, 464-8602, Japan
K. Mishima, T. Ino, KEK, Tsukuba, Ibaraki, 305-0801, Japan
S. Yamashita, ICEPP, University of Tokyo, Bunkyo, Tokyo, 113-0033, Japan

Abstract

Low energy neutron accelerator can be realized by the combination of an adiabatic fast passage spin flipper and a gradient magnetic field. Neutrons have magnetic moments, so that the accumulated potential energies are not canceled before and after passage of a magnetic field and their kinetic energies change in case their spins are flipped in the field. This accelerator handles lower kinetic energy neutrons than approximately 300 neV. Currently we have developed the advanced version which makes it possible to handle broader kinetic energy range. The design and measured characteristics are described.

INTRODUCTION

A non-zero neutron electric dipole moment (nEDM) implies the breaking of time-reversal invariance and the larger nEDM than the prediction of Standard model, which is 10^{-30} to 10^{-32} e $\cdot$ cm, is the evidence of new physics. Therefore research and developments are prompted to update the present nEDM upper limit of 2.9×10^{-26} e $\cdot$ cm [1]. In nEDM experiment, polarized ultracold neutron (UCN), whose kinetic energy is 100–200 neV, is stored in an experimental bottle, and then the nEDM is evaluated with the rotation phase shift of UCN spin precession induced in a superposition of a strong electric and a faint magnetic field parallel each other measured by the Ramsey resonance technique. The bottle should be small enough to have less spurious nEDM signals due to nonuniform electric and magnetic field [2]. Therefore spatially high-dense UCN is required in order to decrease the statistical errors. Such UCN is produced with the spallation neutron source and the superthermal converter, which is sometimes a pulsed source and has a very high peak flux.

We also have proposed a nEDM search with a spallation UCN source (J-PARC P33) [3]. In our plan, the repetition frequency of UCN production is 2 Hz. Because even the extremely dense UCN diffuses during transport according to their own velocity distribution, we are developing a neutron accelerator named ĄgUCN rebuncherĄh in order to control the velocity of UCN and to time-focus UCNs on the mouth of the bottle.

UCN REBUNCHER

A neutron has the magnetic dipole moment $\boldsymbol{\mu}$, and hence in a magnetic flux density $\boldsymbol{B}$ it has a potential energy that is expressed by $-\boldsymbol{\mu} \cdot \boldsymbol{B}$. The absolute value corresponds to 60 neV at a magnetic flux density of 1 T. The energy is lost as the neutron escapes from the magnetic field because such a potential energy is conservative. If the spin of the neutron is flipped in the field, the cancellation is prevented and therefore the kinetic energy of the neutron escaping from the field increases or decreases according to its spin direction [4]. If acceleration/deceleration of the pulsed neutron beam with velocity range is modulated suitably and its velocity-position phase space distribution is rotated, the beam is time-focused at some point [5]. This is the mechanism of the UCN rebuncher.

The spin-flip of a neutron and the kinetic energy control can be realized with the combination of a gradient magnetic field and an adiabatic fast passage (AFP) spin flipper [6]. If a neutron flies to x direction, a gradient magnetic field is applied in the z direcition and an alternating magnetic field of the frequency f is applied parallel to the neutron path, the spin-flip occurs around the point of the resonant magnetic field $B_z = hf/2|\mu|$, where h is the Planck constant. If f is modulated, the strength of B_z for the resonance also changes and hence the spin-flip point moves in the gradient field. Thus each neutron gains a different kinetic energy. Consequently, the phase space distribution of neutrons can be controlled.

The spin-flip probability p depends on the adiabatic parameter k, which are given by [5]

$$p = 1 - \frac{1}{1+k^2} \sin^2\left(\frac{\pi}{2}\sqrt{1+k^2}\right), \tag{1}$$

$$k = \frac{-\gamma_n B_1^2}{dB_0/dt} = \frac{-\gamma_n B_1^2}{v\,dB_0/dx}, \tag{2}$$

where γ_n is the gyromagnetic ratio of neutrons, B_1 is the rotating magnetic field strength, dB_0/dt is the temporal change of the static magnetic field for a UCN, v is the neutron velocity and dB_0/dx is the spatial gradient of the static magnetic field. If k is more than 1.4, the spin-flip probability is more than 0.9. An anisotropic-inter-pole magnet we have developed produces the linearly gradient magnetic field of 3.2 T/m [7,8]. A RF field works as the rotating field. Therefore the strength of the RF magnetic field needs to be more than 0.7 mT in order to achieve $k > 1.4$ with the UCN of 5 m/s.

We developed the prototype of the rebuncher and carried out the demonstration experiment of the rebuncher at ILL in

LATEST NEWS ON HIGH AVERAGE RF POWER OPERATION AT PITZ

Y. Renier*, G. Asova[1], P. Boonpornprasert, M. Gross, J. Good, H. Huck, I. Isaev[2], D. Kalantaryan, M. Krasilnikov, O. Lishilin, G. Loisch, D. Melkumyan, A. Oppelt, T. Rublack, C. Saisa-ard[3], F. Stephan, Q. Zhao[4] DESY, Zeuthen, Germany
M. Bousonville, S. Choroba, S. Lederer, DESY, Hamburg, Germany
[1]on leave from INRNE, Sofia, Bulgaria
[2]on leave from NRNU MEPhI, Moscow, Russia
[3]on leave from Chiang Mai University, Chiang Mai, Thailand
[4]on leave from IMP/CAS, Lanzhou, China

Abstract

The Photo Injector Test Facility at DESY in Zeuthen (PITZ) develops, tests and characterizes high brightness electron sources for FLASH and European XFEL. Since these FELs work with superconducting accelerators in pulsed mode, also the corresponding normal-conducting RF gun has to operate with long RF pulses. Generating high beam quality from the photocathode RF gun in addition requires a high accelerating gradient at the cathode. Therefore, the RF gun has to ensure stable and reliable operation at high average RF power, e.g. 6.5 MW peak power in the gun for 650 µs RF pulse length at 10 Hz repetition rate for the European XFEL. Several RF gun setups have been operated towards these goals over the last years. The latest gun setup was brought into the PITZ tunnel on February 10th 2016 and its RF operation started on March 7th. This setup includes RF gun prototype 4.6 with a new cathode contact spring design and an RF input distribution which consists of an in-vacuum coaxial coupler, an in-vacuum T-combiner and 2 RF windows from DESY production. In this contribution we will summarize the experience from the RF conditioning of this setup towards high average RF power and first experience from the operation with photoelectrons.

RF FEED SYSTEM AND GUN 4.6

The RF waveguide distribution system used with gun 4.6 is the two vacuum windows configuration as shown in Fig. 1. This two RF windows solution was installed in 2014 [1] after several break-downs of RF windows in the previous configuration where only one RF vacuum window was used. This solution has the particularity to have the 10 MW directional coupler and the T-combiner in vacuum. Along with the gun installation, two recoated and pre-conditioned DESY RF windows and a new T-combiner have been installed during the winter 2016. A short section with air under 3 bar pressure is realized between the SF_6 gas and the vacuum section, to have an easy exchange between two different setups and to be as close as possible to the XFEL and FLASH setups where there is no SF_6 but air waveguides. This section is also an additional safety, acting as a buffer in case of a leak in the gas vacuum windows, preventing any SF_6 to reach the vacuum system.

* yves.renier@desy.de

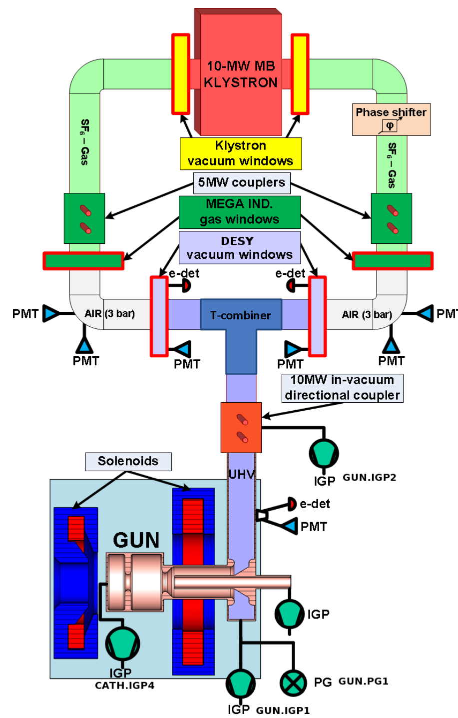

Figure 1: PITZ RF feed system in a two vacuum windows configuration.

The gun 4.6 is a new cavity and uses the new watchband-reloaded cathode spring design [2] where the cathode region has been optimized to avoid any sharp edges. In the original design, sharp edges could be damaged during cathode manipulations and high power operation. The cathode plug is electro-polished to avoid damages to the contact spring eg. caused by bad contact with the cathode or by discharges. As usual, the gun is dry-ice cleaned to reduce the dark current [3].

CONDITIONING

The standard procedure applied for conditioning of RF guns is described in [4]. The control system used is based on DOOCS [5]. Relevant properties are stored by the Data AQuistion system (DAQ). This data is then analyzed to get statistics on conditioning and operation.

ISBN 978-3-95450-169-4

DIELECTRIC AND THz ACCELERATION (DATA) PROGRAMME AT THE COCKCROFT INSTITUTE

G. Burt[1†], R. Letizia[1], C. Paoloni[1], Lancaster University, Lancaster, UK
S.P. Jamison[1], Y. Saveliev[1], ASTeC, STFC Daresbury Laboratory, Warrington, UK
C.P. Welsch[1], University of Liverpool, Liverpool, UK
R.B. Appleby[1], D.M. Graham[1], T.H. Pacey[1], H. Owen[1], G. Xia[1], The University of Manchester, Manchester, UK
A.W. Cross[1], A. Phelps[1], K. Ronald[1], University of Strathclyde, Glasgow, UK
[1]also at Cockcroft Institute, Sci-Tech Daresbury, Daresbury, UK

Abstract

Normal conducting RF systems are currently able to provide gradients of around 100 MV/m, limited by breakdown on the metallic structures. The breakdown rate is known to scale with pulse length and, in conventional RF systems, this is limited by the filling time of the RF structure. Progressing to higher frequencies, from RF to THz and optical, can utilise higher gradient structures due to the fast filling times. Further increases in gradient may be possible by replacing metallic structures with dielectric structures. The DATA programme at the Cockcroft Institute is investigating concepts for particle acceleration with laser driven THz sources and dielectric structures, beam driven dielectric and metallic structures, and optical and infrared laser acceleration using grating and photonic structures. A cornerstone of the programme is the VELA and CLARA electron accelerator test facility at Daresbury Laboratory which will be used for proof-of-principle experiments demonstrating particle acceleration.

INTRODUCTION

In particle physics, future linear colliders such as CLIC or ILC require ultra-short, sub-picosecond, bunches to obtain the luminosity necessary for the particle physics science exploration. In accelerator based x-ray sources, sub-10 fs bunches open new capabilities in femtosecond time-resolved material science. With existing linear accelerators delivering beams on the femtosecond scale already on the km scale, and tens of km scale machines proposed, higher gradient structures are sought for the potential to shrink the size and cost of linear accelerators. Current metallic microwave structures are limited by electric breakdown to around 100 MV/m, and superconducting structures are restricted to even lower gradients. Particle acceleration driven by laser and (laser generated) THz radiation has the potential for GV/m acceleration gradients; The sub-ps to few–fs oscillation periods of THz and laser electromagnetic fields are also well suited for acceleration and control of femtosecond duration electron bunches. While only a very limited number of demonstrations of laser and THz acceleration have been achieved, such approaches remain promising for high gradient acceleration of high energy beams in the long term. In the short-term future, laser and THz acceleration has high potential for applications in generation of femtosecond few-MeV beams for electron diffraction, and for compact soft and hard x-ray sources with intrinsic femtosecond synchronization with lasers.

The Cockcroft Institute has initiated a multi-themed programme, Dielectric and THz Acceleration (DATA), to investigate particle beam acceleration using sub-picosecond electromagnetic fields. The programme is divided into three themes of (i) Laser generated THz acceleration and deflection; (ii) Beam driven (wakefield) THz acceleration in dielectric and metallic structures; and (iii) Dielectric Laser Acceleration. THz electromagnetic fields, with electric field oscillations in the range of 100 fs-1000 fs, will be examined for their potential for efficient and phase-controlled capture and acceleration of electron beams. For the laser generated THz acceleration, both free space and and dielectric waveguide mechanisms are being investigated for acceleration or deflection for beam diagnostics. For beam driven THz sources, the programme is investigating corrugated metallic structures and dielectric waveguides for Wakefield acceleration. Laser-dielectric structures are being examined for their potential in very-high gradient acceleration of high-energy femtosecond beams. In this latter theme we are investigating inverse grating and photonic band-gap structures excited by visible and near-IR lasers. The programme will undertake a range of proof-of-concept demonstrations of laser and THz radiation driven electron acceleration with the VELA and CLARA electron accelerator test facility at Daresbury Laboratory. These test facilities include a 5MeV RF photo-injector gun, a beamline with a suite of diagnostics including a transverse deflecting cavity, and 2 metre long experimental chamber followed by an electron spectrometer. The facilities are currently being upgraded with a second injector and dog-leg transfer line; this new injector will provide beams up to 50MeV. The VELA and CLARA test facilities are described further in reference [1] of this conference.

† Email address: graeme.burt@cockcroft.ac.uk

OPERATION OF THE CEBAF 100 MV CRYOMODULES*

C. Hovater†, T. Allison, G. Biallas, R. Bachimanchi, E. Daly, M. Drury, A. Freyberger, R. L. Geng, G. Lahti, R. Legg, C. Mounts, R. Nelson, T. Plawski, and T. Powers
Jefferson Lab, Newport News, Virginia 23606

Abstract

The Continuous Electron Beam Accelerator Facility (CEBAF) 12 GeV upgrade reached its design energy in December of 2015. Since then CEBAF has been delivering 12 GeV beam to experimental Hall D and 11 GeV to experimental halls A and B in support of Nuclear physics. To meet this energy goal, ten new 100 MV cryomodules (80 cavities) and RF systems were installed in 2013. The superconducting RF cavities are designed to operate CW at a maximum accelerating gradient of 19.3 MV/m. To support the higher gradients and higher Q_L (~ 3×10^7) operations, the RF system uses 13 kW klystrons and digital LLRF to power and control each cavity. This paper reports on the C100 operation and optimization improvements of the RF system and cryomodules.

INTRODUCTION

Since 2014 ten new eight cavity high gradient cryomodules (designated as C100) have been in operation supporting nuclear physics experiments. The cryomodule design is a culmination of the lessons learned from three preproduction high gradient cryomodules and the original 42 CEBAF cryomodules [1]. To meet the 12 GeV energy goals the cryomodules were designed to have an energy gain of 98 MeV, with an additional 10% overhead reaching 108 MV. Each cryomodule consists of eight 7-cell elliptical cavities. The cavities are tuned to 1.497 GHz, and individually controlled by both a mechanical stepper motor and a Piezo tuner (PZT).

The RF system powering and controlling these cryomodules is also a new design [2]. Like most CW SRF accelerators each cavity is powered and controlled by a single klystron and LLRF system. The klystrons produce 12 kW of linear power. The eight klystrons are self-protected with their own interlocks as part of the high power amplifier system. The LLRF controls down convert from the cavity frequency to an intermediate frequency (70 MHz). The cavity signal is then digitized and processed using an FPGA. The RF controls are unique incorporating a digital self-excited loop (SEL) to quickly recover cavities. Controls and interfaces for both the HPA and the LLRF are provided through EPICS.

Since 2014 the cryomodules have performed as needed to provide the energy for the experimental program [3, 4]. Table 1 shows the C100 energy contributions from each cryomodule during the spring 2016 operation period comparing them to their commissioned energies. The lower operational energy is due to a number of challenges that have presented themselves in the operation of the C100 cryomodules. The cryomodules have shown themselves to be sensitive to He pressure variations caused by a combination of RF/resistive heat and the heat capacity limitations of the pipe between the individual cavity helium vessel and the, shared two-phase pipe. When the capacity is exceeded there is a pressure transient which leads result in frequency detuning larger than the klystron power can accommodate. Transient vibration induced microphonics from driven external sources (trucks, cooling towers etc.) with frequency content that falls on the modal resonances of the structure can be a source of unwanted trips. Lastly cavity field emission, becoming dark current, has posed both a radiation damage issue with local cabling & magnets and a vacuum issue in the immediate warm regions downstream from the C100 cryomodules. While these issues have been a challenge they have not prevented CEBAF from delivering electrons for Nuclear physics experiments. We report on the problems and mitigations that are being put into place to overcome them.

Table 1: Cryomodule Energy Gains

Cryomodule	Zone	Commissioned Energy	Operational Energy
C100-1	SL24	104 MV	77.1
C100-2	SL25	122	89.6
C100-3	NL22	108	91.2
C100-4	SL22	93	91.5
C100-5	SL23	121	91.9
C100-6	NL23	111	99.4
C100-7	NL24	103	95.9
C100-8	SL26	110	90.7
C100-9	NL25	105	85.0
C100-10	NL26	106	83.5

CRYOGENIC DETUNING

The C100 cryomodule individual cavity helium vessel piping is designed to accommodate up to 52-62 Watts of RF or electric heat at 2.07 K and a total cryomodule heat load of about 350 which is limited by the end can piping. Above 2.0 K the heat capacity limitation is a strong function of the helium pressure. If the heat in an individual vessel reaches the limit for the heat riser pipe, the helium temperature inside the helium vessel exceeds 2.18 K and there is a pressure transient which causes a microphonic perturbation that is enough to detune the cavity beyond what the klystron can accommodate. In addition the He pressure increases slightly down the LINAC (the C100s are at the end) so the cryomodules at the end of the linac can't

*Authored by JSA, LLC under U.S. DOE Contract DE-AC05-06OR23177. The U.S. Govt. retains a non-exclusive, paid-up, irrevocable, world-wide license to publish or reproduce this for U.S. Govt. purposes.
†hovater@jlab.org

ISBN 978-3-95450-169-4

KLYNAC DESIGN SIMULATIONS AND EXPERIMENTAL SETUP

K. E. Nichols, B. E. Carlsten, A. Malyzhenkov,
Los Alamos National Laboratory, Los Alamos, USA

Abstract

We present design simulations and experimental setup for the first ever experimental demonstration of a bi-resonant klynac; klynac is a term coined for a compact linear accelerator with integrated klystron source utilizing the same electron beam. This device is bi-resonant, one resonant circuit for the klyston input and gain cavities, and one for the klystron output and linac cavities, the schematic is presented in Fig. 1. The purpose of a klynac-type device is to provide a compact and less expensive alternative for an accelerator up to 6 MeV. A conventional accelerator requires a separate RF source and linac and all the associated hardware needed for that architecture. The klynac configuration eliminates many of the components to reduce the weight of the entire system by 60%. We have built an 8-cavity, 2.84 GHz RF structure for a 1 MeV klynac. A 50-kV, 10-A pierce-type electron gun provides the single beam needed. Numerical modelling was used to optimize the design. The separation between the klynac output cavity and the first accelerator cavity was adjusted to optimize the bunch capture and a pin-hole aperture between the two cavities reduces the beam current in the linac section to about 0.1 A. Standard high-shunt impedance linac cavity designs are used. We have fabricated the first test structure and present very preliminary results.

DESIGN PROCESS AND SIMULATIONS

Design

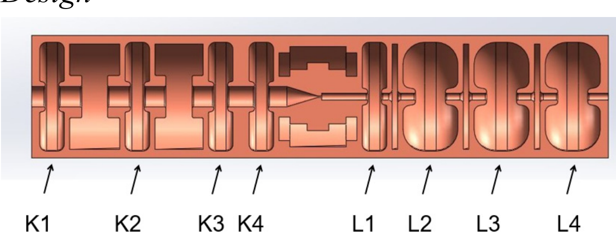

Figure 1: Schematic of the Klynac design. K1, K2, and K3 form one resonant cavity and serve the purpose of gain cavities. K4 is the gain output cavity and L1-L4 are the accelerating cavities, together they form the second resonant circuit. Unmarked cells are coupling cells and have 0 field in the π/2 mode.

The klystron input cavity is K1 which forms a resonant circuit with the two RF gain cavities, K2, and K3. The RF output cavity, K4, as well as the four linac cavities, L1, L2, L3, and L4, form a second resonant structure. Additionally, K4 acts as a conventional klystron output cavity, generating RF power that is then used to drive the linac cavities and accelerate the electron beam. This structure resonates in the π/2 standing-wave mode, therefore the fields in the coupling cavities are negligible and they can be ignored in the design analyses. Note that this mode ensures that successive klystron cavities are 180º out of phase with the previous cavity, but cavity amplitudes can be designed to maximize the extraction power. The cavity locations in the gain section are similarly chosen to maximize harmonic current. An efficiency of 38% was achieved for the gain section, we believe that could be improved upon. The separation between K4 and L1 is adjusted to optimize the bunch capture in L1. An intercepting aperture between cavities K4 and L1 reduces the beam current in the linac section to about 1% of that in the klystron section, this is the amount of beam current that can be accelerated with the power delivered by the gain section. The amount of beam current in the linac section is adjustable by pinching the beam with an external magnetic field. The coupling cell between K4 and L1 is special because it is not open to the axis, it is a toroidal cavity rather than a pillbox cavity [1]. Once the beam reaches L2, it is relativistic. Thus the separation between L2 and L3, and L3 and L4 are close to half the free-space wavelength of the klynac's operating frequency. Standard high-shunt impedance linac cavity designs are used. Both the gap in L1 and the center-to-center separation of L1 and L2 are shortened to provide for better capture of the initially low energy electron beam injected into the linac section.

Table 1: Nominal 1 MeV Klynac Parameters from Simulations

Nominal Design Parameters 1 MeV Klynac	**Value**
RF power generated	160 kW
Number of linac cavities	4
Linac cavity impedance	8.5 MW
Linac cavity transit time factor	0.80
Linac cavity gap voltage	440 kV
Linac electron beam current	0.09 A
RF power dissipated in linac section	69 kW
RF power into beam power	91 kW
Final beam energy	1.00 MeV
RF power generated	160 kW

The cavity voltages in the accelerating cavities were determined from the klynac power balance, which can be approximated as:

BEAM ORBIT ANALYSIS AND CORRECTION OF THE FRIB SUPERCONDUCTING LINAC *

Yan Zhang#, Zhengqi He
FRIB, Michigan State University, East Lansing, MI, USA

Abstract

Beam based alignment (BBA) technique is an important tool for precise beam orbit correction of a high power linac, and it is supplement to a model based or an orbit response matrix (ORM) based orbit correction method. BBA could be applied to the beam orbit analysis and correction of the FRIB linac arcs where a beam orbit offset within 0.1 mm is required to tune the second order achromatic lattice. In this paper, we will first introduce the study of model based beam orbit correction of the linac arcs, and then a more precise orbit correction with BBA. Realistic misalignments of beam elements and beam position monitors (BPMs) are included in the simulation studies.

INTRODUCTION

Beam orbit analysis and corrections are one of the most essential processes applied for beam control in accelerators and beam transport lines, to significantly reduce beam loss and to preserve beam emittance, especially for high power machines. Various beam orbit correction techniques have been developed and demonstrated in particle accelerators including ring and linac, as the requirements to beam orbits for different machines can be substantially different.

We studied various beam manipulation methods in the beam commissioning plan of the FRIB superconducting linac and noted that orbit corrections are very important for the operations with multi charge state beams [1]. Although a beam orbit offset of 1 to 2 mm in the FRIB linac has no issues in simulation studies and likely in operations too, to precisely tune the second order achromat of all the folding segments, an orbit within 0.1 mm is needed. Different orbit correction methods are investigated in simulation studies with realistic misalignments of beam elements and BPMs.

Open XAL online model [2] is applied in the beam orbit analysis and correction. Both model based and beam based orbit correction techniques have been demonstrated in the SNS accelerator systems [3, 4], while different approaches are also planned for the FRIB linac system [5].

MODEL BASED ORBIT CORRECTION

An online model is usually applied to precisely predict beam orbit differences of the real machine, and a model based orbit correction could be conducted using a global optimization of the beam offsets of all the available BPMs, provided that misalignments of all the beam elements and BPMs are well within specifications. However, if errors, misalignments of beam elements or BPMs are outstanding, uncertainties of beam orbit after a model based correction could still be substantial, in which case, iterations of the orbit correction may become necessary, and measurements of the BPM misalignments will be important.

When needed, model based beam orbit correction can be easily extended to measure BPM misalignments. As model predicted beam orbit differences are mainly determined by the injection beam and misalignments of beam elements, series of measurements of beam orbit differences with the linac BPMs can be conducted to reconstruct the model.

The method is simple: different correctors fired in the linac and beam orbit differences measured with BPMs, the same beam steering is applied in the model and compared against model predicted orbit changes, the injection beam and misalignments of the beam elements optimized in the model to reproduce the BPM measurement results. Figure 1 shows an orbit difference exercise in simulation studies.

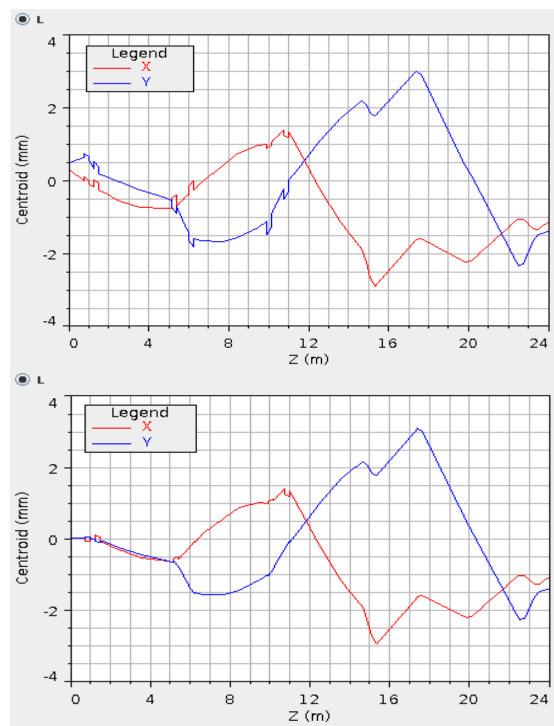

Figure 1: A model based beam orbit differences exercise. Upper: model with an inclined beam and misalignments of quadrupole magnets; Lower: reconstruction using BPMs.

In the above exercises, reconstructed parameters of the injection beam and misalignments of the beam elements differ from those of the original model, mainly because of errors and multiple solutions with limited BPMs. However, misalignments of the BPMs can be identified and corrected with the measurements of beam orbit differences, and after the BPMs are marked a model based beam orbit correction is conducted. The results are shown in Figure 2.

* Work supported by the U.S. Department of Energy Office of Science under Cooperative Agreement DE-SC0000661
# zhangy@frib.msu.edu

ISBN 978-3-95450-169-4

BEAM TUNING OF ACHROMATIC BENDING AREAS OF THE FRIB SUPERCONDUCTING LINAC *

Yan Zhang # and Paul Chu
FRIB, Michigan State University, East Lansing, MI 48824, USA

Abstract

To achieve the design power for the heaviest ion species, it is required to accelerate and transport multi charge state beams simultaneously in the FRIB SC driver linac, which imposes a great technical challenge especially to the folded linac lattice design. An achromatic and isochronous beam optics up to the second order must be established precisely in the bending segments. Because system errors and beam element imperfections always exist in the real machine, beam tuning and optics corrections of the bending areas are critical to high power operation. In this paper, beam tuning algorithms of achromatic arcs of the FRIB driver linac are introduced and the simulation studies discussed.

INTRODUCTION

The FRIB, Facility for Rare Isotope Beams, is currently under construction on the campus of MSU, Michigan State University. The project is funded by the US Department of Energy Office of Science, MSU, and the State of Michigan. The total budget of the project is about 730 million dollars, and it will be completed in 2022 [1].

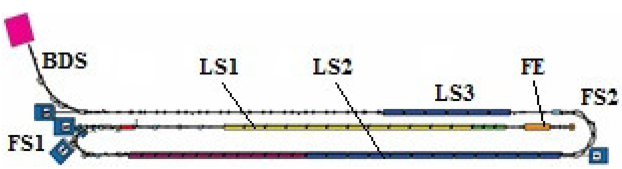

Figure 1: Schematic layout of the FRIB driver linac.

The FRIB driver linac consists of a front end (FE), three linac segments (LS), two 180° folding segments (FS), and a beam delivery system (BDS) which transport beams onto a fragmentation target for the production of rare isotopes. Shown in Figure 1 is a schematic layout of the FRIB linac. For the heaviest ion species, accelerate and transport multi charge state beams simultaneously in the linac are required to achieve the design power of 400 kW, thus the second order achromat is needed to all the folding areas including the BDS, and meanwhile isochronous beam optics should be tuned accurately for the two 180° folding segments.

ACHROMATIC LATTICE

In the design of an achromatic bend, beam particle at the final location shall be independent to the momentum, and the bend will produce the same output beam regardless of the momentum spread. In an isochronous bend, the arrival time of beam particle is independent to the momentum and the transverse location, essentially, injection particles with different momentum and transverse positions arrive at the same time. Using the notations of TRANSPORT [2], first order elements $R_{16} = 0$ and $R_{26} = 0$ in an ideal achromatic system. In an isochronous system, $R_{51} = 0$, $R_{52} = 0$, and $R_{56} = 0$. It is noted that in an isochronous system, $R_{56} = (1-\beta^2)\cdot L$ is generally required for a low energy particle beam as the velocity changes substantially with the momentum. In the FRIB linac however, as the energy and velocity of various charge state beams are similar, so that in the bend different rigidities of those multi charge state beams are analogous to momentum differences, thus $R_{56} = 0$ is required instead, though which is generally for a high energy electron beam.

As charge states of uranium beams from +76 to +80 are equivalent to about ±3% momentum variations, the second order achromat is needed, therefore sextupoles are installed in all the bends. Figure 2 shows transfer matrix elements of the LS1 arc in simulation with MAD-X [3], the symmetric bend totally consists of four 45° dipoles, four quadrupoles, and two sextupoles. In the lattice design, locations of the quadrupoles are selected to have $R_{16} = R_{52}$, and $R_{26} = R_{51}$, therefore once an achromat is established, the bend is also isochronous. Because of compact lattice design, available knobs and spaces are limited, it is not a perfect achromatic system. Sextupole magnets are installed for manipulating second order dispersions, both longitudinal and transverse.

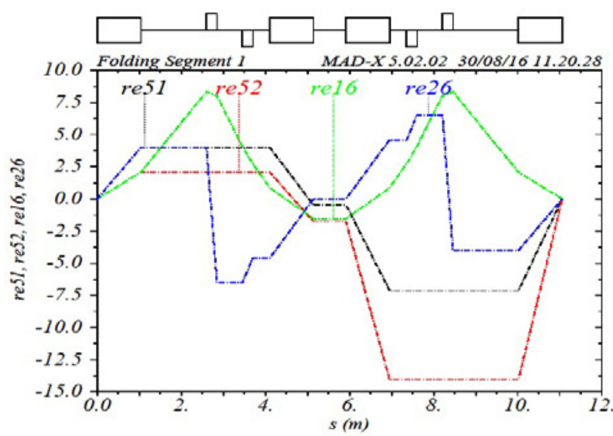

Figure 2: Beam transfer matrix elements R_{16}, R_{26}, R_{51}, and R_{52} of the LS1 lattice in calculation with MAD-X.

BEAM TUNING BASED ON MODEL

Since in the real world beam element imperfections and system errors cannot be completely avoidable, beam tuning of the bending segments becomes important for high power operation of the driver linac. Algorithms of beam tuning and optics corrections have been introduced briefly in the FRIB linac beam commissioning plan [4], while detailed analysis is described in this paper. Figure 3 shows ideal horizontal orbits of difference charge state beams in the

* Work supported by the U.S. Department of Energy Office of Science under Cooperative Agreement DE-SC0000661
# zhangy@frib.msu.edu

BEAM TUNING AND ERROR ANALYSIS OF A SUPERCONDUCTING LINAC *

Yan Zhang #
FRIB, Michigan State University, East Lansing, MI 48824, USA

Abstract

Beam tuning and error analysis of a superconducting linac for heavy ion beams are introduced in this paper. System errors of the beam tuning are analysed numerically, which include random errors of cavities and magnets, and measurement errors of the absolute beam phase, beam bunch length, and transverse beam profiles. Statistical formulas are developed from tedious and time-consuming numerical simulations, and the studies provide advantage tools not only to analyse the errors of linac beam tuning, such as RF phase and amplitude tuning of superconducting cavity, longitudinal and transverse beam matching, but will also be helpful to the linac design with practical beam diagnostics and authentic accelerator lattices.

INTRODUCTION

In the beam tuning of a superconducting linac or other accelerators, imperfections and errors of the accelerator components are unavoidable, thus it can be important to understand the effects and to improve error tolerance in the accelerator design as well as in the practical beam tuning particularly for a high power machine. Usually, intensive numerical computation and simulations with sophisticated accelerator models are needed in the error analysis, which is tedious and can be extremely time-consuming. A simple statistical estimation, even a rough one, can be considered in most cases.

E.g. the effects of random misalignments of a focusing channel in a periodic lattice are analogous to the problem of random walk, and a simple statistical estimation of the amplitude of beam orbit distortions can be expressed as [1]:

$$\delta = \frac{\sigma\cdot\sqrt{N}}{\cos(\frac{\mu}{2})} \tag{1}$$

where, δ is the rms amplitude of coherent orbit distortion, σ is the rms alignment errors of the focusing elements, μ is the phase advance and N number of focusing elements.

As particle acceleration and RF defocusing effects exist, a linac lattice generally is not perfectly periodic, however, Eq. (1) is still a suitable estimation of the linac beam orbit distortion by misalignments of the focusing magnets, prior to any beam orbit corrections.

CAVITY PHASE AND AMPLITUDE

Cavity RF phase and amplitude tuning with beam is one of the primary tasks before operation of a linac. Phase scan and signature matching techniques [2] are widely applied in proton and heavy ion linac. Phase and amplitude tuning of the FRIB superconducting cavity [3] is used here merely as an example, as the method is also valid to other linac.

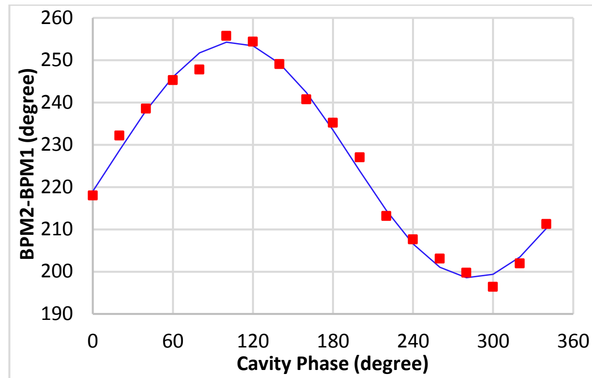

Figure 1: A cavity phase scan and the signature matching.

Figure 1 shows a cavity 2π phase scan and the time-of-flight signature matching in simulations with online model, for a beam energy approximately 17 MeV/u it is almost a pure sinusoidal curve. Errors of the tuning are mainly come from measurement errors of the absolute beam phase with beam phase monitor (BPM) pairs.

To estimate the error of phase scan with random BPM phase measurement errors, cavity RF phase and amplitude are treated as a phasor, the rms error of this phasor is:

$$\delta = \frac{\Delta}{A\cdot\sqrt{N}} \tag{2}$$

where, Δ is random BPM phase errors assumed in uniform distributions, A is the amplitude of BPM phase difference, and N number of measurements in the phase scan ($N \geq 3$).

E.g. in Figure 1, an uniform distribution of random BPM phase error of ±2° is assumed, the amplitude of BPM phase difference is about 28° in the cavity 2π phase scan, number of the BPM phase measurements 18, and we have $\delta \approx 1.7\%$. It means that an rms amplitude error of this cavity is about 1.7%, and an rms phase error is nearly 1° in the tuning.

The amplitude of BPM phase difference in a cavity 2π phase scan can be expressed as:

$$A = \frac{QV_a}{mc^2}\cdot\frac{\omega L}{c\beta^3\gamma^3} \tag{3}$$

where, Q is charge state of the beam particle, mc^2 is the rest energy, c is speed of light, β and γ relativistic parameters; V_a is acceleration voltage of the cavity, ω and L - angular frequency and drift distance of the BPM pairs.

Other errors in a beam time-of-flight measurement with BPM pairs, such as BPM alignment errors and calibration errors, can be summarized as errors of velocity and energy:

$$\frac{dv}{v} = \frac{dL}{L} + \frac{dt}{t}$$
$$\frac{dE}{E} = \gamma(\gamma+1)\frac{dv}{v} \tag{4}$$

where, dL is BPM alignment error, and dt calibration error.

* Work supported by the U.S. Department of Energy Office of Science under Cooperative Agreement DE-SC0000661
# zhangy@frib.msu.edu

ISBN 978-3-95450-169-4

STATUS OF AND PLANS FOR THE BEAM DYNAMICS PROGRAM DYNAC*

E. Tanke, M. Eshraqi, Y. Levinsen, A. Ponton, ESS, Lund, Sweden
S. Valero, Consultant, retired from CEA-Saclay, Paris, France

Abstract

A short introduction to the beam dynamics code DYNAC [1] will be given. Benchmarking of the Radio Frequency Quadrupole (RFQ) model and the relativistic case of a beam transport line with space charge will be discussed.

Recently implemented features, such as a Graphical User Interface (GUI), will be presented and additional planned features to DYNAC and the GUI will be touched upon.

INTRODUCTION

For beam dynamics, the multi-particle code DYNAC contains a numerical method, capable of simulating single and multi-charge state ion beams in accelerating elements as well as an analytical method, capable of modelling protons, single charge state heavy ions and non-relativistic electrons. The code contains three space charge routines, including a 3D version and has been benchmarked against other codes as well as against measurements [2-4]. It is well suited for online modelling and as an aid in view of commissioning [5], [6] and will work on linux, MAC and Windows.

RFQ

The capability in DYNAC for simulating the RFQ Radial Matching Section (RMS) and Fringe Field (FF) regions based on electrical fields directly obtained in using the electrode shape has been added (see Fig. 1).

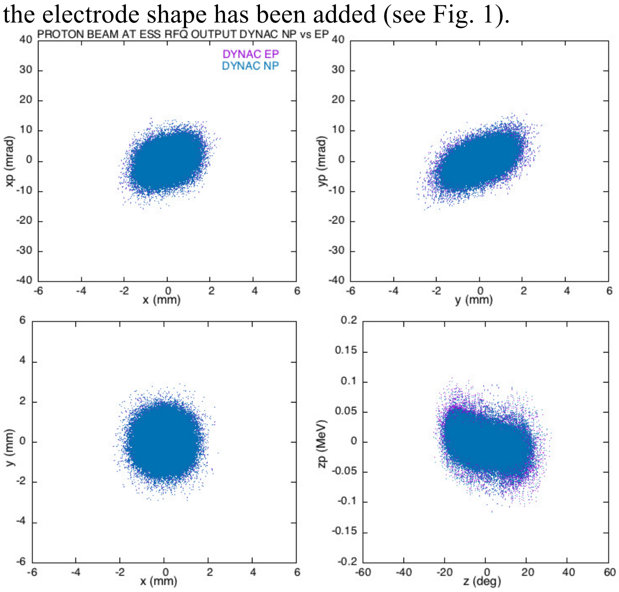

Figure 1: Phase space plots after a fringe field with electric fields directly derived from the electrode profile (EP) and the case where coefficients were used (NP).

For the benchmark of the RFQ, DYNAC results were compared to those obtained from Toutatis [7]. For this purpose, the ~ 4.6 m long 70 mA European Spallation Source (ESS) proton RFQ [8] was taken as test case. This RFQ has a Radial Matching Section (RMS) at the input, followed by a transition cell, 412 accelerating cells, another transition cell and finally a fringe field. The intervane voltage varies from 80 to 120 kV along the RFQ length. The beam is accelerated from 0.075 to 3.62 MeV.

Benchmark Results

The phase space plots at the ESS RFQ output for both DYNAC and Toutatis are shown in Fig. 2. The energy gain differs by ~ 0.1%.

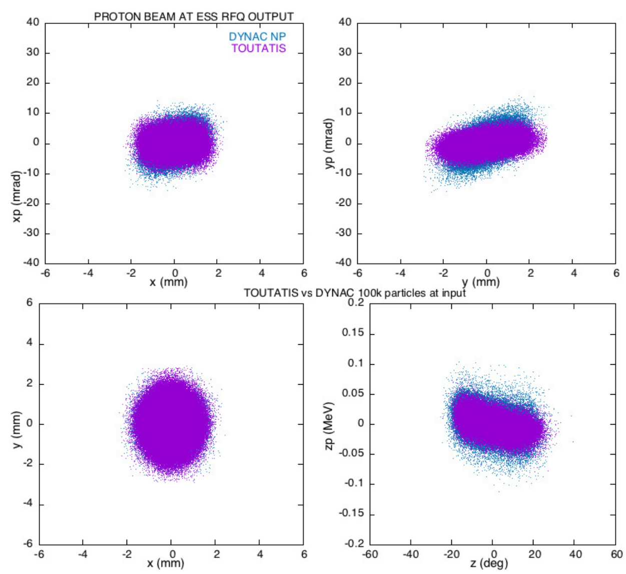

Figure 2: Phase space plots of the proton beam at the output of the ESS RFQ.

Based on a 100k macro particle distribution at the input, a transmission of 99.2% was obtained with Toutatis, whereby only particles that hit the electrodes were eliminated. Optionally one can use radial limits that are defined by a square with an edge equal to two times the minimum aperture. In this case, 98.3% transmission was obtained, but in either case particles that were not or poorly accelerated are still counted. By applying a filter to the output beam such as to eliminate the errant beam, 97.6% was obtained.

For the DYNAC case, the same input distribution was used. Here particles are removed radially when they go beyond an ellipse with the horizontal and vertical apertures as major axis. In addition, particles that are not accelerated are ultimately eliminated as the beam progresses

DISPERSION FREE AND DISPERSION TARGET STEERING EXPERIENCE AT CTF3

D. Gamba*[1], R. Corsini, F. Tecker, P. Skowronski, T. Persson, CERN, Geneva, Switzerland
P.N.Burrows, JAI, University of Oxford, Oxford OX1 3RH, United Kingdom
[1]also at JAI, University of Oxford, Oxford OX1 3RH, United Kingdom

Abstract

One of the goals of the CLIC Test Facility (CTF3) [1] at CERN is to demonstrate the feasibility of the CLIC [2] Drive Beam recombination, which takes place in the Drive Beam Recombination Complex (DBRC). The tight geometry of the DBRC together with its strong optics and the high energy spread of the beam require a careful control of the beam size along the different sections of the DBRC [3, 4]. One of the main contribution to beam size is the dispersion. If uncontrolled, dispersion leads to fast increase of the beam size, hence it may affect the beam current stability of the combined beam. A tool has been implemented at CTF3 to measure and correct dispersion during and after the setup of the machine. Dispersion Free Steering (DFS) has been applied in the upstream Drive Beam LINAC, while Dispersion Target Steering (DTS) has been used in the rings of the DBRC. In the LINAC the weak optics and the wide dynamic aperture of the beamline allow a straightforward correction. In the DBRC the aperture is tighter, and the strong optics produce non-linear dispersion which one needs to take into account. A general overview of current status and future plans in controlling dispersion at CTF3 will be presented.

INTRODUCTION

The ability of controlling dispersion is part of a broader topic, which is the necessity of preserving the beam quality while transporting it over long distances [5]. One of the main sources of beam quality degradation is connected to orbit errors which normally translates in undesired dispersion and emittance dilution.

Dispersion can be used as a convenient observable for steering the beam by means of the DFS technique [6]. DFS is currently one of the main tools for minimising the emittance growth in the CLIC main beam [7]. Experimental verification of DFS were successfully performed at SLAC [8].

One of the main objective of the CLIC Test Facility (CTF3) program [1] is to preserve the emittance of the beam while being recombined in the DBRC. The ability of measuring and controlling the dispersion turned out to be an extremely powerful tool for the set-up and optimisation of the different beam lines.

The layout of CTF3 is shown in Figure 1. Note that the DBRC is composed of a Delay Loop (DL), a Combiner Ring (CR) and connecting transfer lines where clearly dispersion is non-zero by design. Dispersion Target Steering (DTS) is then the natural evolution of DFS to be applied in the DBRC.

* davide.gamba@cern.ch

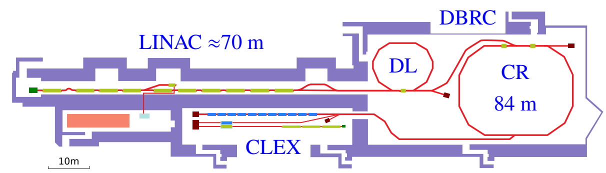

Figure 1: Layout of CTF3 at CERN.

In the following we will give a brief overview of the dispersion measurement tool implemented at CTF3 and its use for DFS, DTS and for machine set-up.

DISPERSION MEASUREMENT

The dispersion in a transfer line can be measured by changing the momentum of the beam with respect to the nominal momentum (p_0) the line is tuned for, and then measuring the mean orbit deviation. The observed orbit displacement (Δx) can be expressed as:

$$\Delta x = D_x \frac{\Delta p}{p_0} + DD_x \left(\frac{\Delta p}{p_0}\right)^2 + o\left(\left(\frac{\Delta p}{p_0}\right)^3\right). \quad (1)$$

One can then fit the coefficients D_x, which is the linear dispersion, and if necessary also the higher order terms (e.g. DD_x). Practically the measurement of D_x is often sufficient to spot errors or mismatches in a beam line.

In transfer lines where dispersion is expected by design another interesting observable is what we call the "nominal" linear dispersion, i.e. the orbit response while scaling *only* the bending magnets. This quantity is not affected by quadrupole misalignments and orbit errors, hence it is a direct measurement, with opposite sign, of D_x in Eq. (1) for the ideally aligned linear machine [4]. Note that the measured quantity is *not* the actual dispersion experienced by the beam, but it is the dispersion contribution of the bending magnets which, in an ideal-linear machine, are the only sources of dispersion. This observable turns out to be useful for optics verification and it can be used to define the target dispersion for DTS.

At CTF3 a MATLAB application to perform online measurements of linear and non-linear dispersion has been developed [4]. The relative energy of the beam with respect to the beam lines can be varied mainly in three ways:

- By scaling all the magnetic elements in the line. Note that this method would not reveal the *incoming* dispersion, but only the dispersion generated within the section of beam line being scaled.

SIMULATING APERTURES IN THE UNIFORM EQUIVALENT EQUIVALENT BEAM MODEL

G. H. Gillespie
G. H. Gillespie Associates, Inc., P. O. Box 2961, Del Mar, CA 92014, USA

Abstract

The uniform equivalent beam model is useful for simulating particle beam envelopes. Beam root-mean-square (rms) sizes, divergences, and emittances of an equivalent uniform beam approximate well the rms properties of more realistic beam distributions, even in the presence of space charge. Envelope simulation codes for high current beams using the model, such as TRACE 3-D, are central to particle optics design. However, the modeling of apertures has required multi-particle simulation codes. Multi-particle codes do not typically have the fitting and optimization capabilities common to envelope codes, so the evaluation of aperture effects is often a secondary study that may result in further design iteration. To incorporate aperture effects into the optics design at the start, a method has been developed for simulating apertures in the context of a uniform equivalent beam. The method is described and its TRACE 3-D implementation is outlined. Comparisons with multi-particle simulations are used to validate the method and examine regions of applicability.

INTRODUCTION

The uniform equivalent beam ("UEB") model [1] provides a useful approximation for simulating particle beam envelopes in transfer lines and accelerator structures. Beam dynamics design often begins with the use of an envelope simulation that utilizes the UEB such as TRACE 3-D [2]. To help incorporate apertures into the initial optics design, a method has been developed for simulating apertures within the context of the UEB model. This paper outlines the method and its implementation in TRACE 3-D. Comparisons with multi-particle simulation codes, with and without space charge, are used to validate the method and examine potential regions of applicability.

It is convenient to examine three cases of a beam passing through an aperture, as illustrated in Fig. 1.

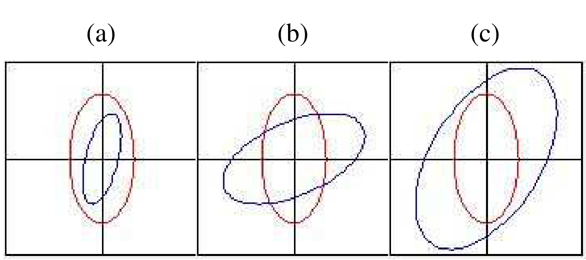

Figure 1: Three cases of beams intercepting an aperture. The apertures are drawn **red** while the beams are in **blue**.

Figure 1 shows an elliptical aperture (**red**) with a vertical (y) to horizontal (x) aspect ratio of 2. Three beam cases are illustrated by **blue** ellipses. Case (a) corresponds to the situation where the beam cross section (i.e. y-x plane) is entirely within the aperture. Case (c) is the situation where the beam covers the aperture, so that the beam cross section is effectively replaced by the aperture cross section. Case (b) illustrates the situation where a part of the beam passes through the aperture ellipse, but a portion of the beam is intercepted and lost.

In the context of the equivalent uniform beam, the spatial particle density is described by an uniformly filled ellipsoid of three dimensions (3-D) for bunched beams, or of two dimensions (2-D) for continuous beams. The Kapchinsky-Vladimirsky [3], or KV, beam is a useful model for continuous beams. The approach to modeling apertures is to determine suitable equivalent uniform beams that approximate the beams which survive after encountering the aperture.

APERTURE METHOD

Transmission Factor T_f

The normalized two-dimensional distribution function, $f(x,y)$, for a beam uniformly distributed within an ellipse, can be represented in terms of the Heaviside step function Θ by:

$$f(x,y) = \Theta[A - B\,(x/x_b)(y/y_b) - (x/x_b)^2 - (y/y_b)^2] \ , \quad (1)$$

where $$A = (1-r_{xy}^2) \ , \quad (2)$$

and $$B = 2r_{xy} \ . \quad (3)$$

The beam ellipse parameters x_b and y_b are the maximum extents of the ellipse in the horizontal and vertical directions, respectively, and are given by the square roots of the beam sigma matrix elements σ_{11} and σ_{33}, respectively. Note that these are not the semi-axes parameters for the ellipse[1]. The parameter r_{xy} is the x-y correlation of the beam: $r_{xy} = r_{13} = \sigma_{13}/(x_b y_b)$.

The aperture transmission function, $T(x,y)$, can similarly be represented by the Heaviside function as:

$$T(x,y) = \Theta[1 - (x/x_a)^2 - (y/y_a)^2] \ , \quad (4)$$

[1] If the semi-axes parameters of the beam ellipse are a and b, then r_{xy} is related to the rotation angle, θ, by:

$$r_{xy} = -\alpha_{xy} / (1+\alpha_{xy}^2)^{1/2} \ ,$$

where $\alpha_{xy} = -(b^2-a^2)\sin(2\theta)/(2ab)$.

The beam ellipse parameters x_b and y_b are given by:

$$x_b = 2^{1/2}ab \,/\, [(b^2+a^2) + (b^2-a^2)\cos(2\theta)]^{1/2} \ ,$$

$$y_b = 2^{1/2}ab \,/\, [(b^2+a^2) - (b^2-a^2)\cos(2\theta)]^{1/2} \ .$$

 ISBN 978-3-95450-169-4

FRIB LATTICE-MODEL SERVICE FOR COMMISSIONING AND OPERATION*

D. Maxwell†, Z. He, G. Shen, Facility for Rare Isotope Beams, East Lansing, USA

Abstract

Accelerator beam simulation is crucial for the successful commissioning and operation of the FRIB linear accelerator. A primary requirement of the FRIB linear accelerator is to support a broad range of particle species and change states. Beam simulations must be performed for these various accelerator configurations and it is important the results be managed to ensure consistency and reproducibility. The FRIB Lattice-Model Service has been developed to manage simulation data using a convenient web-based interface, as well as, a RESTful API to allow integration with other services. This service provides a central location to store and organize simulation data. Additional features include search, comparison and visualization. The system architecture, data model and key features are discussed.

INTRODUCTION

The Facility for Rare Isotope Beams (FRIB) uses a superconducting linear accelerator designed to accelerate all stable ions to energies greater than 200 MeV/u with beam power on target up to 400 kW [1]. This driver accelerator must be highly configurable in order to accommodate a broad range of ion species and charge states. In order meet these requirements for energy and power on target, accelerator beam simulation software will be important to facilitate accelerator configuration and optimization. Management of beam simulation data will be critical for efficient commissioning and reproducible operation of the FRIB driver accelerator.

The FRIB Lattice-Model Service (LMS) has been designed to allow for easy organization and retrieval of beam simulation data. The primary software used for the FRIB driver accelerator design is IMPACT [2] and therefore the LMS initially supports IMPACT simulation data. However, its flexible data model allows it to be easily extended to support additional types of simulation data. Accelerator simulation data can be divided into two parts: the Lattice and the Model.

Lattice

The Lattice consists of the position and orientation of the accelerator elements along with any information needed to fully define the particles trajectory through the accelerator. This includes the element types and any type specific configuration parameters. As well as, the initial beam conditions including the particle species and initial change state.

* This material is based upon work supported by the U.S. Department of Energy Office of Science under Cooperative Agreement DESC0000661, the State of Michigan and Michigan State University.

† maxwelld@frib.msu.edu

Model

The Model is the complete result of executing the beam simulation software with a Lattice as input. The exact content of the Model is specific to each type of beam simulation software. In general the Model includes the following beam parameters at multiple locations along the accelerator: size, position, divergence and energy.

ARCHITECTURE

The LMS must provide users with convenient access to beam simulation data, while being efficient and flexible to meet the demands of commissioning and operation. The overall architecture is adopted from a similar Lattice-Model Service in use at NSCL II [3]. The most significant change from original architecture is the switch from a traditional relational database to a document-oriented database.

The document-oriented database provides a flexible system for storing information and is well suited for storage of beam simulation data. The original relational database scheme was designed to store objects with related arbitrary properties. For example, the Lattice contains a Quadruple element with its magnetic gradient being a property. Likewise, an RF Cavity element with properties amplitude and phase. Through the use of a document-oriented database, more information is now being stored, while the implementation has been greatly simplified. Furthermore, this data model can be more easily extended to support future requirements.

To facilitate convenient access to the simulation data a web interface is provided to users for both submitting new data and for retrieval of existing data. A RESTful API is also provided for programmatic access to simulation data and includes both data submission and retrieval.

IMPLEMENTATION

The LMS is implemented in Python [4] using the Tornado [5] web framework. The use of Python allows for the reuse of existing libraries for reading IMPACT input and result data files. In addition, Python has excellent support for numeric processing, text processing and web applications. Tornado includes a high performance web server which supports modern generator-based asynchronous programming. However, the standard Tornado text template engine was found to be insufficient and instead the more powerful Jinja2 [6] text template engine was used.

The MongoDB [7] document-oriented database is used as it provides excellent performance and integration with Tornado through the use of the Motor [8] client. Motor provides a high performance asynchronous library for interacting with MongoDB.

TRACKING BASED COURANT-SNYDER PARAMETER MATCHING IN A LINAC WITH A STRONG SPACE-CHARGE FORCE

R. Miyamoto*, ESS, Lund, Sweden

Abstract

During the design of a hadron linac, matching at the interfaces of different structures or lattice periods is often performed with the linear approximation of the space-charge force. When space-charge is extremely strong, like in the low energy part of the proton linac of the European Spallation Source, such a matching method is not always good enough and could lead to a residual mismatch at the design level. To avoid this, a matching scheme based on iterations of tracking, thus including the full effect of the space-charge force, is developed. This paper presents the scheme itself as well as its application to the ESS linac.

INTRODUCTION

The European Spallation Source, current under construction in Lund, Sweden, will be a neutron source driven by a proton linac with an unprecedented 5 MW beam power. For such a high power linac, one of the most significant goals of the lattice design is to maintain high beam quality throughout the linac as well as to minimize beam losses as possible. One known cause of beam quality degradation is the mismatch of the Courant-Snyder (CS) parameters at interfaces of sections.

The normal conducting front-end of the ESS linac, which precedes sections with superconducting cavities, consists of an ion source, low energy beam transport, radio frequency quadrupole (RFQ), medium energy beam transport (MEBT), and drift tube linac (DTL) [1]. Housing a fast chopper, collimators, and various diagnostics devices, the MEBT has several functionalities [2] and one of them is to adjust the CS parameters at the DTL entrance to the values matched to the periodic structure of the DTL, the process referred to as *matching*. The matching must be performed not only at the design stage but also for the real machine, in which the beam parameters are not necessarily identical to the design values. Figure 1 shows a schematic layout of the MEBT. For the current baseline lattice, the matching to the DTL was done with the second and third buncher cavities and the last five quadrupoles.

The main simulation tool of the ESS linac is the TraceWin code [3]. The code performs the multiparticle tracking with a 3D space-charge routine, referred to as *PICNIC* [4], and also the fast *envelope calculation*, where only the beam centroid and RMS sizes are propagated under the linearized space-charge and cavity fields. During the design stage, the matching at the interfaces of the sections in the ESS linac had been performed based on the envelope calculation. This is because the contributions to the CS parameters from the nonlinearities are expected not to be significant but it was

* ryoichi.miyamoto@esss.se

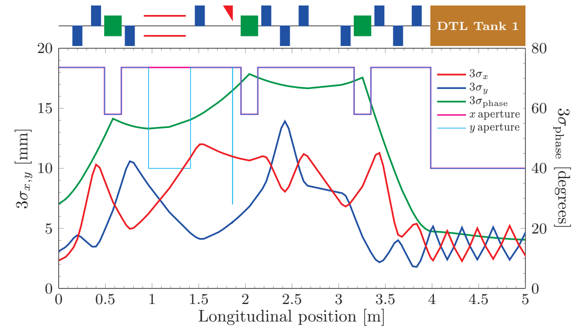

Figure 1: MEBT schematic with 3σ envelopes and apertures. The blue boxes above (below) the line denote focusing (defocusing) quadrupoles, the green boxes do buncher cavities, and the red lines and triangle do a fast chopper and its dump.

found that the MEBT was an exception to this condition. Table 1 compares the CS parameters at the MEBT exit calculated from the envelope calculation and tracking. We can see that all the plane has a discrepancy of 10% level in the mismatch parameter [5] and it is not ideal the lattice by design has such a level of residual mismatches. The causes of these mismatches are the strong space-charge in the MEBT due to the high current (62.5 mA) and low energy (3.62 MeV). For the longitudinal plane, the nonlinearity of the field of the buncher cavities has the same level of a contribution as the space-charge since the bunch length is as long as 60-70 degrees in 3σ at the locations of the buncher cavities (Fig. 1). Because of this situation, we developed a simple scheme to perform the matching with tracking. This paper discusses the scheme itself and sees the impact of the improved matching on the behavior of the beam in the DTL.

Table 1: CS Parameters at the MEBT Exit from the Tracking and Envelope Calculation (The errors for β and α are $\Delta\beta/\beta$ and $[\Delta\alpha - \alpha(\Delta\beta/\beta)]$ for each, with the Tracking case as the reference. $M_{x,y,z}$ is the mismatch parameter.)

Parameter	Tracking	Envelope	Error
β_x [m]	0.222	0.258	0.166
α_x	1.425	1.734	0.072
M_x	—	—	0.087
β_y [m]	0.784	0.896	0.143
α_y	−4.219	−4.876	−0.055
M_y	—	—	0.074
β_z [m]	0.413	0.389	−0.057
α_z	0.125	−0.103	−0.221
M_z	—	—	0.124

ISBN 978-3-95450-169-4

BEAM DYNAMICS SIMULATIONS OF A HIGH CHARGE S-BAND PHOTOINJECTOR FOR ELECTRON BEAM IMAGING EXPERIMENTS

Yanru Wang, Zimin Zhang#, Shuchun Cao, IMP, CAS, Lanzhou, China
Wei Gai, ANL, Argonne, IL, USA
Jiaqi Qiu, Euclid Techlabs, OH, USA

Abstract

A major challenge for high energy density physics is to measure properties of matter under extreme states of temperature and pressure that only occur in a time scale of 10 ns to 1 µs. Here we propose to use a single shot electron beam from an S-band photocathode with enough energy to penetrate the material as a diagnostic capable of time resolution (< ns). In this paper, we report on the beam dynamics simulation of an S-band photocathode electron gun and accelerator (S-band photoinjector) capable of producing up to 10 nC charge with high enough energy. Optimizations of the system parameters, including gun, focusing solenoid and acceleration field are performed using particle tracking code. The beamline is designed to be installed in the Institute of Modern Physics (IMP) electron accelerator centre for high precision electron imaging experimental studies.

INTRODUCTION

High energy density physics aims to study the properties of matter under extreme states of high temperature and high pressure. A new scheme based on high-energy electron beam as a probe was proposed for time-resolved imaging measurement of high energy density materials, especially for high energy density matter and inertial confinement fusion (ICF) [1, 2]. A major challenge is to measure properties of matter under extreme states of high temperature and pressure that only occur in a time scale of 10 ns to 1 µs. A diagnostics system with time-resolved imaging is highly desirable, based on a single shot electron beam from an S-band photocathode with enough energy to penetrate the material and capable of time resolution (< ns).

Here we present the primary beam dynamics simulation design for high charge S-band photoinjector aiming to high quality single-shot electron imaging. A sketch of the S-band photocathode electron gun and accelerator is shown in Fig.1. It consists of a normal-conducting 1.6 cell S-band photocathode radio frequency electron gun and an S-band accelerating tube. The gun cavity is surrounded by a solenoid, which serves for the focusing of the beam as well as for the compensation of the emittance growth caused by space charge effects [3].

Taking into account the requirement of high charge beam with high energy, a parameter optimization has been performed. Simulations showed an rms projected emittance of 2.3 mm mrad/nC achieved at the accelerator exit.

zzm@impcas.ac.cn

Figure 1: The sketch of the S-band photoinjector.

DESCRIPTION & DYNAMICS SIMULATION OF S-BAND PHOTOINJECTOR SETUP

The beam-line consists of the electron gun containing the photocathode, and a second accelerating section called booster cavity. In order to meet the requirement for high charge in S-band photoinjector, a series of beam dynamics simulations have been performed. As an important input for dynamics simulation code, the following parameters have been chosen: round uniform transverse profile are increased gradually from 1.4 mm to 4.5 mm as the bunch charge increases from 1nC to 10nC (thus keeping the same bunch charge density on the photocathode), a Gaussian longitudinal distribution of the cathode laser with 2.9 ps RMS, and assumed kinetic energy of the electrons at the photocathode (for thermal emittance calculation) of 1 eV. The longitudinal centre positions of the main solenoid and the second accelerating section (booster) was fixed in this simulation: 0.22 m and 3.03 m downstream of the photocathode, respectively.

The electron gun consists of a 1.6 cell cavity with a resonance frequency of 2.856 GHz. The field in the gun cavity is showed in Fig. 2. The simulation rf gradient of 40.98 MV/m at the gun cavity with the max gradient of 100 MV/m corresponds to a beam energy of 4.7 MeV at the gun exit for a laser launch phase of 22 deg.

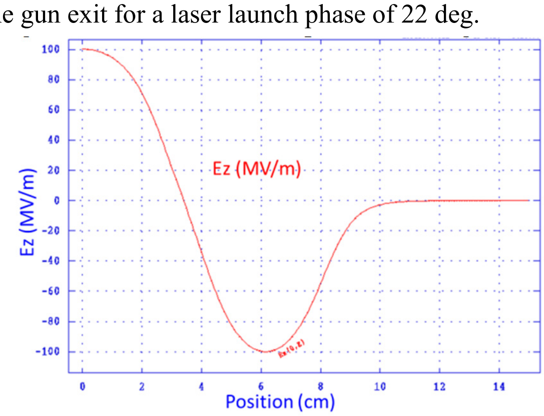

Figure 2: Field in gun cavity.

The gun cavity is surrounded by the main solenoid, which is used to compensate space charge effects in the gun, and the bucking solenoid, which is used to keep the

ISBN 978-3-95450-169-4

DEVELOPMENT STATUS OF FRIB ON-LINE MODEL BASED BEAM COMMISSIONING APPLICATION

Z. He*, K. Fukushima, D. Maxwell, M. Davidsaver, Y. Zhang, G. Shen, Q. Zhao
FRIB, Michigan State University, USA

Abstract

The new software FLAME has been developed to serve as physics model used for on-line beam commissioning applications. FLAME is specially designed to cover FRIB modeling challenges to balance between speed and precision. Several on-line beam commissioning applications have been prototyped based on FLAME and tested on the physics application prototyping environment. In this paper, components of the physics application prototyping environment are firstly described. Then, the design strategy and result of the four major applications: baseline generator, cavity tuning, orbit correction, transverse matching, are discussed.

INTRODUCTION

Facility for Rare Isotope Beams (FRIB) is a new national user facility for nuclear science co-funded by DOE and MSU [1, 2]. In order to handle the special modeling challenges of FRIB driver linac [3–5] while keeping fast speed for on-line purpose, an envelope-tracking based code, the Fast Linear Accelerator Modeling Engine (FLAME) [6] , is developed to provide useful tools for the challenges of FRIB linac modeling and tuning.

The physics application prototyping environment is built for physicists to easily build and test various modeling and tuning applications [7]. The detailed structure of this physics application prototyping environment is discussed in first section. After that, several major physics applications to support FRIB beam commissioning, such as baseline generator, cavity tuning, orbit correction, transverse matching, are developed and discussed in the following section.

PHYSICS APPLICATION PROTOTYPING ENVIRONMENT

The infrastructure of the physics application prototyping environment is described in Fig. 1. A distributed infrastructure is utilized with python to be the middle layer scripting language. A virtual accelerator driven by IMPACT [8] or FLAME is built mimicking the behavior of a real accelerator. The virtual accelerator is wrapped by the same EPICS [9] layer as real accelerator, so that the physics application developed for a virtual accelerator would be directly usable for a real accelerator. The FLAME model service is built onto the python middle layer via its native python interface. Two major kinds of optimizers, Design Analysis Kit for Optimization and Terascale Applications (Dakota) [10] optimizer and Scipy [11] optimizer, are implemented as the optimizer service module. Dakota contains algorithms for optimization with gradient-based local and non-gradient-based local/global methods, written in C++ with a pyDakota [12] python interface. It also has useful features such as hybrid minimization method and native support for MPI parallelization. Scipy also has optimization capability inside package Scipy.optimize, they are easy to use and offers a different set of optimization methods, and can be a good alternative choice. The Dakota optimizer is chosen as the main optimizer in our following discussion. The distributed infrastructure would also allow easy access to any other service needed such as scan service and unit conversion.

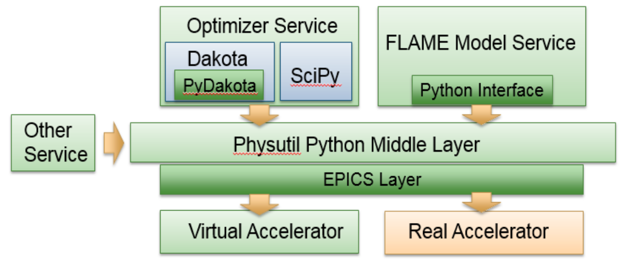

Figure 1: Infrastructure of the physics application prototyping environment.

MAJOR PHYSICS APPLICATIONS PROTOTYPES

In this section, four major physics applications developed with the physics application prototyping environment are discussed, namely baseline generator, cavity tuning, orbit correction and transverse matching.

Baseline Generator

Before beam tuning of FRIB driver linac, we always need a baseline as our tuning goal. Even though a baseline lattice already exists, this design may not be enough to guide FRIB beam commissioning task due to unexpected element fault, change of lattice design requirement, or numerous other situations where the baseline lattice has to be redesigned within a short period of time. Baseline generator is specially designed to handle this problem.

Baseline generation can be reduced to an optimization problem. With FLAME model service and optimizer service in place, all we need is to specify the tuning nob, tuning range, optimizing method and tuning goal. One specific use case is discussed below.

Transverse recovery: in this case, we assume the third superconducting solenoid of LS1 gets failed, causing transverse beam envelopes to blow up as Fig. 2(a). Then, the

* hez@frib.msu.edu

RF-TRACK: BEAM TRACKING IN FIELD MAPS INCLUDING SPACE-CHARGE EFFECTS. FEATURES AND BENCHMARKS

A. Latina, CERN, Geneva, Switzerland

Abstract

RF-Track is a novel tracking code developed at CERN for the optimization of low-energy ion linacs in presence of space-charge effects. RF-Track features great flexibility and rapid simulation speed. It can transport beams of particles with arbitrary mass and charge even mixed together, solving fully relativistic equations of motion. It implements direct space-charge effects in a physically consistent manner, using parallel algorithms. It can simulate bunched beams as well as continuous ones, and transport through conventional elements as well as through maps of oscillating radio-frequency fields. RF-Track is written in optimized and parallel C++, and it uses the scripting languages Octave and Python as user interfaces. RF-Track has been tested successfully in several cases. The main features of the code and the results of its benchmark studies are presented in this paper.

INTRODUCTION

RF-Track was developed to optimize the design and beam transport of the TULIP backward traveling-wave linac [1, 2]. The main requirements were three: (1) being able to track particles in backward-traveling radio-frequency (rf) field maps; (2) being able to transport protons as well as light ions in a fully relativistic regime (β-relativistic, in TULIP, is $\approx$ 0.38); and (3) being able to dynamically tune the rf parameters, like e.g. the rf input power, in order to perform non-trivial optimizations of the linac's transport efficiency.

Given the limited number of codes capable of tracking in oscillating electric and magnetic field maps, the uncertainty on how these codes would handle field maps of backward-traveling structures, and the requirement of a dynamically tunable rf input power, it was decided to develop a new *ad hoc* tool, optimized and tailored for the TULIP project.

RF-Track fulfilled the requirements, and eventually grew to become a general-purpose tracking code that excels for its flexibility, accuracy, and simulation capabilities. Its main features are:

- it is fully relativistic: doesn't make any approximation such as $\beta \ll 1$ or $\gamma \gg 1$;
- it can track particles of arbitrary mass and charge, even in mixed-species beams;
- it implements direct space-charge interaction, computing both the electric and the magnetic fields acting within the particles;
- it implements several integration algorithms: fast algorithms for complex nonlinear optimizations, accurate-but-slow ones for precise tracking;
- it is fast, fully benefiting from modern multi-core CPUs;
- it is programmable, relying on powerful and expressive scripting languages like Octave and Python for its user interface.

The following sections will elucidate each of these points.

RF-TRACK INTERNALS

RF-Track has been developed in C++11, fully exploiting the multi-thread capabilities offered by this language. Every single algorithm in RF-Track has been designed to take full advantage of modern multi-core CPUs.

In an effort aimed at making RF-Track a minimalistic code, yet uncompromised in its scientific throughput, the development has been focused on all physics-related algorithms, relying on powerful and well-established numerical libraries for *all the rest*. Two libraries were chosen to provide numerical algorithms: GSL, the "Gnu Scientific Library", which offers a wide range of mathematical routines such as random number generators, ODE integrators, linear algebra, and more [3]; and FFTW, the "Fastest Fourier Transform in the West", probably the fastest opensource library to compute discrete Fourier transforms ever written [4].

The hundreds of functions and routines that constitute RF-Track are compiled into a single binary file dynamically loadable from the two scripting languages: Octave [5] and Python [6]. These powerful high-level languages are ideal for numerical and scientific experimentations. They offer a large number of *off-the-shelf* toolboxes to perform complex numerical tasks: e.g., multidimensional optimizations, nonlinear fits, complex data processing, etc. The accelerator physics capabilities embedded in RF-Track, together with these expressive and rich scientific languages, make the simulation possibilities offered by RF-Track virtually uncountable.

The interface between the internal C++ code and the aforementioned scripting languages has been obtained using SWIG [7]. A typical RF-Track script, in its Octave version, looks like this:

```
% load the RF-Track library
RF_Track;

% setup the simulation, e.g. a transfer line TL and a beam B0
TL = setup_a_transferline();
B0 = setup_a_beam();

% track B0 through TL, and store the result as B1
B1 = TL.track(B0);

% inquire the final phase space
T1 = B1.get_phase_space("%x %xp %y %yp");

% use Octave's plotting routines to display the results
plot(T1(:,1), T1(:,2), "*");
xlabel("x [mm]");
ylabel("x' [mrad]");
```

As shown, RF-Track's commands can be interleaved with Octave keywords.

CIADS HEBT LATTICE DESIGN*

Y. S. Qin†, W. L. Chen, Y. He, H. Jia, S. H. Liu, Z. J. Wang
Institute of Modern Physics (IMP), Chinese Academy of Sciences, Lanzhou, China

Abstract

CIADS (China Initiative Accelerator Driven System) 600MeV HEBT (High-Energy Beam Transport) will deliver 6 MW beam to the target, with CW (continuous wave) 10 mA beam. The most serious challenges are vacuum differential section and beam uniformization on the target. A novel collimation plus vacuum differential section is proposed in the lattice design. A scanning method is designed for the round beam uniformization on the target.

INTRODUCTION

As a SC LINAC, CIADS will be operated in superconducting temperature (2 K) as shown in Figure 1 [1]. HEBT will transport beam to the target stably and realize the beam-target coupling.

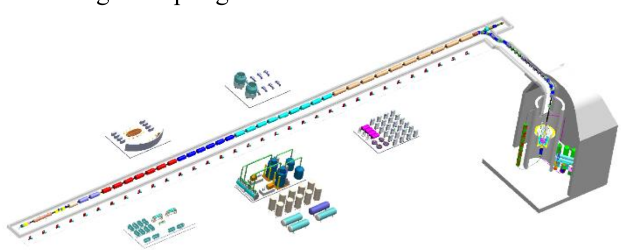

Figure 1: Layout of CIADS.

Because of the high power, we use collimation system to minimize the uncontrolled beam loss along the beam line, especially at the holes of the vacuum differential section. To decrease the risk of target melting, peak power density (PPD) needs to be minimized. The target is granular flow target [2]. The parameters of the HEBT is shown in table 1 as below.

Table 1: HEBT Parameters

Parameter	Value	Unit
Particle	proton	—
Energy	600	MeV
Current	10	mA
Duty factor	100	%
Normalized rms emittance (x/y/z)	0.28/0.28/0.33	π mm.mrad
Input αx/αy/αz	1/1/-1	—
Input βx/βy/βz	20/20/20	mm/π.mrad
Target shape	round	—
FWHM of beam on the target	160	mm

* Supported by National Natural Science Foundation of China (11525523)
† E-mail: marshal@impcas.ac.cn

CONSIDERATION

To decrease beam power loss along the beam line, collimation system is considered. Cross-over lattice is designed to form a small beam waist before the target, where to set the first differential hole and act as the shielding of neutron reflection from the target to protect the accelerator.

The property of the granular flow target leads to three considerations:

1. Vacuum transition

Helium is designed to be heat exchanger and lubrication gas between metallic balls of the granular target [2]. The vacuum degree needs to be kept at 0.5 atm level, while it is 10^{-7} Pa in the SC cavity. This means HEBT should realize vacuum transition about 11 orders of magnitude. Vacuum differential system is adopted in the design.

2. Power density uniformity on the target

To decrease the risk of target melting, the maximum temperature rise of balls should be considered, the same goes for PPD accordingly. The minimum falling speed of the metallic balls and the size of the target depends on PPD, which is the motivation of power density uniformity on the target.

We choose scanning method to decrease PPD on the target. Unlike high-order magnets, scanning method doesn't rely on the beam position or distribution that much, especially when considering beam halo.

3. Beam shape on the target after scanning

To increase effective area, the target surface is designed to be round rather than rectangle or square, which requires uniform distribution in a circular area with diameter 160 mm after scanning.

Simulation shows that when falling down, balls near the center are pressed because of the radial velocity of other balls, which may lead to lower falling speed. A scanning method need to be introduced to balance the situation mentioned above. The distribution should be "hollow" after scanning.

LATTICE DETAILED DESIGN

Considering the function of HEBT, detailed design consists of 4 section: Bending section, Beam collimation section, Vacuum differential section and A2T (Accelerator to Target). Figure 2 shows 10 RMS envelope of the whole HEBT line. There're matching sections between the 4 sections, such that transversal Twiss parameters would match.

IMPROVED BEAM DYNAMICS AND CAVITY RF DESIGN FOR THE FAIR PROTON INJECTOR*

R. Tiede, A. Almomani, M. Busch, F. Dziuba, U. Ratzinger,
IAP, Goethe-University Frankfurt, Germany

Abstract

The FAIR facility at GSI requires a dedicated 70 MeV, 70 mA proton injector for the research program with intense antiproton beams. The main accelerator part consists of six 'Crossbar H-type' (CH) cavities operated at 325 MHz. Recently the beam dynamics has been revised with the goal of fixing all parameters and thus starting the construction of the main linac components. The MEBT behind the RFQ was slightly extended, the gap numbers per CH cavity and the voltage distributions were optimized and the intermediate diagnostics section including a rebuncher cavity at 33 MeV was redesigned. Finally, detailed machine error studies were performed for checking the error sensitivity of the new design and the steering concept. The final parameters obtained from the beam dynamics update are now used for finalizing the CH-DTL cavity design by CST-MWS calculations.

REVISED FAIR PROTON LINAC DTL BEAM DYNAMICS DESIGN

Our group at IAP/Frankfurt University is designing and developing the FAIR Proton Linac in close collaboration with the GSI/FAIR staff, both as a whole [1] [2] [3] and in its main components, like for example the recently power tested coupled CH-DTL prototype cavity [4] [5]. However, when starting the rf design for all six CH cavities, some weak points in the beam dynamics and overall linac layout valid at that time were detected, which lead to the revised beam dynamics design as presented in this paper. The main changes were as follows:

The MEBT section behind the RFQ was slightly extended in length and quadrupole number, including the necessary elements for steering, diagnostics and vacuum. Two identical quadrupole triplet lenses now allow a flexible beam matching into the CH-linac.

The rather long diagnostics and beam cleaning section at 35 MeV has been reduced in length from 3.0 to 1.8 meter, still containing the necessary beam diagnostic, steering and vacuum handling components, as well as a 4 gap, 1.6 MV rebuncher cavity. This section is now positioned at a beam energy of 33 MeV (see next paragraph).

The gap voltage distribution along the whole linac has been moderately changed: The total number of gaps per cavity and the voltage distribution inside each cavity have been optimised with the aim to get more homogeneous on axis gap field distributions and particularly to reduce the maximum field values in the first coupled CH-DTL for safety reasons (from 16.6 to 14.7 MV/m, see Table 1). Moreover, the matching of power requirements of each cavity for using identical amplifiers was improved.

Table 1: Main Parameters of the FAIR Proton Linac DTL

CH-DTL		
f [MHz]	325.224	
energy range [MeV]	3 - 70	
main components	3 coupled CH (CCH), 3 single CH-DTL (CH)	
number of gaps	21 – 30 (CCH); 20 (CH)	
tube inner diam. [mm]	20 - 23	
eff. gap volt. [kV]	270 (CCH1) to 670 (CH)	
max. on axis field [MV/m]	14.7 (CCH1) down to 5.5 (CH6)	
cavity effective length [m]	1.4 to 3.6 (CCH); 2.5 to 3.2 (CH)	
Magnetic quadrupole triplets		
effective length [mm]	375	
eff. gradients [T/m]	45 - 62	
aperture diam. [mm]	30	
Beam parameter		
design current [mA]	75	
	input	output
$\varepsilon_{n,95\%\ \mathrm{transv.}}$ [mm·mrad]	1.35	2.6
$\varepsilon_{\mathrm{rms\ transv.}}$ [mm·mrad]	0.266	0.455
$\varepsilon_{n,95\%\ \mathrm{long.}}$ [keV·ns]	12.0	15.6
$\varepsilon_{\mathrm{rms\ long.}}$ [keV·ns]	2.4	2.9

The above-mentioned measures lead to the final linac parameters as shown in Table 1 and to the beam dynamics results illustrated by Figure 1 and expressed by the emittance numbers shown in Table 1. All simulations were done with the in-house developed code LORASR [6], which is well accepted within the Linac community and has been often benchmarked with other codes.

Figure 1, upper plot shows a transversally well matched beam with small envelope oscillations, except for the typical quadrupole triplet channel pattern. There is also enough safety margin between beam and aperture (in blue), which could be confirmed by error study results (see next chapter). The triplet lenses are either integrated into the CH-cavities (CCH1 to CCH3) or placed externally.

For the particle motion in the longitudinal space the 'combined zero degree' concept was applied [7] [8]. The longitudinal beam envelopes (Figure 2, lower plots) also show stable behaviour with small oscillations particularly at higher energies and small output energy and phase spreads. The emittance growth (see Table 1) is well below or comparable to what was achieved by previous designs.

* Work supported by BMBF (contract no. 05P15RFRBA)

ISBN 978-3-95450-169-4

BEAM DYNAMIC OF TRANSPORT LINE 1+ WITH NEW HRMS FOR THE SPES PROJECT

E. Khabibullina†1, National Research Nuclear University MEPhI, Moscow, Russia
A. Pisent, L. Bellan, M. Comunian, INFN-LNL, Legnaro, Italy
A. D. Russo, INFN-LNS, Catania, Italy
1ITEP, Moscow, Russia

Abstract

SPES (Selective Production of Exotic Species) [1] is integrated Italian facility in LNL (Laboratori Nazionali di Legnaro, Legnaro, Italy) for production of high-intensity and highly charged beams of neutron-rich nuclei for Advanced Studies. The facility is based on 35-70MeV proton cyclotron, an ISOL fission target station and the existing ALPI superconducting accelerator as the post accelerator. In this paper the results of beam dynamic simulation of ^{132}Sn ion beam transport line from Beam Cooler to the Charge Breeder, including HRMS (High Resolution Mass Separator) with mass resolution 1/20000 and electrostatic dipoles are presented.

INTRODUCTION

SPES (Selective Production of Exotic Species) is a CW ion beam facility for neutron-rich radioactive ions production and acceleration to contribute to the study of the nuclear physics processes. The optimization of transport line 1+ from HRMS to Charge Breeder to improve the transportation of these type particles. The considered line 1+ includes:

- HRMS is used to select RNB (Radioactive Nucleolus Beam).
- Dipoles to obtain beam bending which is fixed at the entrance and at the exit of straight periodic transfer line to CB.
- Entrance to Charge Breeder.

The complete layout of the transport line 1+ from High Resolution Mass Spectrometer (HRMS) to Charge Breeder is shown in Fig. 1. The chief purpose of the discussion was to design the matching with new HRMS and with Charge Breeder beam transport line 1+ in carefully way to avoid beam losses.

TRANSPORT LINE 1+ WITH NEW HRMS

HRMS

For the SPES project, the High Resolution Mass Spectrometer has to provide the ^{132}Sn ion beam purifying and ≥97% transmission. New HRMS [1] has a 1/20000 resolution in mass with ± 1 eV energy spread. It will be installed on the High Voltage platform with operating voltage of 260 kV. Developed HRMS is consisting of: two magnet dipoles of R=1.5 m with deflector angle 90°, four electrostatic multipoles, two electrostatic quadrupoles.

The Periodic Transfer Line to Charge Breeder

After HRMS system, there is beam transfer line 1+ [1] to connect HRMS with entrance of Charge Breeder. This transport channel with length of about 45 m has to provide a beam transport without beam losses and with minimum of dispersion (within limits of -80; 80 m). As a bending element the electrostatic dipole was selected. Two triplets after the separator image point and also the electrostatic dipole in transport line help to control the dispersion growth after the HRMS structure. The virtues of this type of dipole, as compared with magnetic dipole, are smaller energy consumption and independence from the ion mass. According to preliminary design of an electrostatic dipole to deflect the beam 90° [2], the main parameters of dipole were chosen. These parameters are shown in Table 1.

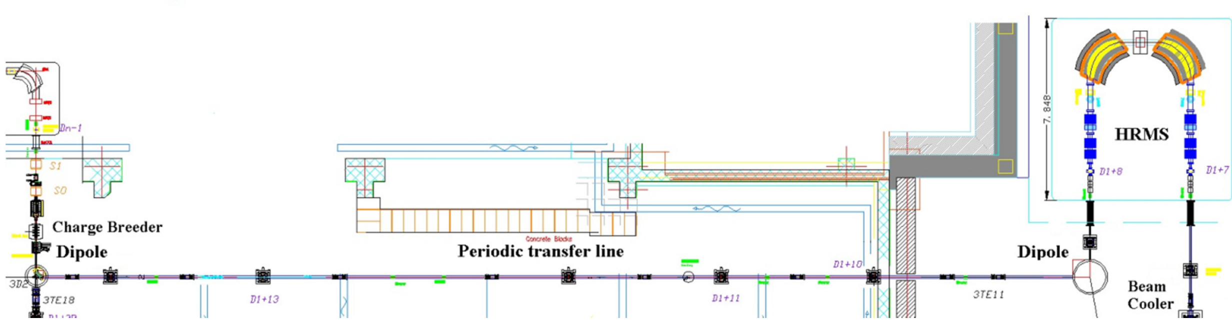

Figure 1: Transport line 1+ from High Resolution Mass Spectrometer (HRMS) to Charge Breeder.

†habi-ka@yandex.ru

PRIMARY BEAM DYNAMIC SIMULATION OF DOUBLE DRIFT DOUBLE BUNCHER SYSTEM FOR SPES PROJECT

A.V. Ziiatdinova[†, 1], National Research Nuclear University MEPhI, Moscow, Russia
M. Comunian, A. Pisent, L. Bellan, INFN/LNL, Legnaro, Italy
[1] also at ITEP, Moscow, Russia

Abstract

SPES (Selective Production of Exotic Species) is a facility intended for production of neutron-rich Radioactive Ion Beams (RIBs) at the National Institute of Nuclear Physics (INFN-LNL, Legnaro, Italy). Exotic nuclei production based on the ISOL (Isotope Separation On-Line) technology using UCx target. Neutron-rich nuclei will be generated by uranium fission under the influence of proton beam from cyclotron. After that, RIBs will be reaccelerated by the ALPI (Acceleratore Lineare Per Ioni). RFQ (Radio Frequency Quadrupole) will be used as a front-end part of the ALPI. Double Drift Double Buncher system is planned to be install before RFQ for transmission increasing. This article is dedicated to beam dynamic simulation and laying-out of transport line at section before ALPI.

INTRODUCTION

SPES project is in progress at the Legnaro National Laboratory of the National Institute of Nuclear Physics (INFN-LNL, Italy). Facility layout is shown in Fig.1.

Therefore, there is complex system for preparing of ion beam before ALPI. This system includes ion beam transport lines, Beam Cooler, Charge Breeder, HRMS and MRMS (high and medium resolution mass separators) and superconductive RFQ [1]. 5 MHz Low Energy Buncher has to be installed upstream RFQ for experiments, which require order of 100 ns beam length. So-called Double Drift Double Buncher system was chosen [2]. It includes two double gap structures (first and second harmonics – 5MHz and 10MHz correspondingly) installed at some distance from each other. The aim of this work was the optimization of beam transport line between MRMS and RFQ. Beam lines from buncher to RFQ before and after optimization are shown on Fig.2.

Optimization tasks:

- beam matching with RFQ
- increasing transmission
- reduce to zero dispersion at the input to RFQ
- particle losses minimization

Beam line includes buncher, magnetic quadruple triplets, solenoid and diagnostic chambers. Matching was carried out by varying the disposition of transport line elements and magnetic forces of focusing elements. The task is complicated by the fact, that disposition varying along beam line is limited because of transport line passes through two walls.

The beam line included 5MHz buncher, two quadruple magnet triplets and solenoid [3]. This work was involved determination of 10MHz buncher and focusing elements location in order to meet the aim.

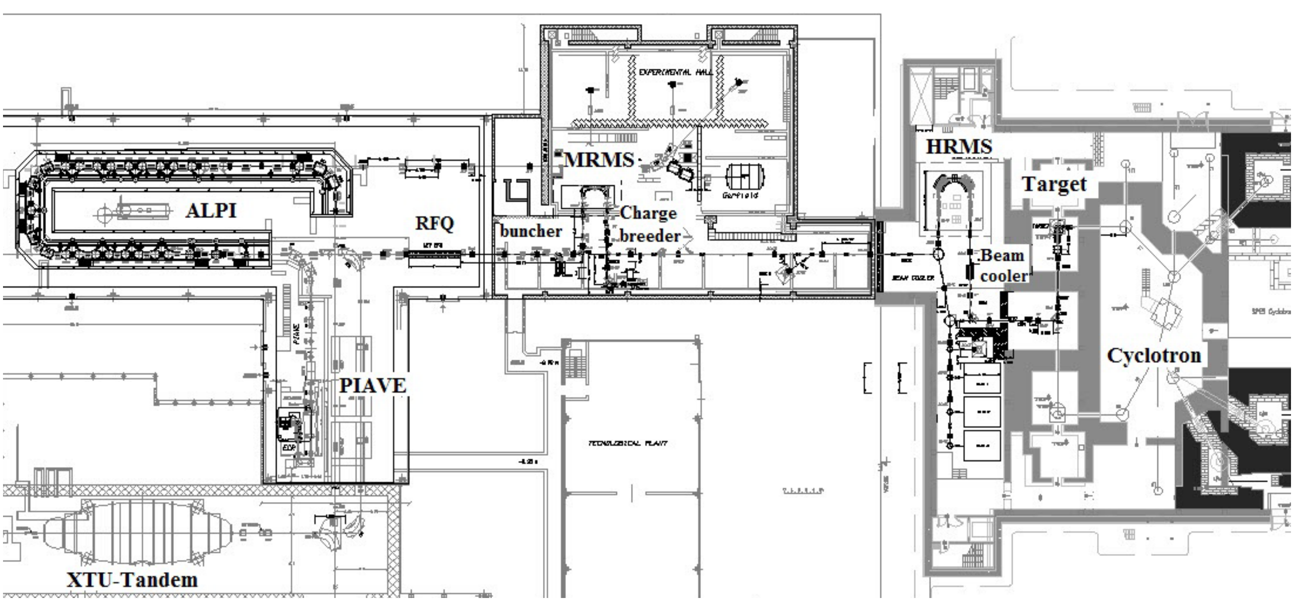

Figure 1: SPES facility layout.

†bishazi@yandex.ru

SEMI-3D BEAM-TRACKING CODE FOR ELECTRON INJECTORS USING BULK-TO-POINT CALCULATION TECHNIQUE FOR SPACE CHARGE FIELDS

A. Mizuno*, H. Hanaki, JASRI/SPring-8, Sayo, Hyogo, Japan

Abstract

A new semi-three-dimensional beam-tracking simulation code for electron injectors using bulk-to-point calculation technique for space charge fields is developed. The calculated space charge fields are not produced by a point charge but a doughnut which has the volume and whose cross-section is ellipsoid. Since the calculation noise which is usually caused by distributions of positions of point charge can be minimized, high accuracy calculation on emittance is realized with small number of electrons. Simultaneously, the calculation time becomes markedly shortened. In this paper, calculation examples for asymmetrical beams are demonstrated by the new code. The accuracy of emittance is also discussed.

INTRODUCTION

The emittance calculation technique is important in the design of electron injectors, particularly very low emittance electron sources such as X-ray free-electron lasers. There have been many analytical solutions [1–4] for beam dynamics, although it is difficult to accurately calculate practical bunch shapes and detailed emittance behavior. On the other hand, particle-tracking simulation codes [5–9] are useful for calculating the dynamics of complex bunch shapes of practical beams. However, the calculated emittances often depend on the number of particles.

These dependences are often caused by the calculation scheme of the space charge field which is produced by a point charge. This scheme makes calculation noise larger. Therefore, the author has developed the two-dimensional beam-tracking simulation code [10] using the calculation technique for space charge fields produced not by a point charge but by a bulk charge.

In this method, a short bunched electron beam is assumed to be an ensemble of several segmentation pieces in both the transverse and longitudinal directions. The trajectory of each electron, which is a point charge and located at each segmentation corner, is solved by the fourth-order Runge-Kutta method. When calculating space charge fields, they are assumed not to be produced by a point charge but by a doughnut that is separated by segmentation meshes. The shape of the entire bunch can be consequently calculated; thus, the emittances can be precisely calculated. These calculation techniques for space charge fields are similar to those used in Ref. [11] but nonlinearity of transverse fields can be calculated in this method. Therefore, highly accurate emittance calculations can be performed.

* mizuno@spring8.or.jp

Asymmetrical beams cannot be calculated by this two-dimensional code, however, calculations for these beams are often required in practical injectors. Therefore, the author upgrades this code to a semi-three-dimensional beam-tracking simulation code which is described in this paper.

OUTLINE OF 2D BEAM-TRACKING CODE

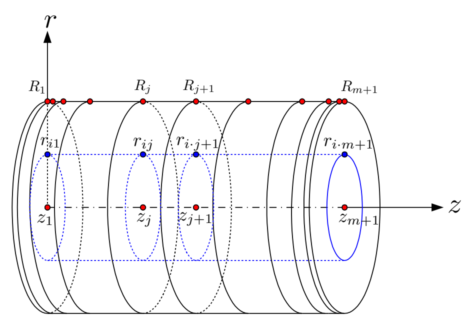

Figure 1: Bunch segmentation model used for the 2D code. This shows initial bunch configuration.

The Initial bunch segmentation model used for the 2D code is shown in Fig. 1. The bunch is divide into m slices in the longitudinal direction and n parts in the transverse direction. Each electron is located at each segmentation corner and tracked by the fourth-order Runge-Kutta method with sum of space charge fields produced by each segmentation doughnut. Charge density of each doughnut is uniform and charge of that is constant throughout calculations. $\langle r^2 \rangle$, $\langle r'^2 \rangle$ and $\langle rr' \rangle$ can be calculated from weighted mean values of the solutions for the each tracked electron; thus the normalized rms emittance that is defined by $\epsilon_r = \langle\gamma\rangle\langle\beta\rangle\sqrt{\langle r^2\rangle\langle r'^2\rangle - \langle rr'\rangle^2}$ can be calculated. In the rest of the paper, m and n are referred to as "segmentation numbers."

The space charge fields produced by the doughnuts can be calculated by subtracting the fields by an inner slice from the fields by an outer slice. These fields from the slice are functions of three variables, r_0/R_s, $2r_0/\gamma L$ and z_0/L [10], where r_0 is a position of the electron, γ, R_s and L are a relativistic factor, a radius and a longitudinal width of the slice respectively. By numerically calculating these fields and preparing as a three-dimensional mapping data file in advance, the fields can be referred in the tracking code by loading the file. Details of the 2D code are described in Ref. [10].

FINAL DESIGN OF THE FULLY EQUIPPED HWR CAVITIES FOR SARAF

G. Ferrand†, L. Boudjaoui, P. Hardy, F. Leseigneur, C. Madec, N. Misiara, N. Pichoff CEA-Saclay, DRF/IRFU/SACM-SIS, Gif-sur-Yvette, France

Abstract

SNRC and CEA collaborate to the upgrade of the SARAF accelerator to 5 mA CW 40 MeV deuteron and proton beams (Phase 2). CEA is in charge of the design, construction and commissioning of the superconducting linac (SARAF-LINAC Project). The SCL is made up of 4 cryomodules: the first two will host each 6 half-wave resonator (HWR) low beta cavities (β = 0.09) at 176 MHz; the last two will host each 7 HWR high-beta cavities (β = 0.18) at 176 MHz. The fully equipped cavity includes the niobium cavity with a helium tank, an input power couplers and a frequency tuning system. The final RF design of the low and high beta cavities will be presented in this poster, as well as the RF design of the couplers, the expected tuning range of the cavities and the multipactor analysis.

INTRODUCTION

The SARAF-LINAC project, managed by CEA (France), is integrated to the SARAF-Phase 2 project managed by SNRC (Israel) and is described in [1].

The beam dynamics studies allowed to define the accelerating voltage, 1.0 and 2.3 MV, the β_{opt}, 0.09 and 0.18, and the flange-to-flange length for RF cavities, 280 mm and 410 mm respectively.

Figure 1 shows the cavity with its helium tank, power coupler and the frequency tuning system.

RF DESIGN

The frequency was defined to be 176.000 MHz in nominal operations. The optimal β, β_{opt}, of the cavities is defined by the β that *maximizes* the R/Q ratio at 176.000 MHz. The target values are *0.091 and 0.181* $\pm$ 0.001. The accelerating fields are defined at β_{opt}. The RF design was first presented in [2]. Optimized simulation results for the low and high beta cavities are detailed in Table 1. RF power loss was computed for a niobium surface resistivity of 40 $n\Omega$ at 4.45 K.

Table 1: Parameters of the Low and High Beta Cavities

	Low β cav.	**High β cav.**
β_{opt}	0.091	0.181
Required E_{acc} (MV/m)	6.5	7.5
Epk_{max} (MV/m)	32.1	33.2
Bpk_{max} (mT)	60.9	60.5
Diss. Power@40nΩ (W)	6.16	14.4
R/Q @ β_{opt} (Ω)	189	280
Stored Energy (J)	4.9	14.4

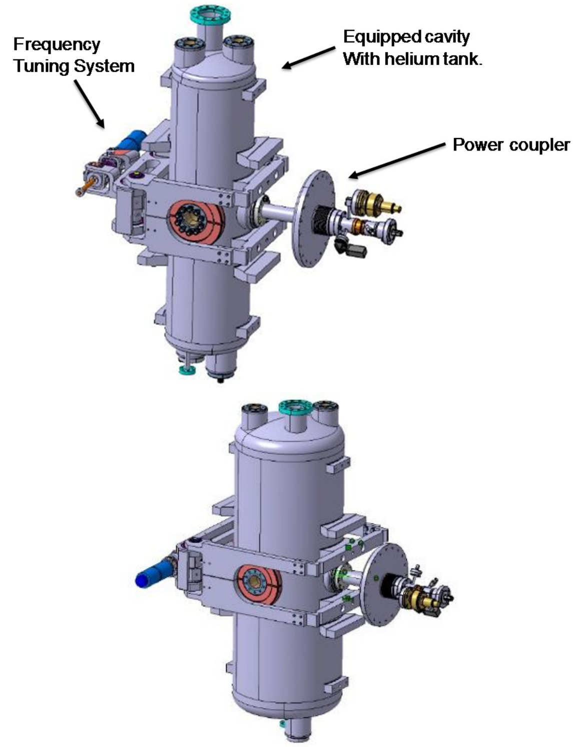

Figure 1: On the top, fully equipped low-beta cavity with power coupler and tuning system. . On the bottom, fully equipped high-beta cavity.

The field maps for the low beta cavity is presented in Figure 2. The peak electric field appears on the beam ports and drift tube. The peak magnetic field appears on the inner conductor, close to the tori.

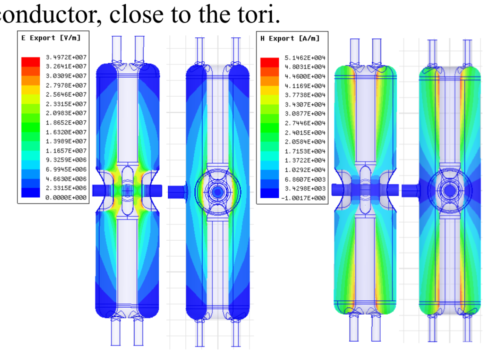

Figure 2: Electric field (left) and magnetic field (right) in the low-beta cavity.

RF - MECHANICAL COUPLING

The cavities will be placed vertically in the cryomodules in accordance with Figure 1. The first presentation of the mechanical design can be found in [2]. Since then, new mechanical simulations were carried out in order to verify the requirements for the frequency tuner system, the sensitivity

ISBN 978-3-95450-169-4

MECHANICAL DESIGN OF THE HWR CAVITIES FOR THE SARAF SRF LINAC

N. Misiara, L. Boudjaoui, G. Ferrand, P. Hardy, F. Leseigneur, C. Madec, N. Pichoff
CEA/DRF/IRFU/SACM-SIS, Gif-sur-Yvette, France

Abstract

SNRC and CEA collaborate to the upgrade of the SARAF accelerator to 5 mA CW 40 MeV deuteron and proton beams (Phase 2). CEA is in charge of the design, construction and commissioning of the superconducting linac (SARAF-LINAC Project). The SCL consists in 4 cryomodules. The first two identical cryomodules host 6 half-wave resonator (HWR) low beta cavities (β = 0.09) at 176 MHz. The last two identical cryomodules will host 7 HWR high-beta cavities (β = 0.18) at 176 MHz. The fully equipped cavity includes the niobium cavity with its helium tank, the couplers and the frequency tuning system. In this paper, the mechanical design and the foreseen qualification procedures for both cavities and tuning systems are presented with compliance, to the best extent, to the rules of Unfired Pressure Vessels NF-EN 13445 (1-5) standards.

INTRODUCTION

The SARAF-LINAC project, managed by CEA (France), integrated to the SARAF-Phase 2 project managed by SNRC (Israel) has been introduced in [1].

This paper focuses on the mechanical design, complying with the European Pressure Equipment Directive (PED), and more specifically to EN-13445. The mechanical design of the Frequency Tuning System (FTS) is also detailed.

Figure 1 shows the cavity with its helium tank, power coupler and frequency tuning system.

PRESSURIZED EQUIPMENT

EN-13445 and Design Cases

The vessel made of niobium constituting the cavity and the He-tank made of titanium are considered as pressure vessels. Materials (Nb, Nb-Ti alloy and Ti), nominal operating conditions (4.45 K) and shapes of the cavities are not covered by the European Standard EN-13445-3, however, this standard was used as guidelines for the mechanical design.

Multiple cases were considered, however, only the most critical cases were computed, called design cases, according to the guidelines of the EN-13445-3. The definition of the design cases is detailed in Table 1. The nominal helium pressure is 1.2 bar and the burst disc opening pressure is 2 bar.

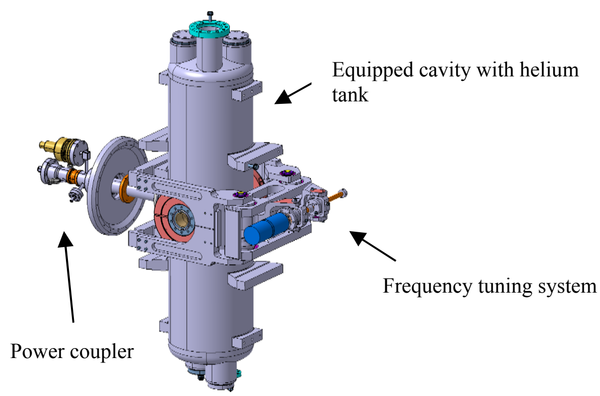

Figure 1: On the top, fully equipped low-beta (LB) cavity with power coupler and tuning system. . On the bottom, fully equipped high-beta (HB) cavity.

Design case 1 corresponds to the pressure test performed on the cavity (Nb-vessel and helium tank assembled) at 2.86 bar at room temperature. The standard defines the test pressure as being 1.43 times the maximum pressure.

Design case 2 corresponds to the test of the FTS on the cavities at 4.45 K. The pressure considered is the opening pressure of the burst disc, i.e. 2 bar.

Table 1: Detail on the Design Cases

	Design case 1	Design case 2
Geometry	LB and HB cavities	Full-equipped LB and HB cavities
Type	Test case	Normal case
Temperature	300 K	4.45 K
Loading	Test pressure: 2.86 bar	Helium pressure: 2 bar FTS effort

As long as the cavity is not at cryogenic temperature (4.45 K), the FTS will remain disengaged by the main security controller.

Material Properties

The material properties considered for the mechanical simulations are detailed in Table 2.

Table 2: Material Properties

Material	Temp [K]	Young mod. [GPa]	Sy [MPa]	Su [MPa]
Nb (ASTM B393)	4.45 293	105	317 40	600 95
Ti Gr 2 (ASTM B265-06)	4.45 293	107	834 275	1117 345
NbTi (ASTM B265-06)	4.45 293	62	- 410	- 450

The material properties presented come from previous studies ([2], [3] and [4]) and are used for simulations. The

SURFACE ROUGHNESS EFFECT ON THE PERFORMANCE OF Nb_3Sn CAVITIES*

R. Porter†, D. L. Hall, M. Liepe, J. T. Maniscalco
Cornell Laboratory for Accelerator-Based Sciences and Education (CLASSE),
Ithaca, NY 14853, USA

Abstract

Surface roughness of current Niobium-3 Tin (Nb_3Sn) superconducting radio-frequency (SRF) accelerator cavities can cause enhancement of the surface magnetic field. This enhancement can push the surface magnetic field beyond the critical field, which, if it occurs over a large enough area, can cause the cavity to quench. This paper presents simulations of the surface magnetic field enhancements in SRF cavities caused by the surface roughness of current Cornell Nb_3Sn cavities, which have achieved record efficiency. Simple, smooth cavity geometry is defined and surface magnetic fields calculated using SLANS2. The cavity geometry is modified with a small rough region for which the geometry is determined from AFM scans of a Nb_3Sn coated sample and the surface fields are calculated again. The calculated surface fields of the smooth and rough cavities are compared to determine the extent of the field enhancement, the area over which the enhancement is significant, and which surface features cause large field enhancement. We find that 1% of the surface analyzed has fields enhance by more than 45%. On average the Q-factor is increased by (3.8 ± 1.0)%.

INTRODUCTION

Nb_3Sn cavities produced at Cornell University [1–3] have rougher surfaces than conventional Niobium cavities. Previous simulations and calculations have shown that both bumps and pits in the surface of a cavity can cause local enhancement of the surface magnetic field [4,5]. If the magnetic field is sufficiently enhanced over a large enough area it could lower the quench accelerating field of the cavity. The increased surface area and changes in local magnetic surface field could also impact the quality (Q) factor of the cavities. When analyzing experimental data the average surface resistance is usually derived from the measured quality factor assuming a smooth cavity surface, so any significant difference could impact previous analysis of Nb_3Sn cavities.

Here we present electromagnetic simulations of the impact of the observed surface roughness of Nb_3Sn cavities on the enhancement of surface magnetic fields and Q-factors. We define the H-field enhancement, β, as $\beta = H_{rough}/H_{smooth}$, where H_{rough} is the surface H-field along the rough surface and H_{smooth} is the surface H-field along the smooth surface. The Q-factor enhancement is defined as Q_{rough}/Q_{smooth}, where Q_{rough} is the Q-factor of the rough cavity and Q_{smooth} is the Q-factor of the smooth cavity.

* Work supported by U.S. DOE award DE-SC0008431
† rdp98@cornell.edu

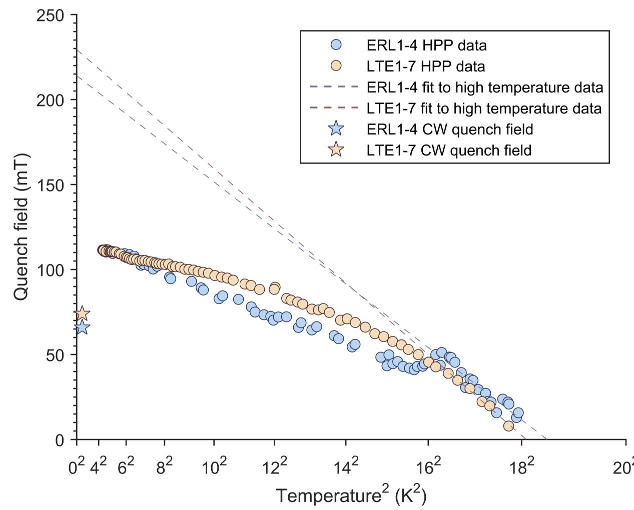

Figure 1: Plot of quench field (calculated from stored energy) versus T^2 from klystron high pulsed power measurements of Cornell Nb_3Sn cavities [6]

THE SUPERHEATING FIELD

Klystron high pulsed power measurements near Tc (see Fig. 1) suggest the superheating field in our Nb_3Sn cavities is ≈230 mT (extrapolated 0 K) [6]. This is significantly lower than theoretical calculations that predict superheating fields of ≈400 mT (at 0 K) [7]. In these results the surface quench field is calculated based on the energy within the cavity, assuming a completely smooth geometry. If the cavity is quenching at locations where the surface H-field is enhanced then the actual H-field causing the quench is higher than what is calculated. Not including field enhancement from surface roughness effects is likely the cause of the lower experiment results.

METHOD

The surface height data was taken from Atomic Force Microscope (AFM) scans of Nb_3Sn samples that were coated at Cornell University (see Fig. 2). The calculation of the surface magnetic was done using the 2D finite element code SUPERLANS2 (SLANS2) [8]. This code calculates non-azimuthally symmetric modes in azimuthally symmetric cavities.

The method of calculation used was based on the work of V. Shemelin [4], in which the surface magnetic fields of pits and bumps were calculated using SLANS2. This was done by creating a model with an elliptical bump or rounded pit in the center of the flat end of an otherwise

ISBN 978-3-95450-169-4

EXPERIMENT OF PLASMA DISCHARGE ON HWR CAVITY FOR IN-SITU SURFACE CLEANING STUDY*

A.D. Wu#, L.Chen, Y. He, T.C. Jiang, C.L. Li, Y.M. Li, F. Pan, Z.X. Shi, Y.K. Song, T. Tan, L. Yang, W.M. Yue, S.H. Zhang, H.W. Zhao, Institute of Modern Physics, Chinese Academy of Sciences, Lanzhou,Gansu 730000, China

Abstract

Hydrocarbons, which migrate from the vacuum bumps system, will absorb on the cavity surface after periods of operation. The contaminants can reduce the surface electron work function. It will enhance the field emission effect and restrict the cavity accelerating gradient. The room temperature in-situ plasma surface processing to clean the hydrocarbon contaminants can act as a convenient and efficient technology for the accelerator performance recovery on line. For better control of the discharge inside the cavity, the experiment works on a HWR cavity to research the ignited discharge between the swarm parameters (gas flow, pressure, forward power).

INTRODUCTION

The Superconducting Linac Injector II for Chinese Accelerator Driven System (C-ADS) was consisted of twelve Have Wave Resonators (HWR) which in two Cryostats. The Injector II operates at 162.5 MHz, and the 10 mA proton beam will be accelerated to 10 MeV on the CW mode. The parameters of HWR cavity for this section are shown in the Table 1[1].

Table 1: Parameters of HWR for the Injector II.

Parameters	Value	Unit
Frequency	162.5	MHz
βopt	0.10	-
Vacc	0.78	MV
Epeak	25	MV/m
Bpeak	50	mT
R/Q0	148	Ω
G	28.5	Ω

FIELD EMISSION

The field emission is one of the limiting for superconducting cavities to reach higher acceleration gradient. Beyond the certain gradient point, the electrons tunneling out from the cavity surface will increase exponential with the gradient value. From the *Fowler-Nordheim Theory*, the field emitted current density was described as Eq. (1) [2].

$$j = a\frac{(\beta E)^2}{\varphi}\exp(\frac{-b\varphi^{3/2}}{\beta E}+\frac{c}{\varphi^{1/2}}) \qquad (1)$$

where, j is the density of the emission current, φ is the surface electron work function, E is the surface electric field, β is the field enhancement factor, and the parameters a=1.54E6, b=6.53E3 and c=10.4 are constants.

The field emission electrons can be weight from its *X-ray* radiation produced by the bremsstrahlung. The field emission effect was measured on the Chinese ADS Injector II facility as shown in the Fig. 1.

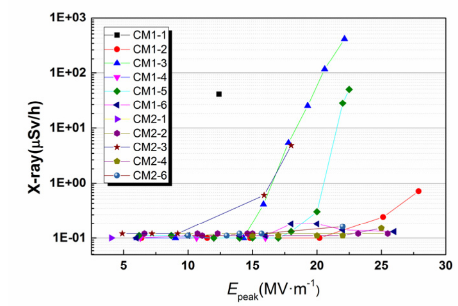

Figure 1: The *X-ray* radiation on C-ADS Injector II.

The target of the *E*peak for operation is 25MV/m, but numbers of the cavities were under restriction of field emission, for the ranging 15 to 20 MV/m. The electromagnetic energy absorbed by field emission electron and dissipated on the cavities wall will increase the cryogenic load.

The electromagnetic energy absorbed by field emission electron and dissipated on the cavities wall will increase the cryogenic load. The in-situ plasma on the superconducting cavities was efficient technology for the performance recover on the elliptical cavities at SNS [3]. Thus the plasma glow discharge experiment was set up at IMP to research the in-situ cleaning for the HWR cavity.

COUPLER COSIDERATION

To accord with the operation on line, a fundamental power coupler (FPC) was chosen to transmit the RF power to the HWR cavity for plasma discharge research. The maximum power of the solid amplifier is 200 Watts, the length of the antenna need to make enough RF power input into the cavity. And to protect the ceramic window, the plasma discharge on the coupler needs to avoid. The length of the antenna to the cavity was simulated with Microwave Studio, the model was displayed as Fig. 2.

* Work supported by Natural Science Foundation of China (Y536070GJ0)
# Email address: antonwoo@impcas.ac.cn

ISBN 978-3-95450-169-4

DEVELOPMENT OF AN HIGH GRADIENT, S-BAND, ACCELERATING STRUCTURE FOR THE FERMI LINAC

C. Serpico, I. Cudin, Elettra – Sincrotrone Trieste S.C.p.A., Trieste, Italy
A. Grudiev, CERN, Geneva, Switzerland

Abstract

The FERMI seeded free-electron laser (FEL), located at the Elettra laboratory in Trieste, is driven by a 200 meter long, S-band linac routinely operated at nearly 1.5 GeV and 10 Hz repetition rate [1]. The high energy part of the Linac is equipped with seven, 6 meter long Backward Traveling Wave (BTW) structures: those structures have small iris radius and a nose cone geometry which allows for high gradient operation [2]. Nonetheless a possible development of high-gradient, S-band accelerating structures for the replacement of the actual BTW structures is under consideration. This paper investigates a possible solution for RF couplers that could be suitable for linac driven FEL where reduced wakefields effects, high operating gradient and very high reliability are required.

INTRODUCTION

The high energy part of the Linac is equipped with seven Backward Traveling Wave (BTW) structures. Small beam apertures and nose cone geometries allow for high gradient operation.

Each structure is powered by a 45 MW, Thales klystron. Pushing the klystron at full power, a gradient of more than 30 MV/m should be achievable. As a matter of fact, BTWs have been found to suffer from increased breakdown activity even when operated at 25-26 MV/m and 50 Hz repetition rate (see Figure 1).

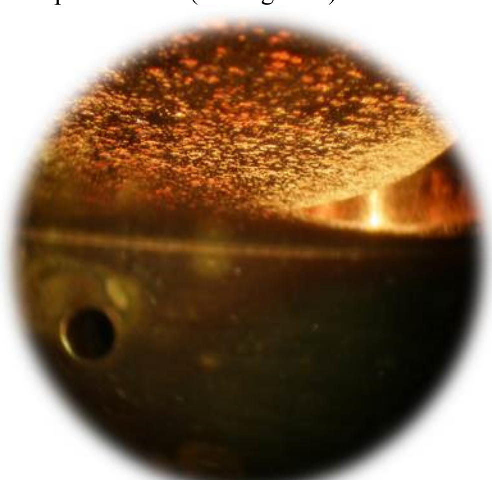

Figure 1: Breakdowns on inner surfaces.

Therefore, a development of new, low wakefields, high gradient and high reliability S-band accelerating structures for the replacement of the existing BTWs is under consideration.

This paper presents the design of an RF coupler that could be suitable for linac driven FELs. After a brief introduction to the field asymmetries and the quadrupole kick in the RF couplers, a dual-feed, electric-coupled (EC) RF coupler is then discussed.

FIELD ASYMMETRY ANALYSIS

The actual impact on the electron beam dynamics produced by field asymmetries in the coupler region can be studied by analyzing the transverse momentum change experienced by the particles passing through the RF coupler [3] [4].

In order to fully evaluate the residual field asymmetries in the coupler region, the following function $F_\varphi(z)$ is introduced [5]:

$$F_\varphi(z) = \left[F_x(r_0, \varphi = 45°, z) - F_y(r_0, \varphi = 45°, z)\right]$$

where $F_x(r_0, \varphi = 45°, z)$ and $F_y(r_0, \varphi = 45°, z)$ are the x- and y-components of the Lorentz force on a charged particle q, moving with velocity $\vec{v}$ at a position given by the cylindrical coordinates $(r_0, \varphi = 45°, z)$ as shown in Figure 2.

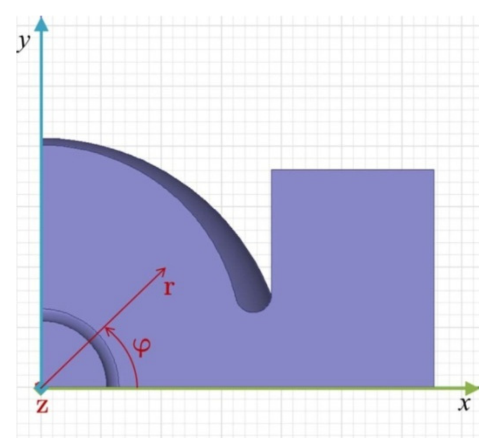

Figure 2: Transverse section of an RF coupler and circular cylindrical coordinates.

This function is then integrated along a line of length L contained in the coupler region. This yields to the quantity:

$$k_q = \frac{1}{qr}\left|\int_0^L F_\varphi(z) e^{j\frac{\omega}{c}z} dz\right|$$

For any ideal quadrupole, the x- and y-components of the Lorentz force at a position $(r_0, \varphi = 45°, z)$ should be equal to zero. So, minimizing the value of k_q will reduce the residual quadrupole kick in the coupler.

DESIGN, MANUFACTURING AND INSTALLATION OF TWO DUAL-FEED ACCELERATING STRUCTURES FOR THE FERMI INJECTOR

C. Serpico, A. Fabris, G. Penco, M. Svandrlik, Elettra Sincrotrone Trieste, Trieste, Italy
B. Keune, RI Research Instruments GmbH, Bergisch Gladbach, Germany

Abstract

FERMI is a seeded Free Electron Laser (FEL) driven by a warm S-band Linac. In the injector region, two 3-meter long Forward Traveling Wave (FTW) accelerating structures, coming from the old Elettra injector, were installed.

In order to improve the e-beam quality at higher bunch charge, it was decided to replace the existing ones with two dual-feed accelerating structures. Those structures have been designed and manufactured by RI Research Instruments GmbH and delivered to Elettra in July 2015.

The following paper will report about the RF design and the manufacturing of the new structures. Details about the RF conditioning and the installation will also be illustrated.

INTRODUCTION

FERMI, the seeded FEL facility located in Trieste, consists of two FEL lines covering the wavelength range between 100 nm down to 4 nm [1].

The FEL is driven by an S-band, warm Linac powered by 15 RF plants. The injector region [2] was equipped with two 3-meter long Forward Traveling Wave structures from the main injector of the Elettra storage ring, namely S0A and S0B.

The existing structures were constant gradient ones, with an average iris radius of 9.73 mm and a shunt impedance of 67.1 MΩ/m [3]. Both the structures were equipped with single-feed RF couplers. Due to this, an evident head-tail kick was affecting the beam, slightly worsening the beam emittance in the injector region.

To further improve the e-beam quality and increase the overall Linac energy as well, it was planned to replace the existing structures with new dual-feed accelerating sections [4] [5] and move the old structures in the high energy part region of the Linac.

The new structures were commissioned to RI Research Instruments GmbH. In the following sections RF design and manufacturing of the structures are described. Also, results from the RF high power conditioning and beam commissioning are reported.

RF DESIGN

Table 1 lists the main rf parameters that are the basis for the structure design. The rf properties for the S-band cells have been simulated with the CST Microwave Studio [6] Eigenmode solver and the SUPERFISH [7] code.

Table 1: RF Design Parameters of the S-band Structures

Parameter	Value	Unit
Cavity length	3375	mm
Operating frequency	2998.01	MHz
Phase advance per cell	$2\pi/3$	-
Nr. regular cells	96	-
Av. shunt impedance (sim.)	60.5	MΩ/m
Gradient @ 16MW (sim.)	14.5	MV/m

The rf design of the travelling wave structures follows the approach described by Paul Scherrer Institute (PSI) for their C-Band structures [8]. A constant accelerating gradient along the structure is maintained by designing the group velocities of the TM010 mode in the accelerating cells in a way that the following equation is satisfied.

$$\frac{v_{g,n}}{\left(\frac{r}{Q}\right)_n} = \frac{v_{g,n-1}}{\left(\frac{r}{Q}\right)_{n-1}} e^{-2\alpha_{n-1}L_{cell}}$$

Here $v_{g,n}$ is the group velocity of the n-th cell, r_n is the shunt impedance, Q_n the quality factor of the n-th cell and L_{cell} the cell length. A MATLAB script was written to derive the exact cell parameters from this iterative design approach.

The rf power is coupled symmetrically to the input coupler cell. The fraction of the power that is not dissipated in the structure is decoupled from the cavity by an also symmetric output coupler cell. Both coupling cells incorporate a racetrack shape cell design to suppress the quadrupole component of the fields to less than 0.01% within the dimension of the beam tube aperture.

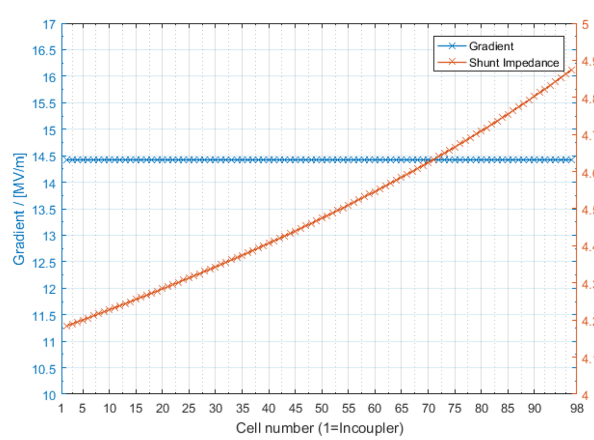

Figure 1: Variation of r/Q and resulting const. gradient.

ISBN 978-3-95450-169-4

MONOPOLE HOMS DUMPING IN THE LCLS-II 1.3 GHz STRUCTURE*

A. Lunin†, T. Khabiboulline, N. Solyak,
Fermi National Accelerator Laboratory, Batavia, USA

Abstract

Developing an upgrade of Linac Coherent Light Source (LCLS-II) is currently underway. The central part of LCLS-II is a continuous wave superconducting RF (CW SRF) electron linac. High order modes (HOMs) excited in SRF structures by passing beam may deteriorate beam quality and affect beam stability. In this paper, we report the simulation results of monopole High Order Modes (HOM) spectrum in the 1.3 GHz accelerating structure. We suggest optimum parameters of the HOM feedthrough for minimizing RF losses on the HOM antenna tip and for preserving an efficiency of monopole HOMs damping simultaneously.

INTRODUCTION

A continuous operation regime of the 1.3 GHz LCSL-II accelerating structure at the nominal gradient of 16 MV/m sets an extra caution on possible overheating of HOM couplers feedthroughs [1]. The HOM feedthrough coupling antenna is made of a solid Niobium, which does not produce significant amount of RF losses until its temperature is keeping below critical and the niobium surface is in a superconducting state. Nevertheless, a radiation of HOMs and an operating mode leaking through the notch filter can cause RF heating of the feedthrough internal parts and then a heating of the antenna itself by a thermal conductivity. This effect may initiate a thermal runaway process when increasing the antenna temperature leads to larger RF losses and generate an additional antenna heating by itself. Eventually it will produce a sharp temperature rise and end up by a cavity quench. In order to avoid such a scenario, one has to minimize the antenna RF heating by using smaller antenna tip and increasing the gap between the antenna and the f-part of HOM coupler. At the same time, we should not compromise the coupler capability to damp the cavity HOM spectrum. Bellow we compare ILC and XFEL design of the HOM feedthrough and analyse various antenna positions for finding optimum parameters.

3 MONOPOLE HOMS SPECTRUM

The detailed study of resonant HOM excitation in the LCLS-II accelerating structure is performed in [2]. For the nominal parameters of LCLS-II linac, the most dangerous are monopole HOMs with high shunt impedances, which may result additional radiation of RF power to the HOM coupler port. Based on it we limited our investigation by the monopole HOMs only. Originally the spectrum of monopole modes in the 2D model of the TESLA 9-cell cavity is presented in [3] for first three TM-monopole passbands. Recently the detailed study of a thermal quench initiated by the overheating of the HOM antenna is published in [4] for various designs of the HOM feedthrough and trapped monopole HOMs below the beam pipe cut-off frequency of 2.942 GHz for the TM01 mode.

Table 1: Parameters of Monopole HOMs

Mode #	Frequency, [GHz]	R/Q [Ω]	Q_{ext}
2-8	2.452	136	8.5e4
2-9	2.458	157	1.7e5
4-1	3.3976	0.025	1.0e4
4-2	3.4073	0.36	4.5e3
5-6	3.8528	4.9	1.0e4
5-7	3.8560	1.6	3.5e4
5-8	3.8578	42	1.4e5
6-1	3.9253	0.05	1.8e4
6-2	3.9453	0.12	5.0e3
7-7	4.7051	0.66	2.2e3
7-8	4.7209	5.8	4.5e4
8-5	4.8829	0.4	1.0e5
8-8	4.8926	0.5	3.8e4

We extend the search of trapped monopole modes beyond the cut-off frequency of a beam pipe. For this purpose we simulate the chain of three cavities where HOMs in the first and last cavities are slightly detuned from the middle cavity in order to approximate the actual spread of the HOM spectrum due to mechanical tolerances. The cavity 3D model is based on actual mechanical drawings including HOM coupler feedthroughs. The results of electromagnetic calculations of monopole HOMs up to the 5 GHz frequency are illustrated in Fig. 1 for modes with highest R/Q values in each passband. One can note that despite the frequencies of second monopole passband in the 1.3 GHz cavity is below the cut-off limit, the RF field is propagating through the beam pipe. The reason is a transformation of monopole TM01 mode in the cavity to the dipole TE11 mode in the beam pipe caused by asymmetries introduced by HOM couplers. The coupled TE11 mode can freely propagate in the interconnecting beam pipe since its frequency is above the cut off limit of 2.252 GHz. The TE11 signal reaches to neighbour cavities and reflects back forming a standing wave pattern, which has a strong influence on a coupling with the HOM ports. Thus, the chain of at least three cavities is required for accurate simulation of

* Operated by Fermi Research Alliance, LLC under Contract No. DE-AC02-07CH11359 with the United States Department of Energy.
† lunin@fnal.gov

REDESIGN OF THE END GROUP IN THE 3.9 GHz LCLS-II CAVITY*

A. Lunin†, I. Gonin, T. Khabiboulline, N. Solyak, Fermi National Accelerator Laboratory, Batavia, USA

Abstract

Development and production of Linac Coherent Light Source II (LCLS-II) is underway. The central part of LCLS-II is a continuous wave superconducting RF (CW SCRF) electron linac. The 3.9 GHz third harmonic cavity similar to the XFEL design will be used in the linac for linearizing the longitudinal beam profile [1]. The initial design of the 3.9 GHz cavity developed for the XFEL project has a large, 40 mm, beam pipe aperture for ensuring a low (< 10^6) cavity loaded quality factor. It is resulted in dipole HOMs with frequencies nearby the operating mode, which causes difficulties with HOM coupler notch filter tuning. The CW linac operation requires an extra caution in the design of the HOM coupler in order to prevent its possible overheating. In this paper, we present the modified 3.9 GHz cavity End Group for meeting to the LCLS-II requirements.

INTRODUCTION

A continuous operation regime of the 3.9 GHz LCSL-II accelerating structure at the maximum gradient of 14.9 MV/m sets an extra caution on possible overheating of HOM couplers feedthroughs [2, 3]. The HOM feedthrough coupling antenna is made of a solid Niobium, which does not produce significant amount of RF losses until its temperature is keeping below critical, but it may initiate a thermal runaway process and end up by a cavity quench due to a leak of an operating mode or a resonant excitation of the cavity HOM spectrum [4]. In order to avoid such a scenario, one has to minimize the antenna RF heating by using smaller antenna tip and increasing the size of the f-part snag. The proposed HOM coupler modification in the 3.9 GHz cavity is illustrated in Fig. 1. The height of antenna tip is decreased from 5 mm to 1 mm and the height of the f-part snag is increased to 7.8 mm in order to make a shallow antenna penetration and, thus, to lower a surface magnetic field. The nominal gap between the antenna and the f-part is chosen equal to 0.5 mm.

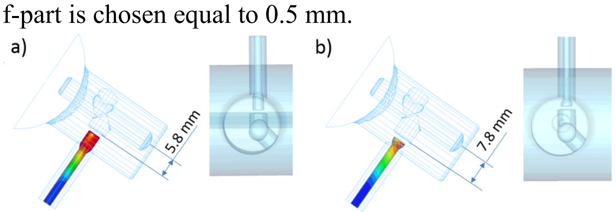

Figure 1: Modifications of the HOM coupler for the 3.9 GHz cavity: a) XFEL design and b) LCLS-II design.

Another drawback of the original XFEL End Group design is an oversized 40 mm aperture of the beam pipe, which has a cut off frequency of the lowest dipole mode very close to an operating mode. Eventually it makes quite difficult tuning the HOM coupler notch filter in a close proximity of dipole HOMs in the cavity End Group [5]. As a remedy, we decided to decrease slightly both apertures of the beam pipe and interconnecting bellows to 38 mm aiming to shift up frequencies of nearby dipole HOMs by at least of 100 MHz Modified design of the 3.9 GHz cavity End Group is illustrated in Fig. 2. The geometry of the cavity end cell remains untouched, while the tapering to a smaller aperture is made within the Nb transition ring.

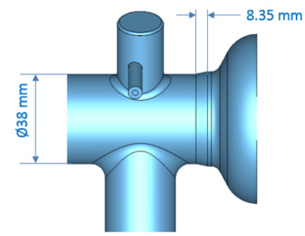

Figure 2: New design of the 3.9 GHz cavity End Group.

OPERATING MODE RF LOSSES

Parameters of operating mode for both designs of 3.9 GHz cavities, XFEL and LCLS-II, are compared in the Table 1. Since only the End Group was modified, there are little changes in the cavity performance

Table 1: Parameters of 3.9 GHz Cavities

Operating Mode Parameters	XFEL	LCLS-II
Frequency, [GHz]	3.9	3.9
Stored Energy, [J]	1	1
R/Q, [Ω]	746	751
Effective Length, [m]	0.346	0.346
Max Electric Field on Axis, [MV/m]	25.4	25.3
Accelerating Gradient, [MV/m]	12.36	12.40
Normalized Surface Electric Field	2.25	2.24
Normalized Surface Magnetic Field, [mT/MV/m]	4.90	4.88

A tail of the operating mode decays to the beam pipe and a remnant surface magnetic field causes ohmic losses in the bellows and connecting flanges. We used ANSYS HFSS software for electromagnetic simulations of the 3.9 GHz cavity [6]. A mechanical model of cavity and bellows connection as well as a distribution of the magnetic field penetrating to the beam pipe are shown in Fig. 3. The result of local G-factors calculations and associated RF losses in the

* Operated by Fermi Research Alliance, LLC under Contract No. DE-AC02-07CH11359 with the United States Department of Energy.
† lunin@fnal.gov

ISBN 978-3-95450-169-4

STATUS OF THE ILC MAIN LINAC DESIGN*

A. Saini†, V. Kapin, N. Solyak, Fermi National Accelerator Laboratory, Batavia, USA

Abstract

The International Linear collider (ILC) is a proposed accelerator facility which is primarily based on two 11-km long superconducting (SC) main linacs. In this paper we present recent updates on the main linac design and discuss changes made in order to meet specification outlined in the technical design report (TDR).

INTRODUCTION

The ILC is a proposed accelerator facility for the study of high energy physics via electron-positron collisions at center–of-mass energy between 200 GeV and 500 GeV. A schematic of the ILC facility is shown in Fig. 1.

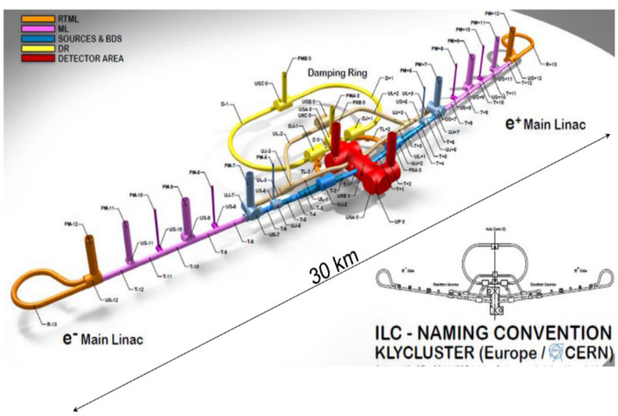

Figure 1: A schematic of ILC facility. All the main sections are presented in different colours.

The heart of the ILC facility is two SC main linacs that accelerate electron and positron from 15 GeV to their final collision energy ranging between 100 to 250 GeV. The ILC technical design report (TDR) [1] establishes technical aspects of the main linac such as geometry, cryogenic segmentation, RF distribution etc. In this paper we present a baseline configuration of the main linac that meets the TDR specifications and discuss the main linac optics.

MAIN LINAC ARCHITECTURE

Each main linac consists of approximately 7,500 nine-cell standing wave niobium cavities operating at frequency of 1.3 GHz. These cavities are installed in two variants of cryomodules named Type-A and Type-B cryomodule. Type-A cryomodule accommodates nine cavities while a Type-B cryomodule consists of eight cavities and a magnet package at the center which is comprised of a quadrupole magnet, a steering corrector magnet and a beam position monitor (BPM). Both cryomodules are approximately 12.6 m long. An arrangement of cryomodules in sequence of type-A type-B type-A forms an RF unit (also called ML unit) and therefore, two successive RF units form a FODO cell. There are 285 (282) ML units in electron (positron) linac. A group of three RF units with a 2.5m cold box at the end makes a cryo string. A periodic arrangement of cryo string is interrupted due to insertion of a 7.5m long warm section. Number of cryo strings between two successive warm sections form a cryo unit. It is comprising of between 11 to 21 cryo strings, with the final cold box being replaced by a 2.5m service box. The length of drift space between the last cryo string of a cryo unit and the first cryo string in following cryo unit is equal to a cryomodule length. Figure 2 shows a segmentation scheme in the main linac.

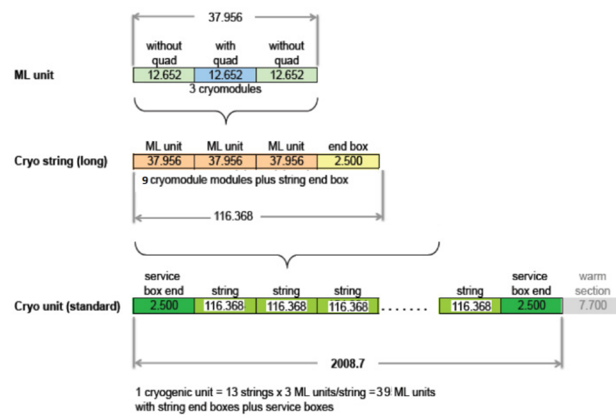

Figure 2: A block diagram of structural segmentation of the main linac.

RF power to the main linac is delivered using the Distribution Klystron Scheme (DKS) [2] which is more preferable choice over the Klystron Cluster Scheme (KCS) [3] for a mountainous topography such as the candidate sites in Japan.

EARTH CURVEATURE IMPLEMENTATION

An essential feature of the ILC linac is that it follows Earth's curvature that simplifies transport of two-phase helium at 2K. A straight variant of the main linacs needs an expensive and complex cryogenic segmentation. In order to implement Earth's curvature in the main linac lattice, a same concept as discussed in [4] is utilized. Each cryomodule in the curved linac is aligned along a line perpendicular to Earth's radius at cryomodule center. It will result in a geometrical kink at the ends of cryomodule. This kink in the lattice is incorporated using a special element in LUCRETIA [5] named GKICK. However, this element is not supported by several optics codes including MAD8 [6]. Thus, a combination of the thin vertical correctors and the thin dipole with same but opposite kick is used to produce equivalent effect. The thin dipole changes both the beam trajectory and the reference frame while the thin corrector cancels out the trajectory change and therefore, leaves only

* Work supported by Fermi Research Alliance, LLC under Contracts No. De-Ac02-07CH11359 with the DOE, USA.
† asaini@fnal.gov

ISBN 978-3-95450-169-4

X-BAND TRAVELLING WAVE ACCELERATING SECTION R&D FOR HTF

K. Jin, National Synchrotron Radiation Laboratory, NSRL USTC, Hefei, Anhui, China

Abstract

Hefei Light Source (HLS) was mainly composed of an 800 MeV electron storage ring and an 800MeV-1GeV constant-gradient accelerator in NSRL. The new Linac with Full Energy Injection and the Top-up Injection scheme has been constructed successfully. And the other functioning as X Ray Free Electron Laser test facility has been considered. In the project, in order to compress the bunch length and to achieve the beam energy distribution linearization. A 15MeV, operation frequency 11.424GHz traveling wave accelerating section as harmonic compensation is being developed. In this paper, the R&D of the x-band accelerating section with collinear load are presented in detail.

INTRODUCTION

The linear accelerators at an X-band frequency are being interested since it gives a reduced accelerator length and reduced average power consumption compared with lower frequencies [1]. A frequency of 9.370GHz, 1.6MeV traveling wave linear accelerator has been fabricated in our Lab. with the view of X-band R&D. It consists of a RF input coupler, 38 disk-loaded accelerating cavities and a constant power-loss collinear load. In this paper, the coupler numerical simulation design, the collinear load study and the accelerator section development are described in detail as following. The manufacture technology and some measurement results are presented. And an operation frequency 11.424GHz traveling wave accelerating section is being developed for the X Ray Free Electron Laser Hefei Test Facility (HTF).

RF INPUT COUPLER DESIGN

The RF coupler is an important component for an accelerator structure. It consists of a tapered rectangular waveguide and a coupling cavity with a coupling aperture. It must be well matched to the feeding waveguide and has synchronous frequency for the proper phase advance in the structure so that ensure the input power is fed effectively and an excellent travelling wave is transmitted in the accelerating cavities train. Therefore the sizes of the coupling cavity and the coupling iris aperture should be designed exactly at operation frequency so that the optimum transmission parameter S21 and scattering parameter S11 are obtained.

In our project, the numerical simulation design of RF coupler assembly was considered. In the wake of the computer program development, special the MAFIA-code [2], it made the three dimensions (3D) S-parameters calculation in time domain becoming possible and the change in dimensions can be easily implemented on the computer. In numerical simulation, a computer model that approximates closely real coupler cavity was built first. It consists of an input coupler, a regular accelerating cavity and an output coupler. Considering the symmetrical, only a half of the structure is needed in calculation. It is necessary to set an appropriate computation period so that assure the electric-magnetic wave can transmitted to end of output coupler (for calculation S21), reflection wave can return to the front end of input coupler (for calculation S11) and the travelling wave in the structure reach to a steady-state. Two main factors of effecting matching and tuning of coupler are coupling cavity diameter and coupling iris aperture. The S-parameters are calculated after each size changed, and the thickness of coupling iris can be obtained by edit a calculation formula in program. Revising the sizes step by step in such a way, in conjunction with microwave measurement by Kyhl method [3], the optimal matching and tuning results are acquired finally. The coupler assembly and time history of S21 are showed in Fig.1 and Fig.2.

Figure 1: RF input coupler assembly.

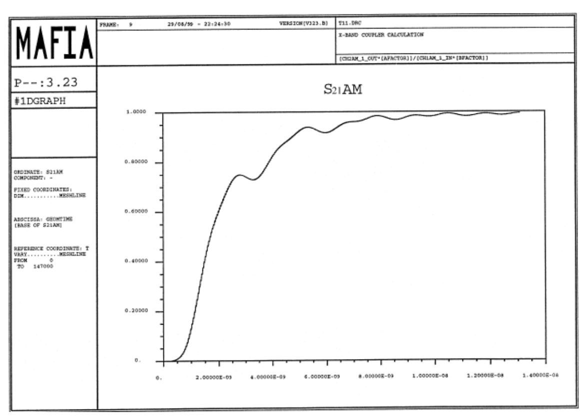

Figure 2: Amplitude of transmission wave vs time.

COLLINEAR LOAD STUDY

The typical operation of a travelling wave electron linear accelerator results in remnant RF power appearing at the termination of the accelerating structure. In general

4 K SRF OPERATION OF THE 10 MeV CEBAF PHOTO-INJECTOR*

G. Eremeev †, M. Drury, J. Grames, R. Kazimi, M. Poelker, J. Preble, R. Suleiman, Y. Wang, M. Wright
Thomas Jefferson National Accelerator Facility, Newport News, VA 23606, U.S.A.

Abstract

Superconducting radio-frequency (SRF) accelerating cavities are often operated in superfluid liquid helium with temperature near 2 K to enhance the cavity quality factor Q_0 and to help manage heat loads, which are particularly important at large SRF accelerator facilities. This 2 K temperature paradigm, however, need not put SRF technology out of the reach of small institutions or even limit SRF operation at large facilities that need 10-100 MeV beam energy. At the Continuous Electron Beam Accelerator Facility (CEBAF) at Jefferson Lab there are regularly scheduled maintenance periods during which cryogenic plant often increases the liquid helium temperature from 2 K to 4 K, reducing power consumption by ~ 50 % and saving megawatts of wall-plug power. During recent maintenance periods, we accelerated a continuous-wave electron beam at the CEBAF photo-injector to a total energy of 6.3 MeV at currents up to 80 µA using two 5-cell niobium cavities in the quarter-cryomodule at 4 K. This contribution describes the SRF and cryogenic performance and uses measured beam quality and energy stability as key metrics. These measurements indicate that 4 K operation of niobium SRF cavities in CEBAF is a sensible and cost effective mode for high quality beam operation, provided the cryogenic load associated with lower Q_0 is manageable for the number of cavities needed to operate. For Jefferson Lab, this enhances our scientific reach allowing additional low-energy ~ 10 MeV experiments each year.

INTRODUCTION

Two cryogenic plants provide liquid helium at 2 K to the CEBAF cryomodules to support 12 GeV beam operations. However, during extended maintenance periods when high energy beam experiments are not performed the cryoplants transition to 4.3 K to reduce their power consumption and save upon operational costs. Cryomodules routinely sit idle during these periods, since it is believed the degraded intrinsic quality factor of superconducting niobium cavities at this temperature precludes productive beam operation. We used several of these maintenance periods to investigate the potential for operating injector cryomodules at 4 K with a couple goals in mind. First, there are a number of experiments which could use low energy ~10 MeV electron beams, e.g. the production of spin-polarized positron beams [1] or the Bubble Chamber experiment [2] aimed at quantifying nucleosynthesis in stars. Second, there is interest in evaluating the performance of Nb_3Sn coated cavities in the accelerator environment using one of the CEBAF cryomodules [3], where the stability of a 2 K cryomodule operated at 4 K needs to be studied.

While operating cryomodules with elliptical cavities at 4 K has been demonstrated, for example TRISTAN [4], LEP [5], and CESR [6] operated for years in such a configuration, a direct comparison of the quality of beams accelerated in the same cryomodule at 2 and 4 K at higher frequencies (where average dissipated power density is higher) had not been studied. In this contribution we describe the SRF gradient reach of the CEBAF injector quarter-cryomodule at 4 K, and compare beam quality and energy stability delivered at 2 K and 4 K.

4 K CRYOMODULE MEASUREMENT

The injector quarter-cryomodule is the first superconducting module at CEBAF, accelerating the beam up to ~ 10 MeV using two 5-cell cavities each operated up to E_{acc} = 10 MV/m. The cavities, designated as #7 and #8 due to their position with respect to RF couplers in the tunnel, were tested at 4 K to determine stable operating gradients. Individually, cavity #7 reached E_{acc} = 9.5 MV/m and cavity #8 reached E_{acc} = 10 MV/m, before being limited by window arcing above E_{acc} = 10.5 MV/m. In both cases the helium liquid level remained stable with the JT valve opened to 70 %, which we considered a heat load limit not to exceed. Next, both cavities were simultaneously powered to E_{acc} = 8 MV/m, again with the JT valve open to 70 %. While the quality factor of the cavities was not measured during these tests, assuming a typical $Q_0 = 3{\cdot}10^8$ at 4.3 K, we estimate about 200 Watts was dissipated into the helium bath for this configuration.

4 K AND 2 K BEAM MEASUREMENTS

After stable operating conditions for the quarter-cryomodule were determined, the injector was setup for beam quality measurements with average intensity ranging from 60 µA at 2 K to 80 µA at 4 K test.

The lower maximum intensity at 2 K was caused by an unrelated operational hardware issue. For convenience the cavities were operated at typical gradients for injector operation, E_{acc}^{cav7} = 5.00 MV/m and E_{acc}^{cav8} = 5.32 MV/m. The electron beam was characterized with diagnostics downstream of the quarter-cryomodule (see Fig. 1). The beam momentum was measured using a spectrometer, by finding the magnetic field (MDL0L02) necessary to deflect the beam a known angle. The (normalized) beam emittance and Twiss parameters were determined using a profile monitor (IHA0L03) to measure the variation of beam size as a function of an upstream quadrupole magnet (MQJ0L02). The energy spread was determined by extracting the dispersive contribution of the beam size as measured at a dispersive location (IHA2D00).

* Authored by Jefferson Science Associates, LLC under U.S. DOE Contract No. DE-AC05-06OR23177.
† grigory@jlab.org

ISBN 978-3-95450-169-4

DESIGN OF A DIELECTRIC-LINED WAVEGUIDE FOR TERAHERTZ-DRIVEN LINEAR ELECTRON ACCELERATION

A.L. Healy*, G. Burt, Cockcroft Institute, Lancaster, UK
S.P. Jamison, R. Valizadeh, STFC Daresbury Laboratory, UK
M.J Cliffe, D.M. Graham, University of Manchester, Manchester, UK

Abstract

A dielectric-lined waveguide has been designed for use as an accelerating structure in terahertz-driven electron acceleration experiments at Daresbury. Experimental verification of acceleration will take place on Versatile Electron Linear Accelerator (VELA). The choice of a rectangular waveguide structure with sidewall dielectric layers enables tuning by varying the spacing between dielectric slabs to account for potential manufacturing errors. Schemes for coupling free-space single cycle THz pulses into the waveguide have been evaluated and optimised through CST simulation.

INTRODUCTION

The use of terahertz (THz) frequencies as an alternative to conventional RF allows for smaller, sub-millimetre structures, with higher accelerating gradients due to increased breakdown limits [1]. Optical frequencies also have this advantage, but the smaller wavelengths result in smaller structures and require manufacturing precision in the sub-micron range. THz wavelengths have the further advantage over optical that an electron bunch of higher charge can be confined within a single acceleration period. Dielectric-lined waveguides (DLWs) can support travelling-wave accelerating modes with phase velocities v_p less than the speed of light. A DLW used for acceleration must maximise interaction between the THz pulse and an electron bunch. There are several points to consider; phase matching of electrons and THz pulse over a wide bandwidth, accelerating gradient, shunt impedance, and ease of fabrication. Other issues include charging of the dielectric and electron bunch injection into a small aperture.

Typical design choice is to use a cylindrical DLW as this maximises the accelerating gradient for a given input power [2]; however this removes the potential for tunability in the case of fabrication errors. Here we consider rectangular DLWs, such as that shown in Fig. 1. The use of CVD diamond as the dielectric allows for thin, few micron dielectric layers, with the benefits of high breakdown field, low loss tangent and highest known thermal conductivity [3]. A rectangular DLW can be tuned to a different operating frequency by varying the dielectric slab separation, which has the added benefit of correcting for any manufacturing errors.

* alisa.healy@cockcroft.ac.uk

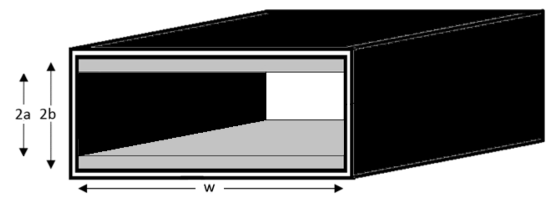

Figure 1: A hollow rectangular DLW of width w, dielectric slab separation $2a$ and dielectric slab thickness $t = b - a$. The waveguide is enclosed with metallic walls.

ACCELERATING MODE

Rectangular DLW modes are longitudinal section magnetic/electric (LSM/LSE) [4], with no H_y/E_y components (normal to the dielectric interface). Field analysis has been performed previously in [2]. The lowest order accelerating mode, with an on-axis longitudinal field component, is the LSM_{11} mode. Figure 2 shows the dispersion relation for the LSM_{11} mode of a rectangular DLW. A THz pulse propagating through the waveguide can co-propagate with an electron at frequencies corresponding to $v_p \leq c$. For an electron travelling at velocity $v_e = v_p = c$, it will travel in phase along the length of the waveguide with one frequency component of the pulse. All other frequencies will shift out of phase with the electron. The phase and group velocities for a rectangular DLW are shown in Fig. 3. To

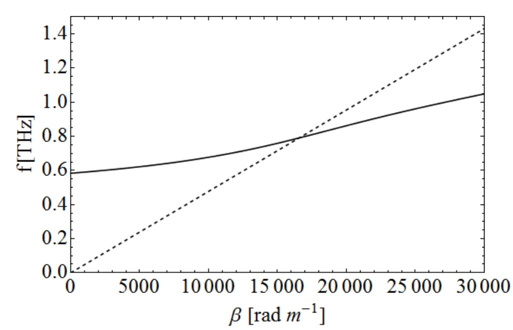

Figure 2: Dispersion relation of the LSM_{11} mode for the optimised waveguide parameters. The dotted line represents $v_p = c$.

understand the effectiveness of the waveguide as an accelerating structure, figures of merit were used. Those considered of most importance were the shunt impedance, r_s, and the accelerating bandwidth, Δf. Shunt impedance is given by

$$r_s = \frac{(V_0 T)^2}{P_{diss}}, \quad (1)$$

COMPACT BEAM POSITION MONITOR FOR ELECTRON AND PROTON MACHINES

M. Znidarcic, M. Cargnelutti, Instrumentation Technologies, Solkan, Slovenia

Abstract

Monitoring and subsequent optimization of the linacs, transfer lines, energy recovery linacs and synchrotrons, requires specific instrumentation optimized for beam position and charge measurements. Libera Spark is the newly developed instrument intended for position and charge monitoring in electron and proton machines. The motivation, processing principles and first results at laboratories are presented.

INTRODUCTION

In this paper we introduce a compact platform that aims to host a wide range of applications like various BPMs, Digitizers, Beam Loss Monitors etc. This paper focuses on a new family of BPMs called Libera Spark.

LIBERA SPARK

Looking at the beam instrumentation used to monitor and stabilize an accelerator, every device suits a specific role, but it is possible to identify some key components that are always present:

- RF front-end and analog signal processing
- Digitalization
- Internal communication buses
- Power supply unit
- Cooling system
- Control system integration layer

In this new development, we take advantage of the latest advances in System on Chip technology to introduce a compact platform (see Fig. 1) that combines a high level of hardware and software integration with our knowledge regarding reconfigurable analog signal processing [2].

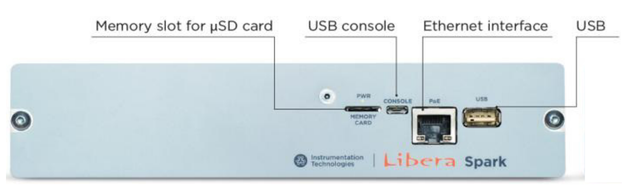

Figure 1: Libera Libera Spark front panel.

HW and SW Integration

Hardware and software are designed taking in account the balance between generality and optimization. This makes possible to add specific features and gives more space for customization, opening at the same time the way for developing different applications, as shown in Fig. 2.

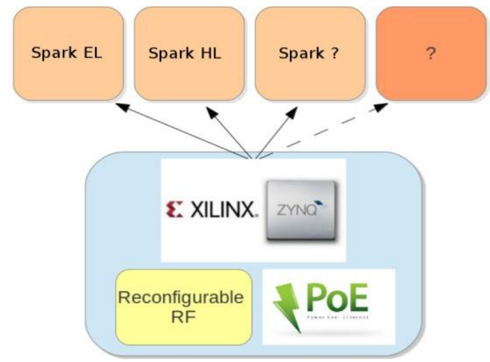

Figure 2: Platform concept based on SoC.

The core part is the SoC Xilinx Zynq 7020 [1] which combines the high-speed processing of the FPGA together with the flexibility of a CPU, all within the same chip. The inner communication between the two entities and the chance to share the same memory removes at the same time two of the biggest bottle-necks that still characterize separate-chip solutions:

- No communication protocols needed
- No data copy between FPGA and CPU.

Basic building blocks are presented in the Fig. 3. Pulses from the pickup electrodes are passed through the analog processing chains. Depending on the beam type, the chain includes a combination of filters, several attenuation and amplification elements etc. By combining hardware components and specific DSP, various applications can reside on a single platform. The following Libera Spark instruments are currently available [3]:

- Libera Spark EL (Linear electron machines, Energy Recovery Linacs)
- Libera Spark HL (Linear proton machines)
- Libera Spark ER (Electron rings)
- Libera Spark HR (Proton rings, proton beam transfers)

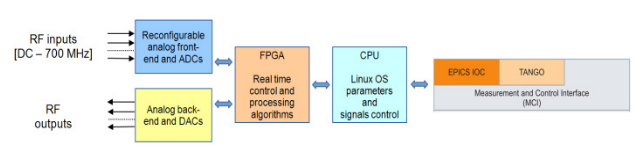

Figure 3: Building blocks.

On the top layer, Libera Spark provides the MCI with a development package and Command Line utilities for open interaction in different control systems. On top of the MCI, various adaptors to different control systems can be implemented (EPICS, Tango, etc.). EPICS interface is part of the standard software package.

ISBN 978-3-95450-169-4

INVESTIGATIONS ON ELECTRON BEAM IMPERFECTIONS AT PITZ

M. Krasilnikov*, Q. Zhao, I. Isaev, P. Boonpornprasert, J. Good, M. Gross, H. Huck, D. Kalantaryan, O. Lishilin, G. Loisch, D. Melkumyan, A. Oppelt, G. Pathak, Y. Renier, T. Rublack, F. Stephan, G. Vashchenko†, DESY, Zeuthen, Germany
C. Hernandez-Garcia, JLab, Newport News, Virginia, USA
G. Asova, INRNE, Sofia, Bulgaria

Abstract

Since more than a decade, the photo injector test facility at DESY, Zeuthen site (PITZ), has developed and optimized high brightness electron sources for modern Free Electros Lasers like FLASH and the European XFEL. Despite a very high performance of the photo injector was experimentally demonstrated, several discrepancies between measurements and beam dynamics simulations have been revealed. Although the optimized measured values of the projected transverse emittance are close to those obtained from the beam dynamics simulations, the corresponding experimental machine parameters show certain systematic deviations from the simulated optimized setup. As a source for these deviations, electron beam imperfections were experimentally investigated. This includes studies on bunch charge production, electron beam imaging using the RF gun with its solenoid, and investigations on the transverse asymmetry of the electron beam generated in a rotationally symmetric gun cavity. Experimental studies were supplied with corresponding beam dynamics simulations. The paper reports on results of these studies.

MOTIVATION

The transverse projected emittance has been experimentally optimized at PITZ for a wide range of bunch charges [1]. The transverse phase space of the electron beam from the 1½-cell L-band RF-gun was measured in details while tuning numerous parameters, like gun gradient (E_{cath}) and phase, main solenoid current (I_{main}), cathode laser pulse temporal profile and transverse distribution. The 2015 measurement program was mainly dedicated to the emittance minimization for 500 pC electron bunches for E_{cath}=53 MV/m applying photocathode pulses with Gaussian temporal profile of ~11 ps FWHM [2]. A typical experimentally optimized electron beam setup is presented in Fig. 1. The transverse projected rms emittance of ~0.8 mm mrad (geometrical average of horizontal and vertical emittance) was obtained from the single slit scan technique [1]. Besides the transverse phase space a bunch current profile was measured using a transverse deflecting system [3]. It is shown in Fig. 1b together with the cathode laser temporal profile. The transverse rms spot size of the photocathode laser was optimized. The results are shown in Fig. 2 together with simulated curves for different models of transverse laser distributions (see section "Photoemission" for more details on these models). For each laser spot size the main solenoid current was optimized. Corresponding measured emittance curves are shown in Fig. 3 together with rms sizes of the electron beam. Results of simulations are shown as well while applying the main solenoid current calibration obtained from the magnetic field measurements. A difference of ~5A in the optimum value for the emittance is clearly seen.

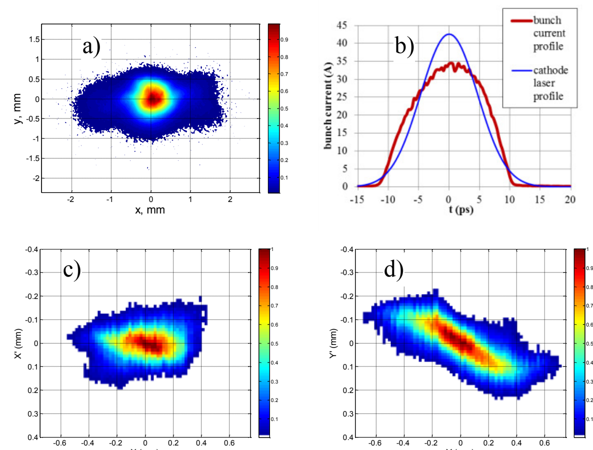

Figure 1: Experimentally optimized setup for 500 pC bunches: a) electron beam transverse distribution at a YAG screen; b) temporal profiles of electron bunch and cathode laser; horizontal (c) and vertical (d) phase space.

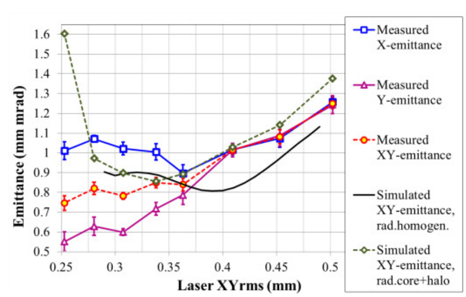

Figure 2: Measured emittance as a function of the transverse rms laser spot size. Simulated curves were obtained applying radially homogeneous laser distributions and using the "core plus halo model".

All these results show electron beam x-y asymmetries in terms of the rms sizes and emittances. The electron beam transverse distribution (Fig. 1a) is strongly deviating from the rotationally symmetric shape expected from the beam dynamics simulations for the rotationally symmetric RF-gun cavity. Also some discrepancies between

* mikhail.krasilnikov@desy.de
† now at DESY, Hamburg

ISBN 978-3-95450-169-4

CONSTRUCTION OF A THIRD RECIRCULATION FOR THE S-DALINAC*

M. Arnold†, T. Kürzeder, J. Pforr, N. Pietralla, M. Steinhorst, TU Darmstadt, Germany
F. Hug, JGU Mainz, Germany

Abstract

The maximum energy of the S-DALINAC will be increased by adding a recirculation beam line and thus recirculating the beam an additional time. All necessary simulations of magnets as well as beam dynamics are finished and summarized. The set-up of the new beam line offers a phase shift of up to 360° and enables to run the S-DALINAC as an once or twice recirculating ERL.

INTRODUCTION

The S-DALINAC is a superconducting electron linear accelerator running since 1991 at TU Darmstadt [1]. It was constructed as a twice-recirculating accelerator with a maximum energy of 130 MeV in cw operation. For a reliable and stable beam operation only 85 MeV (cw mode) were possible due to a lower quality factor of the superconducting cavities than previously anticipated and thus a higher dissipated power to the helium bath. Recirculating the beam an additional time together with lowering the design accelerating gradients from 5 MV/m to 3.75 MV/m will increase the maximum achievable energy close to 130 MeV in cw mode. A floorplan of the three times recirculating S-DALINAC is shown in Fig. 1. The beam is either produced in a thermionic gun with an electrostatic pre-acceleration of 250 keV or in SPIN (S-DALINAC Polarized INjector) - a source for polarized electrons with a pre-acceleration of up to 125 keV [2]. Following both sources the beam is prepared for an acceleration with a time-structure of 3 GHz in a chopper-prebuncher section. In case of a recirculating set-up the beam then is accelerated up to 7.5 MeV in the injector linac. Afterwards it is bend into the main linac with an acceleration of up to 30 MeV per pass. Recirculating the beam up to three times leads to a final energy of up to 130 MeV. Nuclear physics experiments can be performed either with the injector beam at 10 MeV or the main linac beam. In the recirculating operation a maximum beam current of 20 μA can be reached. The transformation from a twice to a three times recirculating set-up required several simulations. In a first step the most important dipoles, the separation and recombination dipole magnets, had to be designed. Additionally six new dipoles for a new beam line were needed. Simulating the whole lattice with all adaptions to new requirements was an important task as well. As the installed pathlength adjustment system of the new second recirculation can move in total a complete RF wavelength of 10 cm, it will enable an energy recovery linac test operation in once or twice recirculating scheme.

* Work supported by DFG through CRC 634 and RTG 2128

† marnold@ikp.tu-darmstadt.de

NEW DIPOLE MAGNETS

Extending the S-DALINAC by one recirculation resulted in the need of new dipole magnets. Replacing existing magnets as the separation and recombination dipoles to fit an additional beam line and strict border conditions were initial points. Furthermore the new beam line had to be equipped with dipole magnets. Both magnet models will be introduced and their positions are indicated in Fig. 1.

Separation Dipole

The new separation dipole magnet and its mirrored version, the recombination dipole, are very complex and demanding magnets. They must fit several conditions on very limited space. Bending four different beams at the same time the separation dipole is additionally a very important magnet of the S-DALINAC. Its main parameters are shown in Table 1. The designed magnetic flux is 0.75 T (0.65 T for 130 MeV) with a pole gap of 30 mm. During their design the magnetic flux inside the yoke as well as the particle tracking of all different beams have been simulated with CST [3]. Furthermore the multipole components along all beam orbits have been investigated. Having a very small width of the yoke at the exit area guaranteeing a good homogeneity of the magnetic field was a challenging task. To ensure the best magnetic field distribution additional shimming was placed in between the beams. A photograph of the installed separation dipole is shown in Fig. 2.

Table 1: Design Values of the Separation Dipole with Beam Energy E, Bending Radius ρ, Bending Angle α, Magnetic Entrance and Exit Wedge Angle $\psi_{1,2}$

E in MeV	ρ in mm	α in $^\circ$	ψ_1 in $^\circ$	ψ_2 in $^\circ$
38.25	189.7	60.000	14.82	-11.87
68.85	341.4	45.000	14.13	-21.40
99.45	493.2	35.035	13.88	-10.25
130.05	644.9	27.000	13.75	4.69

45° Dipole

The new recirculation beam line is placed in between the two existing ones. The bending angles were chosen to eight times 45°. Together with the separation and recombination dipole this leads to six 45° dipoles whose parameters are listed in Table 2. The nominal magnetic flux was set to 0.61 T (maximum magnetic flux of 0.7 T) with a pole gap of 30 mm. In comparison to the separation dipole the 45° dipole is a quite simple one. There are no hard conditions to the magnetic parameters and especially no constraints in space. Setting the bending angle to 45° was the best choice to optimize the usage of remaining space in both arc

THERMAL-MECHANICAL STUDY OF 3.9 GHz CW COUPLER AND CAVITY FOR LCLS-II PROJECT*

I. Gonin†, E.Harms, T. Khabiboulline, N. Solyak, V. Yakovlev, FNAL, Batavia, IL, USA

Abstract

Third harmonic system was originally developed by Fermilab for FLASH facility at DESY and then was adopted and modified by INFN for the XFEL project [1-3]. In contrast to XFEL project, all cryomodules in LCLS-II project will operate in CW regime with higher RF average power for 1.3 GHz and 3.9 GHz cavities and couplers. Design of the cavity and fundamental power coupler has been modified to satisfy LCLS-II requirements. In this paper we discuss the results of COMSOL thermal and mechanical analysis of the 3.9 GHz coupler and cavity to verify proposed modification of the design. For the dressed cavity we present simulations of Lorentz force detuning, helium pressure sensitivity df/dP and major mechanical resonances.

INTRODUCTION

The LCLS-II SCRF baseline linac consists of 35 1.3 GHz, 8-cavity Cryomodules (CM), and two 3.9 GHz, 8-cavity CMs. 3.9 GHz third harmonic superconducting cavities are used to increase the peak bunch current and to compensate nonlinear distortions in the beam longitudinal phase space due to sinusoidal 1.3 GHz accelerating cavity voltage [1]. The fundamental power coupler (FPC) is one of critical component of the third harmonic system developed for the LCLS-II project.

For a 300 uA beam current, a 15.5 MV/m nominal accelerating gradient and a 180 deg beam-to-rf phase, the RF power induced by a beam and radiated to the power coupler is about 1700 W per cavity. If the cavity is detuned by 30 Hz due to microphonics , the required input power from the rf source to maintain the operating gradient would be about 80 W. In whole range of beam parameters, the coupler needs to be rated for at least 1.9 kW of average RF power (in particular, it needs to operate below the peak surface temperature noted below). Therefore in simulations we apply 2 kW of the input RF power in the TW regime.

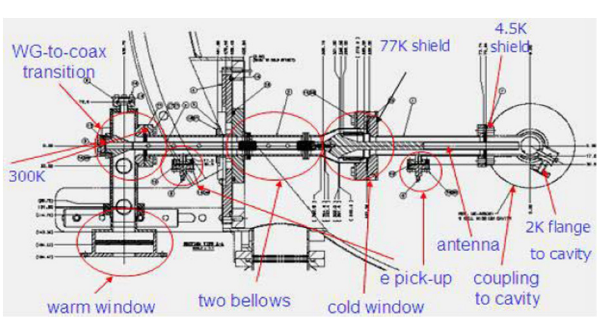

Figure 1: The 3.9 GHz power coupler developed at FNAL.

* Operated by Fermi Research Alliance, LLC under Contract No. DE-AC02-07CH11359 with the United States Department of Energy.

† gonin@fnal.gov

COUPLER THERMAL ANALYSIS

The final design of the 3.9 GHz power coupler is shown in Figure 1. It consists of a 50 Ohm coaxial line with a 30 mm diameter of the outer conductor. Two ceramic windows provide double protection of the cavity from potential damage of the ceramics. The design of the cold (50K) cylindrical window is almost identical to window used in 1.3 GHz XFEL coupler design. Warm pill-box window is installed in waveguide assembly.

Thermally, the power coupler represents a connector from the room temperature (300K) to the superconducting cryogenic environment (2K). Figure 2 shows the thermal model and boundary conditions used in COMSOL simulations [4]. Power dissipation and heat loads were calculated by using temperature dependences (electrical resistance and thermal conductivity) of materials used in coupler.

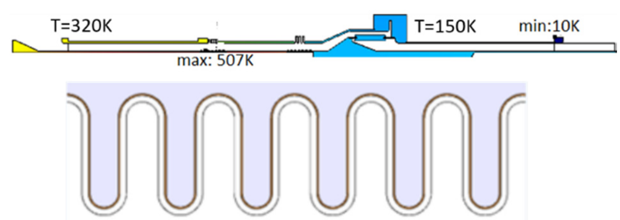

Figure 2: COMSOL thermal analysis model.

Originally, 3.9 GHz power coupler for the FLASH project was designed for pulsed operation (power 50 kW, duration is ~2ms, maximum repetition rate is 10 Hz; average power ~ 1kW). The LCLS-II requirements are CW operation at ~2 kW in quasi - traveling wave regime. At first, we performed COMSOL thermal simulations using LCLS-II parameters without any modifications of the 3.9 GHz coupler. It is resulted in an overheating of the inner conductor of the warm part of the coupler up to 670 K. Thus, we propose the following modifications of the current design:

- Reducing the length of two inner bellows from 20 convolutions to 15 convolutions.
- Increase the thickness of a copper plating in the inner conductor.
- Increase the thickness of ceramics in cold window to move parasitic mode away.

In original design our measurements show that one of the parasitic mode in cold ceramic is pretty close to fundamental mode, which can introduce extra heating of window in CW regime. Last modification is proposed to move nearest parasitic mode off working frequency 3.9GHz.

Figure 3 shows the results of COMSOL thermal simulations for 2kW traveling wave power in coupler and 20, 15 and 10 convolutions of inner bellow vs. copper plating

ISBN 978-3-95450-169-4

STATUS OF THE INJECTION SYSTEM FOR THE CLARA FEL TEST FACILITY

B.L. Militsyn†, D. Angal-Kalinin, R.K. Buckley, R.J. Cash, J.A. Clarke, L.S. Cowie[1], B.D. Fell, P.A. Goudket, T.J. Jones[1], K.B. Marinov, P.A. McIntosh, J.W. McKenzie, K.J. Middleman, T.C.Q. Noakes, B.J.A. Shepherd, R. Valizadeh, A.E. Wheelhouse,
STFC Daresbury Laboratory, Warrington, UK
V.V. Paramonov, Institute for Nuclear Research of RAS, Moscow, Russian Federation
G.C. Burt, Lancaster University and Cockcroft Institute, Lancaster, UK
[1]also at Lancaster University and Cockcroft Institute, Lancaster, UK

Abstract

A description is given of the high repetition rate injection system which is being developed for the proposed CLARA FEL test facility which is under construction at Daresbury Laboratory. The system comprises a 400 Hz High Repetition Rate photocathode Gun providing high brightness electron bunches with a charge of up to 250 pC and a linear accelerator section operating in either booster or bunching mode. The beam is delivered by an interchangeable metal photocathode illuminated with a UV laser.

INTRODUCTION

The Front End of 250 MeV CLARA FEL test facility [1,2] is now under construction at Daresbury Laboratory. The facility is a further development of the VELA electron accelerator which is now in operation [3]. Electron beam for this integrated facility will be provided by two normal conducting S-band photocathode guns: a 10 Hz 2.5 cell gun earlier used as the injector for the VELA machine, and a 400 Hz 1.5 cell High Repetition Rate Gun (HRRG) which has been recently successfully commissioned at Low Power RF.

The initial stage of CLARA will operate with the 10 Hz gun and the linear accelerator section. The beam will be deflected into the existing VELA beamline with an S-bend and directed to the spectrometer line for analysing beam properties or into one of the two VELA user areas. The HRRG will be installed on the VELA beamline for high power RF and beam commissioning with the VELA beam diagnostics suite. The HRRG is equipped with an interchangeable photocathode which allows for the investigation of different metals and to select the best at providing minimal beam emittance at highest quantum efficiency. After commissioning, the 400 Hz gun will be installed onto the CLARA beam line and the 10 Hz gun will be returned to the VELA beam line.

HIGH REPEPTITION RATE GUN

Photocathode Gun Cavity

The high repetition rate photoinjector for CLARA was developed to meet demanding requirements to the beam peak current and pulse duration at the CLARA FEL interaction area [4] and repetition rate required for VELA user experiments. The final design is based on a 1.5 cell normal conducting S-band RF cavity [5]. It has a dual feed RF input coupler with phase adjustment of each feed which has been shown in simulations to supress any dipole component in the coaxial coupler line.

For CLARA FEL experiments very high brightness beams are required. These can be delivered by a photocathode gun with as high value of the cathode surface field as possible. The practical limit in the described design has been set as 120 MV/m which is current state of the art for similar designs. For operation with the VELA beamline a repetition rate of 400 Hz is desired. As demands to the beam brightness are relaxed, a maximum surface field of 100 MV/m has been specified. These requirements imply power handling capabilities of 6.8 kW on the gun cavity. As operation at 400 Hz is not required for CLARA FEL experiments, the maximum cavity power is defined by operation in VELA mode.

Operation of the CLARA seeded FEL requires beam arrival time stability at the point of interaction between the seeding laser and electron beam of less than 64 fs rms [1]. Start to end simulation [1] has shown that to achieve this stability for the magnetic compression scheme the jitter of the beam launching phase in the gun should be better than 0.1° rms; that means that temperature of the cavity should be maintained with stability of better than 0.009° rms. RF amplitude stability must be better than 0.1 % rms [1,6]. To stabilise RF amplitude the gun cavity has a probe port in the second cell for feed-forward amplitude correction.

Cavity Cooling and Temperature Stabilisation

The thermal stabilisation of the gun cavity is achieved via 9 individual cooling channels as shown in Fig. 1, the flow through which can be controlled remotely and used to optimise frequency and field flatness under various operating conditions [5,7].

The cooling of the injector was investigated using advanced computational fluid dynamics techniques in ANSYS CFX. The cell radii are expected to increase by 5.6 μm due to the average steady state RF load of 6.8 kW at 400 Hz and 100 MV/m. This gives a detuning of the resonance frequency of -0.427 MHz which will be compensated for in the water temperature stabilisation system. High resolution thermo-stabilisation for the CLARA HRRG has been designed at Daresbury Laboratory, with

† boris.militsyn@stfc.ac.uk

UPGRADE OF THE KLYSTRON MODULATOR OF THE L-BAND ELECTRON LINAC AT OSAKA UNIVERSITY FOR HIGHER STABILITY

K. Furukawa, G. Isoyama, Osaka University, Janpan
A. Tokuchi, Pulsed Power Japan Laboratory Ltd.,Janpan
R. Kato, KEK, Janpan
K. Kawase, Hiroshima University, Janpan

Abstract

The klystron modulator for the L-band linac is upgraded for higher stability. The two-step charging system for the pulse forming network (PFN) is upgraded by adding a high impedance resonant charging line in parallel with the main line. The charging step of the PFN voltage is reduced considerably near the setting value by switching the main resonance line off so that the charging current flows only through the high impedance line. The second model of the solid-state switch is developed using 60 static-induction thyristors, ten of which are connected in series with six such series connected in parallel to meet maximum specifications of 25 kV and 6 kA. The air-cooling capacity is reinforced so that repetition rate is increased from 10 pps for the first model to 60 pps. The fluctuation and accuracy of the klystron voltage are measured to be 7.8×10^{-6} or 7.8 ppm for the upgraded klystron modulator using a differential amplifier with much higher sensitivity than one used in the previous measurement.

INTRODUCTION

The 40 MeV L-band electron linac is one of the main facilities of the Research Laboratory for Quantum Beam Science, the Institute of Scientific and Industrial Research, Osaka University. It is used mainly for pulse radiolysis in the time range from nanoseconds down to sub-picoseconds and the development and applications of a terahertz (THz) free electron laser (FEL). To generate a highly intense and stable FEL beam, a highly stable electron beam in terms of energy is required. The energy stability of the electron beam accelerated with the linac is dependent on stability of high power RF pulses generated with a klystron. Both the amplitude and the phase of the RF power depend on the voltage applied to the klystron, which is generated using a klystron modulator, so that flatness of high-voltage pulses needs to be high and small fluctuations of the peak voltage are indispensable to generating a highly stable multi-bunch electron beam for FEL.

Figure 1 shows the circuit diagram of the klystron modulator. Electric charge accumulated in the pulse-forming-network (PFN) to a high voltage is discharged using a high-speed switch, and the generated pulse is supplied to the klystron via a step-up transformer, and then a high power RF pulse is generated for accelerating the electron beam in the linac. To obtain the highly stable RF power, the charging voltage of PFN must be accurate and precise, and stable operation of the switch are required.

The switching frequency of the inverter power supply shown in Fig. 1 is 21.75 kHz but the charging frequency is doubled due to the full-wave rectifier, 43.5 kHz. The accuracy of the charging voltage is inversely proportional to the number of pulses sent to PFN, provided that charge per pulse is constant, whereas the charging time is given by the number of pulses divided by the charging frequency, so that a longer time is required for attaining higher accuracy. However, the charging time restricts the maximum repetition frequency of output pulses. Because the repetition frequency of the klystron modulator is 60 pps, the number of charging pulses would be limited to 725 and accordingly the accuracy of the charging voltage would be 0.13 %. To improve the charging accuracy to the order of 10^{-4}, the pulse width was reduced when the charging voltage approached the target value, which solved the contradicting requirements. As for the switch, the thyratron was used for the klystron modulator, which is a discharge tube filled with hydrogen or deuterium and widely used as a high speed and high current switch.

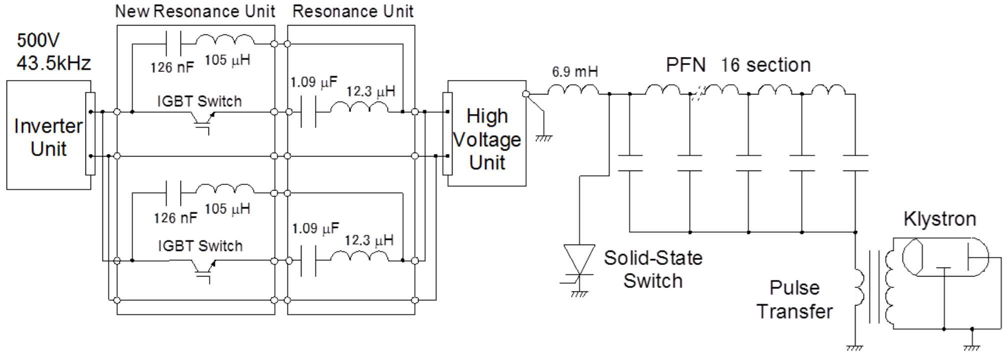

Figure 1: Circuit diagram of the klystron modulator.

CHALLENGES IN REALIZING THE LCLS-II CRYOMODULE PRODUCTION

A. Burrill† (on behalf of LCLS-II Collaboration), SLAC National Accelerator Laboratory, Menlo Park, CA, USA

Abstract

The LCLS-II project requires the assembly and installation of 37 cryomodules in order to deliver a 4 GeV electron beam to the undulators to produce both soft and hard x-ray pulses at a repetition rate up to 1 MHz. All of the cryomodules will operate in continuous wave mode, with 35 operating at 1.3 GHz for acceleration and 2 operating at 3.9 GHz to linearize the longitudinal beam profile. One of the challenges of this project, and the topic of this paper, is coordinating the effort of three DOE labs in order to realize this machine in just a few years time. This coordination is necessary due to the fact that the cryomodules will be assembled at both Jefferson Lab and Fermi Lab, tested, and then shipped to SLAC for installation, commissioning and operation. This paper will report on our experiences to date, issues that have been identified and planned mitigation going forward.

INTRODUCTION

The LCLS-II is a 4 GeV CW X-ray free electron laser (FEL) driven by a superconducting RF linac [1, 2]. It is being built to upgrade the capabilities of the current LCLS, a normal conducting FEL that has been operational at SLAC since 2009. Figure 1 shows the original LCLS layout in the tunnel along with the LCLS-II accelerator. The LCLS-II upgrade will be complementary to LCLS as both accelerators will continue to operate and provide x-rays to the existing user end-stations, albeit not at the same time (in the current operational plan). The upgrade to LCLS-II will expand the operational range of the FEL complex by providing X-ray pulses at up to 1 MHz repetition rate, an increase from the 120 Hz of LCLS, and covering the spectral range from 0.2-1.2 keV and 1-5 keV through two new undulator systems.

The LCLS-II project has a very tight schedule, only 6 years from design through delivery of first beam. In order to accomplish everything that is required to design, build, install and commission a new accelerator in such a short period of time a collaboration between 6 Institutions in the United States has been established. Five Department of Energy (DOE) Laboratories, SLAC, LBNL, Argonne, FNAL and JLab, are each lending their expertise in their respective fields along with Cornell University providing their knowledge of superconducting RF as well as development of an alternative injector for LCLS-II. In the context of this paper the primary contributors are JLab, FNAL and SLAC providing the superconducting RF accelerator components necessary to drive LCLS-II.

THE ACCELERATOR

The superconducting RF (SRF) linac that will drive LCLS-II is made up of 35 – 1.3 GHz cryomodules and 2 - 3.9 GHz cryomodules. Each cryomodule contains 8 superconducting RF cavities. The 1.3 GHZ cavities are based on the TESLA design, most recently used for XFEL, and have been modified for CW operation[3]. The preparation of the cavities has also been modified to incorporate the “High-Q_0 recipe” that utilizes nitrogen doping that can improve the Q_0 of the cavities by roughly a factor of 3 at the operating gradient of 16 MV/m[4].

The modification for CW operation have included modifying the XFEL/TTF-III input coupler, enlarging the exhaust chimney of the helium vessel to handle the larger dynamic heat load, installing 2 cryogenic fill lines to improve the cooldown process and installing 2 layers of magnetic shielding to better achieve the stringent magnetic hygiene requirements that result from using the high Q_0 recipe. The 3.9 GHz cavities, also adapted from XFEL, have also been modified for CW operation, but do not require the additional magnetic hygiene program of the 1.3 GHz cavities.

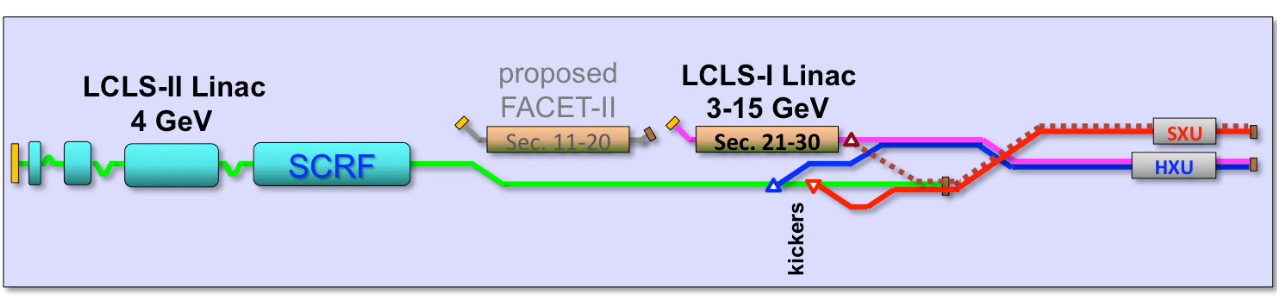

Figure 1: the LCLS-II Linac layout in the tunnel along with the existing LCLS accelerator.

† aburrill@slac.stanford.edu

ISBN 978-3-95450-169-4

COMMISSIONING AND FIRST RESULTS FROM THE FERMILAB CRYOMODULE TEST STAND*

E. R. Harms†, M. Awida, C. Baffes, K. Carlson, S. Chandrasekaran, B. Chase, E. Cullerton, J. Edelen, J. Einstein-Curtis, C. Ginsburg, A. Grassellino, B. Hansen, J. Holzbauer, S. Kazakov, T. Khabiboulline, M. Kucera, J. Leibfritz, A. Lunin, D. McDowell, M. McGee, D. Nicklaus, D. Orris, J. Ozelis, J. Patrick, T. Petersen, Y. Pischalnikov, P. Prieto, O. Prokofiev, J. Reid, W. Schappert, D. Sergatskov, N. Solyak, R. Stanek, D. Sun, M. White, C. Worel, G. Wu,
Fermilab, Batavia, Illinois, USA

Abstract

A new test stand dedicated to Superconducting Radiofrequency (SRF) cryomodule testing, CMTS1, has been commissioned and is now in operation at Fermilab. The first device to be cooled down and powered in this facility is the prototype 1.3 GHz cryomodule assembled at Fermilab for LCLS-II. We describe the demonstrated capabilities of CMTS1, report on steps taken during commissioning, provide an overview of first test results, and survey future plans.

INTRODUCTION

LCLS-II is a next generation hard x-ray light source based on a superconducting RF electron linac operating in continuous wave regime. It is described at this conference in an invited talk [1]. As one of the partner labs Fermilab is responsible for the design of the 1.3 GHz Cryomodules (CM's) as well as assembly and testing for seventeen of the necessary thirty-five CM's. Additionally Fermilab is designing and will assemble and cold test two 8-cavity 3.9 GHz (third harmonic). Both the Cryomodule Test Facility and specifically the CMTS1 test stand have been described previously [2, 3].

SUBSYSTEMS DESCRIPTION & STATUS

Guidance given by the LCLS-II project was to provide a test facility and carry out a testing program on a fast time scale. As such it was deemed best to design CMTS1 similarly to existing SRF test facilities at Fermilab such as the single cavity vertical test areas, HTS, and FAST where both single cavity and 8-cavity cryomodules have been tested and brought into routine operation. CMTS1 thus builds on evolving designs of the various subsystems and has features specifically to support continuous wave cryomodule operation.

Several of the necessary subsystems have been described previously including the cryogenics and distribution, interlocks, girders, and cave infrastructure and are not described further here.

* Operated by Fermi Research Alliance, LLC under Contract No. De-AC02-07CH11359 with the United States Department of Energy.
† harms@fnal.gov

Vacuum

CMTS1 accommodates three separate vacuum systems: beamline, (warm) coupler, and insulating vacuum. The beamline vacuum system is an Ultra High Vacuum (UHV), low-particulate system that achieves characteristic pressures < $1X10^{-8}$ Torr (warm) and < $1X10^{-9}$ Torr (cold) via vacuum stations located at each end of the test stand. Pumpdown/vent-up of the vacuum stations is accomplished with a mass flow control vacuum cart to minimize the possibility of particle transport, and also includes an in-vacuum Faraday cup.

The coupler vacuum system is a conventional unbaked UHV system that achieves characteristic pressures $<1X10^{-7}$ Torr (warm) and $\sim1X10^{-8}$ (cold, no RF), pumped by a single ion pump / titanium sublimation pump (TSP) unit.

The insulating vacuum system is characterized by large volume (~5000l) and high gas loads (up to $6X10^{-2}$ Torr-l/s). Target vacuum levels are $<1X10^{-4}$ Torr (warm) and < $1X10^{-6}$ Torr (cold). A capacitance manometer is available for gas-independent pressure measurement and an RGA is available to differentiate between helium and air leaks. A stand-alone dry roughing system is used to pump between atmospheric pressure and $1X10^{-2}$ Torr.

Magnetic Flux

The pCM is instrumented with 13 Bartington™ *Mag-F* fluxgates [4, 5, 6]. Low field magnetic fields during cooldown are critical to maintaining high Q0. After transportation to and installation at CMTS, the pCM magnetic fields were no higher than 3.5 milliGauss (mG) compared to the specification of < 5mG. Although a demagnetization was not necessary at CMTS1, one was performed at 35 A [6] to confirm the absence of adverse effects of demagnetization on other systems at CMTS. Following this demagnetization, the field readings were all below 1.5 mG and all systems at CMTS were unaffected.

Controls/Timing

General purpose controls for CMTS1 employs the Fermilab ACNET accelerator controls platform. The infrastructure for this system is mature, has a high level of support, and allows for relatively rapid deployment.

ISBN 978-3-95450-169-4

EXAMINATION OF CUTOUTS INNER SURFACES FROM Nb_3Sn COATED CAVITY*

Uttar Pudasaini[1], G. Eremeev[2], Charles E. Reece[2], J. Tuggle[3], M. J. Kelley[1,2,3]
[1]Applied Science Department, The College of William and Mary, Williamsburg, VA 23185, USA
[2]Thomas Jefferson National Accelerator Facility, Newport News, VA 23606, USA
[3]Virginia Polytechnic Institute and State University, Blacksburg, VA 24061, USA

Abstract

The potential for higher operating temperature and higher gradient has motivated SRF cavity researchers to pursue Nb_3Sn as an alternative to niobium for nearly fifty years. Far and away the most common embodiment has been a few micron thick Nb_3Sn layer on the cavity interior surface obtained by vapor diffusion coating, with one or another set of parameters. While many cavities have been made and RF tested, reports of dissecting a cavity in detail to examine the coating and relate it to RF measurements are rare. We coated a BCP-treated single cell cavity in a typical process of tin/tin chloride activation at 500 ºC followed by tin vapor deposition at 1200 ºC. After RF testing, we cut and examined sections from several locations to learn composition, thickness topography of the interior surface. The effect of process variables, such as surface preparation, process temperature and duration, and vapor chemistry needs to be explored.

INTRODUCTION

Nb_3Sn is an intermetallic alloy with superconducting properties to operate at higher temperature of about 4.2 K compared to standard niobium cavities which operate at 2 K. The estimated superheating field of Nb_3Sn also promises higher accelerating gradient than niobium [1]. Researchers had already realized the potential of Nb_3Sn more than 40 years ago, and attempted to fabricate Nb_3Sn coated cavities [2-4]. The vapor diffusion technique was readily successful to deposit a few micron thick Nb_3Sn coating on niobium cavity. These cavities were successful to attain quality factors $>10^{10}$ at few MeV/m gradients, but suffered with precipitous drop with increased gradient [5]. The reason for such degradation is not established so far. We encountered a sharp drop of quality factor in the cavity, C3C4, that was coated with Nb_3Sn during coating system commissioning at Jefferson Lab as shown in Fig. 1 [6]. C3C4 was a BCP treated 1.5 GHz single cell cavity, and coated in a typical process of tin/tin chloride activation at 500 ºC followed by tin vapour deposition at 1200 ºC. Detailed description of coating system and coating process is available in [7].

The cavity was dissected following RF test to pursue material studies of coated interior surface using the cavity cutouts. We aim to correlate the material studies results of cavity cutouts with their RF properties. First results from surface studies of cavity cutouts are presented in here.

* Partially authored by Jefferson Science Associates under contract no. DEAC0506OR23177. Work at College of William & Mary supported by Office of High Energy Physics under grant SC0014475.

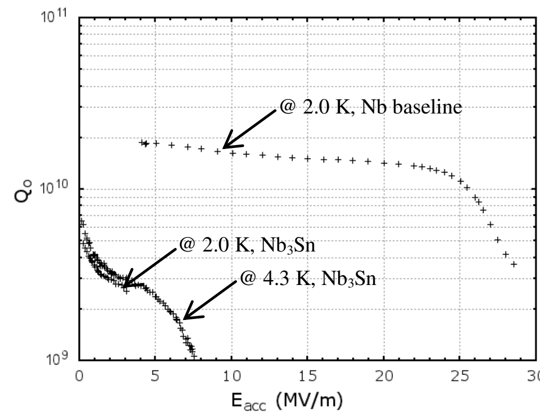

Figure 1: Q_o vs E_{acc} for C3C4 cavity before and after coating. Note the sharp drop of Q_o after coating.

CUTOUT PREPARATION

Temperature mapping of the cavity during RF test was used to choose areas from which to extract cutout samples. They were milled out at machine shop using 3/32 two flute OSG Exomini TiN coated end mill running at 3200 rpm. During the milling process, attempt was made to not cut through, but to leave a thin layer of material in order to reduce contamination and damage to the internal coating surface. This was not always possible due to cavity curvature, but some material was left when the milling was finished. The samples were then removed with pliers, and edges were de-burred with a scalpel or scissor before acetone rinse. The cutouts were again rinsed with methanol, and dried with ionized nitrogen. These cutouts further received ultrasonic cleaning with 2% detergent followed by low pressure ultra pure water rinsing. After drying with ionized nitrogen, these samples received second round of acetone rinse and methanol rinse subsequently. Finally, the cutouts were dried with ionized nitrogen. Several cutouts were prepared from cavity as well as beam pipes for analysis.

EXAMINATIONS AND RESULTS

Prepared cutout samples were examined with a field emission scanning electron microscope (FESEM) with energy dispersive X-ray spectroscopy (EDS) for microstructure and local composition. Atomic force microscope (AFM) was used to investigate surface topography. Electron backscattered diffraction (EBSD) was used to examine the cross-section of cutouts for crystallographic characterization.

ISBN 978-3-95450-169-4

PROGRESS TOWARDS Nb_3Sn CEBAF INJECTOR CRYOMODULE*

G. Eremeev, K. Macha, U. Pudasaini, C.E. Reece, A.-M. Valente-Feliciano
Thomas Jefferson National Accelerator Facility, Newport News, VA 23606, U.S.A.

Abstract

Operations at 4 K instead of 2 K have the potential to reduce the operational cost of an SRF linac by a factor of 3, if the cavity quality factor can be maintained. Cavities coated with Nb_3Sn have been shown to achieve the accelerating gradients above 10 MV/m with a quality factor around 10^{10} at 4 K. Because such performance is already pertinent to CEBAF injector cryomodule, we are working to extend these results to CEBAF accelerator cavities, envisioning coating of two CEBAF 5-cell cavities with Nb_3Sn. They will be installed in an injector cryomodule and tested with beam. The progress on this path is reported in this contribution.

INTRODUCTION

The cryogenic test facility (CTF) at Jefferson Lab provides sub-atmospheric liquid helium for testing purposes in the test lab. The vertical test facility (VTA) in the test lab hosts eight cryogenic dewars for SRF cavity testing with several dewars being often operated simultaneously. The test lab is also home for cryomodule test facility, where assembled cryomodules are RF tested at 2 K, before they are sent for integration into accelerators. The test lab will also soon feature an upgraded injector test facility (UITF), which will serve as a test bed for low energy beam tests in the test lab. All these facilities rely on 2 K helium delivered from CTF. With projected vertical test area and CMTF tests in support of CEBAF, LCLS upgrade work and R&D, as well as UITF beam tests, CTF is expected to be run at full capacity and testing times will be carefully coordinated to fulfill all commitments. Ability to run UITF, which hosts only one accelerating quarter-cryomodule, Fig. 1, at 4 K helium instead of 2 K may increase beam time available to users. Since Nb_3Sn cavities have recently been shown to achieve gradients suitable for this facility at 4 K [1, 2], we are working to demonstrate 4 K operation of a quarter-cryomodule with Nb_3Sn cavities. If cavity performance, demonstrated on single- and two-cell cavities, can be translated to the two CEBAF cavities in a quarter-cryomodule, the cryomodule can be efficiently run with 4 K helium. On the other hand, since long-term cryomodule operation with Nb_3Sn cavities has never been tested, such a run will provide valuable data towards operation of Nb_3Sn cavities in accelerators.

* Authored by Jefferson Science Associates, LLC under U.S. DOE Contract No. DE-AC05-06OR23177. The U.S. Government retains a non-exclusive, paid-up, irrevocable, world-wide license to publish or reproduce this manuscript for U.S. Government purposes.

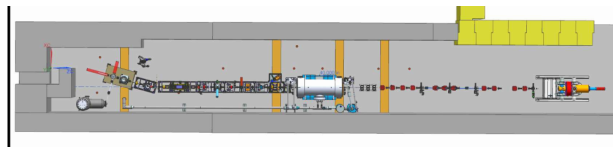

Figure 1: A draft layout of the upgraded injector test facility. The quarter-cryomodule is seen in the center of the picture and will be used to accelerate electron beams up to 10 MeV.

With these goals in mind we are working to upgrade our existing Nb_3Sn coating system to be able to coat CEBAF cavities from the spare CEBAF quarter-cryomodule. In parallel with the system upgrade, we conducted first coating tests of a CEBAF 5-cell cavity, which was modified to fit in our existing coating system. Test results and the progress in the coating system upgrade are reported here.

CAVITY DEPOSITION SYSTEM UPGRADE

The JLab Nb_3Sn coating system needs to be upgraded in order to fit a CEBAF cavity. Our present insert for Nb_3Sn coating, which was designed to coat single-cell R&D cavities, is about 11” ID and has a hot zone, which is about 22” long, [3], while a CEBAF 5-cell cavity is 28 1/4” long and can fit inside a 15” ID cylinder. Hence a new insert was design to allow for a 17” ID and 40” long coating space. The insert is being made out of 4 mm reactor grade niobium sheets. The sheets were cut and rolled to form half cylinders, which were then electron beam welded together. The cylinder is covered by a deep-drawn 4 mm niobium cover on one end, which will also be electron beam welded, and a double O-ring brazed SS flange on the other. In order to extend the hot zone, the furnace is modified to extend the heat shields up. The new heat shields are made out of 0.015” thick molybdenum and are similar in design to the existing ones. The heat shields are supported by a 0.125” SS can on the outside. In order to fit the heat shield extensions, a new door, which sits on the top of the furnace, must be made. The custom door was specified at JLab and is being purchased from Lesker. The door will interface with the existing furnace body on the bottom and will have a O-ring seal on the top, which will mate to a water-cooled zero-length reducer, also purchased from Lesker. The rest of the coating system will re-used. In Fig. 2, the sketch of the upgraded system is shown, where colored components

ISBN 978-3-95450-169-4

INVESTIGATION OF LOW-LEVEL NITROGEN IN NIOBIUM BY SECONDARY ION MASS SPECTROMETRY

J. Tuggle[1], A.D. Palczewski[2], C.E. Reece[2], F.A. Stevie[3], M.J. Kelley[2,4†].
[1]Virginia Polytechnic Institute and State University, Blacksburg, VA, USA
[2]Thomas Jefferson National Accelerator Facility, Newport News, VA, USA
[3]Analytical Instrumentation Facility, North Carolina State University, Raleigh, NC, USA
[4]The College of William and Mary, Willamsburg, VA, USA

Abstract

Understanding the improvement of the SRF cavity quality factor (Q) by low-level nitrogen addition ("N-doping) is attracting much attention from researchers. Precise, repeatable measurement of the nitrogen profile in the parts-per-thousand to parts-per-million range is vital. Secondary Ion Mass Spectrometry (SIMS) is the method of choice because of excellent sensitivity and depth resolution. Accurate quantification must consider sample properties, such as surface topography and crystal structure, as well as calibration of the instrument and data analysis. We report a SIMS study in which, SRF-grade niobium sheet equivalent, polycrystal and single crystal coupons were N-doped.

INTRODUCTION

New and robust characterization programs are needed in order to elucidate N-doping and any thorough investigation of N-doping must include SIMS. It is the only available technique to combine acceptably low detection limits with depth information, giving concentration as a function of depth. However, accurate quantification with SIMS is non-trivial, requiring standards and SIMS experiments as opposed to straight forward analysis common to other analytical techniques. This is due to matrix effects, differential sputtering, surface topography, achieving acceptable backgrounds and other complications.

Matrix Effects

SIMS obtains information by directing a beam of primary ions onto the surface of interest and measuring the mass distribution and intensity of the ejected (secondary) ions. [1] Secondary ion yields can vary five or six orders of magnitude across the periodic table and also several orders of magnitude depending on the bulk material (matrix). Because of this, quantification cannot be based on relative signal intensities only. An implant standard must be created for each species of interest by implanting it into the matrix of interest. Its depth profile can be acquired and dose information can be used to calculate a relative sensitivity factor (RSF) for that species in that matrix. A reference signal from the matrix (here, Nb) is used to adjust for instrumental factors. Example analyses of nitrogen implants in both poly and single crystalline material appear in Fig. 1.

Depth Resolution

Depth resolution is the ability to distinguish between atoms from one depth over atoms from a different depth. Good depth resolution makes SIMS a must-use technique for N-doping. However, many factors may affect depth resolution. Penetration depth of primary beam, raster and gate size, knock-on, crater shape are instrument controlled and require meticulous forethought in choice of analysis conditions.

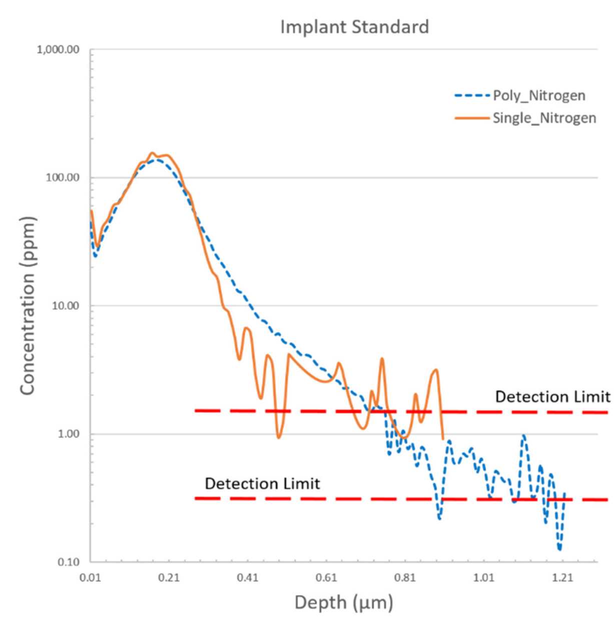

Figure 1: Depth profile of implants used to calibrate N for both polycrystalline and single crystal material.

There are also multiple factors affecting depth resolution which are sample dependent [1]. For example, differing sputter rates between grains of different crystal orientation directly affect the depth resolution achievable in a SIMS analysis. The problem can be reduced by using large grain Nb relative to SIMS crater size. Crater size and grain size must both be taken into consideration. Smaller crater sizes may be used to provide faster analysis when doing relatively deep measurements, but have a negative effect on depth resolution and detection limits due to contributions of the crater edge to the signal. A balance must be found for relative crater, analysis area and grain size. While both implants in Fig. 1 were created and analyzed under the same conditions, the single crystal depth profile shows a sharper implant peak and quicker drop to detection limit, indicative of better depth resolution. Depth resolution was estimated using roughness measurements and TRIM calculations and found to improve from ~109 nm for the polycrystalline implant to ~12 nm for the single crystal implant.

ISBN 978-3-95450-169-4

MATERIAL QUALIFICATION OF LCLS-II PRODUCTION NIOBIUM MATERIAL INCLUDING RF AND FLUX EXPULSION MEASUREMENTS ON SINGLE CELL CAVITIES*

A. D. Palczewski#, F. Marhauser,
Thomas Jefferson National Accelerator Facility, Newport News, VA, USA
A. Grassellino, S. Posen, Fermi National Accelerator Laboratory, Batavia, IL, USA

Abstract

It has been shown that cooldown details through transition temperature can significantly affect the amount of trapped magnetic flux in SRF cavities, which can lead to performance degradation proportional to the magnitude of the ambient magnetic field [1]. It has also more recently been shown that depending on the exact material properties - even when the material used originated from the same batch from the same vendor - and subsequent heat treatment, the percent of flux trapped during a cool-down could vary widely for identical cool-down parameters [2]. For LCLS-II, two material vendors have produced half of the niobium used for the cavity cells (Tokyo Denkai Co., Ltd. (TD) and Ningxia Orient Tantalum Industry Co., Ltd. (NX)). Both vendors delivered material well within specifications set out by the project (according to ASTM B 393-05), which allows yet some variation of material characteristics such as grain size and defect density. In this contribution, we present RF and magnetic flux expulsion measurements of four single cell cavities made out of two different niobium batches from each of the two LCLS-II material suppliers and draw conclusions on potential correlations of flux expulsion capability with material parameters. We present observations of limited flux expulsion in cavities made from the production material and treated with the baseline LCLS-II recipe.

INTRODUCTION

The LCLS-II prototype cavities currently being assembled into the first cryomodules were manufactured by Advanced Energy Systems, Inc. during the ILC R&D activity in the later 2000's out of material from ATI Wah Chang niobium. These cavities had little processing history and have eventually been treated with the now baseline LCLS-II recipe including bulk surface removal by Electropolishing (EP), heat treatment at 800°C for 3 hours and doping with nitrogen for 2 minutes, and finally a light 5-7 micron EP [3,4]. They all passed the current quality factor (Q_0) specification of $2.7\text{x}10^{10}$ at 16 MV/m with multiple cavities reaching $4.0\text{x}10^{10}$ through the use of superconducting flanges, careful environmental magnetic fields, and controlled cooldowns [5-8]. After welding the prototype cavities into the helium vessel, which has been carried out at FNAL, a small drop in the average Q_0 has been experienced, but the average value was still above 3e10 [8].

During the R&D phase, which aimed to develop a robust nitrogen-doping baseline recipe for LCLS-II to be applied by industrial cavity vendors, there were multiple advances in cavity treatment developed simultaneously, apart from the actual recipe development. First, it was shown that when residual magnetic fields are present, quickly cooling a cavity could significantly reduce the residual resistance; depend on the temperature gradient rather than the speed of cooling [1]. Soon after, the sensitivity of the surface resistance due to trapped flux was determined for nitrogen-doped cavities, which revealed a higher value (nΩ/mG) compared to other treatments such as applying EP with 120°C bake as a result of the dependence on the surface mean free path [9-11]. Finally, it was shown that there is a very strong material dependence of the flux expulsion efficiency independent of surface preparation, RRR or material hardness, however a correlation was observed with annealing time and temperature, which also deviated among material from different suppliers. The combination of the above effects was most likely the cause of the wide performance variations in single-cell nitrogen-doping results carried out at JLab in 2014 during the initial LCLS-II R&D [5,6].

Because the treatment history and/or material of the cavities utilized for LCLS-II prototype cryomodules is different compared to production cavities, a clear understanding of the flux expulsion efficiency using the actual recipe with actual production material is needed. In this study, we present the RF and flux expulsion results from four single-cell cavities made from LCLS-II production material (TD, NX) applying the baseline recipe. We show that the LCLS-II material exhibits a wide range of flux expulsion efficiencies depending on the material origin/supplier and batches, but all material trap flux at levels, which would not allow to meet a specification of $Q_0 = 2.7\text{x}10^{10}$ at 16 MV/m in a 5 mG field needed for the project, when applying the original baseline recipe.

LCLS-II MATERIAL

Niobium material being used for LCLS-II production cavities has been thoroughly inspected including Eddy-current scans at DESY (100% of half-cell sheets) resulting in a rejection rate of less than 2% and thus overall with a higher acceptance rate than for the XFEL high-end production for the same vendors (TD, NX). The

* Funding Agency: Authored by Jefferson Science Associates, LLC under U.S. DOE Contract No. DE-AC05-06OR23177.
# ari@jlab.org

ELECTROMAGNETIC DESIGN OF A SUPERCONDUCTING TWIN AXIS CAVITY*

S. U. De Silva[1,2#], H. Park[2,1], J. R. Delayen[1,2], F. Marhauser[2], A. Hutton[2]
[1]Center for Accelerator Science, Old Dominion University, Norfolk, VA, USA
[2]Thomas Jefferson National Accelerator Facility, Newport News, VA, USA

Abstract

The twin-axis cavity is a new kind of rf superconducting cavity that consists of two parallel beam pipes, which can accelerate or decelerate two spatially separated beams in the same cavity. This configuration is particularly effective for high-current beams with low-energy electrons that will be used for bunched beam cooling of high-energy protons or ions. The new cavity geometry was designed to create a uniform accelerating or decelerating fields for both beams by utilizing a TM_{110} dipole mode. This paper presents the design rf optimization of a 1497 MHz twin-axis single-cell cavity, which is currently under fabrication.

INTRODUCTION

The idea of utilizing elliptical shaped rf superconducting accelerating structures with two beam pipes intended for Energy Recovery Linacs (ERLs) applications was first proposed by Noguchi and Kako in 2003 [1]. A similar concept was revisited by Wang, Noonan, and Lewellen in 2007 [2, 3] and recently [4] for based ERL applications. The new proposed superconducting twin-axis cavity allows energy recovery by accelerating and decelerating beams within the same cavity in two beam pipes. The accelerated beam is physically separated from the parallel accelerated/decelerated beam, but interacts with the same rf dipole mode. In an ERL for instance, the low energy beam delivered from the source can be injected into the cavity without requiring a complicated merger structure and thus additional beam line space to bend the beam, while maintaining a small beam emittance.

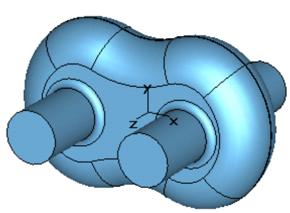

Figure 1: Twin axis cavity.

The new twin-axis cavity geometry, shown in Fig. 1, is designed to create a uniform field for both beams by operating in the TM_{110} rf dipole mode. The electromagnetic fields in the two beam pipes are axially symmetric with a 180 degree phase offset. The on-axis electric field and magnetic field at the cross sectional planes are shown in Fig 2.

*Work supported by DOE Office of Science via Accelerator Stewardship Test Facility Pilot Program (Proposal No. 0000219731). This work used resources of the NERSC center, which is supported by DOE Office of Science Contract No. DE-AC02-05CH11231.
#sdesilva@jlab.org

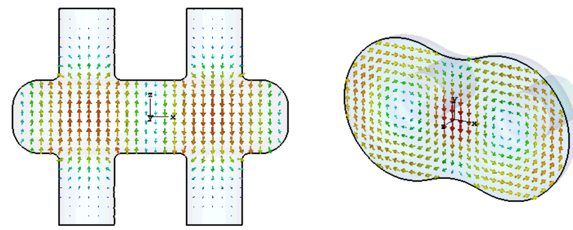

Figure 2: Electric (left) on-axis and magnetic (right) field profile at the cross section of the twin axis cavity.

The beam pipe axis position has been optimized to maximize the on-axis longitudinal electric field component ($E_z(z)$) trying to symmetrize the field across the beam aperture as best as possible, while minimizing the transverse fields ($E_x(z)$ and $H_y(z)$). The optimization of the cavity shape focused on minimizing the transverse component without degrading the accelerating component. Note that the magnetic field is strong at the center of the cavity unlike in conventional accelerating cavities using a TM monopole mode, where the peak surface magnetic field is at the equator.

DESIGN OPTIMIZATION

The initial design of the twin axis cavity was a cylindrical shaped geometry as shown in Fig. 3(a), which then evolved into a racetrack-shaped design with a compressed mid-section. The design has been modified to improve the rf properties, primarily to reduce the peak surface magnetic field.

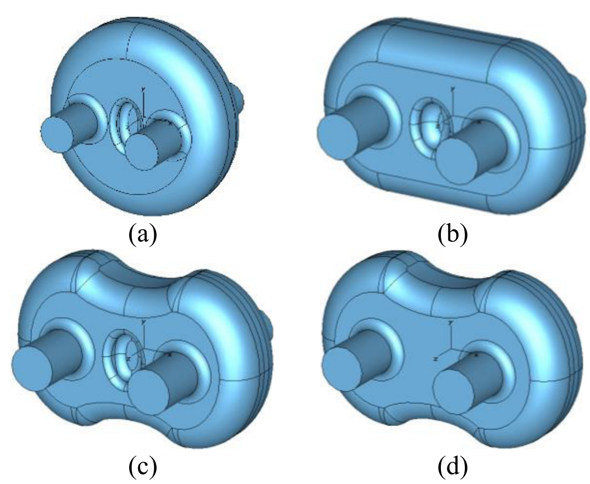

Figure 3: Design evolution of twin axis cavity geometry.

The initial designs (Fig.3(a)–(c)) includes an inward bump to enforce uniformity of the longitudinal fields in each of the two beam pipe. This resulted in an increase in the peak magnetic field. The racetrack-shaped designs

ISBN 978-3-95450-169-4

WAKEFIELD ANALYSIS OF SUPERCONDUCTING RF-DIPOLE CAVITIES*

S. U. De Silva[1,2#], J. R. Delayen[1,2],
[1]Center for Accelerator Science, Old Dominion University, Norfolk, VA 23529, USA.
[2]Thomas Jefferson National Accelerator Facility, Newport News, VA 23606, USA

Abstract

RF-dipole crabbing cavities are being considered for a variety of crabbing applications. Some of the applications are the crabbing cavity systems for LHC High Luminosity Upgrade and the proposed Electron-Ion Collider for Jefferson Lab. The design requirements in the current applications require the cavities to incorporate complex damping schemes to suppress the higher order modes that may be excited by the high intensity proton or electron beams traversing through the cavities. The number of cavities required to achieve the desired high transverse voltage, and the complexity in the cavity geometries also contributes to the wakefields generated by beams. This paper characterizes the wakefield analysis for single cell and multi-cell rf-dipole cavities.

INTRODUCTION

In rf cavities electromagnetic fields are excited by the charged particle beam traversing through the cavity, which then may affect the dynamics of the beam itself. A bunch on-axis can generate longitudinal wakes and a bunch at an offset may generate transverse wakefields [1]. Longitudinal wakefields can cause power losses in the cavity and increase in energy spread in the beam. Similarly transverse effects can amplify the effects leading to beam instabilities.

The wakefield effects can be characterised into wake potentials and wake impedances. These excited wakefields then can be related to the higher order modes (HOMs) present in the cavity.

Wake potential is defined as the change of momentum in a charge particle following a bunch with charge Q_b at a distance s. The longitudinal wake potential is calculated by integrating the longitudinal electric fields as

$$\overrightarrow{W_z}(x,y,s) = \frac{1}{Q_b}\int_{-\infty}^{\infty} \overrightarrow{E_z}\left(x,y,z,t=\frac{s+z}{v}\right)\mathrm{d}z, \tag{1}$$

and the transverse wake potential is given by

$$\overrightarrow{W_t}(x,y,s) = \frac{1}{Q_b}\int_{-\infty}^{\infty}\left[\begin{array}{l}\vec{E}\left(x,y,z,t=\dfrac{s+z}{v}\right)\\ \quad +\vec{v}\times\vec{B}\left(x,y,z,t=\dfrac{s+z}{v}\right)\end{array}\right]\mathrm{d}z. \tag{2}$$

The transverse wakefield is calculated with the integrated the wake potential at an offset from the beam axis and using the Panofsky-Wenzel theorem [2] as shown in Eq. (3).

$$\overrightarrow{W_t}(x,y,s) = -\nabla_t \int_{-\infty}^{s} W_z(x,y,s')\,\mathrm{d}s' \tag{3}$$

Wakefield impedance in frequency domain is derived by applying the Fourier transformation on wake potentials.

$$Z(\omega) = \int_{-\infty}^{\infty} W(t)\exp(-i\omega t)\,\mathrm{d}t \tag{4}$$

The wake potentials are generated for a Gaussian form of bunch charge distribution ($Q(s)$) given in Eq. (5) with bunch length (σ_z) and charge per bunch (Q_b).

$$Q(s) = Q_b\lambda(s) = \frac{Q_b}{\sqrt{2\pi}\sigma_z}\exp\left(-\frac{s^2}{2\sigma_z^2}\right) \tag{5}$$

The frequency spectrum of the Gaussian charge distribution is specified as

$$F(\omega) \sim \exp\left(-\frac{\omega^2\sigma^2}{2c^2}\right) \tag{6}$$

gives the frequency range of which wake potentials are evaluated. The loss factor for the longitudinal wakes are determined by

$$k_z = -\int_{-\infty}^{\infty} W_z(s)\lambda(s)\,\mathrm{d}s\,. \tag{7}$$

Similarly the kick factor for transverse wakefields are defined as

$$k_t = \frac{1}{r_0}\int_{-\infty}^{\infty} W_t(s)\lambda(s)\,\mathrm{d}s \tag{8}$$

where r_0 is the offset from beam axis at which wake potentials are evaluated.

This paper presents the wakefields analysis for the two rf-dipole crabbing cavities of 400 MHz for LHC High Luminosity Upgrade and 952.6 MHz cavity for Jefferson Lab Electron-Ion Collider.

400 MHz CRABBING CAVITY

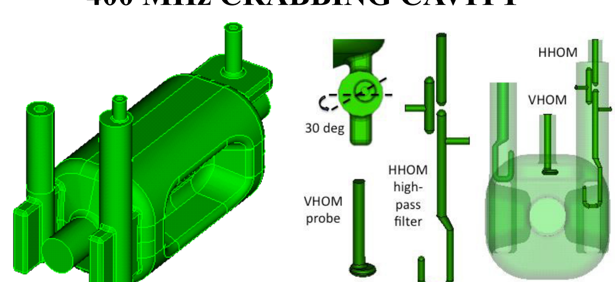

Figure 1: 400 MHz rf-dipole crabbing cavity.

The 400 MHz rf-dipole crabbing cavity shown in Fig. 1 is one of the two crabbing cavities designed for LHC High Luminosity Upgrade [3]. The crabbing cavity is expected

*Work supported by DOE via US LARP Program and by the High Luminosity LHC Project. Work was also supported by DOE Contract No. DE-AC02-76SF00515.
#sdesilva@jlab.org

PREPARATION FOR CAVITY MATERIAL STUDIES AT THE VERTICAL HIGH-TEMPERATURE UHV-FURNACE OF THE S-DALINAC*

R. Grewe†, L. Alff, J. Conrad, T. Kürzeder, M. Major, N. Pietralla,
Technische Universität Darmstadt, Darmstadt, Germany
F. Hug, Johannes Gutenberg-Universität Mainz, Mainz Germany

Abstract

Since 2005 the Institute for Nuclear Physics at the Technische Universität Darmstadt operates a high temperature vacuum furnace. It is designed to reach temperatures of up to 1800°C. It has been used for baking out several niobium superconducting rf cavities at 850°C with proven success. Current research for improving the performance of superconducting rf cavities is focused on nitrogen treatment of such cavities. Nitrogen doping of srf cavtities results in an up to four times higher quality-factor as compared to untreated cavities. At higher temperatures between 1300°C and 1700°C the δ-phase of NbN forms, which is highly interesting for applications to superconducting accelerator technology. The UHV-furnace at the S-DALINAC offers the possibility to treat niobium samples at considerably higher temperatures than what has been done up to now in order to study the effect of delta-phase NbN and N-doping on superconducting properties. The furnace has been refurbished and recommissioned to realize research on nitrogen treatment of niobium samples.

INTRODUCTION

The UHV-Furnace at the S-DALINAC [1] was built at the University of Wuppertal in 1983 [2] and moved to Technische Universität Darmstadt in the year 2002. It was designed for temperatures of up to 1800°C with vacuum pressures lower then 10^{-6} mbar. Since 2005 it has been used for hydrogen bakeout of several superconducting niobium cavities at 850°C with proven success [3]. Due to technical constraints the temperature was limited to 850°C. Beginning in 2015 the furnace has been upgraded and recommissioned to operate at temperatures of up to 1800°C again [4].

Research on doping of niobium cavities with nitrogen at temperatures of 850°C results in a up to 4 times higher quality factor compared to untreated cavities [5]. At even higher temperatures in the range between 1300°C and 1700°C the δ-phase of NbN forms [6]. The δ-phase is highly interesting for superconducting accelerator technology applications.

In 2016 the furnace was further upgraded to allow nitrogen treatments of niobium samples and cavities at temperatures of up to 1800°C. The following sections introduce the furnace and the upgrades made.

* Work supported by the Federal Ministry of Education and Research through grant No. 05H15RDRBA.

† rgrewe@ikp.tu-darmstadt.de

UHV-FURNACE

The cross-section in Fig. 1 illustrates the main parts of the furnace [7]. The inner part of the uhv-furnace is a hot-pot made of niobium. The niobium samples or srf cavities are held by a niobium support system, which is mounted at the top of the furnace. Heat-shields made from ten layers of niobium sheets around the hot-pot minimize the radiation heat flow from inside the furnace to the outer water cooled casing.

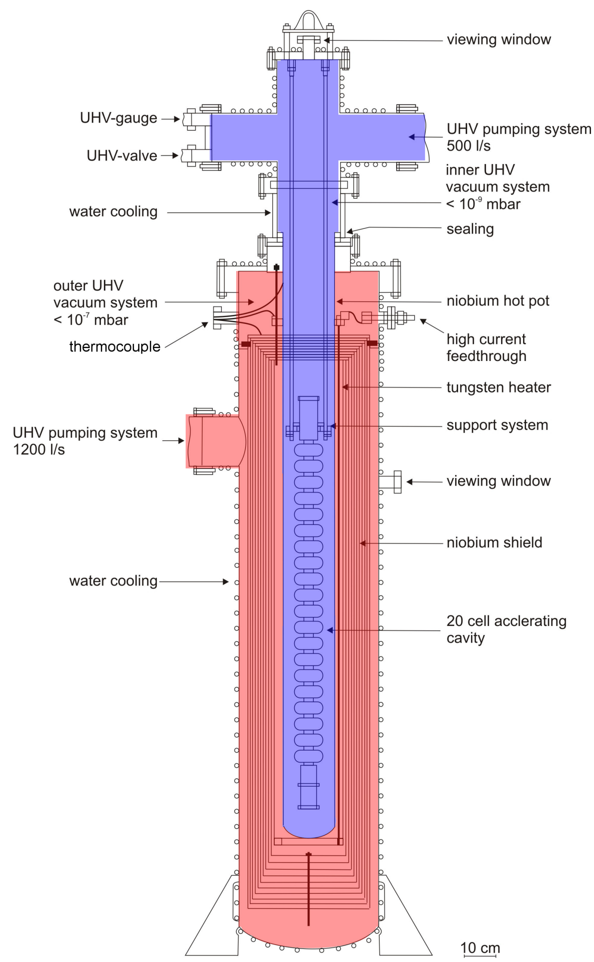

Figure 1: Schematic drawing of the UHV-Furnace. The inner hot-pot vacuum vessel is shown in blue, the insulating vacuum in red.

The furnace has two vacuum systems, an outer insulating vacuum and a separate hot-pot vacuum to reduce contamination of niobium samples or cavities, as indicated in Fig. 1 with pressures below 10^{-6} mbar. A turbomolecular pump

ISBN 978-3-95450-169-4

FABRICATION OF SUPERCONDUCTING SPOKE CAVITY FOR COMPACT PHOTON SOURCE

M. Sawamura#, R. Hajima, QST, National Institutes for Quantum and Radiological Science and Technology, Tokai, Ibaraki, Japan
T. Kubo, T. Saeki, KEK, High Energy Accelerator Research Organization, Tsukuba, Ibaraki, Japan, SOKENDAI (The Graduate University for Advanced Studies), Hayama, Kanagawa, Japan,
H. Hokonohara, Y. Iwashita, H. Tongu, Kyoto University, Uji, Kyoto, Japan

Abstract

We are developing electron beam drivers used for laser Compton scattered (LCS) photon sources. For realizing a wide use of LCS X-ray and γ-ray sources in academic and industrial applications, we adopt the superconducting spoke cavity to electron beam drivers. The spoke cavity has advantages such as relative compactness in comparison with an elliptical cavity of the same frequency, robustness with respect to manufacturing inaccuracy due to its strong cell-to-cell coupling, the better packing in a linac to install couplers on outer conductor. On the other hand the spoke cavity has disadvantage of more complicated structure than an elliptical cavity. Though our proposal design for the photon source consists of the 325 MHz spoke cavities in 4K operation, we have begun to fabricate the half scale model of 650 MHz spoke cavity in order to accumulate our cavity production experience by effective utilization of our limited resources. We fabricated the die set, performed press forming test and measured the formed shape. In this paper, we present our fabrication status.

INTRODUCTION

We are developing laser Compton scattering (LCS) X-ray and gamma-ray sources combined with an energy-recovery linac (ERL) and a laser. The LCS X/γ-ray source is expected for application of non-destructive assay system of nuclear materials with nuclear resonance fluorescence [1], analysis of nano-structure, drug development, medical diagnostics, and so on. We are developing the superconducting spoke cavity for LCS photon sources [2]. Spoke cavities have many advantages such as shortening the distance between cavities, small frequency detune due to micro-phonics and easy adjustment of field distribution for strong cell coupling. We have optimized the cavity shape with genetic algorithm [3], fabricated the die set for the half-spoke on the basis of die design simulation and started press forming test.

The spoke cavity for the compact X-ray source was originally designed at 325 MHz, which can be operated at 4 K. We have, however, recently changed our R&D plan to fabricate a 650 MHz cavity prior to 325 MHz one. This is because a 650 MHz cavity can be fabricated almost "in-house" at the KEK machine shop and suitable for accumulating our cavity production experience within limited resources. Once we learn the design and production process of spoke cavities at 650 MHz, we can easily apply our expertise to production of spoke cavities with difference frequencies.

FABRICATION OF DIE SET

Press forming process consists of three steps such as moving the inner punch, moving the center die and the inner punch together, and moving the outer punch. To realize these steps in a sequence of one slide action the press machine requires a die cushion to control the die center motion and the die set requires a spring functioning component such as a gas spring to control the inner punch motion by the load.

We planned at the beginning to use the press machine of AMADA SDE1522 in KEK, which specifications are shown in Table 1. The die height of the press machine was not enough to mount the die set of half size of original 325MHz-design die set, we have redesigned the die set by changing the type and number of the gas springs and reducing the thickness of the die set as thin as possible. Though the press machine changed to AIDA NC1-15 due to operator's schedule, this machine has similar specifications to AMADA SDE1522.

The components of the die set which contact with the sheet metals are made of extra super duralumin of A7075 or ANP79. The other components of the die set which support the whole structure are made of SS400. The assembled die set mounted to the press machine is shown in Figure 1.

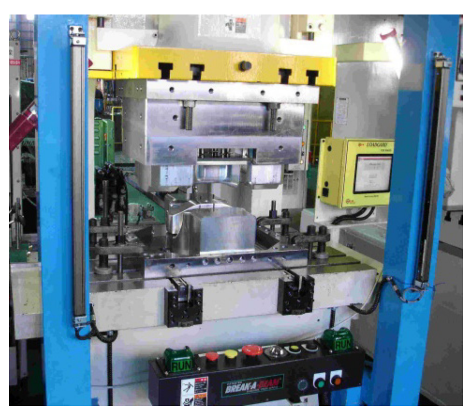

Figure 1: Assembled die set was mounted to press machine.

#sawamura.masaru@qst.go.jp

STUDY ON MULTILAYER THIN FILM COATING ON SUPERCONDUCTING CAVITY

Y. Iwashita, Y. Fuwa, H. Tongu, Kyoto ICR, Uji, Kyoto),
H. Hayano, T. Kubo, T. Saeki (KEK/SOKENDAI, Ibaraki),
M. Hino (Kyoto KURRI, Osaka),
H. Oikawa (Utsunomiya University, Utsunomiya)

Abstract

Multilayer thin film coating to enhance performance of superconducting cavities is under investigation. We proposed a method to deduce a set of the parameters to exhibit good performances. In order to verify the scheme, characteristic measurement setup using the third order harmonic detection method for superconducting thin foil is under preparation.

INTRODUCTION

Multilayer thin film coating is a promising technology to enhance performance of superconducting cavities (see Fig.1). Figure 1 shows the simplest case of two layers of an insulator and a superconductor. The magnetic field B_0 applied from the left vacuum space is partially shielded by the first superconducting thin layer denoted by SC1, where SC1 would have higher $Bc1$ than SC2 (assumed as Nb in the paper) such as NbN or Nb3Sn. Then the magnetic field level felt by the bulk part can be less than B_0, hence the B_0 can be higher than $Bc1$ of SC2. Until recently, principal parameters to achieve the sufficient performance had not been known, such as the thickness of each layer [1]. Reference. 1, however, derived the enhancement factor of the amplitude of the applicable magnetic field as a function of the thicknesses of the insulator and the superconductor layers assuming the characteristics of the superconductor layers. Using the theory, the optimum thickness set of the layers can be found.

In order to verify the scheme, we are trying to make $Bc1$ measurements of thin film coatings at Kyoto University. The third order harmonic detection seems a first choice for that purpose [2,3].

EXPERIMENTAL SETUP

A coil located on a superconducting sample generates magnetic field (see Fig.2). The magnetic field more than the critical field $Bc1$ causes penetration of flux into the superconducting material. By detecting a third order harmonic voltage component in the electromotive force of the coil that is driven by AC current source, the $Bc1$ will be evaluated. While an external DC field could optionally be applied, it also was not adopted in our case as the same as Ref. 3. At the temperature just below the critical temperature, the flux penetration starts at the less magnetic field (see Fig.3)

A rough sketch of the cryogenic stage is shown in Fig. 4. A sample plate is put between the two Cu plates, where the top plate has an exciting coil at the center. The two plates clamp the sample with three coil springs to

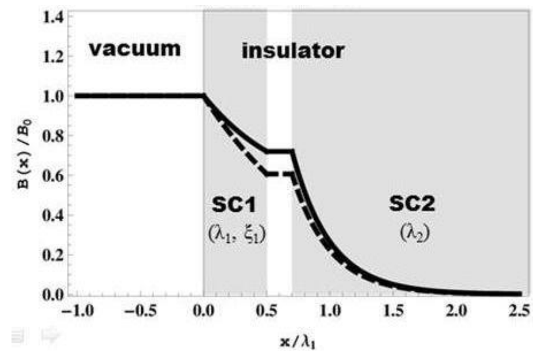

Figure 1: The multilayer thin film coating on superconducting bulk surface. The simplest case of two layers of an insulator and a superconductor is shown. The solid line shows the RF magnetic field amplitude as a function of the coordinate along the axis normal to the surface (see Ref. 1).

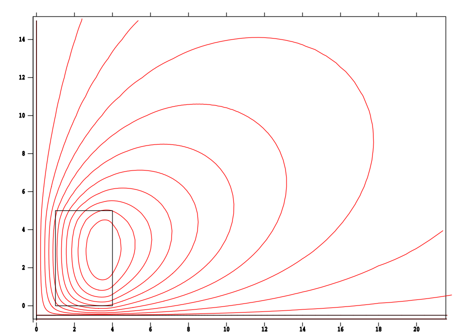

Figure 2: Superconducting material does not allow for a magnetic flux to penetrate when the magnetic field B is less than the critical field Bc1.

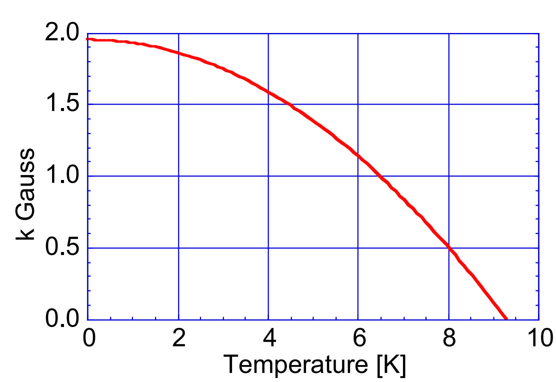

Figure 3: Temperature dependence of a critical field.

ISBN 978-3-95450-169-4

STUDY OF THE SURFACE AND PERFORMANCE OF SINGLE-CELL Nb CAVITIES AFTER VERTICAL EP USING NINJA CATHODES

V. Chouhan†, Y. Ida, K. Ishimi, K. Nii, T. Yamaguchi, Marui Galvanizing Co. Ltd, Himeji, Japan
H. Hayano, S. Kato, H. Monjushiro, T. Saeki, M. Sawabe, KEK, Tsukuba, Japan
F. Furuta, M. Ge, T. Gruber, J. Kaufman, J. Sears, CLASSE, Cornell University, Ithaca, USA
P. Carbonnier, F. Eozenou, Y. Gasser, L. Maurice, C. Servouin, CEA-Saclay, Gif-Sur-Yvette, France

Abstract

A 1.3 GHz single-cell niobium (Nb) coupon cavity was vertically electropolished (VEPed) with three different Ninja cathodes which were specially designed for VEP of 1.3 GHz superconducting RF elliptical (ILC/Tesla type) cavities. The cathodes were fabricated to have different surface areas and different distances between cathode surface and the equator. The Ninja cathode prepared with an enhanced cathode surface area was covered with a meshed shield to avoid bubble attack on the surface of the cavity cell. It has been turned out that the anode-cathode distance and the cathode area affect surface morphology of the equator. A smooth equator surface was obtained in the cases in which the cathode surface was geometrically close to the equator or instead the cathode surface area was sufficiently larger. Two 1.3 GHz ILC/Tesla type single-cell cavities VEPed with the Ninja cathodes and using optimized conditions showed good performance in vertical tests.

INTRODUCTION

Electropolishing (EP) is a promising technique for final surface treatment of niobium (Nb) accelerating cavities. In order to prepare 17,000 cavities for the proposed ILC project a simple and inexpensive EP system is required. EP of a cavity with vertical EP (VEP) technique can be carried out with a simple and less expensive setup as well as at a higher EP rate in comparison to horizontal EP technique. However non-uniform removal of Nb, bubble traces and non-uniform surface roughness are the serious issues in VEP. We are making our effort for the last few years to solve these issues. In our study accumulation of H_2 bubbles on Nb surface was found the main cause of asymmetric removal [1]. We could successfully minimized asymmetric removal in 1-cell cavity and obtain smooth surface of a cavity with our unique i-Ninja cathode [2,3]. Here we report VEP of 1.3 GHz ILC/Tesla type Nb single-cell coupon cavity with three different types of Ninja cathodes which maintain different distances from Nb surface in a cavity cell and contain different surface areas. Vertical test (VT) results are shown for two vertically elecropolished (VEPed) 1.3 GHz ILC/Tesla type single-cell cavities.

NINJA CATHODES AND CAVITIES

Three types of Ninja cathodes, namely Ninja cathode 1, 2 and 3, were prepared. The Ninja cathode-1 consisted of 4 insulating wings while the Ninja cathode-2 was designed with 4 partial metallic wings acted as a cathode and remain near equator surface. The Ninja cathode-3 developed recently contained insulating wings like Ninja cathode-1 whereas a surface area of the cathode was intentionally kept larger compared to the Ninja cathode-1 and 2 both. Moreover the cathode-3 was covered with a meshed shield so as to guide the H_2 gas bubbles along the cathode in upward direction. Schematics of the Ninja cathodes are shown in Fig. 1.

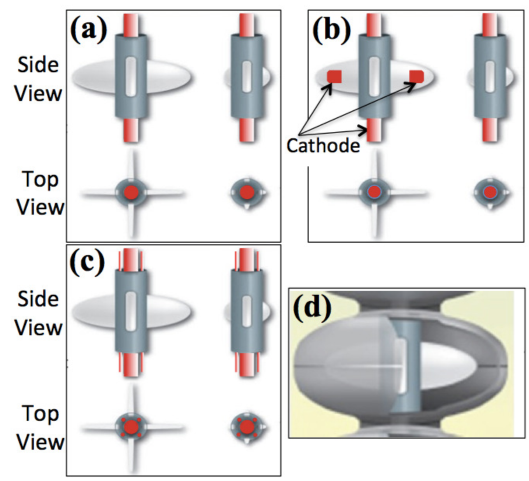

Figure 1: (a) Ninja cathode-1, (b) Ninja Cathode-2 (c) Ninja Cathode-3 and (d) A Ninja cathode in a cavity cell.

A coupon cavity having 6 coupons at its different positions [1,3] was used for VEP experiments to obtain adequate VEP parameters. Other two 1-cell cavities NR1-2 and C1-19, which belong to Cornell University and CEA-Saclay, respectively, were also VEPed using the Ninja cathodes and our adequate VEP parameters. A VEP system used for VEP of the coupon cavity and the C1-19 cavity was detailed elsewhere [3]. The NR1-2 cavity was VEPed with a VEP setup at Cornell University.

RESULTS AND DISCUSSION

Polarization Curves

In order to compare effect of the Ninja cathodes polarization curves were obtained for the coupons and cavity while the cathodes were rotated at a speed of 50 rpm. The speed was chosen based on the previous VEP experiments as found effective to reduce asymmetric removal of Nb along the cavity length [2,3].

† vchouhan@e-marui.jp

ISBN 978-3-95450-169-4

FABRICATION OF 9 CELL COUPON CAVITY FOR VERTICAL ELECTROPOLISHING TEST

S. Kato†, H. Hayano, H. Inoue, H. Monjushiro, T. Saeki, M. Sawabe, KEK, Ibaraki, Japan
V. Chouhan, Y. Ida, K. Nii, T. Yamaguchi, Marui Galvanizing Co. Ltd, Himeji, Japan

Abstract

We have been using single cell coupon cavities to establish vertical electropolishing (VEP) process for a couple of years. A series of in-situ measurements of an EP current at an individual coupon in a coupon cavity can help determination of appropriate EP conditions. VEPed coupons which are surface analysed with XPS, SEM and the other tools can also bring lot information and expertise to development of VEP cathode and optimization of VEP conditions. This time we fabricated the world's first 9-cell coupon cavity where 3 sample coupons at the equators and 6 sample coupons at positions close to the irises can be installed. VEP of this coupon cavity with a newly developed Ninja cathode brought useful information for improvement of the VEP facility and optimization of the VEP conditions.

INTRODUCTION

Needless to describe, it is quite obvious that inner surface quality of a SRF cavity fatefully decides the cavity performance. Therefore deep investigation of the hidden inner surface using surface analytical tools is mandatory to develop good cavities or good surface treatment. For this purpose, so called a coupon cavity is a very strong tool. Surface analysis of coupons brings us reduction of research and development cost and time because the surface analysis helps failure cause investigation very well. In case of electropolishing (EP), in-situ measurements of EP current at each coupon can be carried out and help determination of appropriate EP conditions. We fabricated 4 single cell coupon cavities up to now and proved these ideas for different projects [1-5] while one is being used in DESY for centrifugal barrel polishing [6]. In this report, fabrication of the world's first 9-cell coupon cavity for improvement of VEP will be mainly described.

DISMANTLING OF 9-CELL CAVITY

A 9-cell coupon cavity was designed in order that each set of three sample coupons is installed to the 1st, 5th and 9th cell as shown in Fig.1. In a VEP process, these three cells correspond to the top, centre and bottom cells, respectively. For the 9-cell coupon cavity, a vertical tested 1.3 GHz Nb 9-cell SRF cavity was reused. First, the end plates and the magnetic shields were removed with both a turning machine and an electrical discharge machine (EDM) (Fig. 2). Then using the EDM, the cavity was precisely dismantled into five components, that is, a) the 1st cell including the end group with the short beam pipe, b) the 2nd, 3rd, 4th cells, c) the centre cell, d) the 6th, 7th, 8th cells and e) the 9th cell including the end group with the long beam pipe as shown in Fig.1. The stiffener rings at the cut positions were removed in advance. The dismantlement was needed otherwise it was impossible to make holes for coupons and to weld support legs on the cavity with electron beam welding (EBW).

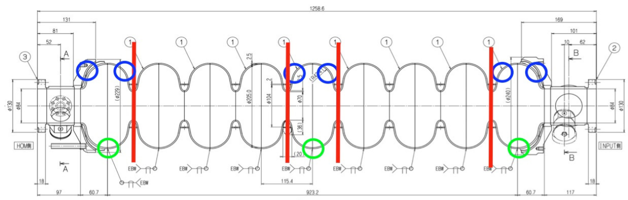

Figure 1: Schematic of the 9-cell coupon cavity. Red lines, blue circles and green circles show the cut positions and the coupon positions at the 1st, 5th and 9th cells, respectively.

Figure 2: Removal of the end plate with an EDM.

SAMPLE COUPON HOLES

For the 9-cell coupon cavity, the same size of coupons that have an analysis diameter of 8 mm and have been being used for 1-cell coupon cavities in KEK for a couple of years was adopted, considering its compatibility.

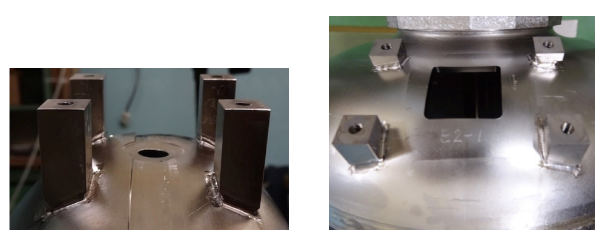

Figure 3: Coupon holes and the support legs for the equator position (left) and the position close to the iris (right).

Totally 9 holes for sample coupons were prepared at three positions of the equators and at the two symmetrical positions close to the irises (Fig.3 and 4). The equator holes to which the coupons with Viton O-rings fit in order to electrically insulate the coupons and to seal EP solution

† shigeki.kato@kek.jp

DEVELOPMENT OF NEW TYPE "NINJA" CATHODE FOR Nb 9-CELL CAVITY AND EXPERIMENT OF VERTICAL ELECTRO-POLISHING

K. Nii#, V. Chouhan, Y. Ida, T. Yamaguchi, Marui Galvanizing Co., Ltd., Himeji, Japan
K. Ishimi, Marui Galvanizing Co., Ltd., Kashiwa, Japan
H. Hayano, S. Kato, H. Monjushiro, T. Saeki, M. Sawabe, KEK, Tsukuba, Japan

Abstract

Marui Galvanizing Co., Ltd. has been improving Vertical Electro-Polishing (VEP) technologies and facilities for Nb 9-cell superconducting accelerator cavities for International Linear Collider (ILC) in collaboration with KEK. This time, we developed new type Ninja cathode in order to improve VEP uniformity of Nb 9-cell cavity inner surface based on the results of 1-cell cavity VEP experiments. In this article, we will report construction of new type "Ninja" cathode for a Nb 9-cell cavity and the experiment of VEP using this.

INTRODUCTION

Marui Galvanizing Co., Ltd. has been improving Vertical Electro-Polishing (VEP) technologies and facilities for Nb SRF cavities in collaboration with KEK. So far, we developed our original cathode "i-cathode Ninja" (Ninja), low cost and high durability VEP facilities made by PVC and performed VEP experiments for parameter optimization [1] - [6].

Regarding 9-cell cavity VEP, we had a problem that the cavity surface temperature during VEP became over 30 degrees C (it is said that the optimized temperature for Nb electro-polishing (EP) is around 20 – 25 °C). To solve this problem, we developed an EP solution cooling system and a cavity water cooling system and added them to our VEP facility. Then the cavity surface temperature during VEP was able to be kept around 20 – 25 °C successfully [6]. The polished surface looked like improved, however the removal thickness distribution was not improved.

This time, in order to improve removal thickness distribution and polished surface state, we developed new type Ninja cathode and performed a VEP experiment using this Ninja and a 9-cell coupon cavity.

IMPROVEMENT OF NINJA CATHODE

To improve uniformity of cavity removal thickness distribution and polished surface state, Ninja cathode was improved in several points. First, wings were made with insulating material and the Ninja cathode was covered with mesh sheet to prevent babble diffusion. Second, cathode surface area inside the mesh sheets was enhanced to perform good, uniform EP of whole cavity inner surface. And additional point, the wing number per cell was decreased from 4 to 3 for the purpose of easy fabrication and use in VEP.

Regarding first and second points, we performed 1-cell cavity VEP experiments using the same concept Ninja cathode. Then good, uniform inner surface state and uniform removal thickness distribution were achieved [7]. This time, preparing the same concept Ninja cathode for a 9-cell cavity, we performed a VEP experiment. Figure 1 shows the schematic view of Ninja cathode.

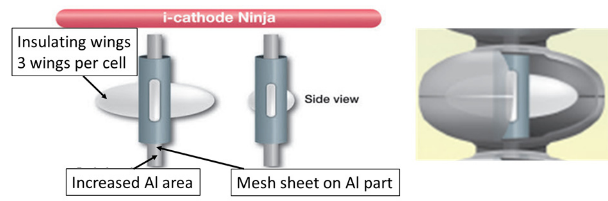

Figure 1: Schematic view of Ninja cathode.

9-CELL COUPON CAVITY

In order to optimize VEP parameters, a 9-cell coupon cavity was fabricated newly [8]. In this cavity, Nb coupons are set on equator positions of 1st, 5th and 9th cell. View ports with Nb coupon are set near iris of 1st, 5th and 9th cell. Figure 2 shows the photo of a 9-cell coupon cavity. These Nb coupons are separated electrically from cavity, so EP current can be measured for individual coupon. And after VEP, coupons can be removed for surface analysis.

Figure 2: Photos of a 9-cell coupon cavity (upper), coupon holders and view ports near iris (lower left), a coupon holder near equator (lower right).

VEP EXPERIMENT

We performed a VEP experiment using new type Ninja cathode and a 9-cell coupon cavity. Table 1 shows the conditions of this VEP experiment. This condition follows the best condition of 1-cell cavity VEP. And Figure 3 shows the VEP setup of this experiment. Top PVC part was put into negative pressure for bubble removal.

#keisuke_nii@e-maui.jp

ISBN 978-3-95450-169-4

DESIGN AND FABRICATION OF BETA=0.3 SSR1 FOR RISP*

Z. Yao†, R. E. Laxdal, B. Waraich, V. Zvyagintsev, TRIUMF, Vancouver, Canada
R. Edinger, PAVAC, Richmond, Canada

Abstract

A 325MHz β=0.30 balloon variant of single spoke resonator, which was proposed to suppress multipacting around operational gradient, was chosen as the prototype cavity of SSR1 for Rare Isotope Science Project (RISP). It was also demonstrated to achieve good RF and mechanical properties by geometry optimization for both cavity and helium jacket. The details of RISP SSR1 design will be reported in this paper, accompanying with some particular considerations of fabrication for this new member to the spoke family.

INTRODUCTION

RISP has been proposed as a multi-purpose accelerator facility at the Institute for Basic Science (IBS), Korea, for research in atomic and nuclear physics, material science, bio and medical science, etc. It can provide various energy beams of exotic rare isotopes up to uranium. [1] The facility consists of three independently phased superconducting linacs. The high energy section SCL2 of the driver linac uses two types of 325MHz single spoke resonators with geometry β at 0.30 and 0.51. It accepts beam at an injection energy of 18.5MeV/u and accelerates to 200MeV/u for uranium.

A prototype cavity of the lower β single spoke resonator SSR1 has been designed at TRIUMF under collaboration with IBS, and is being fabricated at PAVAC. The cavity, shown in Figure 1, is termed the balloon variant due to the conformal shape of the outer conductor that obviates the need for a central spool. The balloon variant is proposed to suppress multipacting in the accelerating gradient range of several MV/m by pushing the secondary electron trajectories to the unstable resonance regime. [2] It also provides a more inherently robust mechanical structure.

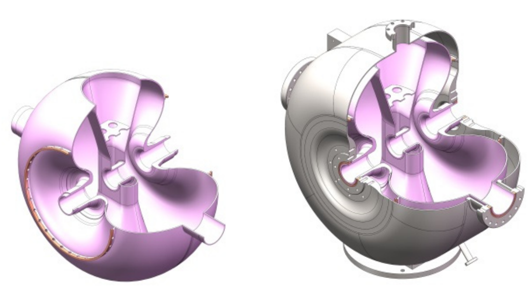

Figure 1: Cross sections of bare cavity (left) and jacketed cavity (right) of RISP SSR1.

SSR1 is designed to operate in continuous wave (CW) mode at 2K with thepeak electric field limited by specification to ≤35MV/m to reduce the likelihood of field emission. The design specifications are listed in Table 1.

* Work supported by RISP-TRIUMF Collaboration
† zyyao@triumf.ca

Table 1: Design Specifications of RISP SSR1.

Parameters	Value
Operating frequency	325 MHz
Geometry β	0.30
Operating temperature	2K
Q_0	$>5\times10^9$
E_{peak}	35 MV/m
V_{acc}	>2.5 MV
df/dp	<10 Hz/mbar
Frequency tuning range	±100 Hz
Q_{ext}	8×10^6
RF bandwidth	40 Hz
Beam aperture	50 mm
Pressure envelop at 300K	2 bar
Pressure envelop at 2K	5bar

RF DESIGN

The operational E_{peak} is limited at 35MV/m as per specification, to avoid field emission and provide stable operation. Minimizing E_{peak}/E_{acc} is a main goal of the RF design to achieve higher cavity gradient and energy gain for the beam.

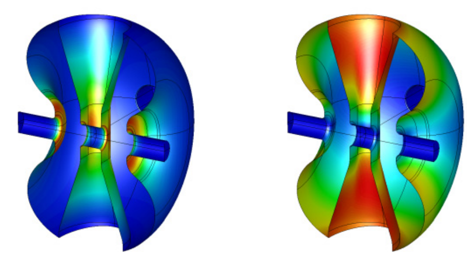

Figure 2: Electric (left) and magnetic (right) field distribution of SSR1.

Geometry Optimization

The major difference of the balloon SSR1 to the conventional spoke resonators is the shape of outer conductor. It is proposed for multipacting suppression, which is mostly effective on the minimum electric field regions. On the other hand, these areas do not affect cavity RF parameters so much as that of the spoke bar. The geometry optimization is similar to conventional spoke designs. The optimization around the beam aperture region is to minimize E_{peak}, while that around the spoke base is to minimize B_{peak}. Geometry factor and R/Q are dependent on the ratio of the inner and outer conductor's dimensions. An elliptical spoke base is chosen to make uniform the magnetic field distribution around the perimeter, which narrows the width of the lowest order multipacting barrier. [2] It decreases the peak magnetic field as well.

CAVITY PROCESSING AND PREPARATION OF 650 MHz ELLIPTICAL CELL CAVITIES FOR PIP-II*

A. M. Rowe†, S. Chandrasekaran, A. Grassellino, O. Melnychuk, M. Merio, D. Sergatskov
Fermi National Accelerator Laboratory, Batavia, IL, USA
T. Reid, Argonne National Laboratory, Lemont, IL, USA

Abstract

The PIP-II project at Fermilab requires fifteen 650 MHz SRF cryomodules as part of the 800 MeV LINAC that will provide a high intensity proton beam to the Fermilab neutrino program. A total of fifty-seven high-performance SRF cavities will populate the cryomodules and will operate in both pulsed and continuous wave modes. These cavities will be processed and prepared for performance testing utilizing adapted cavity processing infrastructure already in place at Fermilab and Argonne. The processing recipes implemented for these structures will incorporate state-of-the art processing and cleaning techniques developed for 1.3 GHz SRF cavities for the ILC, XFEL, and LCLS-II projects. This paper describes the details of the processing recipes and associated chemistry, heat treatment, and cleanroom processes at the Fermilab and Argonne cavity processing facilities. This paper also presents single and multi-cell cavity test results with quality factors above 5E10 and accelerating gradients above 30 MV/m.

INTRODUCTION

The Fermilab and Argonne SRF cavity processing and testing infrastructure is well-suited to provide superior RF performance for PIP-II R&D and production cavities of all types from the 62.5 MHz half-wave and 325 MHz single spoke to 650 MHz multi-cell elliptical cavities. In particular, the elliptical cavity processing infrastructure originally developed for 1.3 GHz cavities was easily adapted to 650 MHz elliptical cavities. Combining the flexible infrastructure with the experience gained processing and testing 1.3 GHz elliptical cavities for the various R&D programs and LCLS-II, resulted in cavity performance results in single and multi-cell 650 MHz elliptical cavities comparable to typical high Q0 and high gradient 1.3 GHz cavities but without the long R&D path.

This paper describes the major processing details developed for PIP-II 650 MHz elliptical cell cavities at the Fermilab and Argonne facilities. Electropolishing, heat treatment, cleanroom processing, and vertical test data are presented that demonstrate performance well above the required operating gradient E_{acc} = 17.7 MV/m and quality factor > 2.0 E10 at 2 °K for 650 MHz cavities.

ELECTROPOLISHING

Low-Beta EP Tool Adaptation

A second electropolishing (EP) system was commissioned at Argonne in 2011 for the processing of low frequency (72.75 MHz) quarter wave resonators (QWRs) for the ATLAS Intensity Upgrade (AIU) project [1]. Initially built for co-axial low-beta cavities, the tool was based on previous experience with the horizontal processing of 1.3 GHz elliptical cavities for the ILC R&D program which made for a natural transition to larger elliptical cavities, specifically 650 MHz single and five-cell cavities as seen in Figure 1 [2]. Due to the large radius of the 650 MHz cell, consideration was given to the cathode design. A fluted 1100 series aluminum cathode donut was implemented to increase the overall cathode surface area for better electropolishing in the equator region of the cavity. These cathode donuts are clam-shelled to the 1100 series aluminum cathode at the center of each cell.

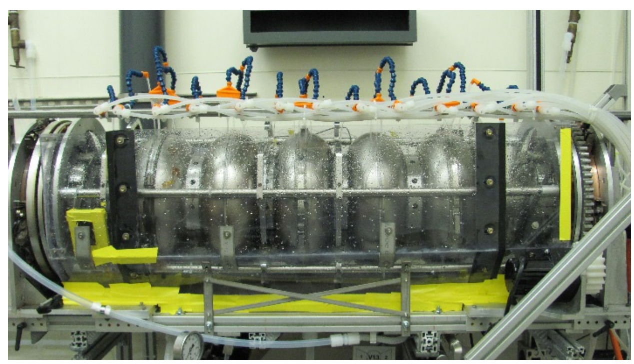

Figure 1: 650 MHz five-cell cavity EP with water cooling.

External Water Cooling

The addition of external water cooling improves process control and stability and minimizes temperature gradients across the cavity that result in non-uniform material removal. A 10 kW chiller is used to spray water through up to thirteen independently controlled spray heads made from standard machine coolant hoses. The total flow rate is up to 40 l/min for five-cell cavities. Each cooling line has its own throttle valve that allows for in-situ changes to the amount of cooling water flow needed at individual beam tubes, irises, and equators. Shields made of polycarbonate minimize splashing and protect the rotary bearings. A stainless steel drip tray underneath the cavity directs the water where it is pumped back to the chiller.

* Work supported by United States Department of Energy under contract DE-AC02-07CH11359
† arowe@fnal.gov

ISBN 978-3-95450-169-4

ADVANCED VERTICAL ELECTRO-POLISHING STUDIES AT CORNELL WITH FARADAY*

F. Furuta, M. Ge, T. Gruber, J. Kaufman, M. Liepe J. Sears, ,
CLASSE, Cornell University, Ithaca, New York, USA
T. Hall, M. Inman, S. Snyder, E. J. Taylor, Faraday Technology, Inc., Clayton, Ohio, USA

Abstract

Cornell's SRF group and Faraday Technology, Inc. have started collaborations on two phase-II SBIR projects. Both projects are aiming for the development of advanced Vertical Electro-Polishing (VEP) for Nb SRF cavities, such as HF free or acid free VEP protocols. These could be eco-friendlier alternatives for the standard, HF-based EP electrolyte used, and could bring new breakthrough performance for Nb SRF cavities. Here we give a status update and report first results from these two projects.

INTRODUCTION

Electro-Polishing (EP), especially Horizontal EP, is applied on niobium SRF cavities in many projects as a high-performance surface treatment procedure. As an alternative, Cornell's SRF group has led the development of Vertical Electro-Polishing (VEP) which requires a much simpler setup and is less expensive compared with the conventional Horizontal EP [1]. Both, Horizontal and Vertical EP are currently done with hydrofluoric (HF) acid based electrolyte, which is the mixed acid of sulphuric acid and hydrofluoric acid in 9~10:1 ratio in weight. As the SRF projects become bigger, the impact of large usage of hazardous HF based acid on niobium cavities for the environment becomes not negligible. Therefore, R&Ds on a less hazardous or more eco-friendly niobium surface process has been performed and has made good progress [2, 3]. As part of recent progress on this eco-friendlier advanced EP work, Faraday Technology, Inc. and Fermi National Laboratory (FNAL) demonstrated a high gradient of 44MV/m with 1.3GHz TESLA single cell cavity, which was processed by Pulse forward/pulse reverse EP (Bipolar-EP) with HF free electrolyte at Faraday Technology, Inc. [4]. RF test was performed by FNAL [5]. The collaboration of Faraday Technology, Inc. and FNAL was supported by funds from the American Recovery and Reinvestment Act (ARRA). For further R&D on advanced EP, now Cornell's SRF group and Faraday Technology, Inc. have started collaborations on Bipolar-EP with HF free/acid free electrolyte. Thise collaboration is supported by the Department of Energy's (DOE) phase-II Small Business Innovation Research (SBIR) program. In this paper, we report an status update and present the plans for these projects in details.

* Work is supported by DOE awards DE-SC0011235 (1002) and DE-SC001342 (1023).
†ff97@cornell.edu

VEP SYSTEM AT CORNELL

Overview

Figure 1 shows a 1.3GHz TESLA shape single cell cavity (left) and a 9-cell cavity (right) installed in Cornell VEP system. The Cornell VEP system can process 1.3GHz single-/multi-cell cavities with up to 9-cells. During the VEP process, the cavity has temperature controlled water cooling on the cavity outside wall and EP acid agitation (0~1Hz) by a paddle on a stirring tube, which is shown in the middle of Fig. 1. A HF based EP electrolyte is used, but no circulation is applied on the electrolyte during the process. Figure 2 shows a typical EP current profile during a single cell cavity VEP at Cornell. EP voltage is fixed at 12V. The temperature of the cavity outside wall is kept below 20degC.

Figure 1: Cornell's VEP system.

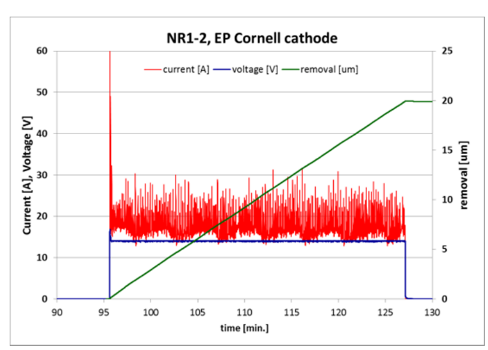

Figure 2: Typical EP current profile for a single cell VEP.

ISBN 978-3-95450-169-4

FABRICATION AND TESTING OF A NOVEL S-BAND BACKWARD TRAVELLING WAVE ACCELERATING STRUCTURE FOR PROTON THERAPY LINACS

S. Benedetti[#], T. Argyropoulos, C. Blanc Gutierrez, N. Catalan Lasheras, A. Degiovanni, D. Esperante Pereira, M. Garlasche', J. Giner Navarro, A. Grudiev, G. Mcmonagle, A. Solodko, M. Timmins, R. Wegner, B. Woolley, W. Wuensch, CERN, Geneva, Switzerland

Abstract

Compact and more affordable, facilities for proton therapy are now entering the market of commercial medical accelerators. At CERN, a joint collaboration between CLIC and TERA Foundation led to the design, fabrication and testing of a high gradient accelerating structure prototype, capable of halving the length of state-of-art light ion therapy linacs. This paper focuses on the mechanical design, fabrication and testing of a first prototype. CLIC standardized bead-pull measurement setup was used, leading to a quick and successful tuning of the prototype. The high power tests will soon start in order to prove that the structure can withstand a very high accelerating gradient while suffering no more than 10^{-6} breakdown per pulse per meter (bpp/m), resulting in less than one breakdown per treatment session.

INTRODUCTION

High gradient structures are limited mostly by breakdown (BD) phenomena. CLIC proposed [1] a new method to asses this limit, considering a Modified Poynting Vector (S_c) instead of the maximum Surface Electric Field. This theory was fully verified at high frequency (12 and 30 GHz) by CLIC with many experiments of structures designed for electron linacs. In this structure, the theory is applied to structures designed for particle velocities well below c. TERA Foundation addressed the issue at 3 GHz, hinting that such theory could still be valid at this lower frequency [2].

The test of this prototype, hereafter presented together with the mechanical design and fabrication, is thus of key importance in defining the upper limits in terms of accelerating gradient of S-Band cavities, and in verifying the S_c model in the 3 GHz and the low phase velocity regime.

MECHANICAL DESIGN

The mechanical design had to face a number of challenges, from the required micron-precision tolerances, to the slenderness of the inter-cell wall with respect to the mass of the 'nose'. The latter presents a critical geometrical feature both for machining and for the bonding/brazing steps. Inter-cell wall thickness remarkably affects the accelerating efficiency of a cavity, so it has to be chosen the minimum possible. A series of high-temperature creep tests was thus carried out. More precisely, an experimental campaign was performed to define the minimum septum thickness that can withstand the creep-induced deformation during the hydrogen bonding heat cycle (with a maximum temperature of 1050 °C). A value of 2 mm was eventually chosen for the septum thickness. A machining test was also performed – with a prototype cell being produced in order to validate the following series.

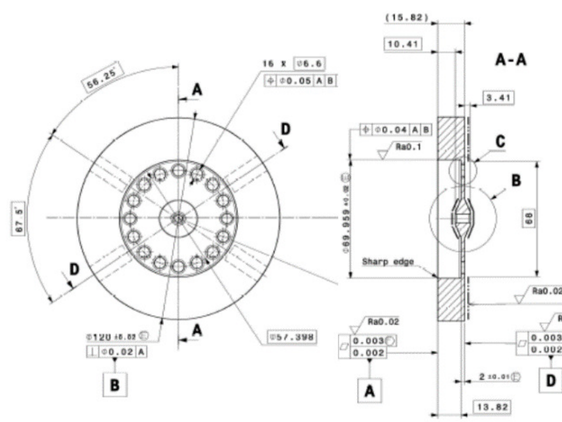

Figure 1: Mechanical drawing of one disk.

Tuning of the structure is made by four dimple tuners per RF cell (Fig.1 left). The number and size of the tuners was determined by an RF sensitivity and tuning analysis. The dimple tuners have a diameter of 10.5 mm, and wall thickness of 1.6 mm. This last parameter has to allow enough deformation of the cavity outer walls to produce a tuning effect, but without rupture. A series of numerical calculations and tests was also carried out on geometries with different diameter/wall thickness ratio, in order to find the best compromise between allowable tuning volume and safety in terms of possible rupture of the copper wall.

A weakly coupled thermo-structural analysis on the full structure was performed by importing the HFSS® electromagnetic field distribution to the thermal and structural packages of ANSYS® (Fig. 2).

The heat dissipation is limited by the peculiar RF design [3], which has 16 coupling holes in each RF cell outer region. As a result, the temperature distribution in the structure is mainly driven by this thermal resistance. Four cooling plates were designed. To prevent plastic deformation, a maximum thermal load of 0.75 kW is allowed, which corresponds to a duty cycle of about 0.075 10^{-3} at a maximum gradient 50 MV/m. Further developments could consider a thicker septum, at the price or reduced rf performance, in case a higher duty cycle is required.

[#] stefano.benedetti@cern.ch, also at EPFL, Lausanne, Switzerland

ISBN 978-3-95450-169-4

DESIGN OF A 750 MHZ IH STRUCTURE FOR MEDICAL APPLICATIONS

S. Benedetti#, CERN, Geneva and EPFL, Lausanne, Switzerland
A. Grudiev, A. Latina, CERN, Geneva, Switzerland

Abstract

Low velocity particles are critical in every hadron accelerator chain. While RFQs nicely cover the first MeV/u range, providing both acceleration and bunching, energies higher than few MeV/u require different structures, depending on the specific application. In the framework of the TULIP project [1], a 750 MHz IH structure was designed, in order to cover the 5-10 MeV/u range. The relatively high operating frequency and small bore aperture radius led the choice towards TE mode structures over more classic DTLs. Hereafter, the RF regular cell and end cell optimization is presented. An innovative solution to compensate dipole kicks is discussed, together with the beam dynamics and the matching with the 5 MeV 750 MHz CERN RFQ [2]. This structure was specifically designed for medical applications with a duty cycle of about 1 ‰, but can easily adapted to duty cycles up to 5 %, typical of PET isotopes production in hospitals.

INTRODUCTION

R&D developments in low beta linear accelerators sparked in the last two decades. Alvarez drift tube linacs (DTL) are usually the preferred solution after the RFQ for pulsed operation. An alternative to DTLs are H-mode linacs, operating in the TE_{110} mode – inter-digital H (IH), or in TE_{210} mode – cross-bar H (CH), as RFQs. Different hybrid solutions – quasi-Alvarez DTL, H-mode linac with PMQ focusing – were studied [3,4]. Ultimately, the choice of the best accelerating structure depends on the application. Medical linear accelerators are characterized by pulsed, low current beam, and have thus a small aperture radius. In addition, a high accelerating gradient is desirable, in order to reduce the overall length of accelerators that have as a final target medical rooms in hospital. This set of parameters – small aperture and high gradient – is unique amongst low beta accelerators, and thus call for a specific design.

COMPARISON BETWEEN STRUCTURES

The 5 MeV 750 MHz CERN proton RFQ represented the starting point of this study. From preliminary beam dynamics considerations, it was decided to use accelerating structures with 2.5 mm aperture radius. The operating frequencies considered were 750 MHz, as the RFQ, and 3 GHz, as the high-beta accelerating structures already designed [5]. The intermediate harmonics were not considered.

RF regular cells with a simplified geometry were optimized in terms of Shunt Impedance (ZTT), considering both DTL and H-mode cavities at the two different frequencies, when applicable (Fig. 1). The results obtained clearly showed the advantage of IH-mode structures in the 5 to 20 MeV/u range. As we will discuss in the following section, the optimization of IH structures is more complex than the optimization of DTL cavities, for which the gap is the most important parameter. As a result, a detailed cavity optimization remarkably increased the ZTT of the 750 MHz IH solution considered (dark red curve in Fig. 1).

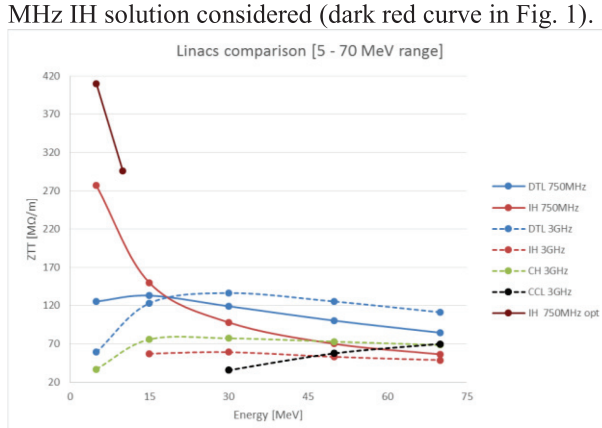

Figure 1: ZTT comparison between different RF cavities.

REGULAR CELL DESIGN

The optimization of TE cavities is more challenging with respect to TM mode ones because of the current flowing in the conductor walls. A DTL RF cell has its ZTT optimum for a given gap, and for stem radius and drift tube thickness the smallest possible. This is not, in absolute terms, the case for IH cavities. For instance, a large stem radius is beneficial because it reduces the Ohmic losses, but it also affects the gap region electric field, thus reducing the ZTT. A careful RF optimization was carried out in order to maximize the ZTT, for a cell length of $\beta\lambda/2$ corresponding to 2.5, 5 and 10 MeV.

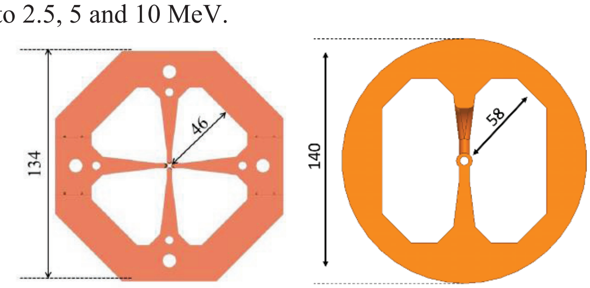

Figure 2: Comparison between the 5 MeV 750 MHz RFQ cell cross section and the IH one.

stefano.benedetti@cern.ch

STUDY AND DEVELOPMENT OF CW ROOM TEMPERATURE REBUNCHER FOR SARAF ACCELERATOR

B. Kaizer*, L. Danon, Z. Horvitz, A. Perry, O. Mazor, J. Rodnizki, SNRC, Yavne, Israel
E. Dunin, E. Farber, A. Friedman, Ariel University, Israel
M. Di Giacomo, J-F. Leyge, M. Michel, P. Toussaint, GANIL/SPIRAL2, Caen, France

Abstract

The SARAF 176 MHz accelerator is designed to provide CW proton/deuteron beams up to 5 mA current and 40 MeV accelerated ion energy. Phase I of SARAF (up to 4-5 MeV) has been installed, commissioned, and is available for experimental work. Phase II of SARAF is currently in the planning stage and will contain larger MEBT with three rebunchers and four cryomodules, each consisting of SC HWRs and solenoids. Phase II MEBT line is designed to follow a 1.3 MeV/u RFQ, is 4.5 m long, and contains three 176 MHz rebunchers providing a field integral of 105 kV. Different rebuncher configurations have been studied in order to minimize the RF losses and maximize the shunt impedance. Different apertures have also been tested with a required of 40 mm diameter by beam dynamics. The simulations were done using CST Microwave Studio. CEA leads the design for SARAF phase II linac including the MEBT rebunchers and has studied a mixed solid copper and Cu plated stainless steel, 3-gap cavity. SNRC is developing a 4-gap OFHC copper rebuncher as a risk reduction. Both designs are presented and discussed in the paper.

REBUNCHER REQUIREMENTS

Main requirements for the MEBT rebunchers are reported in Table 1 [1].

Table 1: Rebuncher Requirements

Requirement	value	units
Frequency	176	MHz
CW Effective Voltage	105	kV
Pulsed Effective Voltage	160	kV
Drift tube aperture	40	mm
Flange to flange distance	280	mm
Optimal β	0.053	

REBUNCHER TYPE

In order to find the most suitable resonator type, a Cu-plated stainless steel 3-gap split spoke geometry and OFHC copper 4-gap cylindrical geometry rebuncher have been studied. The basic structure of the 3-gap rebuncher consists of an outer horizontal cylinder tank with 2 stems which form three acceleration gaps (Fig. 1). The basic structure of the 4-gap rebuncher consists of a vertical cylinder, a fork and a bottom stem which form four acceleration gaps (Fig. 2). For both structures different apertures (30 and 40 mm) have been tested. The rebunchers were designed for $\beta_{beam} = 0.0528$ which corresponds to particle energy of 1.3 MeV/u.

* boazka@soreq.gov.il

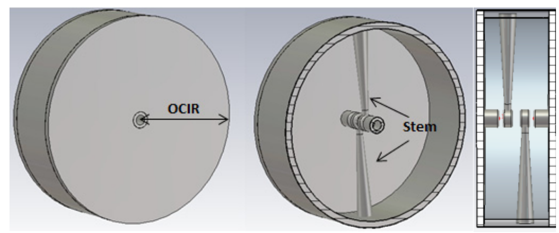

Figure 1: The basic structure of the 3-gap rebuncher.

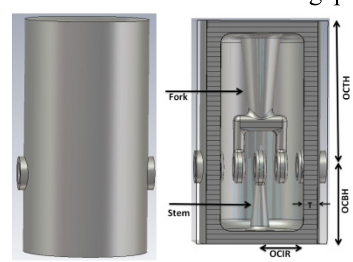

Figure 2: The basic structure of the 4-gap rebuncher.

OPTIMIZATION STUDY

After completion of initial design of the cavity structure for both 3-gap and 4-gap rebunchers, a thorough process of optimization was performed. This optimization process was done using parameter sweeps in CST Microwave Studio [2] and included all the parameters of the resonator structure. These parameters include among others: the structure of the stems and the fork (shape, length and radius), the structure of the drift tube rings (shape, length and radius), the acceleration gap dimension, the outer tank dimensions and the blending radius etc. The EM fields for both structures optimized so that the beam receives the specified energy gain within minimum RF fields, $\frac{E_{pk}}{E_{acc}}, \frac{B_{pk}}{E_{acc}}$, minimum RF losses and maximum shunt impedance.

The optimization was derived for each set of sub component parameters individually. Following each sub-component study, the cavity height was adjusted to reach the linac frequency (Outer Conductor Top Height in case of a 4-gap type, and Outer Conductor Inner Radius in case of a 3-gap type). This is due to the relative low sensitivity of these parameters to the figure of merits under study,

SIMULATION OF GAS AND PLASMA CHARGE STRIPPERS*

O. S. Haas†, O. Boine-Frankenheim[1]
Institut für Theorie Elektromagnetischer Felder (TEMF), Technische Universität Darmstadt,
Schloßgartenstr. 8, 64289 Darmstadt, Germany
[1]also at GSI Helmholtzzentrum für Schwerionenforschung GmbH, Beam Physics Department,
Planckstr. 1, 64291 Darmstadt, Germany

Abstract

Charge stripping of intense heavy ion beams is a major challenge in current and future linear heavy ion accelerators. Conventional stripping techniques are limited in their applicability, e.g. solid carbon foils suffer from short lifetimes at high intensities. One possible alternative is the use of a plasma as a stripping medium, which the presented work focuses on. The main goal of the studies is the prediction of the final charge state distribution of the ion beam. Rate equations were implemented numerically, taking into account different models for ionization, recombination and energy loss processes. First quantitative results are presented in form of an overview of the charge state distributions of different charge stripping media. For fixed projectile properties and target phase, it is observed that the mean charge state q_0 decreases for increasing nuclear charge Z_T of the target. Plasmas show significantly increased q_0 for the same Z_T. The width d of the charge state distributions is larger for higher Z_T. The latter is caused by multiple loss of the projectile and decreases the maximum stripping efficiency by typically less than a factor of 2.

INTRODUCTION

Future facilities like the FAIR project at GSI (see Ref. [1]) require viable methods for charge stripping of intense heavy ion beams at fairly low beam energies of 1 MeV/u to 10 MeV/u. Typically 80 – 90% of the beam can be lost in the charge stripping process due to a large fraction of the beam being in unwanted charge states, thus warranting a theoretical study of charge state distribution widths of different gases and plasmas.

PROBLEM FORMULATION

The analytical considerations in this section on the charge state distribution of the projectile is based on Ref. [2]. The evolution is given by the system of rate equations

$$\frac{\mathrm{d}F_q(t)}{\mathrm{d}t} = \sum_{q'} F_{q'}(t)\alpha_{q',q} - F_q(t)\sum_{q'}\alpha_{q,q'} , \qquad (1)$$

where $F_q(t)$ are the relative fractions of the charge state q, and the $\alpha_{q,q';q',q}$ are the projectile charge changing rates. In most cases charge changing processes are fast and energy loss can be disregarded, then the charge state distribution approaches an equilibrium with mean charge q_0. First we assume only single electron loss and capture processes and an exponential dependence of the rates on the charge state

$$\alpha_{q,q+1} = A_{q,q+1}\exp\Big(-b_{q,q+1}(q-q_0)\Big) \qquad (2)$$

$$\alpha_{q,q-1} = A_{q,q-1}\exp\Big(b_{q,q-1}(q-q_0)\Big) , \qquad (3)$$

where $b_{q,q+1}$, $b_{q,q-1}$, $A_{q,q+1}$ and $A_{q,q-1}$ are positive constants according to the respective charge changing process. The equilibrium charge state distribution is in this case Gaussian with the standard deviation

$$d_0 = \sqrt{\frac{1}{b_{q,q+1}+b_{q,q-1}}} . \qquad (4)$$

Graphically in a semi-log plot of the rates the mean charge q_0 is given by the intersection point, and the width d_0 by the slopes. Numerically we solve the matrix of the rates $\alpha_{q,q'}$ with a singular value decomposition for the equilibrium charge states or integrate directly the rate equations with a high-order adaptive Runge-Kutta scheme for a time resolved evolution of the charge states.

As we will see later in the presented work at typical energies of 1 MeV/u to 10 MeV/u multiple loss cross sections can be almost as large as the single charge changing processes, but multiple electron capture is negligible. The multiple loss rates are approximately given by are roughly given by

$$\alpha_{q,q+n} \approx k_0^{n-1}\alpha_{q,q+1} , \qquad (5)$$

where n is a positive integer representing the n-electron loss or capture process, and $0 < k_0 < 1$.

The standard distribution width of the charge state distribution including multiple loss rates is then given by

$$d = kd_0 \qquad (6)$$

$$k \approx \left[\frac{\sum_{n=1}^{n=n_{\max}} n^2 k_0^{n-1}}{2\sum_{n=1}^{n=n_{\max}} nk_0^{n-1}} + \frac{1}{2}\right]^{1/2} . \qquad (7)$$

From this one can deduct that in case of large multiple loss rates the inclusion of high n is required to get an accurate value of d, e.g. if $k_0 = 0.7$ rates up to roughly $n_{\max} = 10$ should be included.

For heavy ion projectiles it is reasonable to take the limit $n_{\max} \to \infty$ for k, which enables us to derive a very simple expression

$$k \approx \left[\frac{1}{1-k_0}\right]^{1/2} . \qquad (8)$$

* Work supported by the BMBF as part project 05P15RDRBA.
† haas@temf.tu-darmstadt.de

LEBT COMMISSIONING OF THE J-PARC LINAC

T. Shibata, K. Ikegami, Y. Liu, T. Maruta, F. Naito, A. Takagi, High Energy Accelerator Research Organization (KEK), Tsukuba, Japan
H. Asano, Y. Kondo, A. Miura, H. Oguri, K. Ohkoshi, Japan Atomic Energy Agency (JAEA), Naka-gun, Tokai-mura, Japan

Abstract

After J-PARC Linac update for increase of beam energy and current update in 2013 and 2014, sequences of beam commissioning has been made for optimization of RFQ transmission rate. The beam commissioning has been made by iteration of scanning 6 adjustable parameters scan. In the commissioning on January 2016, the highest current ratio between LEBT and MEBT (up- and down-stream of RFQ) up to 92.7 ± 3.3 % has been observed in the 40 mA beam current operation. In addition, numerical analysis has been made for H- beam transport in ion source and low energy beam transport to clarify beam t characteristics.

INTRODUCTION

In J-PARC Linac, a series of upgrades has been done in 2013 and 2014 to increase negative hydrogen ion (H^-) beam energy and current. In the beam energy upgrade, ACS (Annular-ring Coupled Structure Linac) is installed to the Linac which increased the beam energy from 181 MeV to 400 MeV [1]. The peak current upgrade in 2014 is made by exchanging ion source (IS) from arc driven source with LaB_6 (lanthanum hexaboride) filament to Radio Frequency (RF) source which results in increase in the beam current extracted from IS up to 45 mA in user operation (40 mA H- current from Linac) [2]. Also, structure of RFQ (Radio Frequency Quadrupole Linac) system is changed from Bolt type to Brazed type with new beam design for higher beam energy [3].

A sequences of beam commissioning in IS and LEBT (Low Energy Beam Transport) parameters has been made after J-PARC upgrade to keep high RFQ transmission rate. In this proceedings, the commissioning in 40 mA operation on Jan. 2016 is reported.

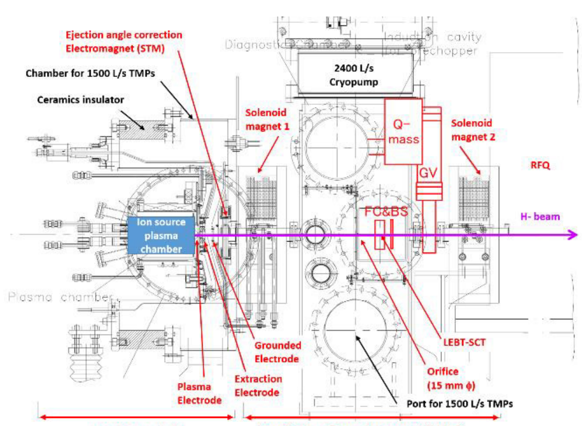

Figure 1: Schematic drawing of J-PARC ion source and LEBT.

LEBT CONSTRUCTION

Figure 1 shows the schematic drawings of IS and LEBT in the Front-End of J-PARC. In LEBT, two solenoid coils are located around beam ducts in up- and down-streams of LEBT chamber. The solenoid coils (SOL 1 and 2) has double pancake 90 turns conducting wire with maximum current 820 A to flow in application of 17 V from power supply which produces B_{max} = 1.1 T in axial direction inside. At the exit of IS, steering electromagnets (STM) are located for adjustment of ejecting angle from IS in vertical and horizontal directions. The LEBT chamber is divided into two region by orifice with aperture 15 mm ϕ in order to decrease conductance of H_2 gas flowing from IS to RFQ. The upstream part of LEBT chamber is pumped by a pair of TMP of 1500 L/s, while the downstream part is connected to Cryopump with pumping speed up to 2400 L/s. Installation of the orifice produces variation of H_2 gas pressure between up- and down-streams in an amplitude of order (~ 10^{-4} Pa and 10^{-5} Pa at up- and down-streams, respectively).

BEAM COMMISIONING IN FRONT-END

In the beam commissioning, 6 adjustable parameters in the followings are optimized for improvement of beam transmission in RFQ;

- Extraction voltage : 9.5 – 10.2 kV
- Acceleration voltage : 41.5 – 45.5 kV
- STM vertical & horizontal current : -10 – 10 A
- SOL 1 & 2 current : 490 – 820 A.

The H^- beam current is measured by SCT (split-core current transformers) (1) in LEBT chamber just after the orifice aperture and (2) in MEBT, at the exit of RFQ. In the commissioning, ratio between current measured in (1) and (2) are calculated. This ratio is not exactly the RFQ transmission rate, but strong relation takes place between these parameters. Error of this current ratio may take place at time averaging of the SCT currents. The current measurement is made at the very end part of beam pulse to obtain steady state value. On the other hand, beam current ramp-down (at the end of the beam pulse) takes place with temporal fluctuation in range of a few μsec. This leads to inclusion of decreased current into the time averaging. From careful investigation of the beam pulse waveforms, error bar of the current ratio I_{MEBT}/I_{LEBT} is estimated to be around ± 3.3 % in the present case.

As there are 6 adjustable parameters, it is difficult to make optimization in one scanning event. Instead, scanning of each parameters are made repeatedly for a few times in order to obtain iteration. Initially, scan for SOL 1

ISBN 978-3-95450-169-4

OPERATING STATUS OF INJECTOR II FOR C-ADS PROJECT

Liepeng Sun#, Longbo Shi, Xianbo Xu, Chenxing Li, Zhouli Zhang,
Wenbin Wang, Liang Lu, Aimin Shi, Yuan He, Hongwei Zhao
Institute of Modern Physics, Chinese Academy of Sciences, Lanzhou 730000, China

Abstract

The Radio Frequency Quadrupole system has been designed and constructed for C-ADS (Chinese Accelerator Driven System) Injector II in Institute of Modern Physics (IMP), Chinese Academy of Sciences, which has been running for more than one year until now. It is a quadrilateral four-vane resonator with two equal couplers operating in CW mode. In the paper, RF system upgrade will be presented in detail，especially the two-port configuration was introduced and the conditioning based on two new sets of solid-state amplifier instead of the original tetrodes power source due to system hardware upgrade are described in the paper.

INTRODUCTION

Since 2011 Chinese Accelerator Driven System (C-ADS) project has been developed in order to solve the nuclear waste disposition and energy shortage crisis [1], which carried out by two institutes from Chinese Academy of Sciences. According to the arrangement of the project, IMP (Institute of Modern Physics) would build a 25-50 MeV demo facility named Injector II by the end of 2016. Injector II consists of Ion Source, LEBT (Low-Energy Beam-Transport), RFQ, MEBT (Medium-Energy Beam-Transport) and SC (Superconducting) section. And as the first accelerator, a four-vane RFQ which accelerated CW 10mA proton beam up to 2.1 MeV and with an operating frequency of 162.5MHz in June 2014, whose power source is traditional tetrode amplifier at the beginning of operation. Now two 80kW solid-state amplifier (SSA) as new power source instead of tetrode one, and by the end of May, 2016, the conditioning had been completed after RF system setting up. The RFQ cavity is shown in Fig. 1.

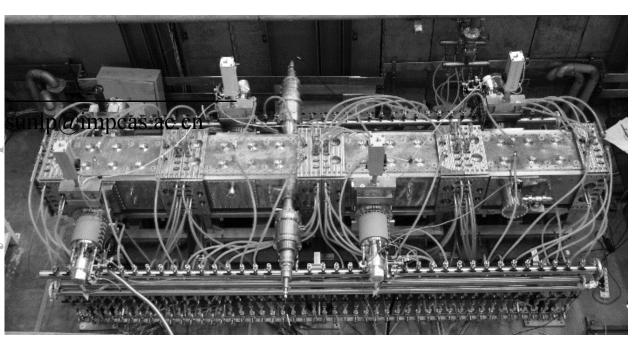

Figure 1: The four-vane RFQ cavity with two couplers.

#sunlp@impcas.ac.cn

NEW POWER SOURCE

According to the design for C-ADS, the failure time are limit strictly by several hours in one year. And previous tetrode amplifier has some problems, such as high sparking risk in input/ output cavity, running pressure while high intensity current due to no circulator and so on. However, since the dissipated power in RFQ cavity is very high, the SSA must be designed to output very high power in spite of two couplers feeding power into resonator. Finally, two new 80kW SSA were decided considering the power margin and beam loading, which were developed by two different manufacturers in order to verify the technologies on high power combining.

Figure 2: Two sets of 80kW solid-state amplifier.

New two power sources delivery the power to the cavity other than old tetrode amplifier, which split the power into two couplers from one power source.

According to the design of RFQ, new parameters of SSA were decided and optimized, which is shown in Table 1, and every module in it must stand the long-term full power reflection and hot swapping (insertion and extraction without ceasing electricity).

Table 1: Specifications of Solid-State Amplifier

Requirement	Target value	Comment
Nominal frequency	162.5MHz	±1MHz
Duty cycle	100%	Pulsed mode possible.
Max. transmitted power	80kW	VSWR≤1.5.
Max. reflected power in operation	10.5kW	Full power reflection possible.
Output noise	≤-60dBc	Dummy load
Harmonic suppression	≤-30dBc	Dummy load
Amplitude stability	$\leq\pm1\times10^{-3}$/24h	Close loop
Phase stability	$\leq\pm1\times10^{-3}$/24h	Close loop
RF impedance	50 ohms	All components

ISBN 978-3-95450-169-4

PROGRESS AND OPERATION EXPERIENCES OF THE J-PARC LINAC

Kazuo Hasegawa*, for the J-PARC Linac group, J-PARC, JAEA/KEK, Tokai-mura, Japan

Abstract

The J-PARC linac started beam commissioning in 2006 and had delivered beam to users since 2008 at an energy of 181 MeV. The linac with an energy of 400 MeV and higher peak beam current of 50 mA was required to reach the goal of the J-PARC project. We installed a new accelerating structure, Annular-ring Coupled Structure (ACS) in 2013 for energy upgrade. The ion source and the Radio Frequency Quadrupole linac (RFQ) were replaced to increase the beam current in 2014. As a result of these, the linac provides beams to demonstrate a 1-MW-equivalent beam at the RCS and also beams for user programs at higher beam power. The progress and operation experiences of the J-PARC linac are presented.

INTRODUCTION

The J-PARC facility consists of a linac, a 3 GeV Rapid Cycling Synchrotron (RCS), a 30 GeV Main Ring synchrotron (MR) and three experimental facilities [1]. The linac started beam commissioning in 2006. The present linac consists of a negative hydrogen ion source, a 3 MeV RFQ, a 50 MeV DTL (Drift Tube Linac), a 191 MeV SDTL (Separated-type DTL) and a 400 MeV ACS (after the upgrade) as shown in Fig. 1. RF frequencies are 324 MHz and 972 MHz for the low energy section (RFQ, DTL and SDTL) and for the high energy section (ACS), respectively. A proton beam from the RCS is injected to the Materials and Life Science Experimental Facility (MLF) for neutron and muon experiments. The MR has two beam extraction modes; a fast extraction for the neutrino beam line (NU) for the Tokai-to-Kamioka (T2K) experiment, and a slow extraction for the Hadron Experimental Facility (HD).

The goal of the J-PARC project is to deliver a 1 MW beam from the RCS and a 0.75 MW beam from the MR. To achieve the goal, the linac peak current and energy should be 50 mA and 400 MeV, respectively, while initial configuration provided a 30 mA and 181 MeV beam. Therefore, we took the energy upgrade, and then, the peak current upgrade [2].

PROGRESS OF PERFORMANCE

Operation in the Early Days

Beam commissioning of the linac started in November 2006 and 181 MeV acceleration was achieved in January 2007. The progress at that time seemed to be smooth. But trip rates of the RFQ unexpectedly increased in autumn 2008 and the incident limited the operation days and power ramp-up. The beam current was limited to 5 mA, and the RCS beam power for the MLF users was 20 kW. The history of the beam power of the MLF is shown in Fig. 2. Note that the small bars in 2008 and 2009 are not

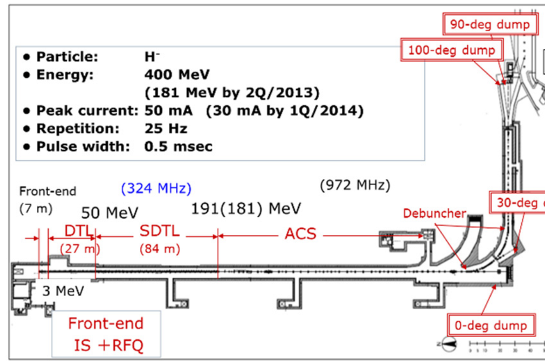

Figure 1: Configuration and main parameters of the J-PARC Linac.

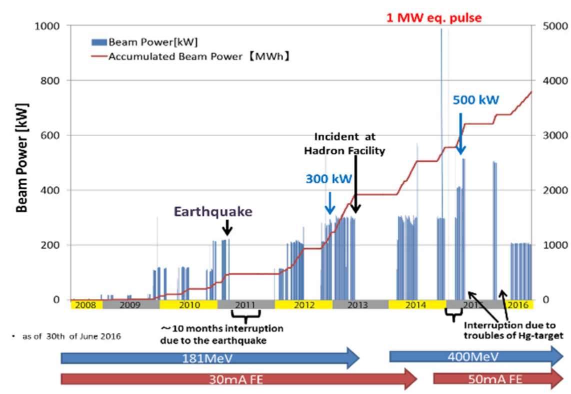

Figure 2: Beam power history for the MLF. (by courtesy of the MLF group).

noises but our suffering days. This was mostly settled by the vacuum improvement work during the summer shutdown of 2009 [3]. We increased the beam power in November 2009; beam pulse length from 0.1 to 0.2 msec, and peak beam current from 5 to 15 mA, thus giving a 6 fold increase from 20 to 120 kW. Since then, we had kept stable operation for users, concretely 90 to 95% availability.

Earthquake in 2011

Based on the stable operation, we planned to step up the beam power to the MLF. We increased the power from 120 to 200 kW in November 2010. The linac beam current and average power were 15 mA and 12 kW, respectively. We also performed 400 kW (equivalent current beam) acceleration in January 2011 for the next step up.

But we had a crisis after two months; the Great earthquake in March 2011. The J-PARC facilities were severely damaged [4]. Thanks to the significant effort of restoration, we resumed beam operation in December and user operation in January 2012 [5].

We started beam operation sooner, but several aftereffects were left. The number of trips in the RFQ was seri-

* hasegawa.kazuo@jaea.go.jp

COMMISSIONING OF THE HIGH INTENSITY PROTON SOURCE DEVELOPED AT INFN-LNS FOR THE EUROPEAN SPALLATION SOURCE

L. Neri, L. Celona, S. Gammino, D. Mascali, G. Castro, G. Torrisi, O. Leonardi, L. Allegra, A. Amato, G. Calabrese, A. Caruso, F. Chines, G. Gallo, A. Longhitano, G. Manno, S. Marletta, A. Massara, A. Maugeri, S. Passarello, G. Pastore, A. Seminara, A. Spartà, G. Vinciguerra, INFN-LNS, Catania, Italy
M.J. Ferreira, ESS, Lund, Sweden
Ø. Midttun, University of Bergen, Bergen, Norway and ESS, Lund, Sweden

Abstract

At the Istituto Nazionale di Fisica Nucleare – Laboratori Nazionali del Sud (INFN-LNS) the commissioning of the high intensity Proton Source for the European Spallation Source (PS-ESS) started some weeks ago. Beam stability at high current intensity is one of the most important parameter for the first steps of the ongoing commissioning. Commissioning plan and preliminary characterization are also presented, with the aim to satisfy the requirement above.

DESCRIPTION

The design of PS-ESS and LEBT involved many efforts from different institutions with the aim to get a source highly reliable and satisfying the ESS requirements. The mechanical and functional interfaces between the different groups of INFN-LNS, ESS and CEA-IRFU were properly addressed and the layout shown in the Figure 1 is now complete. All details are finalized, most of the elements have been already delivered and few other parts are under construction. The source is equipped with a flexible magnetic system consisting of three coils independently energised [1]. The plasma chamber is coupled with a matching transformer to optimize the microwave matching and enhance the electric field on plasma chamber axis. The entire source body is supported with a double pin joint to permit a higher degree of freedom both during alignment and maintenance procedures. The insulating column is made with a single alumina gap. The external surface has an innovative design that permit to reduce the electric field up to 6.5 kV/cm. The so called "triple point" (i.e.: the junction between the alumina the metal and the vacuum) been designed to achieve an electric field lower than 5.5 kV/cm taking into account our previous experiences. Inside this element the tetrode extraction system is placed. It is composed by the plasma electrode located at the exit of the plasma chamber, and a set of three electrodes supported by the first element of the LEBT. There are two grounded electrodes and one repeller electrode in the middle of them. All the electrodes are water cooled. The first element of the LEBT houses two turbo molecular pumps (TMP), water and electrical utilities for the extraction system, a Residual Gas Analyzer (RGA), three different type of vacuum gauges, a burst disk and the gas injection needed to improve the space charge compensation of the LEBT. The design of this part was focused to be as compact as possible [2]. This element is the most important part for the alignment of the entire source. The beam will be then transported through the 2.4 m long LEBT with two solenoids; magnetic steerers are hidden inside each solenoid to reduce the total length of the LEBT [3]. The two LEBT solenoids are identical as well. A bellow and a gas injection are integrated in their design. Both pipes are followed by a gate valve that will permit maintenance operations without breaking the vacuum. The Iris is a six blade diaphragm that will be used to reduce the beam current injected inside the following part of the accelerator (Radio Frequency Quadrupole, RFQ) without changing the source conditions.

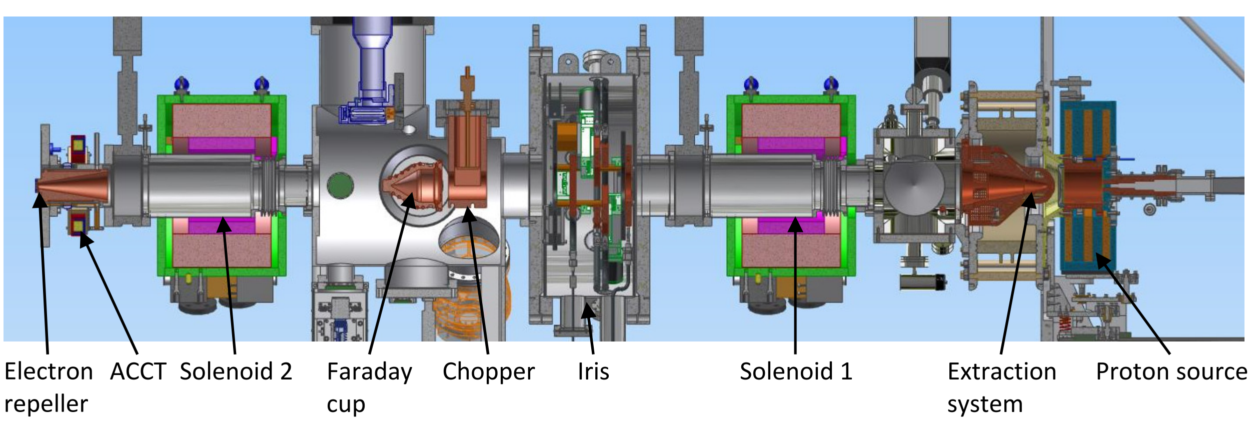

Figure 1: Experimental setup of PS-ESS with the relative LEBT.

ISBN 978-3-95450-169-4

COMMISSIONING PLANS FOR THE ESS DTL

M. Comunian†, F. Grespan, A. Pisent, L. Bellan[1], INFN-LNL, Legnaro, Italy
M. Eshraqi, R. Miyamoto ESS, Lund, Sweden
[1]also at Dipartimento di Fisica e Astronomia, Università degli Studi di Padova, Padova, Italy

Abstract

The Drift Tube Linac (DTL) of the European Spallation Source (ESS) is designed to operate at 352.2 MHz with a duty cycle of 4% (a beam pulse of 2.86 ms, 14 Hz repetition rate) and will accelerate a proton beam of 62.5 mA pulse peak current from 3.62 to 90 MeV. This article describes the commissioning strategy plans for the DTL part of the linac, techniques for finding the RF set point of the 5 Tanks and steering approach. Typical beam parameters, as proposed for commissioning purposes, are discussed as well and how the commissioning sequence of the Tanks fits together with ongoing installation works in the tunnel.

INTRODUCTION

In the ESS accelerator the initial warm linac section is composed by Ion Source, Low Energy Beam Transport line (LEBT), Radio Frequency Quadrupole (RFQ), Medium Energy Beam Transport line (MEBT) and DTL [1].

Table 1. DTL Main Parameters

Tank	1	2	3	4	5
Cells	61	34	29	26	23
E0 [MV/m]	3.00	3.16	3.07	3.04	3.13
L [m]	7.62	7.09	7.58	7.85	7.69
R Bore [mm]	10	11	11	12	12
LPMQ [mm]	50	80	80	80	80
BPM	6	3	2	2	2
EMD	12	6	4	4	4
PMQ	30	16	14	13	11
Ptot [kW]	2191	2191	2196	2189	2195

INFN-LNL is in charge of the design and production of the DTL [2]. The DTL is a 38.8-m long system, divided in five Tanks. Each Tank is a standalone structure, composed of four 2-m-long modules made of AISI 304L stainless steel with internal electro-copper deposition.

The Drift Tubes are positioned in the girder, a precisely machined aluminum alloy structure, which is housed in the upper part of each module. Drift Tubes (DT) are equipped with various components: Beam Position Monitor (BPM), Electro Magnetic Dipole (EMD), and Permanent Magnet Quadrupole (PMQ). The PMQs are placed in the F0D0 layout. The BPM and EMD are placed in the empty tubes. An ACCT as Beam Current Monitor (BCM) is present in each inter-tank section, installed in the end plates where PMQ are not present as shown in Fig. 1.

The main DTL parameters and final distribution of elements Tank by Tank are reported in Table 1.

In the next paragraphs, the authors describe a scientific proposal for the ESS DTL commissioning, developed in order to verify the required performances of the machine. At present time, this plan of measurements is not the reference-commissioning plan of ESS.

ESS DTL INSTALLATION AND COMMISSIONING SEQUENCE

The installation and commissioning of the ESS linac will start in 2017 and the first proton beam at 570 MeV is scheduled to be delivered to the target by the second quarter of 2019. Further details of the overall commissioning plan can be seen in [3]. Commissioning of a large-scale machine, such as the ESS linac, within a relatively short time imposes challenges on many areas including planning and preparations for the beam commissioning.

Each DTL Tank will be assembled and tuned in the ESS RATS facility. Vacuum and cooling systems will be tested in the RATS as well. DTL Tank will be then transported to the tunnel and aligned in its final position, where the high power RF conditioning will take place. The sequence of Tank installation in the tunnel will be Tank4, Tank1, Tank3, Tank2, and Tank5.

The ESS DTL will be commissioned with beam in 3 phases:

1. First phase, Tank1 will be commissioned, using the diagnostic plate already used for 3.62 MeV commissioning. For this reason, Tank2 cannot be installed and conditioned before this phase, while RF conditioning of Tank3 and Tank4 can in principle proceed during Tank1 beam commissioning.
2. During the second phase, Tank2 to Tank4 will be commissioned.
3. Third phase is the full commissioning out of Tank5.

EMD AND BPM DISTRIBUTION

EMDs and BPMs have been recently redistributed inside the 5 Tanks, in order to have more BPMs and EMDs and ease the beam steering in Tank 1, where the phase advance per cell is much larger than the other tanks and a small number of BPMs and EMDs could cause an overshooting issue. The first BPM is located before the first EMD in order to set up the last MEBT elements (Figure 1).

The constrains of this analysis were to keep 15 BPMs and 15 EMDs pairs in the DTL section and to have at least 2 BPMs per Tank for time-of-flight measurement.

CIADS NORMAL TEMPERATURE FRONT-END DESIGN*

W. L. Chen†, W. P. Dou, Y. S. Qin, H. Jia, S. H. Liu, Z. J. Wang, Y. He,
Institute of Modern Physics (IMP), Chinese Academy of Sciences, Lanzhou, China

Abstract

The design and construction with several tens of megawatts superconducting accelerator is the developing direction in the further. The superconducting section follows with the RFQ and MEBT, which needs good enough beam quality. The normal temperature front ends are redesigned for China Initiative Accelerator-Driven Subcritical System (CIADS). The LEBT transports a 35 keV, 10 mA DC proton beam to the RFQ, after the RFQ acceleration the MEBT transports a 2.1 MeV 10 mA CW proton beam to the superconducting DTL. The "Point Source" is proposed in the beam scrape application during the LEBT section to get the ideal transverse beam parameters. To get the ideal longitudinal beam parameters, the new RFQ is designed with little emittance. Collimators are installed in the new MEBT to scrape the outer sphere beams which may turn to halo. Details of the beam dynamics simulations will be given.

INTRODUCTION

A project named China Accelerator Driven Sub-Critical System (C-ADS) has been proposed to treat the spent nuclear fuel and began construction since 2011 [1]. Under three years commissioning, the demo facility had accelerated 10 mA CW proton beam to 2.56 MeV, 2.7 mA CW proton beam had accelerated up to 5.17 MeV, and recently the 10 mA, 10 MeV CW proton beam is under commissioning.

The layout of the demo facility is shown in Fig. 1. As the proton beam out of the ECR ion source coupled with H_2^+ and H_3^+, which are the unwanted particles and will be lost in the downstream. Also, another question is the H_2 removal from the ion source to the RFQ and even to the downstream superconducting cavity. After long-time operation with residual gas RFQ performance may decline has reported by SNS and SARAF [2, 3]. For high power accelerator, the beam loss must be controlled in low order, this paper presents the detailed description about a new structure LEBT for eliminate the unwanted particles and how to decrease the transverse and longitudinal emittance in CIADS normal temperature front end.

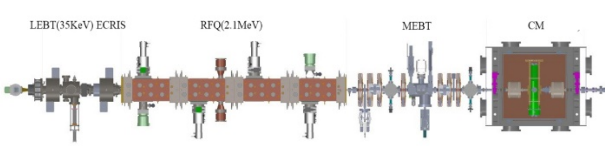

Figure 1: The layout of the ADS LEBT and parts of RFQ.

LEBT SYSTEM

The 10 mA proton DC beam with the energy of 35 keV is extracted from a 2.45 GHz ECR ion source, after the LEBT transmission, match to the RFQ accelerator. The LEBT is used to transport and match the proton beam to the RFQ. Table 1 shows the key parameters of the front end. To meet the proton fraction requirement, a bending magnet and collimator have been considered to substantially reduce the contaminants, such as H_2^+ and H_3^+ [4]. In the previous design, the bending magnet rotation angle and edge angle is chosen with 20° and 6°. It can match well for the symmetry requirement both in X and Y positon. Typical values of the initial parameters from the ion source are listed in Table 2. The space charge compensation is about 0.87 at the vacuum of 1.3E-3 Pa, all these beam parameters refer to the C-ADS accelerator commissioning experience. Figure 2 shows the CIADS LEBT layout.

Solenoids are effective for focusing the low energy beam, especially in LEBT section, but the beam quality decreases with the emittance growth, which contributed by the spherical aberration of the solenoid lens [5]. A "point source" concept is proposed in CIADS LEBT design, which means the beam out of the ion source follows the linear transmission approximation. An aperture is install just after the ion source and before the first solenoid to scrape off the outer parts of the beam particles. This concept is simulated with the initial beam particles generated randomly in 4-dimensional ellipse with Gaussian distribution. The model considered with the space charge effect, the simulation results are shown in Fig. 3.

Table 1: Required Parameters Before the RFQ

Parameters	Numbers	Units
Energy	35	KeV
Current	20	mA
Repetition frequency	50	Hz
Pulse width	CW	-
Twiss parameter α	c	-
Twiss parameter β	0.0479	mm/π.mrad
$\epsilon(nRMS)$	<0.2	π.mm.mrad
Proton fraction	>95	%

* Supported by National Natural Science Foundation of China (11525523)

† E-mail: chenweilong@impcas.ac.cn

ISBN 978-3-95450-169-4

COMMISSIONING OF THE RI PRODUCTION BEAM LINE OF KOMAC*

Hyeok-Jung Kwon†, Han-Sung Kim, Sang-Pil Yun, Young-Gi Song, Yong-Sub Cho
Korea Multi-purpose Accelerator Complex,
Korea Atomic Energy Research Institute, Gyeongju, South Korea

Abstract

A radioisotope (RI) production beam line has developed at Korea Multi-purpose Accelerator Complex (KOMAC) in 2015 and the commissioning started in 2016. The beam parameters of the beam line are 100 MeV beam energy with a maximum 30 kW beam power, which is driven by KOMAC 100 MeV proton linac. The main components of the beam line are a beam transport system, a target transport system, a cooling system for target and hot cell. KOMAC has a plan to commission the beam line and get an operation license in 2016 and start user service in 2017. In this paper, the development and initial commissioning results of the RI production beam line are presented.

INTRODUCTION

One of the utilization fields of the 100 MeV proton beam is the production of the radioisotopes. Major facilities for RI production based on the high power linac include the BLIP (Brookhaven Linac Isotope Producer) at Brookhaven Nation Laboratory and the IPF (Isotope Production Facility) at Los Alamos National Laboratory. [1, 2]

KOMAC started the beam service to users with 2 beam lines from 2013. To satisfy the user requirement, KOMAC developed a new beam line for RI production. In 2015, the construction of the RI production beam line was finished and the commissioning of the beam line is underway. The main components of the beam line are a beam transport system, a target transport system, a cooling system for target and hot cell. All of the components were installed and the test of each component was carried out including RI production test with low power proton beam.

Two RIs are considered to be produced at KOMAC in initial stage. One is a Sr-82 which is used for PET imaging and can be produced from RbCl. The other is Cu-67 which is used for cancer therapy and can be produced from Zn or ZnO. Both of them are efficiently produced through 100 MeV proton beam.

BEAM LINE DEVELOPMENTS

The specification of the RI production beam line is shown in Table 1 and the layout is shown in Fig. 1. [3]

Beam Transport System

The beam transport system consists of 2 sets of 45 degree bending magnets, vacuum box, beam diagnostics and beam window. 2 sets of wobbling magnets are not installed yet. They will be installed after initial operation test. 2 sets of 45 degree bending magnet are different from each other. The pole tip field of the 1st bending magnet is 0.8 T with C type yoke whereas that of 2nd magnet is 1.5 T by using H type yoke because the 1st bending magnet shares two beam lines whereas the 2nd one is only for RI production beam line in limited space. A strip-line type beam position monitor is installed after the 2nd bending magnet and a movable Faraday cup is installed in the vacuum box. Two sets of proportional counter were installed before and after the 2nd bending magnet as a beam loss monitor. A beam window is installed at the end of the beam transport line. The main role of a beam window is separating the beam line vacuum from the water cooling target assembly. The material of the beam window is AlBeMat with 0.5 mm thickness. Before the beam window, vacuum sensor for activating a fast closing valve was installed to protect the accelerator when there is a rupture of the beam window. The beam transport system after installation is shown in Fig. 2.

Table 1: Specification of the RI Production Beam Line

Parameter	Value
Energy [MeV]	100
Peak current [mA]	20
Pulse width [us]	500
Rep. rate [Hz]	30
Duty factor [%]	1.5
Ave. current [mA]	600
Peak power [MW]	2.0
Ave. power [kW]	30
E per pulse [J/pulse]	1000
Target Dia. [mm]	100
Beam size FWHM [mm]	14.2*12.4
Scanning Method	Wobbling
Beam window	AlBeMat

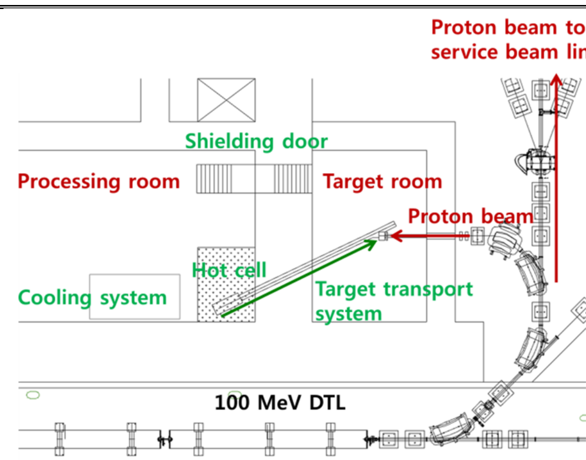

Figure 1: Layout of the RI production beam line.

* Work supported by Ministry of Science, ICT & Future Planning of the Korean Government.
† hjkwon@kaeri.re.kr

ISBN 978-3-95450-169-4

EUROPEAN SPALLATION SOURCE (ESS) NORMAL CONDUCTING FRONT END STATUS REPORT

W. Wittmer*, P. M. Gustavsson, F. Hellström, G. Hulla, ESS, Lund, Sweden
Ø. Midttun, University of Bergen, Norway
L. Celona, S. Gammino, L. Neri, INFN/LNS, Catania, Italy
A. C. Chauveau, D. Chirpaz-Cerbat, O. Piquet, B. Pottin, CEA, Gif-sur-Yvette, France
I. Bustinduy, C. De la Cruz, P. J. Gonzalez, G. Harper, S. Varnaseri, ESS-Bilbao, Spain
F. Grespan, A. Pisent, INFN/LNL, Legnaro, Italy
P. Mereu, INFN-Torino, Italy

Abstract

The European Spallation Source (ESS) will deliver first protons on target by mid 2019. Civil construction of the accelerator tunnel has made good progress and will allow starting installation of the normal conducting frond end (NCFE) by end of 2017. To achieve these milestones the design of all major beam line components have been completed and the construction of the subsystems begun. We report on the advancement of the subsystems and the commissioning progress of the microwave discharge Proton Source (PS-ESS).

ION SOURCE AND LEBT

A 2.45 GHz – 0.1 T PS-ESS has been designed and assembled at INFN-LNS in order to produce pulsed beams of protons up to 74 mA nominal current, at 75 keV of energy, with a transverse emittance containing 99 % of the nominal proton current below 2.25 π mm mrad. The specified beam stability between pulses during normal operation (in terms of current and emittance) shall be within ± 3.5 % variation and ± 2 % with respect to beam current, when averaged over a period of 50 µs.

The reliability goal for the overall accelerator is set to be better than 95 %. To meet this requirement the source's reliability has to be in excess of 99 %. This was a major design driver optimizing both MTBF and MTTR. The main disassembly procedure, as described in [1], can be performed without removing cooling pipes, sensor cables and all 500 A cables of the magnetic system as shown in Fig. 1. This allows venting and replacing of both extraction system and plasma chamber within the required time as specified in the contract between ESS and INFN.

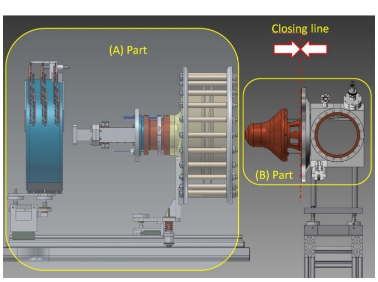

Figure 1: PS-ESS assembly schema. The solenoid and plasma chamber with extraction electrode chamber can be slided to gain fast access to all parts of this area.

Status and Initial Results

All major components of the source and LEBT have either been completed or are in their final stage of manufacturing. The source has been fully assembled in the test area in Catania as shown in Fig. 2, while only the first part of the LEBT, as needed during the initial stage of the commissioning, is assembled and ready for testing. This setup will house, once all devices have been delivered, a Faraday cup (FC), a Doppler shift monitor (DSM), an emittance measurement unit (EMU), and a beam stop.

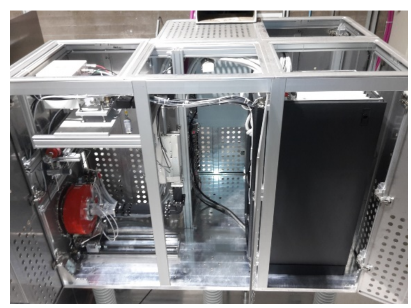

Figure 2: Picture of PS-ESS high voltage platform.

In June first plasma was achieved and thereafter plasma conditioning of the chamber performed. The obtained stability of the microwave power adsorbed by the plasma [2] is a first promising result to achieve the beam stability requested by ESS.

Next Steps

The first commissioning phase will focus on the characterization of the beam current generated by the source utilizing the FC and DSM. The EMU is scheduled to be delivered and installed in November. This will be followed by the second phase during which the main objective is to characterize the source's emittance as a function of different source parameter configurations. The plasma chamber conditioning is ongoing and the tests under thermal load have so far shown satisfactory results. Results of initial tests have been very promising and both INFN and ESS teams are confident for PS-ESS to reach the performance needed by the ESS.

* walter.wittmer@esss.se

DEVELOPMENT OF H^0 BEAM DIAGNOSTIC LINE IN MEBT2 OF J-PARC LINAC

J. Tamura*, A. Miura, T. Morishita, J-PARC, JAEA, Ibaraki, Japan
H. Ao, FRIB, MSU, Michigan, USA
T. Maruta, T. Miyao, J-PARC, KEK, Ibaraki, Japan
Y. Nemoto, Nippon Advanced Technology Co.,Ltd., Ibaraki, Japan

Abstract

In the Japan Proton Accelerator Research Complex (J-PARC), H^0 particles generated by collisions of accelerated H^- beams with residual gases are considered as one of the key factors of the residual radiation in the high energy accelerating section of the linac. To diagnose the H^0 particles, new beam line for analyzing H^0 and H^- particles was designed. The analysis line consists of four dipole magnets for giving the H^- beam chicane orbit, and a wire scanner monitor (WSM) for measuring the horizontal shift of the H^- beam. In the 2015 summer maintenance period, the new analysis line was installed in the second medium energy beam transport (MEBT2), which is the matching section from separated-type drift tube linac (SDTL) to annular-ring coupled structure linac (ACS). In the beam commissioning, we experimentally confirmed that the accelerated H^- beams are horizontally shifted in the analysis line as designed, and measured the H^0 signal obtained by the WSM plate as H^0 particles penetrating the plate.

INTRODUCTION

In J-PARC linac, H^0 particles generated by collisions of accelerated H^- beams with residual gases are considered as one of the key factors of the residual radiation in the ACS accelerating section [1]. Figure 1 shows the layout of the J-PARC linac accelerating structure. The H^- beam is accelerated to a beam energy of 190 MeV by the SDTL and to 400 MeV by the ACS. Although the lower energy beam has the larger cross section of the electron stripping in the residual gas scattering, the vacuum pressures in the SDTL section and the ACS section are around 10^{-6} Pa and 10^{-7} Pa, respectively. The beam loss at the ACS section was clearly related to the vacuum pressure of the SDTL sections [2].

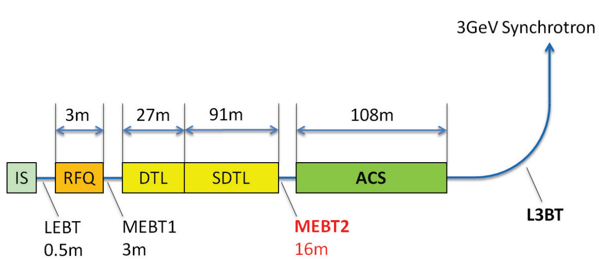

Figure 1: Layout of J-PARC linac accelerating structure.

To diagnose the H^0 particles generated in the SDTL section, we are developing a new diagnostic line in the upstream part of the MEBT2, which is the matching section from the SDTL to the ACS. We call this diagnostic line MEBT2 chicane. In the 2015 summer maintenance period, the new beam line for analyzing H^0 and H^- particles, which is the first stage of the MEBT2 chicane, was installed. In this paper, the configuration of the installed analysis line and the preliminary results of the beam analysis experiment are reported.

DEVELOPMENT OF MEBT2 CHICANE

In the new analysis line of the MEBT2, H^- and H^0 particles are analyzed by the shift bump magnets. The H^- beam is horizontally shifted by the first two dipole magnets (fig. 2) and returned to the original orbit (Z-axis) by the last two dipole magnets. It is noted that the horizontal displacement of $\Delta X \geq 20$mm of the accelerated H^- beam is required because the inner diameter of the beam duct is 37mm before the MEBT2 and is 40mm after the MEBT2. To confirm the horizontal shift of the H^- beam, a WSM and a non-destructive beam position monitor (BPM) are installed between the two sets of the dipole magnets. These components had to be installed within 3m long. The MEBT2 chicane installed in the 2015 summer maintenance period is shown in Fig. 3. The rectangular beam ducts with dimensions of $-50\text{mm} \leq X \leq 50\text{mm}$ and $-20\text{mm} \leq Y \leq 20\text{mm}$ are installed in these dipole magnets. The new beam line is evacuated by a turbo-molecular

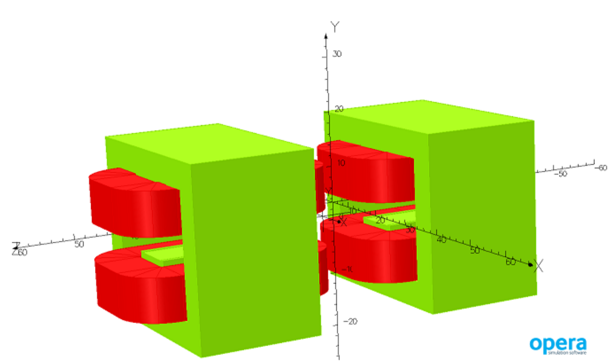

Figure 2: Designed dipole magnets for MEBT2 chicane.

* jtamura@post.j-parc.jp

ISBN 978-3-95450-169-4

HIGH-GRADIENT X-BAND STRUCTURES FOR PROTON ENERGY BOOSTER AT LANSCE

S. S. Kurennoy, L. J. Rybarcyk, LANL, Los Alamos, NM 87545, USA
V. A. Dolgashev, SLAC, Menlo Park, CA 94025, USA

Abstract

Increasing energy of proton beam at LANSCE from 800 MeV to 3 GeV improves radiography resolution ~10 times. Using superconducting RF cavities with gradients ~15 MV/m after the existing linac would result in a long and expensive booster [1]. We propose accomplishing the same with a much shorter cost-effective booster based on normal conducting high-gradient (~100 MV/m) RF accelerating structures. Such X-band high-gradient structures have been developed for electron acceleration and operate with typical RF pulse lengths below 1 µs. They have never been used for protons because typical wavelengths and apertures are smaller than the proton bunch sizes. However, these limitations do not restrict proton radiography (pRad) applications. A train of very short proton bunches with the same total length and charge as the original long proton bunch will create the same single radiography frame, plus pRad limits contiguous trains of beam micro-pulses to below 60 ns to prevent blur in images. For a compact pRad booster at LANSCE, we explore feasibility of two-stage design: a short S-band section to capture and compress the 800-MeV proton beam followed by the main high-gradient X-band linac.

INTRODUCTION

Proton radiography employs high-energy proton beams to image material behavior under extreme conditions. It was invented and developed at LANL, and by now the pRad program at LANSCE has performed hundreds of successful experiments, both static and dynamic. While the LANSCE 800-MeV linac accelerates both protons and H^- ions, the pRad uses H^- beam, which is presently the only beam species that can be chopped in the front end and directed to the pRad facility. For dynamic experiments, pRad uses multiple pulses from the linac, which, coupled with multiple optical viewing systems, produce movies up to a few tens of frames. Each short pRad beam pulse consists of several successive bunches from the linac, which follow at the linac DTL repetition rate of 201.25 MHz, to multiply the pulse total intensity. This is because the H^- bunch current at 800 MeV is limited to about 10 mA, mainly by the ion source, but also by losses in the linac. On the other hand, the pRad pulses are restricted to 60 ns in length, i.e. contain no more than 12 linac bunches, to prevent image blur. The future plans for LANSCE include a proton RFQ in a new injection line with a chopper that will deliver higher proton bunch currents, up to 30 mA. The new 750-keV 4-rod RFQ [2] has been recently delivered to LANL; its initial RF tests will be performed within next several months.

Increasing the beam energy for pRad at LANSCE from present 800 MeV to 3 GeV would provide significant improvements: for thin objects the radiography resolution would increase about 10 times, and much thicker objects could be also imaged [1]. A superconducting (SC) option for a pRad booster to 3 GeV was considered in [1]. Assuming a typical real-estate gradient of 15 MV/m, it leads to a rather long booster, ~150 m. This option is also expensive, in part because it requires a new cryogenic plant at LANSCE. We propose a much shorter and cheaper booster based on high-gradient (~100s MV/m) normal-conducting RF accelerating structures operating at low duty factors.

HIGH-GRADIENT STRUCTURES

High-gradient (HG) normal-conducting structures have been developed for accelerating electrons, e.g. [3]. Such structures operate at very high RF frequencies, usually in X band or higher, with short RF pulses – shorter than 1 µs. The work at SLAC and other labs demonstrated gradients 100-150 MV/m in both traveling-wave and standing-wave X-band cavities at 11.4 GHz with RF pulses of 100s ns [3]. A short standing-wave copper accelerating structure, cut along its axis for autopsy after high power tests, is shown in Fig. 1. Even higher gradients, up to 300 MV/m, were measured at 115-140 GHz, though with very short RF pulses of a few ns [4]. At such high RF frequencies, the structure aperture sizes are tiny, ~1 mm. In X band, the aperture diameter can exceed 1 cm; e.g., the beam aperture diameter of the cavity in Fig. 1 is 11.3 mm. The structure gradients are limited by various factors, most important of them are the peak surface electric field, peak pulse heating, and the modified Pointing vector, see in [3, 4].

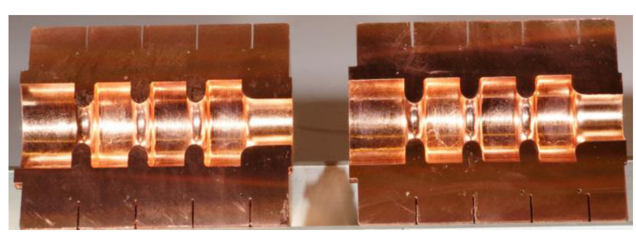

Figure 1: Cut of HG X-band copper accelerator cavity [3].

The HG structures have never been used for protons because their typical wavelengths and apertures sizes are smaller than the usual proton bunch sizes. However, these limitations of HG structures do not restrict their use for pRad applications. The pRad at LANSCE employs up to 12 long bunches from the 800-MeV proton linac to produce a single frame. Obviously, if a linac H^- bunch is

ProBE: PROTON BOOTING EXTENSION FOR IMAGING AND THERAPY*

S.Pitman[1†], R. Apsimon[1], G. Burt[1], Lancaster University, Lancaster, UK
A. Green, H. Owen[1], University of Manchester, Manchester, UK
A. Grudiev, A. Solodko, W.Wuensch, CERN, Geneva, Switzerland
[1]also at The Cockcroft Institute, Daresbury, UK

Abstract

Proton beam therapy is an alternative to traditional x-ray radiotherapy utilised especially for paediatric malignancies and radio-resistant tumours; it allows a precise tumour irradiation, but is currently limited by knowledge of the patient density and thus the particle range [1]. Typically X-ray computed tomography (CT) is used for treatment planning but CT scans require conversion from Hounsfield units to estimate the proton stopping power (PSP), which has limited accuracy . Proton CT measures PSP directly and can improve imaging and treatment accuracy. The Christie Hospital will use a 250 MeV cyclotron for proton therapy, in this paper a pulsed linac upgrade is proposed, to provide 350 MeV protons for proton CT within the facility. Space constraints require a compact, high gradient (HG) solution that is reliable and affordable.

INTRODUCTION

The precise dose delivery achievable with proton therapy requires accurate treatment planning to obtain the greatest benefit. Presently, margins defined around treatment volumes are greater in treatment planning than they might be, to account for uncertainties in CT scans. Proton CT (pCT) can reduce this margin of error by directly measuring the PSP of the tissue between the beam and the patient treatment volume (PTV). While head-and-neck and paediatric pCT is within the energy reach of current 230-250 MeV proton therapy machines, full adult pCT would require around 330-350 MeV to ensure the Bragg peak is outside of the patient.

The Christie Hospital (Manchester, UK) will soon have a 250 MeV cyclotron providing gantries with protons for treatment. A pulsed linac upgrade in 3 metres of space within the planned facility is proposed, to provide 350 MeV protons for pCT. This 3 m space must contain all aspects of this booster accelerator including radio-frequency (RF) cavities and beam focusing; such a system will require an RF linac with an accelerating gradient higher than any currently-existing structure at that particle velocity. The ProBE project was initiated to study the feasibility of such a linac.

RF DESIGN

Studies of high-beta cavities have shown that moving to higher frequencies (such as X band) can increase the gradient via the increased shunt impedance (R_s) per unit

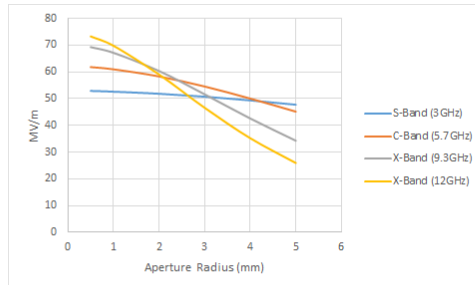

Figure 1: Aperture vs accelerating gradient based on shunt impedance and power per unit length.

length, provided the aperture is small enough [2]. It was not clear if this trend would continue at lower beta, hence we initially investigate a disk-loaded cavity with a medium beta (β=0.6) using CST Microwave Studio; S-band, C-band and X-band frequencies were all considered. Single-cell pillbox cavities were simulated with their septum thicknesses scaled inversely proportional to frequency from 1-4 mm. Due to the limited space and high gradient requirement, we chose to use one 50 MW klystron was per 1 m of linac. This and R_s per unit length were used to calculate the maximum gradient of each single cell.

The maximum gradient is strongly reliant on the aperture radius as can be seen in Figure 1, especially for X-band structures. However, nose cones can be added to increase the R_s of a structure at the expense of peak fields. The next step would be to add nose cones and decrease the gap to increase R_s until the peak fields at maximum gradient fall within reasonable limits. Based on results from the TERA collaboration on re-entrant cavities [3] it was decided to focus on the modified Poynting vector (S_c) as the key measure of peak fields [4], and a maximum value of 4 W/m^2 was chosen for the optimisation. It is also not entirely clear what the minimum septum thickness can be and how it scales with frequency, hence this parameter was varied during the optimisation. Proton imaging requires relatively low beam current (pA) so initially small apertures of 3.5 mm were utilised to maximise gradient, which we revisited later.

The results seen in Figure 2 show that these maximum gradients have very high peak surface electric fields (E_{peak}) which are thought to contribute to RF breakdown. HG tests performed on S-band and C-band cavities elsewhere have suggested that higher E_{peak} than the traditional Kilpatrick limit [5] can be reached within the S_c constraint; however the E_{peak} values seen in Figure 2 are still much higher than that [6,7]. To set a conservative limit, the breakdown rate (BDR)

* Work supported by STFC-IPS, Cockcroft Institute & The Christie Charity
† Sam.Pitman@cern.ch

ISBN 978-3-95450-169-4

FIRST HIGH POWER TESTS AT THE 325 MHz RF TEST STAND AT GSI

G. Schreiber, E. Plechov, J. Salvatore, B. Schlitt, A. Schnase, M. Vossberg,
GSI, Darmstadt, Germany

Abstract

A dedicated RF test stand for testing RF components and accelerating structures at 325 MHz has been put into operation at GSI. It allows testing the klystrons and circulators as well as the RFQ and the CH-acceleration cavities for the planned FAIR Proton Linac (p-Linac) and further cavity projects. The system integration has been completed and first high power tests with the CH prototype cavity were successfully performed. The operation parameters are 2 Hz repetition rate and 200 microseconds pulse length. Investigations on the critical path from wave guide to coaxial high power cavity coupler have been made. Performance measurements of the klystron, circulator and directional couplers with up to 2.7 MW on dummy load and the following conditioning process of the CH-prototype cavity with its coupled RF structures will be presented. Additionally the results of the conditioning of a ladder RFQ prototype are shown.

INTRODUCTION

The 325 MHz test stand at GSI was successfully operated in 2015 [1]. A Thales TH 2181 klystron is able to deliver up to 3 MW RF peak power. A linac 4 klystron modulator was rented from CERN and integrated into the GSI test stand and its interlock systems. All peripheral components, such as circulator, RF load and wave guides have been tested up to the nominal power [2].

Wave Guide Directional Coupler Calibration

Two pairs of directional couplers for measuring the forward and reflected RF power have been installed at the klystron output. Three pairs of directional couplers inserted into the wave guides between circulator and acceleration cavity are used for RF measurements, interlocking and cavity tuning. To achieve an accurate RF power measurement all wave guide WR2300 directional couplers have been calibrated with a special procedure [3]. An external compensation circuit has been installed to improve the directivity of the couplers up to -50 dB even with coaxial-N-transitions and waveguide loads providing a limited matching of worse than S_{11} = -30 dB. Precise power measurements and a reliable klystron protection at VSWR<1.2 in case of failure of the circulator are now assured. A transition from wave guide to coax 6-1/8 inch allows the connection to the coaxial RF cavity coupler. An additional directional coupler in this coaxial section allows a comparison with the wave guide couplers.

P-LINAC CH CAVITY – LOW-LEVEL MEASUREMENS

The FAIR Proton Linac CH prototype cavity [4], developed by the IAP University of Frankfurt [5], was installed at the test stand in the concrete shielded bunker and connected to the water cooling distribution (Fig. 1). The cavity consists of two CH cavities (CH1/CH2) with a RF coupling cell in-between. Fourteen fixed and three movable tuners are foreseen. The movable tuners are located at each cavity part and at the coupling cell. The RF power is fed into the coupling cell by an inductive loop [6]. Field flatness measurements have been done for the installation of the tuners by bead pull measurements.

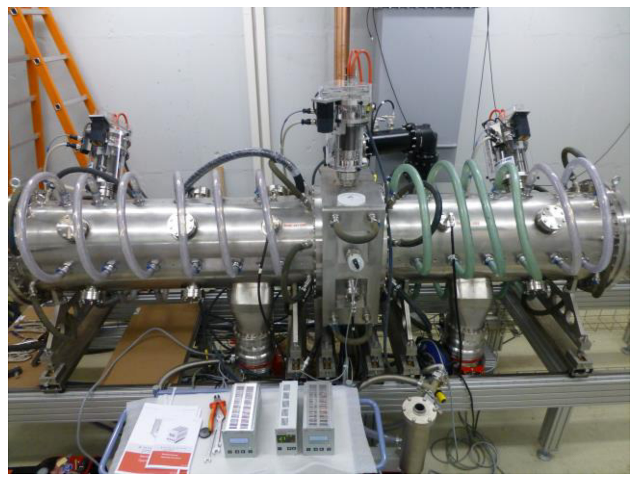

Figure 1: CH Cavity with three movable tuners and coaxial input line (black coloured).

Additional low-level measurements with a 4-port network analyser have been performed to investigate the tuner characteristics. The signal was applied to the RF input coupling loop. The RF pick-up probes at the coupling cell (S_{21}), CH1 (S_{31}) and CH2 (S_{41}) are shown in Fig. 2.

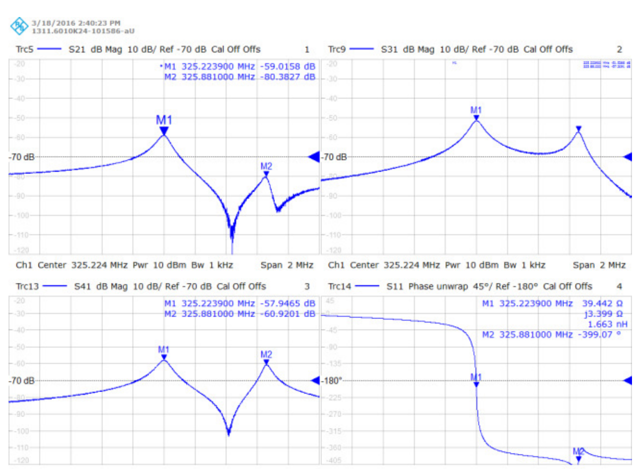

Figure 2: Low-level measurements, coupling cell (S_{21}, up left), CH1 (S_{31}, up right), CH2 (S_{41}, low left) and phase at the coupling cell input.

ISBN 978-3-95450-169-4

IMPLICATION OF MANUFACTURING ERRORS ON THE LAYOUT OF STABILIZATION SYSTEM AND ON THE FIELD QUALITY IN A DRIFT TUBE LINAC - RF DTL ERROR STUDY

R. De Prisco*, A. Karlsson, Lund University, Lund, Sweden
M. Eshraqi, Y. I. Levinsen, R. Miyamoto, ESS, Lund, Sweden

Abstract

The field flatness and the layout of the stabilization system in a drift tube linac are strongly dependent on the manufacturing errors that affect the local resonant frequency. In this paper a methodology is presented to study, firstly, the sensitivity of the resonant frequency and of the field flatness to each geometrical parameter of the drift tubes; then a set of tolerances for each parameter is found and a stabilization system layout is defined in order to keep the field flatness within an acceptable limit.

INTRODUCTION

The manufacturing errors of each part of a Drift Tube Linac, DTL, affect the Radio Frequency, RF, parameters. For this reason it is crucial to analyze the impact of these errors on the frequency and on the field flatness. According to the chosen tolerances it is possible, finally, to define the layout of the stabilization system.

In this paper the study is done for the ESS DTL [1] on which the first author has directly worked. The ESS DTL is an in-kind contribution from INFN/LNL [2, 3]. It is composed of five RF cavities (or tanks) that are used to accelerate a proton beam of 62.5 mA from 3.62 MeV to 89.68 MeV at 352.21 MHz; the transverse focusing system is composed of permanent magnet quadrupoles arranged in a F0D0 lattice.

IMPACT OF THE FIELD FLATNESS ON THE BEAM DYNAMICS

Four error studies are performed to evaluate the impact of the accelerating field flatness on the beam dynamics of the ESS DTL. For each study a set of 1000 simulations are performed using the tolerances defined in [4] and gradually increasing only the tolerance of the field flatness from 1% to 4% (steps of 1%). It is important to underline that *the error studies are executed by using fieldmaps* [5] obtained applying errors on the geometric parameters of the DTL and solving the Maxwell equations in each tank for each simulation.

In addition the four studies are repeated considering the error on E_0 as a random variable uniformly distributed within its tolerance as done in [6].

The results of the studies are reported in Fig. 1: it is clear that modeling the error on E_0 as a random variable, uniformly distributed within its tolerance, underestimates of the emittance growth and the beam losses within the

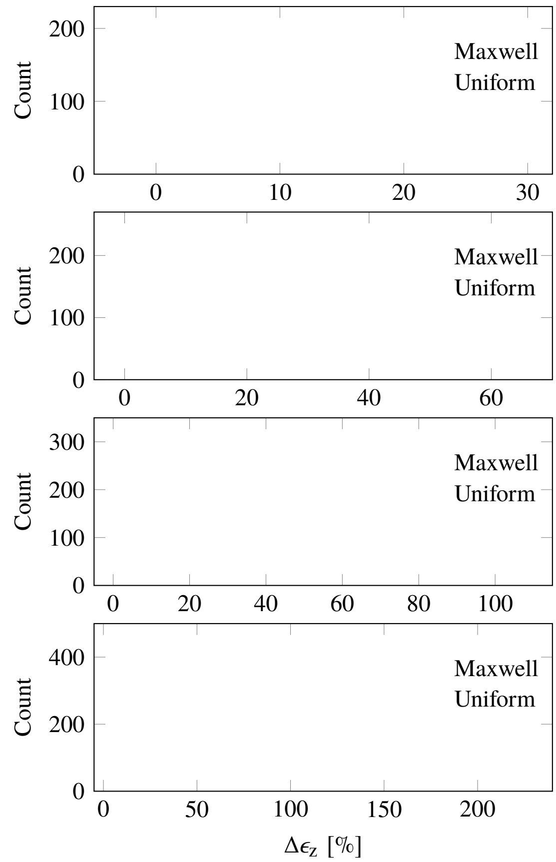

Figure 1: Additional longitudinal RMS emittance growth for the four error studies. The tolerance of the accelerating field flatness increases, from top to bottom, from 1% to 4%.

DTL. In addition the DTL output particle distribution is an inaccurate input for the downstream sections: this can lead to a dangerous underestimation of the emittance growth and of the beam losses in the rest of the ESS LINAC.

Keeping the DTL accelerating field flatness within 1% guarantees the ESS constraint on the losses (<1 W/m) is preserved for the entire ESS LINAC. The effect of a higher value of the flatness tolerance of the ESS DTL on the beam loss and on the emittance growth for all the sections following the DTL should be carefully investigated.

In the following sections a list of tolerances for all the drift tube geometrical parameters is found and a methodology to define the layout of the stabilization system is defined to keep the flatness within 1%.

* renato.deprisco@esss.se

INTEGRATION OF INTERFACES AND STABILIZATION SYSTEM IN THE DESIGN OF A DRIFT TUBE LINAC

R. De Prisco*, A. Karlsson, Lund University, Lund, Sweden
M. Eshraqi, Y. I. Levinsen, R. Miyamoto, ESS, Lund, Sweden

Abstract

Making an accurate Radio Frequency, RF, design of any accelerating structure is fundamental to ensure that electromagnetic and beam dynamics requirements will be achieved. This is essential for the most complicated accelerating structures like the Drift Tube Linac, DTL; in this case a meticulous design facilitates the RF commissioning too. In this paper the influence of the interfaces and of the field stabilization system on the RF design is analyzed and an advanced design methodology to mitigate field degradation is presented.

INTRODUCTION

A *preliminary design* of a DTL is usually done by considering the cavity as a stand alone object without the presence of the stems, of the stabilization system and of the interfaces (power couplers and vacuum grids) with the external systems. The preliminary design is very useful to reach the desired RF properties of the cavities and to optimize the *nominal* accelerating field [1]. Once the preliminary design is done it is necessary to *integrate* in the design the stems, the stabilization system and all the cavity interfaces, compensating their detuning, to keep the same properties and the same optimized accelerating field of the preliminary design.

In this paper the detuning induced by the stems, by the stabilization system and by the interfaces is evaluated; then its influence on the accelerating field is calculated; finally the integration of all the mentioned components in the design of the European Spallation Source, ESS, DTL design [2], on which the first author has directly worked, is proposed. The ESS DTL is an in-kind contribution from INFN/LNL [3,4]. It is composed of five RF cavities (or tanks) that are used to accelerate a proton beam of 62.5 mA from 3.62 MeV to 89.68 MeV at 352.21 MHz; the transverse focusing system is composed of permanent magnet quadrupoles arranged in a F0D0 lattice.

GLOBAL AND LOCAL FREQUENCIES

We can imagine the DTL tank as composed of N consecutive cells, each with its own resonant frequency, *local frequency*, such that the frequency of the tank is f_0, *global frequency* (for the ESS DTL f_0 is 352.21 MHz). As thoroughly discussed in [5], the desired flatness of the accelerating field in each DTL tank can be reached by properly tuning the frequencies of all the cells: at the end of the preliminary design a vector of N frequencies, *nominal local frequencies*, f_{0n}, with $n \in [1; N]$, is defined for each tank in order to get the *nominal accelerating field*, $E_{0,\mathrm{nom}}$ [1].

The insertion of the stems, post couplers and all the interfaces modifies the nominal local frequencies and induces undesired accelerating field tilts. To prevent these undesired tilts it is necessary to retune each cell such that the nominal local frequencies are preserved.

3D VS 2D SIMULATIONS

It is possible to use 2D simulations if the DTL can be considered cylindrically symmetric about the beam axis. This means that the detuning of the post couplers, the stems and the interfaces can be evaluated only with 3D simulations.

The Drift Tube, DT, geometry is accurately described in [6] in which the sensitivity of each geometrical DT parameter is calculated for the ESS DTL. Due to the fact that the DTs are located in a region in which the electromagnetic field changes rapidly and due to the fact that the ratio between the length of each DT parameter and the tank diameter is much smaller than 1, resolution requirements can lead to a very big number of mesh elements. For a fixed resolution, a 2D simulation requires less computational resource or, vice versa, fixed the computational resources, a 3D simulation, for a very complex structure, as each tank of the ESS DTL, could be performed only by decreasing the resolution requirements.

We define Δf as the difference between the frequency calculated with a 2D simulation, using $9 \cdot 10^3$ surface elements, and the frequency calculated with 3D simulation, using a tetrahedral mesh for the first *half* cell just 3.76 cm long, in Low Energy, LE, side, of the ESS DTL.

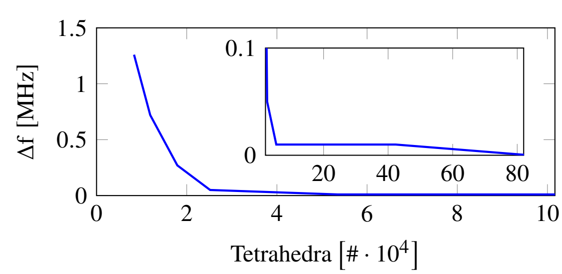

Figure 1: Dependence of the difference between the resonant frequencies, calculated by 3D and 2D simulations, from the 3D mesh elements for the first half cell, in LE side, of the first tank.

It is clear from the Fig. 1 that to have a *good resolution of each DTL cell* the amount of tetrahedra becomes enormous since each cell of the ESS DTL has a very detailed structure and since each tank is longer than 7 m [2]. In case of less

* renato.deprisco@esss.se

ISBN 978-3-95450-169-4

A 3 MeV LINAC FOR DEVELOPMENT OF ACCELERATOR COMPONENTS AT J-PARC

Y. Kondo*, H. Asano, E. Chishiro, K. Hirano, T. Ishiyama, T. Itou, Y. Kawane, N. Kikuzawa, S. Meigo, A. Miura, S. Mizobata, T. Morishita, H. Oguri, K. Ohkoshi, Y. Sato, S. Shinozaki, K. Shinto, H. Takei, K. Tsutsumi, JAEA, Tokai, Naka, Ibaraki, Japan
Z. Fang, Y. Fukui, K. Futatsukawa, K. Ikegami, T. Maruta, T. Miyao, K. Nanmo, T. Shibata, T. Sugimura, A. Takagi, KEK, Oho, Tsukuba, Japan
T. Hori, Nippon Advanced Technology Co., Ltd., Tokai, Japan
A. Ohzone, Hitachi Industry & Control Solutions, Ltd., Omika, Hitachi, Ibaraki, Japan
M. Mayama, Y. Sawabe, Mitsubishi Electric System & Service Co., Ltd., Tsukuba, Japan

Abstract

We have constructed a linac for development of various accelerator components at J-PARC. The ion source is same as the J-PARC linac's, and the RFQ is a used one in the J-PARC linac. The beam energy is 3 MeV and nominal beam current is 30 mA. The accelerator has been already commissioned, and the first development program, laser-charge-exchange experiment for the transmutation experimental facility, has been started. In this paper, present status of this 3-MeV linac is presented.

INTRODUCTION

The Japan Proton Accelerator Research Complex (J-PARC) is a multi-purpose facility for particle physics, nuclear physics, materials and life science, and study of transmutation. The J-PARC accelerator [1] consists of a 400-MeV linac, a 3-GeV rapid cycling synchrotron, and a 50-GeV main ring. The energy and peak beam current of the linac are 400 MeV and 50 mA, respectively. They were already achieved but to upgrade the J-PARC accelerator, components such as scrapers of beam chopper at the medium energy transport (MEBT) should be developed, and beam tests are necessary for these developments. However, the actual J-PARC linac is user operation machine, therefore, it is almost impossible to use it for the beam test of the components.

To this end, we constructed a 3-MeV linac on the first floor of the J-PARC linac building. This linac consists of a negative hydrogen (H^-) ion source, a low energy beam transport (LEBT), an radio frequency quadrupole (RFQ) linac, and a diagnostics bean line. A four-vane-type RFQ used for the J-PARC linac until the summer of 2014 (J-PARC RFQ I) is used for this 3-MeV linac: The design peak beam current of this RFQ is 30 mA, and replaced by a newly developed 50-mA RFQ. The duty factor of this linac is 0.6%, which corresponds to 0.5 kW. The accelerator itself has a capacity of at least 1 kW. However, the beam power is limited by radiation dose, because there are no radiation shields between the accessible area during the operation.

At first, we are planning to conduct experiments of the laser-charge-exchange development for the transmutation experimental facility. Then, this linac will be used for the development of scrapers, bunch-shape monitors, laser profile monitors, and others. We will be able to install new devices into the actual J-PARC linac after the full testing. Developments of ion sources can be carried out at this system, and also RFQs in the future.

In this paper, details of this linac and the preliminary result of the first application are described.

EXPERIMENTAL APPARATUS

Figure 1 shows a photograph of the 3-MeV linac.

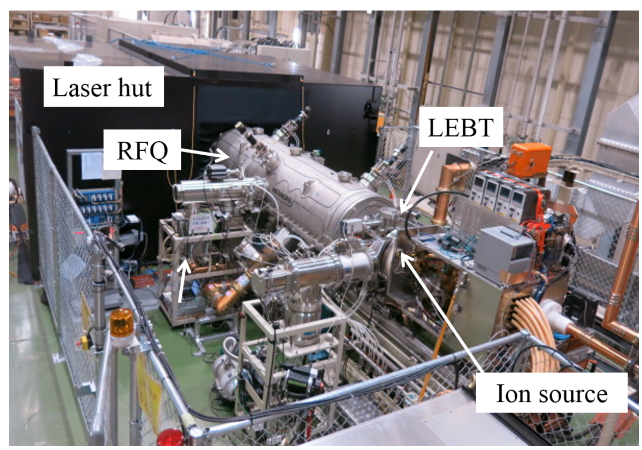

Figure 1: Photograph of the 3-MeV linac.

The same RF driven ion source for the J-PARC linac [2] is employed. The plasma is driven by a pulsed 2-MHz RF power, and a 30-MHz continuous wave RF is also used to ignite the plasma. A 60-kW solid-state amplifier system is used as the RF source. The extraction energy is 50 keV. The LEBT is equipped with two solenoid magnets, and the space charge neutralization effect is also used to focus the beam. The beam current injected to the RFQ is measured using a movable Faraday cup or a slow current transformer located between the two solenoid magnets.

Table 1 lists the parameters of the RFQ.

The cavity of J-PARC RFQ I is contained in a large vacuum vessel [3]. The cavity is not longitudinally segmented, and the vane length is 3115 mm. It consists of four vanes and they are bolted together. The material of the cavity is

* yasuhiro.kondo@j-parc.jp

THE EFFECT OF DTL CAVITY FIELD ERRORS ON BEAM SPILL AT LANSCE*

L. J. Rybarcyk†, R. C. McCrady, Los Alamos National Laboratory, Los Alamos, NM, 87545 USA

Abstract

The Los Alamos Neutron Science Center (LANSCE) accelerator comprises two (H+ and H-) 750-keV Cockcroft-Walton style injectors, a 201.25-MHz, 100-MeV drift-tube linac (DTL) and an 805-MHz, 800-MeV coupled-cavity linac (CCL). As part of the LANSCE Risk Mitigation project a new digital low-level radio frequency (LLRF) control system is being deployed across the linac, starting with the DTL. Related to this upgrade, a study was performed where specific cavity field errors were simultaneously introduced in all DTL tanks about the nominal stable, low-spill, production set points to mimic LLRF control errors. The impact of these errors on the resultant beam spill was quantified for the nominal 100 µA, 800-MeV Lujan beam. We present the details of the measurement approach and results that show a rapid increase in total linac beam spill as DTL cavity field phase and amplitude errors are increased.

INTRODUCTION

The LANSCE facility employs a room temperature 800-MeV linac to produce both proton and H- beams for several user programs. The linac consists of a 100-MeV, 201.25-MHz, four-tank DTL structure followed by a 800-MeV, 805 MHz, 44 module CCL structure. During normal operations, beam spill along the linac, proton storage ring (PSR) and beamlines to the target can be attributed to several factors, one of which is cavity field error. During normal operation, linac machine parameters are usually tweaked to achieve a stable, low-loss tune. These tweaks include adjustments to many of the linac RF phase and amplitude set points. Although these new set points result in relatively low beam spill during operations, cavity field errors can introduce deviations about these nominal values and may result in excursions in beam performance, including increased spill along the linac.

An effort is currently underway to upgrade the linac LLRF control system with a modern digital equivalent. The legacy analog system used along the linac has provided nominal amplitude and phase control estimated to be better than 0.1% and 0.1˚, respectively, during the steady-state portion of a typical 625 µs beam macropulse. During the beam turn-on transient, LLRF amplitude and phase errors typically exceed these values but remain below the fast-protect trip point of 1% and 1˚, respectively. Although the new digital system is expected to achieve same or better performance, the question arose about the impact of larger control errors, i.e. cavity field errors, on beam spill during operations. The work reported here was aimed at quantifying the beam spill associated with larger cavity field errors in the DTL.

EXPERIMENT DETAILS

The experiment was conducted on the LANSCE linac and beam lines that provide 800-MeV beam to PSR and the Lujan Center neutron spallation target. The "Lujan" beam, nominally 100 µA with a duty factor of 20 Hz x 625 µs, is "chopped" in the 750-keV low-energy beam transport (LEBT) to provide an extraction gap for the PSR. The chopping results in a typical beam "minipulse" with 290 ns out of 358 ns. During these measurements, we used the duty factor and the minipulse countdown, i.e. "1-of-n" to reduce the average beam current well below the 100 µA in order to keep the beam on when spill was excessive and interruptions would have otherwise occurred. All results were renormalized to an average beam current of 100 µA.

Beam current and loss monitors along the CCL and downstream beam lines were used to document the average current and spill levels, respectively. We also recorded the status of the beam fast-protect system to ensure that beam was uninterrupted during the measurements.

We used a simplified approach to introduce errors in the DTL cavity fields during these measurements, where the errors are static offsets in amplitude and phase from the nominal production set points. For the purpose of these measurements we assumed that the same LLRF controllers would simultaneously allow a distribution of errors with the same maximum magnitude in percent of amplitude and degrees of phase on all DTL modules, e.g. 0.5% and 0.5˚, respectively. Initially, we used HPSim [1] to simulate beam spill along the CCL due to these types of DTL cavity field errors. In the model the linac was configured to approximate the linac operating at production levels. A typical set of simulations consisted of 1000 different combinations of random, uniformly distributed errors up to the maximum amplitude and phase, respectively on all DTL modules. The simulated beam losses were extracted from all runs so that rms and maximal values could be determined. From these data, we observed a correlation between the extreme beam loss and maximal cavity errors. Initially, we considered the above approach for the experiment, i.e. 1000 different error combinations. However, limited beam-development time and risk of failure to the existing mechanical phase-shifter packages led us to choose a different approach. Instead, we introduced only maximal static field errors in each DTL cavity as deviations about their nominal production set points. For each maximal static error a total of 2^4 different combinations consisting of either same-sign (+,+ or -,-) or opposite-sign (+,- or -,+) intra-tank (amplitude, phase) errors were applied to the DTL. Although limited

* Work supported by the United States Department of Energy, National Nuclear Security Agency, under contract DE-AC52-06NA25396.

† lrybarcyk@lanl.gov

ISBN 978-3-95450-169-4

ENERGY STABILITY OF ERLS AND RECIRCULATING LINACS

R. Eichhorn†, J. Hoke, Z. Mayle, CLASSE, Cornell University, Ithaca, NY, USA

Abstract

Energy recovery linacs can be seen as a hybrid between a linear and a circular accelerator. It has been shown in the past that an appropriate choice of the longitudinal working point can significantly improve the energy stability of a recirculating linac. In this contribution we will expand the concept of energy recovery linacs and investigate the energy spread of the beam as well as the recovery efficiency stability which can be a more demanding quantity in a high current ERL.

INTRODUCTION

The principle of phase focusing in longitudinal phase space is well known and essential for the operation of circular machines like synchrotrons and storage rings. It is also applied in low and medium beta linear accelerators. However with high beta linacs, the acceleration of the particles is usually done on-crest.

Recirculating linacs and energy recovery linacs usually also use on-crest acceleration with a beam transport system tuned to isochronisity. In that case, the machine has no inherent longitudinal stability, and as a result the bunch length and the stability of the RF field inside the accelerating cavities determine the energy spread of the beam.

As pointed out earlier for recirculating linacs [1,2], the choice of an off-crest synchronous phase together with a non-isochronous beam transport system can offer a longitudinal stability, thus reducing the effects of amplitude and phase jitter of the accelerating cavities in the linac. We will apply this concept to energy recovery linacs and also investigate the role of path length variations that may be caused by thermal drifts.

LONGITUDINAL TRACKING

Concept

For our simulations we assumed a particle distribution entering a linac at low energy. This beam is assumed to be accelerated 5 times and decelerated again. The linac is modelled to have several cavities operated and powered individually at a certain gradient and at a given synchronous phase, which we define with respect to the maximum field. Each cavity is assumed to have a certain field stability in terms of amplitude and phase jitter. The recirculation arcs are represented by their longitudinal dispersion and are assumed to have an integer (half integer for the highest energy arc before the beam is decelerated again) wavelength. For some of the simulations, a random error to the path length was added to simulate thermal effects. Figure 1 gives a layout of the machine scenario.

† r.eichhorn@cornell.edu

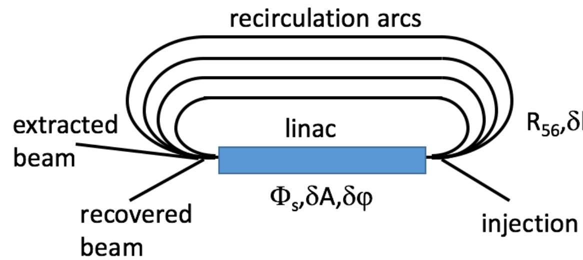

Figure 1: Recirculating linac/energy recovery linac scenario calculated within this paper. R_{56} and Φ_S are the parameters under which the linac and the arcs are operated. δA and δφ are the jitters that are applied to the cavity fields and δl is the random path length variation.

The particle bunch was tracked through the machine within an "inner" calculation loop. This sent a single particle bunch through a simulated linac for N passes. We used an "outer" calculation loop to reiterate the "inner" loop with randomized jitters in the cavity field as well as in path length variation. Every data point given represents the outcome of the outer loop calculation, which is an overlay of all phase space distributions. It represents the beam properties to be expected when accelerating many bunches. Our code was programmed in Python® to assure quick execution. All parameters are easy to change, and a reference ("ideal") particle is tracked to ensure consistency. We also benchmarked our code by reproducing results from earlier calculations.

Parameters

We ran our simulations using realistic parameters and a configuration planned for the C-BETA project [3]. The injection energy in this case is 6 MeV, the energy spread was assumed to be 10^{-3} and the phase spread to be 0.5°. We represented the beam by 1000 particles with Gaussian distributions in energy and phase.

The linac in the case of the C-BETA linac houses six cavities, oscillating at 1.3 GHz and providing a gradient of 6 MV. Random errors for the phase between ±0.5° and for the amplitude between $\pm 10^{-4}$ were assumed. For every inner loop a constant but different amplitude and phase error was allotted to every cavity. This is due to the fact that the fluctuations of the field are typically driven by microphonics and occur on the time scale of milliseconds or more, while the accelerated beam passes through the machine in some 100 microseconds or less. For calculations with path length variations, we assumed individual contributions for every recirculation, being constant within the inner loop. In the outer loop, field errors and path length contributions were re-assigned and the resulting phase space can be seen as an average over a period of

X-BAND PHOTONIC BAND GAP ACCELERATING STRUCTURES WITH IMPROVED WAKEFIELD SUPPRESSION*

Evgenya I. Simakov#, Los Alamos National Laboratory, Los Alamos, NM 87545, U.S.A.

Abstract

We designed a new photonic band gap (PBG) accelerating structure with elliptical rods and improved wakefields suppression. The experimental characterization of the wakefield spectrum in a PBG accelerator with an electron beam was recently performed at Argonne Wakefield Accelerator facility, and the superior wakefield suppression properties of the PBG structure were demonstrated. In 2013 the team from MIT and SLAC demonstrated that the X-band PBG structures with elliptical rods have reduced breakdown rate compared to PBG structures with round rods, presumably due to the reduced surface magnetic fields. However, the structure with elliptical rods designed by MIT confined the dipole higher order mode in addition to the accelerating mode and thus did not have superior wakefield suppression properties. We demonstrate that PBG resonators can be designed with 40% smaller peak surface magnetic fields while preserving and even improving their wakefield suppression properties as compared to the structure with round rods. The structure will be fabricated, tuned, and tested for high gradients and for wakefield suppression.

INTRODUCTION

The next generation of linear accelerators has to address the unprecedented requirements on electron beam's quality, acceleration gradients, and peak currents. The accelerating cavities for the future machines must be able to provide acceleration for the high currents while at the same time preserving the tightly focused low emittance beam. The higher order mode (HOM) wakefields that get excited more easily by the high current electron bunches can affect the quality of the beam and must be suppressed. Photonic Band Gap [1] (PBG) cavities have the unique potential to filter out HOM power and greatly reduce wakefields. The first ever demonstration of acceleration in a PBG resonator was conducted at Massachusetts Institute of Technology (MIT) in 2005 [2]. Since then, a number of important PBG accelerator experiments have been conducted which improved our understanding of the PBG accelerators, their limitations, and ability to suppress wakefields.

The first experimental observation of excitation and suppression of wakefields in a PBG accelerator structure was recently conducted at the Argonne Wakefield Accelerator [3]. It was demonstrated that the Q-factors of most major HOMs could be reduced to about 100 in the structure consisting of 16 PBG resonators with the accelerating frequency of 11.700 GHz. However, previous experiments by the team from MIT and SLAC [4] demonstrated that because of the relatively high peak surface magnetic fields on the rods of the PBG structure, the performance of the PBG accelerator may not be optimal at high gradients. The MIT team suggested that if the shape of the six innermost rods of the PBG structure was changed from round to elliptical, then the peak surface magnetic fields would be reduced and the high gradient performance of the PBG resonator would improve [5].

MIT came up with the new design for the PBG resonator with six elliptical rods and tested it at high gradients demonstrating better performance as compared to the resonators with round rods [5]. However, the question remained if the new MIT resonator would be as effective with regards to the HOM suppression as the original PBG resonator with round rods.

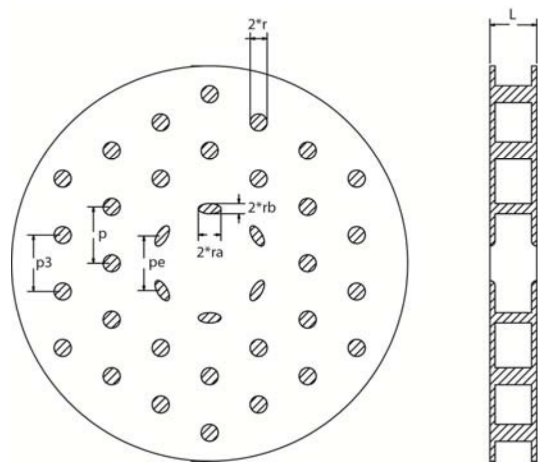

Figure 1: A schematic of the PBG resonator with six elliptical rods.

DOE HEP funded a project at Los Alamos National Laboratory (LANL) to conduct the thorough investigation of the X-band PBG resonators with elliptical rods and design and test a resonator with elliptical rods, reduced peak surface magnetic fields, and improved suppression of wakefields.

DESIGN OF 11.7 GHZ TW PBG RESONATOR WITH ELLIPTICAL RODS

We started the design of the new PBG resonator with the optimization of the shape of the elliptical rod for the minimal magnetic field. Similar optimization was already conducted by our team for the case of the

*Work is supported by the U.S. Department of Energy (DOE) Office of High Energy Physics.

#smirnova@lanl.gov

ELECTRO-MECHANICAL MODELING OF THE LCLS-II SUPERCONDUCTING CAVITIES*

O. Kononenko†, C. Adolphsen, Z. Li, T. Raubenheimer, C. Rivetta, SLAC National Accelerator Laboratory, Menlo Park, USA

Abstract

The 4 GeV LCLS-II superconducting linac will contain 280, 1.3 GHz TESLA-style cavities operated CW at 16 MV/m. Because of the low beam current, the cavity bandwidth will be fairly small, about 32 Hz, which makes the field stability sensitive to detuning from external vibrations and He pressure fluctuations. Piezo-electric actuators will be used to compensate for the detuning, which historically has been difficult at frequencies above a few Hz due to excitation of cavity mechanical resonances. To understand this interaction better, we have been doing extensive modeling of the cavities including mapping out the mechanical modes and computing their coupling to Lorentz forces, external vibration and piezo actuator motion. One goal is to reproduce the measured detuning response of the piezo actuators up to 1 kHz, which is sensitive to how the cavities are constrained within a cryomodule. In this paper, we summarize some of findings.

INTRODUCTION

The LCLS-II project [1] has adopted TESLA-style superconducting cavities [2] for the 4 GeV CW linac being built at the SLAC National Accelerator Laboratory. It will deliver high-brightness, high-repetition-rate electron beams that will drive an X-ray FEL. When operating the narrow bandwidth (BW) TESLA cavities at 16 MV/m, feedback systems [3] will be used to stabilize the cavity fields and frequencies. The BW of the latter is limited by the response of the cavity mechanical resonances.

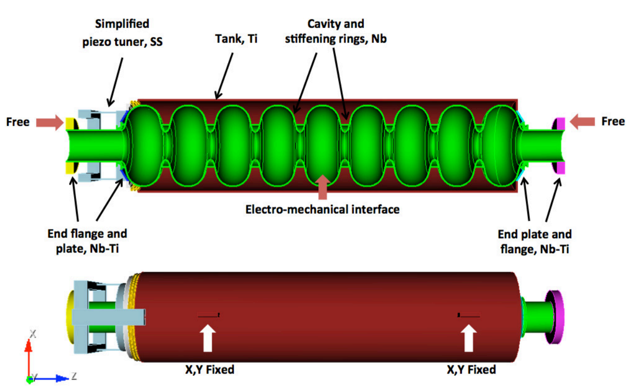

Figure 1: 3D mechanical model of the TESLA cavity.

To understand this effect better, we performed extensive analysis of the coupled electro-mechanical interaction between the RF fields, cavity motion and deformations. The massively-parallel ACE3P simulation suite [4] was used to determine mechanical eigenmodes of the cavity, their coupling to Lorentz and piezo tuner [5] forces as well as to calculate the corresponding RF responses.

In this paper the 3D cold mechanical model of the superconducting TESLA cavity in a helium vessel is considered, where the piezo-electric tuner is replaced by the spring of equivalent stiffness, i.e. 30 N/um [5]. The model, material details and boundary conditions are shown in Fig. 1.

We also study the corresponding vacuum model of the cavity, which is used to calculate RF detuning due to mechanical deformations - see Fig. 2.

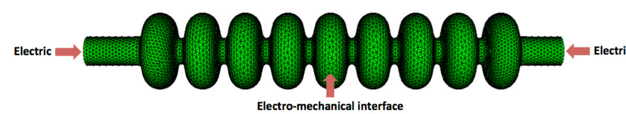

Figure 2: Meshed vacuum model of the TESLA cavity.

The electro-mechanical interface, essentially the cavity internal surface shown in Fig. 1 and Fig. 2, serves as the boundary between the RF and mechanical simulations.

MECHANICAL EIGENMODES

Using the mechanical model we have simulated eigenmodes of the TESLA cavity. The frequencies of the first 20 modes are shown in the Table 1.

Table 1: Eigenmodes of the cavity, longitudinal modes are listed in red.

Mode #	Frequency [Hz]	Mode #	Frequency [Hz]
1	51	11	260
2	57	12	265
3	103	13	299
4	133	14	350
5	145	15	351
6	179	16	386
7	185	17	395
8	221	18	438
9	239	19	441
10	254	20	463

In Fig. 3 we show the surface displacements, indicated in magnitude and direction by the color scale and arrows, for the transverse mode at 57 Hz as well as for two longitudinal modes at 239 Hz and 299 Hz.

It should be noted here that this simulation doesn't take into account any damping or friction nor the effect of the liquid helium within the tank.

* Work supported by DOE Contract No. DE-AC02-76SF00515
† Oleksiy.Kononenko@slac.stanford.edu

MESA - AN ERL PROJECT FOR PARTICLE PHYSICS EXPERIMENTS*

F. Hug#, K. Aulenbacher, R. Heine, B. Ledroit, D. Simon
Johannes Gutenberg-Universität Mainz, Mainz, Germany

Abstract

The Mainz Energy-recovering Superconducting Accelerator (MESA) will be constructed at the Institut für Kernphysik of the Johannes Gutenberg University of Mainz. The accelerator is a low energy continuous wave (CW) recirculating electron linac for particle physics experiments.

MESA will be operated in two different modes serving mainly three experiments: the first is the external beam (EB) mode, where the beam is dumped after being used with the external fixed target experiment P2, whose goal is the measurement of the weak mixing angle with highest accuracy. The required beam current for P2 is 150 µA with polarized electrons at 155 MeV. Additionally a so called beam-dump experiment (BDX) is planned to run in parallel to P2.

In the second operation mode MESA will be run as an energy recovery linac (ERL). The experiment served in this mode is a (pseudo) internal fixed target experiment named MAGIX. It demands an unpolarized beam of 1 mA at 105 MeV. In a later construction stage of MESA the achievable beam current in ERL-mode shall be upgraded to 10 mA.

Within this contribution an overview of the MESA project will be given highlighting the latest accelerator layout and the challenges of operation with high density internal gas targets.

INTRODUCTION

The MESA accelerator has been planned since approx. 2009 [1] and has undergone several design changes during that time as the layouts and requirements of the experiments have been refined as well [2,3]. MESA is planned to be constructed inside of existing underground halls formerly used by one experimental setup (A4) at the microtron MAMI [4]. Since A4 has been decommissioned the existing halls are free now and can be used by MESA. MAMI nevertheless will continue operation in parallel. In

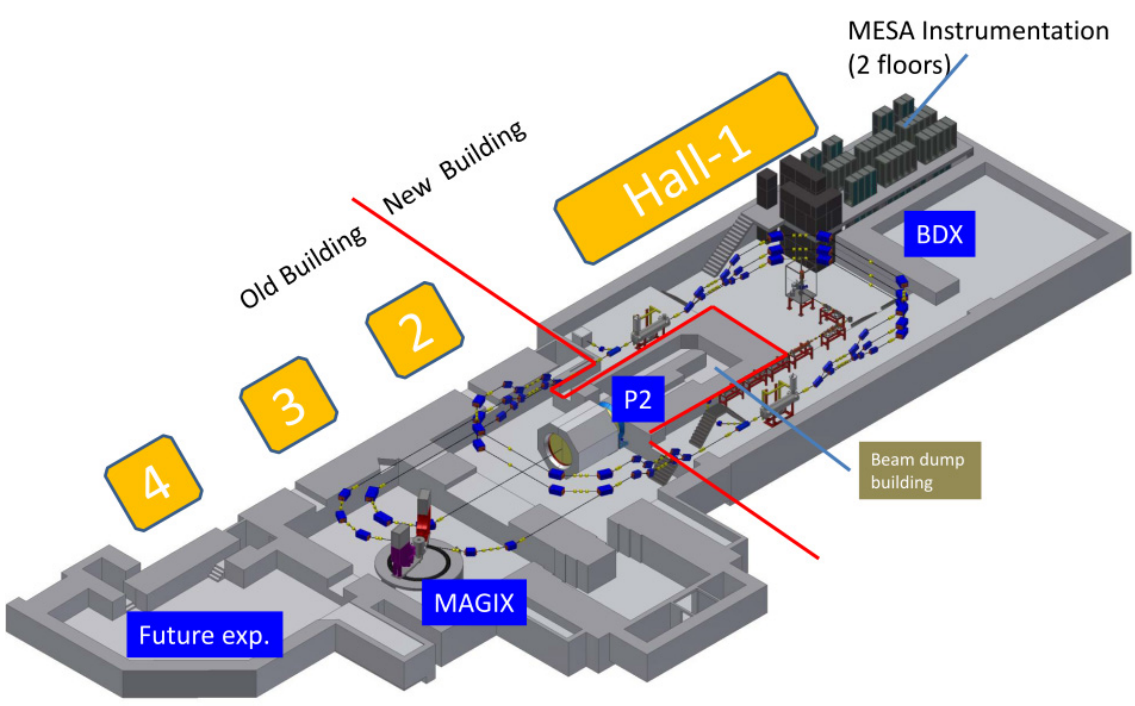

Figure 1: Layout of the MESA accelerator and planned experiments. The accelerator will be located in two existing (No. 2&3) and one new (No. 1) underground halls. The boundary between the old and new part of the building is marked by a red line. Hall 4 can be used at a later stage for additional experiments if needed. Construction of new Hall 1 will start in 2018.

*Work supported by DFG through CRC 634, RTG 2128 and PRISMA cluster of excellence
#hug@kph.uni-mainz.de

ISBN 978-3-95450-169-4

COMMISSIONING STATUS OF THE CHOPPER SYSTEM FOR THE MAX IV INJECTOR

D. Olsson*, J. Andersson, F. Curbis, L. Isaksson, L. Malmgren, E. Mansten, S. Thorin
MAX IV Laboratory, Lund, Sweden

Abstract

The MAX IV facility in Lund, Sweden consists of two storage rings for production of synchrotron radiation, and a short-pulse-facility (SPF). The two rings are designed for 3 GeV and 1.5 GeV, respectively, where the initial beam commissioning of the former has recently been completed, and commissioning of the latter was started in September 2016. Both rings will be operating with top-up injections delivered by a full-energy injector. In order to reduce losses of high-energy electrons along the injector and in the rings during injection, only electrons that are within a time structure where they can be accumulated in the ring buckets are accelerated. Electrons outside this time structure are dumped before they reach the first LINAC structure by a chopper system. The performance of the chopper system during commissioning of the 3 GeV ring is presented in this paper.

INTRODUCTION

The MAX IV injector consists of 39 travelling-wave S-band LINAC structures that are fed via SLED systems [1]. It provides top-up injections for two storage rings at 3 GeV and 1.5 GeV, respectively. The injector also operates as a driver for a short-pulse-facility (SPF) [2], and might be the driver for a future free-electron laser (FEL) [3]. Initial beam commissioning of the 3 GeV ring was completed in the summer of 2016, and the facility will soon open up for the user community. The beam commission of the 1.5 GeV was started in September 2016.

For ring injections, the electron source is a thermionic S-band RF gun that delivers an electron pulse with a length of $\approx 1\ \mu s$ [4]. This electron pulse is bunched with an S-band structure, and only a fraction of its charge can be accumulated in the rings during injection. The RF systems in both rings are operating at 100 MHz, and the number of S-band bunches that can be accumulated in each ring bucket depends on parameters such as available RF voltage and the radiation losses. In its final state, the number of S-band bunches that can be accumulated in each bucket in the 3 GeV ring might vary between 4 and 7, while the number might be as high as 19 in the 1.5 GeV ring [5]. Due to the SLED systems, the accelerated electron pulse has an energy chirp [6] which limits the number of ring buckets that can be injected during each LINAC shot because of the finite momentum acceptance in the transport lines to the rings [7].

Electrons that can not be accumulated during injection are dumped before they reach the first LINAC structure by a chopper system. The electron losses at high energies, as well as the emitted bremsstrahlung, are by that minimized. Apart from protecting personnel and sensitive electronic equipment from radiation, it also reduces radiation-induced demagnetization of the permanent magnets in insertion devices (IDs). Such magnet degradation does not only reduce the undulator/wiggler parameter, K, but does also result in an extra broadening of the spectral lines since the demagnetization is often non-uniform along the IDs [8] [9].

THE CHOPPER SYSTEM

The chopper system consists of two planar striplines with corrector magnets placed around them, as seen in the schematic overview in Figure 1. By adjusting the strengths of the correctors and the shape of the counter propagating TEM waves that are fed to the striplines, only the S-band bunches within the desired time structure experience a net deflecting force that is zero when passing each stripline. S-band bunches that are outside this time structure are vertically deflected and dumped at a downstream located adjustable aperture.

The first stripline is fed with a superposed signal consisting of one 100 MHz, one 300 MHz, and one 700 MHz signal. These three signals can be generated as harmonics (in a comb generator) from any of the 100 MHz main RF signals of the two rings. By doing so, the superposed signal is always phase locked to the RF system of the ring that is being injected. After the three signals have been generated, they are amplified and combined in a cavity filter and fed to the first stripline, as shown in Figure 1. Note that the combined signal is circulated through both stripline electrodes, and the total electrical length is adjusted so that the propagating mode in the stripline is an odd (differential) TEM mode at odd harmonics of 100 MHz. By adjusting the amplitudes of the three signals, it is possible to change the number of S-band bunches per 10 ns period that enters the main injector, i.e. the number of S-band bunches that are injected into each ring bucket. This is illustrated in Figure 2, where the vertical displacement at the position of the aperture is shown for the driving scheme that has been used during commissioning of the 3 GeV ring. With this driving scheme, only 3 S-band bunches per 10 ns period pass the boundaries of the aperture, while the rest are dumped. In [5], other driving schemes are presented where up to 15 S-band bunches per ring bucket are injected.

By feeding two high-voltage pulses with different polarities to the second stripline, the total length of the electron pulse that enters the main injector can be adjusted, i.e. the number of ring buckets that are injected during each LINAC shot. These pulses are generated by commercial switch

* email: david.olsson@maxiv.lu.se

HIGH POWER RF REQUIREMENTS FOR DRIVING DISCONTINUOUS BUNCH TRAINS IN THE MaRIE LINAC*

J. Bradley III, A. Scheinker, D. Rees, R. L. Sheffield, LANL, Los Alamos, NM, U.S.A.

Abstract

The MaRIE project Pre-Conceptual Referenced Design is based on a superconducting linac to provide 12 GeV electron bunches to drive an X-ray FEL. Dynamic experiments planned for MaRIE require that the linac produce a series of micropulses that can be irregularly spaced within the macropulse, and these patterns can change from macropulse to macropulse. Irregular pulse structures create a challenge to optimizing the design of the RF and cryogenic systems. General formulas for cavities with beam loading can overestimate the power required for our irregular beam macropulse. The differing beam energy variations allowed for the XFEL and eRad micropulses produce cavity voltage control requirements that also vary within the macropulse. The RF pulse driving the cavities can be tailored to meet the needs of a particular beam macropulse because the macropulse structure is known before the pulse starts. We will derive a toolkit that can be used to determine the required RF power waveforms for arbitrary macropulse structures. We will also examine how the irregular RF power waveforms can impact RF and cryogenic system cost trade-offs.

OVERVIEW OF THE PRESENT MaRIE DESIGN

The purpose of the Matter-Radiations Interactions in Extremes (MaRIE) project is to investigate material properties in extreme conditions and record how these conditions evolve over time. Long macropulses are important because the conditions of interest change over a time-scales of 1 ms, but also can change very quickly at any time within this time period.

The Pre-conceptual Reference Design uses a superconducting 12 GeV linac to drive a 42 keV X-ray FEL with a train of up to 0.2 nC electron bunches with an average current of 8 mA over a macropulse of 69ns to 700µs (1000µs goal) [1]. The linac is made up of 1.3 GHz TESLA style cavities operating at the ILC design point of 31.5 MV/m, (implying 32.7 MV/cavity, 121.713 J/cavity, and 367 active cavities).

The main linac will also accelerate electron radiography (eRad) micropulses that will be interleaved with the micropulses driving the X-ray FEL.

CHALLENGES UNIQUE TO PLANNED OPERATION MODES AT MaRIE

The MaRIE linac is a pulsed machine with irregularly spaced micropulses within each macropulse [1]. The irregular spacing provides a particular challenge to the RF system driving the accelerating cavities.

The exact micropulse structures for MaRIE are still subject to modification at this point in the project, but in general they are as follows: The X-Ray FEL will use a train of up to 0.2 nC electron bunches with an average current of 8 mA over the macropulse, but in the last part of the macropulse the spacing between micropulses decreases dramatically. In the last 230 ns the pulse spacing can be as small as 2.3 ns. The power feeding the main linac cavities is sized for a continuous 8 mA beam, so the concentration of pulses in the last part of the macropulse will cause the cavities in the main linac to lose energy and the accelerating voltage to droop. A 0.01% electron beam energy tolerance sets a limit on the allowable energy depletion of an electron bunch on the cavity voltage for a succeeding bunch [2].

One design option is for simultaneous electron radiography (eRad) with 2 nC micropulses. These larger charge bunches are interleaved in the same macropulse with the smaller charge bunches that drive the X-ray FEL, further complicating the RF drive requirements. Each eRad micropulse is separated from following micropulses with a spacing of at least 23 ns.

CONTINUOUS AND DISCONTINUOUS BEAM LOADING FORMULAS

Continuous Beam Loading Model

The forward RF power required by a cavity with heavy continuous beam loading [3] assuming: $Q \gg Q_e$, on-crest operation and neglecting microphonics simplifies to the well known power requirement formula for flattop operation

$$P_{f\_maintain} \approx \frac{V_{eff}^2}{4Q_e\left(\frac{R}{Q}\right)}\left(1+\frac{I_b\left(\frac{R}{Q}\right)Q_e}{V_{eff}}\right)^2$$

Discontinuous Beam Loading Model

The discontinuous beam loading model essentially applies a piecewise approximation to the continuous beam model. The following assumptions apply: a cavity/coupler system with time constant $\tau_L = 2Q_L/\omega$ and an external coupling $Q_e \ll Q_0$, a micropulse with charge q_n enters the cavity at t_n, then the micropulse decreases the cavity stored energy $U(t_n)$ from the value just before the bunch enters by the energy the bunch removes from the cavity, $V_c(t_n)\,q_n$; and that this happens instantaneously; finally the forward power between t_n and t_{n+1} is held constant at P_{f_refill}. The cavity stored energy for $t_n < t < t_{n+1}$ is then

$$U(t) = \frac{4P_{f\_refill}Q_e}{\omega}\left(1-\mathrm{e}^{-\frac{t-t_n+t_{fill\_n}}{\tau_L}}\right)^2$$

*Work supported by the NNSA, U. S. Department of Energy under contract DE-AC52-06NA25396.

MEASUREMENT OF THE TRANSVERSE BEAM DYNAMICS IN A TESLA-TYPE SUPERCONDUCTING CAVITY*

A. Halavanau[1,2], N. Eddy[2], D. Edstrom[2], A. Lunin[2], P. Piot[1,2], J. Ruan[2], N. Solyak[2]
[1] Department of Physics and Northern Illinois Center for Accelerator & Detector Development, Northern Illinois University, DeKalb, IL 60115, USA
[2] Fermi National Accelerator Laboratory, Batavia, IL 60510, USA

Abstract

Superconducting linacs are capable of producing intense, ultra-stable, high-quality electron beams that have widespread applications in Science and Industry. Many project are based on the 1.3-GHz TESLA-type superconducting cavity. In this paper we provide an update on a recent experiment aimed at measuring the transfer matrix of a TESLA cavity at the Fermilab Accelerator Science and Technology (FAST) facility. The results are discussed and compared with analytical and numerical simulations.

INTRODUCTION

Several projects are foreseen to incorporate TESLA-type cavities [1, 2]. These include electron- [3], muon- [4], and proton-beam accelerators [5]. The transverse beam dynamics associated to these accelerating cavities has been explored in the last decade [6, 7]. Recently, we attempted to characterize the transfer matrix associated to a TESLA cavity and some preliminary measurement were reported in Ref. [8]. In this paper we improve our previous measurement and confirm that the measured transfer matrix is well described by the by Chambers' [9] model. We especially find that the inclusion of spatial harmonics as discussed in [10–14] is not relevant for the TESLA cavity.

In brief, we consider the transfer matrix R of the cavity in the transverse trace space to be defined as $\mathbf{x}_f = R\mathbf{x}_i$ where $\mathbf{x} \equiv (x, x')$ and the subscript i (resp. f) corresponds to the coordinates upstream (resp. downstream) of the cavity. According to the Chambers' model, the elements of 2×2 matrix R are [9, 12–14]:

$$\begin{aligned}
R_{11} &= \cos\alpha - \sqrt{2}\cos(\Delta\phi)\sin\alpha, \\
R_{12} &= \sqrt{8}\frac{\gamma_i}{\gamma'}\cos(\Delta\phi)\sin\alpha, \\
R_{21} &= -\frac{\gamma'}{\gamma_f}\left[\frac{\cos(\Delta\phi)}{\sqrt{2}} + \frac{1}{\sqrt{8}\cos(\Delta\phi)}\right]\sin\alpha, \\
R_{22} &= \frac{\gamma_i}{\gamma_f}[\cos\alpha + \sqrt{2}\cos(\Delta\phi)\sin\alpha],
\end{aligned} \tag{1}$$

where $\alpha \equiv \frac{1}{\sqrt{8}\cos(\Delta\phi)}\ln\frac{\gamma_f}{\gamma_i}$, $\gamma_f \equiv \gamma_i + \gamma' z$ is the final Lorentz factor, and $|R| = \gamma_i/\gamma_f$.

The analytical solution (1) is obtained under the assumption of axially symmetric field. It is not the case in a real RF cavity which includes input-power and high-order-mode (HOM) couplers needed to respectively couple the RF power to the cavity and damp the HOM fields excited by the beam.

To investigate the impact of couplers further, a 3D electromagnetic model of the cavity – including its auxiliary couplers – was implemented in HFSS [15]. The simulated 3D electromagnetic field map was imported in ASTRA [16] particle-tracking program. The map was computed over a the domain $x = y = \pm 10$ mm from the cavity axis and over $z = 1395$ mm along the cavity length. The respective mesh size were taken to be $\delta x = \delta y = 0.5$ mm and $\delta z = 1$ mm. In our previous studies it was found, via numerical simulation, that the main effect of the 3D model is to induce some beam steering. However, we did not find significant deviations in the cavity transverse-focusing properties from the 1D (i.e. without including 3D effect) model. In particular, simulations indicated a good agreement of the transverse focusing with the analytical model from Chambers [8].

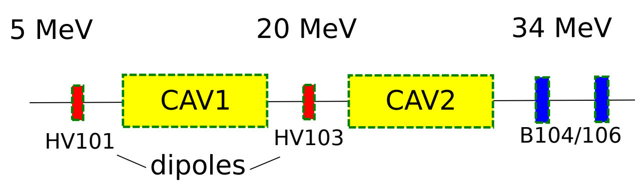

Figure 1: Experimental setup under consideration: two SRF-cavities(CAV1/CAV2) and beam position monitors (BPM 104/106) used in measurements.

EXPERIMENTAL SETUP & METHOD

The experiment was performed at the FAST injector [17] and is the continuation of studies performed earlier at Fermilab A0 photoinjector facility [6] and FAST facility [8]. A significant change from our previous experiment was the addition of a second cavity and the modification of some of the diagnostics.

In brief, an electron beam photoemitted from a high-quantum efficiency is rapidly accelerated to 5 MeV in a L-band RF gun. The beam is then injected in TESLA cavity (CAV1) with average accelerating gradient limited to $\bar{G}_{rf} \simeq 15$ MeV/m and further accelerated to a maximum energy of ~ 34 MeV in the second cavity (CAV2); Fig. 1.)

A priori to performing the experiment, a beam-based alignment through both cavities was performed. The procedure was accomplished using a conjugate gradient algorithm available within SCIPY library and using PyACL framework [18]. In order to measure the transfer matrix, beam-

* This work was supported by the US Department of Energy under contract DE-SC0011831 with Northern Illinois University. Fermilab is operated by the Fermi research alliance LLC under US DOE contract DE-AC02-07CH11359.

ISBN 978-3-95450-169-4

SUPERCONDUCTING TRAVELING WAVE CAVITY TUNING STUDIES*

R. Kostin[1†], A. Kanareykin[1], St. Petersburg Electrotechnical University LETI, St.Petersburg, Russia
P. Avrakhov, Euclid Techlabs, Bolingbrook, IL, USA
V. Yakovlev, N. Solyak, Fermilab, Batavia, IL, USA
[1]also at Euclid Techlabs, Bolingbrook, IL, USA

Abstract

Superconducting traveling wave cavity (SCTW) can provide 1.2-1.4 times larger accelerating gradient than conventional standing wave SRF cavities [1]. Firstly, traveling wave opens the way to use other than Pi-mode phase advance per cell which increase transit time factor. Secondly, traveling wave is not so sensitive to cavity length as standing wave, which length is limited to 1 meter because of field flatness degradation. 3 cell SCTW cavity was proposed [2] and built for high gradient traveling wave demonstration and tuning studies. This paper describes analytical model that was used for cavity development. Tuning properties and requirements are also discussed.

INTRODUCTION

The accelerating gradient in RF cavities plays a key role in high energy accelerators [3], since the cost of the project is highly dependent on its length. The current design of an SRF based linear collider uses superconducting Tesla type [4] accelerating cavities with accelerating gradients of 31 MV/m. The Tesla cavity length is restricted to 1 meter because of field flatness degradation and consists of only 9 cells. There is an unavoidable gap between cavities which decreases the average accelerating gradient.

A superconducting traveling wave cavity (SCTW) was proposed to increase the accelerating gradient [1]. However, it requires a feedback waveguide to transfer RF power from the output of the cavity back to its input section. Traveling wave (TW) cavities have lower field flatness sensitivity to the cavity length and, thus can be much longer. Our investigations showed [5] that a 10 meter long TW cavity would have a better field flatness than even a 1 meter standing wave (SW) cavity if it can be fabricated and cleaned with the required tolerances. Thus, if the technology allows building such a long cavity it might increase the accelerating gradient by 22% eliminating beam pipes empty of RF power between cavities. A TW cavity can operate at any phase advance, and, as is well known, a smaller phase advance provides a higher transit time factor. We investigated the phase advance dependence on the accelerating gradient of the SCTW cavity and it was found that 105 degrees gives an optimal accelerating gradient gain of 24% [5]. Overall, a TW cavity may increase the gradient by up to 46% compared to a conventional SW cavity.

The first approach to a TW cavity was a single cell cavity. It was manufactured to prove the feasibility of cleaning the feedback waveguide. The cavity was cleaned at Argonne National Lab and tested at Fermilab at the vertical test stand in liquid helium. A 26 MV/m accelerating gradient was reached [5], which is comparable to Tesla single cell cavities with the same treatment. This opened the way to build a next generation TW cavity – a 3-Cell SCTW cavity [2] to demonstrate operation in the TW regime in a superconducting cavity with a high gradient. Two cavities were built. Traveling wave was successfully adjusted in one of them at room temperature [6]. The other cavity will be tested in liquid helium and requires siffening ribs on the waveguide. The welding process will be finished by Fall 2016.

Tuning properties of the 3-Cell TW cavity were investigated [7, 8]. Analytical model of 3-Cell traveling cavity which was used in these studies is presented and discussed in the paper. It was found that suppression of microphonics caused by external pressure variation is possible by power redistribution in the input couplers. A feeding scheme with power redistribution capability is proposed and discussed. A 2D tuner required for Lorentz force compensation was designed, manufactured and tested [9]. Its analytical representation in the model is also presented.

ANALYTICAL MODEL

Analytical model was created to investigate traveling wave adjustment in resonator with feedback waveguide and at the same time include effects of mechanical deformations, such as microphonics, Lorentz force and tuner. The model is based on S-matrix formalism and utilizes S-parameters calculated in finite element (FE) codes. The model is suitable for any resonator but will be discussed in details on example of the 3-cell SCTW cavity which schematic is depicted on Figure 1.

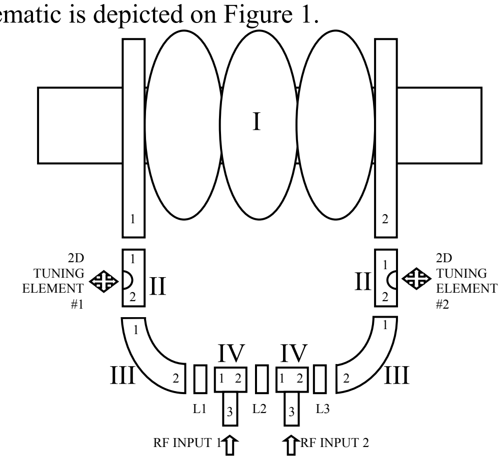

Figure 1: 3-Cell schematic for analytical model.

* Work supported by US DOE SBIR # DE-SC0006300
† r.kostin@euclidtechlabs.com

ISBN 978-3-95450-169-4

GENERATION OF COHERENT UNDULATOR RADIATION AT ELPH, TOHOKU UNIVERSITY

S. Kashiwagi†, T. Abe, F. H. Hama, Hinode, T. Muto, K. Nanbu, I. Nagasawa, H. Saito, Y. Saito, Y. Shibasaki, K. Takahashi, Research Center for Electron Photon Science (ELPH), Sendai, Japan

Abstract

A test accelerator as a coherent terahertz source (t-ACTS) has been under development at Tohoku University, in which an intense coherent terahertz (THz) radiation generated by an extremely short electron bunch [1]. Velocity bunching scheme in a traveling accelerating structure is employed to generate femtosecond electron bunches [2]. Spatial and temporal coherent radiation in THz region can be produced by the electron bunches with small transverse emittance. A long-period undulator, which has 25 periods with a period length of 10 cm and a peak magnetic field of 0.41 T, has been also developed and installed to provide intense coherent THz undulator radiation. By optimizing the bunch length, we found that it is possible to generate a coherent undulator radiation that contains only the fundamental wave from numerical studies. Beam experiment was performed to generate and observe the coherent undulator radiation from extremely short electron bunches. Coherent undulator radiation from 2.6 to 3.6 THz was demonstrated. The preliminary results of the experiment will be reported in this paper.

INTRODUCTION

The relativistic and sub-picosecond electron pulses allows direct production of high intensity, coherent, narrow-band terahertz (THz) radiation by passing the electron beam through an undulator [1]. Using the coherent and narrow-band THz radiation, the various polarization states can be produced for scientific research and applications.

The total radiated power from an electron bunch of N electrons can be written as

$$P(\lambda) = [N\{1 - f(\lambda)\} + N^2 f(\lambda)] \cdot P_0(\lambda), \tag{1}$$

where P_0 (λ) is the radiated power from a single electron. The function of f(λ) is bunch form-factor for Gaussian bunch with rms bunch length (σ_b) and it is given by

$$f(\lambda) = \left|\exp\left(-2\pi^2 \frac{{\sigma_b}^2}{\lambda^2}\right)\right|^2. \tag{2}$$

As the compressed electron bunch is shorter than the radiation wavelength, f(λ) is not zero and the radiation power from the electron bunch P(λ) has a coherent term that is proportional to N^2.

The accelerator system of t-ACTS consists of a specially designed S-band RF gun [3], an alpha magnet with energy slit, a 3m-long accelerating structure, 2.5m-long linearly-polarized undulator with 25 periods. We experimentally confirmed the production of short electron bunch by measuring the bunch length using a streak camera and analysing spectrum of coherent transition radiation in THz region [4-6]. Generation of coherent undulator radiation is studied and demonstrated at t-ACTS.

UNDULATOR RADIATION FROM SHORT ELECTRON BUNCHES

An electric field and spectrum of undulator radiation can be calculated from an electron beam motion and the undulator parameters. The Lienard Wiéchert potential describes the electromagnetic effect of a moving charge. To obtain the electron beam motion, a magnetic field of undulator is derived by a three-dimensional magnetic field calculation program with magnetic charge method [7], and the electron trajectory in the undulator field is calculated with relativistic equation of motion using the Runge-Kutta method. The radiation field and spectrum are calculated for Gaussian bunch with σ_t = 100 fs. An electron energy, K-value and number of periods of undulator were 30 MeV, 3.88 and 25, respectively. Wavelength of fundamental radiation was approximately 120 μm (2.5 THz). Figure 1 shows the electric fields and spectrum of undulator radiation, respectively. By adjusting the bunch length relative to wavelength of fundamental radiation, the higher harmonics can be supressed and the time profile of the electric field become almost sinusoidal wave as in case of σ_t = 100 fs.

We evaluate the intensity of coherent undulator radiation for the case of 100 fs Gaussian bunch. Macropulse duration is 2.0 μs and it contains about 5700 microbunch. Radiation wavelength for fundamental is 120 μm (2.5 THz) and the pulse duration of the radiation is 10 ps

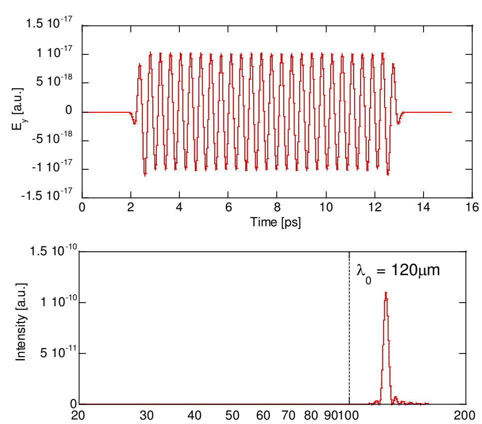

Figure 1: Electric field (up) and radiation spectrum (down) of undulator radiation from Gaussian bunch of σ_t=100 fs.

†kashiwagi@lns.tohoku.ac.jp

INTRA BUNCH TRAIN TRANSVERSE DYNAMICS IN THE SUPERCONDUCTING ACCELERATORS FLASH AND EUROPEAN XFEL

T. Hellert, M. Dohlus, W. Decking, DESY, Hamburg, Germany

Abstract

At FLASH and the European XFEL accelerator superconducting 9-cell TESLA cavities accelerate long bunch trains at high gradients in pulsed operation. Several RF cavities with individual operating limits are supplied by one RF power source. Within the bunch train, the low-level-RF system is able to restrict the variation of the vector sum voltage and phase of one control line below 3E-4 and 0.06 degree, respectively. However, individual cavities may have a significant spread of amplitudes and phases. Misaligned cavities in combination with variable RF parameters will cause significant intra-pulse orbit distortions, leading to an increase of the multi-bunch emittance. An efficient model including coupler kicks was developed to describe the effect at low beam energies. Comparison with start-to-end tracking and experimental data will be shown.

INTRODUCTION

There are several ways for getting a proper description of the transverse beam dynamics in a RF accelerating structure, e.g. using tracking algorithms [1] or simplified analytic models [2]. Assuming knowledge of the electromagnetic field distribution and the initial conditions of the particles, tracking provides accurate solutions, even for very low particle energies. Since the track step has to be small compared to a cell length, many steps are required, which needs considerable computation time for simulations with high dimensional parameter scans. Established simplified analytic models on the other hand may calculate the beam transport by few matrix multiplications. However, they are based on assumptions, most importantly ultra-relativistic beams, which do not apply at most particle injectors. Thus, a major challenge is to set up a model for low particle energies $\gamma = [10 \ldots 200]$, which is simple enough in order to calculate its output within Milliseconds, yet able to reproduce key features of RF dynamics such as RF focussing and coupler kicks.

MODEL DEVELOPMENT

Our approach uses a combination of numerically calculated axial symmetric beam transport matrices and discretized coupler kicks, coefficients of which are derived via a Runge-Kutta tracking algorithm using a high precision 3D field map of the TESLA cavity. Once the parameterized coefficients for the beam transport matrices and coupler kicks are evaluated, the final model uses the matrix formalism to calculate the beam transport through an accelerating module consisting out of 8 cavities in the order of ms for 400 bunches.

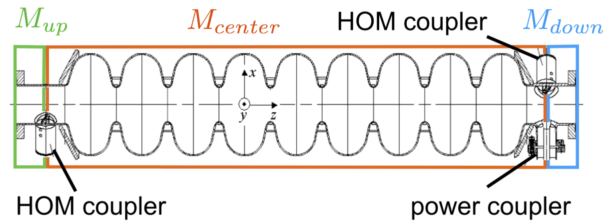

Figure 1: Longitudinal cross-section of a TESLA cavity. Highlighted are the HOM and power couplers and the transfer matrices as used for the model function.

3D-Field-Map

For the TESLA cavity two field maps are available. The axial symmetric field map describes the accelerating mode without geometric disturbances [3]. The 3D field map [4] describes this mode including the fields induced by both HOM and power coupler. Let $E_{[f/r]}^{[sin/cos]}$ being the sine and cosine like parts of the resonating electric field for the forwarded and reflected wave, respectively, and $A_{[f/r]}$ and $\phi_{[f/r]}$ amplitude and phase of the forward and backward wave from/to the fundamental mode coupler. The overall electric field component for the general case with given accelerating voltage V_0 and phase ϕ in respect to the beam can then be calculated with

$$E(t) = \Re\left[V_0/\overline{V}_r\, e^{i(\omega t+\phi)} \cdot \left(E_r^{cos} - i\Gamma \cdot E_r^{sin}\right)\right] \qquad (1)$$

from the 3D field map provided by [4] for the pure decay mode, thus no incoming wave. $\overline{V}_r$ normalizes the field to the Eigenmode-solution of the field map. The voltage standing wave ratio

$$\Gamma = (A_r e^{i\phi_r} - A_f e^{i\phi_f})/(A_r e^{i\phi_r} + A_f e^{i\phi_f}) \qquad (2)$$

describes the ratio between the difference of the forwarded and reflected wave in respect to the overall accelerating field. The magnetic component behaves analogously, using similar symmetry properties of the field components.

Beam Transport in Axial Symmetric RF Cavities

The change of transverse coordinates of a particle induced by an axial symmetric cavity can be written in terms of a matrix formalism. Using the Maxwell equations, a *quasi*-3D field map can be calculated from [3]. A Runge-Kutta algorithm is used to solve the equation of motion for one cavity for an ensemble of initial particles, entering the cavity at different offsets and angles. The calculation of the beam transport matrix then becomes a linear regression problem. The energy gain ΔE of a particle in the TESLA cavity is determined by the accelerating mode and is to a very good

ISBN 978-3-95450-169-4

REVIEW ON TRENDS IN NORMAL CONDUCTING LINACS FOR PROTONS, IONS AND ELECTRONS, WITH EMPHASIS ON NEW TECHNOLOGIES AND APPLICATIONS

F. Gerigk*, CERN, Geneva, Switzerland

Abstract

In recent years superconducting (SC) cavities seem to rise in popularity. While these cavities can save operating costs and shorten the length of linacs, there are many applications and circumstances where normal conducting (NC) cavities are superior. This talk reviews some of the NC Radio Frequency (RF) linacs, which have been either recently commissioned, or which are currently under construction or in the design phase. Focus will be given to the choice between NC and SC cavities and to emerging normal conducting technologies and their applications.

PARAMETER RANGE FOR NC LINACS AND THEIR APPLICATIONS

The choice between NC and SC linacs is made according to power efficiency, real estate gradient, capital investment, maintenance/ running cost, local expertise, and the interest in "doing something new". While the last one may not sound very scientific, engineers are often more attracted to work on SC cavities, which are perceived as challenging and innovative, while NC linacs are considered as not very high-tech.

The above mentioned criteria depend very much on operational parameters such as beam pulse length, bunch current, final energy, duty cycle, and final energy, which also determine the transition energy between NC and SC cavities in the case of hadron linacs.

Parameters

Beam pulse length The filling time t_{fill} of a cavity together with the beam pulse length t_{pulse} determines the RF duty cycle and therefore the RF power consumption. For the cryogenic duty cycle of SC linacs one has to add not only t_{fill} but also the decay time t_{dec} [1] in order to calculate the power consumption of the cryogenic system (see Fig. 1). The filling time is generally proportional to Q/f with Q being the quality factor of the cavity and f the RF frequency. In case of TW NC structures t_{fill} is determined by the group velocity of the RF wave and the structure length, yielding very small values in the <1 µs range. SW NC structures typically need 10 s of µs until the reflected RF waves have stabilised and in SC SW structures one is typically in the range of 100 s of µs or even ms. It is therefore clear that the combination of short µs-range pulses and SC cavities is not very efficient.

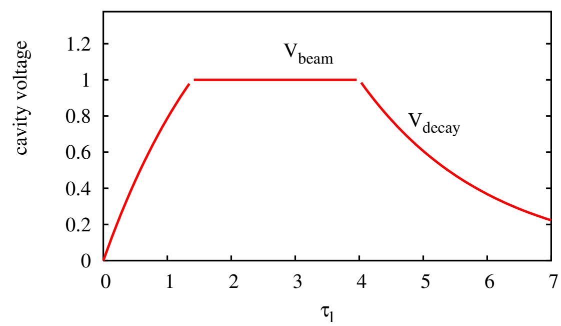

Figure 1: Voltage profile in a pulsed cavity.

Bunch current The power dissipated in the surface of NC SW structures is determined by its accelerating voltage V_{acc}, effective shunt impedance ZT^2, and its length L according to

$$P_d = \frac{V_{acc}^2}{ZT^2 L}. \quad (1)$$

For high currents (e.g. $>$ 100 mA) the beam power $P_b = I \cdot V_{acc}$ can be larger than P_d and then the power efficiency of a NC linac can often be better than a SC alternative. High beam currents may also require to operate SC cavities at a modest gradient in order to protect the power coupler from too high peak power values, which is another argument against SC cavities at high bunch current.

Accelerating gradient/final energy A high-energy linac needs high accelerating gradients in order to limit its length and cost. For short pulses in the µs range NC TW or SW structures are usually the most efficient choice. For longer pulses in the ms range one can choose SC structures. NC TW structures are used routinely at ≈ 30 MV/m for the acceleration of electrons. Even though much higher gradients (60-70 MV/m) can be operated reliably they are rarely used because of the increased cost of high peak power RF systems. SC structures also approach usable gradients of around ≈ 30 MV/m with a good example being the XFEL cryomodules, which achieved an average 27.9 MV/m during testing [2]. More R&D may push the gradients of SC cavities higher but also here the cost of high peak power RF systems may put a natural limit to the gradients being used in operational machines.

TW NC cavities for proton acceleration are so far not used in low-energy linacs, mostly because of the need to adapt the structures to the different energies. However, several projects [3, 4] are working on this option and the coming years may see the first NC linacs operating routinely with 50 MV/m.

* frank.gerigk@cern.ch

EXPERIENCE WITH THE CONSTRUCTION AND COMMISSIONING OF LINAC4

J. B. Lallement for the Linac4 team, CERN, Geneva, Switzerland

Abstract

In the framework of the LHC Injector Upgrade program, CERN is presently commissioning Linac4, a 160MeV H- ion linac, which will replace the present 50 MeV proton linac (Linac2) as injector to the PS Booster during the next LHC long shut-down. The installation of the machine has proceeded in parallel with a staged beam commissioning at the energies of 3, 12, 50, 100 and finally 160 MeV, foreseen for fall 2016. A seven month long reliability run will take place during 2017 to assess potential weak points and find mitigations. The lessons learnt during its construction, the main outcomes of the beam commissioning and the remaining steps toward its connection to the PS Booster are presented in this paper.

THE LINAC4 PROJECT

The Linac4 project started in 2008 with the goal of building a new 160 MeV H^- ion linear accelerator to replace the present 50 MeV Linac2 as injector of the CERN PS Booster (PSB). The main motivations were to increase the beam brilliance in the PSB and in all the LHC injector chain to fulfil the requirements of the High-Luminosity LHC upgrade program [1]. Moreover, the new charge exchange injection into the PSB (H^- ions instead of protons from the Linac2) would reduce the beam losses at injection and increase the operational flexibility.

Linac4 is a pulsed, normal-conducting 80 m long linac. A sketch of the Linac is shown in Fig. 1. It is composed of a 3 MeV pre-injector comprising a 45 keV ion source, a Low Energy Beam Transport (LEBT), a 4 vane Radio Frequency Quadrupole (RFQ) resonating at 352 MHz and a 3.6 m long Medium Energy Beam Transport (MEBT) housing a fast beam chopper. The chopper modifies the beam pulse structure, by removing some selected mircro-bunches at 352 MHz with the purpose of considerably reducing the losses during the beam capture at 1 MHz in the PSB. The linac front-end is followed by a conventional 50 MeV Drift Tube Linac (DTL) with a permanent magnet quadrupole focusing channel, a 102 MeV Cell-Coupled DTL (CCDTL) and a 160 MeV π-mode structure (PIMS) [2]. The main Linac4 parameters are given in Table 1.

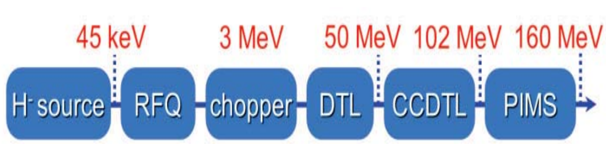

Figure 1: Linac4 sketch.

The beam commissioning was staged in 6 main steps of increasing energy. At the time of writing, the last step, the commissioning of the PIMS, is about to start. It will be completed by the end of 2016 and will be followed by a 7 month run to improve machine performances and assess reliability. The connection to the PSB will take place during the next LHC Long Shut down (LS2) starting from January 2018. It will then become the sole injector for the CERN proton accelerator complex.

Table 1: Linac4 Design Parameters

Ion Species	H^-	
Length	80	m
Output Energy	160	MeV
Frequency	352.2	MHz
Repetition rate	1.1 (max. 2)	Hz
Pulse length	400 (max. 1200)	µs
Linac pulse current (max.)	40	mA
Chopping factor	62	%
RMS Trans. Emittance	0.4	mm.mrad

LINAC4 BUILDING BLOCKS

Source

The Linac4 caesiated surface ion source driven by an external RF antenna solenoid has reached a stable and reliable performance adequate to the needs of the LHC but is still undergoing developments to improve the current for the requirements of future high-intensity beams in the PSB. Many different prototypes were tested and operated in the past years with constantly increasing performances [3]. It is operated in a pulsed mode at 1.2 s interval, keeping the beam output as stable and reliable as possible. It can today reliably deliver a 50 mA beam out of which 35 mA are within the RFQ acceptance. Optimisation, systematic measurements and prototypes testing are presently on-going on a dedicated test stand, made of a LEBT and an emittance meter (slit and grid). During the last years a very useful tool has been deployed on the source. This system regulates the source parameters (e.g. the gas injection and the RF power) while monitoring some given observables like the electron/H^- ratio with the aim of delivering a constant flat pulse of current of the desired intensity and duration. It will also be used to perform the monthly cesiation needed for the correct functioning of the source.

RFQ

The Linac4 RFQ was designed and manufactured at CERN [4]. Its RF design and tuning has been made in collaboration with CEA Saclay. Consisting of a 3 m long structure made of three brazed sections, it accelerated a

HIGH POWER OPERATION OF SNS SC LINAC*

M.A. Plum, Oak Ridge Spallation Neutron Source, Oak Ridge, TN, US

Abstract

The SNS superconducting linac (SCL) provides 972 MeV, 1.5 MW H⁻ beam for the storage ring and neutron spallation target. It has now been in operation for 11 years, and we have gained experience in long-term operational aspects. Three inter-related aspects are gradient changes, errant beams, and trip rates. In this presentation we will provide an update on our progress to mitigate these aspects, and also report on the overall status of the SCL.

INTRODUCTION

The SNS SCL today accelerates an H^- ion beam from 186 to 972 MeV using a total of 81 superconducting 6-cell cavities [1]. The first 33 cavities are contained within 11 cryomodules and are optimized for β = 0.61 (245 MeV), and the remaining 48 are contained within 12 cryomodules and are optimized for β = 0.81 (662 MeV). SCL commissioning began in 2005, and by 2009 the beam power reached 1 MW. The design beam power of 1.4 MW was first reached in 2013. The design beam energy of 1 GeV has not yet been reached for high intensity production conditions, but we are making steady progress through plasma processing [2].

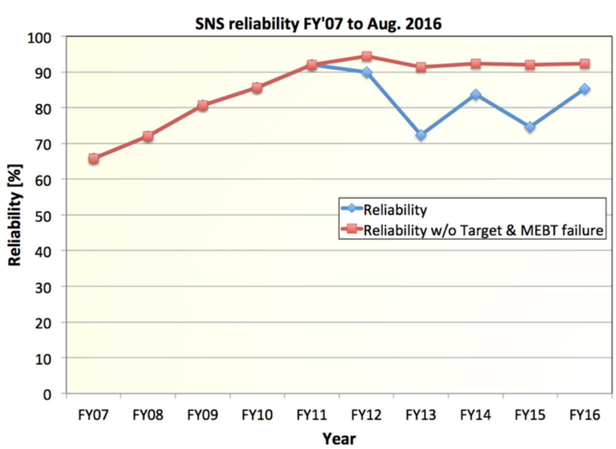

Figure 1: SNS reliability since 2007.

During the 11 years of operation we have learned a lot about operating a high intensity superconducting hadron linac. Highlights include: 1) a previously unrealized beam loss mechanism (intra-beam stripping) was found to be the source of surprisingly high beam loss [3]; 2) errant beam events were found to degrade the SCL cavities [4]; 3) warm linac RF cavity field collapse was found to be the cause of most of the errant beam events [4], and 4) a plasma processing technique was developed to improve cavity gradients [2]. In this paper we will review and update the status of errant beam events at SNS and discuss how to mitigate them, then broaden the discussion to include beam trips in general, and finally conclude with a discussion of beam energy, beam loss and activation.

Since 2011 the linac reliability has been very good, as shown in Fig. 1. It has exceeded 90% in every year except 2014 when it took several weeks to recover from a water leak in the medium energy beam transport a couple meters downstream of the RFQ.

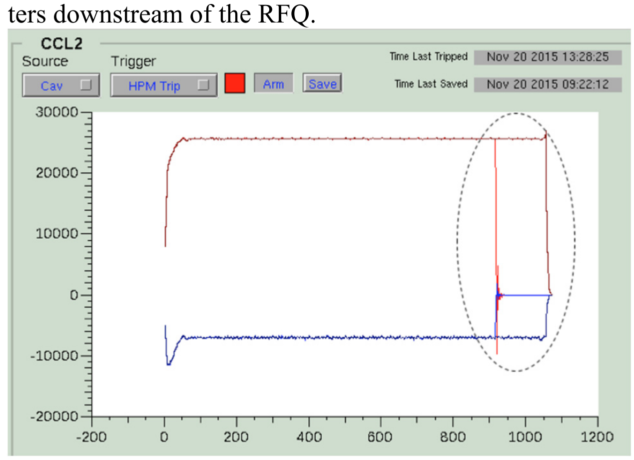

Figure 2: Example of RF field collapse in the warm linac – in this case in cavity CCL-2. The region circled by the dashed line shows the time of the field collapse. A normal pair of I/Q waveforms is superimposed on the field collapse waveforms. The x-axis is in units of microseconds.

ERRANT BEAMS

We define an errant beam event to be an event that causes sudden beam loss due to an off-normal occurrence. For example, at SNS errant beam events often arise in the warm linac in the form of RF field collapse, most likely caused by an arc within the cavity or at the vacuum window. This field collapse causes beam loss to occur in the SCL. The onset of the beam loss is often just a few microseconds in duration, and the beam loss continues until the beam is terminated by the Machine Protection System – typically 7 or 8 µs today. An example is shown in Fig. 2, which shows field collapse in warm Coupled Cavity Linac module CCL-2. In this particular case the beam loss was spread over the first ~75% of the SCL, as shown in Fig. 3, and the event lasted for about 15 µs, as shown by the beam current monitors (BCMs) in Fig. 4. Most errant beam events cause complete loss of beam in the SCL – i.e. 100% of the beam enters the SCL, 0% exits the SCL

* This manuscript has been authored by UT-Battelle, LLC under Contract No. DE-AC05-00OR22725 with the U.S. Department of Energy. The United States Government retains and the publisher, by accepting the article for publication, acknowledges that the United States Government retains a non-exclusive, paid-up, irrevocable, worldwide license to publish or reproduce the published form of this manuscript, or allow others to do so, for United States Government purposes. The Department of Energy will provide public access to these results of federally sponsored research in accordance with the DOE Public Access Plan (http://energy.gov/downloads/doe-public-access-plan).

STATE OF THE ART, STATUS AND FUTURE OF RF SOURCES FOR LINACS

Erk Jensen, CERN, Geneva, Switzerland

Abstract

This paper tries an overview of recent developments in RF sources for linear accelerators of different scales and for various applications, spanning a frequency range from about 100 MHz to X-band, spanning duty factors from about 10^{-3} to CW, and spanning power levels from a few kW up to hundreds of MW average. Exciting recent trends include new bunching concepts for klystrons, promising a significant increase of efficiency, and better power combiners paving the way to MW-class solid-state power amplifiers.

INTRODUCTION

Since I had the opportunity to make a similar overview presentation and paper on RF source status and developments for Linacs in 2010 [1], I will focus in the following report on recent progress, trends and developments in the field while omitting what has not significantly changed since 2010. For this reason, the following status report does not try to be comprehensive. The subsequent part on future developments is of course very personal since I cannot tell the future, but am happy to share what I personally find relevant and important for the future of RF sources for linacs.

CERN LINAC 4

Linac 4 is part of the upgrade of the CERN accelerator chain to eventually reach higher luminosity in the LHC. It will replace the 38-year-old Linac2, which accelerates protons to 50 MeV, and will accelerate H− ions through an RFQ (3 MeV), a DTL (50 MeV), a CCDTL (100 MeV) and a series of pi-mode structures (PIMS) to 160 MeV. At the time of writing the whole Linac4 hardware is ready for beam commissioning to 160 MeV, a 20 mA H− beam has reached 107 MeV in July 2016. Linac4 operates at 352 MHz with an RF pulse length of initially 600 µs, later up to 1.2 ms, and a repetition rate of initially 0.83 Hz with the possibility to later operate at 2 Hz (duty cycle $5 \cdot 10^{-4}$ to $2.4 \cdot 10^{-3}$).

The Linac4 352 MHz RF source consists of eleven 1.3 MW klystrons recuperated from LEP and adapted for pulsed operation, and eight new, state-of-the-art, 2.8 MW peak power klystrons [2]. In a later stage, when the LEP klystrons will have reached their end of life, every two LEP klystrons will be replaced by one new 2.8 MW klystron. The power distribution scheme for this later scheme, in which one klystron will power two accelerating structures, is sketched in Fig. 1. It features the use of a magic-tee and existing circulators and was optimized for small sensitivity on imperfections in circulators and power loads.

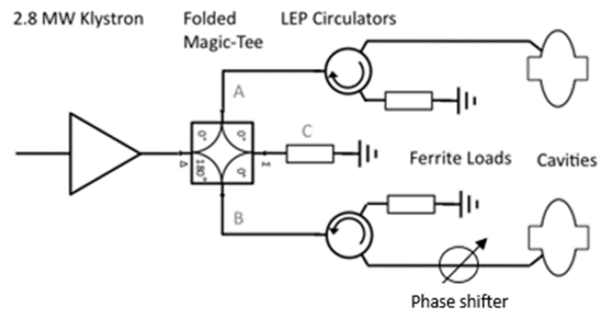

Figure 1: Powering two structures from one 2.8 MW klystrons in Linac4.

Since the LEP klystrons were not designed for pulsed operation, necessary modifications included retuning individual klystron cavities, the replacement of the HV tank, a new mod-anode voltage divider and an improved modulator that allows adjustments to cope with perveance and performance varying between individual klystrons. Figure 2 shows a recent view of the Linac4 klystron gallery.

Figure 2: View of CERN Linac4 klystron gallery.

ESS

The proton accelerator of the European Spallation features a normal-conducting front-end with RFQ and DTL similar to Linac4, operating also at 352 MHz, but with 3.5 ms RF pulses with a repetition rate of 14 Hz (duty cycle $4.9 \cdot 10^{-2}$). After the DTL (90 MeV) follow 352 MHz superconducting spoke cavities, and the main part of the linac (220 MeV to 2 GeV) consists of 704 MHz elliptical cavities, of which 36 are low-beta cavities which will be powered by 1.5 MW klystrons and 84 high-beta cavities to be powered by 1.2 MW multi-beam IOTs.

Since ESS targets a total average beam power of 5 MW, energy efficiency has clearly been a main concern, and ESS have taken the opportunity offered by their schedule (target: 2023) to invest in R&D of multi-beam IOTs with industry [3]. Inductive Output Tubes (IOTs) feature a grid control like tetrodes and output cavities like klystrons.

ISBN 978-3-95450-169-4

PULSED HIGH POWER KLYSTRON MODULATORS FOR ESS LINAC BASED ON THE STACKED MULTI-LEVEL TOPOLOGY

C. A. Martins[1], Goran Göransson, Marko Kalafatic, ESS ERIC, Lund, Sweden
Max Collins, Lund Technical University, IEA Division, Lund, Sweden
[1]also at Lund Technical University, IEA Division, Lund, Sweden

Abstract

ESS has launched an internal R&D project in view of designing, prototyping and validating a klystron modulator compatible with the requirements based on a novel topology named SML (Stacked Multi-Level). This topology is modular and based on the utilization of High Frequency (HF) transformers. The topology allows for the usage of industrial standard power electronic components at the primary stage at full extent which can easily be placed and wired in a conventional electrical cabinet. It requires only few special components like HF transformers, rectifiers and filters (i.e. passive components) to be placed in an oil tank. This arrangement allows scaling up in average and pulse power to the required levels while keeping the size, cost, efficiency and reliability of the different modules under good control. Besides the very good output pulse power quality, the AC grid power quality is also remarkably high with a line current harmonic distortion below 3%, a unitary power factor and an extremely reduced line voltage flicker below 0.3%. A reduced scale modulator prototype has been built and validated experimentally.

INTRODUCTION

The European Spallation Source is a multi-disciplinary research facility in the field of materials science currently under construction in Lund, Sweden. The spallation process will be achieved thanks to utilization of the world most powerful Linac which will provide 2.86 ms long proton pulses at 2 GeV at a pulse repetition rate 14 Hz, representing an average beam power of 5 MW in the target (Fig. 1) [1].

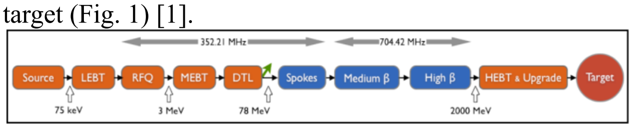

Figure 1: ESS linear accelerator layout.

The Linac will require, amongst others, the following High Power RF amplifiers:

- 1 Klystron for the RFQ;
- 5 Klystrons for the DTL tanks;
- 36 Klystrons for the Medium Beta;
- 84 Klystrons or IOT's for the High Beta

Due to the pulsed nature of the Linac, all klystron modulators will also be pulsed with a pulse width of 3.5ms, allowing for RF stabilisation and filling time of the cavities.

In order to save costs and reduce the footprint on the RF Gallery, largely influenced by the modulators, ESS has decided to launch an internal R&D project in collaboration with Lund Technical University for the development of modular high power modulators able to power up-to 4 klystrons in parallel, each rated for1.2MW RF.

These requirements translate into an electrical pulsed power of 11.5MW to be delivered by each modulator and an average power, absorbed from the AC grid, of 660kVA.

The following powering scheme has been adopted:

- Mod. #1: RFQ & DTL tank #1 klystrons in //;
- Mod. #2, #3: DTL tank #2,#3 & #4,#5 klystrons;
- Mod. #4..#12: Medium Beta klystrons;
- Mod. #13..#33: High Beta klystrons or IOT's;

All modulators are expected to be identical in their ratings, topology and interfaces.

On the contrary of many Linac components like klystrons, RF cavities, RF distribution systems including waveguides, magnets, vacuum systems, cryogenics, etc. that once designed for the peak power depend very slightly on the machine average power, the modulators which have to produce the peak power at their outputs and absorb a constant average power at their inputs represent one of the most challenging pieces of equipment. The challenges consist mainly in combining high pulse power, fast rise-times, high flat-top accuracy and AC grid power quality (low current harmonic distortion, very low flicker). These requirements, once combined with a compact design, low cost per kW peak and kW Average and high reliability, contribute to a worldwide unique set of specifications that led to the development of a novel topology called Stacked Multi-Level (SML), which is described below.

ESS MODULATOR REQUIREMENTS

Table 1 summarises the main requirements of the ESS klystron modulators. Additionally, the following design goals have been identified as crucial to achieve the above mentioned objectives and were on the basis for the SML topology choice:

- Safety, health and environmental sustainability (safe and reliable energy storage; biodegradable dielectric materials);
- Highly demonstrated and qualified power semiconductors (like IGBT's), power stacks and passive power components (inductors, capacitors) for higher reliability;
- Easy accessibility to components for maintenance and easy replacement of modules (MTTR < 3 hours);

ISBN 978-3-95450-169-4

RESONANCE CONTROL FOR FUTURE ACCELERATORS*

Warren Schappert*, Fermilab, Batavia, IL

Abstract

Many of the next generation of particle accelerators (LCLS II, PIP II) are designed for relatively low beam loading. Low beam loading requirement means the cavities can operate with narrow bandwidths, minimizing capital and base operational costs of the RF power system. With such narrow bandwidths, however, cavity detuning from microphonics or dynamic Lorentz Force Detuning becomes a significant factor, and in some cases can significantly increase both the acquisition cost and the operational cost of the machine. In addition to the efforts to passive environmental detuning reduction (microphonics) active resonance control for the SRF cavities for next generation linear machine will be required. State of the art in the field of the SRF Cavity active resonance control and the results from the recent efforts at FNAL will be presented in this talk.

CAVITY DETUNING

SRF cavities are manufactured from thin sheets of niobium to allow them to be cooled to superconducting temperatures. The thin walls make cavities susceptible to mechanical distortions from:

- Pressure variations in the surrounding helium bath
- Radiation pressure from the RF field (Lorentz Force Detuning)
- External vibration sources (microphonics)

As the walls distort, the resonant frequency of the cavity shifts from the design frequency according to the Slater rule.

Detuned cavities are more expensive to operate. If sufficient RF power is not available to maintain a constant gradient during the expected peak cavity detuning, the beam will be lost. Providing sufficient power to overcome detuning increases both the capital and the operating costs of the machine.Figure 1 shows the capital cost of the LCLS-II RF plant as a function of RMS detuning. The cost increases rapidly once the RMS detuning exceeds a few Hz.

Table 1 lists a number of SRF accelerators being planned or currently under construction [1]. Each machine can be assigned to one of four broad classes depending on the operating mode and cavity bandwidth:

- Wideband CW;
- Wideband Pulsed;
- Narrowband CW; and
- Narrowband Pulsed.

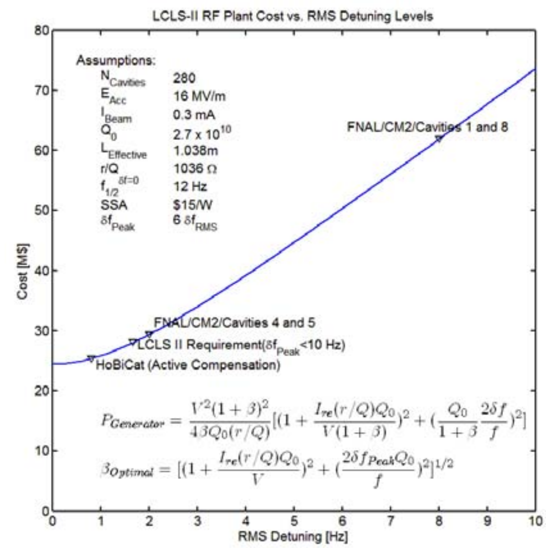

Figure 1: LCLS-II RF Plant Cost as a Function of RMS Detuning.

Minimizing cavity detuning is critical for narrowband machines, both CW and pulsed. Detuning can be one of the major cost drivers for such machines. Narrowband pulsed machines such as PIP-II present a unique challenge because of radiation pressure from the RF pulse can itself drive significant levels of cavity vibration. If such vibrations cannot be suppressed, the cost of operating such a machine may become prohibitive.

ACTIVE COMPENSATION

Active compensation of cavity detuning has been used successfully to stabilize cavity resonant frequencies in the presence of vibration sources. A fast mechanical actuator, often a piezo stack, applies pressure to cavity in an attempt to cancel all or part of the cavity wall distortions induced by external sources. The use of piezo actuators for active detuning compensation of Lorentz force detuning was pioneered at DESY [2] but is now in wide use at SRF accelerators around the world.

Measuring Cavity Detuning

In order to successfully compensate for detuning, the frequency shift of the cavity must be accurately determined. This can be done using the complex baseband forward, reflected, and probe RF signals. The complex differential

*This manuscript has been authorized by Fermi Research Alliance, LLC under Contract N. DE-AC02-07CH11359 with U.S. Department of Energy.
#warren@fnal.gov

HIGH-GRADIENT RF DEVELOPMENT AND APPLICATIONS

W. Wuensch, CERN, Geneva, Switzerland

Abstract

The CLIC collaboration has made significant progress in understanding the phenomena which limit gradient in normal-conducting accelerating structures and to increasing achievable gradient in excess of 100 MV/m. Scientific and technological highlights from the CLIC high-gradient program are presented along with on-going developments and future plans. I will also give an overview of the range of applications that potentially benefit from high-frequency and high-gradient accelerating technology.

INTRODUCTION

The CLIC collaboration has been developing the technology necessary for a multi-TeV range electron-positron collider [1]. A priority of this effort has been to increase the gradient achievable in normal-conducting accelerating structures to above 100 MV/m. Such gradient gives a 3 TeV center of mass energy collider with a total length of 50 km and allows optimization of gradient for cost and power consumption for lower energies. For example the 380 GeV initial energy stage of CLIC has an optimum gradient of around 70 MV/m [2].

The underlying strategy has been to take "classical" rf accelerating technology, so that a post-LHC facility can be proposed and built in a timely fashion, understand its fundamental limits, design optimized accelerating structures and demonstrate feasibility with high-power test prototypes. Many other technological challenges have been addressed by the CLIC collaboration - including rf power generation using a drive beam, micron-precision alignment and nano-meter level vibration stabilization - but this report restricts itself to the issue of gradient in the accelerating structures.

The effort to increase gradient has to take into account the numerous requirements given by the overall design of the CLIC facility. These include that accelerating structures must preserve quality of very low emittance beams, operate with high rf-to-beam power efficiency (high beam-loading), contain features which suppress higher-order-modes (HOMs) and run very stably with a breakdown (vacuum arcing) rate of the order of 10^{-7} 1/m or below [1]. These requirements impose many constraints on the accelerating structures which make the gradient more difficult to achieve.

A photograph of one cell of a prototype structure is shown in Fig. 1 and an assembled structure is shown in Fig. 2. The CLIC collaboration has now successfully operated a number of prototype accelerating structures in the range of 100 MV/m, and the results will be summarized in the section on test results. Most importantly, the accumulated results demonstrate that a 3 TeV CLIC is feasible in terms of accelerating gradient. But the results also show that high-gradient X-band accelerating systems can be useful in a wide variety of applications beyond linear colliders. These applications include XFELs, compact Compton sources and hadron therapy linacs. I will return to applications in towards the end of the report.

Figure 1: One cell of a CLIC high-power test accelerating structure. The part is made from OFE copper using a diamond tool and has micron-level tolerances. The four waveguides provide higher-order-mode damping (although no terminating loads are present here) and the outer cell wall is formed by four convex segments to minimize enhancement of surface current.

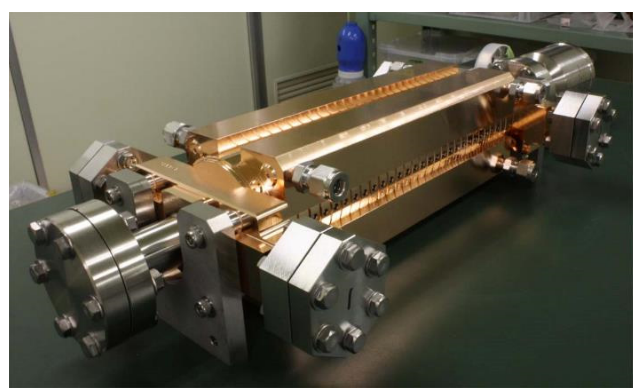

Figure 2: Fully assembled CLIC high-power test accelerating structure. This structure was designed by CERN, fabricated and tested at KEK and bonded at SLAC.

This report covers some of the main themes of the CLIC high-gradient accelerating structure development program and highlights of progress which has made. The different areas of the program can be summarised as follows:

- **Dynamics of metal surfaces under high electromagnetic fields** – Normal conducting rf structures are limited by a number of effects including vacuum arcing and pulsed surface heating. Important insights into these phenomena have come from material science and have given important input to establishing high-

ISBN 978-3-95450-169-4

BEAM COMMISSIONING RESULTS FROM THE R&D ERL AT BNL*

D. Kayran[#,1,2], Z. Altinbas[1], D. Beavis[1], S. Belomestnykh[1,2], I. Ben-Zvi1[2], D.M. Gassner[1], L.R. Hammons[1,2], J. Jamilkowski[1], P. Kankiya[1], R. Lambiase[1], V.N. Litvinenko[1,2], R. Michnoff[1], T. A. Miller[1], J. Morris[1], V. Ptitsyn[1,2], T. Seda[1], B. Sheehy[1], K. Smith[1], E. Wang[1], Wencan Xu[1]
[1]Collider-Accelerator Department, Brookhaven National Laboratory, Upton, NY 11973, USA
[2]Physics & Astronomy Department, Stony Brook University, Stony Brook, NY 11794, USA

Abstract

BNL R&D ERL beam commissioning started in June 2014 [1]. The key components of R&D ERL are the highly damped 5-cell 704 MHz superconducting RF cavity and the high-current superconducting RF gun. The gun is equipped with a multi-alkaline photocathode insertion system. The first photocurrent from ERL SRF gun has been observed in November 2014. In June 2015 a high charge 0.5 nC and 20 uA average current were demonstrated [2]. In July 2015 gun to dump beam test started. The beam was successfully transported from the SRF gun through the injection system, then through the linac to the beam dump. All ERL components have been installed. In October 2015, SRF gun cavity has been found contaminated during severe cathode stalk RF conditioning. This cavity has been sent for repair and modification for later use in low-energy RHIC electron cooler (LEReC). LEReC scheduled to start commissioning in early of 2018 [3]. We present our results of BNL ERL beam commissioning, the measured beam properties, the operational status, and future prospects.

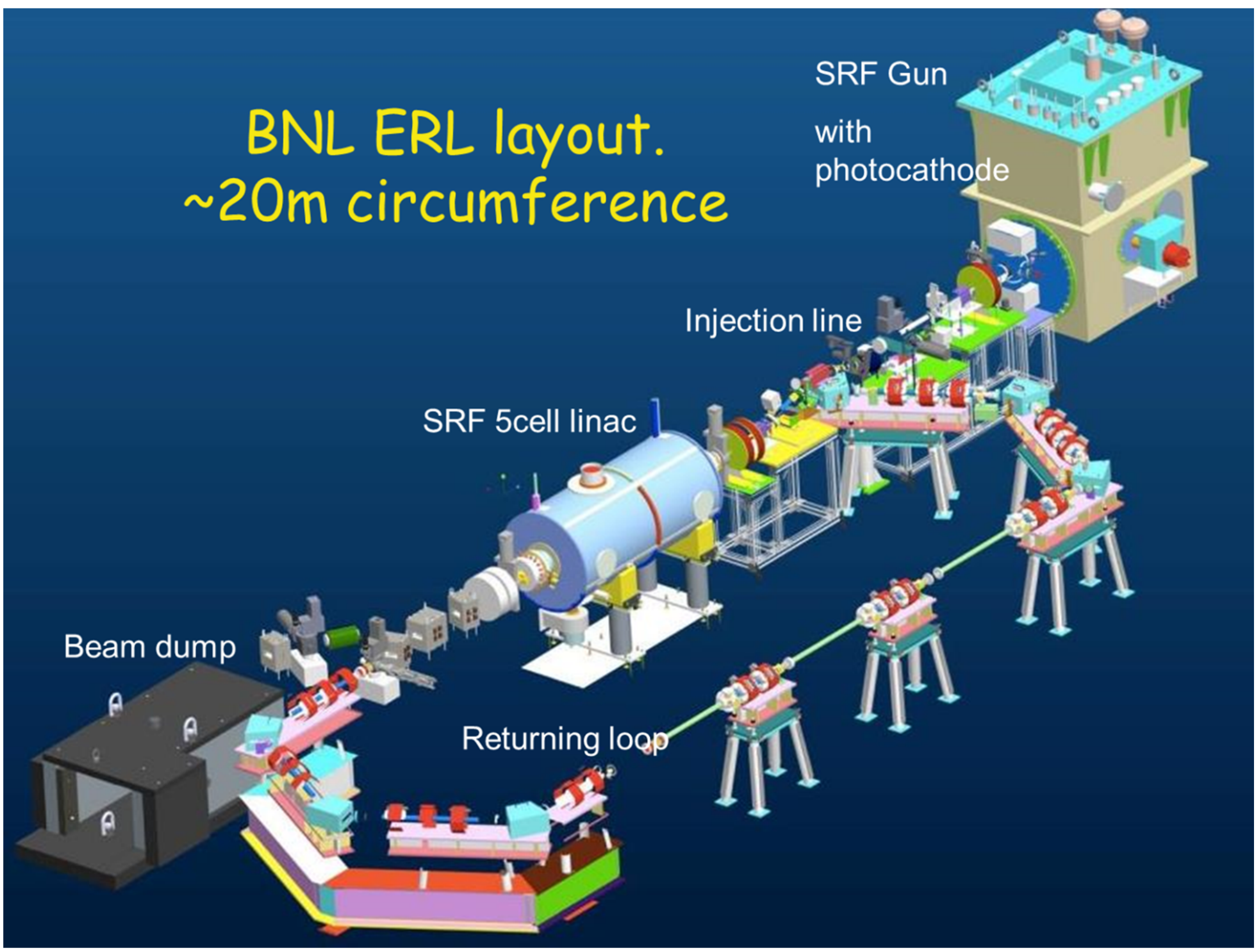

Figure 1: Schematic layout of the R&D ERL at BNL.

* This work is supported by Brookhaven Science Associates, LLC under Contract No. DE-AC02-98CH10886 with the U.S. DOE.
#dkayran@bnl.gov

APPLYING TRANSVERSE GRADIENT UNDULATORS TO SUPPRESSION OF MICROBUNCHING INSTABILITY

D. Huang, H. Deng, C.Feng, D. Gu, Q. Gu, Z. Zhao
Shanghai Institute of Applied Physics, Shanghai 201800, China

Abstract

The microbunching instability developed during the beam compression process in the linear accelerator (LINAC) of a free-electron laser (FEL) facility has always been a problem that degrades the lasing performance, and even no FEL is able to be produced if the beam quality is destroyed too much by the instability. A common way to suppress the microbunching instability is to introduce extra uncorrelated energy spread by the laser heater that heats the beam through the interaction between the electron and laser beam, as what has been successfully implemented in the Linac Coherent Light Source and Fermi@Elettra. In this paper, a simple and effective scheme is proposed to suppress the microbunching instability by adding two transverse gradient undulators (TGU) before and after the magnetic bunch compressor. The additional uncorrelated energy spread and the density mixing from the transverse spread brought up by the first TGU results in significant suppression of the instability. Meanwhile, the extra slice energy spread and the transverse emittance can also be effectively recovered by the second TGU. The magnitude of the suppression can be easily controlled by varying the strength of the magnetic fields of the TGUs. Theoretical analysis and numerical simulations demonstrate the capability of the proposed technique in the LINAC of an x-ray free-electron laser facility.

INTRODUCTION

X-ray free-electron lasers (FELs) hold great promise as ultra-short, tunable, intensity radiation sources for advanced user applications and open up new frontiers of ultra-fast and ultra-small sciences at the atomic scale. In the recent years, the successful user operation of the first FEL facilities in soft and hard x-ray regimes announced the birth of the x-ray free-electron laser. In the x-ray FEL process, the required high intensity electron beams of sub-picosecond (sub-ps) length are usually obtained by compressing longer beams in magnetic bunch compressors at relativistic energies. The bunch compressor manipulates longitudinal phase space of the electron beam with a considerable energy chirp by introducing the dependence of a particle's longitudinal position on its energy. As the result, the bunch can be significantly compressed in the bunch compressor due to the momentum compaction factor therein. On the other hand, due to existence of the longitudinal space charge (LSC), the coherent synchrotron radiation (CSR) and structural impedance in the beam transportation and compression process, the initial small energy and density perturbation in the electron bunch can be amplified with a large gain factor in many cases, which results in the increase of the fragmentation of the longitudinal phase space and dilute the emittance. This process of amplification is usually known as the microbunching instability, and it will seriously degrade the FEL performance thereafter.

The TGU is an undulator with a transverse gradient between the magnetic poles. In this paper, by investigating the transport matrix and the beam dynamics in a TGU, a simple and inexpensive technique based on transverse-to-longitudinal phase space coupling is proposed to suppress the microbunching instability of an electron beam. It is found that by adding a TGU right before the magnetic bunch compressor where large energy chirp exists, the gain of the microbunching instability developed in the electron beam can be effectively suppressed by the additional slice energy spread and the density mixing from the transverse spread introduced by the TGU. Meanwhile, the additional slice energy spread and the transverse emittance growth introduced by the first TGU can also be recovered very well by another TGU right after the compressor. Compared with the other techniques, this method is quite simple and could be easily applied to all existing FEL facilities in addition to a laser heater.

METHODS

The TGU is an undulator with a transverse gradient between the magnetic poles. The original idea of the TGU was a tool to prevent gain degradation in FEL oscillators due to the large energy spread of the electron. Recently, the idea has been applied to laser-plasma accelerator-driven high-gain FELs for the design of compact x-ray FEL devices. The TGU can be realized by canting the poles of a regular undulator and the gradient is usually made in the horizontal direction. Because the electrons at different horizontal positions feel different magnetic fields, the path length of an electron traversing a TGU depends on its transverse coordinates at the entrance of the TGU, as the result, the transverse-to-longitudinal phase space coupling is introduced. Ignoring the vertical effects, the first-order transport matrix of the TGU in $(\vec{x}, x', \vec{z}, \delta_\gamma)$ phase space can be derived as

$$\mathbf{R}_{\mathbf{TGU}} = \begin{bmatrix} 1 & L_T & 0 & \tau L_T/2 \\ 0 & 1 & 0 & -\tau \\ \tau & \tau L_T/2 & 1 & -\tau^2 L_T/6 \\ 0 & 0 & 0 & 1 \end{bmatrix} \quad (1)$$

where L_T is the effective length of TGU and τ is the strength of TGU. In the TGU transport matrix (1), one can see that the effective elements R_{31} and R_{24} are of the same value but in opposite signs.

Assuming a TGU is placed right before the first dipole of a magnetic bunch compressor where the energy chirp is

CBETA: THE CORNELL/BNL 4-TURN ERL WITH FFAG RETURN ARCS FOR ERHIC PROTOTYPING*

G. H. Hoffstaetter†, J. Barley, A. Bartnik, I. V. Bazarov, J. Dobbins, B. Dunham, R. G. Eichhorn, R. Gallagher, C. Gulliford, Y. Li, M. Liepe, W. Lou, C. E. Mayes, J. R. Patterson, D. Sabol, E. Smith, K. Smolenski, Cornell University (CLASSE), Ithaca, NY, USA
I. Ben-Zvi, J. S. Berg, S. Brooks, G. Mahler, F. Meot, M. Minty, S. Peggs, V. Ptitsyn, T. Roser, D. Trbojevic, N. Tsoupas, J. Tuozzolo, H. Witte, BNL, Upton, NY, USA
D. Douglas, JLab, Newport News, VA, USA

Abstract

The Cornell-BNL ERL Test Accelerator (CBETA) is a 4-turn Energy Recovery Linac with a FFAG return arc that is being built at Cornell University in collaboration with BNL.

Cornell University has prototyped technology essential for any high brightness electron ERL. This includes a DC gun and an SRF injector Linac with world-record current and normalized brightness in a bunch train, a high-current CW cryomodule, a high-power beam stop, and several diagnostics tools for high-current and high-brightness beams, e.g. slit measurements for 6-D phase-space densities, a fast wire scanner for beam profiles, and beam loss diagnostics. All these are now available to equip a one-cryomodule ERL, and laboratory space has been cleared out and is radiation shielded to install this ERL at Cornell. BNL has designed a multi-turn ERL for eRHIC, where beam is transported more than 20 times around the RHIC tunnel. The number of transport lines is minimized by using two non-scaling (NS) FFAG arcs.

A collaboration between BNL and Cornell has been formed to investigate eRHIC's NS-FFAG optics and its multi-turn ERL by building a 4-turn, one-cryomodule ERL at Cornell. It has a NS-FFAG return loop built with permanent magnets and is meant to accelerate 40mA beam to 150MeV.

INTRODUCTION

CBETA is being constructed at Cornell University. It will be the first ever multi-turn Energy Recovery Linac (ERL) with superconducting RF (SRF) acceleration. And it will be the first ERL based on Fixed Field Alternating Gradient (FFAG) optics [1]. It will be a unique resource to carry out accelerator science and enable exciting research in nuclear physics, materials science and industrial applications. Initially it will prototype components and evaluate concepts that are essential for Department of Energy (DOE) plans for an Electron-Ion Collider (EIC).

Two DOE labs, BNL and JLAB, have EIC projects and both need an ERL as an electron cooler for low-emittance ion beams. For eRHIC at BNL, a new electron accelerator would be installed in the existing RHIC tunnel, colliding polarized electrons with polarized protons and ^{3}He ions, or with unpolarized ions from deuterons to Uranium. The electron beam can either be stored in a ring for a ring-ring collider or it can be provided by an ERL for a linac-ring collider. Because experiments have to be performed for all combinations of helicity, bunches with alternating polarization have to be provided for the collisions. An electron ring can provide these conditions only when it is regularly filled by a linac. The ring-ring as well as the linac-ring design therefore have a recirculating linac with return loops around the RHIC tunnel. Significant simplification and cost reduction is possible by configuring these loops with non-scaling (NS-FFAG) optics of large momentum aperture.

CBETA will establish the operation of a multi-turn ERL as well as that of an FFAG lattice with large energy acceptance. Many effects that are critical for designing the EIC will be measured, including the Beam-Breakup (BBU) instability, halo-development and collimation, growth in energy spread from Coherent Synchrotron Radiation (CSR), and CSR micro bunching. In particular, CBETA will use an NS-FFAG lattice that is very compact, enabling multiple passes of the electron beam in a single recirculation beamline, using the SRF linac four times.

Because the prime accelerator-science motivations for CBETA are essential for an EIC, and address items that are perceived as the main risks of eRHIC, its construction is an important milestone for the NP division of DOE and for BNL.

CBETA brings together the resources and expertise of a large DOE National Laboratory, BNL, and a leading research university, Cornell. CBETA will be built in an existing building at Cornell, using many components that have been developed at Cornell under previous R&D programs for a hard x-ray ERL [2] that were supported by the National Science Foundation (NSF), New York State, and Cornell University. These components are a fully commissioned world-leading photoemission electron source, a high-power injector, and an ERL accelerator module, both based on SRF systems, and a high-power beam stop. The only elements that require design and construction from scratch are the FFAG magnet transport lattices of the return arc.

THE CBETA HALL AT CORNELL

Cornell's Wilson laboratory has the experimental hall L0E that has already largely been freed up for the installation of CBETA. It was originally constructed as the experimental

* Supported by NSF award DMR-0807731, DOE grant DE-AC02-76SF00515, and New York State.
† gh77@cornell.edu

DEVELOPMENTS ON THE 1.4 MeV/u PULSED GAS STRIPPER CELL

P. Scharrer[1,2,3*], W. Barth[1,2], M. Bevcic[2], Ch. E. Düllmann[1,2,3], L. Groening[2], K. P. Horn[2], E. Jäger[2], J. Khuyagbaatar[1,2], J. Krier[2], A. Yakushev[2]
[1] Helmholtz-Institut Mainz, 55099 Mainz, Germany
[2] GSI Helmholtzzentrum für Schwerionenforschung, 64291 Darmstadt, Germany
[3] Johannes Gutenberg-Universität Mainz, 55099 Mainz, Germany

Abstract

The GSI UNILAC in combination with SIS18 will serve as a high-current, heavy-ion injector for the FAIR facility. It must meet high demands in terms of beam brilliance at a low duty factor. As part of an UNILAC upgrade program dedicated to FAIR, a pulsed gas stripper cell was developed, aiming for increased beam intensities inside the post-stripper.

The pulsed gas injection is synchronized with the beam pulse timing, enabling a highly-demanded increased gas density. First tests using uranium beams on a hydrogen target showed a 60 %-increase in the stripping efficiency into the desired 28+ charge state. In 2015, the setup was improved to achieve yet increased target thicknesses and enhanced flexibility of the gas injection.

Recently, the pulsed gas cell was used with various ion-beams, to test the capabilities for operation at the GSI UNILAC. The stripping of ions in different gases at different gas densities was successfully tested in mixed-beam operation. Charge fractions, beam emittance, and energy-loss were systematically measured using uranium, bismuth, titanium, and argon beams on hydrogen, helium, and nitrogen targets. Selected results are presented.

INTRODUCTION

The GSI Universal Linear Accelerator (UNILAC) will serve as part of an injector system for the future Facility for Antiproton and Ion Research (FAIR), currently under construction at GSI in Darmstadt, Germany [1]. For operation at FAIR, the UNILAC has to deliver high-intensity $^{238}U^{28+}$-ion beams at a low duty cycle (approx. 100 μs beam pulse length, $\leq$ 2.7 Hz repetition rate) and an excellent beam brilliance.

In the course of an extensive upgrade program for the UNILAC [2], a new setup for the gas stripper at 1.4 MeV/u beam energy was developed to replace the previously existing N_2-jet gas stripper [3]. The aim was to increase the output beam brilliance for $^{238}U^{28+}$ ions. Pulsed gas valves, as originally designed for automotive aplications, were utilized to realize a pulsed gas injection, synchronized with the beam-pulse transit through the stripper. The pulsed gas injection enabled higher gas densities for the stripping process because the low repetition rates still result in a decreased effective gas load compared to the previously used continuous jet. This allowed for the practical use of lighter gases as stripper target, like H_2 and He, which require an increased mass flow into the stripper to achieve sufficient target thicknesses. This would overload the pumping system if applied continuously. By using H_2 as a stripper gas, the stripping efficiency for $^{238}U^{28+}$ ions could be significantly increased, still preserving a sufficient beam quality [4].

At the GSI UNILAC, various different ion beams, from protons up to uranium, are accelerated to be delivered to a wide range of experiments with varying requirements. In routine operation at the UNILAC, the gas stripper has to be used for all available projectile ions. Therefore, the pulsed gas stripper was tested with a selection of ion beams, including ^{238}U, ^{209}Bi, ^{50}Ti, and ^{40}Ar, using different gas targets, including H_2, He, and N_2.

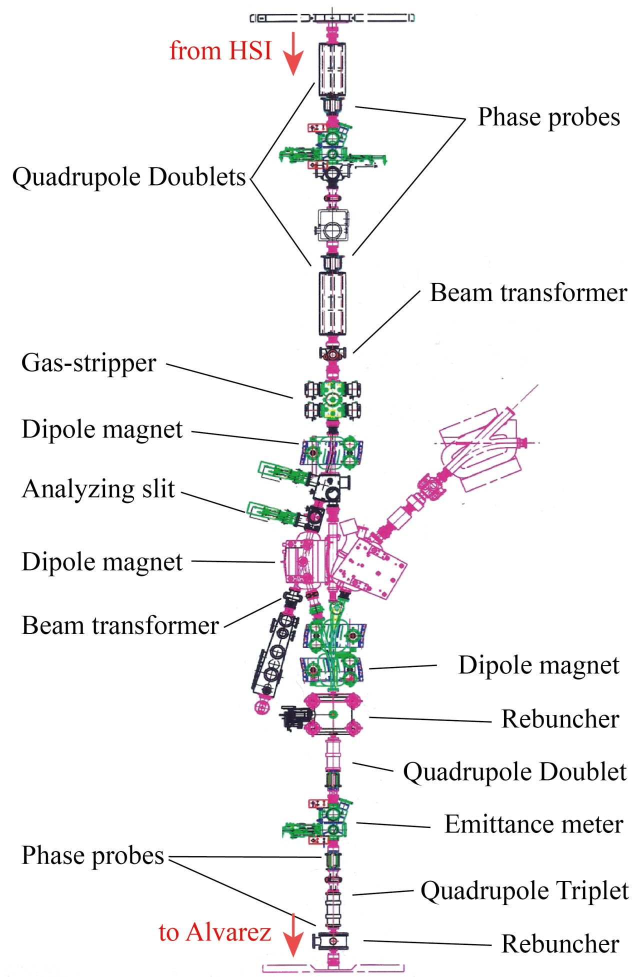

Figure 1: Stripper section of the GSI UNILAC

* p.scharrer@gsi.de

ISBN 978-3-95450-169-4

ON THE ACCCELERATION OF RARE ISOTOPE BEAMS IN THE REACCELERATOR (REA3) AT THE NATIONAL SUPERCONDUCTING CYCLOTRON LABORATORY AT MSU*

A.C.C. Villari†, G. Bollen, D.B. Crisp, M. Ikegami, A. Lapierre, S.M. Lidia, D.J. Morrissey, S. Nash, R.J. Rencsok, R. Ringle, S. Schwarz, R. Shane, C. Sumithrarachchi, T. Summers and Q. Zhao

Facility for Rare Isotope Beams, National Superconducting Cyclotron Laboratory, Michigan State University, East Lansing, MI 48824-1321, USA

Abstract

The ReAccelerator ReA3 has run continuously for one year delivering rare isotopes and stable beams for experiments at the National Superconducting Cyclotron Laboratory (NSCL) at the Michigan State University (MSU). Beams of rare isotopes are produced and separated in-flight at the NSCL Coupled Cyclotron Facility (CCF) and subsequently stopped in a gas cell. The rare isotopes are then continuously extracted as 1+ (or 2+) ions and transported into a beam cooler and buncher, followed by a charge breeder based on an Electron Beam Ion Trap (EBIT). In the charge breeder, the ions are ionized to a charge state suitable for acceleration in the superconducting radiofrequency (SRF) linac, extracted in a pulsed mode and mass analyzed. The extracted beam is bunched to 80.5 MHz and then accelerated to energies ranging from 300 keV/u up to 6 MeV/u, depending on their charge-to-mass ratio. Alternatively, ions of stable isotope can be accelerated by injecting stable ions from an external ion source in the EBIT. ReA3 has provided stable ^{14}N, ^{40}Ar, ^{39}K and ^{78}Kr as well as the rare isotope beams of ^{34,46}Ar, ^{37,46}K and ^{75}Ga for a total of 11 experiments since August 2015. This contribution focuses on the properties and techniques used to accelerate and transport the rare-isotope beams and will show average results obtained during the preparation of these experiments in the ReA facility.

INTRODUCTION

The National Supeconducting Cyclotron Laboratory NSCL [1] is a facility dedicated to the production of rare isotope beams via projectile fragmentation. The In-flight technique for production of rare isotopes provides excellent production performance for fast medium-to-high-energy beams. Optimal beam properties and intensities are obtained when the primary beam is in the range of several hundreds of MeV per nucleon, where the reaction probability for projectile fragmentation and/or fission are high, whilst the kinematics provides fragments with high longitudinal and low transversal momentums with low dispersion. The fragments, therefore, maintain the primary beam momentum and have, consequently, high energy.

Another important characteristic of the in-flight technique is that the rare isotope production is independent of the chemical property of the fragments. As they are produced in-flight, the fragments leave the production target without any chemical interaction, which is different from Isotope On-Line Separator (ISOL) approach [2]. Lower-energy beams can be produced using degraders. However, this approach has limitations due to energy and angle straggling after the degraders, generating poor beam characteristics, i.e. large emittance with poor energy resolution.

Gas-stoppers [3] followed by a reaccelerator combine the advantages of the in-flight technique, fast and no chemical dependence, with the delivery of high quality beams as available from the ISOL technique. This combination allows the generation of high-quality beams of virtually any isotope, including those that have very short half lives.

Rare isotope ions produced by projectile fragmentation are energy degraded and stopped in a gas-stopper cell with helium, re-extracted and re-accelerated. The combination of a gas-stopper cell and the new reaccelerator ReA3 [4] of the NSCL is unique worldwide and provides energies ranging from 300 keV/u to up to 6 MeV/u, depending on their charge-to-mass ratio of the ions. This contribution focuses on the properties and techniques used to stop, reaccelerate and transport rare isotope beams and shows results obtained during the first year of the ReA3 facility.

GAS-STOPPER TECHNIQUE

In order to convert the fast, rare-isotope beam into a low-energy, high-quality beam, the fast ions are sent through a momentum compression beam line consisting of a set of solid degraders, a dipole magnet and subsequently stopped in a gas stopper filled with helium gas. The ions are transported inside the gas stopper via electric and radio-frequency fields and extracted through a small orifice (1.3 mm diameter) via a supersonic jet. The gas

* Based on work supported by NSF under grant PHY-11-02511 and the Michigan State University.
† email address: villari@frib.msu.edu

FIRST EXPERIMENTS AT THE CW-OPERATED RFQ FOR INTENSE PROTON BEAMS

P. P. Schneider*, D. Born, M. Droba, C. Lorey, O. Meusel, D. Noll, H. Podlech, A. Schempp, B. Thomas, C. Wagner, Institute of Applied Physics (IAP), Frankfurt am Main, Germany

Abstract

This contribution describes the first experiments with the CW-operated RFQ [1], which is designed to accelerate protons from 120keV to 700keV for the FRANZ-Project [2]. The commissioning is done using the RF and ion beam scrubbing technique. In the first phase, the acceptance of the RFQ is scanned and the performance of the RFQ without space-charge effects is evaluated with a 2mA proton beam. The second phase will increase the beam current up to 50mA and a third phase with a machine upgrade for a beam current of up to 200mA is planned. The configuration of a high-current RFQ [3] transporting beam current increasing from 2mA with no space-charge forces to a beam with high space-charge effects gives a unique insight in the beam optics of the space-charge effects. The measurements are done with a slit-grid emittance scanner for the transversal phase-space, a Faraday Cup for the transmitted current and a momentum spectrometer to measure the energy spread. The results set the basis for later experiments on variations of the beam current and the future coupling of the RFQ with an IH-structure [4].

INTRODUCTION

The CW-operated RFQ, which is the main component of this paper and seen in Fig. 1, is part of the accelerator driven neutron source at the Stern-Gerlach-Zentrum (SGZ) at Goethe-University Frankfurt [2]. It is located downstream the LEBT[1]-section, which matches protons with an energy of 120 keV into the RFQ. The device is operated in CW-mode at 175 MHz to be able to deliver a continuous beam or short pulses from the Chopper [5] with $\tau = 100$ ns at a repetition rate of 250 kHz. The connected RF-amplifier can deliver up to 250 kW for a maximum beam current of about 200 mA and for the possibility of coupling and supplying a downstream IH-structure [4] inductively with RF-power from the same amplifier. Yet, the present rods are designed to accelerate up to 50 mA protons. The required high power requires a sophisticated thermal design and cooling technique [3, 6].

INSTALLATION

The RFQ is installed and tuned, the 122 water-cooling channels are connected and a pre-conditioning up to 300 W is done [7]. Following this, the RFQ is integrated and aligned into the beam line. To ensure the proper vacuum conditions, two turbomolecular pumps with a throughput of 1400 L/s are connected. In addition the RF connection, coupling and controlling [8] of the amplifier is ensured.

* schneider@iap.uni-frankfurt.de
[1] Low Energy Beam Transport

Figure 1: A glimpse at the RFQ with its matching section.

EXPERIMENTAL SETUP

To verify the performance of the RFQ, an experimental setup with various diagnostic possibilities is available. In front of the RFQ an insulated cone is mounted at the end of the LEBT-Section to prevent the RFQ from transversal mismatched beam. The loss current at this cone can be measured. Downstream the RFQ, a diagnostic train – schematically drawn in Fig. 2 – is installed. As first device, a slit-grid emittance meter measures the transversal phase space. Subsequent, a Faraday Cup (FDC) detects the transmitted current. As the FDC has a 1 mm aperture, a fraction of the beam can pass to a momentum spectrometer to survey the longitudinal phase space. Additionally, a mass spectrometer is mounted at the emittance meter and analyses the composition of the residual gas. At a distance of approximately 10 m, a Low Energy Photon Spectrometer (LEPS) is used to detect the x-ray photons coming from the RFQ.

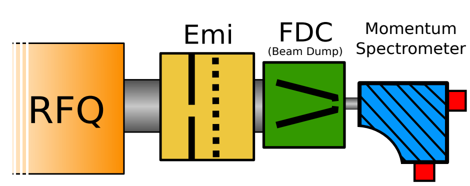

Figure 2: Scheme of the diagnostic train.

COUPLING

The amplifier measures forward and reflected power (S_{11}-measurement), in addition, a pickup measures the RF power transmission through the RFQ (S_{21}-measurement). In Fig. 4 on the left the results for pickup and forward power are shown. In the optimal case, the pickup to forward power graph gives a straight line. Some measurements indicate that this is not the case due to conditioning effects. The longer the machine runs, the measurements become more stable, which indicates positive conditioning effects.

ISBN 978-3-95450-169-4

HIGH PERFORMANCE NEXT-GENERATION Nb_3Sn CAVITIES FOR FUTURE HIGH EFFICIENCY SRF LINACS*

Daniel L. Hall†, John J. Kaufman, Matthias Liepe, James T. Maniscalco, Ryan Porter
Cornell Laboratory for Accelerator-Based Sciences and Education (CLASSE),
Ithaca, NY 14853, USA

Abstract

A 1.3 GHz ILC-shape single-cell Nb_3Sn cavity fabricated at Cornell has shown record performance, exceeding the cryogenic efficiency of niobium cavities at the gradients and quality factors demanded by some contemporary accelerator designs. An optimisation of the coating process has resulted in more cavities of the same design that achieve similar performance, proving the reproducibility of the method. In this paper, we discuss the current limitations on the peak accelerating gradients achieved by these cavities. In particular, high-pulsed-power RF testing, and thermometry mapping of the cavity during CW operation, are used to draw conclusions regarding the nature of the quench limitation. In light of these promising results, the feasibility and utility of applying the current state of the technology to a real-life application is discussed.

INTRODUCTION

The A15 superconductor Nb_3Sn is a promising alternative for niobium in superconducting RF cavities. With a transition temperature of 18 K and a superheating field of approximately 400 mT [1, 2], the material has the potential for both greater efficiency at 2.0 and 4.2 K operation as well as higher operating gradients. The Cornell Nb_3Sn program began in 2009 [3–5], coating bulk niobium cavities with tin to form a thin Nb_3Sn layer using the vapour diffusion method [6].

In this paper we present the the latest performance results from the 1.3 GHz single-cell cavities in use at Cornell. We also discuss the limitation in accelerating gradient, currently understood to be due to a localised surface defect. Surface analysis of samples has revealed a number of features that could potentially lead to cavity quench, examples of which are given here. We conclude with a discussion on the next steps that will be taken to identify the current cause of quench in the single-cell cavities shown here.

SINGLE-CELL CAVITY PERFORMANCE

There are currently three 1.3 GHz single-cell cavities in use on the Cornell Nb_3Sn program. Of these, one, designated ERL1-4, is of Cornell ERL design, with the other two, LTE1-6 and LTE1-7, are of ILC design. Two more ILC single-cell cavities have recently been completed and are currently undergoing baseline testing in preparation for coating with tin.

The coating apparatus used at Cornell University is described in detail in Ref. [7], but will be surmised here: a niobium coating chamber, containing the cavity/sample to be coated, sits within an ultra-high vacuum (UHV) furnace. At the base of the coating chamber is a recessed area containing a crucible filled with tin. The recessed area is surrounded by a secondary heating element that allows the tin crucible, referred to as the source, to be held at a temperature higher than that of the furnace and coating chamber. The generation of a temperature gradient between source and chamber alters the ratio of the rate of arrival of tin at the surface of the niobium being coated and the rate of growth of the Nb_3Sn layer.

An optimisation of the coating cycle [8] has resulted in all three of the single cell cavities achieving accelerating gradients of greater than 16 MV/m with high efficiency at 4.2 K. The continuous wave (CW) performance of these cavities can be seen in Fig. 1. All three cavities quench at approximately the same accelerating gradient of 17-18 MV/m. Processing of the cavity by continuously quenching over an extended period of time does not result in an increase in the quench field.

In high pulsed power (HPP) testing, the cavity is filled with energy as quickly as possible in an attempt to overcome thermal limitations [9]. During HPP tests, ERL1-4 [10] and LTE1-7 achieved fields higher than those achieved during CW testing, with both achieving fields of approx. 110 mT at 4.2 K, corresponding to an accelerating gradient of 25 MV/m in an ILC cavity. At higher temperatures close to the transi-

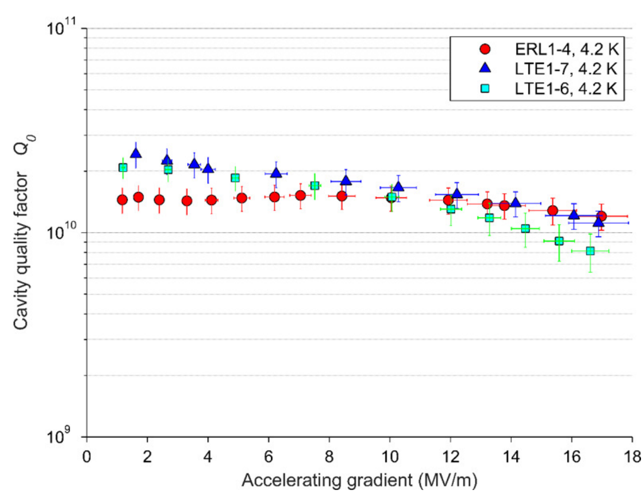

Figure 1: Quality factor vs. accelerating gradient at 4.2 K bath temperature for the three single-cell 1.3 GHz cavities on the Cornell program.

* This work supported by U.S. DOE award DE-SC0008431.
† dlh269@cornell.edu

ON MAGNETIC FLUX TRAPPING IN SUPERCONDUCTORS

R. G. Eichhorn†, J. Hoke, Z. Mayle, CLASSE, Cornell University, Ithaca, USA

Abstract

Magnetic flux trapping on cool-down has become an important factor in the performance of superconducting cavities. We have conducted systematic flux trapping experiments on samples to investigate the role of the orientation of an ambient magnetic field relative to the niobium's surface.

INTRODUCTION

According to the perfect Meissner effect, a superconductor is expected to expel all magnetic flux when it becomes superconducting. However, it is well known that superconducting cavities made from Niobium trap some of the magnetic flux during the transitions to its superconducting state while being exposed to an external magnetic field. The trapped flux will result in normal conducting vortices, which add significantly to the total surface resistance. As a result, shielding of an SRF cavity against the earth's magnetic field is essential, and usually magnetic flux strengths below 0.5 μT are required for high Q cavity performance.

Recently, flux trapping has gained an increasing interest: it was found that the amount of flux being trapped depends on the cool-down speed and also on the surface preparation details.

Our research now indicates a third factor: the orientation of the magnetic field with respect to the superconductor surface.

EXPERIMENTAL SET-UP

To investigate the role of field orientation in flux trapping we designed a simple and flexible set-up. It consisted of a sample, clamped into position by a copper frame, two solenoids that could either be oriented parallel or orthogonal to the sample, 4 flux gate sensors to measure magnetic field components (axial with respect to the sensor) and two cernox sensors to measure the temperature of the sample during the thermal cycle. Details of the set-up are shown in Fig. 1.

The solenoids consisted of wire coiled 25 times around cylinders of stainless steel. Each solenoid had a diameter of 3.8 cm and was mounted to the insert via stainless steel screws. During our tests we operated the solenoids at 0.05 A when mounted orthogonal (Fig. 1 (a)) and at 0.4 A when mounted parallel (Fig. 1 (b)). During the experiment the whole ensemble was placed inside a helium dewar which was well shielded against external magnetic fields. In every trial, we cooled the sample down to 4.2 K with various magnetic field configurations, and recorded the fluxgate readings and how they

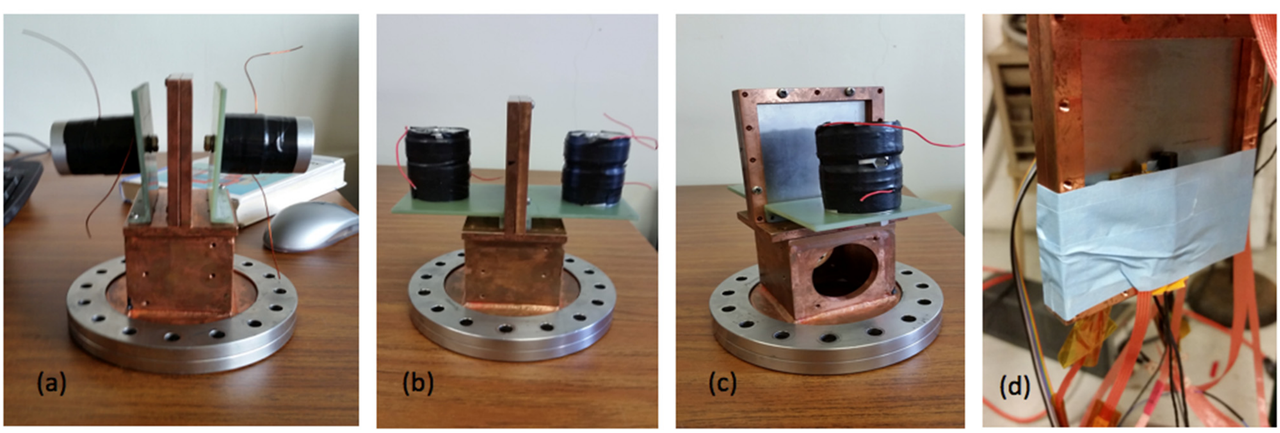

Figure 1: Experimental set-up: (a) solenoids placed orthogonal to the sample (enclosed in a copper clamp), (b) solenoids parallel to the sample, (c) more detailed view of the set-up showing the sample, (d) location of the transversal flux gate heads and the temperature sensor.

† r.eichhorn@cornell.edu

STATE OF THE ART ADVANCED MAGNETRONS FOR ACCELERATOR RF POWER SOURCE

Hideyuki Obata, Kuniyoshi Furumoto, Hiroyuki Miyamoto
New Japan Radio Co., Ltd., Saitama, Japan

Abstract

X ray sources for linear accelerators continue to be a necessary requirement for industries such as medical, inspection, and non-destructive test equipment. Future requirements for such sources are; low cost, compact packaging and high performance of the RF source for electron acceleration. The magnetron has proven to be a perfect source over other RF sources for linear accelerator use. It advantageous are; simple design, low cost per output, small size and proven performance. These meet all required characteristics for accelerator designers. New Japan Radio Co., Ltd. has improved and modified its linac magnetrons' performance and characteristics enabling easy matching to the linac modulator, high stability, long life and maximum output power.

This paper will provide a detailed explanation on the improved magnetron design methodology and its effects on the performance of these magnetrons installed in linac systems. These technologies have been utilized successfully on a commercial level worldwide over the last few years. The technology has been deployed into linac systems operating in S and X band and soon C band, at various output power levels.

INTRODUCTION

Magnetrons have been practically installed into electron accelerator systems since the 1950's. [1] In that period, out of all oscillating devices the S band magnetron was chosen for its proven performance at high output power, high efficiency and compact size. The design of a magnetron only requires a small interaction space to convert DC electrical power into high frequency microwaves by applying a magnetic field perpendicular to the electrical field.

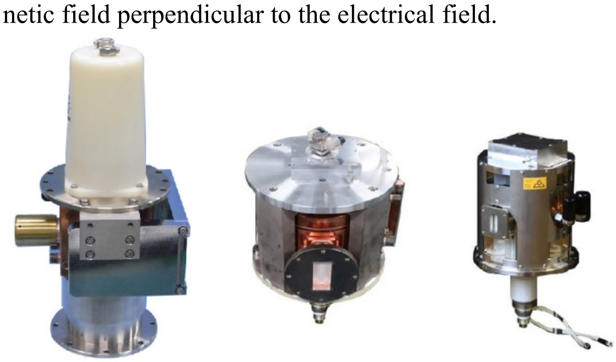

Figure 1: S band, C band, and X band magnetrons.

These photographs include external or built in magnet. The size of the resonant cavity can then be relatively small when designing for high frequency oscillation. The cavity size of magnetron is dependent on the oscillation frequency, so high frequency of microwave oscillation only requires a small resonant cavity. The chosen microwave oscillating frequency is left to the discretion of the linac designing engineer. The package size of a magnetron basically becomes compact in frequencies of S band, C band and X band as shown in Fig. 1. Each band of oscillation frequency for linac design is shown in Table 1.

Table 1: Each Band of Oscillation Frequency for Linac

Frequency band	S	C	X
Frequency (MHz)	2993 to 3002	5702 to 5722	9275 to 9325

High frequency of C band and X band offer an advantage for compact size and light weight design. These higher frequencies can reduce the size and weight not only for magnetron itself but also the RF circuit, RF transmission waveguide devices, accelerator, and shielding in the linac system. A compact light weight linac system can be easily deployed into portable systems, controlled movable radiation beam systems and utilized for installation into narrow spaces. [2] The cost of accurate piece parts required by the magnetron have been minimized by advanced high machining technology enabling high frequency output power at a reasonable cost.

Advanced thermal design of the interior of the magnetron avoids overheating allowing for higher average input power which will enable the magnetron to operate effectively at high frequency and high microwave power at high pulse duty cycles.

CONVENTIONAL DESIGN

Type of Designed Structures

The hole and slot type magnetron has been installed into S band linac systems since early development. [3] This type of design requires a large size of copper block material then mechanically cut the holes and slots to create the anode resonant cavity as shown in Fig. 2. This large size of anode has the advantage of high thermal endurance due to its large thermal capacity. This anode structure can accept high input power without overheating, so high average output power can be obtained easily for an S band hole and slot type magnetron. This hole and slot type design is difficult to deploy into C and X band high powered, tuneable frequency magnetrons because a wide cathode surface area is required for low current density which extends the cathode's lifetime of high power magnetrons. The hole and slot

ISBN 978-3-95450-169-4

METHODS FOR BUNCH SHAPE MONITOR PHASE RESOLUTION IMPROVEMENT

A. Feschenko, S. Gavrilov†
Institute for Nuclear Research of the Russian Academy of Sciences, Moscow, Russia

Abstract

Bunch shape monitors, based on secondary electron emission, are widely used for measurements of longitudinal bunch profiles during linac commissioning and initial optimization of beam dynamics. The typical phase resolution of these devices is about 1º. However it becomes insufficient for new modern linacs, which require a better resolution. Some methods developed for a phase resolution improvement are discussed.

INTRODUCTION

The technique of a coherent transformation of a temporal bunch structure into a spatial charge distribution of low energy secondary electrons through RF-modulation was initially implemented by R. Witkover [1] for BNL linac. An energy (longitudinal) RF-modulation of secondary electrons was used. In the Bunch Shape Monitor (BSM) [2], developed in INR RAS, a transverse RF-scanning is used. The general principle of BSM operation has been described elsewhere and is clear from Fig. 1.

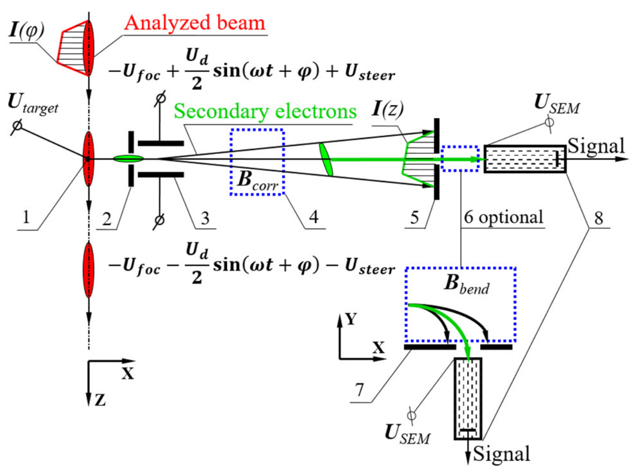

Figure 1: BSM scheme: 1 – tungsten wire target, 2 – inlet collimator, 3 – RF-deflector combined with electrostatic lens, 4 – correcting magnet, 5 – outlet collimator, 6 – optional bending magnet, 7 – registration collimator, 8 – secondary electron multiplier.

Secondary electrons are scanned by a deflecting RF-field and their position Z depends on its phase and amplitude:

$$Z = Z_0 + Z_{max} sin\varphi. \tag{1}$$

BSM resolution can be defined as a full width at a half maximum of a spread function for infinitely short bunches. Due to a finite phase resolution the measured distribution is smoothed and a fine bunch structure can be lost.

By differentiation of Eq. (1) the phase resolution can be written as: $\Delta\varphi = \Delta Z/(Z_{max} cos\varphi)$, assuming, that ΔZ is a FWHM size of the electron beam. Substituting φ from Eq. (1) one can write the phase resolution for the coordinate of the outlet collimator $Z = Z_c$ as:

$$\Delta\varphi = \frac{\Delta Z}{Z_{max}\sqrt{1-\frac{(Z_c-Z_0)^2}{Z_{max}^2}}}. \tag{2}$$

Evidently, the phase resolution can be improved, if the steering voltage U_{steer} is adjusted to direct the electrons into the outlet collimator, when the deflecting RF-field is off. In this case $Z_c = Z_0$, and the resolution equals:

$$\Delta\varphi = \frac{\Delta Z}{Z_{max}}. \tag{3}$$

The value of a maximum deflection Z_{max} can be found from electrical and mechanical parameters of the detector, so the main problem is to estimate accurately the size ΔZ of the electron beam and to propose ways for its decreasing. Sometimes instead of FWHM ΔZ it is more convenient to use the double RMS size $2\sigma_z$.

Modern ion linacs under construction, such as FRIB MSU or ESS ERIC are foreseen to operate with RMS bunch lengths of about 10÷20 ps at medium energies and even shorter at high energies, and at least 0.5° phase resolution is required for reliable bunch shape diagnostics in these linacs.

RF & STATIC ELECTRIC FIELDS

The main unit of BSM is RF-deflector. The deflector is combined with the electrostatic lens thus enabling simultaneous focusing and RF-scanning of the electrons. Typically, BSM deflectors are RF-cavities, based on parallel wire lines with capacitive plates. An electrical length of the deflectors is usually λ/4 or λ/2.

To improve the uniformity of both deflecting and focusing fields in Y-direction, thus improving a phase resolution, the new λ-type symmetric cavity has been developed for BSM-ESS (Fig. 2).

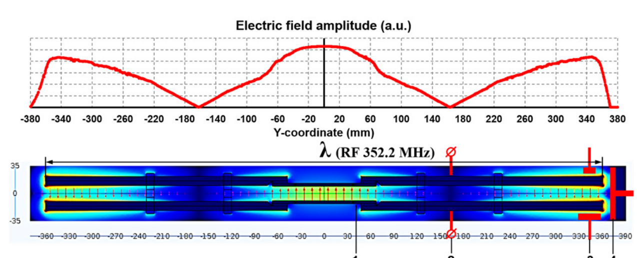

Figure 2: E-field distribution in λ-type deflector.

† s.gavrilov@gmail.com

ISBN 978-3-95450-169-4

ESS DTL BEAM DYNAMICS COMPARISON BETWEEN S-CODE AND T-CODE

M Comunian, L. Bellan[1], A. Pisent, F. Grespan, INFN-LNL, Legnaro, Italy
[1]also at Dipartimento di Fisica e Astronomia, Università degli Studi di Padova, Padova, Italy

Abstract

The Drift Tube Linac (DTL) for the ESS accelerator will accelerate protons up to 62.5 mA average pulse current from 3.62 to 90 MeV. The 5 tanks composing the DTL are designed to operate at 352.21 MHz in pulses of 2.86 ms long with a repetition rate of 14 Hz. The accelerating field is around 3.1 MV/m, constant in each tank. Permanent magnet quadrupoles (PMQs) are used as focusing element in a F0D0 lattice. The empty drift tubes accommodate Electro Magnetic Dipoles (EMDs) and Beam Position Monitors (BPMs) in order to implement beam corrective schemes. This paper presents the beam dynamics comparison over the 5 tanks between t-code PARMELA and the s-code Tracewin code.

INTRODUCTION

The following analysis was performed in order to check the consistency of the incremental law of particle velocity with the cell geometry of DTL, since we noticed that for the same value of cell lengths; different definitions gave different values of synchronous phase.

In order to bypass the intrinsic problem of the s-code (where equations of motion are integrated in space) with the relative synchronous phase definition, we decided to use a t-code (equations of motion integrated in time) with the absolute phase definition. This allowed us to check the correlation between space and time and the DTL self-consistency generation.

In the ESS DTL, the synchronous phase is ramped on Tank 1 from -35° to -26°, then it is kept constant at 25° up to the end of DTL, except for the inter-tank regions where one gap is missed and the phase is used to match the beam in the longitudinal plane, as shown in Figure 1. About transverse plane, the values of the PMQs of the F0D0 channel are fixed to obtain an equipartitioned beam evolution and a good phase advance matching with the RFQ at low energy side and with the SC linac at high energy side. The RMS input emittances are: Trans./Long. = 0.28/0.36 mm mrad (0.1436 π deg MeV). The emittance growth is $\Delta\varepsilon_{\perp,rms} = 2\%$, and $\Delta\varepsilon_{l,rms} = 1\%$ [1].

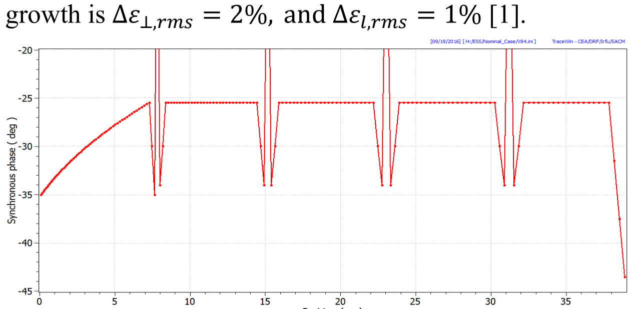

Figure 1: Synchronous Phase along the DTL.

SYNCHRONOUS PHASE DEFINITION

The ESS DTL was generated by GenDTL code. This code uses the full field map obtained from Superfish to synchronise the cell lengths with a given RF phase law. Starting from the nominal cell lengths and the other acceleration parameters given by GenDTL-SuperFish, we recalculated the synchronous phase values with the Wangler-Carne formula [2,3], to check the self-consistency of this model. The agreement of the two methods is better than 1 deg, with the larger error concentrated in the tank-to-tank interface (Figure 2).

To evaluate the effects of such difference on the beam, we track the particles through the entire DTL, using full tank field maps, so that the geometry itself sets-up the synchronous phase.

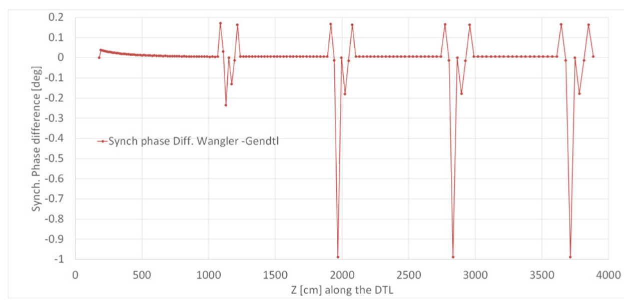

Figure 2: synchronous phase difference between Wangler-Carne formula and nominal phase law.

COMPARISON S-CODE T-CODE

Software's used for the comparison are Parmela [4] and TraceWin [5]. Both are PIC codes, with a 2D (r-z) grid mesh. The mesh size was adjusted as indicated in the reference [6], in order to minimize the 6D RMS emittance growth.

The input distribution was a not stationary waterbag, of 62.5 mA proton beam at 352.21 MHz @ 3.62 MeV. The input emittance was $\varepsilon_{n,\perp,rms}$ = 0.2797 mm mrad while the Twiss parameters were $\alpha_x = 0.0525$ $\beta_x = 0.1823$ mm/mrad, $\alpha_y = 0.0354$ $\beta_y = 0.9527$ mm/mrad. The longitudinal emittance was $\varepsilon_{l,rms}$ = 0.1545 deg MeV, $\alpha_l = -0.0175$ $\beta_l = 269.3992$ deg/MeV.

Due to the bunch distance over the bunch length (20°/360°= 0.15 ns/2.8 ns) the head and tail effect of the previous and subsequent bunches could be neglected.

The five DTL tanks were modelled in two different methods:

- The first method uses the field maps: magnetostatic for the PMQ (obtained by Comsol Simulation) and RF for

ISBN 978-3-95450-169-4

EFFECT OF NUMBER OF MACRO PARTICLES ON TIME EVOLUTION OF PHASE SPACE DISTRIBUTION*

T. Miyajima†, KEK, Tsukuba, Ibaraki 305-0801, Japan

Abstract

In particle tracking simulation with space charge effect, the macro-particle model, which has same mass-to-charge ratio, is widely used, since it does not require any symmetry of beam shape. However, selection of proper number of macro-particles is important, because the accuracy depends on it. Emittance, which is calculated by phase-space distribution, is especially affected by the number of macro-particles. In order to study the relation between the number of macro-particles and the resolution in the phase space, we defined a transformation, which describes reduction process of macro-particle number, and analyzed static phase space distribution. As a next step, we studied the effect of the macro-particle number on the dynamics of the phase space distribution for 1D charged particle distribution in the rest frame. The numerical result shows that the number of macro-particles affected the phase space distribution around the head and the tail of the bunch.

INTRODUCTION

In an accelerator, the motion of a charged particle beam which consists of N particles can be described by a trajectory on $6N$ dimension phase space. Since an actual beam contains enormous number of particles, for example $N \sim 4.8 \times 10^8$ electrons in an Energy Recovery Linac with 77 pC operation, degree of freedom in a simulation and a theoretical analysis is reduced using an approximation. In order to analyze the charged particle beam, a beam model is used to reduce number of degrees of freedom, e.g. charged disk model, charged cylinder model and macro-particle model [1]. The macro-particle model, which does not depend on the symmetry in the beam, is versatile method to describe it.

In numerical simulation, the macro-particle model, which has same mass-to-charge ratio, is widely used, since it does not require any symmetry of beam shape. However, the estimation of proper number of macro-particles is one of the important issues, since it affects the resolution of the phase space distribution of the beam. Then, we defined a transformation, particle pair transformation, to reduce macro-particles. Using the transformation, we studied the relation between the number of macro-particles and the resolution in the phase space for 1D and 2D charged particle distributions in the rest frame [2]. In the previous study, the static electric field was calculated from the transformed particle distributions with the reduced macro-particle number by the particle pair transformation. The result shows that the strength of the electric field at the edge of the distribution is affected by the number of macro-particles.

The next topics is to study the effect of the macro-particle number on the dynamics of the phase space distribution. In this paper, we report the time evolution of the 1D charged particle distribution in the rest frame with different the number of macro-particles.

MACRO PARTICLE MODEL

The equation of motion of an electron in electro-magnetic field, $\boldsymbol{E}$ and $\boldsymbol{B}$, is

$$c\frac{m_e}{e}\frac{d(\gamma\boldsymbol{\beta})}{dt} = \boldsymbol{E} + \boldsymbol{v} \times \boldsymbol{B}, \tag{1}$$

where, m_e and e are the mass and the charge of an electron, c is the speed of light, $\boldsymbol{v}$ is the speed of the electron, $\beta = v/c$ and $\gamma = 1/\sqrt{\beta^2 - 1}$. Here, the electron beam consists of N electrons. In order to describe the electron beam by the macro-particle model with M macro-particles, we have to preserve the mass-to-charge ratio. The macro-particle contains $a(= N/M)$ electrons, and the mass and charge are $m_m = am_e$, $q_m = ae$, respectively. The equation of motion of the single macro-particle is

$$c\frac{m_m}{q_m}\frac{d(\gamma\boldsymbol{\beta})}{dt} = \boldsymbol{E} + \boldsymbol{v} \times \boldsymbol{B}. \tag{2}$$

It is the same equation as the single electron, Eq. (1), because $m_e/e = m_m/q_m$. Therefore, the description of the beam motion by macro-particle model corresponds to an approximation by M charged particles with the mass, am_e, and the charge, ae.

PARTICLE PAIR TRANSFORMATION

In this section, we describe a particle pair transformation to describe the replacement of an particle distribution by macro-particles [2]. The original distribution consists of n_0 macro-particles with the mass, m_{m0}, and the charge, q_{m0}. The procedure of the transformation has the following five steps.

1. Calculate the center of the original particle distribution.
2. Choose the most distant particle from the center, and the nearest neighbor particle from it.
3. Calculate the average position about the above two particles.
4. Replace the two particles by a new macro-particle with $m_{m1} = 2m_{m0}$ and $q_{m1} = 2q_{m0}$ on the average position.
5. Repeat step. 2 to step. 4 until all the original particles are replaced.

Figure 1 shows the particle pair transformation for one dimensional particle distribution. After the transformation, the number of transformed particles is reduced to $n_1 = n_0/2$. After i-th transformation, the number of transformed particles is reduced to $n_i = n_0/i$.

* This work was supported by JSPS KAKENHI Grant Number 26600147.
† tsukasa@post.kek.jp

FREQUENCY SPECTRA FROM SOLENOID LATTICE ORBITS*

C. Richard†, National Superconducting Cyclotron Laboratory, East Lansing, USA
S. Lidia, Facility for Rare Isotope Beams, East Lansing, USA

Abstract

Multi-charge state heavy ion beams have been proposed to increase average beam intensity in rare isotope drive linacs [1]. However, the dynamics of multi-charge state beams make it challenging to optimize the beam quality in low energy linacs. One of the primary complications is that the multiple charge states introduce different focusing effects in the beam dynamics. This leads to a large frequency spectrum in the transverse motion of the beam centroid. Matlab simulations are used to describe how the frequency spectrum of the centroid transforms when the reference charge state is changed in accelerating, space charge free solenoid lattices. These frequency shifts can then be used to predict the behavior of beam of known composition using the frequency spectrum of BPM signals.

INTRODUCTION

Multicharge state beams have been proposed to increase beam intensity in ion accelerators [1]. While the dynamics of individual charge states are understood, there is no formalism for analysing the orbits of multicharge state beams. Beam position monitor (BPM) measurements of multicharge state beams look only at the center of the beam, not the distribution of beam. Therefore the individual charge states cannot be resolved from these measurements and the center will be the weighted average of each center of the individual charge states.

The orbit of each charge state in the beam is straightforward to compute. For a magnetic quadrupole lattice, where the x and y dynamics are uncoupled, the multicharge state center evolution can be simulated. However, in a solenoid lattice the x-y coupling makes the analysis more difficult. The problem can be simplified using the Larmor frame. However, this requires the solutions of each charge state to be transformed into the lab frame. The orbits in the lab frame are rather complex. Therefore, instead of trying to average multiple positions, it is simpler to view the solution in the frequency domain. In the frequency domain, the multicharge state orbits can be represented by the superposition of the frequency spectra from each charge state. Also, rotations into different frames turn into splitting of peaks by adding and subtracting the rotation frequency from the original peak.

Therefore, by understanding the how the frequency spectra of the positions of each charge state evolve with the lattice parameters, it is possible to formulate a model to predict the behavior of the centroid of a multicharge state beam.

* Work supported by Michigan State University and the National Science Foundation under Grant No. PHY-1102511.
† richard@nscl.msu.edu

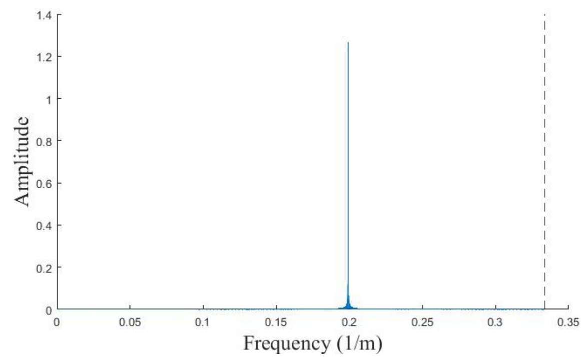

Figure 1: Frequency Spectrum from Hill's equation with κ=4, η=1/3, L = 1.5 and cos(σ)=0.3. The dashed line is at 1/(2L).

MAPPING SOLUTION

A simple method for generating single particle beam obits in a periodic, hard edge, solenoid beam line is to use the transfer matrix, M. For a solenoid lattice of length L, focusing strength κ, and occupancy η the x offset and velocity in the Larmor frame is given by the transfer matrix [2]:

$$\begin{bmatrix} x \\ x' \end{bmatrix}_{s=(n+1)L} = M \begin{bmatrix} x \\ x' \end{bmatrix}_{s=nL} \tag{1}$$

where

$$M = \begin{bmatrix} \cos(\sqrt{\kappa}L\eta) - \sqrt{\kappa}L(1-\eta)\sin(\sqrt{\kappa}L\eta) & \frac{1}{\sqrt{\kappa}}\sin(\sqrt{\kappa}L\eta) - L(1-\eta)\cos(\sqrt{\kappa}L\eta) \\ -\sqrt{\kappa}\sin(\sqrt{\kappa}L\eta) & \cos(\sqrt{\kappa}L\eta) \end{bmatrix} \tag{2}$$

$$\kappa = \left(\frac{qB}{2m\gamma\beta c}\right)^2 \tag{3}$$

where q is the charge of the particles, B is the magnetic field of the solenoid, m is the mass of the particles, ß is the normalized velocity, and γ is the relativistic factor.

The transfer matrix can generate beam orbits for long, periodic beam lines very quickly. Because of the fixed step size a discrete Fourier transform was used to determine the frequency spectrum of the positions (Fig 1). The transform was calculated using the fast Fourier transform (FFT) function in Matlab [3].

However, the step size is fixed at the lattice period length. This large step size causes aliasing which must be accounted for. The aliasing causes all frequencies to be mapped to a frequency between $-\frac{1}{2L}$ and $\frac{1}{2L}$. The aliased spectrum was found to only include none peak. Therefore

ISBN 978-3-95450-169-4

SOURCE AND LEBT BEAM PREPARATION FOR IFMIF-EVEDA RFQ

L. Bellan †,1, M. Comunian, E. Fagotti, A. Pisent, F. Grespan, INFN-LNL, Legnaro, Italy
P-Y. Beauvais, P. Cara, H. Dzitko, F4E, Garching, Germany
A. Marqueta, F. Scantamburlo, IFMIF/EVEDA Project Team, Rokkasho, Japan
B. Bolzon, N. Chauvin, R. Gobin, F. Senee CEA, Gif-sur-Yvette, France
R. Ichimiya, A. Kasugai, M. Sugimoto, QST, Rokkasho Fusion Institute, Rokkasho, Japan
[1]also at Dipartimento di Fisica e Astronomia, Università degli Studi di Padova, Padova, Italy

Abstract

The commissioning phase of the IFMIF-EVEDA RFQ requires a complete beam characterization with simulations and measurements of the beam input from the IFMIF-EVEDA ion source and LEBT, in order to reach the RFQ input beam parameters. In this article, the simulations results of the complex source-LEBT with the corresponding set of measurements and their impact on the commissioning plan will be reported.

THE IFMIF-EVEDA PROJECT

The Linear IFMIF Prototype Accelerator (LIPAc) is a high intensity deuteron linear accelerator [1]; it is the demonstrator of the International Fusion Material Irradiation Facility (IFMIF) machine within the Engineering Validation Engineering Design Activities (EVEDA) scope. It is presently in an advanced installation phase at Rokkasho under the Fusion Energy Research and Development Directorate National Institutes for Quantum and Radiological Science and Technology (QST), in the prefecture of Aomori, Japan. LIPAc has been designed and constructed mainly in European labs with participation of JAEA in the RFQ couplers. It is composed of an injector delivered by CEA-Saclay [2], a RFQ [3] designed made and delivered by INFN on April 2016, a superconducting Linac designed by CEA-Saclay [4], RF power, Medium and High Energy Beam Transfer lines and a beam dump designed by CIEMAT [5]. The coordination of the European activities is managed by F4E and, on Rokkasho site, the Project Team supported by QST is responsible for coordination, integration and commissioning.

SOURCE AND LEBT

The injector is composed of a 2.45 GHz ECR ion source based on the CEA-Saclay SILHI source design and a LEBT line of about 2.05 m (distance from plasma electrode to RFQ entrance flange). The LEBT is composed of two solenoids with H/V integrated steerers, two diagnostic boxes (one between two solenoids and the second one after the injection cone) and the RFQ injection cone, equipped with repeller electrode. The first diagnostic box contains the following devices:

- Self-polarized Faraday Cup,
- Doppler-Shift Spectroscopy diagnostic,
- Neutralising gas injection device (H2 or Kr gas),
- Chopper
- 4-Grid analyser, for space charge compensation measurement.

The diagnostic box is equipped with:

- Allison-Scanner emittancemeter, placed 300 mm after the RFQ injection point (it will be placed between the two solenoids during RFQ commissioning),
- ACCT for pulsed current diagnostic at RFQ entrance (it will be placed at the end of the RFQ during commissioning),
- Self-polarised beam stop for current measurement.

The diagnostics employed in this section may be biased due to the beam power (14 kW for deuterons) and to the large quantity of electrons inside the beam pipe. Distributed power deposition along the LEBT components may induce thermal effects, which induce deformation on the diagnostics. Moreover, the electrons in the LEBT produced by residual gas ionization and collisions, can give rise to over/under estimation of the beam current reading. Both these effects may be a significant source of errors in beam parameters measurements. Therefore, it is very important to compare the diagnostics output and the simulations prediction, in order to check the understanding of the physics behaviour. The target values are 140 mA (70 mA proton) deuteron beam @ 100 keV (50 keV proton) with $\varepsilon_{n,rms}$ = 0.25 mm mrad and a correct converging beam at RFQ input: mismatch factor [6] lower than 10%. A pulsed beam will be used for RFQ commissioning, so the reproducibility of LEBT beam at different duty cycle up to cw is necessary. Finally a proton beam (50 keV, 70 mA) well characterized would help for beam commissioning.

BEAM DYNAMICS SIMULATION AND MEASUREMENT OF SOURCE AND LEBT

The simulation results presented here are relative to an 86 mA (read from the power supply) hydrogen beam extracted beam at 50 keV, with an estimated proton fraction of 72% (from Doppler shift spectrometer) respect to H2 and H3 measured between the two solenoids of the LEBT ($Q = 3.23\times10^{-3}$ generalised perveance, 55 mA proton beam at beam stop). The emittance measurement done within the maximum transmission area of the BS and the simulation with AXCEL-INP [7] program were used in order to find the Twiss parameter and emittance after 20 cm from the plasma electrodes. The software used for LEBT simulation was TraceWin[8], which is a PIC code with single species transport of 55 mA proton beam. 10000 macroparticles were used and the mesh was

† luca.bellan@lnl.infn.it

PHASE-SPACE TRANSFORMATION FOR A UNIFORM TARGET IRRADIATION AT DONES*

C. Oliver †, A. Ibarra, Centro de Investigaciones Energéticas, Medioambientales y Tecnológicas (CIEMAT), Madrid, Spain
A. Gallego, Universidad Complutense, Madrid, Spain
N. Chauvin, CEA/DRF/IRFU, Gif-sur-Yvette Cedex, France
P. Cara, Fusion for Energy, Garching, Germany

Abstract

In the framework of the EU Roadmap, a DEMO Oriented Neutron Source (DONES) [1] has been proposed to provide a high neutron intense neutron source with a suitable neutron spectrum to understand the degradation of advanced materials under DEMO and future fusion plants irradiation conditions. DONES will be based on the International Fusion Materials Irradiation Facility IFMIF [2], being only one accelerator considered. The HEBT will be devoted to the transport, bending and shaping of the 40 MeV, 125 mA CW deuteron beam to the free surface of the rapidly flowing lithium target. To produce a forward peaked source of fusion-like neutrons, which stream through the target into the test cell, a rectangular uniform distribution across the flat top of the beam profile is required, being the footprint tailored in both the vertical and horizontal directions according to the target design. Different methods for beam uniformization in IFMIF accelerator has been proposed in the past [3]. Two main concerns in DONES will be the minimization of particle losses over the whole HEBT and the effect of the different shaping techniques on such strong space charge regime, especially on the beam halo modulation. A review of the different methods for the beam shaping of the high power, high space charge DONES HEBT beam will be depicted. A final solution will be proposed.

DONES HEBT REQUIREMENTS

The need of a rectangular flat top beam profile on the liquid-Lithium target determines the design of the High Energy Beam Transport (HEBT) line between the superconducting linac and the Liquid Lithium target. Two beam size configurations (20x5 cm2, 10x5 cm2) with 5% top density uniformity are demanded at the Lithium surface. Additionally constraints in the beam tails (to avoid a sudden increase in the deposited power in the Lithium target as well to eliminate heating of the adjacent structure) are imposed. A sketch of the required horizontal and vertical beam profile at target is shown in Fig. 1.

The high space charge, high power beam imposes two additional concerns in the HEBT design: the minimization and safe control from the radioprotection point of view of losses as well the space requirement for beam diagnostics [4].

* This work has been carried out within the framework of the EUROfusion Consortium and has received funding from the Euratom research and training programme 2014-2018 under grant agreement No 633053.
† concepcion.oliver@ciemat.es

BEAM SHAPING

Different techniques of providing an arbitrary spatial beam distribution starting from a given input beam can be found. Active techniques based on pencil beam scanning, used in some other projects as ESS [5], have been shown to be not an option for DONES given the possible disruption of the liquid Lithium by the pressure waves [6].

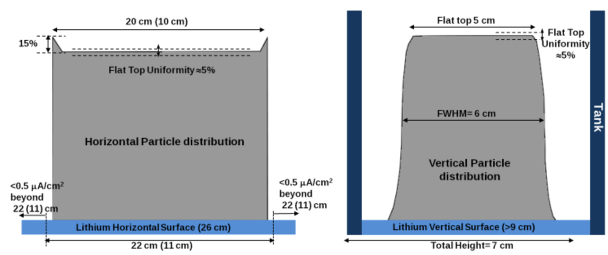

Figure 1: DONES horizontal (left) and vertical (right) beam requirements at the Lithium target.

The use of non-linear magnetic fields to shape the beam to a required beam profile has been considered the best option [7]. Although previous studies showed the advantage of using special dipoles, called “step-like field magnets” [8], which remove the scrapers and their associated shielding, the need of a magnet prototype and the impact on the DONES timeline has pushed to the traditional non-linear magnet solution.

The use of standard high order multipoles to obtain a uniform beam has been well documented and used in several facilities [9, 10]. Whereas particles in the center of the beam distribution are unaffected by the non-linear magnets, the divergence of particles far from the center is modified such, after the subsequent transport, the beam edges are folded into the core.

The lowest-order non-linear magnets are desirable to reduce the magnet aperture and technology difficulties as well possible beam losses. However, octupoles optimized to improve the beam uniformity would have an undesirable large effect on the particles in the very far beam tail, which will be excessively folded, producing losses downstream the octupole. To counteract this effect, critical in DONES given the halo produced by the high space charge, duodecapoles nee to be introduced. With both type of multipoles, the beam uniformity will be almost controlled by the octupoles whereas the maximum beam extension (and the minimum pipe aperture) will be limited by the duodecapoles.

AN RFQ BASED NEUTRON SOURCE FOR BNCT*

X. W. Zhu†, Z. Y. Guo, Y. R. Lu#, H. Wang, Z. Wang, K. Zhu, Y. B. Zou
State Key Lab Nuclear Physics and Technology
Peking University, Beijing 100871, China

Abstract

Boron Neutron Capture Therapy (BNCT) [1, 2], promises a bright prospect for future cancer treatment, in terms of effectiveness, safety and less expanse. The PKU RFQ group proposes an RFQ based neutron source for BNCT. A unique beam dynamics design of 162.5 MHz BNCT-RFQ, which accelerates 20 mA of H+ from 30 keV to 2.5 MeV in CW operation, has been performed in this study. The Proton current will be about 20 mA. The source will deliver a neutron yield of $1.76 \times 10^{13}\ n/sec/cm^2$in the $^7_3Li(p,n)^7_4Be$ reaction. Detailed 3D electromagnetic (EM) simulations of all components, including cross-section, tuners, pi-rods, and cut-backs, of the resonant structure are performed. The design of a coaxial type coupler is developed. Two identical RF couplers will deliver approximately 153 kW CW RF power to the RFQ cavity. RF property optimizations of the RF structures are performed with the utilization of the CST MICROWAVE STUDIO [3].

BEAM DYNAMICS

BNCT treatment requires sufficient fluxes of thermal (< 0.5 eV) or epithermal (0.5 eV ~ 10 keV) neutrons for its application. The 4-vane proton RFQ will accelerate a 15 mA beam to 2.5 MeV at 162.5 MHz in CW operation for safety margin, and it is also demanded that the design should keep high transmission up to 20 mA.

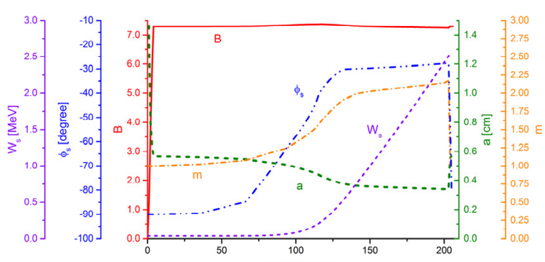

Figure 1: Main parameters of the BNCT RFQ beam dynamics.

The beam dynamics design of BNCT RFQ adopts the New Four-Section Procedure (NFSP) design strategy [4], and the main design parameters are shown in Fig. 1.

Based on the PARMTEQM code [5], 10^5 input macro particles are put into the multiparticle dynamics simulations. Fig. 2 shows the simulation results at 20 mA.

Table 1 summarizes the detailed simulation results, where the Kilpatrick factor is only 1.24, quite reliable for CW operation. The modest inter-vane voltage is kept constant at 65 kV, and does bring benefits to ease the thermal management, which the bottleneck in CW RFQ operation. The transverse focusing strength B is kept constant to simplify the cross-section design, which makes it easier to tune the cavity, and constant transverse radius of curvature allows to machine the vanes with flying cut. The design has a transmission of 99.6% at 20 mA. However, even at 40 mA, which is twice as large as the design value, the transmission is still as high as 96.6%. Tolerance analyses have been completed; the analyses indicate the RFQ design well tolerates the twiss parameters, mechanical and field errors.

Clearly, the design and simulation results satisfy all requirements well for the BNCT RFQ.

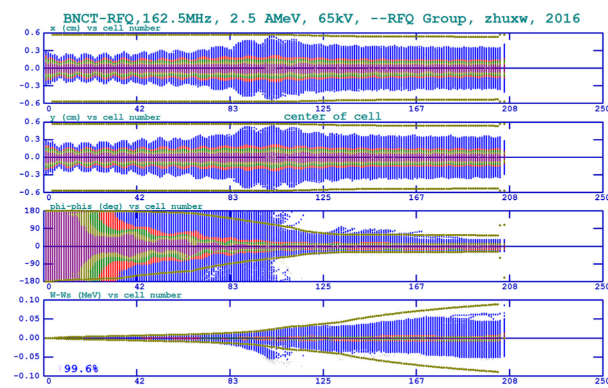

Figure 2: PARMTEQM simulations of the RFQ at 20 mA.

Table 1: RFQ Parameter List

BNCT RFQ	Value
Input energy	35 keV
Output energy	2.5 MeV
Frequency	162.5 MHz
DC current	20 mA
Vane voltage	65 kV
Vane length	523.4 cm
RF power (PEC)	103 kW
Beam Power	50 kW
ε_t(norm. rms, exit)	0.25 mm mrad
ε_l(norm. rms, exit)	0.0655 MeV deg
$E_{s,max}/E_k$	1.24

RF STRUCTURE

The RFQ resonator design aims to satisfy the requirements given by beam dynamics. These studies involves iteration of RF electromagnetic simulations to provide good mode stabilization, right operating frequency, and coupling. Both 2D SUPERFISH code and CST MICRO-

* Work supported by 2014CB845503
† zhuxw13@pku.edu.cn
# yrlu@pku.edu.cn

ISBN 978-3-95450-169-4

ELECTRON DRIVEN ILC POSITRON SOURCE WITH A LOW GRADIENT CAPTURE LINAC

Masao Kuriki*, Takaomi Kakita, Tohru Takahashi,
Hiroshima University, Higashi-Hiroshima, Japan
Kentaro Negishi,Iwate University, Morioka, Japan
Toshiyuki Okugi, Tsunehiko Omori, Masanori Satoh, Yuji Seimiya, Junji Urakawa, Koaru Yokoya,
Accelerator Lab., KEK, Ibaraki, Japan
S. Kashiwagi, Tohoku University, Sendai, Japan

Abstract

ILC (International Linear Collider) is e+ e- linear collider in the next high energy program promoted by ICFA. In ILC, an intense positron pulse in a multi-bunch format is generated with gamma ray from Undulator radiation. As a technical backup, the electron driven positron source has been studied. By employing a standing wave L-band accelerator for the capture linac, an enough amount of positron can be captured due to the large aperture, even with a limited accelerator gradient. However, the heavy beam loading up to 2 A perturbs the field gradient and profile along the longitudinal position. We present the capture performance of the ILC positron source including the heavy beam loading effect.

INTRODUCTION

ILC (International Linear Collider) [1] is an e+ e- linear collider with 500 GeV CME in the first phase and 1000 GeV in the second phase. This is only way to realize the e+ e- collision beyond 350 GeV CME beyond the limitation of a storage ring collider and is an official future project promoted by ICFA. ILC realize the high luminosity as high as $3.0 \times 10^{34} cm^{-2} s{-1}$ with a limited average current, 50 µA. This current is much less than that in a storege ring, but it is a technical challenge, especially for positron source, because it corresponds to 50 times of that in SLC [2]. In the current design [1], the positron is generated by Undulator radiation driven by more than 150 GeV energy electron beam. The high energy electron driver (>150 GeV) is sharedleading a possible long commissioning time for the positron source because it can be operated after the electron main linac is establsihed. To avoid this limitation, an electron driven positron source has been studied.

In the electron driven positron source, the electron driver can be a dedicated several GeV linac. solving the problem related to the beam sharing. The biggest technical challenge on the electron driven positron source is the possible damage on the positron production target. In the undulator positron production, 7.8×10^{13} positrons are generated in 0.8 ms (macro pulse length). If we assume the same time strcture for the electron driven positron source, any taraget can not survive with this heavy thermal heat load and a shock wave induced by the incident beam [3].

Omori et al. proposed a new e-driven scheme relaxing the target load [4] by extending the effective macro pulse length from 0.8 ms to 64 ms. In this scheme, positrons are accelerated by normal conducting accelerator and heavy beam loading is expected. Satoh et al. [5] proposed a beam loading compensation for the travelling wave linac by amplitude modulation. Urakawa [6] proposed a fast amlitude modulation method by combining two RF sources with a fast phase switching. Seimiya, Kuriki, et al. [7] showed that an enough positron, 3.0×10^{10} per bunch can be generated by assuming the beam loading compensation.

In this study, we propose the electron driven positron source for ILC based on the preceding studies [4, 7]. In this study, we assume RF power source off-the-shelf or developoed by exisiting technology. Comparing to the preceding studies, the accelerator gradient is much lower. In addition, we re-evaluated the accelertor gradient and the beam loading compenstation ability on the L-band standing wave accelerator which is used in the capture linac (the 1st accelerator section) after the target by newly developed a multi-cell cavity model. In the following sections, we explain the whole system, a new model for standing wave accelerator based on the multi-cell, and the simulation results.

THE ELECTRON DRIVEN ILC POSITRON SOURCE

Figure 1 shows schematically the electron driven ILC positron source [7]. The positron is generated by inpinging the 4.8 GeV electron beam on W-Re target. AMD (Adiabatic Matching Device) is attached at the downstream of the target to compensate the transverse momentum of the generated positron. This is composed from axially symmetric longitudinal magnetic field is peaked (5 T) at the entrance and decayed down to 0.5 T which is kept over the capture linac which is composed from 28 of L-band standing wave accelerator tubes. Chicane is placed after the capture linac to remove electrons and positrons with a large energy deviation. The booster accelerates the beam up to 5 GeV. It is composed from L-band and S-band traveling wave tubes. ECS (Energy Compressor System) is composed from 4 chicanes and 3 L-band RF structures. This is very important to obtain a good positron yield.

The positron is generated in 1 µs macro-pulse containing 136 bunches with 6.15 ns bunch spacing. This pulse is

* mkuriki@hiroshima-u.ac.jp

MULTISPECIES SIMULATION OF THE FRIB FRONTEND NEAR THE ECR SOURCES WITH THE WARP CODE

K. Fukushima*, S. M. Lund, FRIB, Michigan State University, MI 48824, USA
C. Y. Wong, NSCL, Michigan State University, MI 48824, USA

Abstract

The linear accelerator in the Facility for Rare Isotope Beams (FRIB) will use Electron Cyclotron Resonance (ECR) sources. ECR sources generate a high-brightness DC beam with high charge states. However, the ECR sources produce numerous species that must be collimated to one or two target species with minimal degradation in beam quality. The first stage of this collimation is accomplished in a tight 90° dipole bend with a wide aperture and slanted pole faces to provide additional focusing. We report on simulations carried out with the Warp PIC code [1–3] for operation with high-rigidity Uranium ions. These simulations use linked 2D xy-slice runs in the straight section upstream of the bend and steady-state 3D simulations in the dipole bend. Simulations with ideal (sector) and full 3D field maps of the dipole magnet are contrasted. Issues associated with placing a 3D dipole field with an extended fringe field on a bent coordinate system are addressed. Placement of the dipole bend is optimized consistent with the 3D field and is found to closely correspond to the ideal field center. Minimal problems are found (small centroid shift and distribution distortions) due to 3D space charge effects in the initial species separation within the bend when using simple fractional neutralization factors in the anticipated range.

INTRODUCTION

In the FRIB front-end, diagnostic systems are limited due to the source operating on a high-voltage stand and the many-species beam distribution emerging from ECR source being DC. Therefore it is desirable to develop improved numerical models to better understand uncertainties and support front-end commissioning.

SIMULATION DESCRIPTION

Lattice

Figure 1 (upper panel) shows the front-end lattice from the ECR source through the first bending magnet and (lower panel) the corresponding axial magnetic (from ECR and solenoids; blue) and electrostatic (from grated gap; red) axial accelerating fields in straight section. Parameters of the two solenoids and one electrostatic (ES) gap are listed in Table 1. These elements have short length with wide apertures, so nonlinear fields are significant. Note that fringe fields neighboring elements can overlap — particularly the ECR and the first solenoid. Fields of these elements are calculated in 2D by the finite element codes LORENTZ [4] (ECR solenoids) and Poisson [5] (iron solenoids and ES gap) and imported on a high-resolution r-z mesh.

Table 1: Lattice Element Parameters

Component	Length [cm]	Aperture r [cm]
Solenoid (0.6 [T])	29.6 (coil) 39.52 (iron)	7.75 (coil) 8.00 (iron)
ES Gap (50 [kV])	27.6	9.921 (upstream) 7.620 (downstream)
Bend (0.17 [T])	99.7456 (core) 63.5 (curvature)	20.5 (horizontal) 5.0 (vertical)

The iron bending magnet is modeled with Opera [6] (electromagnetic design software) in 3D. Figure 2(a) shows the vertical dipole field B_y on longitudinal axis ($x = 0$ and $y = 0$) along the center-line of the element, and Fig. 2(b) shows the variation of B_y as a function of the radial coordinate x at the element center ($y = 0$ and $z = 3.047$). B_y varies due to slanted iron poles of the magnet. This magnet has significant nonlinearity and an extended fringe field.

Uranium Beam Emerging from ECR

A multi-species beam beam emerges from the ECR with U with $Q = 25$ to 40 and O (from support gases) with $Q = 1$ to 4 [2]. Two desired "target" species to retain are U^{33+} and U^{34+}. Table 2 summarizes parameters applied to all species emerging from the ECR source. This normalized canonical angler momentum and normalized thermal rms emittance of U^{33+} corresponding to these parameters are 0.381 mm-mrad and 0.042 mm-mrad, respectively.

Table 2: Simple Symmetric Ion Distribution

Initial distribution	Waterbag
Ion temperature	3.0 [eV]
Magnetic field at ion birth	1.65 [Tesla]
RMS size (x, y)	(2.0, 2.0) [mm]
Neutralization factor	75 [%]

PIC SIMULATIONS

In our simulations, we assume an initial Waterbag distribution including space-charge adaption for each charge state [7]. 2D slice (xy) Warp PIC simulations using the model described in Ref. [2] are carried out from the ECR source to before bending magnet. The xy distribution is then used to continuously inject a 3D distribution into the dipole to carry out 3D steady state simulations (advanced twice the ~2 μs dipole transit time of the slowest species).

* fukushim@frib.msu.edu

ONGOING STUDIES OF THE SUSI ECR ION SOURCE AND LOW ENERGY BEAM TRANSPORT LINE AT THE MSU NSCL*

Alfonse N. Pham†, Jesse Fogleman, Bryan Isherwood, Daniela Leitner[1],
Guillaume Machicoane, Derek Neben, Shane Renteria, Jeffry Stetson, Larry Tobos
National Superconducting Cyclotron Laboratory, Michigan State University, East Lansing, MI, USA
[1]also at Lawrence Berkeley National Laboratory, Berkeley, CA, USA

Abstract

Heavy ion accelerator laboratories for nuclear science and rare isotope research require a wide array of high intensity heavy ion beams. Due to their versatility and robustness, Electron Cyclotron Resonance (ECR) ion sources are the choice injectors for the majority of these facilities worldwide. Steady improvements in the performance of ECR ion sources have been successful in providing intense primary beams for facilities such as the National Superconducting Cyclotron Laboratory (NSCL). However, next generation heavy ion beam laboratories, such as the Facility for Rare Isotope Beam (FRIB), require intensities that are approaching the limits of current possibility with state of the art ion source technology. In this proceedings, we present the ongoing low energy beam transport characterization efforts of a superconducting ECR ion source injector system at the MSU NSCL.

INTRODUCTION

The Coupled Cyclotron Facility (CCF) at the NSCL [1] utilizes two superconducting cyclotrons to accelerate primary ion beams up to 160 MeV/u corresponding to beam power deposition on production target of up to 1 kW for rare isotope production. The parallel operation of the two ECR ion source injector systems allow for the delivery of primary beams, from helium up to uranium, to the CCF while permitting development on the other source. The Advanced Room TEMperture Ion Source (ARTEMIS) [2] operating at 14.5 GHz uses normal conducting solenoids for axial confinement and permanent magnet hexapoles for radial confinement, whereas the Superconducting Source for Ions (SuSI) [2] operating at 18 GHz from a klystron and 24 GHz from a gyrotron uses superconducting solenoids and hexapoles for confinement of the plasma.

The production of rare isotopes often require expensive and difficult to obtain stable isotopes as primary beams, therefore research efforts are focused on improving the understanding of heavy ion beam transport in the low energy section of injector systems to minimize systematic beam loss. In this proceedings, we will focus on the superconducting SuSI ECR ion source and its corresponding low energy beam transport line, related beam diagnostics, and beam transport simulation efforts.

* Research supported by Michigan State University and National Science Foundation Award PHY-1415462.
† pham@nscl.msu.edu

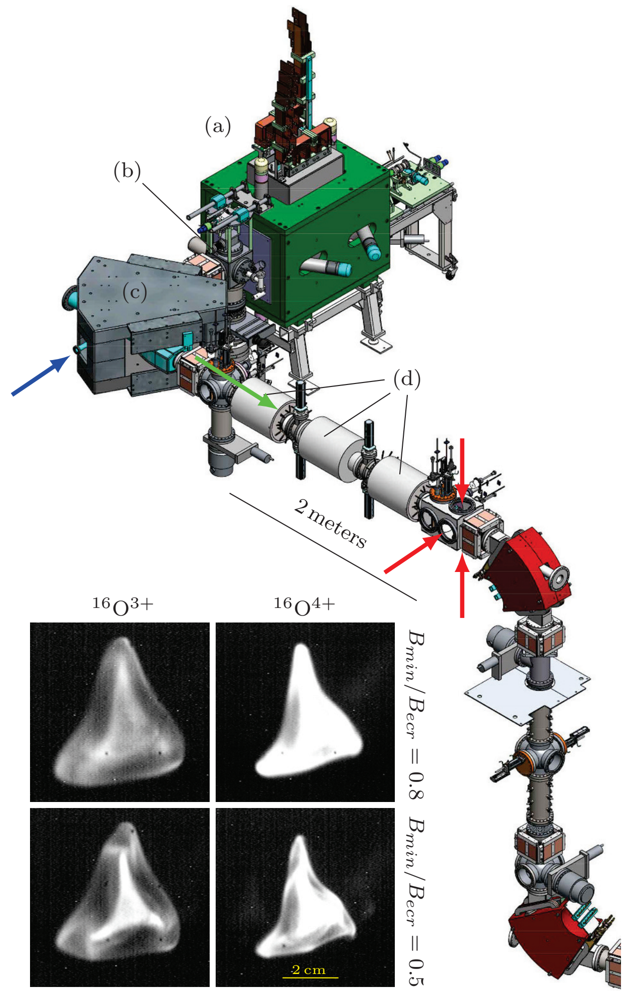

Figure 1: (color) Diagram of the SuSI ECR Ion Source Injector showing (a) the ion source, (b) extraction system, (c) *A/Q* spectrometer, (d) solenoid triplet, blue arrow indicate the location of the HPGe detector, red arrows indicates the location of emittance scanners and scintillator screen, and green arrow the direction of the beam.

BEAM LINE MEASUREMENTS

The relevant portion of the SuSI injector system, shown in Fig. 1, consists of the ECR ion source held at high voltage up to 30 kV, triode extraction system, an Einzel lens, solenoids, steerers, and collimation apertures and slits. The diagnostics on the beam line include Faraday cups for beam current measurements, a high-resolution *A/Q* spectrometer for ion species separation, an Allison scanner [3] for beam

SELF-CONSISTENT PIC MODELING OF NEAR SOURCE TRANSPORT OF FRIB*

Chun Yan Jonathan Wong†, National Superconducting Cyclotron Laboratory, East Lansing, USA
Steven M. Lund, Kei Fukushima, Facility for Rare Isotope Beams, East Lansing, USA

Abstract

Self-consistent simulation studies of the FRIB low energy beam transport (LEBT) system are conducted with the PIC code Warp. Transport of the many-species DC ion beam emerging from an Electron Cyclotron Resonance (ECR) ion source is examined in a realistic lattice through the Charge Selection System (CSS) which employs two 90-degree bends, two quadrupole triplets, and slits to collimate non-target species. Simulation tools developed will support commissioning activities on the FRIB front end which begins early operations in 2017. Efficient transverse (xy) slice simulation models using 3D lattice fields are employed within a scripted framework that is readily adaptable to analyze many ion cases and levels of model detail. Effects from large canonical angular momentum (magnetized beam emerging from ECR), thermal spread, nonlinear focusing, and electron neutralization are examined for impact on collimated beam quality.

INTRODUCTION

The Facility for Rare Isotope Beams (FRIB) is designed to accelerate heavy ions to 200 MeV/u with 400 kW CW on target [1, 2]. The beam is produced by one of two electron cyclotron resonance (ECR) ion sources at the front end: ARTEMIS [3] and VENUS [4]. Each ion source is followed by a charge selection system (CSS) where non-target species passing the first dipole are removed in a high-dispersion region between two 90-degree dipoles. Schematics of the post-ECR and CSS lattices are embedded in Fig. 2 and 1.

Beams emerging from an ECR exhibit complex evolution because: 1) the high-current, many-species beam has strong space charge; 2) the beam is born in a high magnetic field and thus carries large canonical angular momentum; 3) the beam is partially neutralized by electrons from the ionized residual gas; and 4) the lattice is dispersive, has strong acceleration, substantial applied field nonlinearities, and fringe fields overlap for some elements. To better understand how to preserve beam brightness and optimize the CSS, a framework of code tools has been developed using the open-source PIC-code Warp [6]. This paper describes the Warp simulations (see [7, 8] for more details) and how an envelope model is employed for beam matching. Simulations contrasting the performance of the CSS under various initial beam conditions illuminate the impact of canonical angular momentum and space charge. Implications for beam collimation and further transport downstream are discussed.

* Work supported by the U.S. Department of Energy Office of Science under Cooperative Agreement DE-SC0000661 and the National Science Foundation under Grant No. PHY-1102511.

† wong@nscl.msu.edu

FRONT END MODEL IN WARP

Initial Conditions & Loading

Table 1 lists beam parameters used in the Warp simulations. An initial axisymmetric waterbag distribution adapted for space-charge [12] is injected with no centroid offset at the extraction point of the ECR. Each species' envelope extent fills the puller electrode aperture (i.e. $R_{\text{puller}} = 2\sigma_x$ where $\sigma_x^2 = \left\langle x^2 \right\rangle$). The 35kV extraction potential sets the kinetic energy of each species, and the longitudinal velocity spread and radial (thermal component) emittance arise from a 3eV ion temperature. The average canonical angular momentum of each species is set by assuming all ions are born at the same magnetic field, i.e. $\langle P_\theta \rangle = q \left\langle r^2 \right\rangle_{\text{birth}} B_{\text{birth}}/2$, where $B_{\text{birth}} = \int_{z(\text{peak 1})}^{z(\text{peak 2})} B_z(r=0)dz$ is the average axial B-field between the peaks of the solenoidal field of the ECR. Since the B-field at launch differs from B_{birth}, for $\langle P_\theta \rangle = \text{const}$ as specified, an angular velocity is injected upon each ion of the species with:

$$\theta_0' = \left[\frac{\left\langle r^2 \right\rangle_{\text{birth}}}{\left\langle r^2 \right\rangle_{\text{launch}}} B_{\text{birth}} - B_{\text{launch}} \right] / (2[B\rho]). \qquad (1)$$

Here, $[B\rho]$ is the particle rigidity, and we assume $\left\langle r^2 \right\rangle_{\text{birth}} = \left\langle r^2 \right\rangle_{\text{launch}}$. Simulated beam species and currents for U operation are given in Ref. [5].

Table 1: Beam Parameters of U^{34+} Based on VENUS

At launch	
Temperature	3 eV
$\langle P_\theta \rangle / (mc)$	0.305 mm−mrad
$\varepsilon_{r-\text{rms-norm}}$	0.015 mm−mrad
$\sigma_r = \sqrt{2}\sigma_x$	2.82 mm
$\sigma_r' = d\sigma_r/dz$	0
$\mathcal{E}$ (before/after ES Gap)	5.00 / 12.00 keV/u
$[B\rho]$ (before/after ES Gap)	7.13×10^{-2} / 1.10×10^{-1} Tm

Lattice Design & Matching Methodology

The beam line can be divided into two distinct sections: the axisymmetric transfer line from the ECR to the CSS, and the CSS which produces large dispersion for species selection.

ISBN 978-3-95450-169-4

FINAL ACCEPTANCE TEST OF SRF PHOTO-INJECTOR COLD STRING FOR THE bERLinPro ENERGY RECOVERY LINAC *

A. Neumann†, D. Böhlick, P. Echevarria, A. Frahm, F. Göbel, T. Kamps, J. Knobloch, O. Kugeler, M. Schuster, J. Ullrich, A. Ushakov
Helmholtz-Zentrum Berlin, Germany
A. Matheisen, M. Schalwat, M. Schmökel
DESY, Hamburg, Germany
E. Zaplatin
Forschungszentrum Jülich, Jülich, Germany
G. Ciovati, P. Kneisel
JLab, Newport News, Virginia, USA
A. Burrill
SLAC, Menlo Park, California, USA

Abstract

Helmholtz-Zentrum Berlin (HZB) is currently designing and building an high average current all superconducting CW driven ERL as a prototype to demonstrate low normalized beam emittance of 1 mm mrad at 100 mA and short pulses of about 2 ps. In order to achieve these demanding goals HZB started a staged program for developing this class of required high current, high brightness SRF electron sources. In this contribution we will present the current status of the module assembly and testing of the prototype SRF photo-injector cavity cold string. The steps taken to install the cathode insert system with the cavity in the clean room and the following horizontal test of the cold string as final acceptance test prior installation into its cryostat are shown. First beam in a dedicated diagnostics test stand called Gunlab are planned for this winter.

SRF PHOTO-INJECTOR FOR bERLinPro

The high average current all superconducting CW driven energy recovery linac (ERL) bERLinPro is foreseen as a prototype to demonstrate low normalized beam emittance of 1 mm·mrad at 100 mA and short pulses of about 2 ps [1]. It is currently being constructed at HZB in Berlin. In the first stage the photo-injector delivering the beam consists of a 1.4-cell superconducting cavity [2] using a high quantum efficiency (QE) normal conducting multi-alkali cathode [3] implementing a modification of HZDR's cathode insert design [4]. The medium power prototype cavity fabricated by JLab [5] utilizes CW-modified TTF-III couplers allowing an average current up to 5 mA. The purpose of this prototype is mainly to demonstrate the beam dynamics goals and the insertion of a high QE semi-conductor cathode in an SRF cavity. The final high power version is currently in its design and drafting phase. Table 1 summarizes the main RF figures of merit and parameters of operation of the first cavity and the actually achieved values estimated by combining CMM based measurements with RF simulation tools as Superfish and CST [6]. It took quite some effort to reach that stage as production proved to be challenging. This is described in several papers and not repeated here [5, 7, 8]. Here, the final cold string assembly of the cavity is described and the acceptance testing in the horizontal cavity test stand HoBiCaT [9]. In the next months the module will be completed and integrated with the diagnostic beamline of Gunlab [10] to fully study the injector beam's phase space prior to its move to the bERLinPro underground accelerator hall.

Table 1: RF Design Parameters and the Values Estimated for the Prototype Cavity as Produced

Parameter	Design	As built
TM_{010} freq. (MHz)	1300	1300
$R/Q(\Omega)$ $\beta = 1$	150	132.5
$G(\Omega)$	174	154
P_{forward} max. (kW)	20	20
E_{peak}/E_0	1.45	1.66
$B_{\text{peak}}/E_{\text{peak}}$ (mTMV^{-1}m)	2.27	2.18
E_{kin} (MeV)	3.5	2.5-3

THE COLD STRING ASSEMBLY

Figure 1 displays the assembly and testing steps for the gun cavity at JLab and HZB to completely monitor the performance with respect to achievable field level and surface resistance or unloaded quality factor Q_0 during the different construction steps. After helium vessel welding the cavity performed good enough in the final vertical test at JLab, and the critically coupled horizontal RF tests at HZB, to be further prepared for cold string mounting. As shown in the 3D models and pictures below the assembly comes in several stages, where the first part of cold string mounting is

* Work supported by German Bundesministerium für Bildung und Forschung, Land Berlin, and grants of Helmholtz Association

† Axel.Neumann@helmholtz-berlin.de

‡ E_0 is the peak on axis field. The cold string test had an administrative limit of 29 MV/m.

S-BAND BOOSTER DESIGN AND EMITTANCE PRESERVATION FOR THE AWAKE e^- INJECTOR

Oznur Mete Apsimon*†, Robert Apsimon†, Graeme Burt†, Lancaster University, Lancaster, UK
Guoxing Xia†, The University of Manchester, Manchester, UK
Steffen Doebert, CERN, Geneva, Switzerland
†also at The Cockcroft Institute, Sci-Tech Daresbury, Warrington, UK

Abstract

AWAKE is a proton driven plasma wakefield acceleration experiment at CERN which uses the protons from the SPS. It aims to study the self modulation instability of a proton bunch and the acceleration of an externally injected electron beam in the plasma wakefields, during the so called "Phase II" until the technical stop of LHC and its injector chain (LS2) in 2019. The external electron beam of 0.1 to 1nC charge per bunch will be generated using an S band photo injector with a high QE semiconducting cathode. A booster linac was designed to allow variable electron energy for the plasma experiments from 16 to 20 MeV. For an rf gun and booster system, emittance control can be highlighted as a challenging transmission task. Once the beam emittance is compensated at the gun exit and the beam is delivered to the booster with an optimum beam envelope, fringing fields and imperfections in the linac become critical for preserving the injection emittance. This paper summarises the rf design studies in order to preserve the initial beam emittance at the entrance of the linac and alternative mitigation schemes in case of emittance growth.

INTRODUCTION

The Advanced Wakefield Accelerator (AWAKE) project offers an experimental program to study proton beam driven plasma wakefield acceleration (PDPWA). It is currently being built at CERN with the collaboration of many institutes [1]. This project aims to use the proton beam from the SPS accelerator which also serves as the LHC injector alongside with many other experiments at CERN. Plasma wakefields will be induced by the 400 GeV SPS beam and a seeding laser. After establishing the wakefields in a 10 m long plasma, a second beam, the so-called witness beam will be injected into the plasma. The witness beam, which consists of single electron bunch of 0.1 to 1 nC with energies ranging from 16 to 20 MeV, will be accelerated through the plasma [2]. An rf gun based electron injector will provide the witness beam for the AWAKE experiment. The injector system consists of a 3 GHz standing wave (SW) structure based on the existing PHIN gun and a constant gradient travelling wave structure as booster linac. Baseline beam specifications and parameter ranges for systematic plasma experiments which should be delivered by the injector system are summarised in Table 1.

* o.mete@lancaster.ac.uk

Table 1: Specifications for the Simulation Studies for the Baseline and the Parameter Range of Interest

Parameter	Baseline	Range
Beam energy (MeV)	16	10-20
Energy spread (σ, %)	0.5	-
Bunch length, (σ, ps)	4	0.3-10
Beam focus size, (σ, µm)	250	250-1000
Norm. emittance (rms, mm-mrad)	2	0.5-5
Bunch charge, (nC)	0.2	0.1-1

A photo injector is an electron source that uses laser pulses in order to extract electrons from the surface of a metallic or a semiconductor cathode (such as Cu and Cs_2Te). Electrons can escape the cathode surface if the laser pulses provide sufficient energy for electrons to overcome the potential barrier of the surface. The cathode plug is placed in one end of an RF cavity. This RF cavity is used for the rapid acceleration of the electrons after the production. Photo injectors can produce high brightness, low emittance electron beam; this is a mature technology, first implemented in the 1980s. There have been many improvements since then motivating the photo injectors as versatile and reliable electron sources. Some historical highlights and overview of photo injectors can be found in [3–5].

CERN's Super Proton Synchrotron (SPS) will provide the proton beam for the experiment, various modifications were implemented on the corresponding beamline which previously provided protons for neutrino experiments [6,7]. Commissioning of the experiment and data taking will take place in 2016-2017 with protons during the so called "Phase I" [8,9].

In Phase II of the experiment the electron beam will be injected into the plasma to be captured and accelerated by plasma wakefields. The injector consists of an S-band RF gun and traveling wave booster linac. Photoelectrons emerging from a semiconductor cathode will be accelerated to 6.6 MeV by the 2+1/2 cell RF gun with 100 MV/m accelerating gradient. Consequently, the electron beam will be transported to the constant gradient travelling wave booster linac which allows to span the energy range requested by the plasma experiments.

BOOSTER DESIGN

An S-band booster linac, ATS, was designed as a travelling wave structure with constant gradient of 15 MV/m through the entire structure (Fig. 1-a). It consists of 30 cells

ISBN 978-3-95450-169-4

FIELD FLATNESS AND FREQUENCY TUNING OF THE CLARA HIGH REPETITION RATE PHOTOINJECTOR

L.S. Cowie[1], P.A. Goudket, T.J. Jones[1], B.L. Militsyn,
STFC, Daresbury Laboratory, Warrington, UK
G. Burt,Cockcroft Institute, Lancaster University, UK
B. Keune, Research Instruments GmbH, Bergisch Gladbach, Germany
[1]also at Cockcroft Institute, Lancaster University, UK

Abstract

The High Repetition Rate Photoinjector, designed for the CLARA FEL at Daresbury Laboratory, was tuned at the manufacturers for both field flatness and frequency. Due to the high average power in the gun cavity of 6.8 kW the cavity requires significant cooling, achieved by water channels in the cavity body. These channels prohibit the use of tuning studs to tune the cavity. The cavity was tuned by taking pre-braze clamped low power RF measurements and using the data to trim the cavity cells to the optimum length for both field flatness and frequency. The optimum field flatness is 100% and the design frequency is 2998.5 MHz. Both cells were trimmed in 4 stages, resulting in a post-braze frequency of 2998.51 MHz and field flatness of 98%.

INTRODUCTION

CLARA is a new FEL test facility being developed at STFC Daresbury Laboratory in the UK [1]. The main motivation for CLARA is to test new FEL schemes that can later be implemented on existing and future short wavelength FELs. Particular focus will be on ultra-short pulse generation, pulse stability, and synchronisation with external sources.

The High Repetition Rate Gun (HRRG) was developed at Daresbury Laboratory to meet demanding requirements in bunch length and emittance for bunches of up to 250 pC. For operation at 100 Hz for CLARA FEL experiments the cathode surface electric field required is 120 MV/m. The field is lowered for the 400 Hz mode to 100 MV/m. Consequently, the photoinjector must have high power handling capabilities.

The final design is a 1.5 cell normal conducting S-band RF photoinjector [2]. It has a dual feed RF input coupler with phase adjustment of each feed to supress any dipole component in the coaxial coupler line. The cavity schematic can be seen in Fig. 1.

Operation of the CLARA requires a very stable beam arrival time at the FEL. The RF amplitude stability must be 0.1 % and the phase stability 0.1° rms, imposing a temperature stability requirement of 0.009 °C rms [3]. The RF cavity has a probe in the second cell for feed-forward amplitude correction and a thermo-stabilisation system of water channels built into the copper cavity structure and fed by a high resolution control system developed at Daresbury.

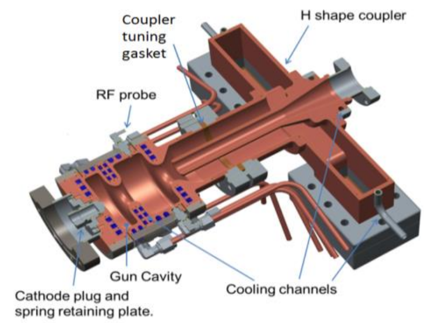

Figure 1: Schematic of the HRRG cavity showing water channels, probe, coupler tuning gasket and removable cathode plug.

Field flatness, which is defined as the ratio of electric field amplitude in cell 1 to cell 2, is essential to reach the highest possible beam momentum and evenly disperse the RF losses in the cavity. Optimum field flatness is achieved when the maximum field amplitudes are equal in each cell. Due to the extensive water channels in the cavity structure there is no scope for the tuning studs typically used to tune the field profile and frequency of a cavity. It was therefore proposed to tune the cavity before brazing using clamped RF measurements and trimming the cell lengths.

TUNING METHOD

The cavity was tuned before brazing at the manufacturers, Research Instruments GmbH [4]. Clamped low power measurements of the operating mode frequency and field were performed at 23 °C with a Cu photocathode plug and the data was used to trim the length of the cells to optimise both RF parameters. Both cells were manufactured with extra length to provide a tuning range that would cover the frequency spread possible due to the radial tolerances. The extra length for each cell was proportional to its length, keeping the field amplitude in each cell of the design cavity equal. The extra length on cell 1 was chosen to be 200 µm and on cell 2 was 422 µm.

Simulations were performed to model the effect of trimming the length of each cell on frequency and field flatness. An algorithm was developed from the simulation results to calculate the amount of length to trim from each cell to reach the target frequency and field flatness from the measured result.

The trimming was performed over 3 steps covering 1/3 of the required frequency correction each, with CMM dimensional measurements and RF measurements taken after each step. This was done to test the method so that correc-

ISBN 978-3-95450-169-4

BEAM INSTABILITIES IN ELECTRON CYCLOTRON RESONANCE ION SOURCES*

Bryan Isherwood†, Eduard Pozdeyev, Guillaume Machicoane, and Yoshi Yamazaki
National Superconducting Cyclotron Laboratory, East Lansing, MI, USA
Facility for Rare Isotope Beams, East Lansing, MI, USA

Abstract

Accelerator facilities for radioactive beams and low energy nuclear physics such as FRIB require intense, stable ion beam currents in order to achieve required reaction rates for rare and undiscovered isotopes. Presently, the only way to produce intense continuous wave beams of highly-charged, medium to heavy-mass ions is with Electron Cyclotron Resonance Ion Sources (ECRIS). The complex nature of these devices causes temporal instabilities to occur, most notably: slow and fast instabilities. Slow instabilities and drifts, occurring over hours, decay the beam current intensity due to variations in ambient and hardware conditions. These drifts require beam operators to constantly monitor and tune ECRIS plasma parameters in order to maintain experimental beam requirements. Fast instabilities, in the form of ms oscillations, occur at operational parameters needed for high-intensity, high-charge state beams. These oscillations cause sudden drops in beam current of the order of 30%. We present here initial results of recent measurements to investigate these instabilities. Results for slow instabilities indicate a linear decay of beam intensity following a sharp current drop due to a brief source conditioning period. Results for fast instabilities show a relationship between the frequency and amplitude of beam oscillations and the electric potential of the plasma chamber bias disk.

INTRODUCTION

ECR ion sources' are the principle devices used in accelerator facilities to generate high intensity, high charge state ion beams. However, instabilities within the system diminish the reliability of modern accelerator facilities by introducing unexpected beamline behaviors. We investigate two types of instabilities: slow intensity drifts and periodic beam instabilities. The slow intensity drift is characterized by a steady continuous change in beam current intensity, typically a decrease, occurring on the order of hours. This effect usually manifests itself following the initial ignition of the plasma but can also be seen when changing plasma parameters. Significant enough drifts lead to increased experimental uncertainty and dead time in beam applications as the constantly changing beam must be tuned regularly. Periodic beam oscillations caused by cyclotron instabilities within the ion source plasma cause catastrophic losses of beam intensity on the order of 30%. These instabilities are characterized by emission of microwave, bremsstrahlung, and visual light radiation from the plasma and ultimately a drop in measured beam current [1]. Oscillations of this type also lead to experimental uncertainties within beamline systems by interfering with RF technologies. The remainder of this report is dedicated to an explanation to the beam current oscillation phenomenon as well as results from a recent measurement designed to explore the effects of different plasma parameters on both instabilities.

* Work supported by the U.S. Department of Energy Office of Science under Cooperative Agreement DE-SC0000661 and the National Science Foundation under Cooperative Agreement PHY-1102511.

† Isherwoo@nscl.msu.edu

THEORY BACKGROUND

While at this time a mathematical description for the slow drift of the ion beam is unknown, great strides have recently been made in understanding physical processes behind the instabilities responsible for the observed beam current oscillations. Cyclotron instabilities ignite within the system when the energy of slow quasi-longitudinal extraordinary wave modes undergo rapid growth [2]. This process can be represented by

$$\frac{dE_\mu}{dt} \approx < \gamma - \delta > E_\mu \qquad (1)$$

where E_μ is the energy of the emitted microwaves and γ and δ are the growth and decay rates, respectively [1]. As the system enters a regime where $\gamma > \delta$, the plasma will begin to amplify the intensity of microwave emissions. Electrons with energies in the range of 10 - 100 keV interact with these microwaves and escape confinement. As a result the beam current is diminished while the electron population of the system recovers.

MEASUREMENT

Measurements were taken using an AECR-U type source, known as ARTEMIS, powered by a 14.5 GHz klysteron source [2]. A 90° analyzing magnet steered the beam to a faraday cup 14 feet downstream of the ion source (Figure 1).

Slow Beam Drift

Several measurements using an argon beam were taken in order to evaluate this effect, each time the system was allowed to evolve for several hours following the plasma's ignition. A set of 5 semiconductor temperature sensors (DS1820) were placed on the source and return water coolant lines for both the plasma chamber and coils as well as the gas inlet line. These thermal sensors were connected to a wireless driver (Embedded Data Systems: OW-SERVER) which communicated with an external computer. The faraday cup

THE TRIUMF ARIEL RF MODULATED THERMIONIC ELECTRON SOURCE

F. Ames†, Y. Chao[1], K. Fong, S. Koscielniak, N. Khan, A. Laxdal, L. Merminga[1], T. Planche, S. Saminathan, D. Storey, TRIUMF, Vancouver, BC, Canada
C. Sinclair, Cornell University, Ithaca, NY, USA
[1]present address SLAC, Menlo Park, CA

Abstract

Within the ARIEL (Advanced Rare IsotopE Laboratory) at TRIUMF, a high power electron beam is used to produce radioactive ion beams via photo-fission. The electron beam is accelerated in a superconducting linear accelerator (linac) up to 50 MeV. The electron source for this linac provides electron bunches with charge up to 15.4 pC at a repetition frequency of 650 MHz leading to an average current of 10 mA at a kinetic energy of 300 keV. The main components of the source are a gridded dispenser cathode (CPI –Y845) in an SF6 filled vessel and an in-air HV power supply. The beam is bunched by applying DC and RF fields to the grid. Unique features of the gun are its cathode/anode geometry to reduce field emission, and transmission of RF power for the modulation via a dielectric (ceramic) waveguide through the SF6. The source has been installed and first tests with accelerated beams have been performed. The complete phase space of the beam has been characterized for different source conditions.

THE ARIEL PROJECT AT TRIUMF

Within the ARIEL project [1] two additional target stations to produce rare isotopes via the ISOL method will be built. Together with the existing ISAC facility (Isotope Separation and ACceleration) they will allow the simultaneous delivery of up to three beams to experiments. One target station will use an additional proton beam from the TRIUMF cyclotron, while the other one will produce rare isotopes via photo-fission of actinide targets or (γ,n/p) reactions. The photo-fission will be achieved by using Bremsstrahlung from up to 50 MeV electrons hitting a converter target in front of the isotope production target. The electron beam will be produced by a superconducting linac operating at a frequency of 1.3 GHz. For the final beam power at the converter target of up to 0.5 MW, it will operate at a continuous beam current of 10 mA.

ELECTRON SOURCE REQUIREMENTS

The electron source should allow continuous beam operation up to an average current of 10 mA. The minimum energy for injection into the accelerator has been determined by electron optics simulations to be 250 keV. In order to operate in a safe regime above this limit, and as it deemed technically not too challenging, the operating voltage of the source has been set to 300 kV.

The beam will be modulated at a frequency of 650 MHz. This is to match to the accelerator structures at half of the cavity frequency. At an average current of up to 10 mA it results in a bunch charge of up to 15.4 pC. With an additional room temperature buncher cavity in front of the injector module the requirement for the pulse length at the source is <±16º of RF phase at 650 MHz, corresponding to 137 ps. The normalized transverse emittance should be about 5 μm.

An additional requirement is the capability to change the duty factor of operation between 0.1% -100% by superimposing a macro-pulse structure at Hz to kHz frequency. It will allow beam tuning and set up at the full bunch charge but at lower average beam power.

The lifetime of the isotope production targets are expected to be up to 5 weeks. Thus, to minimize down time, the maintenance intervals for the source should exceed this time.

ELECTRON SOURCE IMPLEMENTATION

General Concept

A thermionic dispenser cathode has been proven in many applications that it can operate stable and reliable over an extended period of time and doesn't require the extreme vacuum conditions of a photo cathode. Although the brightness which can be achieved with a thermionic cathode is lower, this is not a limiting factor for our application.

When equipped with a grid in front of the cathode surface the beam can be modulated at high frequency. The method has been developed by Bakker et al. [2] for the FELIX accelerator already in 1991 and more recently in 2011 it has been considered for future high intensity accelerators by P. Sprangle et al. [3]. It uses a superposition of DC and RF voltages at the grid. The negative DC voltage blocks the electrons from passing the grid and the source becomes conducting only during a short interval determined by the RF voltage.

RF Modulation of the Beam

Ideally the electron current emitted from the cathode should depend on the voltage applied to the grid following a characteristic curve of a triode. As a good approximation for the estimation of bunch charge and length a linear dependence has been assumed already in [2]. It can be written as:

$$\mathrm{I}(t) = g_{21}(U_g - U_c), \quad (U_g - U_c) \geq 0\,. \tag{1}$$

† email address ames@triumf.ca

LOW-TEMPERATURE PROPERTIES OF 2.6-CELL CRYOGENIC C-BAND RF-GUN COLD MODEL CAVITY*

T. Sakai†, T. Tanaka, K. Nogami, K. Takatsuka, K. Nakao, M. Inagaki, LEBRA, Nihon University, Funabashi, Japan
M. Fukuda, T. Takatomi, D. Satoh, N. Terunuma, J. Urakawa, M. Yoshida, KEK, Tsukuba, Japan

Abstract

Development of a cryogenic C-band photocathode RF gun cavity has been conducted at Nihon University in collaboration with KEK. Improvement of the RF input coupler and the 2.6-cell accelerating structure from the first cold model has been performed using the 3D simulation code CST Studio. The high-purity copper cavity was fabricated at KEK with ultraprecision machining and diffusion bonding technique. The low level RF properties of the cavity measured at room temperature have been in good agreement with the predictions based on the CST Studio calculation. The experiments of 20 K cooling of the cavity have begun at Nihon University since the late summer of 2016. Preliminary 20 K cooling tests have shown the RF properties consistent with the simulation by CST Studio.

INTRODUCTION

Development of a cryocooled 2.6-cell π-mode C-band photocathode RF electron gun has been advanced at Nihon University in collaboration with KEK [1].

In the new cold model cavity, as a major difference from the one fabricated in 2015, the corners of the new cavity cells have been modified to be rounded off for increasing RF power efficiency [2, 3]. Based on the low temperature characteristics data of high-purity copper materials available from NIST [4], the dimensions of the RF input coupler and the 2.6-cell π-mode cavity were determined by the simulations using SUPERFISH [5], CST Studio [6] and GPT [7]. The structure of the input coupler has been modified to improve the VSWR characteristics and the conversion efficiency from the rectangular TE_{10} to the circular TM_{01} mode. The cavity was completed at the Mechanical Engineering Center in KEK by ultraprecise machining and diffusion bonding technique. After low power tests at the room temperature, low temperature cooling experiments of the cavity down to approximately 20 K have been carried out at LEBRA in Nihon University since the late summer of 2016.

PROPERTIES OF THE NEW 2.6-CELL COLD MODEL CAVITY

The field simulation of the first cold model cavity with CST-Studio suggested that, in addition to a large reflection in the coupler, non-negligible TE_{11} mode electric field was excited on the circular waveguide axis. As a result of careful coupler dimension search, the TE_{11}/TM_{01} electric field amplitude ratio on the circular waveguide has been reduced from 17% to approximately 2% in the new model [8].

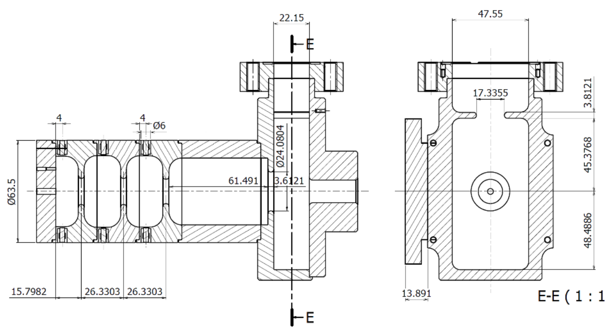

Figure 1: Cross-sectional view of the 2.6-cell π-mode cold model cavity.

The dimensions of the input coupler have also been modified to improve the VSWR characteristics and the conversion efficiency from TE_{10} to TM_{01} mode. The frequency separation from the TM_{01} π/2 mode has been expanded from 20 MHz to 46 MHz [9]. The low temperature surface resistance of the copper cavity has been estimated from the theory of the anomalous skin effect [10]. The linear expansion ratio of copper between 20 K and 296.65 K, $L_{296.65\mathrm{K}}/L_{20\mathrm{K}} = 1.0033529$, was deduced from the resonant frequency shift that occurred at a cooling-test cavity, which is slightly different from the estimate obtained from the

Table 1: Specifications for the 2.6-cell Cryogenic C-band Photocathode RF Gun with Input Coupler

RF frequency @ 20 K	5712	MHz
Source peak RF power	4	MW
Q_0	73029 @ 20 K	
	13310 @ 297 K	
Shunt impedance	603 @ 20 K	MΩ/m
	113 @ 297 K	MΩ/m
Coupling coefficient	19.3 @ 20 K	
	3.52 @ 297 K	
Cavity length	68.2	mm
RF pulse duration	2	μs
RF pulse repetition rate	50	Hz
Maximum field on axis	95	MV/m
Output beam energy	0.73	MW
RF duty factor	0.01	%
Maximum beam charge	0.5	nC/bunch
Laser pulse repetition rate	357	MHz
Laser pulse length	10-20	ps
Maximum beam energy	3.5	MeV

* Work supported by the Photon and Quantum Basic Research Coordinated Development Program of the Japanese Ministry of Education, Culture, Sports, Science, and Technology (MEXT).
† sakai@lebra.nihon-u.ac.jp

UPS STUDY FOR CSK2SB PHOTOCATHODE

Masao. Kuriki†, Lei Guo, Masahiro Urano, A.Yokota, HU/AdSM, Higashi-Hiroshikma, Japan
Taro Konomi, Yuji Seimiya (KEK, Ibaraki), Kentaro Negishi, Iwate University, Morioka, Japan

Abstract

CsK2Sb photo-cathode is one of the ideal cathode for accelerators requiring the high brightness electron beam. It can be driven with a green laser which can be generated as SHG from solid state laser. The QE (Quantum Efficiency) of photo-electron emission is as high as more than 10% with 532 nm light. The material is robust and the typical operational lifetime is more than several months. It is also vital against the high intensity beam extraction. The photo-cathode is generated as a thin film in-situ and the material property and optimized condition for the cathode formation is not understood well. In this article, we present UPS analysis of CsK2Sb cathode for deeper understanding.

INTRODUCTION

CsK2Sb is a photocathode, which is generated by evaporation in a high vacuum environment as a thin film on a substrate. The initial beam performance is very important in an accelerator based on a linear accelerator, because the performance strongly depends on the initial beam. The material is paid attention as a high performance photo-cathode material, because it can be driven with a visible light, quantum efficiency of the photo-emission (QE) is as high as more than 10% with 532 m laser [1], and it is robust comparing to other material.

To achieve the best performance of a photo-cathode material, we should understand what determines the cathode performance. Betes investigated that the property of Cs3Sb photocathode [2]. He found that the cathode performance depends on the chemical state, which can be extracted from XPS (X-ray Photo-electron Spectroscopy) spectrum. The ratio of cross sections of Cs5s Cs5p states has a correlation to the cathode performance, QE. The ratio shows the crystalline condition of CS3Sb and the result shows that the ion crystalline Cs3Sb gives a better performance. Ettema and Groot calculated CsK2Sb's band structure [3]. It is shown that Sb 5p band located at top of the valence band and the cross section of this band has a large influence to the cathode QE. In this article, we perform Ultraviolet Photoelectron Spectroscopy (UPS) experiment for CsK2Sb with UPS to evaluate correlation between the surface state and the cathode performance, what Betes did for Cs3Sb. UPS is one of the experimental way of studying material's surface electron state [4]. The experimental setup is schematically shown in Fig. 1. Monochromatic UV light obtained by a Synchrotron facility with a monochrometer, illuminates the sample and the kinetic energy of the photo-electron is measured by an electro- static analyser.

†mkuriki@hiroshima-u.ac.jp

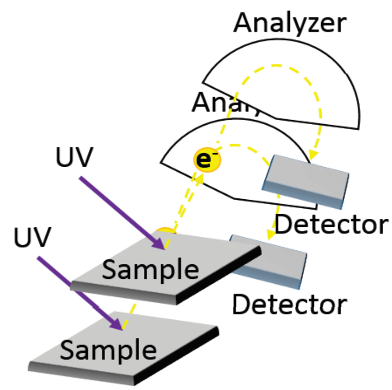

Figure 1: An image of an UPS system. Generated electrons are divided its kinetic energy through analysed by static electrical field in the analyser and counted by CCD.

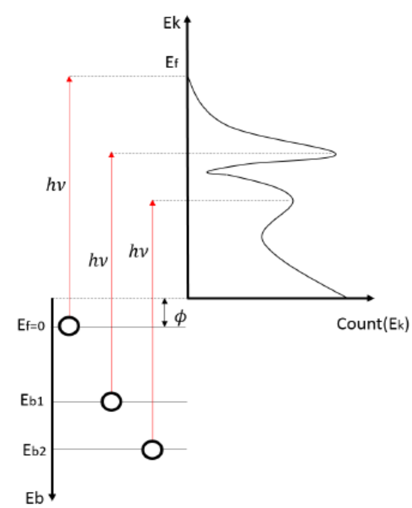

Figure 2: This figure shows UPS principle. In the figure, Ef means Fermi level, Eb means electron's binding energy. hv is photon's energy in the UV. Φ is a sample's work function.

By sweeping the energy of the analyser, an UPS spectrum is obtained. The UPS spectrum reflects the band structure of the material as shown in Fig. 2.

EXPERIMENT

The experiment was carried out at UVSOR BL2B beamline [6]. UVSOR is a synchrotron radiation facility with 750 MeV electron beam energy in Okazaki, Japan. 59eV UV light was used to take the UPS spectra. The cathode is generated by evaporation in an evaporation chamber, which is specially designed for this experiment [5]. This chamber is connected to UPS chamber where UPS spectrum was taken, and the cathode sample is transferred to

 ISBN 978-3-95450-169-4

DESIGN AND IMPLEMENTATION OF AN AUTOMATED HIGH-PRESSURE WATER RINSE SYSTEM FOR FRIB SRF CAVITY PROCESSING*

I. Malloch#, E. Metzgar, L. Popielarski, S. Stanley, Facility for Rare Isotope Beams (FRIB), Michigan State University, East Lansing, MI 48824, USA

Abstract

Traditionally, high-pressure water rinse (HPR) systems have consisted of relatively simple pump and rinse wand actuator systems intended to clean superconducting radio frequency (SRF) cavities during processing prior to test assembly. While these types of systems have proven effective at achieving satisfactory levels of cleanliness, large amounts of operator touch-labor are involved, especially in SRF cavities with complex geometries, where several fixture changes and cavity manipulations may be required. With this labor comes the risk of cavity damage or contamination, and the expense of the operator's time. To reduce this operator intervention and maximize cavity cleanliness and process throughput, a new, fully-automated, robotic HPR system has been commissioned in the Facility for Rare Isotope Beams (FRIB) cavity processing facility. This paper summarizes the design and commissioning process of the HPR system, and demonstrates improvements to the FRIB processing facility through the minimization of cavity contamination risk and reduction of technician labor through system automation. Comparative cavity RF test results are presented to further demonstrate system effectiveness.

INTRODUCTION

High-pressure rinsing (HPR) has been performed successfully at FRIB for many years on a research and development scale. The simple rinse system used previously, consisting of a rotary table and a rinse wand attached to a linear actuator, could be adapted for use with a wide variety of cavities, and served its purpose well. However, though flexible, this system required a large amount of fixtures to be used to support and align the cavities.

This reliance on fixtures was detrimental in two ways. First, the need to frequently change and manipulate fixtures during the rinse cycles increased the possibility of damage and contamination to the cavity. Operator error in fixture assembly and/or improper alignment could easily have caused cavity damage due to impact from the wand, and the repeated fastening and unfastening of bolts, dowel pins, and locking levers, as well as the rotating sprockets, bearings, and chains were a source of particulate contamination risk.

The second concern was the high labor cost associated with the operation of this system. The heaviest of the FRIB cavities weighs more than 90 kg, and, as such, requires more than one operator to manipulate in the fixture. The large amount of operator touch labor associated with these manipulations was not sustainable for the high-volume of processing required for the FRIB project. For these reasons, an automated rinse system was procured and installed to improve the efficiency and quality of the cavity rinsing process. The use of this system is anticipated to save more than 2500 person-hours of labor over the course of the project, as shown in Table 1 below.

Table 1: Labor Savings from New HPR System

Cavity Type	FRIB Production Cavity Quantity	R&D HPR Hours per Cycle	Robot HPR Hours per Cycle	Total Hours Saved
β=0.041	12	4	1	36
β=0.085	100	4	1	300
β=0.29	72	9	1	576
β=0.53	148	9	1	1184

Net Labor Savings (hrs)	2096
20% Reprocessing Labor (hrs)	419.2
Total Labor Savings (hrs)	**2515.2**

DESIGN AND INSTALLATION

Design and Procurement Process

While proposing designs, three primary concepts were focused on safety, quality, and efficiency. The most important of these, safety, would be achieved by minimizing the handling of the cavities required by the operator, and by barring the operator from entering any areas containing stored energy hazards. Quality would be achieved by analyzing the design for its ability to clean the cavities thoroughly, and efficiency by minimizing the amount of operator labor required to run a rinse cycle.

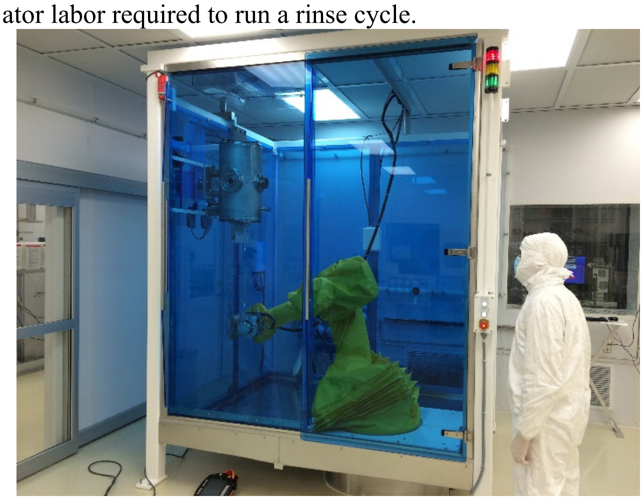

Figure 1: Robotic high-pressure rinse system, installed.

The HPR system went through several design iterations before the design was finalized. The initial designs were all

* This material is based upon work supported by the U.S. Department of Energy Office of Science under Cooperative Agreement DE SC0000661, the State of Michigan and Michigan State University.

malloch@frib.msu.edu

LOW TEMPERATURE NITROGEN BAKING OF A SRF CAVITY*

P. N. Koufalis†, F. Furuta, M. Ge, D. Gonnella[1], J. J. Kaufman, M. Liepe, J. T. Maniscalco, R. D. Porter
Cornell University, CLASSE, Ithaca, NY, USA
[1] also at SLAC National Accelerator Laboratory, Menlo Park, CA, USA

Abstract

We present the effects of a low temperature 160 °C nitrogen bake on the performance of a single-cell 1.3 GHz niobium cavity. The cavity demonstrated the same increase in quality factor, Q_0, and anti-Q-slope typical of cavities nitrogen-doped at 800°C reaching a maximum Q_0 of 3.6×10^{10} at $E_{acc} = 16$ MV/m and $T = 2.0$ K. Compared to the doping procedures in the high temperature regime, this method requires no post-treatment chemical etching.

INTRODUCTION

Impurity doping has been a topic of recent interest in the superconducting radio frequency (SRF) community, with much of the current focus on nitrogen as an interstitial impurity in bulk-niobium cavities. Previous experiments [1–3] have shown that nitrogen doping has the potential to increase cavity quality factor, Q_0, by a factor of two or more and gives rise to the so-called "anti-Q-slope". Until very recently, nitrogen doping has typically been done in the temperature regime ($T \geq 800$ °C) where niobium nitrides form on the surface, necessitating post-treatment chemical etching. Our focus here is on the nitrogen bake of a SRF cavity in the low temperature regime ($T \leq 200$°C) based on previous work at Fermilab [4] where nitride formation is not an issue and post-treatment chemistry is not needed. We show that low temperature nitrogen baking leads to cavity performance on par with cavities prepared in the high temperature regime.

CAVITY PREPARATION

A single-cell ILC-shaped 1.3 GHz bulk-niobium cavity, LTE1-4, received a chemical etching to ensure the removal of any contaminants or prior dopants, followed by a low temperature nitrogen bake at 160 °C and subsequently a long annealing period. The preparation procedure is outlined below:

1. Outside buffer chemical polish (10 min)
2. Inside vertical electropolish (16 µm)
3. 800 °C (12 hr in UHV)
4. 160 °C (48 hr in 35 mTorr N_2)
5. 160 °C (168 hr in UHV)

The degassing step (i.e. $T = 800$°C) removes hydrogen introduced by the BCP and EP and diffuses the oxygen from the oxide layer deep into the bulk. The nitrogen baking step exposes the the cavity surface to nitrogen gas and the annealing step allows for any nitrogen taken up by the surface diffuse further into the bulk

RF TESTING

Following the low temperature nitrogen bake, the cavity was rinsed on a high-pressure rinsing system before being assembled and tested. Measurements of cavity Q_0 vs. E_{acc} were taken at $T = 2.0$ K and are shown in Fig. 1. Anti-Q-slope and improvement in Q_0 are evident. The Q_0 continued to rise to a maximum of 3.6×10^{10} at $E_{acc} = 16$ MV/m before gradually decreasing.

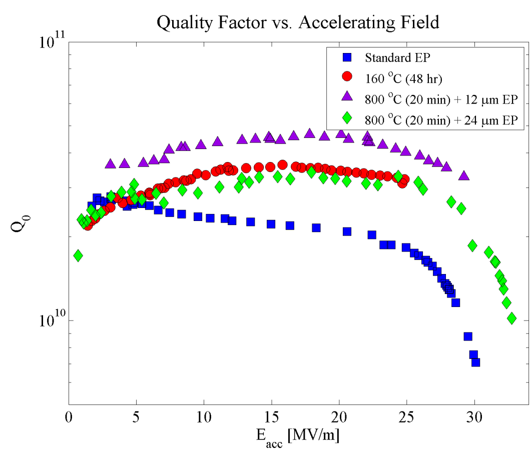

Figure 1: Cavity Q_0 vs. E_{acc} at $T = 2.0$ K. Both the high and low temperature treatments in a nitrogen atmosphere produce an anti-Q-slope and increased Q_0 compared to the baseline test (squares) of a standard niobium cavity.

For comparison, Q_0 vs. E_{acc} data taken previously from two high temperature (800 °C) doped cavities are shown in Fig. 1. A standard bulk niobium cavity is shown as well to serve as a performance baseline. The two doped cavities were treated in a nitrogen atmosphere at 800 °C for 20 min followed by a 30 min anneal at the same temperature in ultra-high vacuum. Each had a different amount of post-treatment material removal via vertical electropolishing. The cavity with the low temperature nitrogen treatment performs similarly to the doped cavity with the 24 µm EP removal in the medium field region but does not quite reach the same level of performance as the cavity with the 12 µm of material removal. Both quantitatively and qualitatively, the low temperature treatment and high temperature doping produce very similar results.

Figure 3 shows the deconvolution of R_{BCS} and R_0 at 2.0 K where these are the temperature dependent and independent

* Work supported by NSF Award PHYS-1416318
† pnk9@cornell.edu

AN ANALYSIS OF FAST SPUTTERING STUDIES FOR ION CONFINEMENT TIME*

Derek Neben†, Guillaume Machicoane, Guy Parsey, Alfonse Pham,
Jeffry Stetson, and John Verboncoeur
National Superconducting Cyclotron Laboratory, Michigan State University, East Lansing, MI, USA

Abstract

Existing heavy ion facilities such as the National Superconducting Cyclotron Laboratory at Michigan State University rely on Electron Cyclotron Resonance (ECR) ion sources as injectors of highly charged ion beams. Long ion confinement times are necessary to produce dense populations of highly charged ions due to the steadily decreasing ionization cross sections with increasing charge state. To further understand ion extraction and confinement we are using a fast sputtering technique first developed at Argonne National Laboratory (ANL) [1] to introduce a small amount of uranium metal into the plasma at a well-defined time. We present an analytical solution to the coupled ion density rate equations for using a piecewise constant neutral density to interpret the fast sputtering method.

INTRODUCTION

ECR Ion Sources (ECRIS) are injectors of choice for many heavy ion accelerators worldwide. These ion sources can ionize elements to higher charge states with greater brightness than other source types, and metallic beams such as uranium or calcium are routinely produced. A pure metal or a metallic compound is vaporized into a support plasma, typically consisting of a naturally gaseous element like oxygen. Well-developed techniques for metal vaporization include laser ablation, sputtering, and neutral beam ovens. Two methods, sputtering and laser ablation, have been developed at ANL to probe ion characteristic timescales in an ECR plasma [1, 2]. Repetitive short bursts of neutral metal vapor were added to the established stable gaseous plasma and observed as pulses of extracted metallic beam current. Each charge state of the metal contaminant was resolved through a dipole magnet and collected on a Faraday cup. The measured beam current was sampled with an oscilloscope. We present an analytical solution that attempts to deconvolve ion confinement from beam current waveforms. We consider the following reactions: single electron impact ionization

$$A^i + e = A^{i+1} + 2e, \tag{1}$$

charge exchange

$$A^i + A = A^{i-1} + A^+, \tag{2}$$

and electron recombination

$$A^i + e = A^{i-1} + E_\gamma \tag{3}$$

for our analysis of ion density. In Eq. (1), (2), (3), A denotes a molecule or atom, i represents the charge state, e the electron, and E^γ the radiated photon energy.

ANALYTICAL SOLUTION FOR ION DENSITY

A reaction rate is defined by

$$\int_\infty \sigma_{i\to j}(E) v f_e(E) dE = n_e < \sigma v >_{i\to j} . \tag{4}$$

The Electron Energy Distribution Function (EEDF) is assumed to be isotropic in velocity space and rewritten in terms of energy $f_e(E)$. The reaction rate is calculated by weighting the EEDF by cross section $\sigma(E)$ and center of mass scalar velocity v. We assume no energy dependence on the particle location and therefore electron density n_e may be treated as a scalar and is separated from the EEDF explicitly. We may write all the source and sink rates for a single ion species as

$$\begin{gathered} dn_i/dt = n_e n_{i-1} < \sigma v >_{i-1\to i} + \\ n_0(t) n_{i+1} < \sigma_{cx} v >_{i+1\to i} + n_e n_{i+1} < \sigma_r v >_{i+1\to i} \\ - n_e n_i < \sigma v >_{i\to i+1} - n_0(t) n_i < \sigma_{cx} v >_{i\to i-1} \\ - n_e n_i < \sigma_r v >_{i\to i-1} - n_i/\tau_i \end{gathered} \tag{5}$$

wherein: n_i is the density of the i^{th} ion, σ_{cx} is the charge exchange cross section between ions and neutrals, σ_r is the recombination cross section between ions and electrons, σ without subscript represents an ionization cross section, and the ion confinement time for the i^{th} species is written as τ_i. Since Eq. (5) is cumbersome, it may be simplified to

$$dn_i/dt + \gamma_i n_i = \alpha_i n_{i-1} + \beta_i n_{i+1} \tag{6}$$

by creating effective rate coefficients α, β, and γ that are multiplied to respective ion densities. These rate coefficients carry units of inverse time and are real and positive. Additionally, α and β act as particle sources into the i^{th} charge state while γ represents an effective sink from the i^{th} charge state.

Expansion in Charge State

Due to cross coupling in ion density within Eq. (5), a complete analytical solution across all charge states is not practical. Therefore, we consider here only a small subset of charge states. We will include the effects of the neighboring charge states by taking a time derivative of Eq. (6) to produce

$$d^2 n_i/dt^2 + \gamma_i dn_i/dt = \alpha_i n_{i-1}/dt + \beta_i n_{i+1}/dt. \tag{7}$$

The ion species n_i under analysis, from the beginning, was assumed to be a sufficiently small perturbation that the rate coefficients are fixed in time by the more numerous support

* Work supported by Michigan State University and the National Science Foundation: NSF Award Number PHY-1415462

† neben@nscl.msu.edu

ISBN 978-3-95450-169-4

DEVELOPMENT OF 6 MeV EUROPEAN S-BAND SIDE-COUPLED INDUSTRIAL ELECTRON LINEAR ACCELERATOR AT RTX & KAERI

P. Buaphad[1,2,3]*, Y. Kim[2,†], K. B. Song[1], H. D. Park[1], S. Y. Yoo[1], S. S. Cha[2], and Y. Joo[2,3]
[1]Radiation Technology eXcellence, Daejeon 34025, Korea
[2]Korea Atomic Energy Research Institute, Daejeon 34057, Korea
[3]University of Science and Technology, Daejeon 34113, Korea

Abstract

There are growing demands on low energy electron linear accelerator (linac) for industrial applications. Most of industrial electron linacs require a compact structure and limited undesirable neutron production to avoid huge lead shielding. Radiation Technology eXcellence (RTX) and Korea Atomic Energy Research Institute (KAERI) have developed a 6 MeV compact side-coupled linac by using 2998 MHz European S-band RF technology to meet those requirements. To design the linac structure, the 3D CST MICROWAVE STUDIO (CST-MWS) was used for various electromagnetic simulations, and ASTRA code was used for particle beam dynamics simulations. After various optimizations, the shunt impedance of 61 MΩ/m is obtained at 2998.38 MHz. With a peak RF power of 2.2 MW and a 47 cm-long structure, electron beam with a peak current of 150 mA can be accelerated from 25 keV to 6 MeV. For the industrial linac, the electron beam spotsize at an X-ray target, located 5 cm downstream of the linac structure exit should be smaller than 2 mm (FW). In addition, it can supply an X-ray dose rate of 8 Gy/min at 1 m after the X-ray target. In this paper, we describe the design concepts and optimization of the 2998 MHz side-coupled industrial linac structure.

INTRODUCTION

The Non-Destructive Testing (NDT) is an analysis technique widely used in industry to evaluate the properties of materials, components without causing any damage [1]. Generally, the NDT method uses ultrasonic, X-ray, gamma, neutron, or eddy-current to examine a sample. However, the X-ray NDT can inspect materials with a higher resolution [2, 3]. Recently, the X-ray NDT systems based on low energy S-band electron linear accelerator (linac) have been playing more and more important roles in industrial applications [4]. Therefore, the demands of low energy electron linac for industrial activities have been increasing rapidly. The industrial electron linacs are required a self-shielding system and reasonably compact for easy system relocation [1].

As shown in Fig. 1, for the NDT system, recently, Radiation Technology eXcellence (RTX) [5] and Korea Atomic Energy Research Institute (KAERI) have been developing an industrial electron linac with a nominal energy of 6 MeV and an X-ray radiation dose rate of 8 Gy/min at 1 m. Our linac is a 47 cm-long standing wave accelerating structure, which uses the side-coupled coupling technology. It is primarily aimed to be operated in the $\pi/2$ mode, and it can accelerate electrons up to 6 MeV. This electron energy can give a sufficiently high yield of the X-ray to penetrate a 30 cm-thick steel [1]. This paper describes the design of electron linac with a side-coupled structure, and the beam dynamics of electrons in the linac structure.

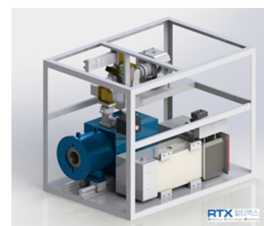

Figure 1: The compact industrial NDT system based on the European S-band electron linac.

AN INDUSTRIAL ELECTRON LINAC

The main components of the European S-band industrial electron linac are a DC electron gun, a 2998 MHz RF accelerating structure based on the side-coupled coupling, and an RF magnetron. The ALTAIR A102414 electron gun is used as its electron source, and it can be applied the maximum gap voltage of 25 kV. This electron gun is connected directly to the accelerating structure, so the wall of its first cell acts as the anode of the electron gun. The accelerating structure is designed by coupling 9.5 cells together through side-coupled cells. The first 2.5 cells are bunching ones where their relativistic speeds are less than 0.98. The first half cell plays an important part of the accelerating structure. When the DC-injected electron beam from the gun enters the half cell, it is confronted with the maximum electric field and receives energy gain effectively. The magnetron that we have chosen for the NDT systems is an MG6090 tunable S-band magnetron made by e2v technologies. It can supply a 3.1 MW RF power at an RF frequency from 2993 MHz up to 3002 MHz for an RF pulse length of 5 µs and an RF pulse repetition rate of 200 Hz. The RF output power is coupled to the WR-284 type waveguide with internal dimensions of 72.14 mm × 34.04 mm.

DOSE RATE OF X-RAY RADIATION

The compact industrial electron linac as the X-ray source works in a pulsed mode, and the dose rate of the X-ray pulses

* buappika@kaeri.re.kr
† yjkim@kaeri.re.kr

LCLS-II CRYOMODULES PRODUCTION AT FERMILAB*

T. Arkan†, C. Grimm, J. Kaluzny, Y. Orlov, T. Peterson, K. Premo,
Fermi National Accelerator Laboratory, Batavia, USA

Abstract

LCLS-II is an upgrade project for the linear coherent light source (LCLS) at SLAC. The LCLS-II linac will consist of thirty-five 1.3 GHz and two 3.9 GHz superconducting RF continuous wave (CW) cryomodules that Fermilab and Jefferson Lab (JLab) will assemble in collaboration with SLAC. The LCLS-II 1.3 GHz cryomodule design is based on the European XFEL pulsed-mode cryomodule design with modifications needed for CW operation. Fermilab and JLab will each assemble and test a prototype 1.3 GHz cryomodule to assess the results of the CW modifications, in advance of 16 and 17 production 1.3 GHz cryomodules, respectively. Fermilab is solely responsible for the 3.9 GHz cryomodules. After the prototype cryomodule tests are complete and lessons learned incorporated, both laboratories will increase their cryomodule production rates to meet the challenging LCLS-II project requirement of approximately one cryomodule per month per laboratory. This paper presents the Fermilab Cryomodule Assembly Facility (CAF) infrastructure for LCLS-II cryomodule production, the Fermilab prototype 1.3 GHz CW cryomodule (pCM) assembly and readiness for production assembly.

INTRODUCTION

The LCLS-II main linac 1.3 GHz cryomodule (CM) is based on the XFEL design, including TESLA-style superconducting accelerating cavities, with modifications to accommodate CW (continuous wave) operation and LCLS-II beam parameters [1]. Two prototype cryomodules (pCM) were planned for assembly at Fermilab and JLab to confirm the design modifications. The 3.9 GHz CM assembly will follow the 1.3 GHz CMs, for efficiency.

At Fermilab, the pCM was assembled between September 2015 and June 2016. For the prototype cryomodule, 8 ILC style bare cavities were processed with a high-Q0 recipe and then vertical-test qualified at Fermilab's Vertical Test Stand (VTS) [2]. The qualified bare cavities were jacketed in a helium vessel at the CAF TIG welding glove box [3]. The dressed cavities were tested and qualified for cavity string assembly at VTS and/or at Fermilab's Horizontal Test Stand (HTS) [4].

For the 16 production cryomodules, the cavities will be fabricated, surface processed, jacketed with a helium vessel, and assembled (ready to be tested at VTS) at the cavity vendors. Qualified cavities will arrive at the CAF for string assembly. To date, Fermilab has received eight cavities from the cavity vendors, and five of those cavities were vertical test qualified and delivered to the CAF to start cavity string assembly of the first production module.

The procurement responsibilities for cryomodule components for the prototypes and production cryomodules are divided between Fermilab and JLab. SLAC is managing the fundamental power couplers procurement. Each laboratory is responsible for procuring a specific component for all 35 cryomodules. The components for 16 and 17 CMs will be drop shipped from vendor(s) to Fermilab and JLab, respectively. Acceptance Criteria Strategy (ACS) documents have been jointly developed for each major component procurement to establish common incoming QC guidelines. The incoming QC and acceptance of the component is done by each laboratory. At Fermilab, an LCLS-II CM supply chain manager coordinates the life cycle of the procured components from receipt, acceptance, storage, and kitting, to delivery to CAF production floors.

CRYOMODULE ASSEMBLY FACILITY

The CAF consists of two assembly/production floors: CAF-MP9 and CAF-ICB. CAF-MP9 (see Figs. 1 and 2) houses the cleanroom which consists of a ~250 square meter cleanroom complex which has Class 10 (ISO 4), 100 (ISO 5) and 1000 (ISO 6) areas. There are two workstations (WS) setup in the cleanroom: WS0 is for coupler cold end assembly to the qualified dressed cavity and WS1 is for cavity string assembly. After the string is assembled, it is rolled to WS2 for cold mass assembly phase-I.

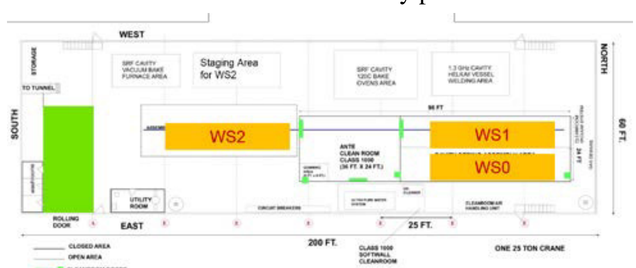

Figure 1: CAF-MP9 layout.

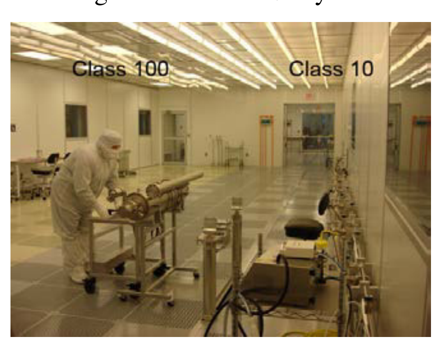

Figure 2: CAF-MP9 cleanroom.

*Work supported, in part, by Fermi Research Alliance, LLC under Contract No. DE-AC02-07CH11359 with the United States Department of Energy and the LCLS-II Project
†arkan@fnal.gov

ISBN 978-3-95450-169-4

AN ITERATIVE LEARNING FEEDFORWARD CONTROLLER FOR THE TRIUMF E-LINAC*

M. Laverty, K. Fong, TRIUMF, Vancouver, BC, Canada

Abstract

In the TRIUMF e-linac design, beam stability to within 0.1% within 10 usec in pulse mode is a design requirement. Traditional feedback control systems cannot respond within this time frame, so some form of feedforward control is needed. Even conventional feedforward may not be sufficient due to differences between the required feedforward signal and the actual beam-loading current. For this reason, an adaptive feedforward system using an iterative learning controller was developed for the e-linac LLRF. It can anticipate repetitive beam disturbance patterns by learning from previous iterations. The design and implementation of such a control algorithm is outlined, some simulation results are presented, and some preliminary test results with an actual cavity are illustrated.

INTRODUCTION

Some background information on the TRIUMF electron linac is first outlined. The design of the feedforward system is then described. Some simulation results are presented. Finally some test results using the system with an actual cavity are detailed.

THE TRIUMF E-LINAC

A diagram of the current e-Linac accelerator showing the installation stages is shown in Fig. 1.

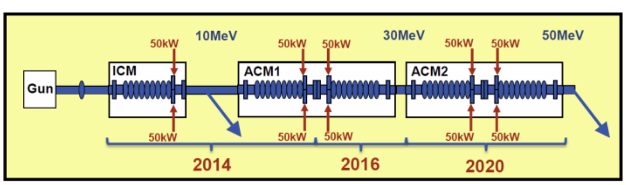

Figure 1: TRIUMF e-Linac schematic[1].

The system includes an electron gun biased at 300 kV, capable of 10 mA CW, and modulated at 650 MHz. A dielectric waveguide is used to carry the rf to the gun. An injector cryomodule containing a single 9-cell 1.3 GHz cavity follows. Next come two accelerating cryomodules each containing two 1.3 GHz 9-cell cavities. The accelerating cryomodules are each driven by a single klystron with power splitting and phase adjusters for the four couplers. Each cavity operates at 10 MeV for a total of 50 MeV of acceleration or 0.5 MW of beam power.

* TRIUMF receives federal funding via a contribution agreement through the National Research Council of Canada

THE ITERATIVE LEARNING CONTROLLER

Figure 2 shows a block diagram of a typical iterative learning controller[2]. The rf components have been omitted for simplicity. The lower part of the diagram represents a conventional feedback controller. The upper part of the diagram includes the ILC controller and its associated memories for the error signal and output drive.

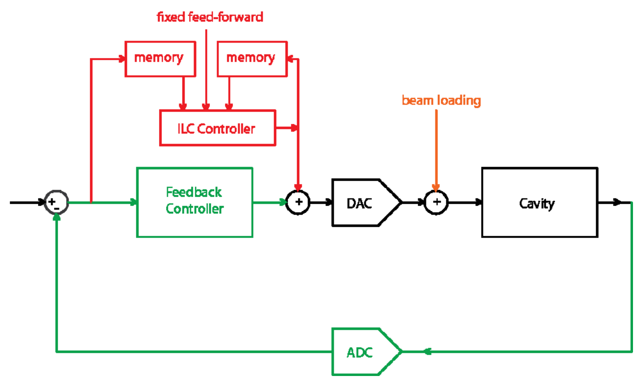

Figure 2: Iterative Learning Controller.

The ILC operates on the premise that the beam loading effect is repetitive from pulse to pulse. This makes it possible to "learn" the corrections needed to be applied to the drive for the next beam pulse. The learning function combines the drive and error signals from the previous iteration and constructs the correction signal to be applied to the present iteration. The ILC cannot correct for pulse to pulse variations in the system, cavity microphonics, or rf amplifier drive fluctuation. This means the conventional feedback controller is still required in the control system.

Initially, both causal (time delay <= 0) and non-causal (time delay > 0) learning functions were examined. The former yielded results that appeared to converge initially, but then rapidly diverged and became unstable. This had been predicted theoretically from stability plots, and was confirmed in a time domain simulation (Fig. 3).

Figure 4 shows the comparable simulation results for a simple non-causal learning function. The learning function converges fairly rapidly without displaying the instability evident in the previous example. The learning function used for this simulation is a simple three sample moving average given by this discrete time equation:

$$u_{k+1}(T) = u_k(T) + \frac{1}{3}\left[e_k(T+1) + e_k(T+2) + e_k(T+3)\right]$$

ISBN 978-3-95450-169-4

MEASUREMENTS AND ANALYSIS OF CAVITY MICROPHONICS AND FREQUENCY CONTROL IN THE CORNELL ERL MAIN LINAC PROTOTYPE CRYOMODULE*

M. Ge†, N. Banerjee, J. Dobbins, R. Eichhorn, F. Furuta, G. Hoffstaetter, M. Liepe, P. Quigley, J. Sears, V. Veshcherevich, Cornell University, Ithaca, New York, USA.

Abstract

The Cornell Main Linac cryomodule (MLC) is a key component in the CBETA project. The SRF cavities with high loaded-Q in the MLC are very sensitive to microphonics from mechanical vibrations. Poor frequency stability of the cavities would dramatically increase the input RF power required to maintain stable accelerating fields in the SRF cavities. In this paper, we present detailed results from microphonics measurement for the cavities in the MLC, discuss dominant vibration sources, and show vibration damping results. The current microphonics level meets the CBETA requirement of a 36MeV energy gain without applying fast tuner compensation.

INTRODUCTION

The Cornell-BNL FFAG-ERL Test Accelerator (CBETA) [1, 2] is designed and now under construction at Cornell University to prove the FFAG-ERL concept for BNL's future Nuclear Physics facility, eRHIC [3]. One of the important components in CBETA is the Cornell Main Linac Cryomodule (MLC) prototype [4-6] which will provide 36MeV energy gain for a single-turn beam of the CBETA. The MLC consists of six 1.3GHz 7-cell SRF cavities. However there are several effects that can limit the cavity accelerating voltages in beam operation below their ultimate quench limit. Microphonics, known as frequency perturbation of SRF cavities, is one of the main sources of field perturbation, driving the RF power required for high Q_{ext} cavity operation in an ERL. If we only consider the effect of microphonics, the relation between the required RF forward power ($P_{forward}$) and the frequency detuning ($\Delta\omega = \omega_c - \omega$) at an accelerating voltage (V_{acc}) is determined by Eq. (1) [7],

$$P_{forward} = \frac{V_{acc}^2}{4 \cdot R/Q \cdot Q_L} \cdot \frac{\beta + 1}{\beta} \left\{ 1 + \left(2Q_L \cdot \frac{\Delta\omega}{\omega} \right)^2 \right\}, \quad (1)$$

where R/Q is the ratio of cavity shunt impedance (R) to its intrinsic quality factor (Q_0), Q_L is the loaded quality factor, β is the coupling coefficient which is defined by Eq. (2),

$$\beta \equiv \frac{Q_0}{Q_{ext}} = \frac{Q_0}{Q_L} - 1, \quad (2)$$

and Q_{ext} is the external quality factor of the input power coupler. The Q_{ext} for the MLC is $\sim 6 \times 10^7$. Comparing to $Q_0 \sim 2 \times 10^{10}$, gives a β of about 1000. Thus $Q_L \approx Q_{ext} \sim 6 \times 10^7$.

It can be seen from Eq. (1) that the RF power is approximately proportional to the square of frequency detuning ($\Delta\omega$), i.e. $P_{forward} \sim (\Delta\omega)^2$, for large detuning. Hence poor frequency stability demands significantly more RF power to sustain the cavity at an accelerating voltage. The maximum output of the High Power RF Amplifiers (HPA) driving the cavities of the MLC is 5kW per cavity; nominally, the RF amplifiers should work at 2 to 3 kW to leave sufficient overhead for residual beam loading compensation.

MICROPHONICS MEASUREMENTS

Experimental Set-up

The location of the MLC and 2K pumping skid in the testing area (L0E) is shown in Fig. 1. The pumping skid is about 15m away from the MLC. The position of the six cavities in the MLC is shown in Fig. 1 (insert). The cavities #1, #3, and #5 are un-stiffened cavities; and the cavities #2, #4, and #6 have mechanical stiffening rings between the cells [8]. The chimney from the 2K two-phase (2K2P) line to the helium-gas return pipe is located between cavities #3 and #4.

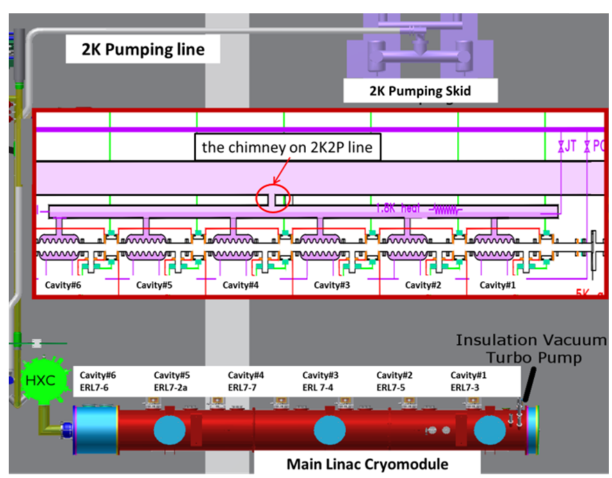

Figure 1: Cryogenic operation diagram of the MLC with the 2K pumping skid and 2K pumping line. The position of the cavities in the MLC is shown in the middle subplot.

The microphonics measurements were carried out when the cavities were cooled to temperature of 1.8K with the resonant frequency tuned to 1300MHz, but without applying any fast tuner compensation; the accelerating gradients (E_{acc}) of the cavities was set to ~1.3MV/m.

* Work supported by NSF Grant NSF DMR-0807731
† mg574@cornell.edu

PERFORMANCE OF THE NOVEL CORNELL ERL MAIN LINAC PROTOTYPE CRYOMODULE*

F. Furuta†, J. Dobbins, R. Eichhorn, M. Ge, D. Gonnella‡, G. Hoffstaetter, M. Liepe, T. O'Connell, P. Quigley, D. Sabol, J. Sears, E. Smith, V. Veshcherevich,
CLASSE, Cornell University, Ithaca, New York, USA

Abstract

The main linac cryomodule (MLC) for a future energy-recovery linac (ERL) based X-ray light source at Cornell has been designed, fabricated, and tested. It houses six 7-cell SRF cavities with individual higher order-modes (HOMs) absorbers, cavity frequency tuners, and one magnet/BPM section. Cavities have achieved the specification values of 16.2MV/m with high-Q of 2.0e10 in 1.8K in continuous wave (CW) mode. During initial MLC cavity testing, we encountered some field emission, reducing Q and lowering quench field. To overcome field emission and find optimal cool-down parameters, RF processing and thermal cycles with different cool-down conditions have been done. Here we report on these studies and present final results from the MLC cavity performance.

INTRODUCTION

Cornell University has proposed to build an Energy Recovery Linac (ERL) as driver for a hard x-ray source because of its ability to produce electron bunches with small, flexible cross sections and short lengths at high repetition rates. The proposed Cornell ERL is designed to operate in CW at 1.3GHz, 2ps bunch length, 100mA average current in each of the accelerating and decelerating beams, normalized emittance of 0.3mm- mrad, and energy ranging from 5GeV down to 10MeV, at which point the spent beam is directed to a beam stop [1, 2]. The design of main linac prototype cryomodule (MLC) for the Cornell ERL had been completed in 2012. Figure 1 shows the 3D model of the MLC. The key parameters are listed in Table 1. Table 2 shows the surface preparations of the MLC 7-cell cavity. The fabrication and testing of MLC components (cavity, high power input coupler, HOM dampers, tuners, etc.,) and assembly of the MLC cold mass had been completed in 2014 [3, 4]. RF tests with different cool down conditions, including the first cool down, have been performed in 2015. In this paper, we summarize the results from these tests.

Table 1: MLC Parameters

Item	Parameter
Number of 7 cell cavities	6
Accelerating gradient	16.2MV/m
R/Q (linac definition)	774 Ohm
Q_{ext}	6.0×10^7
Total 2K/5K/8K loads	76 W / 70 W / 150 W
Number of HOM loads	7
HOM power per cavity	200 W
Couplers per cavity	1
RF power per cavity	5 kW
Amplitude/phase stability	10^{-4} / 0.05°
Module length	9.8 m

Table 2: Surface Preparation of the 7-Cell Cavities

Process	Parameter
Bulk BCP	140 μm
Degassing	650 degC, 4days
Frequency tuning	Field flatness >90%
Light BCP	10 μm
Baking	120degC, 48hrs
HF rinse	10 min.

HTC STUDIES

In parallel with the MLC fabrication, a one-cavity Horizontal Test Cryomodule (HTC) was also developed. The HTC is powerful tool to investigate cavity performance in a horizontal cryomodule with various conditions, especially under the different cool down protocols. A prototype 7-cell cavity for the Cornell ERL and high-Q 9-cell cavities for the LCLS-II project at SLAC have been tested in the HTC [5, 6, 7] and important lessons have been learned for. The HTC studies revealed two key features

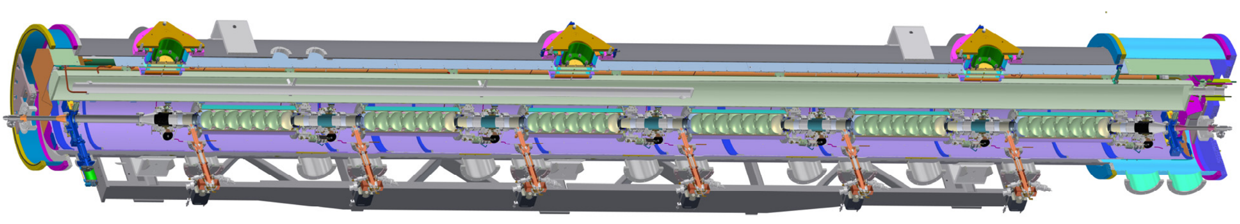

Figure 1: The Main Linac Cryomodule (MLC)

* Work is supported by NSF awards NSF DMR-0807731 and NSF PHY-1002467
†ff97@cornell.edu
‡Now at SLAC National Accelerator Laboratory

HOM MEASUREMENTS FOR CORNELL'S ERL MAIN LINAC CRYOMODULE*

F. Furuta[†], R. Eichhorn, M. Ge, D. Gonnella[‡], G. Hoffstaetter, M. Liepe, P. Quigley, V. Veshcherevich, CLASSE, Cornell University, Ithaca, New York, USA

Abstract

The main linac cryomodule (MLC) for a future energy-recovery linac (ERL) based X-ray source at Cornell has been designed, fabricated, and tested. It houses six 7-cell SRF cavities with individual higher order-modes (HOMs) absorbers, cavity frequency tuners, and one magnet/BPM section. All HOMs in a MLC prototype have been scanned in 1.8K. The results show effective damping of HOMs, and also agree well with simulation results and previous HOM scan results on one 7-cell cavity prototype test cryomodule. Here we present detailed results from these HOM studies.

INTRODUCTION

Cornell University has proposed to build an Energy Recovery Linac (ERL) as driver for a hard x-ray source because of its ability to produce electron bunches with small, flexible cross sections and short lengths at high repetition rates. The proposed Cornell ERL is designed to operate in CW at 1.3GHz, 2ps bunch length, 100mA average current in each of the accelerating and decelerating beams, normalized emittance of 0.3mm- mrad, and energy ranging from 5GeV down to 10MeV, at which point the spent beam is directed to a beam stop [1, 2]. For this type of high current machine, the suppression of high order modes (HOMs) excited by the beam in the SRF cavities is essential, because HOMs can lead a deflection of the beam. Especially the dipole modes, which can make a transverse kick on the beam bunch and start a bunch oscillation around the design orbit, need to be damped strongly to avoid resulting beam break up (BBU).

HOM ABSORBER IN MLC

MLC

Figure 1 (Top) shows an image of the Cornell ERL main linac cryomodule (MLC) prototype. The design had been completed in 2012. It is 9.8 m long and houses six 1.3 GHz 7-cell superconducting cavities, three of them are stiffened cavity, another three are un-stiffened, with individual HOM beamline absorbers located between the cavities. Each cavity has a single 5kW coaxial RF input coupler, which transfers power from a solid-state RF power source to the cavity (the designed Q_{ext} is $6.0x10^7$). Due to the high beam current combined with the short bunch operation, a careful control and efficient damping of higher order modes (HOMs) is essential. Therefore, HOM beamline absorbers are installed at the beam pipe

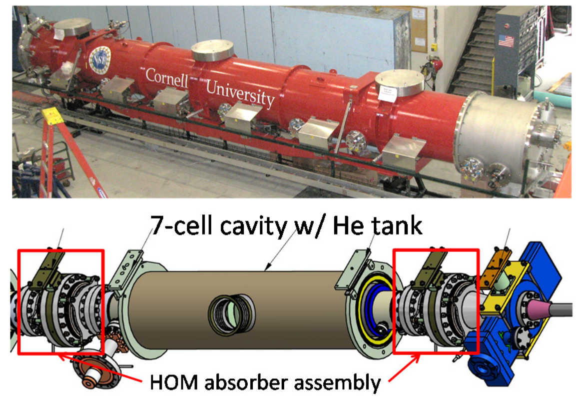

Figure1: MLC prototype (top), and 3D image of a one-cavity section of the string assembly (bottom).

ends of each cavity (Fig. 1, bottom). The specification values of the 7-cell cavities in the MLC are Q_0 of $2.0x10^{10}$ for the fundamental mode at 16.2MV/m, 1.8K. The fabrication and testing of MLC components (cavity, high power input coupler, HOM dampers, tuners, etc.,) and assembly of MLC cold mass have been completed in 2014 [3, 4, 5]. Initial cool down and RF tests have been performed in 2015, and reported in reference [6].

HOM Absorber

Figure 2 shows a cross section view of the production version of the Cornell HOM absorber. For these production versions, the absorbing material is Silicon Carbide, SC-35® from Coorstek [7]. Two prototypes where initial-

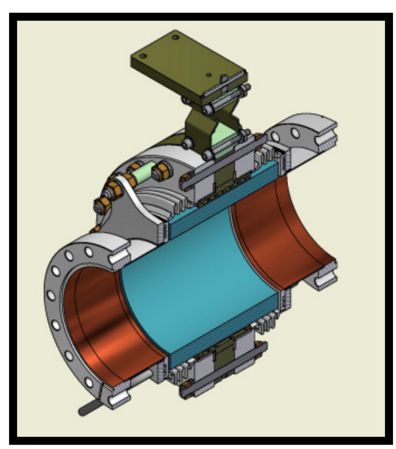

Figure 2: Cornell's HOM beamline absorber used in the main linac cryomodule (MLC). The absorbing material is SC-35 from Coorsteck, shrink-fitted into a Ti cylinder.

* Work is supported by NSF awards NSF DMR-0807731 and NSF PHY-1002467
† ff97@cornell.edu
‡ Now at SLAC National Accelerator Laboratory

LIFETIME STUDY OF CsK2Sb ROBUST PHOTO-CATHODE FOR A HIGH BRIGHTNESS ELECTRON SOURCE

Masao Kuriki†, Yuji Seimiya (KEK, Ibaraki), Lei Guo, Katsuhiro Moriya, Masahiro Urano, Atsuki Yokota (HU/AdSM, HigashiHiroshima), Kentaro Negishi (Iwate University, Morioka, Iwate)

Abstract

CsK_2Sb photocathode is one of the ideal cathode for accelerators requiring the high brightness electron beam. It can be driven with a green laser generated as SHG of a solid state laser. The QE (Quantum Efficiency) of photoelectron emission is as high as more than 10% with 532nm light. In this article, the robustness of the cathode is studied. Two indexes of lifetime regarding to time and extracted charge density were evaluated experimentally. The result shows that the cathode is robust enough for a high brightness accelerator.

INTRODUCTION

Next generation accelerator project based on Linac such as linear colliders, ILC [1], FEL [2] and ERL [3] are under being studied and developed in recent years. In the linac, the electron beam performance can be superior to what is in a storage ring, but the beam quality from the electron gun has to be better than that in the storage ring. In addition, we have to provide a large current beam which is equivalent to that in the storage ring, too.

Photo-cathode electron gun is a device which generates electron beam by photoelectric effect by laser light. This electron gun has superior performance (low emittance, short pulse, spin polarization, etc.) by high operability with laser. For example, in a linear colliders (ILC and CLIC), polarized electron plays an important role and the photo-cathode is the only way to generate such beam practically. The photo-cathode with an optimized laser (spot size, temporal length, and wavelength) gives a minimum emittance. To provide such high performance beam with a required time structure and intensity, quantum efficiency (QE) of photoelectric effect (ratio of the numbers of laser photon and photo-electron) of the cathode should be high enough and should be maintained for a reasonable period. Otherwise, we need a huge power laser and/or frequent cathode replacement. The QE and the robustness are always practical issues for the photo-cathode. For example, NEA (Negative Electron Affinity)-GaAs [4] has a high QE (more than 10% at 530nm), but the cathode function is easily lost by residual gas molecules such as H_2O, O_2, etc. On the other hand, metal cathode (Cu, Mg, Pb and so on) is much robust, but QE is typically low (10^{-4}~10^{-5}) and need UV light for the excitation. Therefore, they are not suitable to generate high current electron beam.

Recently, multi-alkali photocathode is paid attention for the high brightness beam generation. This cathode is formed by evaporation with more than two kind of alkali metals. The high robustness is already demonstrated [5] and QE is as high as more than 10% at 532 nm [6]. According to these reasons, this cathode is suitable to generate a high brightness electron beam for FEL, ERL, and X-ray source by laser Compton scattering.

In Hiroshima University, CsK2Sb multi-alkali photocathode for the electron source of Linac is studied to establish the technique to develop the high performance cathode and understand the property of the cathode [6]. In this article, the CsK2Sb cathode was evaporated on a substrate in a high vacuum environment and examined the cathode performance to evaluate the cathode robustness.

EXPERIMENTAL SETUP

Multi-alkali Test Chamber

In this chapter, we explain the multi-alkali test chamber in Hiroshima University. This test chamber is made from SUS and the inner surface was electrically polished. Ultra-high vacuum in order of 10-9 Pa is kept with a NEG pump and an ion pump. Figure 1 shows the schematic drawing of the evaporation system in the test chamber [5]. The cathode is evaporated on a 31 mm x 31 mm substrate made of SUS304 whose surface was finished with the electrical polishing. The substrate is mounted on a holder with a ceramic heater for the heat cleaning and temperature control. The holder is electrically isolated from the ground and is biased with a DC voltage supply to measure the beam current. The typical bias voltage is -100 V. The evaporation head where the sources are mounted, generates the metal vapour symmetry to the substrate and the quartz thickness monitor. Owing to this system, we can monitor the amount of the evaporated metal on the substrate simultaneously. Laser light can be introduced through a view port to observe photo-electron emission during the evaporation. To monitor the vacuum environment, an extractor vacuum gauge and QMS (Quadruple Mass Spectrometer) are placed.

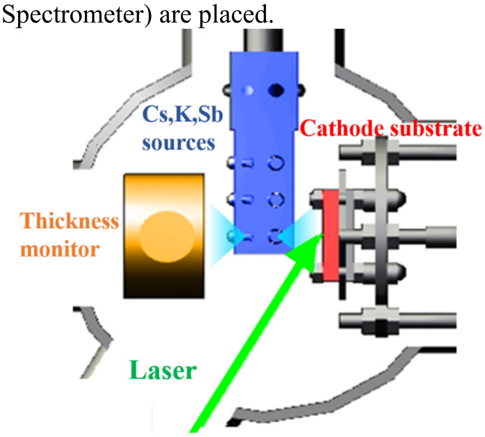

Figure 1: Layout of inside of the evaporation chamber.

† mkuriki@hiroshima-u.ac.jp

DESIGN OF A GAMMA-RAY SOURCE BASED ON INVERSE COMPTON SCATTERING AT THE FAST SUPERCONDUCTING LINAC*

D. Mihalcea[1], B. Jacobson[2], A. Murokh[2], P. Piot[1,3], and J. Ruan[3]
[1] Department of Physics and Northern Illinois Center for Accelerator & Detector Development, Northern Illinois University DeKalb, IL 60115, USA
[2] Radiabeam Technologies, Santa Monica, CA 90404, USA
[3] Fermi National Accelerator Laboratory, Batavia IL 60510, USA

Abstract

A watt-level average-power gamma-ray source is currently under development at the Fermilab Accelerator Science & Technology (FAST) facility. The source is based on the Inverse Compton Scattering of a high-brightness 300-MeV beam against a high-power laser beam circulating in an optical cavity. The back scattered gamma rays are expected to have photon energies up to 1.5 MeV. This paper discusses the optimization of the source, its performances, and the main challenges ahead.

INTRODUCTION

The range of x- and γ-ray applications, already impressive, could increase even further pending the availability of small-footprint sources. High dose, high brightness and monochromatic x-rays can be generated via synchrotron radiation at large accelerator facilities which are extensively used for fundamental scientific research. More compact sources could have a large variety of applications for national defense industry and medicine. The most promising process which can be at the base of future compact x- and γ-ray is the Inverse Compton Scattering (ICS) [1,2]. Essentially, ICS consists of head-on collision between an electron beam and a laser. The energy of the scattered photons [3] is much higher than of the incident photons because of a double-Doppler frequency upshift:

$$\omega_s = \frac{4\gamma^2}{1 + \frac{a_0^2}{2} + \gamma^2\theta^2}\omega_L, \tag{1}$$

where ω_s and ω_L are the frequencies of the scattered radiation and of the laser respectively, γ the relativistic factor of the electron beam, a_0 the normalized vector potential ($a_0 \equiv \frac{eA}{mc}$) and θ the observation angle with respect to the electron beam. Although ICS also needs an electron accelerator, the $\propto \gamma^2$ dependence of the scattered photon energies makes this technique promising because only a small to medium size accelerator is needed. For example, at FAST the electron energy reaches about 300 MeV and after the collision with infrared laser pulses ($\hbar\omega_L \simeq 1.2$ eV) the scattered photon energy is $\hbar\omega_L \leq 1.5$ MeV.

* This work was sponsored by the DNDO award 2015-DN-077-ARI094 to Northern Illinois University. Fermilab is operated by Fermi Research Alliance, LLC. for the U.S. Department of Energy under contract DE-AC02-07CH11359.

The other γ-ray source properties can be similar to those produced at large electron facilities. At FAST we expect that each single electron pulse to produce a γ-ray pulse with brightness in excess of 10^{20} photons/[s-(mm-mrad)^2-0.1%BW]. In normal operation FAST linac delivers trains of about 3,000 pulses each second. Under some approximations [4] valid for most experimental conditions including those at FAST the γ-ray brightness can be expressed in terms of laser and electron beam parameters:

$$B_x \propto \frac{N_\gamma}{\sigma_L^2}\gamma^2\frac{N_e}{\Delta t_e \epsilon_{n,x}^2}, \tag{2}$$

where N_γ is the number of photons in the laser pulse, σ_L is the laser transverse size (rms), γ electron beam relativistic factor, N_e number of electrons in the bunch, Δt_e electron pulse length and $\epsilon_{n,x}$ electron beam normalized transverse emittance. At FAST γ and Δt_e are fixed at about 600 and 3 ps rms respectively.

Under similar approximations [4] the scattered photon dose depends on the laser and electron beam properties as

$$N_x \approx \frac{N_e N_\gamma \sigma_T}{2\pi(\sigma_e^2 + \sigma_L^2)}, \tag{3}$$

where N_e, N_γ, σ_L have the same meaning as in Eq. (2), σ_T is the total Thompson scattering cross section and σ_e is the electron beam transverse size (rms).

The monochromaticity of the scattered beam, more often referred as bandwidth is defined as the relative energy spread of the scattered photons in the observation direction. In practice bandwidth is heavily dominated by the electron beam angular spread [3]:

$$BW(\%) \approx \frac{\epsilon_{n,x}^2}{\sigma_e^2} \tag{4}$$

In the next section we describe some of the experimental challenges. The following section contains results of simulations aimed to optimize the performances of the scattered radiation and the last section contains the conclusions.

EXPERIMENTAL CHALLENGES

The laser beam used for ICS experiment originates from the IR laser system used to extract the electrons from the photocathode after conversion to UV (266 nm). The IR-to-UV conversion efficiency is small (~ 10%) so that most

ISBN 978-3-95450-169-4

SUMMARY OF THE TEST AND INSTALLATION OF 10MW MBKS FOR THE XFEL PROJECT

V. Vogel, L. Butkowski, S. Choroba, A. Cherepenko, J. Hartung, V. Kachaev, R. Wagner, S. Wiesenberg, DESY, Hamburg, Germany

Abstract

For the European XFEL project, horizontal multi-beam klystrons (MBK) which produce RF power up to 10 MW, at an RF frequency of 1.3 GHz, 1.5 ms pulse length and 10 Hz repetition rate, were chosen as RF power sources. All MBKs have been manufactured by two companies, 22 tubes from Thales Electron Devices and 7 tubes from Toshiba Electron Tubes & Devices. In this article we will give a summary of the tube testing, conditioning and installation in the underground linear accelerator tunnel.

INTRODUCTION

After the successful test of three horizontal MBK prototypes [1 and 2] in 2008-2011, two companies started klystron delivery for the European XFEL project in 2012. At present all ordered klystrons are manufactured, 26 klystrons are required for first installation. The main parameters of the MBKs are given in Table 1.

Table 1: Main Parameters of the L-band MBK for XFEL

Parameters	Design	Test
Central frequency (MH	1300	1300
RF pulse length (ms)	1.5	1.5
Efficiency (%)	> 63	63-68
Average RF power (kW	150	155
Output power (MW)	10	9.9-10.5
Bandwidth (MHz)	3	>3

After delivery each klystron was connected to a connection module (CM) [3, 4 and 5], which consists of an oil tank, filament transformer and diagnostics, and afterwards tested on one of the MBK test stands at DESY [6, 7, and 8]. The average time of testing for each MBK was about 320 hours with the exception of several tubes, which needed more time for conditioning and retest. The tubes were tested up to full RF power and full RF pulse length with a repetition rate of 10 Hz. Figure 1 shows one of the klystrons with the CM (grey) and HV cable between the CM and the HV pulse transformer (red) inside the XFEL injector underground building. Two coaxial cables of the same type with an additional screen and ferromagnetic cores were used at the test stands for the test of all klystrons for more than 13000 hours.

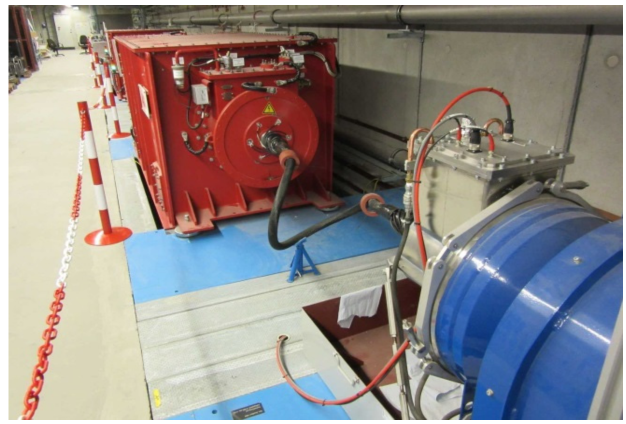

Figure 1: Connection between HV transformer and MBK.

The cables did not show any sign of degradation or increased level of partial discharge in the HV cables itself or the connectors.

MBK TEST AND INSTALLATION

At the start of the XFEL klystron design DESY demanded a mechanical design and interfaces allowing for fast replacement of the klystrons in the accelerator.

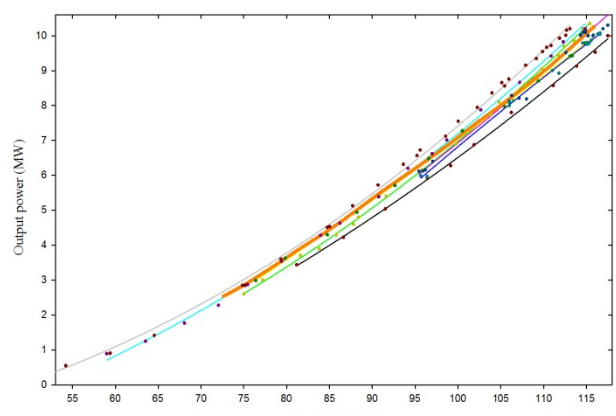

Figure 2: Saturated power of the Toshiba E3736H.

Another very important part of mechanical design is the protection of all sensitive parts of the klystron during transportation and installation in an underground tunnel. Since 2012 when the test of the first series MBKs at DESY site was started no problems occurred during transportation and installation.

COMMISSIONING OF THE COMPACT 14MEV LINAC FOR AN FEL-BASED THZ SOURCE

Y.J. Pei, L. Shang, Z.X. Tang, Z.M. Wang, Z.Y. Zhao, J. Liu, D.C. Jia, W. Wei, P. Lu, G.R. Huang, K. Jin, B.G. Sun, X.Y. He, Y.L. Hong
National Synchrotron Radiation Laboratory, USTC, Hefei 230029, China
T.N. Hu, Q.S. Chen, P. Tang, B. Qin, L. Cao, Y.Q. Xiong, W. Chen, J. Li, Z.Y. Yang, Y.B. Wang, F. Zhu, Y.J. Liang, J.J. Chen, J. Zha, Q. Zhang, B. Tang, S.W. Hu
Huazhong Unversity of Science & Technology,Wuhan 430074, China

Abstract

This paper will describe the commissioning of a compact LINAC of 14MeV which is used for FEL to produce THz radiation through 30μm to 300μm. Main design parameters are given in this paper. The compact LINAC of 14MeV was composed of novel EC-ITC-RF gun, constant gradient travelling wave accelerator with a collinear absorbing load, focusing system, RF power system, beam diagnostic system, vacuum system, control system and so on. The LINAC was installed on November of 2014. Now the LINAC has been operating and commissioning for THz radiation test. So far, the facility is running well and the main beam parameters tested are coincident with design parameters of the LINAC.

GENERAL DESCRIPTION OF THE FACILITY

The facility is designed for producing a THz radiation with wavelength of 30um~300um. In order to satisfy the strict requirements of high performance of electron beam for THz-FEL and obtain a more compact layout for the facility, HUST (Huazhong University of Science and Technology) and NSRL (National Synchrotron radiation Laboratory)/USTC (University of Science and Technology of China) are cooperating to do R &D work. The facility is main composed of a novel EC-ITC RF gun, transverse focusing system, constant gradient travelling wave LINAC with an input coupler offset and a collinear absorbing load to improve the electric field to be symmetry. Besides, other inevitable sub-systems are established either, such as beam diagnostics system, microwave power system, vacuum system, control system and so on. The layout of the facility is shown as Figure 1 [1,2,3] .

Table 1: Measuring Parameters of the LINAC

parameter	unit	value
energy	MeV	13.58
Current	A	0.665 (macro pulse) 29~47 (micro pulse)
Width of beam	us ps	1~2 (macro pulse) 5~8 (micro pulse)
Repeat frequency	pps	2-10
Charge per pulse	pC	~230
Energy spread	%	0.332
Nor. emittance	mm mrad	24.1
Input power	MW	24

The building for the machine was finished in July 2014 and all parts of the LINAC were tested. In August of 2014, we started to install the machine and got the first beam from the LINAC, which energy was of 13.4MeV, macro pulse current was of 1.1A. After that, we started to commission the LINAC, improve diagnostic system and test its parameters in detail. The parameters of the LINAC we've measured are listed in Table 1.

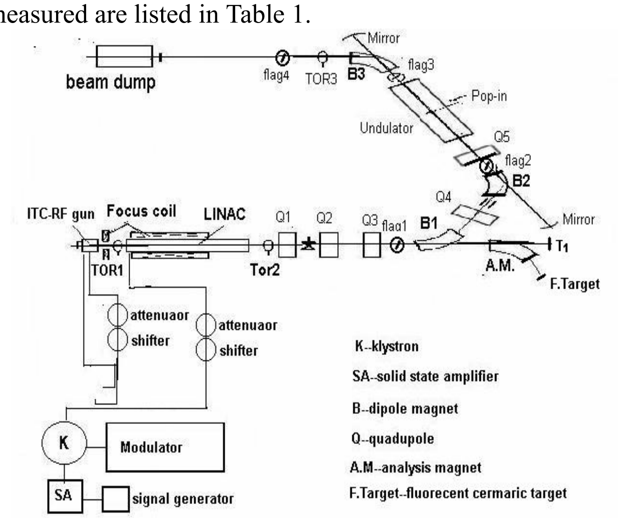

Figure 1: Layout of the facility.

BEAM PARAMETER MEASUREMENT

Energy and Energy Spread Measurement

We employ an analysis magnet, Flag1 and a fluorescent target (F. Target) located at the end of the vacuum chamber (see Figure 1) to measure the energy and the energy spread. The transmission matrix of the energy analysis system can be expressed by Eq. (1),

$$\begin{pmatrix} x_1 \\ x_1' \\ (\frac{\Delta p}{p})_1 \end{pmatrix} = \begin{pmatrix} m_{11} & m_{12} & m_{13} \\ m_{21} & m_{22} & m_{23} \\ m_{31} & m_{32} & m_{33} \end{pmatrix} \begin{pmatrix} x_0 \\ x_0' \\ (\frac{\Delta p}{p})_0 \end{pmatrix} \quad (1)$$

In the system, m_{12} is designed to 0, and m_{11} should be designed close to 0. Then, by observe the beam spot on Flag1 and F. Target, beam radii at these two positions can be obtained, so that the energy is easy to be obtained by means of magnet calibration and the energy spread can be calculated by Eq. (2),

PARTICULATE STUDY ON MATERIALS FOR CLEANROOM ASSEMBLY OF SRF CAVITIES*

L. Zhao, T. Reilly,
Thomas Jefferson National Accelerator Facility, Newport News, VA 23606, USA

Abstract

Reducing particulates is an important aspect for cleanroom operation. Knowing that it is impossible to completely eliminate all particulates in a clean room, efforts have been made to prevent particulates from entering SRF cavities during high pressure rinsing (HPR) and assembly. At Jefferson Lab, one practice to achieve this goal has been clamping covers to cavity open flanges during assembly. Several cover materials that have been used are examined and alternative candidate materials are under development. Clamps as a known particulate generator are carefully examined and cleaning efficiency of different methods is studied. Cover tests were done on different cavity flanges, including an LCLS-II beam pipe flange, which helps the selection of cover materials for prototype and production of the project.

BACKGROUND

The battle with field emission has been a long journey for the SRF community [1-3]. Even with newly developed facilities and tools, understanding [4] and controlling [5] particle contamination is still an on-going topic. During HPR and assembly at Jefferson Lab, open ports on cavities are covered to prevent particulates entering clean cavities. The cover material has evolved over time and with projects. For CEBAF cavities (C50 and C100), stainless steel covers with O-ring were used. Screws were used to keep the covers in place. Figure 1 (left and middle) shows two examples of these covers. In recent years, niobium blanks (Fig. 1, right) have been used on various cavity shapes, attached to cavity openings with stainless steel spring clamps. This option is much simpler and less flange dimension dependent than the O-ring design.

Since metal-to-metal contact can generate significant amount of particles, other candidates such as plastic materials are being considered.

EXPERIMENT

Investigation of Plastic Covers

Polyvinylidene fluoride (PVDF) and polytetrafluoroethylene (PTFE) are widely used in ultrapure water industry and semiconductor industry. At Jefferson Lab they are commonly used plastics in cavity processing especially chemical polishing tools, because of their excellent chemical resistance and reasonable mechanical strength. Our search for alternatives started with these two materials.

Figure 1: Stainless steel covers with O-ring (left, middle) and niobium blank (right).

Similar to common plastics, longer time is needed to blow clean PVDF and PTFE with an ionized nitrogen gun compared with metals. Bulk PTFE has only moderate stiffness and low surface friction, which can be a problem when a large force is applied. Other forms of PTFE products are available commercially, such as expanded PTFE (Gore-Tex), which preserves the chemical property but is very stretchable, enabling it to be used as gaskets. PVDF has higher mechanical strength but is less stretchable.

Figure 2 shows particle counts on PVDF covers of different dimensions. The smaller diameter was 70 mm, and the bigger diameter was 140 mm. The surface was lathed. The particle counter was set at 10 seconds/cycle and the flow rate was 1.0 cfm. The horizontal axis is the clean-up time needed for a cover, i.e. how long it took to blow down to zero counts. The vertical axis is the total amount of particles (≥0.3 μm) recorded through the clean-up time of the cover. The two axes are not necessarily functions of each other. Rather, the plot shows two parameters that indicate the cleanliness of a part. Points near the upper right corner indicate the surface has more particles and it takes longer to clean up. Points at lower left corner indicate the surface has fewer particles and it cleans up quickly. Apparently, geometry and dimension also play a role in surface particle counts. For the same surface finish, parts with more corners and holes have larger total counts.

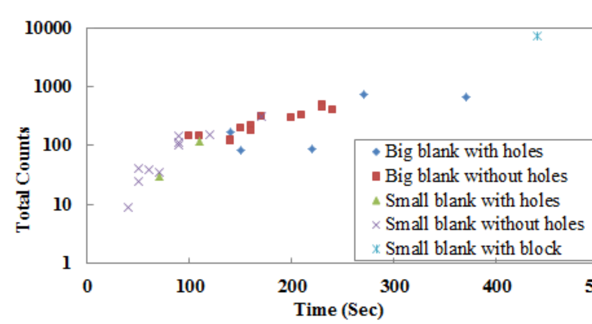

Figure 2: Total particle (≥ 0.3 μm) counts and cleaning-up time on PVDF covers in two diameters and different designs.

PVDF Covers with Different Surface Finish

The machined PVDF surface was difficult to blow clean. Noticing that the as-received manufactured surface

---

* Work supported by Jefferson Science Associates, LLC under U.S. DOE Contracts DE-AC05-06OR23177 and DE-AC02-76SF00515 for the LCLS-II Project
† lzhao@jlab.org

IMPURITY CONTENT OPTIMIZATION TO MAXIMIZE Q-FACTORS OF SUPERCONDUCTING RESONATORS*

M. Martinello†, M. Checchin, FNAL, Batavia, IL, USA and IIT, Chicago, IL, USA
A. Grassellino, O. Melnychuk, S. Posen, A. Romanenko, D.A. Sergatskov, FNAL, Batavia, IL, USA
J.F. Zasadzinski, IIT, Chicago, IL, USA

Abstract

Quality factor of superconducting radio-frequency (SRF) cavities is degraded whenever magnetic flux is trapped in the cavity walls during the cooldown. In this contribution we study how the trapped flux sensitivity, defined as the trapped flux surface resistance normalized for the amount of trapped flux, depends on the mean free path. A systematic study of a variety of 1.3 GHz cavities with different surface treatments (EP, 120 °C bake and different N-doping) is carried out. A bell shaped trend appears for the range of mean free path studied. Over-doped cavities fall at the maximum of this curve defining the largest values of sensitivity. In addition, we have studied the trend of the BCS surface resistance contribution as a function of mean free path, showing that N-doped cavities follow close to the theoretical minimum. Adding these results together we show that the 2/6 N-doping treatment gives the highest Q-factor values at 2 K and 16 MV/m, as long as the magnetic field fully trapped during the cavity cooldown is lower than 10 mG.

INTRODUCTION

Recently, a new surface treatment implemented on superconducting cavities, called nitrogen-doping, shows unprecedented values of quality-factors ($Q_0 > 4 \cdot 10^{10}$) at medium values of accelerating field (E_{acc} = 16 MV/m) [1]. However, it was shown that whenever external magnetic is trapped in nitrogen-doped cavities, the Q_0 degradation is more severe than in standard-treated niobium cavities such as 120 °C baked and electro-polished (EP).

To understand this peculiar behavior, it is necessary to analyze the RF surface resistance, $R_s = G/Q_0$. R_s is given by two contributions, one temperature-dependent called BCS surface resistance (R_{BCS}), and one temperature-independent called residual resistance (R_{res}).

Surprisingly, in nitrogen-doped cavities R_{BCS} decreases with the increasing of the accelerating field. This results in an increasing of Q-factor with accelerating field called anti-Q-slope [1] .

The residual resistance term R_{res} is the one affected by trapped magnetic flux [2]. The amount of trapped flux depends on both the value of external magnetic field which surrounds the cavity during the SC transition, and on the cooldown details, which affects the magnetic flux trapping efficiency [3–5]. Fast cooldowns, with large thermal gradients along the cavity length, facilitate magnetic flux expulsion, while slow and homogeneous cooling through transition leads to full flux trapping.

In this paper both the trapped flux and the BCS surface resistance contributions are studied for cavities subject to different surface treatments: electro-polishing (EP), 120 °C baking, and N-doping with different time of nitrogen exposure and EP removal. Details on the N-doping treatment can be found elsewhere [1, 6].

The findings here reported allow a better understanding of which surface treatment is required to maximize the Q-factor for a certain RF field, taking into account the external DC magnetic field trapped during the cooldown. More details of this study may be found in Ref. [7].

EXPERIMENTAL PROCEDURE

All the cavities analyzed are single cell 1.3 GHz Tesla-type niobium cavities.

In order to estimate the trapped flux surface resistance, every cavity was RF tested, at least, after two different cooldowns: i) compensating the magnetic field outside the cavity in order to minimize its value during the SC cavity transition, ii) cooling slowly the cavity with about 10 mG of external magnetic field applied.

After each of these cooldowns, the cavities were tested at the Vertical Test System (VTS) at Fermilab. Curves of Q-factor versus accelerating field were always acquired at both 2 and 1.5 K.

A schematic of the instrumentation used to characterize the trapped flux surface resistance may be found in Fig. 1 of Ref. [8]. Helmholtz coils are used to adjust the magnetic field around the cavity, Bartington single axis fluxgate magnetometers to monitor the external magnetic field at the cavity equator, and thermometers to measure the temperature distribution during the cooldown.

The residual resistance may be considered as a sum between the trapped flux surface resistance, R_{fl}, and the "intrinsic" residual resistance, R_0, which does not depends on trapped flux.

At 1.5 K the BCS surface resistance contribution becomes negligible, therefore $R_{res} = G/Q(1.5K)$.

If during the cooldown the amount of trapped flux is successfully minimized, then: $R_{fl} \simeq 0$ and $R_{res} \simeq R_0$. In order to obtain very low value of trapped flux, the magnetic field outside the cavity was compensated during the cooldown through the SC transition. Alternatively, the measurement was done after a complete magnetic flux expulsion ($B_{SC}/B_{NC} \sim 1.74$ at the equator). We have observed that these two methods gave the same results within the mea-

* Work supported by the US Department of Energy, Office of High Energy Physics.
† mmartine@fnal.gov

ISBN 978-3-95450-169-4

ENHANCEMENT OF THE ACCELERATING GRADIENT IN SUPERCONDUCTING MICROWAVE RESONATORS*

M. Checchin[1,2,†], M. Martinello[1,2], A. Romanenko[1], A. Grassellino[1], S. Posen[1] and J. F. Zasadzinski[2]
[1] Fermilab, Batavia, IL 60510, USA
[2] Illinois Institute of Technology, Chicago, IL 60616, USA

Abstract

The accelerating gradient of superconducting resonators can be enhanced by engineering the thickness of a dirty layer grown at the cavity's rf surface. In this paper the description of the physics behind the accelerating gradient enhancement by meaning of the dirty layer is carried out by solving numerically the the Ginzburg-Landau (GL) equations for the layered system. The calculation shows that the presence of the dirty layer stabilizes the Meissner state up to the lower critical field of the bulk, increasing the maximum accelerating gradient.

INTRODUCTION

The possible enhancement of the accelerating gradient by meaning of layered structures in accelerating cavities was introduced by A. Gurevich [1]. He showed that high κ (GL parameter) superconducting layers separated by insulating layers (SIS structure) deposited at the rf surface can in principle enhance the superheating field, and allow for higher gradients.

In the same direction T. Kubo [2, 3] and S. Posen *et al.* [4] explored thoughtfully the behavior of the SIS structure. T. Kubo in particular, described also the SS structure [3, 5], i.e. a high κ (dirty) superconducting layer on top of a low κ (clean) bulk superconductor. He approached the problem in the high κ approximation by meaning of the London equations as done for the SIS structure, showing that the dirty layer can in principle enhance the superheating field even if no insulating layer is present.

In the present paper an alternative description of the SS structure is presented. The approach here is different since the calculation is carried out numerically from the GL equations, where the dirty layer is assumed to behave as a perturbation on the magnetic induction profile in the material. We show that the dirty layer stabilizes the superconductor against the vortex nucleation, and shifts the lower critical field of the whole structure up to the bulk's value, increasing the magnetic field range in which the Meissner state is stable.

THE BEAN-LIVINGSTON BARRIER FOR NON-CONSTANT κ

Let us assume a semi-infinite superconductor, where the normal to the surface directed towards the material bulk is $\hat{x}$, the external magnetic field is applied along the z direction and the screening currents are flowing along the y direction. On top of such superconductor we assume the presence of a thin superconducting dirty layer with higher κ than the bulk (grown by diffusion of impurities for example), so that the κ profile of the system can be described by the analytic form:

$$\kappa(x) = -\frac{\kappa_s - \kappa_b}{1 + e^{-(x-x_0)/c}} + \kappa_s \,, \tag{1}$$

which corresponds to a sigmoidal function, where κ_s and κ_b are the superficial and bulk GL parameters, c is a constant that defines the steepness of the function (normally $c = 0.018$) and x_0 corresponds to the inflection point assumed as the thickness of the dirty layer.

Since we are dealing with dimensionless units $x = \mathrm{depth}/\lambda$, with λ the penetration depth $\lambda = \lambda_0\sqrt{1 + \xi_0/l}$, l the mean free path, $x_0 = d/\lambda$, $\xi_0 = 38$ nm and $\lambda_0 = 39$ nm [6].

Forces Acting on the Vortex

The forces acting on a vortex penetrating from the surface can be calculated in first approximation by implementing the same description of C. P. Bean and J. D. Livingston [7]. The repulsive force (with respect the surface) due to the interaction of the vortex with the magnetic induction profile in the material is:

$$\mathbf{f_f}(x) = -\frac{4\pi}{\kappa(x)}\frac{\partial\, b_f(x)}{\partial x}\,\hat{\mathbf{x}} \,, \tag{2}$$

where $b_f(x) = a'(x)$ is calculated numerically from the GL equations modified in order to account also for the variation of κ with x:

$$\begin{aligned} &\frac{1}{\kappa^2(x)} f'' - a^2 f + f - f^3 = 0 \\ &\mathbf{a}'' - f^2\mathbf{a} = 0 \,, \end{aligned} \tag{3}$$

where f and $\mathbf{a}$ are respectively the dimensionless order parameter and vector potential as defined in [8], while the boundary conditions are the same assumed in [9].

The attractive force is instead calculated as:

$$\mathbf{f_v}(x) = \frac{4\pi}{\kappa(x)}\frac{\partial\, b_v(2x)}{\partial x}\,\hat{\mathbf{x}} \,, \tag{4}$$

where $b_v(r) = a'(r) + (1/r)a(r)$ is the magnetic induction of the image-vortex.

In order to maintain the description mono-dimensional, we calculate the magnetic induction profile from the cylindrically symmetric GL equations. Such approach is carried

* Work supported by the US Department of Energy, Office of High Energy Physics.
† checchin@fnal.gov

ISBN 978-3-95450-169-4

OPTIMAL NITROGEN DOPING LEVEL TO REACH HIGH Q_0*

D. Gonnella†‡, T. Gruber, J. Kaufman, P.N. Koufalis, M. Liepe§, and J.T. Maniscalco

CLASSE, Cornell University, Ithaca, NY 14853, USA

Abstract

New continuous wave (CW) accelerators such as LCLS-II at SLAC require many SRF cavities operating in the medium field region at unprecedented high Q_0. In order to achieve this demanding goal, nitrogen-doping of the SRF cavities will be used. Nitrogen-doping has been shown to affect the BCS resistance both by a lowering of R_{BCS} at low fields and by the introduction of an anti-Q slope which enables the Q_0 to continue increasing as the RF field is increased. The exact strength of this anti-Q slope is heavily dependent on the doping recipe and specifically the mean free path of the RF penetration layer of the doped cavities. In addition to its effect on R_{BCS}, the mean free path affects the amount of residual resistance obtained due to trapped magnetic flux. We have analyzed nine cavities prepared with different levels of nitrogen-doping to understand how BCS and residual resistance are affected by changes in the mean free path. Here we present a model based on these experimental results to predict the optimal doping level to reach the maximum Q at 16 MV/m[1] based on the ambient magnetic field conditions. We find that if the cavities can be cooled with small amounts of trapped flux, moderate nitrogen-doping is better, while if they will have large amounts of trapped flux, lighter dopings should be used.

INTRODUCTION

Nitrogen-doping has been shown to dramatically improve the intrinsic quality factor, Q_0, of SRF cavities in the medium field region [1]. This improvement in Q_0 is due to two effects: a lowering of the low field temperature dependent BCS resistance, R_{BCS}, by a lowering of the electron mean free path, and an introduction of an anti-Q slope which allows R_{BCS} to decrease further by resulting in a decreasing R_{BCS} as the electric field is increased [2]. These two effects have resulted in cavities repeatably reaching Q_0's higher than 4×10^{10} at 2.0 K and 16 MV/m compared with less than 2×10^{10} in cavities prepared with standard methods. In addition to these benefits on R_{BCS} however comes a higher sensitivity of residual resistance to trapped magnetic flux, $R_{res,B}/B_{trapped}$ [3]. That is the amount of residual resistance, R_{res}, that a cavity will have for a given amount of trapped magnetic flux in its walls.

Both of these effects, a lowering of R_{BCS}, and an increase in R_{res} from trapped flux are heavily dependent on the exact doping level of the cavity. This doping level can be quantified with the electron mean free path: nitrogen-doping directly leads to a lowering of the mean free path [2]. Here we summarize the experimental data measured on single-cell cavities at Cornell which represent a large spread in doping level in order to combine these two effects and find the optimal nitrogen-doping level to minimize the total surface resistance for a given amount of trapped magnetic flux.

CAVITIES TESTED

A total of nine single-cell cavities of varying levels of nitrogen-doping were tested. For each cavity the BCS resistance at low and high fields and $R_{res,B}/B_{trapped}$ were measured. The mean free path was also extracted for each cavity. For a full description of the experimental methods used to measure these properties and a table listing them see [2].

DEPENDENCE OF BCS RESISTANCE ON MEAN FREE PATH

The temperature dependent component of surface resistance is called the BCS resistance, denoted R_{BCS}. At low fields its behavior is well-explained by standard (non-field dependent) BCS theory [4]. At higher fields however there does not exist a theory that fully encompasses the parameter space. Nitrogen-doped cavities have been shown to possess an anti-Q slope which is a result of a decreasing R_{BCS} with increasing E_{acc}. A few theories have been proposed, aiming at explaining this anti-Q slope. A promising theory by Gurevich is discussed in comparison to experimental data in [5]. At low fields, R_{BCS} for nitrogen-doped cavities closely follows the mean free path dependence predicted by BCS theory [2]. At high fields however there is a deviation. This is shown in Fig. 1 which shows R_{BCS} at 16 MV/m and 2 K for the cavities tested. Also shown is the low field BCS prediction and an adjusted BCS prediction. This adjustment comes from assuming a logarithmically decreasing R_{BCS} with E_{acc} which has been shown to approximate the anti-Q slope well [2]. In addition to this logarithmic dependence on field, the strength of the anti-Q slope is heavily dependent on mean free path with larger anti-Q slopes corresponding to lower mean free paths [2]. It can be seen that this adjustment shows very good agreement with the experimental data suggesting that R_{BCS} at higher fields is still governed by BCS theory with a small correction. The Gurevich theory which provides this correction results in the same qualitative behavior. For full details see [5]. While low field BCS theory predicts a minimum in R_{BCS} at mean free paths of

* Work supported by the US DOE and the LCLS-II High Q_0 Program and NSF Grant PHY-1416318

† gonnella@slac.stanford.edu

‡ Now at SLAC National Accelerator Laboratory, 2575 Sand Hill Road, Menlo Park, CA 94025 USA

§ mul2@cornell.edu

1 16 MV/m and 2 K were chosen to study due to this being chosen as the operating temperature and gradient for LCLS-II.

ISBN 978-3-95450-169-4

MAGNETIC FIELD MANAGEMENT IN LCLS-II 1.3 GHZ CRYOMODULES*

S. K. Chandrasekaran†, A. Grassellino, C. Grimm, G. Wu, Fermilab, Batavia, Illinois, USA

Abstract

The ambient magnetic field at the SRF cavity surface of the LCLS-II 1.3 GHz cryomodules is specified to be less than 0.5 µT (5 mG). Multiple methods were designed to lower the magnetic fields inside the prototype cryomodule. The resulting ambient magnetic field components in this cryomodule just prior to its first cool down was <0.15 µT (1.5 mG), as measured using fluxgates inside and outside the cavity helium vessels.

INTRODUCTION

Trapped magnetic fields on the RF surface of a SRF cavity can limit the quality factors (Q) achieved, due to increased RF surface resistance. The LCLS-II 1.3 GHz cryomodule specifications [1] therefore require the ambient magnetic fields to be less than 0.5 µT (5 mG), to obtain a Q of $2.7\text{x}10^{10}$ at 16 MV/m. The methodologies used to meet this specification include a 2-layer passive magnetic shield, an active longitudinal compensation scheme, and a strict magnetic field control program. The effectiveness of these methods are evaluated in the two prototype cryomodules (pCM), one at Fermi National Accelerator Laboratory (Fermilab) and one at Thomas Jefferson National Accelerator Facility (JLab). The Fermilab pCM is fully assembled and currently installed at the Fermilab Cryomodule Test Stand 1 (CMTS1). The JLab pCM is currently being assembled, and the results from this prototype shall be presented by JLab colleagues in a later publication.

MAGNETIC INSTRUMENTATION

The two pCMs are populated with 13 Bartington® Instruments Mag-F fluxgates each [2, 3]. Of the eight cavities in the pCM, four are instrumented with 2 fluxgates each inside the helium vessels, attached to the outer surface of the cavity, as illustrated in Figure 1. The first fluxgate is placed perpendicular to the cavity axis, in a vertical plane perpendicular to the cavity axis, and close to the bottom equator. The second fluxgate is placed at 45° to the cavity axis, in a vertical plane parallel containing the cavity axis.

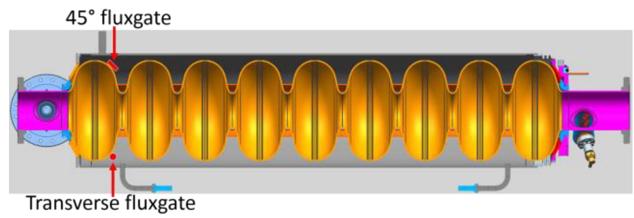

Figure 1: The two fluxgate locations within the cavity helium vessel. These fluxgates are mounted on the outside surface of the cavities.

An additional 5 fluxgates are placed external to the cavity helium vessels, between the two layers magnetic shields, parallel to the cavity axis and close to the vertical plane containing the cavity axis. The locations of these 5 fluxgates in the pCM are illustrated in Fig. 2.

The fluxgates inside the helium vessel have three functions: (1) to monitor the magnetic fields during assembly of the cryomodule and qualify the magnetic control program, (2) to quantify magnetic flux expulsion of the cavities during cool down, and (3) to monitor magnetic field generated by thermoelectric currents at the superconducting critical temperature of the niobium cavity at 9.2 K.

MAGNETIC SHIELDING

The magnetic shielding design for these cryomodules was optimized computationally [4] to reduce the ambient magnetic field at the cavity to less than 0.5 µT (5 mG). This shield scheme assumes a low carbon steel vacuum vessel is used for the cryomodules. These calculations assumed a relative permeability (μ_r) of 12,000 for the magnetic shielding material. The shields were designed to envelope the outside surface of the helium vessels of the cavities, but also had to accommodate several components attached to the cavities, including the fundamental power coupler, the cavity support bearing brackets, the end lever tuner to cavity attachment arms, beam tubes, etc. A 3-dimensional CAD model of the resulting magnetic shield used in the pCM is illustrated in Figure 3.

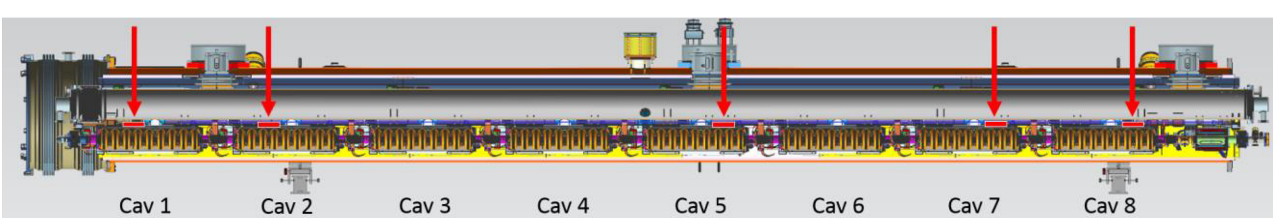

Figure 2: The locations of the five fluxgates external to the cavity helium vessels.

* Operated by Fermi Research Alliance, LLC under Contract No. De-AC02-07CH11359 with the United States Department of Energy.
† saravan@fnal.gov

ALTERNATIVE DESIGN FOR THE RISP PRE-STRIPPER LINAC*

B. Mustapha†, P.N. Ostroumov, Z.A. Conway, M.P. Kelly, and A. Plastun,
Argonne National Laboratory, Lemont, IL, USA,
J.-H. Jang, H. Jin, J.-W. Kim and H.J. Kim, RISP, IBS, Korea

Abstract

In a collaborative effort between Argonne's Linac Development Group and the RISP project team at the Korean Institute for Basic Science, we have developed an alternative design for the pre-stripper section of the RISP driver linac. The proposed linac design takes advantage of the recent accelerator developments at Argonne, namely the ATLAS upgrades and the Fermilab PIP-II HWR Cryomodule. In particular, the state-of-the-art performance of QWRs and HWRs, the integrated steering correctors and clean BPMs for a compact cryomodule design. To simplify the design and avoid frequency transitions, we used two types of QWRs at 81.25 MHz. The QWRs were optimized for β ~ 0.05 and ~ 0.11 respectively. Nine cryomodules are required to reach the stripping energy of 18.5 MeV/u. Following the lattice design optimization, end-to-end beam dynamics simulations including most important sources of machine error were performed. The results showed that the design is tolerant to errors with no beam losses observed for nominal errors.

INTRODUCTION

The baseline design for the RISP pre-stripper linac [1], named SCL3, uses QWRs and HWRs with room-temperature quadrupole focusing between cryostats containing one or two cavities. In this alternative design, we propose long cryomodules containing 7 or 8 cavities each with SC solenoid focusing. This design has the potential of significantly reducing the length and construction cost of the linac while satisfying the same beam requirements.

QWR CHOICE & EM DESIGN

Based on the frequency and the velocity range of the RISP pre-stripper linac, QWR type cavities are an ideal match for this section. In addition, using only QWRs will avoid a frequency transition in the middle of the linac if HWRs are used. At ANL, we have successfully developed and operated QWR resonators in the same frequency and velocity ranges as the ones required for the RISP pre-stripper linac [2]. Therefore, the design and fabrication of the RISP QWRs will require little to no R&D.

Two QWR types are required for the RISP pre-stripper linac, a low-β and a high-β, with β ~ 0.05 and 0.11, respectively. Both cavities are designed for 81.25 MHz frequency with 40 mm diameter aperture. The EM design of the two QWRs was performed based on the design optimization procedure developed at ANL [3]. The main RF parameters, such as the shunt impedance and peak fields, were optimized by varying the geometry parameters of the cavities. The proposed geometries have tapered inner and outer conductors spreading the magnetic field over a larger area which helps reduce the peak surface magnetic field. It is important to note that tapering the outer conductor does not add to the real-estate of the linac but uses the available space between elements.

Table 1 lists the RF parameters of the optimized designs for both QWRs while the geometry and the EM field distributions are shown in Figure 1.

Table 1: RF Design Parameters of the Two QWRs

Parameter	Low-β	High-β
β_{opt}	0.05	0.11
L_{eff}	18.5	40.5
E_{peak}/E_{acc}	5.6	5.6
B_{peak}/E_{acc}	7.7	7.3
R/Q (Ω)	493	552
G (Ω)	23	32

Following the design optimization of the cavities, the EM fields were extracted and used for beam simulations of the linac. This step is important to study the beam steering effects expected from these QWRs and apply the steering corrections by tilting the faces of the drift tubes. For the low-β, the required angle is 1 deg, while it is 4 deg for the high-β QWR.

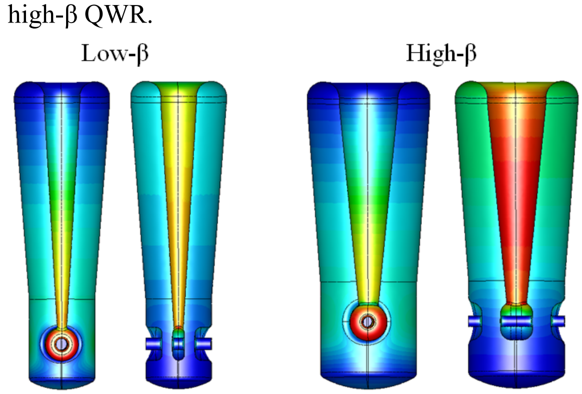

Figure 1: Geometries and EM field distributions for both types of QWRs.

LINAC LATTICE DESIGN

Ion beam acceleration from 500 keV/u to 18.5 MeV/u requires 2 types of QWRs as discussed in the

* This work was supported by the work-for-other grant WFO8550H titled "Pre-conceptual design, cost and schedule estimate of the 18.5 MeV/u Pre-stripper linac for the RISP/IBS.
†corresponding author: brahim@anl.gov

FRIB HWR TUNER DEVELOPMENT*

S. Stark†, A. Facco[1], S. Miller, P. Ostroumov, J. Popielarski, K. Saito, B. Tousignant, T. Xu
FRIB, Michigan State University, East Lansing, MI, USA
S. Gerbick, M. Kelly, Argonne National Laboratory, Argonne, IL, USA
[1] also at INFN-Laboratori Nazionali di Legnaro, Legnaro (PD), Italy

Abstract

During the last two years the HWR pneumatic tuner development at FRIB evolved from the first prototypes to the final production design. A lot of warm testing and several cryogenic integrated tests with cavity were performed to optimize the tuner features. The main challenges included the bellow bushings binding and very tight space limitations for the assembly on the rail. The final design, based on the acquired experience, was prepared in collaboration with ANL and entered the preproduction phase.

FIRST PNEUMATIC TUNER PROTOTYPE AT FRIB

First pneumatic tuner prototype was prepared in spring 2014 (Fig.1). The design followed ANL guidelines [1]. We started the systematic study of the tuner in June 2014 using a HWR53 cavity.

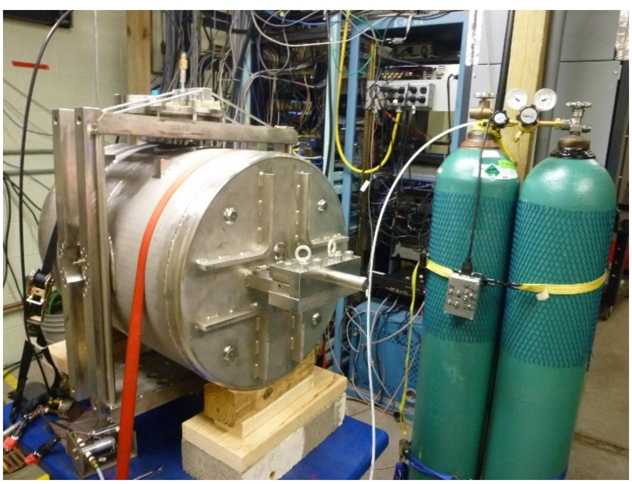

Figure 1: Pneumatic tuner prototype.

We used FRIB LLRF controller interfaced with PC to drive the valve system and acquire helium gas pressure and frequency data. For evaluation purposes we developed 3 types of sequences:

- Full range scanning with frequency and pressure registration up to 15 cycles per hour (can be executed in superconducting state and nearly critical coupling at room temperature)
- Full range scanning up to 150 cycles per hour with pressure registration
- Small range (1-2 psi) scanning 1800 cycles per hour with pressure registration. The pressure floor could be changed using the pressure regulator

During the first warm testing runs the main part of tuning mechanism including frame, arms and cables seemed to work fine and to be under control. We only had to reinforce the planes as they were flexing and enlarge the spacing for frame to move without touching the arms. We had to concentrate on the bellows lifetime as the most critical parameter for FRIB project. We started with the bellows with 3 guides for the movable flange (Fig. 2).

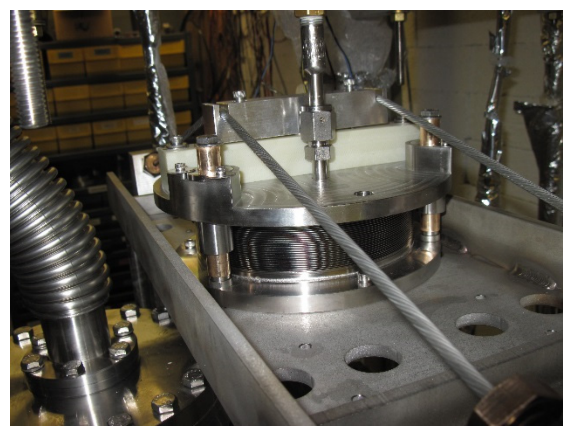

Figure 2: Initial bellows model.

We have got one of the bellows broken in the first convolution after 500 full cycles. After that all new bellow flanges are EB welded instead of TIG to reduce the overheating and bellows damage probability, and the profile for welding had been modified.

The main problem we encountered was the friction and binding between the guides and the flange.

Used testing sequence consisted of about 200-300 full range cycles and about 2000 each small range cycles in at least 3 pressure regions.

Several guide bar-bushing combinations and solutions were tested (Fig.3).

- Nitronic bar and bushing
- Nitronic bar and Bronze bushing
- Nitronic bushing and Bronze bar (ANL style)
- Nitronic bushing and Bronze bar of larger diameter
- Nitronic/Dicronite bushing and Bronze bar
- Nitronic/Dicronite bar and bushing
- Nitronic/Dicronite bushing and Nitronic bar

* Work supported by the U.S. Department of Energy Office of Science under Cooperative Agreement DE-SC0000661, the State of Michigan and Michigan State University
† stark@frib.msu.edu

ISBN 978-3-95450-169-4

FIRST FRIB β = 0.53 PROTOTYPE COLDMASSS BUILD*

D. Victory#, K. Elliott, B. Oja, J. Popielarski, M. Wilbur,
Facility for Rare Isotope Beams (FRIB), Michigan State University, East Lansing, MI 48824, USA

Abstract

The β = 0.53 coldmass consists of eight Superconducting Radio Frequency (SRF) β = 0.53 cavities, eight Fundamental mode Power Couplers (FPC), and one 8 T solenoid. This is the first coldmass with this version of cavity and it has brought new challenges to overcome. The Facility for Rare Isotope Beams (FRIB) contains 18 cryomodules with β = 0.53 cavity coldmasses, and this type of coldmass is the highest power and most produced ones in FRIB. During the final cleaning stage and the cavity assembly, particle detection equipment is used to verify the cavity cleanliness levels for cavity certification test and for coldmass assembly. This method allows for cleanliness detection of specific areas inside the cavity at any time a vacuum flange is off. The fixtures, techniques and procedures used to build the β =0.53 coldmasses will be presented.

INTRODUCTION

The FRIB linear accelerator consists of 3 β = 0.041 coldmasses, 11 β = 0.085 coldmasses, 12 β = 0.29 coldmasses, and 18 β = 0.53 coldmasses. Coldmasses of each type have been assembled except for the β = 0.29 variant at this time. All of the β = 0.041 coldmasses have been assembled and are being installed into cryomodules. Three β = 0.085 coldmasses have been fully assembled with two tested. The last β = 0.085 cryomodule was tested with no field emission increase from vertical test.

The β = 0.53 coldmass took over a year to complete from the first cavity arrival. The design and process were based on a prototype cryomodule previously built, but new fixtures and procedures were developed with new designs to successfully build the coldmass.

FRIB BASELINE CAVITY PROCESS

Incoming Cavity Process

All cavities and coldmass components are subject to inspection through an Acceptance Criteria List prior to processing. Critical dimensions are measured with a Coordinate Measurement Machine. Machined mounting surfaces are measured to ensure proper placement of the cavity on the alignment rails. Other inspection includes surface finish quality test, and detection of scratches, dings, and inclusions.

Cavities are degreased after inspection to remove any residual grease and oil from the fabrication process. A 1% solution of Micro-90tm detergent is used in an ultrasonic cleaner at 100°F for 60 mins.

* This material is based upon work supported by the U.S. Department of Energy Office of Science under Cooperative Agreement DE SC0000661, the State of Michigan and Michigan State University.
# victory@frib.msu.edu

Cavity Etching and Heat Treatment

The β = 0.53 cavity is etched with buffered chemical polish to remove 120 microns. This process is also used to tune the cavity. For this purpose, the process is divided into several steps [1]. A final etch cleans up the surface by removing 30 microns of material. After etching the cavity goes into the cleanroom and 150 minutes high pressure rinsing takes place with 93 bar water. The high pressure rinse robot manipulates a wand that enters into the 7 ports on the cavity.

After the bulk etch process is completed, the cavity is placed in a vacuum furnace. This furnace operates at 600°C for 10 hours to remove the deposited hydrogen on the surface of the niobium.

Cavity Assembly

After the high pressure rinse, the cavity is dried overnight in an ISO 5 cleanroom. The cavity ports are covered with clean plastic caps to prevent particles from entering during assembly. The assembly starts on the bottom of the cavity and goes up to reduce the contamination from handling hardware above open ports. The vertical test setup includes a matched radio frequency power coupler and the cryomodule diagnostic pickup loop coupler. Cavities and vacuum components are verified to be clean with a surface particle detector to less than 0.2 0.3μm particles/cm^2.

The cavity is mounted on a vertical test insert with a flexible coupling to make the vacuum connection (Fig. 1). The vacuum system on the insert allows for manual slow pump and purge processes to pump out and purge at 1 mbar/s. A helium mass spectrometer is used to verify the seal and weld leak rates before cooled down to 2 K with liquid helium.

Figure 1: β = 0.53 cavity for vertical test on test insert with Fundamental mode Power Coupler (FPC).

FIRST FRIB β=0.041 PRODUCTION COLDMASS BUILD*

K. Elliott#, S. Miller, B. Oja, J. Popielarski, L. Popielarski, D. Victory, M. Wilbur, T. Xu, Facility for Rare Isotope Beams, East Lansing, USA
M. Wiseman, Thomas Jefferson National Accelerator Facility, Newport News, USA

Abstract

Three β=0.041 cryomodules (CMs) are required for the Facility for Rare Isotope Beams (FRIB) accelerator. Clean-room assembly of all three coldmasses for these cryomodules has been completed. The cleanroom assembly includes; the superconducting radio frequency (SRF) cavities, the superconducting solenoids, fundamental-mode power couplers (FPC), beam position monitors, alignment rail, and transport cart. This paper will provide an overview of the techniques and procedures used to assemble this cavity string to be put to practical use in the FRIB accelerator.

INTRODUCTION

The β=0.041 cryomodules (CMs) are the lowest β CMs, being the first superconducting accelerator components of the FRIB accelerator. There will be three of the β=0.041 CMs. The core of the CM is referred to as the coldmass. Generally speaking, the lowest β coldmass is the most difficult to manufacture and to assemble for its tight space. The coldmass assembly is done in an ISO 5 cleanroom. The coldmass is considered complete once the physical assembly matches the assembly drawing, and is under vacuum and leak checked.

COLDMASS COMPONENTS

The completed β = 0.041 coldmass is shown in Figure 1. It can be seen from the figure that four β = 0.041 superconducting RF (SRF) cavity vessels and two superconducting (SC) solenoid vessels are mounted on the alignment rail.

Figure 1: Completed β=0.041 coldmass.

*This material is based upon work supported by the U.S. Department of Energy Office of Science under Cooperative Agreement DE SC0000661, the State of Michigan and Michigan State University.
#elliott@frib.msu.edu

Alignment Rail and Cart

The alignment rail is a stainless steel structure on which the cavities are mounted and aligned along the beam axis. The cart is a simple assembly which the alignment rail is mounted on to allow easy transportation and manipulation of the entire coldmass. The alignment rail undergoes numerous inspections upon arriving from the vendor. The cooling lines, which are welded to the rail, are leak checked. A coordinate measurement machine (CMM) verifies that the alignment features of the rail are within tolerance. The alignment rail is measured for residual magnetic field. Once the rails are accepted they are cleaned with a high pressure solution of ultra-pure water and Micro90 detergent, then brought into the cleanroom. Surface particle counts are taken on the rails after they enter the cleanroom to confirm that the rails are adequately clean and will not risk contaminating the SRF cavities.

SRF Cavities

The SRF cavities are of quarter wave resonator (QWR) structure with a resonant frequency of 80.5 MHz. They undergo a similar battery of acceptance tests as the rails, with the notable addition of a cavity surface inspection by borescope, and frequency measurement. After the cavities are accepted they will receive a bulk etching of 120 µm by buffered chemical polish (BCP). Then they are heat treated in a vacuum furnace at 600°C for 10 hours, and precision machined for beam line alignment. The cavities can be fine-tuned by preferential etching [1]. After all of the aforementioned steps are completed the cavity proceeds through the final processing steps, including an ultrasonic cleaning, light etch of at least 30 µm, and high pressure rinse with ultrapure water (UPW) for 150 minutes at a pressure of 93 bar [2].

The cavity typically dries overnight following the high pressure rinse. It is then assembled and installed to the testing insert. The beam line space is evacuated to ultrahigh vacuum and leak checked, then the test insert is removed from the cleanroom and prepared for cryogenic testing.

The test insert provides a platform which mimics actual CM operation. Liquid helium is supplied to the cavity helium vessel to make the cavity superconducting. A friction mass damper is installed to the cavity's inner conductor, just as it would be in the CM. During the cryogenic testing numerous performance parameters are measured to confirm that they are within specification. The cavity should not have any leaks from the helium jacket. The cavity frequency should be within the tuneable range provided by the stepper motor. In particular, the cavity quality factor, Q, should meet or exceed FRIB specification of 1.4×10^9 at

ISBN 978-3-95450-169-4

RF ANALYSIS OF ELECTROPOLISHING FOR EXFEL CAVITIES PRODUCTION AT ETTORE ZANON SpA

A. Sulimov, DESY, Hamburg, Germany
A. Gresele, M. Giaretta, A. Visentin, Ettore Zanon S.p.A., Schio, Italy

Abstract

After successful finishing of superconducting cavities mass production at Ettore Zanon S.p.A. (EZ) for the European XFEL (EXFEL), the authors had the possibility to provide a detailed analysis of the electropolishing (EP) process. The analysis of EP material removal is based on specified RF measurements and was used for the determination of both, the ratio between cavity's iris and equator and uniformity in different cells. A comparison of the RF measurements results with mechanical measurements is presented.

STATISTICS

The measurements of cavity weight before and after the EP process during serial cavity production at EZ allowed us to calculate the average value of removed material from the cavity surface on the level of (154 ± 6) µm. The minimal and maximal values are correspondingly 143 µm and 183 µm.

The results of the statistical analysis of more than 300 cavities are presented on Figure 1.

The relative errors of frequency changes (δF_{pi}) and frequency sensitivity determination ($\delta(dF_{pi}/d\,\overline{R})$) are about 15 %. It means that the average value of removed material from the cavity surface can be determined with relative error of 30 %, which corresponds to the values (153 ± 44) µm.

The usage of additional RF measurements helps to estimate also the average values in different cavity regions (irises and equators) [1].

One can notice that the pi-mode frequency change (dF_{pi}) not only depends on the average amount of removed material from the inner cavity surface but also on the ratio of removed material between iris and equator – *dRi/dRe*. Extra material removal from the iris reduces the pi-mode frequency deviation due to EP and it has to be taken into account in the analysis of the mean removal value along a cavity.

ALGORITHM OF ANALYSIS

The three calculation methods will be described in this part:

- removed material along one cell;
- mean removal along a cavity;
- removed material in different cavity cells.

Removed Material Along One Cell

The amount of removed material along one cell is a function:

$$dR_{cell} = f(z), \tag{1.1}$$

which is determined in the range $z \in [-\frac{L_c}{2}, \frac{L_c}{2}]$, where L_c is the length of a cell.

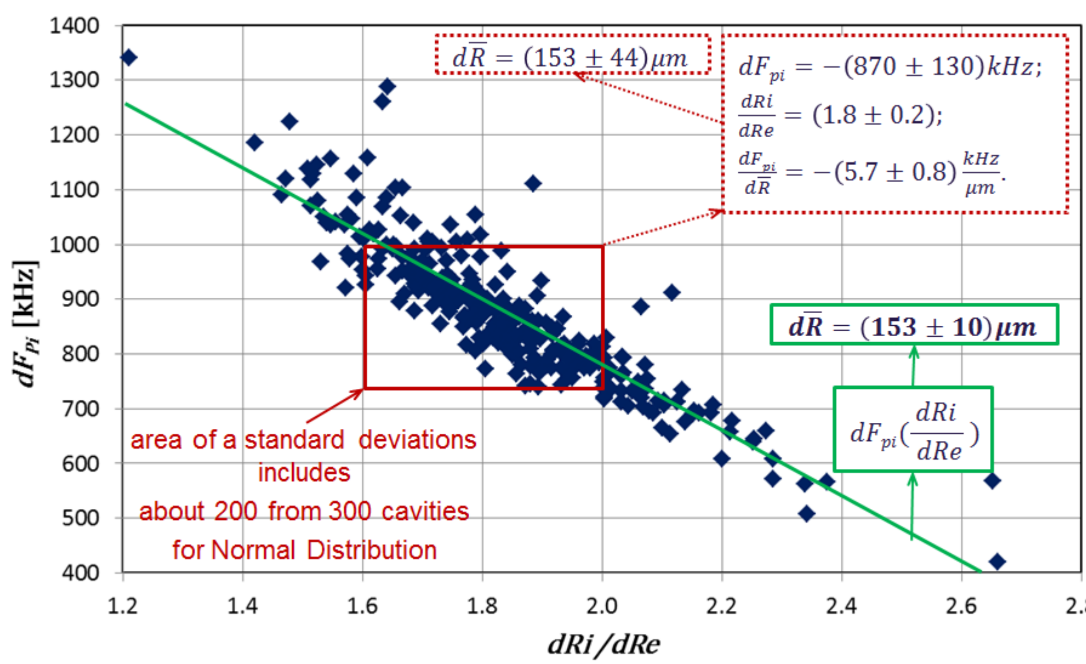

Figure 1: Deviation of EXFEL cavities parameters during EP at E.ZANON (for 300 cavities).

THE DTL POST COUPLER – AN INGENIOUS INVENTION TURNS 50

S. Ramberger*, CERN, Geneva, Switzerland
M. R. Khalvati, School of Particles and Accelerators, IPM, Tehran, Iran

Abstract

In September 1967, the patent for "A method and device for stabilization of the field distribution in drift tube linac" has been filed by Edward A. Knapp, Donald A. Swenson, and James M. Potter of Los Alamos National Laboratory [1]. It is this invention which to a good part led to the success of highly efficient Alvarez drift tube linacs (DTLs) in that it considerably reduces field errors. The explanation for why the post coupler when tuned correctly has such a strong stabilizing effect has been given at the time in an accompanying paper by describing the modal confluence of the accelerating mode band with the post-coupler mode band, turning a comparatively sensitive 0-mode structure into a stable $\pi/2$-mode like structure. As ingenious as the invention of the post coupler appears, as poor has been the way of finding its optimum length by relying mainly on trial and error. With the design of the Linac4 DTL at CERN, a new technique has been derived by a DTL equivalent circuit model. Understanding stabilization on an almost cell by cell level provides a new way of optimizing post couplers of an entire structure with few measurements and even without the extraction of the circuit model itself. Previous approaches to post-coupler stabilization are reviewed and the new, straightforward and accurate technique is described and demonstrated in the stabilization of the Linac4 DTL structures.

INTRODUCTION

Within two years after WWII, Luis Alvarez developed the first Drift Tube Linac (DTL) based on ideas of Ising and Widerøe [2]. While beams of ions had been accelerated by RF power before, it was with the availability of strong RF sources at 200 MHz that had been developed for radar applications during the war that such a structure could be built with reasonable dimensions as necessary for the acceleration of proton beams. In order to achieve sufficient acceleration, high gradients were required, that could only be maintained in cavities. Alvarez had the idea to attach one cavity to the next and to suppress end walls in order to reduce losses. He built the first DTL empirically from model cavities that he excited in the TM_{010} mode and he adjusted the dimensions in order to find the proper drift tube and resonator length.

In the following years, the theory of RF acceleration was further developed and beams of ever higher intensity could be accelerated. The invention of strong focusing in the early 1950s sorted out the issues with grid focusing [3] and soon after, new drift tube geometries were found analytically which lead to higher shunt impedances [4]. Already at that time, permanent magnet quadrupoles have been considered as focusing elements and computers were used to optimize the RF design.

EQUIVALENT CIRCUIT MODEL

For the injection into synchrotrons, effective beam transport and beam quality were of particular importance and in the 1960s with new machines just having come on-line, it became clear that field stability and beam loading needed to be better understood. It turned out that beam loading not only had an influence on the absolute field level but also on the variation of fields within the cavity. Modal analysis and equivalent circuits were used for a better understanding of the cavity behavior [5].

The equivalent circuit of yet unstabilized drift tube cells has been developed in [6] that topologically is that of a transmission line with series resonators Z_n and shunt elements Y_n' (Fig. 1):

$$Z_n = j\omega L_n + \frac{1}{j\omega C_n} \quad (1)$$

$$Y_n' = j\omega C_n' + \frac{1}{j\omega L_n'} \quad (2)$$

where L_n and C_n represent the equivalent circuit elements for drift tube n, and L_n' and C_n' are the elements of the stem and the shunt capacitance between drift tubes and tanks respectively. Certainly, the elements when extracted do not fully scale with cell lengths as they are the result of a quasi-static approximation and also contain other stray contributions. Note that losses have been neglected.

Infinite circuit structures can be analyzed by transmission line theory in order to get an idea about the average wave transmission on fully distributed elements or more correctly by Floquet's theorem thus representing an infinite chain of equal basic cells (Fig. 1) [7]. The propagation constant and thus the dispersion diagram can be directly extracted from Z and Y'. When using transmission line theory, the π-mode is not represented.

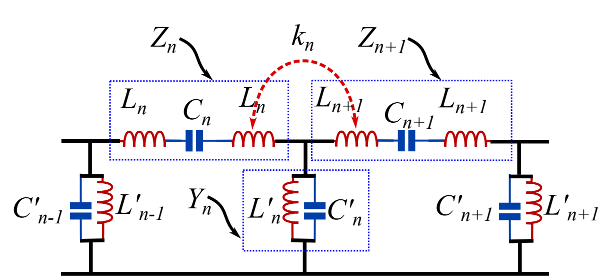

Figure 1: DTL equivalent circuit without post couplers.

* Suitbert.Ramberger@cern.ch

ISBN 978-3-95450-169-4

THE RF SYSTEM OF THOMX*

M. El Khaldi, H. Monard, R. Marie, F. Wicek
LAL, Orsay, France
M. Diop, R. Lopes, A. Loulergue, M. Louvet, P. Marchand, F. Ribeiro, R. Sreedharan
SYNCHROTRON SOLEIL, Gif-sur-Yvette, France

Abstract

The RF system of the ThomX electron storage ring consists in a 500 MHz single cell copper cavity of the ELETTRA type, powered with a 50 kW CW solid state power amplifier (SSPA), and the associated Low Level RF feedback and control loops. The low operating energy of 50/70 MeV makes the impedances of the cavity higher order modes (HOMs) particularly critical for the beam stability. Their parasitic effects on the beam can be cured by HOM frequency shifting techniques, based on a fine temperature tuning and a dedicated plunger. A typical cavity temperature stability of ± 0.05°C within a range from 30 up to 70 °C can be achieved by a precise control of its water cooling temperature. On the other hand, the tuning of the cavity fundamental mode is achieved by changing its axial length by means of a motor-driven mechanism. A general description of the system and the state of its progress are reported together with some considerations of the effects of beam cavity interactions.

INTRODUCTION

ThomX is a Compton source project of hard X rays (45/90 keV). The machine is composed of a 50/70 MeV injector Linac and a storage ring where an electron bunch collides with a laser pulse accumulated in a Fabry-Perot resonator. The final goal is to provide an X-rays average flux of 10^{11}-10^{13}ph/s. The ThomX project [1] was recently funded and a demonstrator is being built on the Orsay university campus.

The proposed RF system for the ThomX storage ring is described in [2]. It consists in a 500 MHz single cell cavity of the ELETTRA type [3], powered with a 50 kW CW solid state power amplifier (SSPA), and the associated Low Level RF feedback and control loops [4].

When a bunch traverses a high Q resonator like a RF cavity, it excites its higher order modes (HOMs). The induced long term electromagnetic wakefields act back on the bunch over many revolutions and therefore can cause beam instabilities resulting in degradation of the beam quality or even beam losses.

In a low energy ring like ThomX, the natural damping time is so weak (~ 1 s) that a stationary stable condition can never be reached during the beam storage time, which is as short as 20 ms. On the other hand, it is sufficient to maintain the instability growth time larger than the beam storage time in order to keep at tolerable level the effect on the beam. That requires very strong attenuation of the cavity HOM impedances, typically by a few 10^3.

There are essentially two methods of coping with such HOM impedances, either a strong de-Qing of the HOM resonances [5, 6] or a tuning of their frequencies away from the beam spectral lines to prevent resonant excitations [7]. With the former it is difficult to reach attenuation factors larger than a few 10^2 over a wide frequency range. The latter, which consists in controlling the HOM frequencies, is better suited to a small circumference machine like ThomX, where the beam spectral lines spacing (16.7MHz) is very large as compared to the HOM bandwidth. As far as the HOM density is not too high and that they can be tuned far enough from the beam spectral lines ($\delta f >> f_{HOM}/Q_o$), it should be possible to reduce their effective impedances, R_{eff} ("as seen" by the beam), down to tolerable levels:

$$R_{eff} \approx R_s / (2Q_o.\delta f / f_{HOM})^2 << R_s \qquad (1)$$

That led us to choose the ELETTRA type cavity which allows applying this technique in combining three tuning means. The HOM frequencies are precisely controlled by proper setting of the cavity water cooling temperature within a range from 30 up to 70 °C with a stability of ± 0.05 °C, while the fundamental frequency is recovered by means of a mechanical tuner which changes the cavity length. Besides, a movable plunger provides another degree of freedom for tuning the HOM frequencies.

In order to insure a fine control of the HOM frequencies, a good knowledge of their characteristics is mandatory. The main parameters of the fundamental and the HOMs have therefore been calculated using the Eigenmode solver of the 3D Electromagnetic HFSS [8] and CST MWS [9] codes and compared with the measured values on the cavity [10]. As it will be hard to cope with all these modes only by applying the tuning technique, one relies on the longitudinal and transverse feedbacks in order to bring additional damping.

STORAGE RING RF SYSTEM

The selection of 500 MHz as RF frequency leads to a quite good compromise in terms of cavity fundamental and HOM impedances, space requirements as well as the availability of RF power sources and other components.

500 MHz RF Cavity

One 500 MHz single cell cavity of the ELETTRA type, powered with a 50 kW CW SSPA, will provide the required RF voltage of 500 kV. It is made out of OFHC

*Work supported by the french "Agence Nationale de la Recherche" as part of the program "investing in the future" under reference ANR-10-EQPX-5, and also by grants from Région Ile-de-France.

ISBN 978-3-95450-169-4

MANUFACTURING, ASSEMBLY AND TESTS OF THE LIPAC MEDIUM ENERGY BEAM TRANSPORT LINE (MEBT) *

I. Podadera †, P. Abramian, B. Brañas, J. Calero, J. Castellanos, J. M. García, D. Gavela, A. Guirao, J. L. Gutiérrez, D. Jiménez-Rey, M. Lafoz, D. López, L. M. Martínez, E. Molina, J. Molla, C. de la Morena, C. Oliver, D. Regidor, A. Soleto, F. Toral, R. Varela, V. Villamayor, M. Weber, CIEMAT, Madrid, Spain
O. Nomen, Institut de Recerca en Energia de Catalunya, IREC, Barcelona, Spain

Abstract

LIPAc [1] is a 9 MeV, 125 mA CW deuteron accelerator which aims to validate the technology that will be used in the future IFMIF-DONES accelerator [2]. The acceleration of the beam will be carried out in two stages. An RFQ will increase the energy up to 5 MeV before a Superconducting RF (SRF) linac made of a chain of eight Half Wave Resonators bring the particles up to the final energy. Between both stages, a Medium Energy Beam Transport line (MEBT) [4] is in charge of transporting and matching the beam between the RFQ and the SRF. The transverse focusing of the beam is controlled by five quadrupole magnets with integrated steerers, grouped in one triplet and one doublet. Two buncher cavities surrounding the doublet handle the longitudinal dynamics. Two movable scraper systems are also included to purify the beam optics coming out the RFQ and avoid losses in the SRF. In this contribution, the final integrated design of the beamline will be shown, together with the auxiliaries. The manufacturing of all the components and the integration in the beamline will be depicted. The final tests carried out to the beamline prior to the installation in the accelerator will be also reported.

MANUFACTURING & TESTS

The challenging requirements from beam dynamics [3] due to the high space charge along the MEBT causes a very compact and complex mechanical design [4]. In less than two meters, the MEBT contains five combined magnets, two movable scrapers, two re-buncher cavitities and four beam position monitors, as main components. Moreover, due to the activation, the time required for maintenance of the components should be minimized with easy access to the most delicate pieces.

Magnets

The mechanical design and the manufacturing was performed by the company ANTEC from an electromagnetical design [5]. The main challenges of the design were the limiting longitudinal space, which complicates the design of the coils and the electrical and hydraulical connections. Further information of the manufacturing can be found in [6] (see Fig. 1). Each magnet has followed a complete set of tests in the company: water cooling tests, insulation, coils impedance at several frequencies, metrology. All the magnets passed the tests prior to the magnetic analysis. Later, the magnets were tested in two magnetic test benches in ALBA-CELLS [14]. The analysis showed slightly higher harmonics in some magnets. However, after redoing some beam dynamics analysis it was seen there was no influence in the beam, therefore the magnets were accepted for assembly in the beamline.

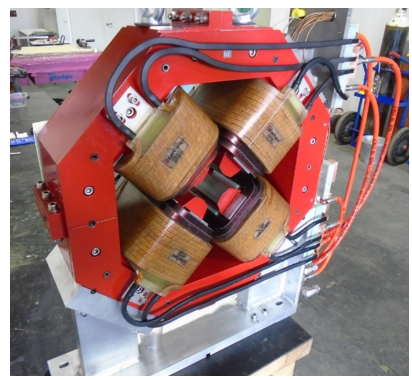

Figure 1: Picture of one of the MEBT combined magnets.

Re-buncher Cavities

Two re-buncher cavities with an E_0LT of 350 kV are necessary to match the beam with the SRF LINAC. The design was really challenging due to the limited space and the high voltage required. It was necessary to search for a special design of 5-gap IH resonant cavity with less than 10 kW dissipation power and low power density in the walls [8]. The re-buncher cavities were manufactured and integrated mainly by the Spanish company DMP (Fig. 2). The two re-buncher cavities have been tested following the same procedure. A complete set of tests (vacuum, water cooling, metrology) was performed in factory after each fabrication step [9]. Later, a smooth RF conditioning up to full power was carried out successfully at ALBA-CELLS RF laboratory [10]. The final Solid State Power Amplifer (SSPA) -developed by bTESA- was used as RF supply [11].

Scrapers

The mechanical design, manufacturing (see Fig. 3) and integration were performed by the company AVS from the thermomechanical and cooling design of the blades [12].

* This work has been funded by the Spanish Ministry of Economy and Competitiveness under the Agreement as published in BOE, 16/01/2013, page 1988 and the project FIS2013-40860-R
† ivan.podadera@ciemat.es

DESIGN AND OPERATION OF PULSED POWER SYSTEMS BUILT TO ESS SPECIFICATIONS

Michael Kempkes, Marcel Gaudreau, Matthew Munderville, Ian Roth, Diversified Technologies, Inc., Bedford, MA, USA
Julien Domenge, Jean-Luc Lancelot, SigmaPhi Electronics, Vannes, France

Abstract

Diversified Technologies, Inc. (DTI), in partnership with SigmaPhi Electronics (SPE) has built three long pulse solid-state klystron transmitters to meet spallation source requirements. Two of the three units are installed at CEA Saclay and the National Institute of Nuclear and Particle Physics (IN2P3), where they will be used as test stands for the European Spallation Source (ESS). The systems delivered to CEA and IN2P3 demonstrate that the ESS klystron modulator specifications (115 kV, 25 A per klystron, 3.5 ms, 14 Hz) have been achieved in a reliable, manufacturable, and cost-effective design. There are only minor modifications required to support transition of this design to the full ESS Accelerator, with up to 100 klystrons. The systems will accommodate the recently-determined increase in average power (~660 kW), can offer flicker-free operation, are equally-capable of driving Klystrons or MBIOTs, and are designed for an expected MTBCF of over ten years, based on operational experience with similar systems.

INTRODUCTION

Diversified Technologies, Inc. (DTI), in partnership with SigmaPhi Electronics (SPE), has designed and installed advanced, high voltage solid-state modulators for European Spallation Source (ESS)-class klystron pulses (Figure 1). These klystron modulators use a series-switch driving a pulse transformer, with an advanced, patent-pending regulator to maintain a precise cathode voltage as well as a constant load to the external power grid. The success of the design in meeting the ESS pulse requirements (Table 1) is shown in Figure 2.

Figure 1: DTI's prototype solid-state ESS-class klystron modulator, developed under a DOE SBIR grant.

Table 1: ESS Klystron Modulator Requirements

Specification	
Voltage	-115 kV
Current	25 A per Klystron
Pulse Width	3.5 ms
Frequency	14 Hz (max)
Average Power	160 kW (per Klystron)
Droop	< 1%
Pulse Repeatability	< 0.1%

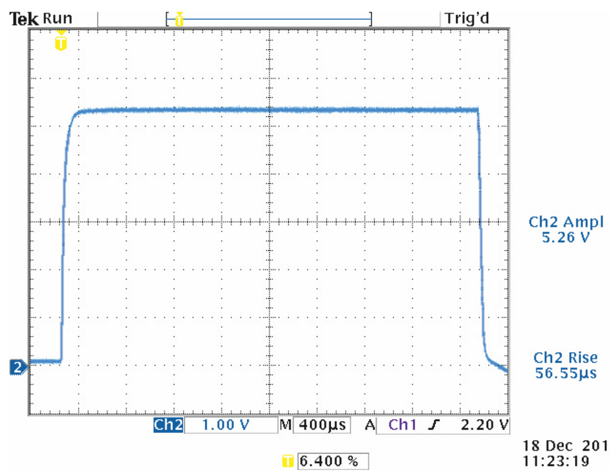

Figure 2: Modulator pulse at 108 kV, 3.5 ms, 0.07% flattop into a Thales TH2179A klystron during site acceptance testing at IN2P3, 18 December 2015.

The DTI/SPE klystron modulator is now a fully proven design, delivering significant advantages in klystron performance through:

- Highly reliable operation, demonstrated in hundreds of systems worldwide, and predicted to significantly exceed ESS requirements
- Flicker- and droop-free operation over a range of operating parameters
- All active electronics in air for easy maintenance

With the delivery of these initial modulators, the transition to production for the ESS system itself is straightforward.

DESIGN

The heart of the DTI/SPE modulator design is a high voltage solid-state switch driving a pulse transformer. The switch is made of seven series-connected IGBT modules, and operates at 6.7 kV. This design enables a measured

THYRATRON REPLACEMENT

Dr. Ian Roth, Dr. Marcel Gaudreau, Michael Kempkes, Matthew Munderville,
Diversified Technologies, Inc., Bedford, MA, USA

Abstract

Semiconductor thyristors have long been used as a replacement for thyratrons in low power or long pulse RF systems. To date, however, such thyristor assemblies have not demonstrated the reliability needed for installation in short pulse, high peak power RF stations used with many pulsed electron accelerators. The fast rising current in a thyristor tends to be carried in a small region, rather than across the whole device, and this localized current concentration can cause a short circuit failure. An alternate solid-state device, the insulated-gate bipolar transistor (IGBT), can readily operate at the speed needed for the accelerator, but commercial IGBTs cannot handle the voltage and current required. It is, however, possible to assemble these devices in arrays to reach the required performance levels without sacrificing their inherent speed. Diversified Technologies, Inc. (DTI) has patented and refined the technology required to build these arrays of series-parallel connected switches. DTI is currently developing an affordable, reliable, form-fit-function replacement for the klystron modulator thyratrons at SLAC capable of pulsing at 360 kV, 420 A, 6μs, and 120 Hz.

BACKGROUND

The Stanford Linear Collider (SLC) has used thyratrons in its klystron modulators since its inception in 1963. While the thyratrons function, they need replacement every 10,000 hours at a cost of $13,000 each, plus labor. Furthermore, periodic maintenance is required to adjust their reservoir heater voltage over the thyratron lifetime. As the Stanford Linear Accelerator Center (SLAC) continues to run its accelerator over the next two decades, replacing the thyratrons with a solid-state switch that would last 25 years or more, and does not need maintenance, would provide significant savings – both in the avoided cost of thyratrons as well as the labor in replacing and adjusting them.

SLAC is presently funding the development of a solid-state switch, based on thyristor technology to replace the thyratrons (Figure 1), meeting the requirements of existing klystron modulators (Table 1). The difficulty is that a fast rising current in a thyristor tends to be carried in a small region, rather than across the whole device, and this localized current concentration can cause a short circuit failure.

Work supported by DOE under contract DE-SC0011292

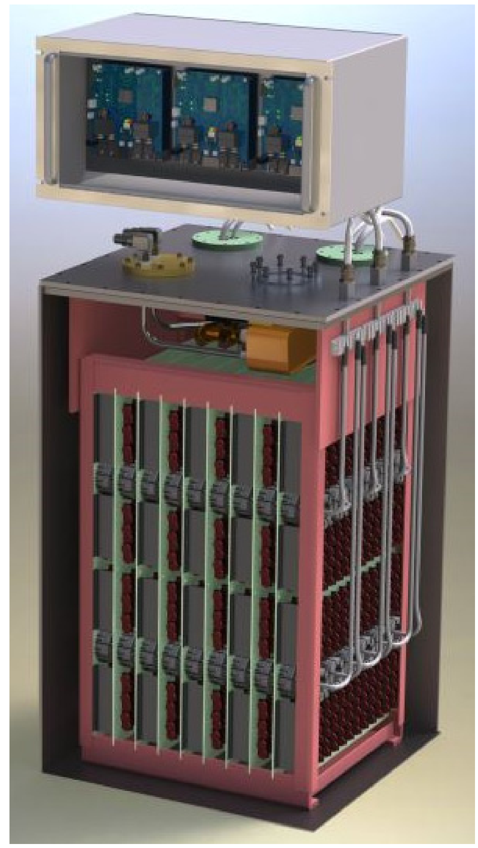

Figure 1: DTI solid-state replacement for the L-4888 thyratron used at SLAC. The switch, which operates at 48 kV and 6.3 kA, fits in the same location as the legacy thyratron assembly.

Table 1: ESS Klystron Modulator Requirements

Specification	
Voltage	48 kV
Current	6.3 kA
Pulse Width	6 μs
Risetime	1 μs, 10 A/μs
Frequency	120 Hz

DESIGN

An alternate solid-state device, the insulated-gate bipolar transistor (IGBT), can readily operate at the speed needed for the accelerator, but commercial IGBTs cannot handle the voltage and current required. It is, however, possible to assemble these devices in arrays to reach the required performance levels without sacrificing their inherent speed. Diversified Technologies, Inc. (DTI) has patented and refined the technology required to build these arrays of series-parallel connected switches. DTI has shipped more than 500 systems leveraging this tech-

ISBN 978-3-95450-169-4

DESIGN, FABRICATION, INSTALLATION AND OPERATION OF NEW 201 MHZ RF SYSTEM AT LANSCE*

J. T. M. Lyles#, W. Barkley, R. Bratton, M. Prokop, D. Rees
AOT Division, Los Alamos National Laboratory, Los Alamos, NM, USA

Abstract

The LANSCE RM project has restored the proton linac to high power capability after the RF power tube manufacturer could no longer provide devices that consistently met the high average power requirement. Diacrodes® now supply RF power to three of the four DTL tanks. These tetrodes reuse the existing infrastructure including water-cooling systems, coaxial transmission lines, high voltage power supplies and capacitor banks. Each final power amplifier (FPA) system uses a combined pair of LANL-designed cavity amplifiers using the TH628L Diacrode® to produce up to 3.5 MW peak and 420 kW of average power. A new intermediate power amplifier (IPA) was developed using a TH781 tetrode. These amplifiers are the first production of new high power 200 MHz RF sources at accelerators in three decades. Design and prototype testing of the high power stages was completed in 2012, with commercialization following in 2013. Each installation was accomplished during a 4 to 5 month beam outage each year starting in 2014. Simultaneously, a new digital low-level RF control (dLLRF) system was designed and tested, and placed into operation this year, meeting the stringent field control requirements for the linac. The rapid-paced installation project changed over from old to new RF systems while minimizing beam downtime to the user facility schedule.

BACKGROUND

The LANSCE drift tube linac (DTL) uses four Alvarez cavities powered at 201.25 MHz, to accelerate both protons (H^+) and negative hydrogen ions (H^-) from 0.75 to 100 MeV before injection into a 805 MHz coupled-cavity linac (CCL). Pulsed RF power must be capable of 15% duty factor (DF) and as high as 3.3 MW of peak RF power, with corresponding average power capability of 480 kW per cavity. This is in contrast to the high-peak/low-average power proton injector linacs at 200 MHz used at Fermilab, CERN, RAL and BNL. Over the past 25 years, manufacture of reliable RF amplifier triodes operating at this average power has been unpredictable. Both premature loss of cathode emission and ceramic cracking have occurred in numerous tubes run at our power levels. In 2006, the operating point of the power amplifiers (PA) had to be reduced in order to hold operating costs on budget (for all-too-frequent tube replacements). This led to the decision to operate LANSCE at half of its design original duty factor, until a solution was ready. This report discusses the solution from the LANSCE Risk Mitigation project - to double the linac duty factor by replacing the original 201.25 MHz amplifiers with modern power amplifier circuits and to modernize the low level RF controls for these amplifiers.

RF SYSTEM IMPROVEMENTS

Power Amplifiers

A previous report explained the reasoning behind the choice of the TH628L Diacrode® from Thales Electron Tubes as the active device for this application [1]. Combining the outputs of two FPAs (Fig. 1) provides suitable headroom in peak and average power, allowing the tubes to operate well within their rating. Increased amplifier reliability and tube lifetime results from this pairing.

A matching cavity amplifier circuit was developed with technical assistance from the Thales tube product engineering team. The common-grid circuit configuration uses a full wavelength double-ended coaxial line output circuit. This enables the Diacrode® to double the RF power available over a traditional single-ended tetrode [2]. The mechanical and electrical design and testing of the FPA, IPA and supporting electronics were discussed elsewhere [3][4]. Continuous RF testing in 2012-13 demonstrated 2.5 MW peak power at 12% duty factor and up to 3 MW at lower average power to validate the design and test the cathode emission capabilities of the tube. Each FPA operates at less than 1.85 MW in the DTL RF Stations.

Figure 1: Dual final power amplifiers.

Continental Electronics Corporation manufactured seven PAs per our design in 2013-2015 [5]. Four IPAs were produced by Betatron Electronics, Inc. These units use a Thales TH781 tetrode and matching TH18781 cavity amplifier. One IPA drives two FPAs at each RF station. All amplifiers conveniently reuse the same cooling water plant, the HV power supplies, capacitor banks, crowbar

* Work supported by the United States Department of Energy, National Nuclear Security Agency, under contract DE-AC52-06NA25396
# jtml@lanl.gov

COMMISSIONING OF XBOX3: A VERY HIGH CAPACITY X-BAND RF TEST STAND

N. Catalan Lasheras, C. Eymin, G. McMonagle, S. Rey, I. Syratchev, B. Woolley, W. Wuensch, CERN, Geneva, Switzerland
J. Giner Navarro, D. Esperante Pereira, T. Argyropoulos, Instituto de Física Corpuscular (IFIC), Valencia, Spain
M. Volpi, Melbourne University, Australia
J. Tagg, National Instruments, Switzerland

Abstract

The Compact Linear Collider (CLIC) beam-based acceleration baseline uses high-gradient travelling wave accelerating structures at a frequency of 12 GHz. In order to prove the performance of these structures at high peak power and short pulse width RF, two klystron-based test facilities have been put in operation in the last years. The third X-band testing facility at CERN (Xbox3) has recently been commissioned and has tripled the number of testing slots available. Xbox3 uses a novel way of combining relatively low peak power (6 MW) but high average power klystron units whose power is steered to feed four testing slots with RF to the required power with a repetition rate of up to 400 Hz. Besides the repetition rate, peak power, pulse length and pulse shape can be customized to fit the test requirements. This novel way of combining pulsed RF high power can eventually be used for many other applications where multiple test slots are required.

INTRODUCTION

The performance target for the normal conducting accelerating structures of a 3 TeV final energy version of CLIC is a maximum breakdown rate of 3×10^{-7}/(pulse·m) at the nominal average gradient of 100 MV/m in order to limit luminosity loss to less than 1% [1, 2]. An extensive program aiming at testing 40 structures by 2019 is being carried out to understand and control the RF breakdown rate in prototype CLIC accelerating structures. The original klystron-based test facilities in Japan and the US are being complemented by the construction of three new test facilities at CERN called Xbox1, Xbox2, and Xbox3 [3, 4]. Rather than using high peak voltages and currents in the klystrons as the previous two facilities, Xbox3 uses a combination of low peak power klystrons. The average power is recovered by increasing the pulse width and repetition rate. The required peak power is achieved by combining the output power of multiple klystrons and through pulse compression [5]. This process allows the production of 60 MW, 200-300 ns pulses at much higher repetition rates than would be possible with the single XL5 klystron used in previous Xboxes. In this paper, we will describe the combination scheme used in Xbox3. The two following sections will deal with the testing and commissioning of LLRF and control system. The last section will be dedicated to describe our experience during the global commissioning of the facility.

COMBINATION SCHEME

To recreate the power produced by the drive beam and Power Extraction Transfer Structure (PETS) into the CLIC accelerating structures, we require a rectangular pulse longer than 180 ns with a peak power of 60 MW. We use as in the previous test facilities pulse compression which can multiply the peak power by a factor four, when compressing a 3.5 µs pulse down to 300 ns [6]. The original Xbox3 layout combined four 6 MW power klystrons through a chain of hybrids to reach the required power for a test bench [7]. The phase into the klystrons is changed every pulse to direct the power to any of the four branches after the chain of hybrids. The high repetition rate (400 Hz) is used to feed the test benches sequentially with a final repetition rate of 100 Hz. However, given the good performance of the klystron/modulator system and the pulse compression obtained in Xbox2, we decided to separate the four-in-four system into two independent test facilities combining two-in-two. By construction, if any of the power sources fails, the operation of the full test facility is compromised. By building the Xbox3 as two separate facilities, we can double the general availability of the benches. The geometry and location of the elements in the waveguide network has been kept so that going back to a four-in-four operation is possible in the future by installing the two additional hybrids. The devices under test (DUT) are then placed after the pulse compressors with a stainless steel RF load at the output to terminate the waveguide network. Directional couplers, pumping ports and vacuum gates complete the network. A layout of the final Xbox3 configuration is shown in Fig. 1.

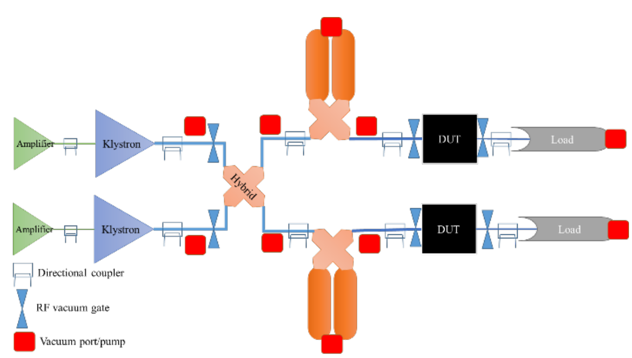

Figure 1: Schematic of the high power RF network of half the Xbox3 in two-in-two mode.

STATUS AND LESSON LEARNED FROM MANUFACTURING OF FPC COUPLERS FOR THE XFEL PROGRAM

S. Sierra†, C. Lievin, C. Ribaud, Thales Velizy, France
G.Garcin, G.Vignette, THALES,Thonon les Bains, France
M.Knaak, M.Pekeler, L.Zweibaeumer, RI Research Instruments, Bergisch Gladbach, Germany
A.Gallas,W.Kaabi, LAL, Orsay,France

Abstract

For the XFEL accelerator, Thales, RI research Instrument GmbH and LAL are working on the manufacturing, assembly and conditioning of Fundamental power couplers (FPC), 670 couplers have been manufactured. The main characteristics of these couplers are remained at 1.3 GHz.

The paper describes the full production activity from the starting of the program, lessons learned from a mass production and different steps necessaries for obtaining a rate up to 10 couplers a week.

We propose also some other way to be optimized for a future possible mass production of such components. With comparison of processes and adaptation which could benefit to an increase rate, if needed, including some of them which could be studies from the coupler definition to the manufacturing process in order to obtain a stable and possible increased rate or lower cost of production by decreasing the risks on programs.

INTRODUCTION

Fundamental coupler main parameters are [1]:

- RF frequency: 1.3 GHz
- Peak Power: 150 kW
- Pulse length: 1.3 ms
- Repetition rate 10 Hz
- Tuning : ± 10 mm
- Coupling (Qext) $2x10^{6} \rightarrow 2x10^{7}$
- Two ceramics windows

The main metallic sub-assemblies of a coupler are the Warm External Conductor (WEC), Warm Internal Conductor (WIC), The Cold External conductor (CEC) and the antenna, see Fig. 1.

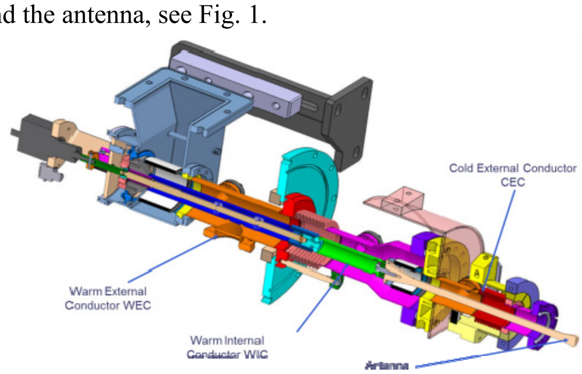

Figure 1: Coupler general layout.

COUPLER MANUFACTURING

Main steps in the coupler fabrication, already described [2], consist in parts assemblies, copper coating of RF surfaces, TiN coating of ceramics windows then all parts are EB welded and clean in an ISO 4 room before being sent to LAL for RF conditioning at 1 MW peak before assembly on cryomodule at IRFU.

Thales Production

The XFEL couplers sub-assemblies are based on a brazing technology. This technology allows having a better reproducibility than a welded one, which is more operator dependant and also could be performed by batches, which is useful for a mass production.

Once the sub-assemblies are brazed and prepared, the three main one (WEC, WIC and CEC) are copper coated, as illustrated in Fig. 2.

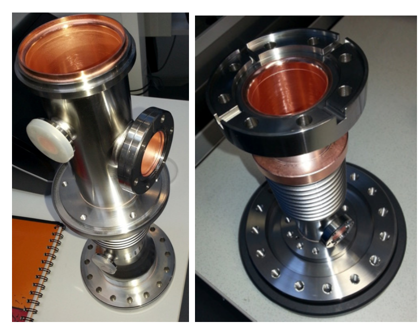

Figure 2: Warm and Cold External conductor.

Thickness and tolerances on WEC and CEC are of 10 µm ±20 % on tubular parts and ± 30% on bellows, For WIC thickness is of 30 µm ±20 % on tubular parts and ±30% on bellows. RRR value initial specification was from 30 to 80.

For copper coating acceptance on visual criteria a special document have been establish on order to have common and objective criteria [3].

This document defines the tooling for control and objective criteria on what is acceptable and what is not acceptable. These criteria are illustrated by pictures giving examples of parts of pieces with real cases observed during inspection of subassemblies.

This is a major document for common understanding on acceptance of pieces during the program. This document is of particular interest for the gap existing between perfect pieces and enough good ones to be used.

DESIGN OF 4-VANE RFQ WITH MAGNETIC COUPLING WINDOWS FOR NUCLOTRON INJECTOR LU-20

V. Koshelev, G. Kropachev, T. Kulevoy[1†], D. Liakin, A. Plastun,
Institute for Theoretical and Experimental Physics of NRC Kurchatov Institute, Moscow, Russia,
S. Vinogradov, Moscow Institute of Physics and Technology, Dolgoprudniy,
Moscow Region, Russia
S. Polozov, - National Research Nuclear University - Moscow Engineering Physics Institute,
Moscow, Russia
A. Butenko, Joint Institute for Nuclear Research, Dubna, Moscow Region, Russia
[1]also at National Research Nuclear University - Moscow Engineering Physics Institute,
Moscow, Russia

Abstract

Alvarez-type linac LU-20 is used as Nuclotron injector. In the framework of NICA project the high voltage electrostatic pre-injector for LU-20 has been replaced by RFQ linac. The RFQ was designed by the team of ITEP and MEPhI (Moscow, Russia) and was manufactured in VNIITF (Sneginsk, Russia). The engineering design of the 4-vane RFQ linac with magnetic coupling windows and details of its manufacturing are presented and discussed.

INTRODUCTION

The new accelerator complex Nuclotron-based Ion Collider fAcility (NICA) is under development and construction at Joint Institute for Nuclear Research [1]. New complex is assumed to operate with two injectors: Alvarez-type DTL LU-20 as injector for light ions (mainly polarized deuterons) and new linac HILAc for heavy ions. To provide polarized deuterons acceleration, the modernization of LU-20 was carried out. The old 700 kV electrostatic for-injector was replaced by an RFQ with coupling windows (see Fig.1) [2]. The RFQ has been developed by a team of specialists from Institute for Theoretical and Experimental Physics (ITEP) and Moscow Engineering-Physics Institute (MEPhI). The RFQ was designed to accelerate ion beams with charge -to-mass ratio ≥ 0.3. It has to accelerate polarized deuteron beam with current up to 15 mA. The RFQ injects beam into Alvarez-type DTL LU-20 for following acceleration. The RFQ resonant frequency is 145.2 MHz, the same as LU-20 one. The RFQ has to provide the operation mode with RF pulse length of 150 μs and pulse repetition rate not higher than 1 pps. The RFQ was fabricated, assembled and aligned at Zababakhin All-Russian Scientific Research Institute of Techinical Physics (VNIITF). The design of the RFQ as well as the fabrication procedures are presented and discussed.

[†]email: kulevoy@itep.ru

RFQ DESIGN

The RFQ cavity has a length of 2230 mm and consists of three nearly identical segments of 695 mm length and input/output flanges. A complete design of the central segment as well as the cutaway view showing the relative location of electrodes is given in Fig. 1.

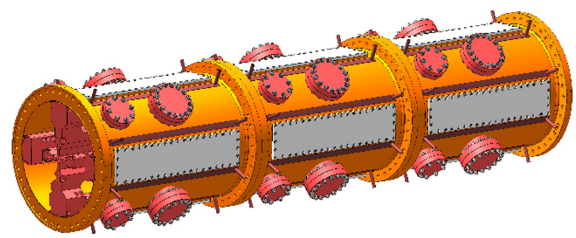

a)

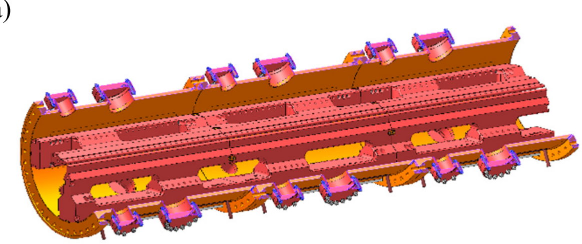

b)

Figure 1: Design of RFQ tanks.

Electrodes

Each electrode line is divided into three sections, therefore twelve electrode units were fabricated for the RFQ. Eight of them have the identical design (except modulation at the tip). Two pairs of electrodes differ from each other in geometry of open half-windows at front and rear end of the resonator. The adjacent electrodes are installed in the tank as it is shown in Fig. 1b. One can see that their half windows are located at the opposite ends of the tank.

ISBN 978-3-95450-169-4

DEVELOPMENT AND MEASUREMENTS OF A 325 MHz LADDER-RFQ*

M. Schütt, M. Obermayer, U. Ratzinger
Institut für Angewandte Physik, Johann Wolfgang Goethe Universität, Frankfurt, Germany
A. Schnase, GSI, Darmstadt, Germany

Abstract

In order to have an attractive alternative to 4-Vane RFQs above 200 MHz, we study the possibilities of a Ladder-RFQ. The 325 MHz RFQ is designed to accelerate protons from 95 keV to 3.0 MeV according to the design parameters of the p-Linac for the research program with cooled antiprotons at GSI-FAIR, Darmstadt, Germany. Therefore a dedicated 70 MeV, 70 mA proton injector is required. In the low energy section, between the ion source and the main linac an RFQ will be used operating at 325.224 MHz. This particular high frequency for an RFQ creates difficulties, which are challenging in developing a cavity. In order to define a satisfying geometrical configuration for this resonator, both from the RF and the mechanical point of view, different designs have been examined and compared. Very promising results have been reached with a ladder type RFQ, which has been investigated since 2013 [1, 2]. Due to its geometric size the manufacturing as well as maintenance is not that complex compared with brazed cavities. The manufacturing, copper-plating and assembly of a 0.8 m prototype RFQ has been finished. We present recent measurements of the rf-field, frequency-tuning, field flatness as well as results from power measurements.

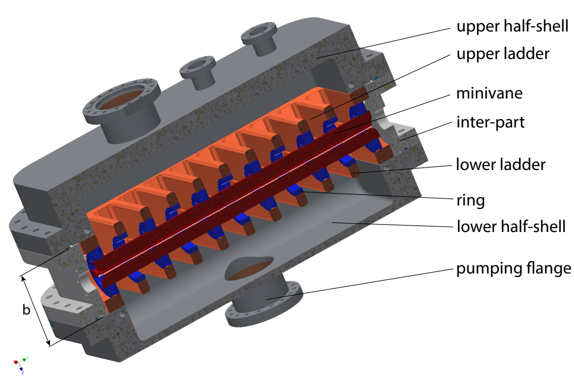

Figure 1: Isometric view of the Ladder-RFQ. The copper carrier-rings (coloured in blue) guarantee the electrode positioning as well as the RF contact. The ladder structure consists of bulk copper components. Any brazing or welding processes were avoided on the copper structure.

INTRODUCTION

The idea of the Ladder-RFQ firstly came up in the late eighties [3, 4] and was realized successfully for the CERN Linac3 operating at 101 MHz [5] and for the CERN antiproton decelerator ASACUSA at 202 MHz [6]. Within the 4-Rod design the challange is to minimize dipole components and to have geometrical dimensions which are suitable for a mechanical manufacturing and assembling.

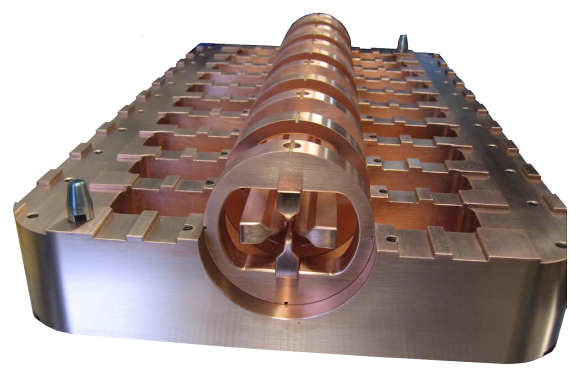

Figure 2: Front view of the Ring-System. The steel-tank and the upper half-shell are removed.

At frequencies above 250 MHz the 4-Vane-type RFQ is used so far. Many versions for low and high duty factors have been realized successfully until now. Draw backs are the high costs per meter, the complexity as well as the challenging RF tuning procedure of that structure: The dipole modes tend to overlap with the quadrupole mode. Safe beam operation conditions result in ambitious mechanical vane tolerances. In the proposed ladder-RFQ version, the ladder spokes show an extended width b which increases the resonance frequency and results in an homogeneous current flow towards the mini-vanes. The mini-vanes are embedded via precisely machined carrier rings into the copper shells (s. Fig. 2). It is even possible to exchange the ring-mini-vane-structure completely by an improved electrode system as demonstrated successfully at the GSI High Current RFQ [7, 8]. To proof the mentioned advantages and the realizability of the Ladder RFQ a prototype was designed and built. The results of the measurements are shown in this paper.

MECHANICAL LAYOUT

The mechanical design consists of an inner copper ladder structure mounted into an outer stainless steel tank. The tank is divided into a lower half-shell carrying the inner resonating structure, an inter-part and the upper half-shell (s. Fig. 1). The lower half-shell will carry and adjust the position of the resonating ladder structure. All parts are metal-sealed. The rf features are mainly determined by the resonating structure, while the dimensions of the tank have no significant influence on the frequency. Further details of the mechanical layout can be seen in [9]. Based on the

* Work funded by BMBF 05P12RFRB9, 05P15RFRBA

RFQ VANE SHAPES FOR EFFICIENT ACCELERATION

Y. Iwashita, Y. Fuwa, ICR, Kyoto Univ. Uji, Kyoto
R. A. Jameson, IAP, Frankfurt am Main

Abstract

RFQ vane shapes for efficient acceleration are under investigation by introducing more terms in addition to the two-term potential. They can incorporate the feature of the trapezoidal shape modulation with less multipole components, while higher acceleration efficiency is expected. A series of electrostatic calculations was carried out for a new 7-term potential ones. They are compared with the two-term scheme and the trapezoidal scheme. The new one exhibits a higher accelerating efficiency with less multipole components.

INTRODUCTION

Design of RFQ has been based on the so-called two-term potential scheme [1]. The two-term potential has the minimum terms of acceleration and focusing in the lowest order:

$$U_2(r,\theta,z)=\frac{V}{2}\{X\left(\frac{r}{a}\right)^2\cos 2\theta+AI_0(kr)\cos(kz)\}$$

where

$$A=\frac{m^2-1}{m^2I_0(ka)+I_0(mka)},\ k=\pi/Lc$$

and a is the minimum radius at z=0 (see Fig. 1)[2]. The vane surface profile can be defined by the equipotential surface of U_2 at the vane voltage $V/2$. These parameters are independently defined at each cell, which may make discontinuities between cells if no care is taken for it.

The acceleration term A and the focusing term X are the functions of only m and Lc/a. A contour plots of A as function of m and Lc/a is shown in Fig.2. Since the acceleration term A does not increase monotonicaly with m in the short cell length region when the minimum aperture a is kept constant, m is usually limited up to 2 or 3 for practical cases. This can be comprehended by observing the vane surface profiles in such regions, where the ridgeline of the equipotential surface breaks [3]. The practical m values is a function of Lc/a, which can be roughly expressed by m < 1.3+0.6(Lc/a-0.75) and is expressed by a red line in Fig. 2.

While the set of Lc/a and m is simple to define the potential, the set of Lc/r_0 and m is often used. In this case, the potential is rewritten as follows:

$$U_2(r,\theta,z)=\frac{V}{2}\{\left(\frac{r}{r_0}\right)^2\cos 2\theta+AI_0(kr)\cos(kz)\}$$

where

$$r_0=a/\sqrt{1-AI_0(ka)},\ A=\frac{m^2-1}{m^2I_0(ka)+I_0(mka)},\ k=\pi/Lc$$

Figure. 3 shows the same contour plot but as a function of Lc/r_0 and m. The large m at short Lc region not for use is expresed by the red curve in Fig. 3.

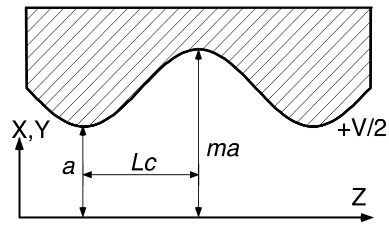

Figure 1: Definitions of vane parameters.

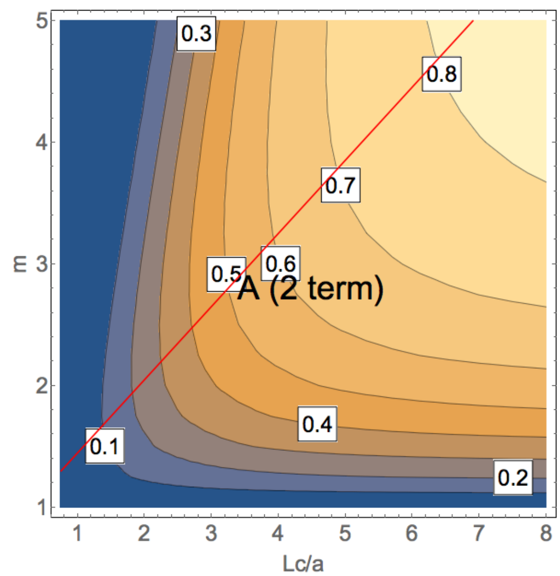

Figure 2: Contour plot of the acceleration term A as a function of Lc/a and m for the two-term potential.

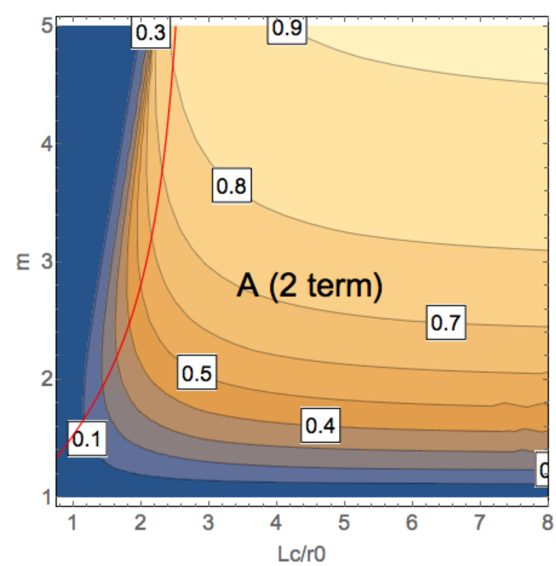

Figure 3: Contour plot of the acceleration term A as a function of Lc/r_0 and m for the two-term potential.

ISBN 978-3-95450-169-4

RESULTS OF OPERATION OF 162.5 MHZ RFQ COUPLERS*

S. Kazakov†, J.P. Edelen, T.N. Khabiboulline, O. Pronitchev, J. Steimel,
Fermi National Accelerator Laboratory, Batavia, USA

Abstract

Two couplers for RFQ of PIP-II Injector Test facility were designed and manufactured. Each coupler is designed to deliver 70 KW, CW to RFQ at 162.5 MHz. First results of couplers' operation are reported.

INTRODUCTION

The PIP-II Injector Test is the prototype front end of the Proton Improvement Project II (PIP-II) linac beign developed at Fermilab. A key element of front end is a 162.5 MHz, continuous wave (CW), normal conducting, radiofrequency quadrupole (RFQ). This is RFQ designed to accelerate up to 10 mA H- ions beam from 30 keV to 2.1 MeV.[1] A photo of the RFQ in the beam line is presented in Fig. 1. The total RF power required for operation is less than 130 kW, CW or pulsed. RF power is delivered through two couplers placed at opposite sides of RFQ cavity. We describe first experience of coupler operation in this paper.

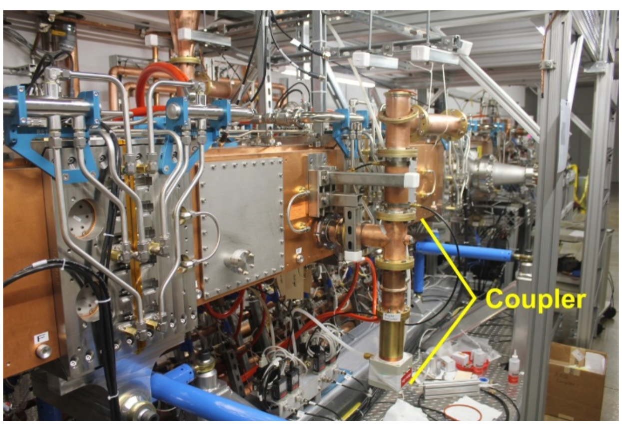

Figure 1: RFQ in test area.

COUPLER DESIGN

Coupler cut view is presented on the Fig. 2 and requirements are listed in Table 1.[2] Each coupler has one ceramic RF window made of alumina, with an outer diameter of 79 mm and inner diameter of 28.6 mm. The thickness of the ceramic is 6 mm. The end of the antenna loop is not grounded and allows a high voltage DC bias to suppress a multipactor. The coupler is designed to operate at 70 kW power level in continues wave (CW) mode and is cooled with forced air. Coupling can be adjusted by rotating the loop relative to the RFQ field.

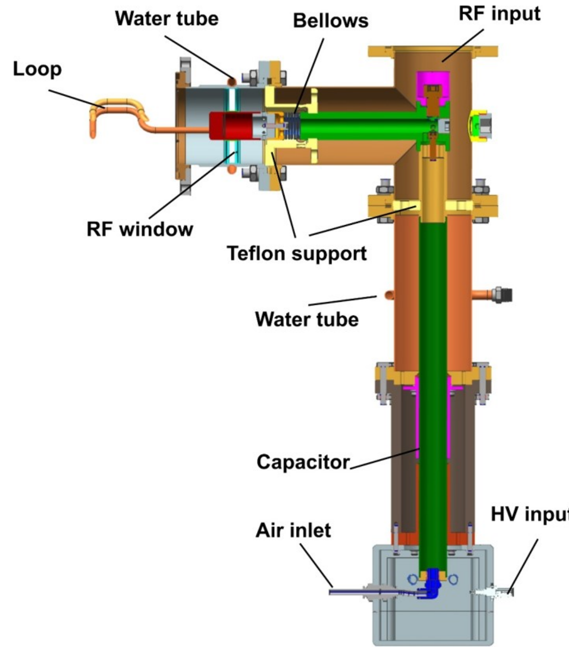

Figure 2: Cut view of RFQ coupler.

Table 1

Parameter	Value
Frequency	162.5 MHz
Operating power	70 kW
Coupling type	Loop
Input diameter	3-1/8 inch
Output port diameter	3-1/8 inch
Input impedance	50 Ohm

HISTORY OF OPERATION

Two couplers were installed in the RFQ cavity. Low power measurements confirmed computer simulations. The orientation angles of loops were close to 45^{O} with zero being orthogonal to beam direction as it was designed.

The first CW run occurred in May 2016. Conditioning began on the 4^{th} of May followed shortly by an amplifier failure that occurred on May 6^{th}. After the repair we continued CW operation for a week. Conditioning started at 17 kV (voltage between vanes) and continued up to 63 kV. We were able to achieve up to 65kV however more conditioning time would be needed in order to operate stably. CW operation was stopped in order to continue pulsed beam operations.

The next attempt to return to CW mode operation was made on August 24-25, 2016. During the conditioning, the behavior of "vacuum" was not as stable as the first run. Pressure bursts were observed periodically during power

* Operated by Fermi Research Alliance, LLC under Contract No. DE-AC02-07CH11359 with the United States Department of Energy.
†skazakov@fnal.gov

ADVANCED DESIGN OPTIMIZATIONS OF A PROTOTYPE FOR A NEWLY REVISED 4-ROD CW RFQ FOR THE HLI AT GSI*

D. Koser†, H. Podlech, IAP University of Frankfurt, 60438 Frankfurt am Main, Germany
P. Gerhard, L. Groening, GSI Helmholtz Centre, 64291 Darmstadt, Germany
O. Kester, TRIUMF, Vancouver, BC, Canada

Abstract

Within the scope of the FAIR project (Facility for Antiproton and Ion Research) at GSI Helmholtz Centre for Heavy Ion Research in Darmstadt, Germany, the front end of the existing High Charge State Injector (HLI) is upgraded for cw operation. The dedicated new 4-Rod RFQ structure is currently being designed at the Institute for Applied Physics (IAP) of the Goethe University of Frankfurt. The overall design is based on the RFQ structures that were originally developed for FRANZ and MYRRHA. Regarding the HLI-RFQ the comparatively low operating frequency of 108 MHz causes a general susceptibility towards mechanical vibrations especially concerning the electrodes because of the necessarily larger distance between the stems. Besides RF simulations and basic thermal simulations with CST Studio Suite, the key issues like mechanical electrode oscillations as well as temperature distribution from heat loss in cw operation are investigated with simulations using ANSYS Workbench. At first instance a dedicated 6-stem prototype is currently being manufactured in order to validate the simulated RF performance, thermal behavior and structural mechanical characteristics.

INTRODUCTION

In general 4-Rod Radio Frequency Quadrupole (RFQ) structures for lower operating frequencies are prone to mechanical oscillations because the usually larger distance between the stems facilitates the bending of the inter-stem electrode segments as well as of the levitating electrode extensions. In case of the currently existing HLI-RFQ, which was originally designed within the scope of an intended HLI cw upgrade, the mechanical vibrations cause strong modulated RF power reflections that severely limit the achievable pulse length and amplitude [1]. Measurements of the velocity profile of the electrode vibrations using a laser vibrometer revealed two main types of vibrational modes at approximately 350 Hz and 500 Hz, respectively [2]. Both mode types could later be confirmed and further investigated by structural mechanical eigenmode and resonance response simulations using ANSYS [3]. Thereby the higher modes at 500 Hz could be identified as radial (relating to the beam axis) oscillations of the electrodes that are easily excitable by the radial electric forces associated with the RF pulse. The lower modes at 350 Hz correspond to tangential (relating to the radial axis) oscillations of the electrodes that are excited by asymmetrically acting forces, e.g. originating from the design inherent uneven voltage distribution between the electrodes caused by the intrinsic asymmetries of a 4-Rod RFQ, leading to an electric dipole field component.

In addition to the difficulties with mechanical vibrations the existing structure is also highly sensitive to changes in thermal load which have a significant and nearly immediate effect on the resonance frequency, thus substantially impairing operational stability.

Overall the existing HLI-RFQ which was commissioned at GSI in 2010 [4] fails to fulfill the requirements for the upcoming cw linac. A completely newly revised 4-Rod RFQ is currently being designed with particular attention on structural mechanical stability regarding the susceptibility towards vibrations, especially the severely RF affecting radial electrode eigenmodes, as well as thermal deformations.

RF- AND STRUCTURAL MECHANICAL DESIGN OPTIMIZATIONS

Starting from the basic FRANZ/MYRRHA-RFQ design the crucial geometric parameters were analyzed regarding their influence on the mechanical electrode mode frequencies as well as on the shunt impedance with the aim to yield maximum mechanical rigidity while still obtaining a tolerable overall power loss and moderate local heat loads.

Dipole Compensation

In principle the RF cells of 4-Rod RFQs are capacitively shortened $\lambda/4$-resonators. The voltage distribution on the stems is an almost linear function of the stem height, leading to a higher voltage on the upper electrodes than on the lower ones [5].

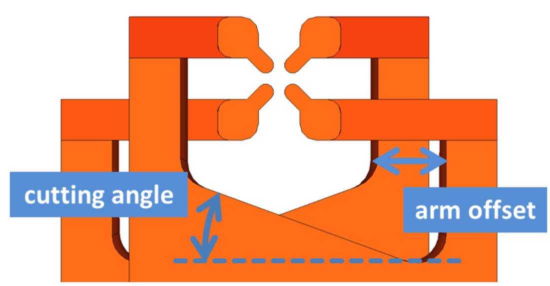

Figure 1: Dipole compensation methods.

One way to compensate the resulting dipole effect is to increase charge transport to the undersupplied electrodes by providing more space for the magnetic field around the stem arms eventually introducing a steeper stem cutting. Another method is to increase the length of the current path to the lower electrodes e.g. by introducing a stem arm offset

* work supported by GSI, BMBF Contr. No. 05P15RFRBA
† koser@iap.uni-frankfurt.de

ISBN 978-3-95450-169-4

PROGRESS OF A 162.5 MHz HIGH-CURRENT RFQ WITH COUPLING WINDOWS *

Qi Fu, Kun Zhu†, Yuanrong Lu†, Zhi Wang, Shuli Gao, Fangjian Jia, Pingping Gan, Haipeng Li,
State Key Laboratory of Nuclear Physics and Technology, Peking University, Beijing, China

Abstract

A 162.5 MHz, four-vane RFQ with magnetic coupling windows has been designed by the RFQ group of Peking University. Clear frequency separation of the resonant modes and smaller transverse dimension are the advantages of the window-type RFQ. The electromagnetic simulations have shown that the average power loss of this 1.809 m long RFQ is about 50 kW in continuous wave mode. Consequently, a water cooling system was designed via the multi-physics analysis. The mechanical design and assembling technology were also presented in this paper.

INTRODUCTION

The copper prototype of a four-vane RFQ with coupling windows, which combines the characteristics of traditional four-vane RFQ and that of four-rod [1], is ready to be manufactured. It will accelerate deuteron from 50 keV to 1 MeV, and operate at 162.5 MHz of mode TE_{210} with Δf of 3.144 MHz from mode TE_{110} [2]. At present, the aircraft aluminium model has been finished and tested. It confirmed the results calculated by either CST MWS or HFSS [3].

The multi-physics analysis is a complete loop of coupled numerical simulations, as shown in Fig. 1 [4]. Surface current induced by magnetic field is simulated in CST MWS, and it is used to calculate the thermal losses, which can be imported to MPS for thermal analysis. Then, the structure stresses and deformation field can be obtained by coupling the optimized temperature field to the Mechanical Solver. Finally, sensitive analysis in CST MWS realizes the estimate for frequency shift caused by structure deformation.

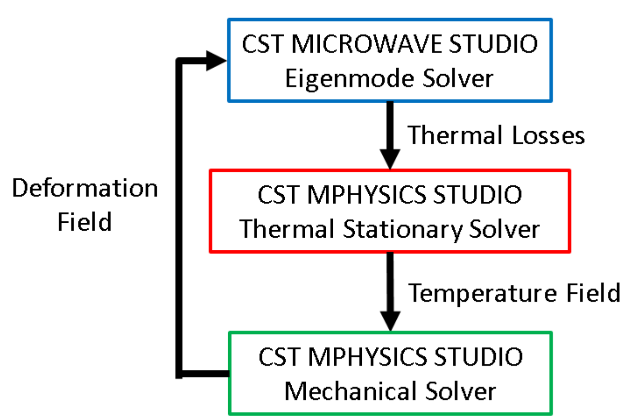

Figure 1: The multi-physics analysis scheme based on CST.

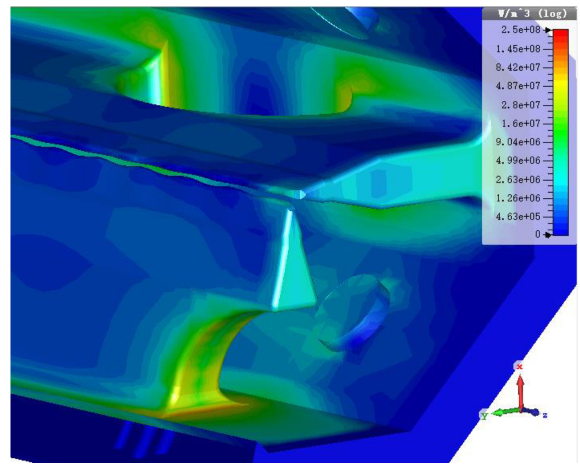

Figure 2: Power loss distribution.

RF ANALYSIS

The electromagnetic performance of this RFQ, calculated by CST MWS, has been shown in earlier paper. For improving the field flatness affected by the vane modulation, the tuners and some optimizations of the coupling windows were considered in recent RF study. The new parameters of this RFQ are summarized in Table 1. The resonant frequency of the RFQ was tuned to 162.522 MHz and Q value nearly 9000 with electric conductivity of 5.0×10^7 S/m. The total power losses of the cavity were 46.5kW, while the inter-vane voltage was normalized to 60 kV.

Table 1: The Main Parameters of the RFQ

Parameters	Value
Frequency [MHz]	162.522
Nearest mode (TE_{110}) [MHz]	165.666
Mode separation [MHz]	3.144
Quality factor	8999.0
Power loss [kW]	46.523
Special shunt impedance [kΩ·m]	69.991
Inner cavity diameter [mm]	340.00
Length of the RFQ vanes [m]	1.809

Loss distribution indicated that the maximum loss appears in the corners of the windows on both cavity ends, as shown in Fig. 2. Thus, a water cooling system was needed to control the temperature in the cavity, especially around the coupling windows.

* Work supported by NSFC, Grand No. 2014CB845503
† Corresponding author: zhukun@pku.edu.cn; yrlu@pku.edu.cn

ISBN 978-3-95450-169-4

ASYMMETRIC FOUR-VANE RFQ*

A. Kolomiets, D. Liakin,
Institute for Theoretical and Experimental Physics NRC "Kurchatov Institute", Moscow, Russia
A. Plastun†, Argonne National Laboratory, Lemont, USA

Abstract

A four-vane resonator is widely used in Radio Frequency Quadrupole (RFQ) accelerators. The field distribution in a long four-vane resonator can be easily perturbed by nearest dipole modes which are excited due to the local geometry errors. This paper describes the electromagnetic properties of a four-vane resonator with an introduced asymmetry between neighboring chambers. The asymmetry provides necessary separation of dipole modes keeping losses and field uniformity of the quadrupole mode similar to those in a conventional four-vane resonator. This feature of an asymmetric resonator is confirmed by analytical results from transmission line model as well as by CST Studio simulations.

4-VANE RESONATOR

A 4-vane resonator was the first radio frequency (RF) structure proposed for an RFQ. This structure is presented in the description of the RFQ invention and in the first publication [1]. The 4-vane resonator is a suitable choice for RFQs used for acceleration of high-intensity beams and for continuous wave accelerators due to the highest RF power efficiency and the most precise distribution of the quadrupole focusing electric field.

Most of RFQ resonators are long regular structures of several operating wavelengths. The properties of the resonators are defined by the properties of a multi-mode transmission line with proper boundary conditions. Both a lumped-circuit model [2] and a 3D computer simulation of a 4-vane resonator show the presence of three propagation modes. These propagation modes (an operating quadrupole mode TE_{21} and two dipole modes TE_{11}) have close critical frequencies, and the main drawback of the conventional 4-vane resonator is that the frequencies of the operating quadrupole mode and dipole modes are close to each other. Usually, the frequency of TE_{110} modes are getting even close to TE_{210} due to the field equalizing undercuts at the ends of the electrodes.

This rapprochement makes the field distribution very sensitive to machining and alignment errors and causes the redistribution of RF power between the operating quadrupole TE_{210} and parasitic TE_{11n} modes. It leads to disturbance of voltage distribution in each chamber of the resonator and unbalance of electrode potentials over its cross-sections.

The separation of long 4-vane structures into short resonantly coupled sections decreases the disturbance effect caused by higher quadrupole TE_{21n} modes [3], but not by the nearest dipole TE_{11n} field. Also the resonant coupling of several 4-vane sections makes the mechanical design of an RFQ linac more complicated.

The ref. [4] explains the need for dipole-free frequency region around the operating frequency in order to provide stable operation of the resonator. This gap is defined as the difference between the operating frequency and the frequency of the closest dipole mode. The gap should be as wide as several percent of the operating frequency. In order to shift out dipole modes' frequencies suppressor loops [4] and stabilizing rods at the ends of the 4-vane resonator [5] are used. These methods allow changing of the boundary conditions at the end of the resonator differently for the dipole and quadrupole modes. It has also been argued that the installation of rods decreases the dipole perturbations considerably.

ASYMMETRIC 4-VANE RESONATOR

Let us consider a conventional cloverleaf 4-vane resonator with cylindrical chambers of radius R_{ch} and quadrupole tips, which is studied in ref. [2]. The spectrum of the resonator (frequencies of quadrupole and dipole modes) can be managed if one makes the equivalent inductances of the adjacent chambers not equal. This could be realized by using different radii for adjacent chambers, while keeping the radii of opposite chambers the same (see Fig. 1). Introduce a coefficient of asymmetry $k_{asym} > 0$, so the radii of the pair of large resonator chambers are $R_{ch1} = R_{ch} \cdot (1+k_{asym})$. The size of the another pair of chambers should be modified in such a way to keep the quadrupole mode frequency unaffected. Assuming that chamber specific inductance is linearly proportional to the cross-section area of a chamber, we get the radii of the small chambers:

$$R_{ch2} = R_{ch}(1+k_{asym}) / \sqrt{1+4k_{asym}+2(k_{asym})^2}\ . \qquad (1)$$

Figure 1 presents cross-sections of the resonators with $k_{asym} = 0$ and $k_{asym} = 0.30$. Computer simulation of the test resonator in the range $0.0 < k_{asym} < 0.30$ has been performed with CST Studio Suite [6]. The frequencies of the dipole modes (black and blue curves) and the quadrupole mode (green line) are shown in Fig. 2. The quadrupole mode is kept at the frequency of 350 MHz in the whole range of k_{asym}. The calculation was done for the test resonator with the following parameters: average radius $R_0 = 4$ mm, width of quadrupole tips $2R_e = 6.4$ mm, length of the vanes $L_{\mathrm{vane}} = 3000$ mm. All results presented in the paper correspond to this test resonator.

It should be mentioned, that the asymmetry coefficient is not limited by 0.30 as shown in Fig. 2. For the asymptotic value $k_{\mathrm{asym}} \to \infty$, we get $R_{\mathrm{ch2}} / R_{\mathrm{ch}} \to \sqrt{1/2}$ and the 4-vane resonator is transformed into the well-known 2H-resonator [7].

* This work was supported by the U.S. Department of Energy, Office of Nuclear Physics, under Contract No. DE-AC02-06CH11357
† on leave from Institute for Theoretical and Experimental Physics

RF DESIGN OF THE NUCLOTRON-NICA 145.2 MHz RFQ

A. Plastun†, V. Andreev, V. Koshelev, T. Kulevoy[1], V. Kuzmichev, D. Liakin, A. Sitnikov, Institute for Theoretical and Experimental Physics of NRC Kurchatov Institute, Moscow, Russia,
A. Butenko, Joint Institute for Nuclear Research, Dubna, Moscow Region, Russia
[1]also at National Research Nuclear University - Moscow Engineering Physics Institute, Moscow, Russia

Abstract

ITEP has designed the Radio-Frequency Quadrupole (RFQ) linac for the JINR NICA Complex (Dubna, Russia) to provide ion beams ($q/A \geq 0.3$) with energy of 156 keV/u for further acceleration by existing Alvarez-type linac. The RFQ is based on a 4-vane structure with magnetic coupling windows in order to avoid a risk of excitation of dipole field components inherent in a conventional 4-vane resonator. The paper presents results of the radio-frequency (RF) design and capabilities used for coarse and fine tuning of the field distribution and resonant frequency during manufacturing and finalizing of the RFQ.

INTRODUCTION

In a framework of the Nuclotron-based Ion Collider fAcility (NICA) project [1] at Joint Institute for Nuclear Research (JINR, Dubna, Russia) upgrade of the accelerating complex front-end is being performed [2]. The upgrade includes replacement of the 700-kV accelerating tube for the LU-20 drift-tube linac (DTL) with an RFQ [3] and development of a brand new heavy ion injector based on a 4-rod RFQ and IH-DTL sections [4].

LU-20 is a conventional Alvarez-type DTL used for acceleration of proton and ion ($q/A \geq 0.3$) beams at the frequency of 145.2 MHz. The RFQ designed by ITEP provides 156 keV/u ion beams for following acceleration by the DTL at 2βλ-mode to the energy of 5 MeV/u [3].

The 145.2-MHz RFQ is based on a 4-vane resonator with magnetic coupling windows [5]. The structure provides both reliable dipole-free range and compactness compared to a conventional 4-vane. Higher RF power losses of the structure is not an issue for the RFQ injector since it operates in a pulsed mode at RF pulse width less than 150 µs and repetition rate not higher than 1 Hz.

RESONATOR DESIGN

The 2-meter long RFQ is built from 3 segments (see Figure 1) or 4.5 periods of the RF structure (see Figure 2). Each segment has a length of 690 mm and tank inner diameter of 400 mm. The average aperture radius $R_0 = 6.5$ mm and the vane tip radius $R_e = 5.2$ mm remain constant along the resonator. The cost-effective mechanical design of the RFQ has assumed vanes made of carbon steel and fastened to stainless steel tanks with screws. The whole resonator (except the vane tips) has been copper-plated after the fine machining. Photograph of the resonator segment #1 with installed vanes is shown in Figure 3.

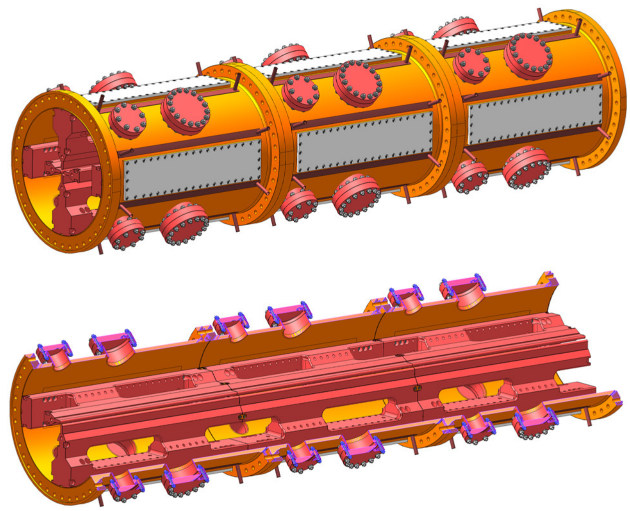

Figure 1: 3D model of the RFQ resonator.

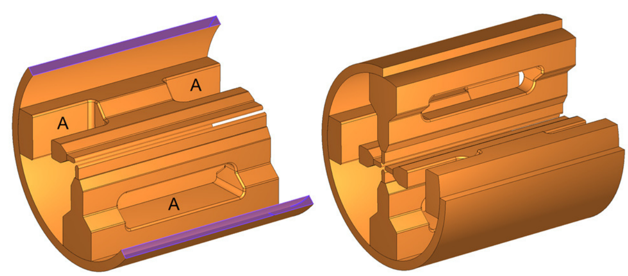

Figure 2: 3D model for the RF period of the 4-vane resonator with coupling windows.

Coupling Windows

Dimensions of the coupling windows have been adjusted in order to provide both reliable frequency range between the operating and nearest dipole modes, and convenient mechanical design. The dipole-free frequency range is required to get proper distribution of the electric field components in the accelerating channel. Dipole field components are suppressed by moving dipole modes of the resonator far away (about 10 MHz higher) from the band of the operational quadrupole mode [6]. This task as well as the whole RF design of the RFQ has been done with CST STUDIO SUITE [7].

Frequency Adjustment

The mechanical design assumed the resonant frequency adjustment during the manufacturing by whittling down the surfaces of coupling windows (surfaces A in Figure 2)

† email: asplastun88@gmail.com

ISBN 978-3-95450-169-4

CRYOMODULE AND POWER COUPLER FOR RIKEN SUPERCONDUCTING QWR

K. Ozeki*, O. Kamigaito, H. Okuno, N. Sakamoto, K. Suda, Y. Watanabe, K. Yamada,
RIKEN Nishina Center, Wako, Japan
E. Kako, H. Nakai, K. Umemori, KEK, Tsukuba, Japan
K. Okihira, K. Sennyu, T. Yanagisawa,
Mitsubishi Heavy Industries Mechatronics Systems, Ltd., Kobe, Japan

Abstract

We report a general description of the cryomodule for the RIKEN superconducting quarter-wavelength resonator, the construction of which is now in progress and is aimed to be completed within this fiscal year.

OVERVIEW

At the RIKEN Nishina Center, the construction of an accelerator system based on the superconducting quarter-wavelength resonator (QWR) is underway with the goal of developing basic technologies for the low-beta superconducting linear accelerator for ions [1]. A cryomodule that can mount two QWRs is now being constructed as a prototype. The fabrication of one QWR has been completed and a performance test has been carried out. The result of the performance test is reported in Ref.2 [2].

The overall structure and the design parameters of the cryomodule are shown in Fig. 1 and Table 1. Detailed design parameters of the QWR are described in Ref. 2. The vacuum vessel has a cylindrical shape. The vacuum of the QWR is separated from that of the whole system. As the first step, one actual QWR and one dummy cavity will be mounted in the cryomodule. The general descriptions of the components of the cryomodule other than the QWR are given in the following section.

Table 1: Design Parameters of the Cryomodule

Resonant freq. of QWR	75.5 MHz
Inner diameter of QWR	300 mm
Cavity height of QWR	1055 mm
Gap length of QWR	60 mm
Beam aperture	40 mmϕ
Operating temperature	4.5 K
Estimated heat flow	5.0 / 15.0 W/resonator (Cavity / Thermal shield)
Assumed Max. RF power	10 kW

COMPONENTS OF CRYOMODULE

Helium Jacket

The QWR is enfolded in the helium jacket. The helium jacket is made of titanium, which has a coefficient of thermal expansion similar to that of niobium, which is the material of the QWR. The space between the QWR and the helium jacket is filled with the liquid helium to cool down the QWR.

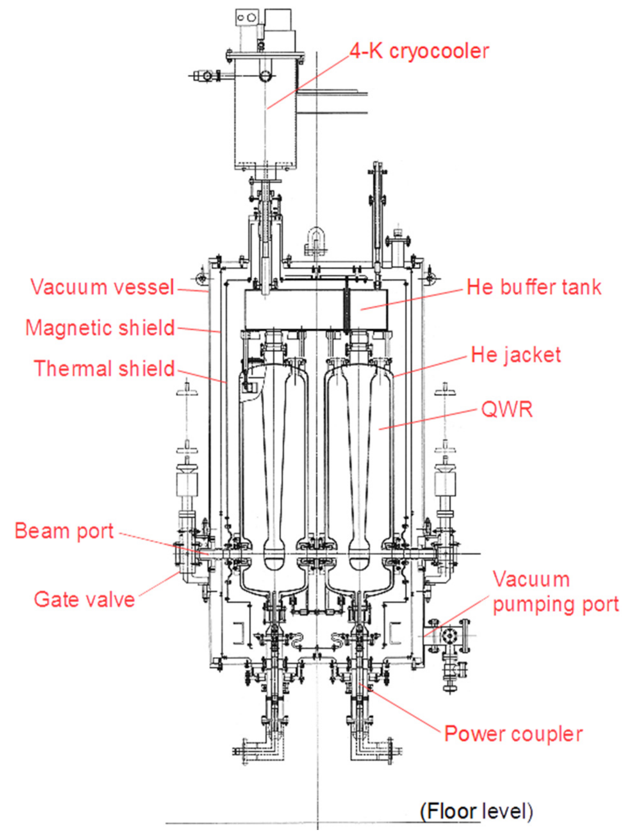

Figure 1: Overall structure of the cryomodule.

4-K Cryocooler

The liquid helium is stored in the helium jacket and the helium buffer tank, and the evaporated helium is recondensed using 4-K GM-JT cryocoolers. The GM-JT cryocooler adopted here is a V316SLCR, manufactured by Sumitomo Heavy Industries, Ltd. (SHI). This GM-JT cryocooler has a cooling power of 4.2 W/5.0 W at 4.3 K (50 Hz/60 Hz). Three GM-JT cryocoolers will be installed to obtain a cooling power of 12 W at 4.5 K (See Table 1).

Thermal Shield

In order to reduce the heat flow into the QWR, the thermal shield is installed in the cryomodule. In the design stage, two types of the thermal shield were compared: the twofold thermal shields (20 and 80 K) cooled down by the double-stage cryocooler and the onefold thermal shield (40 K) cooled down by the single-stage

* email address: k_ozeki@riken.jp

IMPACT MODEL FOR REA AND ITS BENCHMARK WITH DYNAC*

T.Yoshimoto†, and M. Ikegami
FRIB, Michigan State University, East Lansing, Michigan, USA

Abstract

A new online model for the ReAccelerator 3 (ReA3) [1] has been developed for machine tuning using the IMPACT tracking code [2, 3]. A DYNAC [4-6] model was originally applied for REA3 optics analysis. However this model is limited to symmetric cavities, not asymmetric ones such as superconducting Quarter-Wave Resonators (QWRs), which are installed in ReA3. This limitation renders it difficult to effectively tune the ReA3 beamline with DYNAC. To address this situation, a new and more precise model of IMPACT is under development which more closely reflects the actual lattice.

This paper reports benchmarking results of IMPACT and DYNAC model for ReA3 acceleration line from just after RFQ exit to a transport line with a symmetric cavity as a first step before more precise simulations including non-axisymmetric cavities and the RFQ.

INTRODUCTION

Reaccelerator3

ReA3 is a post-target accelerator at the National Superconducting Cyclotron Laboratory (NSCL) and Facility for Rare Isotope Beams (FRIB). It reaccelerates beams of heavy ion isotopes with kinetic energy ranging 3 MeV/u to 6 MeV/u for nuclear experiments. First, an ion bunch is produced up-steam of the transport line and stored in an Electron Beam Ion Trap (EBIT) charge breeder [7], where an electron beam strips electrons. Bunches with higher charge state are extracted from the EBIT and selected by a 90 degree bending magnet in a mass-to-charge separator. A subsequent Multi-Harmonic Buncher (MHB) [8] with a fundamental frequency of 80.5 MHz compresses the beam longitudinally before entering a Radio-Frequency Quadrupole (RFQ) [9, 10]. The RFQ has a frequency of 80.5 MHz and is capable of accelerating 600 keV/u incident ions with *Q/A* ranging from 0.2 to 0.5.

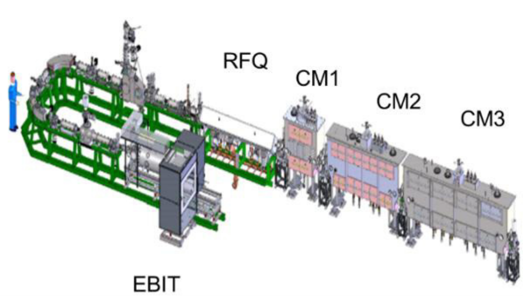

Figure 1: ReA3 beamline at NSCL/FRIB.

† email address: yoshimot@frib.msu.edu

Ion beams extracted from the RFQ are accelerated by three super-conductive CryoModules (CM). CM specification are summarized in Table 1. These cavities are QWRs. Non- axisymmetric electromagnetic field components can kick the beam in vertical direction. In order to correct beam orbit errors caused by this effect and initial beam misalignments, several horizontal and vertical dipole correctors are installed within focusing solenoids. The design relativistic beta β of the CMs vary corresponding to the increasing beam velocity.

Table 1: Components of ReA3 Cryomodule

CM No.	Cavity No	Solenoid/Collector No
CM1	1 (β=0.041)	2/2
CM2	6 (β=0.041)	3/3
CM3	8 (β=0.085)	3/3

Beam tuning

For usual lattice tuning, intercepting monitors such as scintillation detectors and Faraday cups are located outside of CMs because typical beam current is a few hundred pA. Each CM has several cavities and induces accumulated orbit errors. A more precise beam simulation model is required to estimate the beam orbit error along the CMs. In addition, different species with various energies are required to be provided to experimental lines in a short period. This requires effective procedures to change ion species with different charge to mass ratios.

SIMULATION

Single-particle tracking simulations after RFQ section in both case of IMPACT and DYNAC are carried out with eight thousand macro particles. The ion beam species is He^{1+} with 600 keV/u kinetic energy. The Root Mean Square (RMS) measure beam size and angle are 1.25 mm and 1 mrad (both horizontal and vertical) with

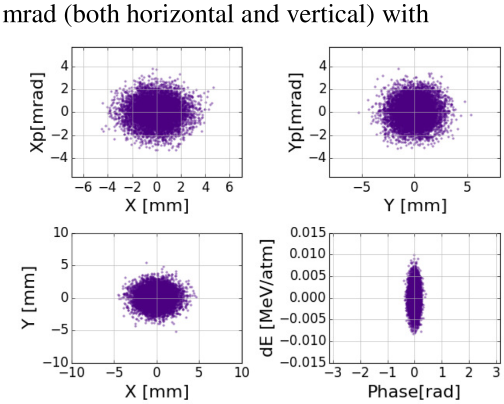

Figure 2: Projections of the initial distribution for the IMPACT and DYNAC simulations.

HIGH CURRENT BEAM INJECTOR FOR CANCER THERAPY*

L. Lu#, L. yang [1], W. Ma[1], T. He[1], L.P. Sun, X.B. Xu, L.B. Shi, C.X. Li, Y. He, H.W. Zhao,
Institute of Moden Physcis (IMP), CAS, Lanzhou, China
[1]also at University of Chinese Academy of Sciences, Beijing, China

Abstract

A hybrid single cavity (HSC) type linac was developed as high current beam injector for cancer therapy. A prototype HSC machine had accelerated 5.2 mA C6+ ions up to 25.7 MeV (2.1MeV/u) with a laser ion source (LIS). sthe ion injection method adopted a direct plasma injection scheme (DPIS). In beam testing, we found the measured beam parameters agreed with simulations. More details of the measurements and the results of the high power test are reported in this paper.

INTRODUCTION

In the last decades, accelerator-driven cancer therapy has considered as a remarkably effective treatment [1]. However, the injection accelerators at existing facilities are large in size and expensive to run [2]. Our team proposed HSC type injector with DPIS as a way to reduce the cost of the cancer therapy facilities, and it was also proposed to use as injector for neutron source[3]. The HSC linac is an interdigital-H (IH) cavity combined a 4-rod type radio frequency quadrupole (RFQ) and a drift tube (DT) structure. The HSC cavity has both merits of RFQ and DT such as a better emittance in transverse, a higher transmission for low energy region in RFQ structure and a better shunt-impedance in DT [4-5], and the power source for HSC acceleration is only one.

The design goal of the prototype HSC linac was to accelerator C^{6+} ions up to 2.1 MeV/u from 25 keV/u in the 1800 mm, the designed resonator frequency was 100 MHz. In the beam conditioning, the linac operated in a pulsed mode, the duty was limited to 5‰ because of the maximum limit of the power source. The input current was designed as 20 mA and the transmission of whole cavity was calculated as 30%. The measured Q and frequency are 91% and 100.49 MHz, respectively. And the calculated shunt impedance based on perturbation measurements is 111.2 MΩ/m, which is 91% of the MWS simulated value of 122.2 MΩ/m. The shunt impedance value of 111.2 M/m for the HSC structure cavity is quite high compared to other linac structures within the same beam velocity region, as shown in Figure 2 [1][6].

Comparing to existing injection systems of cancer therapy facilities, the HSC injector can make the charge stripper (mainly change C^{4+} or C^{5+} ions to C^{6+} ions) and the multi-turn injection useless, moreover, the useless of the multi-turn injection make the synchrotron magnets downsize.

The high power acceleration system of the prototype HSC is shown in Figure 1.

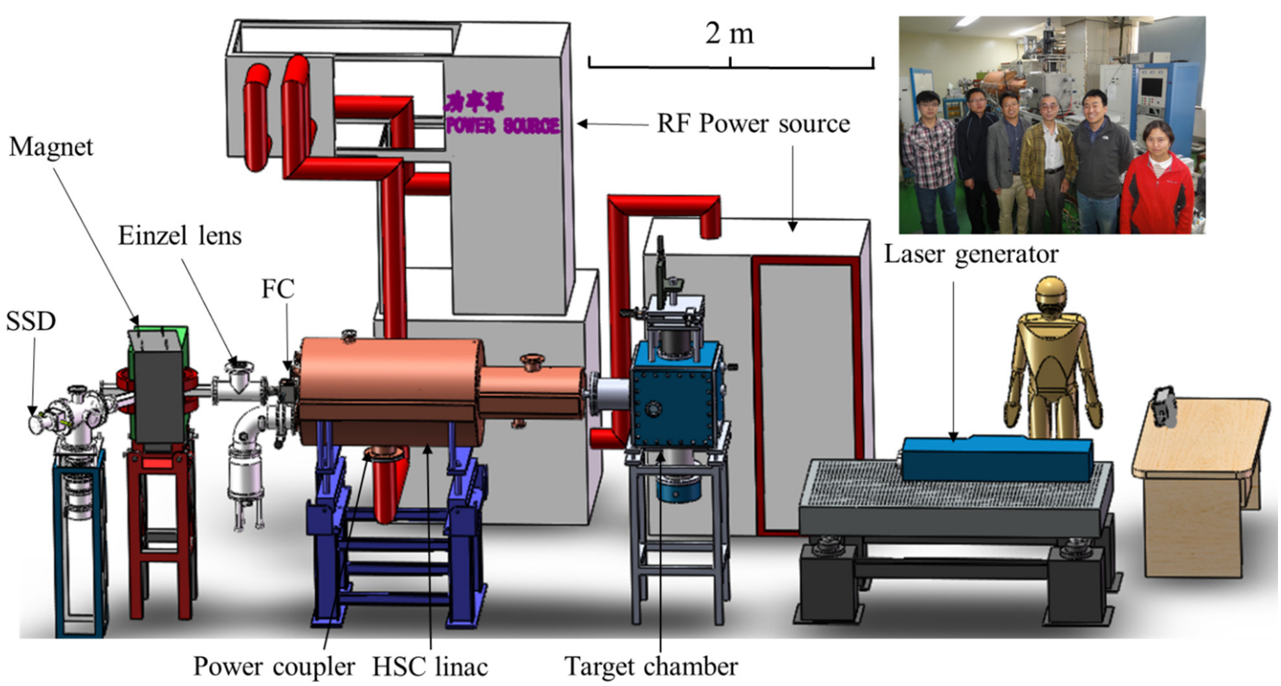

Figure 1: High power acceleration system for prototype HSC linac.

* Work supported by NSFS and Youth Innovation Promotion Association of CAS

luliang@impcas.ac.cn

SOLENOID/MAGNETIC SHIELDING TEST RESULTS IN FRIB-1&2 CRYOMODULES*

D. Luo†, H. Ao, E. Burkhardt, J. Casteel, A. Ganshyn, W. Hartung, M. Holcomb, J. Popielarski, K. Saito, S. Shanab, E. Supangco, M. Thrush
Facility for Rare Isotope Beams, Michigan State University, East Lansing, MI, USA

Abstract

Recently we tested the first two cryomodules for FRIB, which contain $\beta = 0.085$ superconducting quarter-wave resonators and superconducting solenoid packages. Their performance was successfully validated under realistic conditions. This paper reports the solenoid package tests results.

INTRODUCTION

The Facility for Rare Isotope Beams (FRIB) is under construction on the campus of Michigan State University (MSU) [1]. It is a joint project supported by the US Department of Energy and MSU for cutting-edge research in nuclear physics. FRIB requires a 200 MeV per nucleon driver linac with a total of 332 superconducting radio-frequency (SRF) cavities of 4 different types: $\beta = 0.041$ quarter wave resonators (QWRs, 12 cavities), $\beta = 0.085$ QWRs (100 cavities), $\beta = 0.29$ half wave resonators (HWRs, 72 cavities) and $\beta = 0.53$ HWRs (148 cavities). The cavities are housed in a total of 48 cryomodules, including 4 matching cryomodules [2]. The construction started in early 2014 and is expected to be completed in 2022.

In the FRIB cryomodules, superconducting solenoid packages for transverse focusing and steering are interspersed with the cavities. Because of the close proximity, the influence of the solenoid fringe field on cavity performance is a major concern. An example is shown schematically in Figure 1: the $\beta = 0.085$ QWR cryomodule (CM) contains 8 cavities and 3 superconducting solenoid packages. This cryomodule is similar to the cryomodules fabricated for the MSU re-accelerator, ReA3 [3]. An important feature of the cryomodule design is the local magnetic shielding around the SRF cavities [4]. The shields operate at cryogenic temperature ($\simeq$ 25 K).

The cavities and solenoid packages are certified individually via Dewar tests prior to assembly onto the cold mass. After assembly of the cold mass into the cryomodule, the cavities and solenoids are tested again in situ. Two FRIB cryomodules have been tested so far (CM-1, CM-2). For the solenoid packages, the goal is to make sure that all of the coils can reach the FRIB design requirements (Table 1), can operate stably and robustly, and do not adversely impact the SRF cavity performance.

* Work supported by the U.S. Department of Energy Office of Science under Cooperative Agreement DE-SC0000661, the State of Michigan and Michigan State University.

† Luo@frib.msu.edu

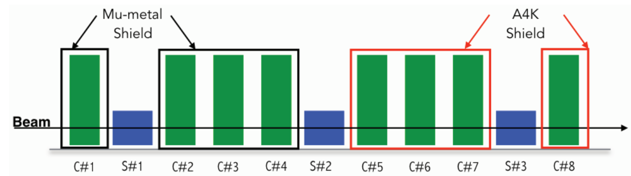

Figure 1: Layout of FRIB-1 Cryomodule (CM-1). C: cavity (green); S: solenoid package (blue). Cavities 1–4 are shielded by mu-metal (black) and Cavities 4–8 are shielded by A4K (red).

Table 1: FRIB 50 cm Solenoid Package Design Requirements. The Fringe Field Requirement Applies at the Magnetic Shield.

Operating temperature	4.5 + 0.5/ − 0.0 K
Solenoid nominal current	≤ 90.9 A
$\int B^2 dz$	≥ 13.6 T^2·m
Peak solenoid field on beam axis	≥ 8.0 T
Fringe field	≤ 270 gauss

LOCAL MAGNETIC SHIELD

As discussed above and illustrated in Figure 1, the SRF cavities are enclosed by local magnetic shields. This approach has two benefits: lower material cost for the shields, and better shielding of the cavities from the remnant magnetic field in the cryomodule.

The need to mitigate the fringe field's effect on the SRF cavity performance sets the shield requirements. For the FRIB QWRs, the magnetic field at the cavity must be ≤ 15 milligauss. Fringe fields higher than ≃ 300 gauss cannot be screened by the shield, hence they will produce a drop in the cavity quality factor after a cavity quench. The magnetic shield requirements are summarized in Table 2.

For the ReA3 cryomodules, the local shields were made of A4K material, with $\mu > 10\,000$ even at cryogenic temperature ($\simeq$ 25 K). However, a recent analysis [5] showed that mu-metal of thickness 1 mm with $\mu > 9000$ at $\simeq$ 25 K can meet the shielding requirements for the FRIB QWRs. Since cryogenic magnetic shields such as Cryoperm and A4K are very expensive compared to mu-metal, switching to mu-metal is economically advantageous, if mu-metal can provide adequate shielding. To evaluate the shielding perfor-

Table 2: FRIB Magnetic Shield Parameters.

Magnetic permeability μ	≥ 10 000 at 25 K
Thickness	1 mm for QWR

ISBN 978-3-95450-169-4

PROGRESS AND DESIGN STUDIES FOR THE ATLAS MULTI-USER UPGRADE*

B. Mustapha†, and P.N. Ostroumov, Argonne National Laboratory, IL, USA
A. Perry, SOREQ-NRC, Israel

Abstract

With the recent integration of the CARIBU-EBIS into ATLAS for more pure and efficient charge breeding of radioactive beams, more effort is being devoted to study the design options for a potential multi-user upgrade. The proposed upgrade will take advantage of the pulsed nature of the EBIS beams and the cw nature of ATLAS, in order to simultaneously accelerate beams with very close charge-to-mass ratios. In addition to enhancing the nuclear physics program, beam extraction at different points along the linac will open up the opportunity for other possible applications. Different beam injection and extraction schemes are presented and discussed.

INTRODUCTION

In the past few years, the requested experimental beam time significantly exceeded the 5000-5500 hours that ATLAS can deliver every year. With the Californium Rare Isotope Beam Upgrade (CARIBU) online, the demand for beam time has more than doubled. Low intensity radioactive beams from CARIBU requires longer experimental run periods which further reduced the number of users served. We believe that there is an immediate need for multi-user capabilities at ATLAS. An analysis of ATLAS operation, when CARIBU beams are accelerated, shows that such an upgrade could deliver ~ 50% more beam time if certain experimental areas were appropriately equipped with instruments. Figure 1 shows the ATLAS floor plan with the possibility of serving two experimental areas simultaneously, namely Area II with beam energies of 4-7 MeV/u and Area III/IV with beams up to the full ATLAS energies.

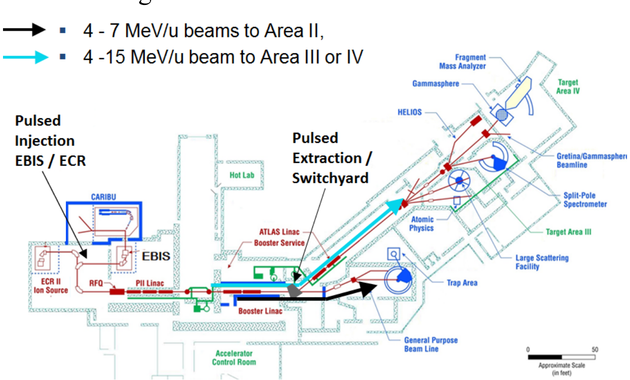

Figure 1: ATLAS floor plan showing the possibility of serving different experimental areas simultaneously.

The recently commissioned CARIBU-EBIS [1] will produce pulsed radioactive beams with ~ 3% duty factor. It will be possible to simultaneously inject stable beams from the ECR ion source in the remaining 97% of the cycle and take advantage of the cw nature of ATLAS. The two beams will have to be within 3% in charge-to-mass ratio. Figure 2 shows the expected time structure of the two beams and their combination.

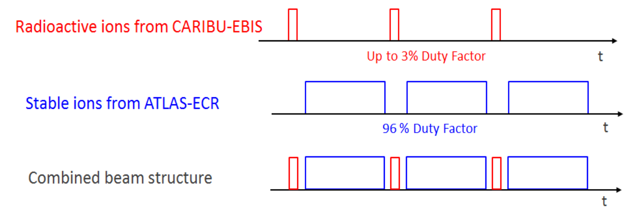

Figure 2: The expected time structure of the CARIBU-EBIS beam, the ECR beam and their combination for injection into ATLAS.

More details about the potential overlap of radioactive and stable beams that could be simultaneously accelerated as well preliminary design solutions for the upgrade were reported earlier [2]. We here report on the progress made in these design studies for both the beam injection at the LEBT and extraction of one of the beams at the Booster.

MODIFIED BEAM INJECTION IN THE LEBT

In order to combine two beams with very close charge-to-mass, one stable from the ECR and one radioactive from EBIS, the LEBT section has to be modified as shown in Figure 3. For the ECR line, an additional 90 deg bend and a 75 deg magnet are used to bring the beam to a 15 deg pulsed electrostatic deflector on the EBIS line. In addition, two sextupoles are required for second order corrections in the dispersive section between the dipoles.

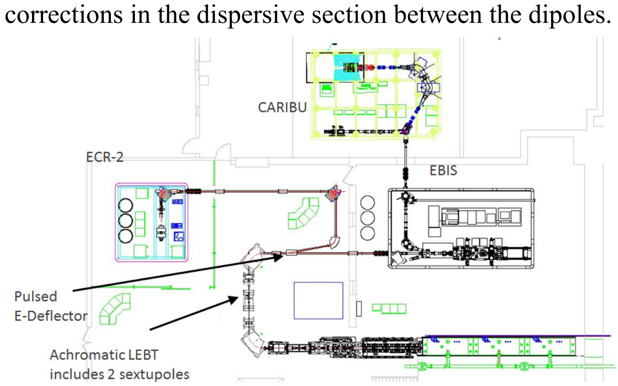

Figure 3: Modified LEBT to combine one stable beam from ECR and one radioactive beam from LEBT.

* This material is based upon work supported by the U.S. Department of Energy, Office of Science, Office of Nuclear Physics, under Contract number DE-AC02-06CH11357. This research used resources of ANL's ATLAS facility, which is a DOE Office of Science User Facility.
†brahim@anl.gov

SIMULATION STUDY ON THE BEAM LOSS MITIGATION IN THE 1ST ARC SECTION OF FRIB DRIVER LINAC*

T. Maruta†, KEK / J-PARC, Tokai, Japan
M. Ikegami, F. Marti, Facility of Rare Isotope Beams, Michigan State University, MI 48824, USA

Abstract

For a high power superconducting (SC) accelerator like FRIB, the extinction of the beam loss inside the cavities is the most important issue for a stable operation. The charge-exchange reaction is unique to heavy ions and potentially generates a loss. Recently we conducted the simulation study to evaluate this loss in the beam transport after 1st linac segment, and then the necessity of one collimation is identified. This paper introduces this study details.

INTRODUCTION

The Facility of Rare Isotope Beams (FRIB) is a high power heavy ion accelerator facility currently being constructed in Michigan State University under cooperative agreement with United States Department of Energy [1]. The driver linac will operate in continuous wave (CW) mode and deliver more than 200 MeV/u all stable heavy ions to the target with beam power of 400 kW.

For a high intensity accelerator, the beam loss mitigation is essentially important. Especially, FRIB intensively employs SC RF cavities after the 0.5 MeV/u Radio Frequency Quadrupole (RFQ), and it is well known that the beam loss inside a SC cavity significantly deteriorates its operable RF voltage. Moreover, the beam loss power density of heavy ions is more severe than proton with same velocity. The energy deposit per unit length is proportional to Q^2/A where Q and A are charge number and mass number, respectively [2]. For example, this density of uranium is 36 times higher than proton. Therefore FRIB must considerably pay attention to potential loss source and distinguish a loss, especially for inside RF cavities for stable operation.

In this paper, we discuss the beam loss originated by charge-exchange reaction in the 1st folding segment (FS1). Since this reaction exchanges a electron with residual gas, the beam ion charge-state, q, varies after the reaction. Then it also varies the magnetic rigidity because it is dependent on the charge-to-mass ratio, q/A. The charge-exchanged ion orbit is distorted and then it could be lost somewhere in downstream. The reaction probability depends on the residual gas pressure. The FS1 is a beam transport connecting 1st and 2nd linac segments (LS1 and LS2). A high power load collimator, namely charge selector, is located in the arc section and pressure level around the selector is estimated to be the worst in the entire driver linac. Therefore significant amount of charge-exchange reaction could occurs around the charge selector. A new collimator position and aperture are optimized by using 3D Particle-In-Cell (PIC) simulation. The simulation studies a charge-exchange reaction of uranium beam. We track the orbits of charge-exchanged ions and loss location in the arc section. Then a new collimator position and aperture size are optimized also by the simulation.

In this paper, the outline of FS1 is explained in the next section. The total power of charge-exchanged ions are estimated from the cross-section and residual gas pressure in 3rd section. The loss location and aperture study by simulation is shown in 4th section. Then we conclude this study in the last section.

* Work supported by the U.S. Department of Energy Office of Science under Cooperative Agreement DE-SC0000661
† tomofumi.maruta@kek.jp

FOLDING SEGMENT 1

The FS1 is a 57 m long beam transport connecting parallelly placed 1st to 2nd linac segments (LS1 and LS2) as shown in Fig. 1. The injection beam energy is 16.6 MeV/u for uranium. A charge stripper is placed upstream of the arc section in order to increase effective acceleration gradient at LS2 and later linac section. In the stripper, beam ions are stripped off their electrons by passing though a thin liquid lithium film. The q/A of heavy ions such as uranium increases more than twice. Meanwhile, the beam ions deposit their energy about 0.2 MeV/u on average in the stripper. In the charge stripper, heavy ions with unwanted charge states are also generated. A horizontal movable collimator, namely charge selector, extinguishes these unnecessary ion. This collimator locates after the 1st 45-degree bending magnet in arc section as shown in Fig. 1. The bending radius of each ion differs by their own q/A due to the magnetic rigidity, which is inversely proportional to q/A. Therefore horizontal position at the bending magnet exit depends on each q/A. Moreover, β_x at the selector is minimized to realize a good q/A separation. The arc section is 11 m long, two fold achromatic and isochronous lattice and each of them is comprised from two 45-degree bending, two quadrupole and one sextupole magnets. The beta functions and momentum dispersion along the arc are shown in Fig. 2.

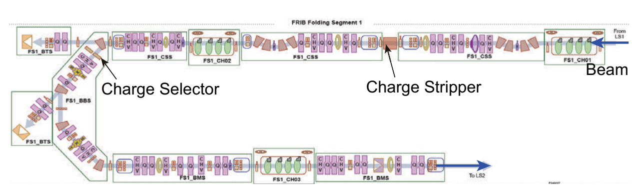

Figure 1: Outline of FS1. The beam is transferred from LS1 (top right) to LS2 (bottom right) passing through 180-degree arc.

ISBN 978-3-95450-169-4

EFFICIENT HEAVY ION ACCELERATION WITH IH-TYPE CAVITIES FOR HIGH CURRENT MACHINES IN THE ENERGY RANGE UP TO 11.4 MEV/U

H. Hähnel†, U. Ratzinger, R. Tiede
Institute of Applied Physics, Goethe University Frankfurt, Germany

Abstract

We propose an efficient design for heavy ion acceleration from 1.4 to 11.4 MeV/u with a design current of 15 emA for a U^{28+} beam as a possible injector for FAIR. The proposed linac is based on IH-DTL cavities and quadrupole triplet focusing. The KONUS beam dynamics concept [1] is used to achieve high acceleration efficiency. By optimization of the transverse focusing scheme and the longitudinal bunch center motion, low emittance growth for the entire linac is achieved. Beam dynamics simulations were performed along with 3D rf simulations of all cavities. The cavities are designed for 108.408 MHz, reaching an effective shunt impedance of 100-200 MΩ/m. The overall length of the linac is just 22.6 m which is almost a third of an alternative Alvarez layout. A mechanical realization concept employing a modular tank design is presented. The proposed design is a viable option for the GSI UNILAC poststripper linac replacement, leaving free space in the UNILAC tunnel for future energy upgrades.

LAYOUT AND COMPONENTS

The whole linac structure was developed with LORASR and CST Microwave Studio. The design comprises five 108 MHz IH-DTL cavities and seven quadrupole triplet lenses [2]. The linac is divided into three mechanically rigid sections (see Fig. 1).

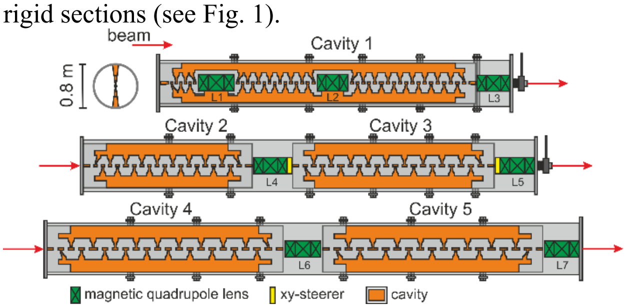

Figure 1: Layout of the IH-DTL linac.

Additionally, the cavities are divided into short modules (as shown in Fig. 2) to allow copper plating and easy alignment of the modules with drift tubes and lenses. The layout features phase probes for all lenses except L1 and L2 and beam steerers between L4 and L5 to ensure optimal beam transport. The power requirements of the cavities were estimated using CST simulations of all sections. The overall consumed power per cavity is 0.82 MW at the beginning of the linac and reaches 1.22 MW towards the end of the linac (see Table 1). At a duty factor of 0.2 % the thermal losses are in the order of 2 kW and could be managed with simple cooling techniques. Significantly higher duty factors are also possible, but would require extensive cooling of the structures.

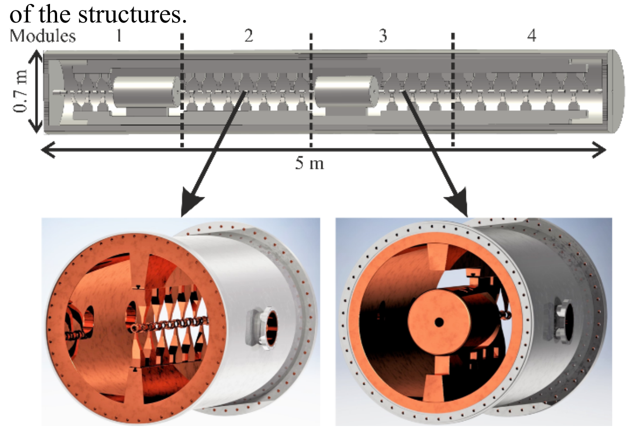

Figure 2: Mechanical design of the modular sections for the first IH-DTL cavity (courtesy of D. Bänsch

At 108.408 MHz the IH-cavities are 0.7-0.8 m in diameter. The design limits were chosen to be state of the art values to provide a reliable and durable machine. On axis electric field in the IH-cavities is at maximum just above 11 MV/m which is a value considered safe for an IH-structure at this frequency. The quadrupole magnets are now limited by < 1.1 T at the pole tip. This provides some operational margin, since tip fields of 1.3 T are possible using current magnet technology. The average accelerating gradient of the whole linac is 3.76 MV/m.

Table 1: Cavity Properties

Cav.	L_{tot} [m]	V_{tot} [MV]	P_{tot} [MW]
1	4.9	19.6	0.8
2	2.8	17.2	1.0
3	3.6	18.7	1.2
4	3.7	18.7	1.2
5	3.9	16.8	1.2

BEAM DYNAMICS

The beam dynamics design was developed using LORASR and is based on the KONUS beam dynamics concept. The combination of a negative synchronous phase section (rebunching) followed by a longer section with a phase close to zero degrees allows for more efficient acceleration. The zero-degree section allows higher accelerating voltages and a significant reduction of radial E-field defocusing of the beam. Meanwhile the rebunching sections ensure longitudinal matching between the different sections. This way the drift length between two succeeding triplet

* Work supported by BMBF 05P15 RFRBA
† haehnel@iap.uni-frankfurt.de

FABRICATION AND LOW TEMPERATURE TEST PLAN FOR RARE ISOTOPE SCIENCE PROJECT*

Wookang Kim, Mijoung Joung, Yoochul Jung, Heetae Kim†, Jongwon Kim, Youngkwon Kim, Ilkyoung Shin, Rare Isotope Science Project,
Institute for Basic Science, Daejeon 34047, Republic of Korea

Abstract

Quarter-wave resonator (QWR), half-wave resonator (HWR) and single-spoke resonator (SSR) cryomodules are used for RAON accelerator. The layout of RAON accelerator and three types of cryomodules such as QWR, HWR and SSR are shown in the linac. SRF test facility which consists of cryoplant, cleanroom, vertical test facility and horizontal test facility is constructed. Cleanroom has high pressure rinsing (HPR), ultrasonic cleaning (USC), buffered chemical polishing (BCP), high vacuum furnace and cavity assemble place. The test plan for cavity and cryomodules is presented.

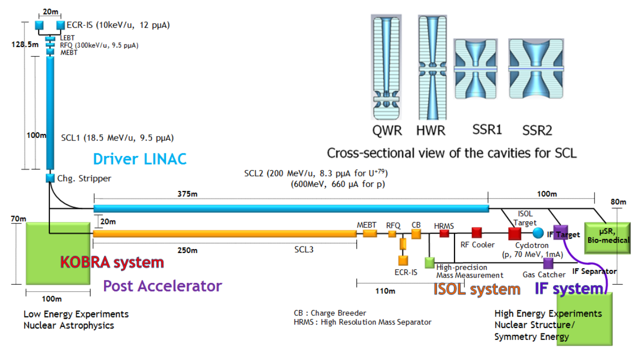

Figure 1: Layout of RAON accelerator.

INTRODUCTION

N-dimensional thermal radiation was studied [1] and the size effect of the thermal radiation was predicted [2, 3]. Properties of superfluid helium fog were studied [4-6] and RAON superconducting radio frequency (SRF) test facility was designed [7]. The RAON SRF test facility consists of cryogenic system, cleanroom, vertical test facility and horizontal test facility. Cavity process and assemble can be performed in the cleanroom. Residual resistivity ratio (RRR) of Nb was measured and the conditions of e-beam welding (EBW) for Nb were studied [8, 9]. Helium leak detection techniques were shown for cryogenic system [10] and a half-wave resonator (HWR) cryomodule was test in low temperature [11].

In this paper, we show the layout of RAON accelerator in which QWR, HWR and SSR cryomodules are installed. Progress of the cryomodules' development is presented and SRF test facility is shown. Cleanroom, vertical test facility and horizontal test facility can be used in the SRF test facility.

RAON ACCELERATOR

RAON accelerator consists of SCL1, SCL2, and SCL3. The layout of the RAON accelerator and the cross-sectional view of cavities are shown in Fig. 1. The types of cavities are QWR, HWR, SSR1, and SSR2. Radio frequencies to drive QWR, HWR, and SSR cavities are 81.25, 162.5, and 325 MHz, respectively. Beta is 0.047, 0.12, 0.30, and 0.51 after QWR, HWR, SSR1, and SSR2 cryomodules from SCL1 through SCL2. Beam energy for H^+ is about 600 MeV and beam energy for U^{+79} is about 200 MeV. Power on target is about 400 kW. It is expected to construct the RAON accelerator in 2021.

TYPES OF CRYOMODULES

Prototypes of cryomodules are fabricated and tested. Fabricated prototypes of the cryomodules are quarter-wave resonator (QWR), half-wave resonator type 1 (HWR1), half-wave resonator type 2 (HWR2), single-spoke resonator type 1 (SSR1), and single-spoke resonator type 2 (SSR2) cryomodules. The types of the cryomodules are shown in the layout of RAON accelerator in Fig. 2. SCL1 and SCL3 are the same, which have QWR, HWR1, and HWR2 cryomodules. SSR1 and

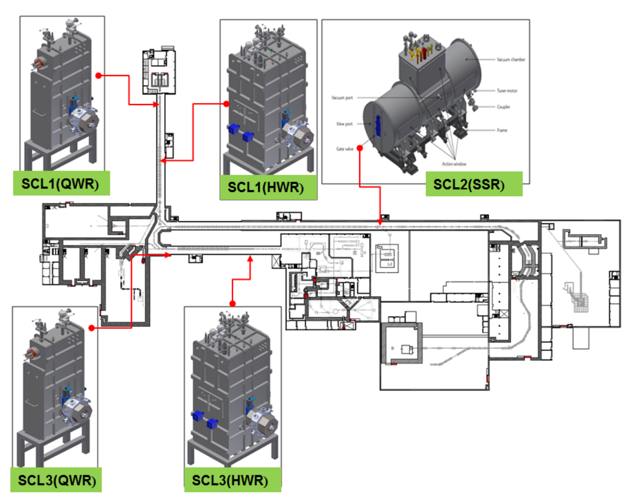

Figure 2: Types of cryomodules in RAON accelerator.

* This work was supported by the Rare Isotope Science Project of Institute for Basic Science funded by the Ministry of Science, ICT and Future Planning (MSIP) and the National Research Foundation (NRF) of the Republic of Korea under Contract 2013M7A1A1075764.
† kim_ht7@yahoo.com

ISBN 978-3-95450-169-4

DEVELOPMENT OF RAON QWR CRYOMODULE FOR LINAC DEMONSTRATION*

Heetae Kim, Jong Wan Choi, Yong Woo Jo, Yoochul Jung, Wookang Kim†,
Youngkwon Kim, Min Ki Lee, Rare Isotope Science Project,
Institute for Basic Science, Daejeon 34047, Republic of Korea

Abstract

Quarter-wave resonator (QWR) cryomodule is developed for linac demonstraction. The plan and layout of the linac demonstration are shown. 3D drawing and P&ID are shown for the quarter-wave resonator (QWR) cryomodule. The QWR cryomodule consists of cavity, coupler, tuner, liquid helium reservoir, thermal shield and magnetic shield. PLC rack is fabricated to control the QWR cryomodules. The PLC controls and monitors pumps, heaters, cryogenic valves, solenoid valves, gate valves and temperature sensors.

INTRODUCTION

Superfluid helium fog was studied below the critical temperature of superfluid, 2.172 K [1-3]. Thermal radiation from n-dimension [4] and the size effect of the thermal radiation [5, 6] were investigated. RAON superconducting radio frequency (SRF) test facility was designed [7]. The RAON SRF test facility consists of cryogenic system, cleanroom, cavity test and cryomodule test. The cleanroom is used for cavity processes and assembles. Residual resistivity ratio (RRR) test of niobium was performed and the conditions of e-beam welding (EBW) were studied [8]. A half-wave resonator type 1 (HWR1) cryomodule was test in low temperature [9].

In this research, we develop QWR cryomodule for linac demonstration. Layout of linac demonstration is presented. In order to control the cryomodules, PLC rack is fabricated and PLC program is developed.

LINAC DEMONSTRATION

Superconducting linac (SCL) demonstration consists of ECRIS, LEBT, RFQ, MEBT, QWR cryomodule, warm section, RF system and cryogenic system. Figure 1 shows the layout of the linac demonstration. The linac demonstration is located in RAON SRF test facility. The SRF test facility includes cleanroom, cryogenic system, vertical test bench, horizontal test bench, etc. Oxygen beam having A/q~3 is used initially and then metal ion such as Bismuth having A/q~7.2 will be used in future. ECRIS beam energy is 10 keV/u, RFQ beam energy is 500 keV/u, and QWR beam energy is 530 keV/u.

* This work was supported by the Rare Isotope Science Project of Institute for Basic Science funded by the Ministry of Science, ICT and Future Planning (MSIP) and the National Research Foundation (NRF) of the Republic of Korea under Contract 2013M7A1A1075764.
† kwko11045@ibs.re.kr

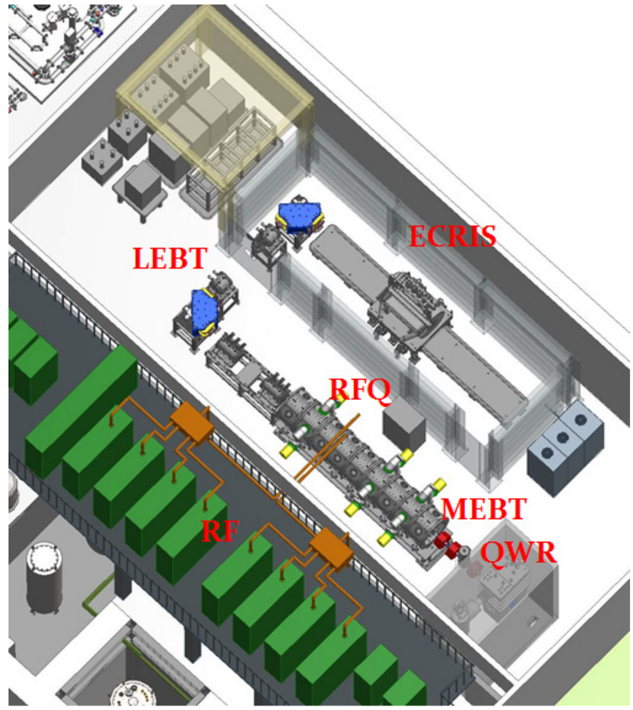

Figure 1: Layout of linac demonstration.

QWR CRYOMODULE

Prototype of QWR cryomdoule was fabricated and the QWR cryomodule is modified for linac demonstration. Figure 2 shows the 3D drawing of the QWR cryomodules. The QWR cryomodule consists of cavity, coupler, tuner, liquid helium reservoir, thermal shield, magnetic shield, etc. The cavity is made of Nb and is operated at the temperature of 4.3 K and the frequency of 81.25 MHz. The Residual resistivity ratio (RRR) value of Nb shows the purity of niobium, which is related to heat transfer during welding process. The RRR degrades during electron beam welding process due to impurity incorporation. Thus, e-beam welding is very important process to fabricate the Nb cavity. In order to improve the quality (Q) factor of Nb cavity, the conditions of e-beam welding which include vacuum level, welding speed, and power were studied [10] and were applied to the cavity fabrication.

SRF test facility has cryoplant, cleanroom, vertical test bench and horizontal test bench. Cleanroom has high pressure rinsing, buffered chemical polishing, ultrasonic cleaning, high vacuum furnace and cavity assemble place. The classes of the cleanroom are 10, 100, 1000, and 10000. The class of cavity assemble place is 10 in which

MAGNETIC FIELD MEASUREMENTS IN A CRYOMODULE WITH NEARBY WARM-SECTION QUADRUPOLE MAGNETS OF RAON HEAVY ION ACCELERATOR

H. J. Cha†, M. K. Lee, I. Chun and J. W. Choi, IBS/RISP, Daejeon, South Korea

Abstract

In order to increase the quality factor of a superconducting cavity, a shielding mechanism against geomagnetic fields in a cryomodule is required. In this paper, we introduce the magnetic properties of Mu-metal specimens for global shielding in the cryomodule. Dramatic reduction of the geomagnetic fields in a real Mu-metal shielding structure is also reported.

INTRODUCTION

The superconducting linac of the RAON is composed of a number of cryomodules in which include niobium cavities and intermediate warm section modules for heavy ion beam collimation and diagnostic [1]. For the acceleration performance of a superconducting cavity, ambient magnetic fields around the cavity should be minimized as possible. In our case, the ambient fields are based on two magnetic factors: one is geomagnetic fields which can be trapped in the cavity surface during a cool-down process and the other is fringe fields from a warm-section quadrupole magnet which can be partially trapped at the cavity quench location [2]. In this study, we focus on the minimization of geomagnetic fields at the cavity position with the global magnetic shielding of a QWR cryomodule.

MAGNETIC PROPERTY MEASUREMENTS OF MU-METAL SPECIMENS

We prepared two kinds of Mu-metal samples: one was processed by just thermal annealing and the other was done by annealing again in hydrogen atmosphere.

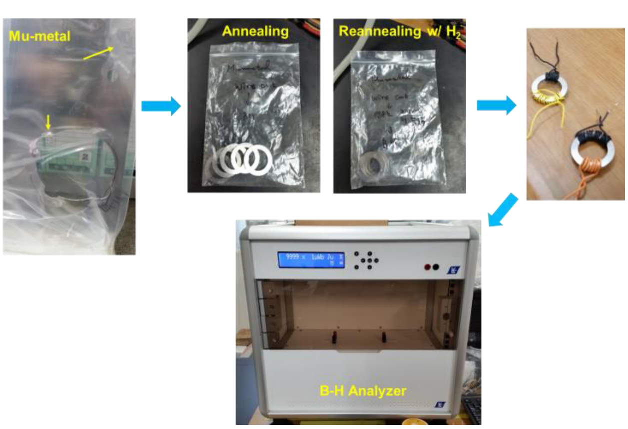

Figure 1: Preparation for magnetic property measurements of Mu metal specimens.

A magnetic analyzer was used for measuring the B-H characteristics of the Mu-metal samples. Yellow arrows in the left-side photograph of Fig. 1 indicate the pressed and stressed spots which can degrade the shielding property of the Mu-metal structure.

Figure 2 shows measurement results for the two kinds of samples. The magnetic property for shielding of the H_2-processed sample (red curve) is superior to that of the just thermally annealed sample (black curve). The treatment for shielding performance of Mu-metal is known to be annealed in the cooling rate of 200 ℃/hr after 1150 ℃ baking in H_2 atmosphere for 4 hours [3].

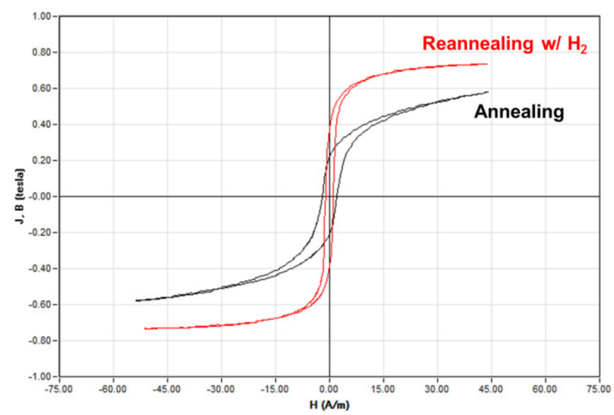

Figure 2: Comparison of measurement results for an annealed sample and a reannealed one with hydrogen supply.

We could also obtain a relative permeability curve for the H_2-processed sample as shown in Fig. 3. Supposed that the geomagnetic field is around 0.5 Oe (50 μT), the permeability of the Mu-metal sample corresponds to be approximately 18,000 in that field. However, it is possible to increase the relative permeability by optimizing the thickness and dimension of a Mu-metal structure as the following equation:

$$B = 1.25DH_0/t \qquad (1)$$

where B is a magnetic flux density induced to a shielding structure, D and t are a diameter and a thickness of the structure (cylinder), respectively, and H_0 is an external magnetic field [4]. The resultant permeability can contribute to improving a shielding factor of the Mu-metal structure.

† hjcha@ibs.re.kr

ISBN 978-3-95450-169-4

STATUS OF RRR ANALYSIS FOR RAON ACCELERATOR*

Yoochul Jung†, Heetae Kim, Wookang Kim, RISP, IBS, Daejeon, South Korea
Jonghwa Lee, Jiwon Seo, Vitzrotech, Ansan, South Korea

Abstract

Residual Resistance Ratio, which is called RRR, is an important parameter representing the purity of superconducting material. Since a thermal quench, which means the superconductivity no longer exists, is induced by thermal accumulation when a local spot exceeds a critical temperature, the purity control near superconducting surface as about nano meter level is critical. Analyzing RRR characteristics is a key to check out how e-beam welding is carried out. Therefore, optimization and analysis of electron beam welding is very important as the first step to produce superconducting cavity. RISP has been producing low beta cavities including half-wave, quarter-wave, and spoke type cavities to construct heavy-ion accelerator, "RAON". We have conducted series of e-beam welding tests and confirmed that RRR is strongly dependent on the vacuum level, welding power, and welding speed. In this paper, we report RRR results from various welded samples for producing niobium superconducting cavities.

INTRODUCTION

Low-beta cavity requires complicated processes such as cavity part forming by using a pressing machine, part welding by e-beam welding, chemical polishing of a cavity [1], heat treatment, high pressure rinsing for cleaning the inner surface of the cavity [5] [3]. Because the superconductivity is strongly dependent on the surface state of the superconducting cavity, the surface of the cavity should be carefully treated. Welding, which is carried out to assemble two or more parts, is basic process to fabricate the superconducting cavity. However, this welding process must be performed systematically and elaborately as well for successful result. In principle, the welding occurs between liquid metals. Therefore, this moment is very vulnerable for a material to be easily contaminated from environment. According to previous studies [4], vacuum level, welding power and welding speed are known as critical factors to determine the success of the welding, needless to say the clean surface of parts to be joined. We performed various welding of niobium by using electron-beam with the same condition as used for producing prototype niobium cavities. And we analyzed the results of the residual resistance ratio with physical property measurement system (PPMS). In this paper, we will discuss the characteristics of RRR measurement as a function of the vacuum level, welding speed, and welding power.

* This work was supported by the Rare Isotope Science Project of Institute for Basic Science funded by the Ministry of Science, ICT and Future Planning (MSIP) and the National Research Foundation (NRF) of the Republic of Korea under Contract 2013M7A1A1075764

† sulsiin@ibs.re.kr

EXPERIMENTAL

Sample Preparation and E-beam Welding

RRR 300 grade niobium sheets (Nb,41) were purchased from ATI, Wah Chang Inc. (Albany,USA). Each Nb sheet has the size as $3 \times 635 \times 1200$ mm^3 ($thickness \times width \times length$). Purchased niobium satisfied the mechanical and chemical specifications for producing Nb superconducting cavity [**?**]. Successfully welded niobium sheet for preparing samples has the size as 200×200 mm^2, which means two identical niobium parts of 100×200 mm^2 were butt-joined by e-beam welding. Welding conditions are summarized in Table 1. Nb samples for RRR measurement have the size as $0.5 \times 0.5 \times 9$ mm^3, and they were cut from the welded Nb sheet perpendicular to the welding line. All dimensions of niobium are summarized in Table 2. Each distance of cut sample was 0, 2, 4, 6, 8, 10, 15, 20, 25, 50 mm from the welding line. This is shown in Figure 1 and Figure 2. Cutting samples was carried out by electrical discharge machining (EDM). Samples were cut from bottom, middle and top part along the welding direction. For instance, twenty samples were cut from the bottom part including both the weld side (front side) and bead side (back side). Ten samples were obtained from one welded sheet. Therefore, sixty Nb samples in total were prepared from the welded Nb sheet.

Table 1: Welding Conditions for Sample Preparation

Items	Values
Voltage (kV)	60 - 120
Current (mA)	30 - 60
Power (kV)	Max. 9
Welded Speed (mm/s)	3-20
Vacuum (Torr)	$2 \times 10^{-5} \sim 5 \times 10^{-6}$

Table 2: Nb Dimensions for RRR Measurement

Items	Dimensions
Nb Sheet	$3 \times 635 \times 1200$mm^3 (T $\times W \times L$)
Welded Sheet	200×200 mm^2
Part for Welding	100×200 mm^2
Nb Sample	$0.5 \times 0.5 \times 9$ mm^3

RRR Experiment

RRR measurement by using physical property measurement system (PPMS) was performed with no magnetic field. Among many definitions of RRR, we defined RRR by measuring the resistance of niobium sample just above 9.2 K, the critical temperature at niobium turns into superconducting

VERTICAL TEST RESULTS ON ESS MEDIUM BETA ELLIPTICAL CAVITY PROTOTYPE

Enrico Cenni#, Guillaume Devanz, Xavier Hanus, Franck Peauger, Juliette Plouin, Dominique Roudier, Luc Maurice, Fabien Eozenou, Christophe Servouin, Stephane Berry, Pierre Bosland, CEA Saclay, Gif-sur-Yvette, France
Christine Darve, ESS, Lund, Sweden
Gabriele Costanza, Lund University, Lund, Sweden

Abstract

The ESS elliptical superconducting Linac consists of two types of 704.42 MHz cavities, medium and high beta, to accelerate the beam from 216 MeV (spoke cavity Linac) up to the final energy of 2 GeV. The last Linac optimization, called Optimus+ [1], has been carried out taking into account the limitations of SRF cavity performance (field emission). The medium and high-beta parts of the Linac are composed of 36 and 84 elliptical cavities, with geometrical beta values of 0.67 and 0.86 respectively. This work presents the latest vertical test results on ESS medium beta elliptical cavity prototypes. We describe the cavity preparation procedure from buffer chemical polishing to vertical test. Finally, magnetic probes (Fluxgate) were installed on the cavity to determine magnetic field background during vertical test. The latest vertical test results showed that the cavity design performance is beyond requirements.

INTRODUCTION

CEA-Saclay is in charge of developing and manufacturing six medium beta elliptical cavities [2] for the superconducting section of ESS Linac. Four of these cavities will be installed in a cryomodule prototype used as demonstrator [3]. Next, 5 high beta cavities [4] will be manufactured and installed (4 of them) into a cryomodule for testing.

As of September 2016, all 6 medium beta cavities have been manufactured, 2 were tested and are ready for helium tank integration. The remaining 4 will be soon delivered to be polished by means of acid etching (buffer chemical polishing). Figure 1 shows a section of a medium beta cavity equipped with the helium tank.

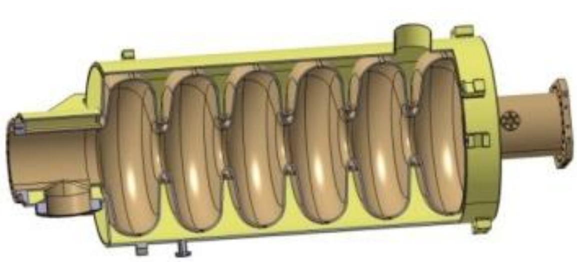

Figure 1: Medium beta elliptical cavity equipped with helium tank (section view).

#enrico.cenni@cea.fr

Table 1 presents all the relevant parameters concerning medium beta cavities design and working conditions.

Table 1: Medium Beta Cavity Design Parameters

Parameter	Value
Frequency	704.4 MHz
Length	1258.8 mm
# cells	6
Operating temperature	2K
Beta	0.67
Nominal E_{acc}	16.7 MV/m
Q_0 at nominal E_{acc}	>$5x10^9$
E_{pk}/ E_{acc}	2.36
B_{pk}/ E_{acc}	4.79 mT/(MV/m)
G	196.63 Ω
Cell to cell coupling	1.2%

CAVITY MANUFACTURING AND PREPARATION

Six cavity prototypes have been manufactured following a dedicated procedure [5].

In Table 2 are shown the average deviations between the measured and simulated length and fundamental mode frequency, for the 6 manufactured cavities.

Table 2: Cavities Manufacturing Deviation Summary

Parameter	Average deviation respect computed values
Length	0.767 mm
π-mode frequency	0.292 MHz

Preliminary results on accelerating mode frequency and length show that the manufacturing process is accurate and reliable, especially into evaluate the welding shrinkage. This allowed us to have a precise estimation of the cavity frequency and length. On the other hand, field flatness measurements just after welding, showed to be different among the two first cavities. P01 had a 56.8% field flatness while P02 had 89.1%. Our goal is to tune all cavities with a field flatness of 95% before the helium tank integration. A dedicated tuning machine was designed to achieve this task, each cell can be tuned independently during the same tuning process.

ISBN 978-3-95450-169-4

RESULTS OF INTENSITY UPGRADE PHASE I FOR 200 MeV H- LINAC AT BROOKHAVEN*

D. Raparia#, B. Briscoe, C. Cullen, T. Lehn, V. Lodestro, A. McNerney, J. Ritter, A. Zelenski,
Brookhaven National Laboratory, Upton, NY, USA

Abstract

The 200 MeV H- Linac has been operational for the last 45 years providing beam to the physics and isotope programs. There is eight folds increase in yearly-integrated intensity delivered to Brookhaven Linac Isotope Producer (BLIP) in the past decade. Recently we have finished intensity upgrade phase I, which resulted 48% more intensity for BLIP and reduced losses along the linac and transfer line to BLIP by several fold. We will present detail of the upgrade and future upgrades plan to further increase in the intensity by factor of two.

INTRODUCTION

The Brookhaven National Laboratory (BNL) 200 MeV drift tube linac (DTL) was built in 1970 [1] with following design parameters for proton: input energy 0.75 MeV, output energy 200.3 MeV, frequency 201.25 MHz, peak beam current 100 mA, beam pulse length (max) 200 µs, RF pulse length 400 µs, pulse repetition rate (max) 10 Hz. Over the 45 years of linac operations, it has gone through several improvements. The major upgrades were; (a) switch to 5 Hz operation [2], (b) change proton to H^- [3], (c) addition of polarized H^- source [4], (d) replacement of the Cockcroft-Walton by Radio Frequency Quadrupole (RFQ) [5], (e) new timing system [6], (f) new 12 inches pressurised coax system [6], (g) RF system improvements [6], new 50 kV power supply, eliminating of DC charge control at 60 kV, new RF control system, phase and amplitude servo redesign, (h) new polarized source OPPIS source and its upgrade, and [7,8], (i) reconfiguration of 35 keV and 750 keV transport lines [9,10,11,12,13].

At present linac provides H^- beam at 200 MeV to polarized proton program for Relativistic Heavy Ion Collider (RHIC) and 66-200 MeV to Brookhaven Linac Isotope Producer (BLIP). The RHIC program needs two pulses every AGS cycle (~4-6 sec), one for injection into the AGS booster and other for 200 MeV polarization measurements located in the High Energy Beam Transport line (HEBT). The rest of the pulses from high intensity source are delivered to BLIP. Requirements for these programs are quite different and are following. (1) RHIC: 200 MeV, 600 µA beam current, up 400 µs pulse length, polarization as high as possible and emittance as low as possible, (2) BLIP: 66-200 MeV, 450 µs pulse length, current as high as possible (~55 mA), uniform beam distribution at the target, and beam losses as low as possible. Many of subsystems of the linac are 45 years old and need to be replaced. Three upgrade programs; reliability, intensity, and beam raster [14, 15], are in progress. Here, we will discuss only intensity upgrade program for BLIP.

INTENSITY UPGRADE

The average current delivered to BLIP is steadily increasing over the years as shown in Fig. 1. To increase the isotope production, there is strong desire to increase the linac current by factor of two. An Accelerator Improvement Plan (AIP) was approved for Phase I of intensity upgrade in 2014. Phase I includes 15 % (5 % in the peak current and 10% in the beam pulse length) increase in average current and evaluations of the linac subsystem for doubling the current [17]. Table 1 summarizes linac parameters for intensity upgrade Phase I (2014), operating 2016 and proposed to increase the intensity by factor of two, Phase II. Both the goals of Phase I, (1) increase in 15% current, and (2) evaluation of the linac subsystem for delivering 250 µA average beam current, were successfully completed on time and within the budget. We have concluded that the linac can deliver 250 µA with upgrades of subsystem describe in section below.

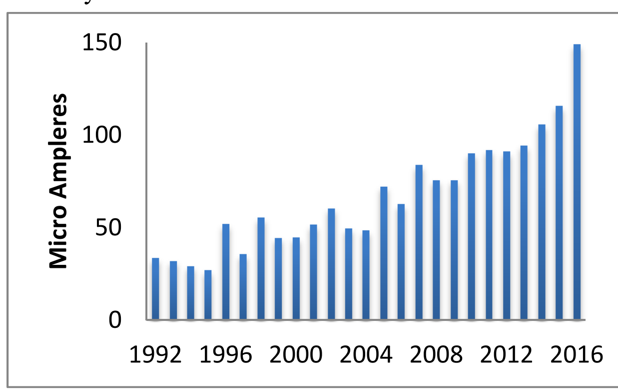

Figure 1: The average current delivered to BLIP for last 15 years (2002-2016).

Table 1: Linac Parameters for Intensity Upgrade Phase I (2014), Operating 2016 and proposed Phase II.

Parameter	**Phase I (Goal)**	**Operation 2016**	**Phase II (Goal)**
In. Energy (MeV)	0.75	0.75	0.75
Out. Energy (MeV)	200	200	200
Peak Cur. (mA)	45	55	45
Beam PL (µs)	**490**	**470**	**900**
RF PL (µs)	**650**	**620**	**1100**
Frequency (MHz)	201	201	201
Rep. Rate (Hz)	6.67	6.67	6.67
Ave. Current (µA)	140	165	250

*Work performed under Contract Number DE-AC02-98CH10886 with the auspices of the US Department of Energy
#raparia@bnl.gov

OPTIMIZING CAVITY CHOICE FOR FRIB ENERGY UPGRADE PLAN*

S. Shanab†, K. Saito, and Y. Yamazaki,
National Superconducting Cyclotron Laboratory, Michigan State University, East Lansing, USA

Abstract

Isotope production yield rate is directly proportional to beam power, especially for heavy ions. Higher beam kinetic energy on target drives more isotope yield. FRIB has an energy upgrade plan up to ≥ 400 MeV/u for Uranium and already prepared a vacant space in the design stage and cryogenic capacity that accommodates for the energy upgrade plan [1]. This upgrade requires an optimized linac design and challenging technology for cavity performance improvement. In this paper, we will approach this issue concerning; maximizing final energy, optimum beta, cavity operating frequency, cryogenic power, fabrication and cost in order to develop a cavity that is suitable for the energy upgrade plan.

INTRODUCTION

The Facility for Rare Isotope Beams (FRIB) is a heavy ion linac under construction at Michigan State University. FRIB is a unique linac in such a way that it accelerates multi-species ions. FRIB baseline design will accelerate ions to energies ≥ 200 MeV/u. It will accelerate all stable ion beams from Proton to Uranium. FRIB has an energy upgrade plan [1] and prepares a vacant space of approximately 74 meters in the design stage and cryogenic capacity to accommodate the plan. Cavity class choice is important for the energy upgrade due to the dependence of transit time factor curve width (velocity acceptance) on number of gaps. For multi-species linac such as FRIB, less gaps increase velocity acceptance as shown in Figure 1 where Transit Time Factor (TTF) versus beta geometry is plotted for varies number of gaps for elliptical cavity. For instance, in FRIB elliptical cavities with high number of acceleration gaps will be inefficient for Protons due to the Proton's beta will fall in the transit time factor curve tail.

Transit time factor model equations are below [2].

$$T = \left(\frac{\beta}{\beta g}\right)^2 sin\left(\frac{\pi N}{2\beta/\beta g}\right)\frac{(-1)^{(N+2)/2}}{N((\beta/\beta g)^2 - 1)} \qquad (1),$$

for odd number of gaps

$$T = \left(\frac{\beta}{\beta g}\right)^2 cos\left(\frac{\pi N}{2\beta/\beta g}\right)\frac{(-1)^{(N-1)/2}}{N((\beta/\beta g)^2 - 1)} \qquad (2),$$

for even number of gaps

*Work supported by the U.S. Department of Energy Office of Science under Cooperative Agreement DE-SC0000661.
†shanab@nscl.msu.edu

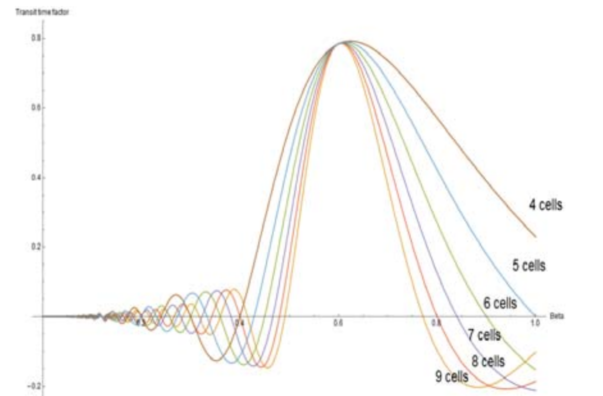

Figure 1: Transit Time Factor (TTF) vs. beta with varying number of cells (gaps) for elliptical cavities.

POSSIBLE CAVITY CLASSES

FRIB energy upgrade linac design has to choose an optimized cavity class: cavity frequency, number of cells for the cavity, and beta geometry for multi-species in order to maximize the benefits for FRIB upgrade. Table 1 compares potential cavity classes where the crucial cavity parameters are quantitatively presented. One can note that the higher operating frequency can allow the higher accelerating gradient. In contrast, compared to elliptical cavities the FRIB beta=0.53 Half Wave Resonator (HWR) has higher transit time factor at beta optimum. Whereas, elliptical cavity has higher acceleration efficiency (R/Q). The cavity aperture is kept the same as the FRIB HWR aperture (40 mm). For elliptical cavity classes, a small aperture lowers cell to cell coupling. FRIB beam current is very low (several mA). This parameter won't play an important role in the energy upgrade plan. An overview of potential cavity classes for FRIB energy upgrade are discussed in next page to see their advantages and disadvantages.

- *FRIB beta = 0.53 Half Wave Resonator (HWR)*

No R&D is needed in this case. FRIB already uses the 0.53 HWR. Eight 0.53 HWR cryomodules will be utilized for the upgrade.

- *Spoke cavity*

Spoke cavity has benefits for low frequency and heavy beam loaded cavities, however these benefits are not so important for FRIB energy upgrade because of the low current machine. Due to the complexity of the cavity shape, cavity production cost is a concern.

ISBN 978-3-95450-169-4

PIP-II INJECTOR TEST: CHALLENGES AND STATUS*

P. F. Derwent†, J.P. Carneiro, J. Edelen, V. Lebedev, L. Prost,
A. Saini, A. Shemyakin, J. Steimel
Fermi National Accelerator Laboratory, Batavia IL 60510, USA

Abstract

The Proton Improvement Plan II (PIP-II) at Fermilab is a program of upgrades to the injection complex. At its core is the design and construction of a CW-compatible, pulsed H- superconducting RF linac. To validate the concept of the front-end of such machine, a test accelerator known as PIP-II Injector Test is under construction. It includes a 10 mA DC, 30 keV H- ion source, a 2 m-long Low Energy Beam Transport (LEBT), a 2.1 MeV CW RFQ, followed by a Medium Energy Beam Transport (MEBT) that feeds the first of 2 cryomodules increasing the beam energy to about 25 MeV, and a High Energy Beam Transport section (HEBT) that takes the beam to a dump. The ion source, LEBT, RFQ, and initial version of the MEBT have been built, installed, and commissioned. This report presents the overall status of the Injector Test warm front end, including results of the beam commissioning through the installed components, and progress with SRF cryomodules and other systems.

THE PIP-II PROJECT

The Proton Improvement Plan-II (PIP-II) is a high-intensity proton facility being developed to support a world-leading neutrino program over the next two decades at Fermilab. PIP-II is an integral part of the U.S. Intensity Frontier Roadmap as described in the Particle Physics Project Prioritization Panel (P5) report of May 2014 [1]. PIP-II is focused on upgrades to the Fermilab accelerator complex capable of providing a beam power in excess of 1 MW on target at the initiation of Long Baseline Neutrino Facility [1,2] operations and is a part of a longer-term concept to achieve multi-MW capabilities at Fermilab. PIP-II is a Department of Energy project following the critical decision (CD) process and guidelines of DOE Order 413.3b [3]. The project does anticipate in-kind contributions from international partners, with significant contributions from India. At the present time, PIP-II received designation of CD-0 ("Mission Need") in November 2015. A Reference Design Report was completed in 2015 [4].

R&D STRATEGY

The R&D Strategy is designed to mitigate technical and cost risks by validating the choices made in the facility design and by establishing fabrication methods for major subsystems and components, including the qualification of suppliers. There are 5 key aspects to the strategy:

1. Development and operational test of PIP-II Front End covering the first 20 MeV.

2. Development and demonstration of cost effective superconducting radio frequency acceleration systems at three different frequencies (162.5 MHz, 325 MHz, 650 MHz) and with RF duty factors ranging from 10% to 100%.

3. Development of a Booster injection system capable of accepting beam pulses from the SC Linac.

4. Development of system designs capable of supporting a 50% increase in the proton beam intensity accelerated and extracted from the Booster/Recycler/Main Injector complex.

5. Development of requisite capabilities at international partner institutions to successfully contribute to SC Linac construction.

In this paper we will describe the first step in this strategy, the development and operational test of the front end (PIP-II Injector Test or PI-Test).

The PI-Test program will develop and perform an integrated system test of the room temperature front end [5, 6] and the first two superconducting cryomodules [7]. The hardware layout is shown in Figure 1.

PIP-II INJECTOR TEST

PI-Test will install and test hardware with the following scope:

- A H^- source capable of up to 10 mA at 30 keV
- A Low Energy Beam Transport (LEBT) using unneutralized transport in the downstream part of the line and beam chopping
- A Continuous Wave RadioFrequency Quadrupole (RFQ) operating at 162.5 MHz and capable of delivering 5 mA at 2.1 MeV
- A Medium Energy Beam Transport (MEBT) with an integrated wide band chopper capable of generating arbitrary bunch patterns at 162.5 MHz
- Two low β superconducting cryomodules, utilizing half wave (HWR) and single spoke resonators (SSR1), capable of accelerating 2 mA of beam to 25 MeV
- Beam dump capable of accommodating 2 mA at full beam energy
- Associated utilities and shielding

The Ion source and LEBT were commissioned in 2015. The RFQ was commissioned during 2016 [9], with the full Medium energy beam transport to follow in 2017. Initial

* Operated by Fermi Research Alliance, LLC under Contract No. DE-AC02-07CH11359 with the United States Department of Energy.
† derwent@fnal.gov

ISBN 978-3-95450-169-4

ASSEMBLY OF XFEL CRYOMODULES: LESSONS AND RESULTS

S. Berry†, O. Napoly
CEA, IRFU, SACM, Centre d'Etudes de Saclay, 91191 Gif-sur-Yvette Cedex, France

Abstract

The industrialized string and module assembly of 103 European XFEL cryomodules has been performed at CEA-Saclay between September 2012 and the July 2016. The general features and achievements of this construction project will be reviewed, including lessons learned regarding organization, industrial transfer, quality control and assembly procedures. An overview of the cryomodule performance and RF test results will be presented.

INTRODUCTION

The accelerator of the European XFEL is assembled out of 101 superconducting accelerator modules being contributed by DESY (Germany), CEA Saclay, LAL Orsay (France), INFN Milano (Italy), IPJ Swierk, Soltan Institute (Poland), CIEMAT (Spain) and BINP, Russia. The 17.5 GeV Linac is made of 808 9-cells cavities at 1.3 GHz and 25 RF stations of 5.2 MW each.

The CEA was in charge of assembly of 103 accelerator modules on the Saclay site and with CEA infrastructure while the workforce is given by an industrial contractor Alsyom. The very challenging delivery rate was to produce one module per week. The performance goal is an accelerating gradient E_{acc} > 23.6 MV/m and a quality factor Q_0 > 1^{10} at 2 K.

In this paper, the preparation phase of this construction project will be briefly reminded, then the achievements including lessons learned regarding organization, industrial transfer, quality control are presented, finally the cryomodules performance are analysed regarding the assembly procedures. Some cryomodules repair activities will also be presented.

Due to their good performances 96 modules are enough to meet the energy goal with some margins. These 96 modules have been installed in the tunnel. More details on the status of XFEL are presented in [1].

PREPARATION PHASE

A set of three building have been refurbished and assembly halls were organised in 7 workstations (WS). The so-called XFEL Village consists of 200 m² clean room complex with 112 m² under ISO4 allows assembling the couplers to the cavity and two cavity strings in parallel; the cryostating will be held on the 1325 m² of assembly platforms and 400 m² are dedicated to storage [2]. During the preparation phase, many automated or demi-automated test benches have been developed. DESY lent CEA nine pumping systems (with mass-spectrometers) and one laser-tracker. INFN developed for the Saclay site two piezo tuner control racks, CEA bought a washing machine to enter parts into ISO4 clean room, and three pumping units (slow-venting) with leak detector in the cleanroom dedicated to non-vacuum experts. CEA developed four RF crates for automatized RF measurements namely RF spectra, transmission and field flatness measurements and Time Domain Reflexion. This crates have been used at different workstations to: control the HOM coupler rejection filter, monitor the cavity tuner installation, tune the HOM and check RF cable integrity.

The breakdown of the total assembly work over 7 workstations aims at:

- balancing almost equally the occupancy of each WS,
- bringing the longest WS occupancy below 5 days, it impacts directly the throughput

Preparation phase was also used to qualify the providers of the parts CEA had in charge: beam vacuum gaskets and fastening, multi-layer insulation and magnetic shielding. For one module, there are 9 422 individual components integrated and over 12 400 individual parts manipulated per cycle time. The use of reliable Enterprise Resource Planning ERP is highly recommended.

PRODUCTION PHASE

Cryomodule Production

A detailed presentation of the cryomodule mass production is given in [3]. The modules delivery to DESY ends on 2016 July the 28th. In total 103 modules were delivered to DESY (including the so-called pre-series cryomodules XM-3, XM-2, XM-1).

Figure 1 shows the number of cryomodule produced as a function of the delivery dates. As indicated in Figure 1, in 2015, one cryomodule was delivered every 4 working days, 52 in total. The Cold Linac will also include two pre-series cryomodules: XM-2 and XM-1.

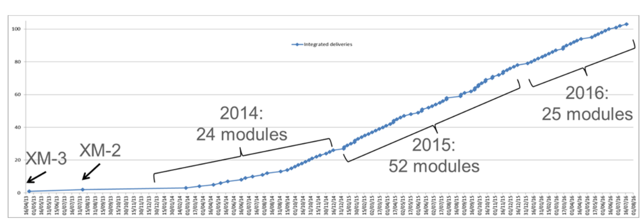

Figure 1: Number of cryomodules delivered vs. the delivery dates, from XM-3, XM-2, XM-1 and XM1-XM100.

Figure 2 shows the production throughput over time. The throughput of one module every 5 days have been reached mid-October 2014 with XM15 confirming that the design of the Assembly Infrastructure was correct.

Thanks to organisational efforts, the 4-day throughput was reached in January 2015 with XM25 and maintained till the completion.

† email address: stephane.berry@cea.fr

THE SUPERCONDUCTING RADIO-FREQUENCY LINEAR ACCELERATOR COMPONENTS FOR THE EUROPEAN SPALLATION SOURCE: FIRST TEST RESULTS

C. Darve†, N. Elias, F. Schlander, European Spallation Source, Lund, Sweden
P. Bosland, C. Arcambal, E. Cenni, G. Devanz, F. Peauger, CEA-IRFU, Paris, France
G. Olry, S. Bousson, P. Duthil, G. Olivier, D. Reynet, CNRS-IPN, Orsay, France
G. Costanza, Lund University, Lund, Sweden
R. Ruber, H. Li, R. Santiago Kern, Uppsala University, Uppsala, Sweden

Abstract

The European Spallation Source requires a pulsed linac with an average beam power on the target of 5 MW, which is about five times higher than the most powerful spallation source in operation today. Over 97 % of the acceleration occurs in superconducting cavities. ESS will be the first accelerator to employ double spoke cavities to accelerate beam. Accelerating gradients of 9 MV/meter is required in the spoke section. The spoke section will be followed by 36 elliptical 704 MHz cavities with a geometrical β of 0.67 and elliptical 704 MHz cavities with a geometrical β of 0.86. Accelerating gradients of 16.7 and 20 MV/m are required in the medium and high-β elliptical cavities, respectively. Initial gradient test results will be presented in which results exceed expected requirements.

THE ESS LINEAR ACCELERATOR

The ESS new facility is composed of a 5 MW proton linear accelerator (linac), a tungsten target to produce neutrons by spallation reaction and experimental neutron beam lines [1]. The ESS Superconducting Radio-Frequency linac has been designed to deliver to the target a time averaged proton beam power of 5 MW at the completion with a nominal current of 62.5 mA with a stage at 1 MW in 2019. The proton linac is a long pulse machine with 2.86 ms beam pulse length and 14 Hz pulse repetition rate giving a duty cycle of 4 %.

Figure 1 shows the layout of the ESS linac, Optimus + [2]. The superconducting linear accelerator lattice redesign has permitted to optimize the layout of the linear accelerator using a transition energy of 90 MeV with the normal conducting linac and reaching 2 GeV at the target. It accelerates a high intensity proton beam using a 50 m long warm linac, which increases the beam energy up to 90 MeV and a 312 m long cold linac to reach the final energy of 2 GeV.

The choice of Superconducting Radio-Frequency (SRF) technology is a key element in the development of the ESS accelerator. The SRF linac is composed of three families of cavity strings, which operate at 2 K [3-5].

In the framework of the ESS-CEA-CNRS cooperation agreement, signed in 2009, IPN Orsay and CEA Saclay are intensively involved in ESS project by leading the design of the whole spoke (WP04) and elliptical cryomodules (WP05) of the linac, respectively. Technology demonstrators are being designed, fabricated and tested for the spoke and the elliptical cavities and cryomodules. Those demonstrators will validate the technologies to be implemented for the ESS SRF linac series production.

According to the agreed In-Kind Contributions the series spoke cavities and cryomodules are fabricated and tested in IPN Orsay before being tested at high power in Uppsala University, then shipped to Lund.

The production of the elliptical cavities is distributed between LASA and STFC, who provide the medium- β and high- β elliptical cavities, respectively. Then, the elliptical cavities are assembled with their fundamental power couplers and cold tuning systems, before being assembled into cryomodules in CEA Saclay, using the experience learned from the X-FEL project. Finally, the cryomodules are shipped to Lund to be tested at high-power in collaboration with the IPJ Polish institute, before being installed in the ESS tunnel.

Since the main components are being fabricated by institutions located outside the Lund area, the integration and interfacing of each resulting components must be carefully planned. Hundreds of requirements have been identified to best integrate the SRF components in the ESS tunnel. The requirements are also used to define the interfaces with the conventional facilities, the control system and to define the operating modes for the ESS SRF linac [6-7].

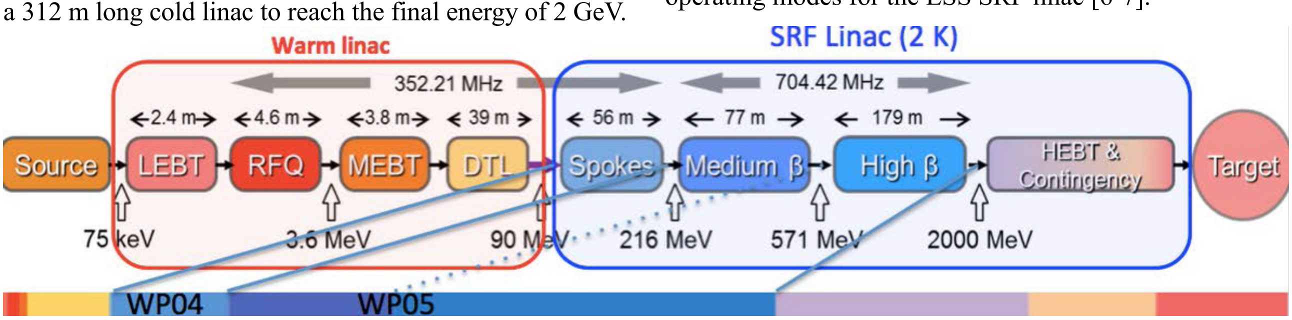

Figure 1: Block diagram of the Optimus+.

†christine.darve@esss.se

ISBN 978-3-95450-169-4

PERFORMANCE ANALYSIS OF THE EUROPEAN XFEL SRF CAVITIES, FROM VERTICAL TEST TO OPERATION IN MODULES

N. Walker[†], D. Reschke, J. Schaffran, L. Steder, M. Wenskat, DESY, Hamburg, Germany
L. Monaco, INFN Milano, LASA, Milano, Italy

Abstract

More than 800 resonators have been fabricated, vertically qualified and operated in module tests before the accelerating module installation in the linac, which will be completed before the conference. An analysis of this experience, with correlation of the final cavity performances with production, preparation and assembly stages, is underway and at the time of the conference a summary of the activities will be available.

INTRODUCTION

The construction of the 17.5-GeV SRF linac for the European XFEL (EXFEL) [1] is now complete. A total of 102 cryomodules (100 series modules and 2 pre-series) have been successfully constructed in a period of three years from 816 1.3-GHz nine-cell Tesla cavities entirely produced by industry and tested at DESY. The completed cryomodules were returned to DESY for testing before installation in the tunnel. Finally 97 of the total 102 cryomodules have been installed; the last four cryomodules were not installed due to schedule constraints.

All individual cavities (cold vertical test) and completed cryomodules (module test) were tested at the purpose-built Accelerator Module Test Facility (AMTF) at DESY [2,3,4]. All testing was performed by a team from IFJ-PAN Krakow, as part of an in-kind contribution to EXFEL. A peak cryomodule production rate of 1.25 cryomodules per week was achieved from the beginning of 2015, successfully matched by AMTF testing rates.

In this paper we present the final production statistics of the cavity cold vertical tests and cryomodule tests. For the cavity production, we present both an analysis of the factors limiting the gradient performance, as well as steps taken to acceptably recover low-performance cavities. The high-power pulsed RF results from the cryomodule tests will then be presented, and a rough comparison of the observed performance in both the vertical and module tests made. Finally the expected installed linac performance will be discussed.

CAVITY PRODUCTION

Industrial Cavity Production

A comprehensive review of the cavity production for the EXFEL can be found in [5]. Here we briefly summarise the key points by way of introduction to the latter sections of this report.

The total cavity production for EXFEL was split equally between two vendors (E. Zanon Spa. (EZ), Italy, and Research Instruments GmbH (RI), Germany), and included both the mechanical fabrication and the surface-polishing chemical treatments. Cavity production followed the so-called "build to print" concept [6], with no cold RF performance requirement of the vendors. DESY accepted the responsibility for recovering low performance cavities. The niobium material was purchased by DESY and after quality control sent to the vendors [7,8].

The cavities were delivered to DESY fully equipped with helium tank, flanges, HOM antennae, pick-up probe, and a fixed-coupling high-Q input coupler antenna, ready for cold vertical testing (see Fig. 1).

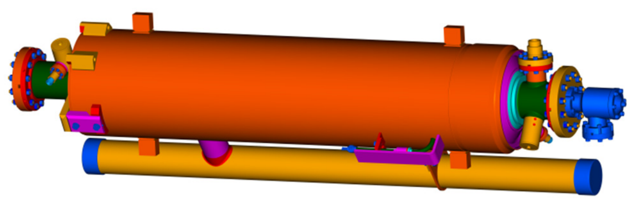

Figure 1: 3-D model of a fully-equipped XFEL cavity as delivered to DESY:

Cavity production differed at the two vendors in the choice of the final chemical surface polishing. The surface preparation at both vendors started with a bulk electro-polishing (EP) followed by 800° annealing, but for the final surface treatment two alternative recipes have been used: EZ applied a final chemical surface removal ("Flash-BCP"), while RI applied a final EP ("Final EP").

Cavity production began in in early 2013 and ramped up to an average total production rate of approximately 30 cavities per month at the end of that year. Production then continued through to the end of 2016. Of the total of 844 cavities successfully produced, 816 were used for the construction of cryomodules. The remainder were special cavities used for infrastructure commissioning and testing, as well as the so-called HiGrade cavities [9], delivered without helium tank and used throughout production for QA and also R&D.

COLD VERTICAL TEST PERFORMANCE

Overview of Cold Vertical Testing

As previously noted, the cavities were delivered to DESY from the vendor ready for cold vertical testing at AMTF. The extensive QA/QC checks performed before and after the vertical test are described here [10]. All of the 816 sent for cryomodule assembly and the 16 remaining HiGrade cavities underwent at least one cold vertical

[†]nicholas.walker@desy.de

ISBN 978-3-95450-169-4

HIE-ISOLDE SC LINAC PROGRESS AND COMMISSIONING IN 2016

W. Venturini Delsolaro, E. Bravin, N. Delruelle, M. Elias, E. Fadakis, J.A. Ferreira, F. Formenti, M. A. Fraser, J.C. Gayde, N. Guillotin, Y. Kadi, G. Kautzmann, T. Koettig, Y. Leclercq, M. Martino, M. Mician, A. Miyazaki, E. Montesinos, V. Parma, J.A. Rodriguez, S. Sadovich, E. Siesling, D. Smekens, M. Therasse, L. Valdarno, D. Valuch, G. Vandoni, U. Wagner, P. Zhang

CERN, Geneva, Switzerland

Abstract

After the first successful physics run with radioactive ion beams at HIE ISOLDE, in October 2015 [1], the staged deployment of the linac continued in 2016 by adding a second cryomodule and by refurbishing the first one. During the physics run with one cryomodule, the second cryomodule was being assembled. The refurbishment of the first cryomodule was made necessary to overcome limits imposed by thermal instabilities of the fundamental coupler lines. A modified design for the power couplers was developed and implemented on all the cavities, after extensive validation tests in a vertical cryostat. The paper will describe the lessons learnt from the first commissioning campaign, in particular concerning the fundamental power coupler, the solution adopted, and the results of the 2106 commissioning campaign with two cryomodules, which will allow reaching 5.5 MeV/u for all the species available at ISOLDE.

INTRODUCTION

The HIE ISOLDE project [1] reached an important milestone in October 2015, when the first radioactive ion beam was delivered to the users [2]. A ^{74}Zn beam was accelerated up to ~4 MeV/u by a single cryomodule hosting 5 superconducting quarter wave resonators and a superconducting solenoid for transverse focusing. This cryomodule, a prototype in all respects, had been entirely designed and assembled at CERN, with industrial partners supplying some of the main components. The heart of it, the Nb sputtered superconducting cavities, were manufactured at CERN [3] starting from copper substrates produced in industry. The cryomodule was installed in the new linac, deployed in 2015 with its cryogenics facilities and high energy beam transfer lines.

LESSONS LEARNT IN 2015

The commissioning campaign of 2015 brought to the surface a problem in the RF power coupling system, which was found to be thermally unstable at the chosen operational bandwidths. When running in self-excided loop mode, with constant forward power, the cavity fields were observed to steadily decrease while the loaded bandwidth was increasing and the resonance frequency dropped (see Fig.1). When running in feedback mode, field and frequency could be kept constant only at the price of constantly increasing the forward power.

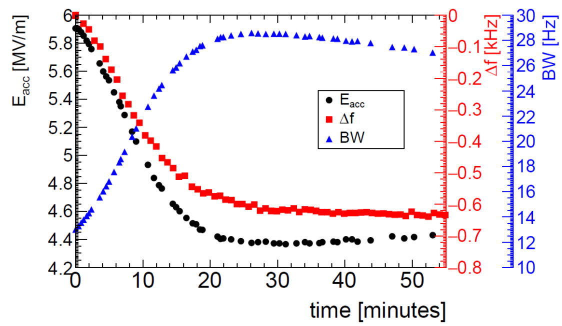

Figure 1: Thermal runaway, as seen in the RF signals.

All these signs were interpreted as the result of the thermal expansion of the coupler antennas.

Detailed thermal and RF models were developed in order to better understand the mechanism at work. The main finding of RF simulations done with CST MS was that a localized RF heating is present on the tip of the capacitive coupling antenna, when the cavity is loaded at the operational bandwidths. The coupler system was modelled with ANSYS, solving the relevant time dependent and non-linear heat equation. The output of the RF simulation was used for the distributed heat source. The calculations showed that the thermal anchoring of the RF cable was not optimal, and that the temperature distribution peaked at the tip of the antenna, reaching 600 K. Dedicated tests in a vertical cryostat confirmed that a thermal runaway could be initiated which would have eventually destroyed the couplers. Figure 2 shows a post mortem dissection of a test coupler after a stress test done for 3 hours at 200 W RF power in the vertical test stand.

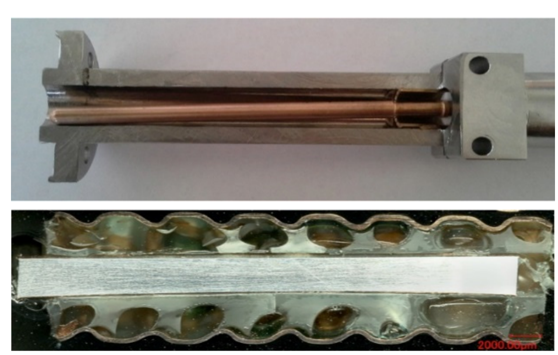

Figure 2: Sections of damaged coupler and RF cable after stress test in vertical cryostat.

ISBN 978-3-95450-169-4

STATUS OF SPIRAL2 AND RFQ BEAM COMMISSIONING

R. Ferdinand, P. Bertrand, M. Di Giacomo, H. Franberg, O. Kamalou, JM. Lagniel, G. Normand, A. Savalle, F. Varenne, GANIL, Caen, France
D. Uriot, CEA/IRFU, Saclay, France
JL. Biarrotte, IN2P3, Orsay, France

Abstract

The SPIRAL2 project beam commissioning is started and the superconducting linac installation is being finalized. In parallel with the installations, the first proton beam was extracted in 2014 and the expected beam performances were achieved from both light and heavy ion sources. The conditioning of the RFQ started in October 2015, and the beam commissioning soon after that. After having briefly recalled the project scope and parameters, the present situation of the RFQ beam commissioning is presented.

INTRODUCTION

GANIL is significantly extending its facility with the new SPIRAL2 project based on a multi-beam Superconducting CW linac driver [1, 2].

This new SPIRAL2 facility has two dedicated experimental areas in the fields of Neutron for Science (NFS) and very heavy and super heavy element production (S3). The SC linac is composed of 12 low β and 7 high β cryomodules, including a β=0.07 cavity and two β=0.12 cavities respectively. The status of the installation and commissioning is explained.

PROJECT STATUS

Beams Requirements

The layout of the SPIRAL2 driver takes into account a wide variety of beams to fulfill the physics requests. It is a high power CW superconducting linac delivering up to 5 mA proton and deuteron beams or 1 mA ion beams for Q/A > 1/3 (Table 1). Our major challenges are to handle the large variety of different beams due to their different characteristics (in terms of particle type, beam currents – from a few µA to a few mA - and/or beam energy), a high beam power (200 kW, CW) and to answer correctly to the safety issues, especially with the deuteron beam.

Table 1: Beam Specifications

Particles	H^+	D^+	ions	option
Q/A	1	1/2	1/3	1/6
Max I (mA)	5	5	1	1
Max energy (MeV/A)	33	20	15	8.5
Max beam power (kW)	165	200	45	51

Injector

The injector is composed of two specialized ECR ion sources and of a warm RFQ connected to the superconducting LINAC. Both ECR sources and their Low Energy Beam Transport lines (LEBT) have been successfully tested and qualified at an earlier stage [3] in the past years at LPSC Grenoble and IRFU Saclay. The two ion sources and their respective LEBT are now installed in the SPIRAL2 building (Fig. 1). The first proton beam was extracted on December 19, 2014. The First heavy-ion beam at was obtained in July 10, 2015 (230 µA argon 9+).

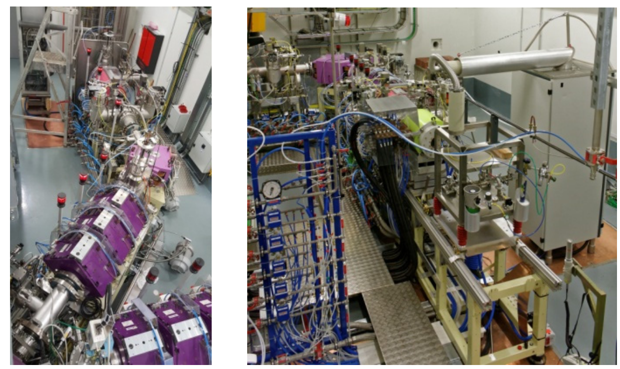

Figure 1: sources and LEBT at GANIL/SPIRAL2. Left : light ion source (H^+, D^+), right : heavy ions (Q/A=1/3).

On December 03, 2015 the 88.0525 MHz RFQ cavity was ready for beam, and the first proton beam was successfully accelerated. The theoretical 100% transmission was obtained after a few hours.

The next step will be to accelerate the Q/A=1/3 heavy ions after completion of the full RF power RFQ conditioning.

LINAC

Eighteen of the nineteen superconducting cryomodules are installed (Fig. 2). The last cryomodule is currently under maintenance (small helium leak).

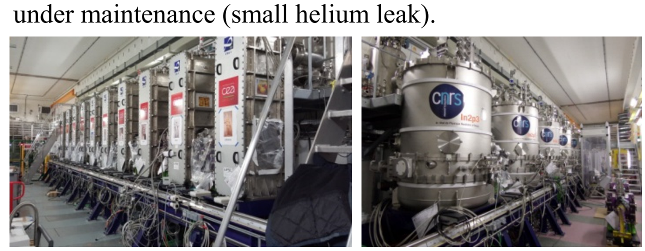

Figure 2: Cryomodules in the linac tunnel.

Warm sections including two quadrupole magnets and a BPM are located between the cryomodules. The first five warm sections also include a longitudinal bunch extension monitor (BEM) to allow a complete beam tuning.

All the valve-boxes needed to be repaired. It was a very long process to manage that delayed the installation by one year.

FRIB CRYOMODULE DESIGN AND PRODUCTION*

T. Xu†, H. Ao, B. Bird, N. Bultman, E. Burkhardt, F. Casagrande, C. Compton, J. Crisp, K. Davidson, K. Elliott, A. Facco[1], R. Ganni, A. Ganshyn, W. Hartung, M. Ikegami, P. Knudsen, S. Lidia, I. Malloch, S. Miller, D. Morris, P. Ostroumov, M. Reaume, J. Popielarski, L. Popielarski, M. Shuptar, S. Shanab, G. Shen, S. Stark, K. Saito, J. Wei, J. Wenstrom, M. Xu, Y. Xu, Y. Yamazaki and Z. Zheng, Facility for Rare Isotope Beams, Michigan State University, East Lansing, MI, USA
M. Wiseman, Thomas Jefferson National Accelerator Facility, Newport News, VA, USA
M. Kelly, Argonne National Laboratory, Lemont, IL, USA
R. Laxdal, TRIUMF, Vancouver, Canada
K. Hosoyama, High Energy Accelerator Research Organisation, Tsukuba, Japan
[1]also at INFN - Laboratori Nazionali di Legnaro, Legnaro (Padova), Italy

Abstract
The Facility for Rare Isotope Beams (FRIB), under construction at Michigan State University, will utilize a driver linac to accelerate stable ion beams from protons to uranium up to energies of >200 MeV per nucleon with a beam power of up to 400 kW. Superconducting technology is widely used in the FRIB project, including the ion sources, linac, and experiment facilities. The FRIB linac consists of 48 cryomodules containing a total of 332 superconducting radio-frequency (SRF) resonators and 69 superconducting solenoids. We report on the design and the construction of FRIB cryomodules.

INTRODUCTION

The Facility for Rare Isotope Beams (FRIB) at Michigan State University (MSU) will advance the frontier of heavy-ion beam power by two orders of magnitude compared to existing accelerators when it reaches its design beam power of 400 kW [1]. In August 2013, the US Department of Energy (DOE) Office of Science approved the project baseline and start of civil construction (CD2-3a) with a total project cost of $730M, funded by DOE, MSU and the State of Michigan. FRIB obtained CD-3b approval from DOE in August 2014, and technical construction began in October 2014. The FRIB linac design has been developed and optimized through several iterations [2-6], with the goal of minimizing the overall project cost while maintaining the design performance and upgrade potential.

Figure 1 shows a schematic of the driver linac, which includes three linac segments with 44 accelerating modules and 2 folding segments with 4 matching cryomodules. The FRIB resonators are optimized for 4 different velocities: $\beta = v/c = 0.041$, 0.085, 0.29, and 0.53. Quarter-wave resonators (QWRs) at 80.5 MHz are used for low velocities and half-wave resonators (HWRs) are used for medium velocities. The cryomodules contain superconducting resonators and superconducting solenoids with a peak field of 8 T for transverse focusing. The solenoids include dipole windings for horizontal and vertical steering. The low-β cryomodules include beam position monitors (BPMs). The cryomodule element counts are listed in Table 1. At completion, FRIB will be one-of-a-kind large scale low-beta and medium-beta superconducting linac.

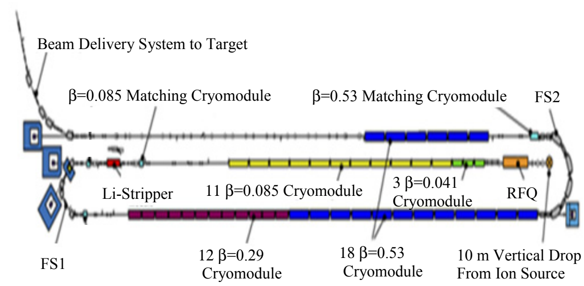

Figure 1: FRIB driver linac. The beam is produced in an ion source (orange), with the first stage of acceleration done in a copper radio-frequency quadrupole (RFQ, orange). Then the beam travels through the SRF cryomodules. Charge stripping is done before the first folding segment (FS1) to improve the acceleration efficiency.

FRIB CRYOMODULE DESIGN

As shown in Figure 2, the FRIB cryomodules consist of a cold mass, baseplate, cryogenic system, thermal shield, magnetic shield, and vacuum vessel. This modular design allows us to use the same construction sequence for all 6 cryomodule types. The design introduces the innovation of a "bottom-up" assembly starting with the baseplate and ending with the installation of the vacuum vessel from the top. The bottom-up approach is different from the more traditional "top-down" approach, in which the cold mass is suspended from a top plate and lowered into a vacuum vessel. The bottom-up design, along with a carefully-engineered kinematic support system, ensures the placement of cavities and solenoids within alignment tolerance, without an actual alignment step, which tremendously reduces the cryomodule assembly time. This design concept was validated with an Engineering Test Cryomodule ETCM [7, 8]. The FRIB cryomodule design also adopted a U-tube interface with cryo-distribution developed by Jefferson Laboratory (JLab) for cryomodules at CEBAF and the Spallation

* Work supported by the U.S. Department of Energy Office of Science under Cooperative Agreement DE-SC0000661
† xuti@frib.msu.edu

PLASMA PROCESSING TO IMPROVE THE PERFORMANCE OF THE SNS SUPERCONDUCTING LINAC

M. Doleans, R. Afanador, J.A. Ball, D.L. Barnhart, W. Blokland, M.T.Crofford, B.D.Degraff, S.W.Gold,B. S.Hannah, M.P.Howell, S-H.Kim, S-W.Lee, J. Mammosser, C.J. McMahan, T.S.Neustadt, J.W.Saunders, S.Stewart, W.H.Strong, P.V. Tyagi, D.J.Vandygriff, D.M. Vandygriff, Oak Ridge National Laboratory, Oak Ridge, TN, USA

Abstract

An in-situ plasma processing technique has been developed at the Spallation Neutron Source (SNS) to improve the performance of the superconducting radio-frequency (SRF) cavities in operation. The technique uses a low-density reactive neon-oxygen plasma at room-temperature to improve the surface work function, to help removing adsorbed gases on the RF surface and to reduce its secondary emission yield. Recently, the plasma processing technique has been applied to one offline cryomodule and to two cryomodules in the linac tunnel. Improvement of the accelerating gradient has been observed in all three cryomodules.

INTRODUCTION

The SRF cavities at the SNS are operated at 805 MHz in pulsed mode with 60 Hz repetition rate [1]. The cavities are packaged in cryomodules hosting 3 or 4 cavities cooled down to 2 K during neutron production. The average accelerating gradient of the 81 cavities installed in the linac tunnel is 12.5 MV/m. Thermal instabilities at the extremities of the cavities induced primarily by field emitted electrons prevent from operating cavities at higher accelerating gradients [2]. Field emission process in SRF cavities has been linked to surface defects and to particulate contamination at the high electric field regions on the RF surface. Surface studies on small samples and residual gas analysis during warm-up of operated cryomodules at the SNS indicate that hydrocarbon contamination can also be present at the niobium surface and measurements using the Kelvin probe method show that such contamination tends to lower the work function of the surface and be an aggravating factor for field emission [3, 4].

The new in-situ plasma processing technique developed at the SNS removes the hydrocarbon contaminants from the niobium surface using a reactive neon-oxygen plasma. The volatile by-products of oxidation are continuously removed from the cavity volume by vacuum pumping. Cold-test of dressed cavities in the horizontal test apparatus at the SNS showed that plasma processing can help increasing their accelerating gradient [3]. The new cleaning technique has since been applied to three SNS cryomodules, one offline cryomodule and two cryomodules in the linac tunnel.

PLASMA PROCESSING OF CRYOMODULES AT THE SNS

The plasma processing technique was developed and tested using individual cavities but was designed to be directly applicable to SNS cryomodules. For example, the plasma processing gas manifolds and RF stations are packaged in carts that can easily be rolled into place to plasma process a cryomodule in the SNS linac tunnel as shown in Figure 1.

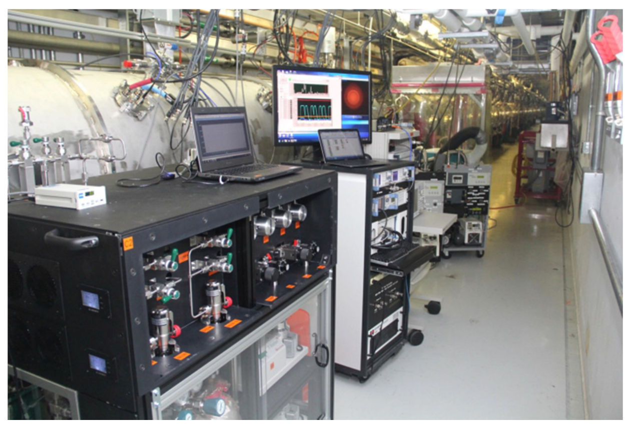

Figure 1: Plasma processing of a cryomodule in the SNS linac tunnel.

The SNS superconducting linac is segmented with a warm section after each cryomodule. The warm sections have quadrupole doublets for transverse focusing of the H^- beam and concomitant beam diagnostics. Sector gate valves are located at the extremities of each cryomodule which allows the vacuum space of a module to be isolated from the rest of the linac, for example when thermal cycling is performed. An ion pump is installed on each cryomodule and on each warm section and a pumping port with a manual valve is available at each pump. The valves are in closed position and capped during normal operation. The sector gate valves and the manual valves are being used to plasma process cryomodules individually without affecting near-by cryomodules and without requiring venting of the beamline.

ISBN 978-3-95450-169-4

OPERATION OF KOMAC 100-MEV LINAC*

Han-Sung Kim†, Hyeok-Jung Kwon, Yong-Sub Cho
Korea Atomic Energy Research Institute, Korea Multi-purpose Accelerator Complex
Gyeongju, Gyeongbuk, Republic of Korea

Abstract

A 100-MeV proton linear accelerator at the KOMAC (Korea Multi-purpose Accelerator Complex) was under development for past 15 years, including preliminary design study period, and was successfully commissioned in 2013. The operation of the linac for user service started in July 2013 with two beam lines: one for a 20 MeV beam and the other for a 100-MeV beam. The linac is composed of a 50 keV microwave proton source, a 3 MeV four-vane-type RFQ (radio-frequency quadrupole) and a 100 MeV DTL (drift tube linac). In 2015, the linac operating time was more than 2,800 hours with an availability of better than 89% and unscheduled downtime was about 73 hours, mainly due to the ion source and HVCM problems. More than 2,100 samples from various fields such as material science, bio and nano-technology and nuclear science, were treated in 2015. Currently, additional beam line for radioisotope production is being commissioned and a new beam line for low-flux irradiation experiments is under construction along with a continuous effort being made to increase the average beam power.

INTRODUCTION

KOMAC is a facility for hadron beam application hosting a 100 MeV proton linac and several low energy ion beam accelerator including a 3 MeV tandem machine and ion implanters. It was established as a branch of KAERI (Korea Atomic Energy Research Institute) in 2013. Gross area of the KOMAC site is 1,100 m by 400 m, which is enough to host a 1 GeV proton machine and 450 m by 400 m was developed up to now for the 100 MeV linac as a first phase as shown in Fig. 1. The remaining are is reserved for future extension [1].

Currently, buildings for a 100-MeV linac, low energy beam applications, utility systems, the electric power station and water treatment are completed and under operation. In addition, a building for guest house is under construction and will be finished at the end of this year. The construction of the administration building is supposed to start in October, 2016.

The user beam service of the linac started in 2013 after the inspection for operation license from government. At first, we started user beam service with two beam lines and target stations, even though KOMAC has design capacity of ten beam lines and target stations. To meet various and dedicated requirements from users, we developed a beam line for radio-isotope production in 2015 and demonstrated a RI production by using low current test run. The commissioning of the RI production beam line is almost completed and it is waiting for the operational license. In addition, a new beam line for low-flux beam applications such as space environment simulation and detector test is under construction. The operational experiences of a 100 MeV proton linac are given and some issues are discussed in this paper.

Figure 1: KOMAC site.

OPERATION OF 100 MEV LINAC

Accelerator

The 100 MeV proton linac is installed in an accelerator building. It consists of a 50 keV microwave ion source, a 3 MeV four-vane-type RFQ and a 100 MeV DTL. The accelerator building is a three-story building; first floor is hosting a linac, second floor is a klystron gallery and third floor is a modulator room. The layout of the accelerator building with a linac is shown in Fig. 2. The main specifications of the 100 MeV linac are summarized in Table 1. One of characteristics of the linac is that there are two beam extraction points; one is at 20 MeV and the other is at 100 MeV.

We use a microwave ion source (2.45 GHz) due to its long life time without maintenance. For the LEBT (low energy beam transport), two solenoids are used to match the beam to the RFQ. The RFQ is a four vane type and used to bunch the beam from the ion source and accelerate the beam up to 3 MeV. Total 11 DTL tanks are installed to accelerate the beam from 3 MeV to 100 MeV. First 4 tanks are used to accelerate the beam up to 20 MeV and driven by a single klystron, which is a unique feature of KOMAC RF network. The power balance is maintained through three magic Tees with 1% precision and the phase of each tank is adjusted by mechanical phase shifters installed at each branch of RF waveguide network from the klystron to each DTL tank. Under these RF environment, the measured normalized rms emittance of 20 MeV beam was 0.23 pi-mm-mrad, which agrees well with the design value of 0.20 pi-mm-mrad.

* Work supported by Ministry of Science, ICT & Future Planning of Korean Government.
† kimhs@kaeri.re.kr

ISBN 978-3-95450-169-4

DEVELOPMENT OF NEW HEAVY ION LINACS AT GSI

L. Groening and S. Mickat
Gesellschaft für Schwerionenforschung, Darmstadt, Germany

Abstract

The heavy ion linac UNILAC at GSI will be upgraded in order to meet the beam requirements imposed by the upcoming FAIR facility. This upgrade includes several innovative techniques and applications. They comprise a new gaseous stripper with enhanced efficiency, full 4d transverse emittance measurements, a round-to-flat beam adaptor, asymmetric transverse focusing along the new Alvarez DTL, optimized shape of the drift tube surface w.r.t. shunt impedance per surface field, and a field stabilization and tuning scheme without post-couplers. Additionally, we report on the development of a super-conducting cw linac which will be dedicated to production of superheavy elements at energies close to the Coulomb barrier.

INTRODUCTION

GSI is currently constructing the Facility for Antiproton and Ion Research (FAIR) [1]. It aims at provision of 3×10^{11}/s uranium ions at 1.5 GeV/u. Due to its high rigidity uranium imposes the highest challenges to the accelerator chain w.r.t. fields and machine protection. The existing UNIversal Linear ACcelerator UNILAC will provide all primary ions but protons. In order to deal with the FAIR requirements in the upcoming decades, the UNILAC needs a considerable upgrade. While FAIR will be served by the upgraded UNILAC at low duty-cycles, the research program on superheavy elements (SHE) requires a linac providing energies at the Coulomb barrier with highest possible duty cycle. To this end a dedicated superconducting cw linac for heavy ions for SHE is under design as well. The following section will introduce the developments related to the upgrade of the UNILAC, while the third section is on the activities and achievements concerning the new cw linac.

DEVELOPMENTS FOR THE UPGRADE OF THE UNILAC

The existing UNILAC (Fig. 1) together with the subsequent synchrotron SIS18 serves as injector for FAIR. Three ion source terminals can be operated in pulse-to-pulse switching mode at 50 Hz. One terminal is equipped with an ECR source providing highly charged ions. Followed by an RFQ and an IH-cavity operated at 108 MHz it forms the High Charge Injector (HLI) providing beams at 1.4 MeV/u. Another terminal houses a Penning source (PIG) providing low intensity beams at intermediate charge states at 2.2 keV/u. The third terminal is dedicated to provision of intense beams of low-charged ions at 2.2 keV/u as well. Intense heavy ion beams are produced in a MEVVA or VARIS. Beams are bunched and pre-accelerated to 120 keV/u along a 9 m long RFQ operated at 36 MHz. Afterwards two IH-cavities provide for acceleration to 1.4 MeV/u, being the exit energy of the High Current Injector (HSI). For uranium the highest particle numbers are obtained by using the charge state $^{238}U^{4+}$. After the IH-DTL the acceleration efficiency is increased by passing the beam through a gaseous stripper which delivers a mean charge state of $^{238}U^{28+}$ at its exit. This increase of charge state is at the expense of intrinsic particle loss. Prior to 2014 about 87% of the uranium ions were stripped to a charge state different from 28+. After dispersive selection of the desired charge state the beam is matched to the subsequent post-stripper Alvarez-type DTL. The latter is operated at 108 MHz and comprises five tanks. Its exit beam energy is 11.4 MeV/u being the injection energy for the synchrotron SIS18. The post-stripper DTL can be fed with beams from the HLI as well. The UNILAC design parameters are listed in Table1.

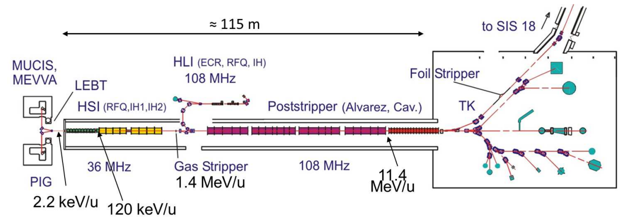

Figure 1: The UNIversal Linear ACcelerator (UNILAC) at GSI.

Table 1: Beam Design Parameters for the Upgraded UNILAC

Ion A/q	≤ 8.5	
Beam Current	1.76·A/q	mA
Input Beam Energy	1.4	MeV/u
Output Beam Energy	3.0 - 11.7	MeV/u
Emit. (norm., tot.) hor/ver	0.8/2.5	µm
Exit tot. Bunch Length	≤ ±30	deg
Beam Pulse Length	200	µs
Beam Repetition Rate	10	Hz
Rf Frequency	108.408	MHz

High Pressure H_2-Stripper

So far, a continuous N_2 jet has been used as stripping medium. The achieved stripping efficiency from $^{238}U^{4+}$ to $^{238}U^{28+}$ was 13%. Since 2014 a pulsed gas stripper cell has been tested [2]. It injects short gas pulses, the length of which matches the beam pulse length into the stripping chamber, producing a high density target without overloading the differential pumping system toward adjacent accelerator systems. Using H_2 the efficiency of stripping into the most populated charge state has been increased from 14(1)% to 21(1)%. Figure 2 compares measured charge state spectra of

SARAF 4-ROD RFQ RF POWER LINE SPLITTING DESIGN AND TEST

J. Rodnizki†, B. Kaizer, Z. Horvitz, L. Weissman, A. Perry, D. Hirschmann, Soreq NRC SARAF, Yavne, Israel

Abstract

The SARAF 3.8 m long 4-rod RFQ is able to accelerate 4mA CW proton beam to 1.5 MeV. During the last years several experiments with CW proton beam up to 2 mA and in the range of 1.9– 4 MeV were run at SARAF linac. The conditions for running CW deuteron beams (250 kW CW dissipated power or a 65 kV inter-rod voltage) have not been achieved yet. Our findings imply that the RFQ coupler was the primary bottle neck. Thus, a project to split the RFQ power line was initiated. In the framework of the project, a 3 dB splitter and two new RF couplers were installed. The RF couplers were manufactured in-house according to an improved design which included better brazing methods and better vacuum and RF sealing. This project is innovative from two points of view: (a) Implementation of two couplers located in two separated RF cells in a 4-rod RFQ. Synchronization of the incident power phase in both couplers was achieved by a single LLRF control channel and phase matching was achieved by adjusting the length of the RF rigid lines. (b) RFQ availability at 200 kW CW was demonstrated. This power range is sufficient for acceleration of a high intensity 5 mA CW deuteron beam to 1.3 MeV/u by a new modulation of the RFQ rods. To our knowledge, SARAF RFQ will be the first 4-rod RFQ capable of running a CW deuteron beam.

INTRODUCTION

The SARAF 176 MHz, 3.8 m long 4-rod RFQ is able to generate a 1.5 MeV 4mA CW proton beam. During the last few years, several experiments with CW proton beam up to 2 mA and in the range of 1.9 – 4 MeV were run at SARAF linac, [1, 2]. In order to run a CW deuteron beam the required RFQ power is 250 kW CW, to reach a 65 kV inter-rod voltage. This amounts to four times the power needed to run a CW proton beam. The maximum reachable value demonstrated few times in recent years, was around 200 kW in CW operation mode using a single RF coupler. In 2014 an extensive conditioning campaign of the SARAF RFQ has achieved stable operation in CW mode for 4.5 hours at 200-205 kW incident power and 50% duty cycle pulsed mode at 250 kW [3]. However, these capabilities could not be maintained for extended times. During 2015, several events of copper evaporation on the ceramics in the coupler RF window were occurred and we could not bring the RFQ back to the same operational level. It became evident that the status of the RF coupler has deteriorated and as a result deuteron beam operation was not possible. Subsequently, it was decided to replace the original single coupler with two improved couplers and to split the coaxial line from the amplifier, as a complementary step to the RFQ improvements reported in [4]. The goal of the project was to reduce the RFQ coupler load and, hence, achieve long term stable operation of the current RFQ.

A proposal for redesign the SARAF RFQ rods with purpose to reduce the integrated RFQ load required for deuteron operation was also under consideration [5]. Defining the available upper limit of this load with the new improved couplers system was another important objective of this work.

THE COUPLERS AND RF SYSTEM

General Layout

The project included installation of a 3 dB RF splitter at 176 MHz (the linac frequency), new RF lines structure and two new upgraded couplers with individual directional couplers (Fig. 1). The 3 dB splitter was adopted due to its ability to isolate crosstalk between the two couplers in order to enable a stable beam operation. The available RF power (up to 300 kW) was split towards the two couplers. A dummy load that is able to absorb 150 kW from the reflected power was connected to the port next to the injected forward power.

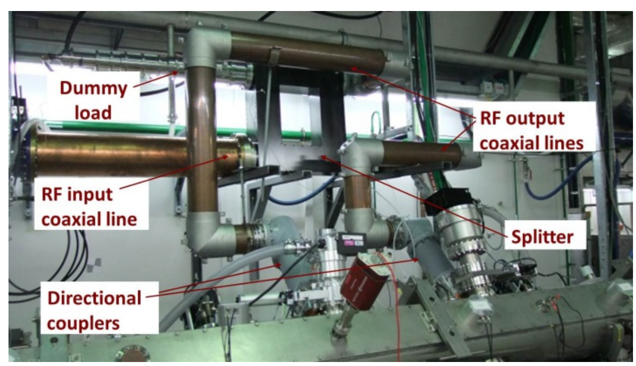

Figure 1: Configuration of the RF lines.

Phase Matching Between Both Couplers Ports

The magnetic phase between adjacent RF cells (total 40 stems along the RFQ with 39 RF cells) is 180º. The shift is due to the eigenmode pattern of the magnetic field, induced by the coupler (Fig. 2). As a result the relative phase between the couplers loops is 180º due to the odd number of RF cells between them.The output ports of the 3 dB splitter have 90º phase shift. By extending the length of the RF line by 1/4 λ the requirded phase matching between the two couplers port is achieved to within a deviation of ~1º, equivalent approximately to a 5 mm deviation in the rigid RF line length. The superposition of the combined induced fields from both ports on the excited RFQ eigenmode may be evaluated by:

$$A\cos(wt-\alpha/2)+A\cos(wt+\alpha/2) = 2A\cos wt\cos\alpha/2$$

† jacob@soreq.gov.il

ISBN 978-3-95450-169-4

TOWARDS COMMISSIONING OF THE IFMIF RFQ

Andrea Pisent, INFN/LNL, Legnaro, Padova, Italy
on behalf of INFN team for IFMIF RFQ construction

Abstract

All 18 sections of the IFMIF RFQ were completed in summer 2015. A 2 m section (the last three modules and one prototype used as RF termination) were RF tested at LNL at the design value of 90 kW/m in cw conditions. The three 3.3 m long supermodules were sent to Japan in January 2016. The RFQ was installed and tuned with fixed tuners to the nominal field frequency and field distribution. The very high design shunt impedance was achieved.

INTRODUCTION

The required acceleration in continuous wave (cw) of 125 mA of deuterons up to 5 MeV poses IFMIF RFQ at the forefront frontier of high intensity injectors [1].

This RFQ is indeed meant to be the injector of a 5 MW deuteron linac (40 MeV final energy) for Fusion Material Irradiation tests. The International Fusion Materials Irradiation Facility (IFMIF) [2] project aims at producing an intense (about 10^{17} s^{-1}) neutron source facility, with spectrum up to about 14 MeV, in order to test the materials to be employed in the future fusion reactors. The facility will be based on two high power CW accelerator drivers, hitting a single liquid lithium target (10 MW power) to yield neutrons via nuclear stripping reactions.

The IFMIF-EVEDA project was funded at the time of the approval of ITER construction (2007); the task is to validate the IFMIF design by the realization of a number of prototypes, including a high-intensity CW deuteron accelerator (called LIPAc, linear IFMIF Prototype Accelerator) for a beam power exceeding 1 MW.

LIPAc is being installed at the QST (ex JAEA) site at Rokkasho (Japan). The accelerating structures of the porotype linac, operating at 175 MHz, are the RFQ and the first Half Wave Resonator cryomodule. The injector is composed by an ECR and a magnetic LEBT, the RF system is composed by similar RF units (8 for the RFQ and 8 for the HWR). The schematic lay out of LIPAc is shown in Fig. 1.

The realization of LIPAc is a strict collaboration between Japan and Europe, The detailed organization of such challenging project is discussed in [3], the main contribution are for QST the infrastructures of the site, for the European institutes (mainly CEA, Ciemat and INFN, coordinated by F4E) the accelerator components.

At present the injector is under commissioning, the RFQ is assembled and tuned, the MEBT and the diagnostic plate are under set up, the RF system is under completion [4]. The commissioning plane foresees four phases; Phase A: 140 mA deuteron current at 100 keV in CW, Phase B: 125 mA deuteron current at 5 MeV at 0.1% duty cycle, Phase C: 9 MeV deuteron current at 9 MeV at 0.1% duty cycle, Phase D: ramp up the duty cycle up to CW. In all phases we plan to characterize and use, together with the d beam, a proton beam with half energy, half current and similar space charge.

Now the commissioning phase A is ongoing, with a diagnostic plate and an Ellison scanner installed immediately after the nominal RFQ input. Such phase is extremely important to establish the correct RFQ input condition and guarantee the required LIPAc performances [5-7].

To allow the LEBT beam operation, the RFQ is installed 3.3 m downstream its nominal position for assembling and tuning. In November the RFQ will be installed in its final position in view of RF conditioning and beam commissioning phase B.

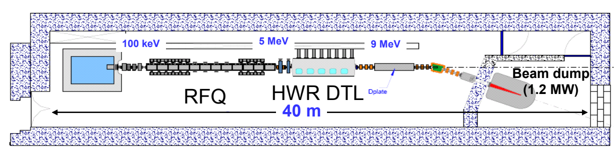

Figure 1: Schematic layout of the IFMIF-EVEDA prototype linac (125 mA, 9 MeV deuterons).

RFQ DESIGN AND MODULE CONSTRUCTION

INFN is in charge of the design and construction of the RFQ system, namely the accelerator structure, the vacuum system, the cooling system used for slow frequency tuning and the local control system. This activity was developed through the LNL labs, by an accelerator Physics group with previous experience in RFQ realization, and Padua, Torino and Bologna sections, with previous experience for mechanical development and realization in large international experiments (like for CERN LHC). The responsibilities were distributed accordingly, with Padua and Torino in charge of the RFQ module mechanical development and engineering integration respectively; about 30 people including physicists and engineers have been involved in RFQ realization.

A specific characteristic of this development has been the use of internal resources and installations, not only for the physical and local control design, but also for all the other steps of the realization, like mechanical design, high precision machining of critical components, QA and

HIGH-FREQUENCY COMPACT RFQS FOR MEDICAL AND INDUSTRIAL APPLICATIONS

M. Vretenar, V. A. Dimov, M. Garlasché, A. Grudiev, B. Koubek, A. M. Lombardi, S. Mathot, D. Mazur, E. Montesinos, M. Timmins, CERN, Geneva, Switzerland

Abstract

CERN has completed the construction of a 750 MHz RFQ reaching 5 MeV proton energy in a length of only 2 meters, to be used as injector for a compact proton therapy linac. Beyond proton therapy, this compact and lightweight design can be used for several applications, ranging from the production of radioisotopes in hospitals to ion beam analysis of industrial components or of artworks. The experience with the construction of the first unit will be presented together with the design and plans for other applications.

INTRODUCTION

In the frame of its new programme for medical applications, CERN has designed and constructed a compact 750 MHz Radio Frequency Quadrupole (RFQ) with the primary goal of providing a low beam loss alternative to cyclotrons as injector for proton therapy linacs operating at high frequency (3 GHz). While this option was already proposed in the past [1], the technical challenges of building and tuning an RFQ at a frequency about a factor of two higher than in conventional RFQs moved the proton therapy linac teams to foresee the use of an available cyclotron as injector to the high-frequency structures [2]. Although easily accessible, this option presents the drawbacks of high beam losses related to the unmatched beam transfer between accelerators operating at very different frequencies and of the need to pulse the cyclotron at the high repetition frequency of the linac.

In recent years, the experience gained at CERN in the construction of the Linac4 RFQ [3] together with the development of a new unconventional beam dynamics approach [4] and an increased confidence in the design and tuning of RFQs that are long with respect to the wavelength, meant the problem could be reconsidered on a new basis. After a preliminary analysis, a multi-disciplinary working group converged on the design of a prototype RFQ at 750 MHz reaching the energy of 5 MeV in only 2 meters [5]. While the RFQ beam optics is optimised for a specific proton therapy accelerator, its overall design is general enough to be used for a wide range of applications; construction techniques and machining tolerances are optimised for industrial production. The compactness, lightweight and standardised simplified construction of this new design open entirely new perspectives for applications of the RFQ technology outside of the scientific environment that would benefit from the RFQ qualities with respect to other low-energy accelerators: minimum beam loss with no need for dedicated accelerator shielding, excellent beam quality, very high reliability and availability, and minimum maintenance.

The construction in the CERN workshops of the prototype RFQ started in 2014 and was recently completed (Fig. 1). The main RFQ design parameters are reported in Table 1; they are based on the application as injector to the proton therapy linac of the LIGHT project [6].

Figure 1: The RFQ assembled on the tuning bench.

Table 1: Main RFQ Parameters

Input/Output Energy	40 keV / 5 MeV
Length	1.964 m
Vane voltage	67.6 kV
Min aperture radius	1 mm
Maximum modulation	3
Final synchronous phase	-15 deg
Output current (max.)	300μA
Beam transmission	30 %
Output transv. rms emit.	0.027 π.mm.mrad
Output phase spread	± 2 deg
Output energy spread	± 20 keV
RF Frequency	750 MHz
RF Power	350 kW
Operation duty cycle	0.4 %
Design duty cycle	5 %

For application in a proton therapy linac, the RFQ frequency needs to be a sub-harmonic of 3 GHz; 750 MHz has been selected because lower frequencies increase the RFQ length while higher frequencies decrease acceptance, increase power loss density and make difficult the machining of the first very short cells. However, the optimum is quite wide and for other applications the same RFQ design could be used at frequencies up to 1 GHz. In order to keep a sufficient beam acceptance at high frequency, the aperture is similar to that of lower frequency RFQs; this allows the machining tolerances to be kept in a range achievable with conventional tools, but results in a small cavity cross-section (45.9 mm inner radius) and limits the shunt impedance. To simplify the tuning, the length of this prototype RFQ has been conservatively limited to 2 m, corresponding to 5 times the wavelength.

THE LINAC LASER NOTCHER FOR THE FERMILAB BOOSTER*

David E. Johnson#, Kevin Laurence Duel, Matthew Gardner, Todd R. Johnson, David Slimmer (Fermilab, Batavia, Illinois), Sreenivas Patil (PriTel, Inc., Naperville, Illinois), Jason Tafoya (Optical Engines, Inc., Colorado Springs, Colorado)

Abstract

In synchrotron machines, the beam extraction is accomplished by a combination of septa and kicker magnets which deflect the beam from an accelerator into another. Ideally the kicker field must rise/fall in between the beam bunches. However, in reality, an intentional beam-free time region (aka "notch") is created on the beam pulse to assure that the beam can be extracted with minimal losses. In the case of the Fermilab Booster, the notch is created in the ring near injection energy by the use of fast kickers which deposit the beam in a shielded collimation region within the accelerator tunnel. With increasing beam power it is desirable to create this notch at the lowest possible energy to minimize activation. The Fermilab Proton Improvement Plan (PIP) initiated an R&D project to build a laser system to create the notch within a linac beam pulse at 750 keV. This talk will describe the concept for the laser notcher and discuss our current status, commissioning results, and future plans.

MOTIVATION

The current Fermilab Booster utilizes multi-turn injection and adiabatic capture to populate all RF buckets in the ring. To minimize losses from the rise time of the 8 GeV extraction kicker, a portion of the beam (about 60 ns. out of 2.2 μs.) in the ring is removed by fast kickers at low energy into an absorber. This empty section of the circumference is called a "Notch". On Booster cycles that are ultimately injected into the MI for the Neutrino and Muon programs this process takes place at approx.400 MeV about a hundred microseconds after capture. To keep the activation of tunnel components to reasonable limit for maintenance, the Booster has an administrative limit on loss power of 525W. The process of creating the notch in the Booster contributes approximately 1/3 (175W) to this limit. Moving this process out of the Booster tunnel to the 750 keV Medium Energy Beam Transport (MEBT) of the linac is expected to reduce the loss to ~17 W, assuming a 90% efficiency in the Linac Notch creation and 10% clean-up in the Booster ring.

LINAC & BOOSTER BEAM

At the completion of PIP, the Fermilab Booster will be operating at 15 Hz. The length of the linac pulse injected into Booster is N*τ where N is the number of injected turns and τ is the Booster revolution period at injection. Creating a notch in the linac pulse requires removing N-1 sections of the linac beam at the Booster revolution period. The spacing between these removed sections should guarantee that when the H- is injected into the Booster, the empty sections fall on top of one another in the ring producing a single notch in the Booster. This process is shown in Fig. 1. The top pane shows the 15Hz linac pulses to be injected into Booster. The bottom pane shows a single linac pulse with 60 ns notches created within the pulse separated by ~2.2 μs, the Booster revolution period. Not shown is the 200 MHz bunch structure in the linac pulse.

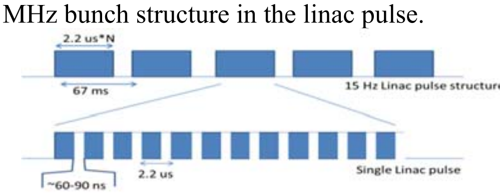

Figure 1: Linac pulse showing the notch structure for a single linac pulse.

LASER NOTCHER CONCEPT

The technique employed to produce the notch is to remove the outer electron of the H- ion using photoionization for the appropriate beam sections. There have been discussions on using lasers to create a notch in the linac beam for some time [1-3]. This technique was demonstrated in 2000. [1] The photoionization cross section has a broad peak centered at 1.51 eV (□=821 nm) photon energy in the center-of-mass frame of the electron with a cross section of 4.2×10^{-17} cm^2. [4] The choice of the lab frame photon energy is dependent of the H- energy and the interaction angle through the standard Lorentz transformation. The laser technology for both solid state (Nd:YAG) and ytterbium (Yb) doped fiber with a laser wavelength of 1064 nm has matured significantly over the last decade such that it is the natural choice for the laser system. The cross section for these photons with CM energy 1.165 eV is 3.66×10^{-17} cm^2, only 13% off the peak. When the probability of interaction between the photons and electrons is high and the mechanism does not depend on the electron intensity [4], the fraction of electrons that are detached from the moving H- ions is given by [5]

$$F_{neut} = {}^{N}\!/_{N_0} = \left(1 - e^{-f_{CM}\sigma(E)\tau}\right), \qquad (1)$$

where f_{CM} is the flux of photons at the interaction point in the rest frame of the H- [photons/cm^2/sec], σ(E) is the photoionization cross section for photon energy E, and τ is the interaction time of the photons and electrons. The center of mass flux can be expressed in lab frame parameters as

$$f_{CM} = \gamma\left(\frac{E_{laser}\lambda_{LAB}}{hc\tau_{laser}}\right)\left(\frac{1}{A_{laser}}\right)(1-\beta\cos\theta), \qquad (2)$$

where $\boldsymbol{E_{laser}}$ is the laser pulse energy, λ_{LAB} is the lab frame wavelength of the laser, τ_{laser} is the laser pulse length, $\boldsymbol{A_{laser}}$ is the laser cross sectional area, γ and β are the usual relativistic parameters, and θ is the interaction angel between the photons and H-. Figure 2 shows the "single

*Operated by Fermi Research Alliance, LLC under contract No. DE-AC02-07CH11359 with the United States Department of Energy.
#DEJ@fnal.gov

RESULTS FROM THE LASERWIRE EMITTANCE SCANNER AND PROFILE MONITOR AT CERN'S LINAC4

T. Hofmann*, G.E. Boorman, A. Bosco, S.M. Gibson, K.O. Kruchinin
John Adams Institute at Royal Holloway, University of London, Egham, United Kingdom
U. Raich, F. Roncarolo, CERN, Geneva, Switzerland

Abstract

A novel, non-invasive, H^- laserwire scanner has been tested during the beam commissioning of CERN's new Linac4. *Emittance* measurements were performed at beam energies of 3 and 12 MeV with this new device and were found to closely match the results of conventional slit-grid methods. In 2015, the configuration of this laserwire scanner was substantially modified. In the new setup the electrons liberated by the photo-detachment process are deflected away from the main beam and focused onto a single crystal diamond detector that can be moved in order to follow the laser beam scan. The beam *profiles* measured with the new laserwire setup at 50 MeV, 80 MeV and 107 MeV are in good agreement with the measurements of nearby SEM grids and wire-scanners. The design of the final laserwire scanner for the full 160 MeV beam energy will also be presented. In Linac4 two independent laserwire devices will be installed in the transfer line to the BOOSTER ring. Each device will be composed of two parts: one hosting the laserwire and the electron detector and the second hosting the segmented diamond detector used to acquire the transverse profiles of the H^0 beamlets.

INTRODUCTION

Laser-based devices offer several diagnostic possibilities for H^- accelerators. Transverse profile measurements are the most commonly used [1] but other measurements as transverse emittance [2], longitudinal bunch profile [3] or energy spread [4] have also been implemented recently. The main advantages are the wide operational ranges in terms of beam energies and intensities and the absence of mechanical parts intercepting the main beam (non-destructive measurements).

In our case the laserwire instruments will be used to measure the transverse profiles and the transverse emittances of the beams at the end of Linac4, at an energy of 160 MeV. These measurements will be used to tune the optics parameters of the accelerator and optimize the matching to the BOOSTER ring, thus maximizing the injection efficiency. Prototypes of the Linac4 laser-scanners have been tested during the commissioning of the machine. Figure 1 illustrates the locations, at the different energies, where the tests have been performed.

The monitor concept is illustrated in Fig. 3: as the thin laser beam crosses the H^- beam, the low energy photo-detached electrons are deflected by a small magnet onto an electron collector, while the neutralized H^0 atoms drift unperturbed to a downstream segmented detector. A dipole magnet, located between the laser and H^0 detector, is then used to separate the H^0 beamlet from the main H^- beam. By scanning the laser through the H^- beam, the beam profile can be obtained from the evolution of the electron signal on the collector and the transverse phase-space can be reconstructed using the H^0 profiles acquired as function of the laser position.

The system is based on a relatively low-power pulsed laser (~kW peak-power), which can be reliably transported to the interaction point (IP) with the H^- beam by an optical fiber.

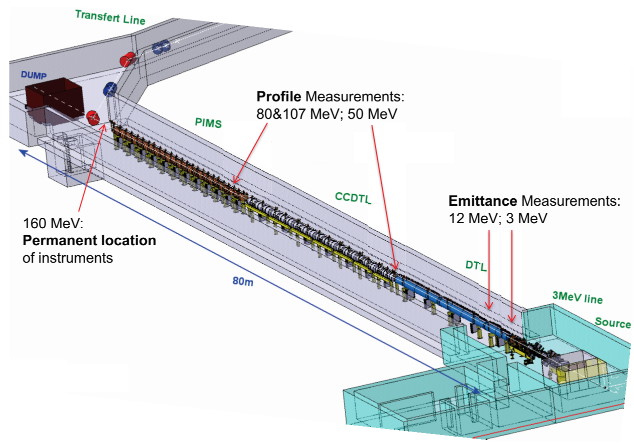

Figure 1: Linac4 facility with beam energies at different commissioning steps. The laserwire instrument has been tested at 3 and 12 MeV for emittance measurements and at 50, 80 and 107 MeV for profile measurements. The final instruments will be installed at Linac4's top energy of 160 MeV.

EMITTANCE MEASUREMENTS

The first prototype was designed to validate the vertical phase-space reconstruction via the H^0 detection and was tested during the 3 and 12 MeV commissioning periods. Figure 2 shows the test setup with a zoom on the laser delivery system situated next to the IP. To detect the profiles of the H^0 beamlets after the bending magnet a polycrystalline (pCVD) diamond strip detector was used (see Fig. 4). This type of detector offers high sensitivity and bandwidth and, most important, an excellent radiation hardness [5].

The Linac4 beam consists of 400 µs long macro-pulses with H^- bunched at 352.2 MHz while the laser generates macro-pulses of 1 ms with 80 ns long pulses repeated at

* thomas.hofmann@cern.ch

ISBN 978-3-95450-169-4

COMPLETE TRANSVERSE 4D BEAM CHARACTERIZATION FOR ION BEAMS AT ENERGIES OF FEW MeV/U

M. Maier†, X. Du, P. Gerhard, L. Groening, S. Mickat, H. Vormann, C. Xiao
Gesellschaft für Schwerionenforschung, Darmstadt, Germany

Abstract

Measurement of the ion beam rms-emittances is done through determination of the second order beam moments. For time being the moments quantifying the amount of inter-plane coupling, as <xy> for instance, have been accessible to measurements just for very special cases of ions at energies below 150 keV/u using pepper pots. This contribution presents successful measurements of all inter-plane coupling moments at 1 to 11 MeV/u. From first principles the used methods are applicable at all ion energies. The first campaign applied skewed quadrupoles in combination with a regular slit/grid emittance measurement device. The second campaign used a rotatable slit/grid device in combination with regular quadrupoles.

INTRODUCTION

Usually just separated measurements of two-dimensional x-x′ and y-y′ sub phase-spaces (planes) are measured, as for simplicity correlations between the two planes, i.e. x-y, x-y′, x′-y, and x′-y′ are often assumed as zero. However, such inter-plane correlations may be produced by non-linear fields such as dipole fringes, solenoids, and titled magnets or just by beam losses. Figure 1 shows the simulation of a coupled and an uncoupled beam with initially identical projected horizontal and vertical rms-emittances though a solenoid channel. This illustrates the fact that initial coupling influences the final horizontal and vertical beam size.

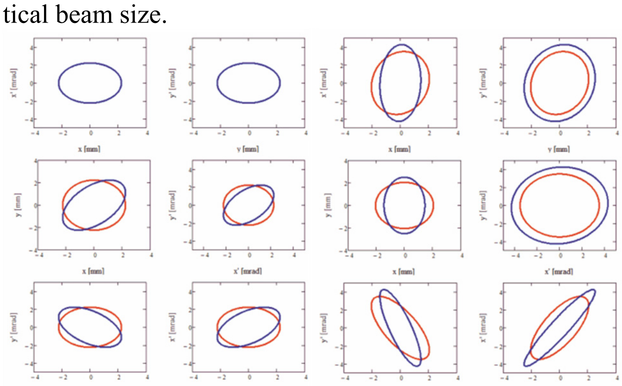

Figure 1: Simulations of an initially uncoupled (red) and coupled (blue) ion beam (left) through a solenoid channel (right).

For some applications [1], to match the round transverse phase space of a Linac beam to the flat acceptance of a synchrotron, inter-plane correlations are a prerequisite. In order to remove correlations that do increase the projected rms-emittance, they must be quantified by measurements.

There is considerable work on measuring four-dimensional distributions using pepper-pots [2-5] for electron beams or ion beams at energies below 150 keV/u, where the beam can be stopped by the pepper-pot mask. However, due to technical reasons this method is not applicable at energies above 150 keV/u, i.e. doubtful readout by temperature-dependent screens and fixed resolutions by holes and screens [6]. In the following we report about the combination of skew quadrupoles with a slit/grid emittance measurement device [7] and on ROSE [8],[9] an alternative method to measure the full 4d beam matrix that additionally features a significantly reduced time needed to perform the measurements.

FOUR-DIMENSIONAL RMS-QUANTITIES

The four-dimensional second-moments beam matrix contains ten unique elements, four of which describe the coupling.

$$C = \begin{bmatrix} XX & XX' & XY & XY' \\ X'X & X'X' & X'Y & X'Y' \\ YX & YX' & YY & YY' \\ Y'X & Y'X' & Y'Y & Y'Y' \end{bmatrix} \tag{1}$$

If at least one of the elements of the off-diagonal submatrix is non-zero, the beam is x–y coupled. Projected rms-emittances ε_x and ε_y are quantities which are used to characterize the transverse beam quality in the laboratory coordinate system and are invariant under linear uncoupled (with respect to the laboratory coordinate system) symplectic transformations. Projected rms-emittances are the rms phase-space areas from projections of the particle distribution onto the planes, and their values are equal to the square roots of the determinants of the on-diagonal submatrices, i.e., phase-space area divided by π:

$$\varepsilon_\mu = \sqrt{<\mu\mu><\mu'\mu'> - <\mu\mu'>^2}\ , \tag{2}$$

where μ refers to either x or y. The dimensionless parameter α relates to the μ−μ′ correlation and the β-function refers to the beam width. They are defined as

$$\alpha_\mu = -\frac{<\mu\mu'>}{\varepsilon_\mu}, \beta_\mu = \frac{<\mu\mu'>}{\varepsilon_\mu}\ . \tag{3}$$

The Eigen-emittances ε_1 and ε_2 are invariant under coupled linear symplectic transformations provided by solenoids and skew quadrupoles for instance [10] . None of the projected emittances can be smaller than the smaller of the two Eigen-emittances. The Eigen-emittances $\varepsilon_{1,2}$ can be expressed as [9].

$$\varepsilon_1 = \frac{1}{2}\sqrt{-tr[(CJ)^2] + \sqrt{tr[(CJ)^2] - 16\det(C)}} \tag{4}$$

$$\varepsilon_2 = \frac{1}{2}\sqrt{-tr[(CJ)^2] - \sqrt{tr[(CJ)^2] - 16\det(C)}} \tag{5}$$

The square matrix J is the skew-symmetric matrix with non-zero entries in the block diagonal off form and is defined as:

MAKING MOLECULAR MOVIE WITH MEV ELECTRONS*

X. Shen†, X. Wang, SLAC National Accelerator Laboratory, Menlo Park, CA 94025, USA

Abstract

Ultrafast electron probes, complementary to x-ray free electron lasers, enable direct insight into structural dynamics in material, chemical, and biological sciences. SLAC National Accelerator Laboratory has constructed a mega-electron-volt (MeV) ultrafast electron diffraction (UED) system to serve ultrafast science experiments and instrumentation development. The system delivers high brightness electron beams of femtosecond pulse duration with outstanding machine stability performance, which enables visualization of ultrafast structural dynamics with atomic time and length scales, i.e., making molecular movies. In this paper, we review the performance of the SLAC MeV UED system, highlight recent results in material science and gas phase experiments, and give an outlook for future developments.

INTRODUCTION

Visualization of structural changes reveals the strong correlation between structure and functionality of matter. Electrons and x-rays with short wavelength (≲1 Å) and short pulse durations (≲100 fs) are the most viable probes for this challenging task with atomic length and time scales. While x-ray mainly interacts with atomic electrons, electrons are sensitive to both electrons and nuclei. Electrons have $10^4 - 10^6$ times larger scattering cross sections and less radiation damage per elastic scattering event [1]. Electrons are charged particles such that they can be easily manipulated by accelerating structures and electro-magnetic lenses in a compact setup. The good properties of electrons have driven development of ultrafast electron diffraction and microscopes (UED and UEM) in the last few decades [2-10].

So far, most UED systems are operating with kilo-electron-volt (keV) DC electron sources. However, due to the strong space-charge forces at such low electron energies, the electron bunches undergo substantial length expansion as it propagates [11]. Therefore, it becomes practically impossible to produce a keV electron bunch with ~ 100 fs pulse duration at the specimen with more than a few hundred electrons [12]. Even with high efficiency single-electron detectors, obtaining a high signal-to-noise ratio diffraction pattern, which generally requires at least 10^6 electrons at the sample, is very difficult in the sense of apparatus stability, sample exposure time, sample heat load deposited by pump pulse, etc.

The temporal resolution barrier due to strong space-charge forces can be overcome by implementing an rf photoinjector as high brightness electron sources [13, 14]. The accelerating field of a rf photoinjector normally exceeds 100 MV/m, which is much higher than the 10-20 MV/m level for the dc photocathode. Electrons extracted in a rf photoinjector are rapidly accelerated to mega-electron-volt (MeV) level, such that the space-charge forces are greatly suppressed. It then becomes possible to group into a bunch of ~ 100 fs duration with up to three orders of magnitude more electrons. Moreover, the relativistic nature of the MeV electron probe naturally solves the problem of velocity mismatch between the pump pulse and probe beam which is critical when it comes to gas phase samples [15]. The more energetic electrons also come with a larger penetration depth, which enables implementation of thicker specimens.

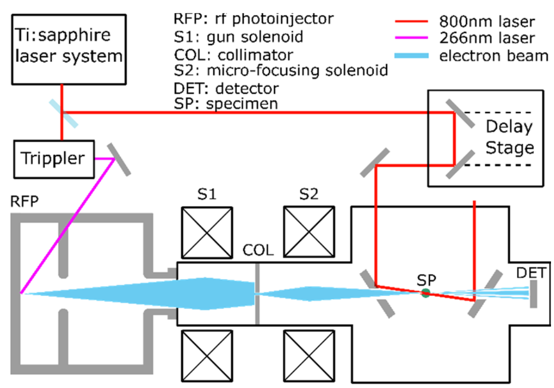

Figure 1: A schematic diagram of the SLAC MeV UED system.

SLAC MEV UED SYSTEM

SLAC recently launched a UED/UEM Initiative [16] aiming at developing the world's leading ultrafast electron scattering instruments. The first stage of the Initiative was to construct an MeV UED system. Figure 1 shows a schematic diagram for the SLAC MeV UED system. A Ti:sapphire laser system produces a 5 mJ 800 nm laser pulse which is split into two parts: a pulse goes to the pump line, while the other pulse is frequency tripled to 266 nm UV laser pulse to illuminate the photocathode at a 70° angle of incidence to generate femtosecond electron bunches. The 80 MV/m accelerating gradient in the rf photocathode rapidly accelerates electron bunches to 3.7 MeV, where the effect of space-charge forces is strongly reduced. The gun solenoid (S1) right after the rf photocathode is used to adjust the beam divergence at the exit of the rf photocathode, which effectively adjusts the beam size on the retractable collimator (COL) located at 0.4m downstream of the gun solenoid. The four pin holes on the collimator, with diameter of 100 um, 200 um, 500 um, and 1000 um, respectively, can be flexibly in-

*Work supported in part by the U.S. DOE Contract DE-AC02-76SF00515 and the SLAC UED/UEM Initiative Program Development Fund.
† xshen@slac.stanford.edu

ISBN 978-3-95450-169-4

THE LOS ALAMOS MULTI-PROBE FACILITY FOR MATTER-RADIATION INTERACTIONS IN EXTREMES*

R. W. Garnett†, Los Alamos National Laboratory, Los Alamos, New Mexico, USA

Abstract

A next-generation signature facility based on multi-probe capabilities is being pursued at Los Alamos. This new facility would enable the first in a new generation of game-changing scientific facilities for the materials community. The new Matter-Radiation Interactions in Extremes (MaRIE) facility would be used to discover and design the advanced materials needed to meet 21st-century national security and energy-security challenges to develop next-generation materials that will perform predictably in extreme environments. The MaRIE facility pre-conceptual reference design includes a new 12-GeV electron linac using a state-of-the-art electron photoinjector and superconducting accelerator technology to drive a 42-keV XFEL to generate x rays of unprecedented flux and quality, coupled with the existing proton-beam capabilities of the LANSCE proton linac, new experimental halls, and new materials fabrication/characterization facilities. A description of this new facility, its requirements, and planned uses and capabilities will be presented.

INTRODUCTION

Los Alamos has been pursuing a next-generation signature facility based on multi-probe capabilities to address the control of performance and production of weapons materials at the mesoscale for quite some time. Many of the uncertainties that remain in our assessment of weapon safety, security, and performance arise from uncertainties in material properties governed at the spatial scales between of atomic structures and those of the engineering continuum (the mesoscale) [1]. The proposed Matter-Radiation Interactions in Extremes (MaRIE) facility will provide this new capability by aiding our ability to understand and test materials response at resolutions necessary to understand the links between materials microstructure and performance in weapons-relevant extreme environments through new and more rigorous science-based approaches to manufacturing and certification without the need for nuclear tests as part of science-based stewardship.

It is expected that experimental data from the MaRIE facility will improve the understanding of interfaces, defects, and microstructure in the mesoscale and provide the ability to offer time-dependent control of processes, structures, and properties. Materials samples will be synthesized and characterized at the mesoscale, and their dynamic behaviour studied in time-dependent extreme conditions through the use of both imaging and diffractive scattering with multiple probes at multiple spatial and time scales. Exascale computing will be combined with experimental results from the MaRIE facility to enable rapid and confident deployment of new components and systems through more cost-effective and more rigorous science-based approaches.

The scientific community has identified that the challenge to accelerated discovery and integration of new materials with enhanced and optimized properties is at the mesoscale, where new tools and approaches are needed to understand this regime [2]. It has become clear that in many important areas the functionality that is critical to macroscopic behaviour begins not at the atomic or nanoscale but at the mesoscale, where defects, interfaces, and non-equilibrium structures dominate materials behaviour [3]. Measurements are therefore needed of scattering off the periodic structure of the material (phase, texture, orientation) as well as imaging of non-periodic structures (defects, material interfaces, and microstructures) to resolve these materials behaviours. These measurements are possible with a brilliant, high-repetition-rate, coherent X-ray source such as proposed for the MaRIE facility.

The expectation is that the proposed MaRIE facility would be sited at the Los Alamos Neutron Science Center (LANSCE). The LANSCE facility has been the flagship facility for large-scale science at Los Alamos National Laboratory for many decades.

THE MARIE FACILITY

The proposed MaRIE facility includes a new 12-GeV electron linac driving a 42-keV X-ray free-electron laser (XFEL), coupled with the existing capabilities of the LANSCE 800-MeV proton linear accelerator (linac), a new experimental hall, and materials fabrication and characterization facilities. The LANSCE accelerator complex currently supports a broad user base including the neutron scattering community, basic science, and national security programs by providing multiple beams to several diverse experimental areas. MaRIE builds upon the success of LANSCE to transform the science of microstructure, interfaces, and defects of materials in extremes. This will be accomplished by providing the necessary extreme environments (pressure, temperature, radiation, etc.) coupled with multiple probes including, charged particles (protons and/or electrons), optical laser photons, coherent X-rays, and state-of-the-art diagnostics. Figure 1 shows a pre-conceptual layout of the MaRIE facility at LANSCE.

* Work supported by the United States Department of Energy, National Nuclear Security Agency, under contract DE-AC52-06NA25396.
† rgarnett@lanl.gov

ISBN 978-3-95450-169-4

THE VELA AND CLARA TEST FACILITIES AT DARESBURY LABORATORY

P. A. McIntosh#, D. Angal-Kalinin, J. A. Clarke, L. S. Cowie, B. Fell, A. Gleeson, S.P. Jamison, T. Jones, B. Militsyn, Y. M. Saveliev, D. J. SCott, N. Thompson and P. Williams
on behalf of the VELA and CLARA development teams.
STFC Daresbury Laboratory, Warrington, WA4 4AD, UK.

Abstract

The Versatile Electron Linear Accelerator (VELA) provides enabling infrastructures targeted at the development and testing of novel and compact accelerator technologies, specifically through partnership with academia and industry, aimed at addressing applications in medicine, health, security, energy and industrial processing. The facility is now fully commissioned and is taking advantage of the variable electron beam parameters to demonstrate new techniques/processes or otherwise develop new technologies for future commercial realization. Examples of facility exploitation include; electron diffraction and new cargo scanning processes. The Compact Linear Accelerator for Research and Applications (CLARA) will be a novel FEL test facility, focused on the generation of ultra-short photon pulses with extreme levels of stability and synchronization. The principal aim is to experimentally demonstrate that sub-cooperation length pulse generation with FELs is viable, and to compare the various schemes being championed. The results will translate directly to existing and future X-ray FELs, enabling attosecond pulse generation. The VELA and CLARA facilities are co-located at Daresbury Laboratory and provide the UK with a unique platform for scientific and commercial R&D using ultra-short pulse, high precision electron and photon beams.

VELA AND CLARA ACCELERATORS

VELA is a high performance, modular injector facility capable of delivering stable, high quality and customisable electron beams into two dedicated, shielded test enclosures (BA1 and BA2) for the development and qualification of advanced accelerator systems [1] (see Fig. 1).

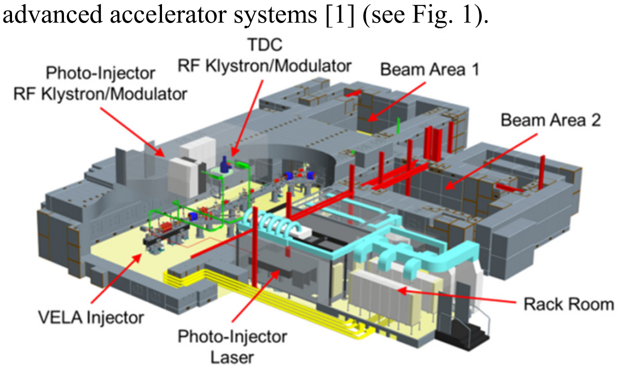

Figure 1: VELA accelerator layout.

CLARA is a dedicated FEL test facility [2] currently under construction, capable of testing new FEL schemes that have the capability to enhance the performance of short wavelength FELs worldwide (see Fig. 2). The primary focus of CLARA is for ultra-short pulse generation, stability and synchronisation. Enhancements in these three areas will have a significant impact on the experimental capabilities of FELs in the future. The wavelength range chosen for the CLARA FEL is 100 – 400 nm, appropriate for the demonstration of advanced FEL concepts on a relatively low energy accelerator.

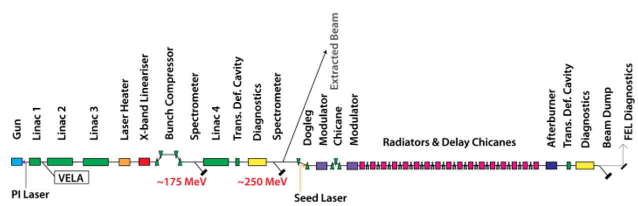

Figure 2: CLARA Design Schematic.

VELA Commissioning and Characterisation

Since achieving first electron beam in early 2013 [3], a number of commissioning and beam characterisation experiments have been completed. VELA has a suite of diagnostics in a specially designed beamline consisting of quadrupoles, YAG screens, BPMs, wall current monitor, Transverse Deflecting Cavity (TDC) and a spectrometer line for 6D beam characterisation (see Fig. 3), which have been used to characterise the RF gun performance and beam transverse and longitudinal phase space.

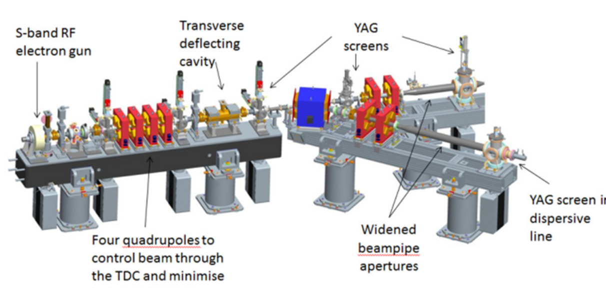

Figure 3: VELA beam diagnostics beamline.

Bunch charges over the range 40 fC (for electron diffraction) to 250 pC with a peak beam energy of ~5 MeV reliably achieved, with 8 MW of RF power in the S-Band RF gun cavity [4]. Dark current, measured throughout commissioning and operation with two different cathodes, has shown continual improvement, decreasing from 1.2 nC to 130 pC per 3 μs RF pulse at a gradient of 70 MV/m. The

EXPERIMENTAL STUDY OF NUCLEATION FOR Nb_3Sn DIFFUSION COATINGS ON NIOBIUM SRF CAVITIES*

Uttar Pudasaini[1], G. Eremeev[2], Charles E. Reece[2], M. J. Kelley[1,2]
[1]Applied Science Department, The College of William and Mary, Williamsburg, VA 23185, USA
[2]Thomas Jefferson National Accelerator Facility, Newport News, VA 23606, USA

Abstract

Nb_3Sn has the potential to achieve superior performance both in terms of operating temperature (4.2 K vs 2 K) and accelerating gradient resulting in significant reduction in both capital and operating costs of SRF linacs. Cavity interior surface coatings are obtained by two step vapor diffusion: nucleation followed by deposition. To gain more understanding of nucleation and its effect on the subsequent coating, we investigated the effect of varying parameters in a typical tin/tin chloride process. We report findings obtained by SEM/EDS, AFM, SAM and other materials characterization approaches.

INTRODUCTION

Nb_3Sn is an alternative superconducting material that has potential to replace traditional niobium in SRF cavities. Critical temperature and predicted superheating field of Nb_3Sn are nearly twice that of niobium which offers the possibility of attaining higher operating temperature and accelerating gradient resulting in significant reduction in both capital and operating cost. Nb_3Sn is a challenging material because of lower thermal conductivity and brittleness. That restricts its application as a cavity material to only coating form. Fabrication of Nb_3Sn cavities by deposition of Nb_3Sn diffusion coatings on niobium cavities dates back to 1970's [1-3], and is the most successful technique so far. Recent performance results of such cavities are very promising, attaining quality factor $>10^{10}$ operating at 4.2 K with gradient more than 10 MV/m [4].

The majority of research institutions working currently to develop Nb_3Sn coated cavities use the diffusion coating technique [5-7]. The essence of the process is to transport tin vapour to the niobium substrate, and provide the high temperature environment to form Nb_3Sn phase, which is determined by binary phase diagram [8]. This coating process is favourable to complicated shaped cavities. It involves two steps: nucleation and deposition. Tin chloride, used as a nucleation agent evaporates at about $500^{\circ}C$ to deposit tin on niobium surface which later acts as Nb-Sn nucleation sites to form Nb_3Sn phase [9]. It is assumed that these nucleation sites grow with influx of tin vapour at higher temperature. An example of Nb_3Sn coating process at Jlab is shown in Figure 1. The first temperature plateau at nucleation temperature of $500^{\circ}C$ is dedicated to nucleation process whereas second temperature plateau for deposition.

* Partially authored by Jefferson Science Associates under contract no. DEAC0506OR23177. Work at College of William & Mary supported by Office of High Energy Physics under grant SC0014475.

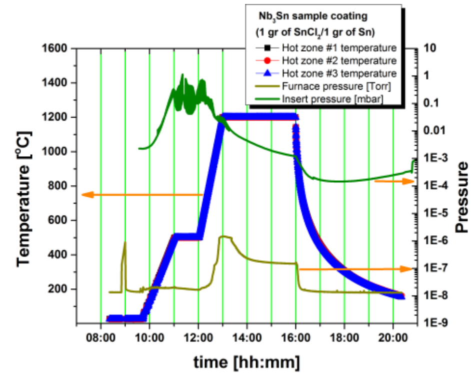

Figure 1: Temperature profile used for coating Nb_3Sn on niobium samples.

The purpose of this work was to gain insight into the nucleation process, and to determine the effects of changing nucleation parameters. We varied nucleation temperature and/or duration at which nucleation temperature was kept constant for same amount of tin and tin chloride. We also investigated the effect of changing the amount of tin chloride in few cases.

EXPERIMENTAL DESCRIPTION

Materials

The samples here were high purity niobium coupons prepared by EDM cutting 3mm thick, high RRR (~300) sheet material of the type used to fabricate SRF cavities. All were subjected to buffered chemical polishing (BCP) with expected minimum removal of 50 µm. These samples further received metallographic polishing, also known as nanopolishing (NP) to obtain smoothest possible surfaces. The average roughness of NP samples was ~2 nm which was measured from 50 µm x 50 µm scan areas using an atomic force microscope (AFM).

Experiments

The same deposition system that is available at Jlab to coat Nb_3Sn on niobium cavities was used in this work. Detailed description of deposition system is available [5]. Experimental setup was very similar to the one used before to deposit Nb_3Sn coatings [10]. One gram of tin and required amount of tin chloride were packaged in niobium foil, and placed on the niobium plate which covered the bottom side of sample chamber. Both ends of the sample chamber were covered by niobium plates after mounting coupons inside, before installing into the furnace insert. The insert was pumped down to attain pressure of 10^{-5} – 10^{-6} Torr range before the heating profile was initiated. The temperature inside the insert was raised at the rate of

INVESTIGATION OF NITROGEN ABSORPTION AND NITRIDE GROWTH ON SRF CAVITY GRADE RRR NIOBIUM AS A FUNCTION OF FURNACE TEMPERATURE*

Ari Deibert Palczewski#, Charles E. Reece, Jefferson National Laboratory, Newport News, VA
Michael Kelley, The College of William and Mary, Williamsburg, VA
James Tuggle, Virginia Polytechnic Institute and State University, Blacksburg

Abstract

The current state of the art processing of niobium superconducting radio frequency cavities with nitrogen diffusion is performed at 800°C in a furnace with a partial pressure of approximately ~20 mTorr of nitrogen. Multiple studies have shown the bulk of the nitrogen absorbed by the niobium forms a thick (1-3 microns) non-superconducting nitride layer which must be removed to produce optimal RF results. The depth profiling of interstitial nitrogen and surface nitrides has already been probed using SIMS measurements for this recipe. These measurements have been successfully modelled by extrapolating data from nitride growth studies performed at atmospheric pressure and temperatures above 1000°C [1]. One open question is whether there is a diffusion-only zone at lower temperature in the ~20 mTorr range in which the niobium will absorb nitrogen but not create a non-superconducting nitride layer; or is the absorption of nitrogen only possible by first forming a nitride buffer layer which then frees up nitrogen for absorption which is what has been shown down to 600°C at atmospheric pressures on long time scales. A systematic study of absorption vs. temperature and correlated SIMS measurements is required to answer this question. We report on measurements of the parabolic rate constant vs. temperature from 400°C to 900°C of cavity grade niobium with metallurgically flat witness samples. Depth profiles of witness samples using SIMS are presented together with SEM imaging for nitride crystals and correlated with N absorption.

INTRODUCTION

In 2012 and 2013 the first two results of surface "doping" on SRF cavities were presented using titanium and nitrogen, showing an unprecedented high Q0, rising with field [2,3]. First theoretical predictions of such low surface resistance, Rs(B), appeared with distinctly decreasing dependence on surface magnetic field [4,5]. The LCLS-II project embarked on a research program 2014-2015 at FNAL, JLab and Cornell University to take advantage of this new phenomenon.

One of the open questions at the time of this study was whether effective doping of niobium without the need for post-heat-treatment chemistry to remove non-superconducting nitrides can be obtained. Multiple studies at 800°C and above show non-superconducting nitrides form in the pressure range ~20 mTorr [6,7], and nitride formation at 1 atm can be produced down to 600°C [8].

In this study we performed nitrogen doping of SRF grade RRR niobium from 400°C to 900°C at ~20 mTorr to model the total absorption and compare with previous studies to 600°C to 1000°C at 1atm pressure N_2. Along with the absorption data, secondary ion mass spectrometry (SIMS) depth profiles of nitrogen and scanning electron microscope (SEM) data analysis of the surface for witness samples are shown. The absorption parabolic rate constant calculations, SIMS profiles and SEM images all show nitride growth dominates over the entire temperature range. Ignoring bulk diffusion, our data at 20 mTorr and short time scales matches the approximate slope of Clenney and Rosa's data, but also shows an order of magnitude lower absorption attributed to the lower pressure in our process [8].

DOPING NB SETUP

Doping was performed on two cavity grade niobium half-cell plates from the Spallation Neutron Source (SNS) stock material manufactured by Tokoyo Denkai with a RRR=250. The original stock material measured 3.99 mm thick × 381 mm diameter. The two plates were as manufactured with no additional heat treatment, chemistry or forming before this study.

Before each doping the plates were chemically etched by HF(48%) : HNO3(60%) : H3PO4(85%) = 1:1:1 buffered chemical polishing to remove the doping from the previous run and remove the damage layer before the first run. The amount of removal before each annealing step is shown in Table 1. The runs were performed in the following order: 400°C, 500°C, 600°C, 700°C, 800°C, 900°C, and then a retest at 600°C. The re-run at 600°C was for sample verification and the plate absorption rate did not change for the two runs at 600°C. For each run, the two plates along with a nano-polish fine grain and large grain 10 mm ×10 mm sample were loaded into the furnace. The furnace was pumped down to 2×10^{-7} Torr before the heaters were turned on. For all runs except 800°C, the furnace was ramped to 800°C at a rate of 5° C/min and held for 2 hours before ramping down/up at a rate of 5C°/min, held for 10 minutes to stabilize the temperature; then doping was performed. For 800°C, the doping proceeded immediately after the 2-hour run.

* Funding Agency: Authored by Jefferson Science Associates, LLC under U.S. DOE Contract No. DE-AC05-06OR23177.
#ari@jlab.org

A COLD BEAD-PULL TEST STAND FOR SRF CAVITIES

A.Vélez, A.Frahm, J.Knobloch, A.Neumann, Helmholtz-Zentrum Berlin, Berlin, Germany

Abstract

Bead-pull measurements represent a final step in the fabrication process of an SRF cavity. These tests allow to characterise the flatness of the field profile in order to mechanically tune the cavity to achieve design specifications. The realization of a bead-pull measurement is always performed at room temperature and therefore it is influenced by the material physical properties resulting into higher surface losses as compared to the superconducting state. Moreover, questions like mechanical deformation due to asymmetrical thermal shrinkage through the cool-down process and the stress created by the tuner actuation have not yet been answered experimentally. In this paper, an upgrade of the former Cold-Bead pull system developed by HZB [1] is presented. This test-stand is capable of holding a 9-cell Tesla cavity at LHe temperature providing a realistic insight to cavity parameters under operation conditions. In addition, a copper test pill-box is placed in series with the multi-cell cavity in order to perform 1.8K calibration of the bead. Test results of the commissioned test-stand prototype are presented on this paper.

INTRODUCTION

Many different mechanical systems have been developed and used by industry and Labs as a working tool to accurately perform final tuning of the cavity geometry in order to fulfil specifications [2,3]. As it is known this process is always performed under "warm conditions" with the focus on the operating fundamental mode as a quality indicator. HZB approach is to develop a test-stand capable of analysing the field profile characteristics of a Niobium prototype in a SC regime. The goal is to be able to validate the future fabricated prototypes while having a deeper insight on the cavity changing response due to environmental conditions such as temperature through the cool-down process. As it is detailed in [1] the cold bead-pull test-stand offers the possibility to analyse and characterize the field profile for the fundamental TM_{010} band within a 1.8K environment as well as high order modes (HOMs). The later measurement becomes often very complicated since it is masked by the high surface resistivity of Niobium above 9.2K. As it is later discussed the presented test-stand is an slight modifications of the former prototype where limitations such as field saturation for the fundamental TM_{010} band due to the size and metallic condition of the bead are solved. The set-up has been commissioned in HoBiCaT [4] by the characterizations of a 1.3GHz 9-cell Tesla cavity with mounted Helium vessel and tuner. As a result accurate field profiles and R/Q values have been obtained. A 1.3GHz Copper pill-box has been placed in series with the measured 9-cell Tesla in order to perform the necessary bead calibration and measure the corrected form factor of the bead under experiment environmental conditions which would allow the correct determination of the R/Q values.

BEAD-PULL TESTS-STAND

Main mechanical modifications required consist on the enlargement of the supporting aluminium structure to hold the two cavities within the HoBiCaT [4] space capabilities (Fig.1). As it is later described the size and material of the bead has also been changed to modify the system´s sensitivity.

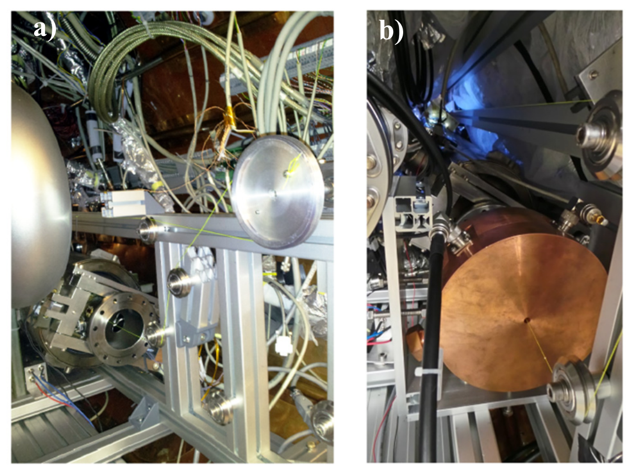

Figure 1: 9-cell Tesla cavity mounted on the test-stand before the installation of the pillbox (a). Pill-box cavity mounted with the wire system inside the HobiCat cryo-module (Niobium 9-cell cavity hidden behind) (b).

The commissioning procedure is performed in two phases. On the first stage the bead is placed at the beginning of the run (pill-box side) and several runs are performed to derive the experimental form factor *(f_{bead})* of the bead by comparing with the simulated eigenmode response (COMSOL Multiphysics [5]). On a second stage and once the form factor is known, the bead is allowed to enter the cavity under analysis to perform the analysis of the selected bands of interest.

Bead Calibration

Due to the high sensitivity of the field response to the used metallic bead under LHe temperature found in the 1st experiment [1] a smaller dielectric bead was chosen (spherical Macor ε_r=6, r=0.75mm, r_{hole}=0.25mm) in order to avoid saturation on the fundamental pass band. As it was already described, a copper pill-box (l=75mm,

MEASUREMENTS OF THE BEAM BREAK-UP THRESHOLD CURRENT AT THE RECIRCULATING ELECTRON ACCELERATOR S-DALINAC*

T. Kürzeder†, M. Arnold, L. Jürgensen, J. Pforr, N. Pietralla, TU Darmstadt, Darmstadt, Germany
F. Hug, JGU Mainz, Mainz, Germany

Abstract

Linear accelerators, in particular those using a recirculating design and superconducting cavities, have to deal with the problem of Beam Break-Up (BBU). This instability can limit the maximum beam current in such accelerators. Knowing the effectiveness of prevention strategies is of great interest especially for future accelerators like energy recovery linacs (ERL) which aim for high beam currents. One option is to optimize the cavities and higher order mode couplers of those machines. In addition one may adapt the beam line lattice for further suppressing BBU. The superconducting recirculating accelerator S-DALINAC at the Technische Universität Darmstadt provides electron beams in c.w. for nuclear physics experiments since 1991. As the SRF components were never optimized for higher order mode suppression the S-DALINAC suffers from BBU at relatively low beam currents of a few μA. While those currents are sufficient for most nuclear physics experiments we can investigate BBU with respect to the beam optics. Measurements were done and different BBU limits were found for different energy settings of the accelerator. First tests were carried out to increase the maximum beam current by varying the beam optics in the first recirculation loop.

INTRODUCTION

The S-DALINAC is a recirculating superconducting linear accelerator located at the Technische Universität Darmstadt. It provides electron beams in c.w. for nuclear physics experiments since 1991 [1]. It consists of a 10 MeV injector and a 40 MeV main linac, both superconducting using 3 GHz elliptical niobium cavities. The linac houses eight 20 cell cavities for the main acceleration, while the injector cryo-module uses beside two of those cavities an additional two cell and five cell structure for pre-acceleration. So far two recirculation beam lines allowed to use the main linac up to three times. Currently a third recirculation is under construction allowing an additional linac pass in future [2]. Figure 1 shows a drawing of the S-DALINAC and Fig. 2 a photograph of one of its cavities. The design beam current in the recirculating mode at 130 MeV beam energy was 20 μA. Early estimations [3] during the design phase of the S-DALINAC predicted no transverse beam break-up (BBU) within the design parameters of beam energy and current, but nevertheless operation experience showed that instabilities occurred, which could be related to BBU. Therefore the S-DALINAC can be used to investigate the behavior of BBU as it shows up at low beam current which ensures that we can do so without the risk of damaging the accelerator.

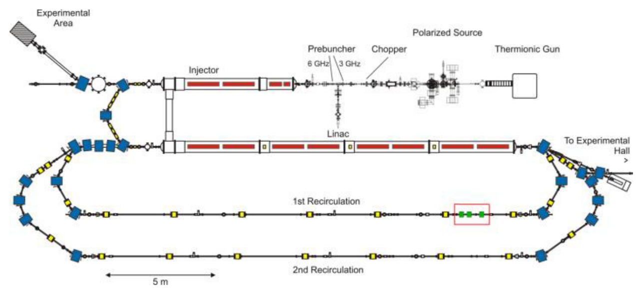

Figure 1: Floorplan of the S-DALINAC with two recirculation beam lines. Three skew quadrupole magnets (green) were installed in the first recirculation line in order to mix the transverse phase space advance.

Figure 2: Picture a of S-DALINAC 20 cell cavity.

BEAM BREAK-UP

When electron bunches travel through an accelerating structure they can excite higher order modes (HOM) in it. Especially in superconducting cavities these modes can have a large quality factor and thus a long lifetime. Such HOMs, for example dipole modes, deflect the beam in transversal direction and the bunches start to oscillate around the design orbit. In case of a recirculating accelerator design the bunches may re-enter the cavity with that offset and the same HOM can be excited even more and thus the deflection becomes even larger. If the deflection becomes too large the beam will be lost and one talks about beam break-up.

Early superconducting accelerators [3,4] have observed this phenomenon and also Energy Recovery Linacs (ERL), were the electron beams also re-enters the same linac to deaccelerate the electrons and gain back their energy, suffer from it [5]. As the excitation of a HOM becomes larger if the bunch charge is larger, BBU limits the maximum beam current in recirculating linac and ERLs. A formula, taken and modified from [6], shows the threshold beam current for a single turn ERL with one HOM:

$$I_{th} = -\frac{2p_b c}{e\left(\frac{R}{Q}\right)Q\frac{\omega}{c}T_{12}sin(\omega t_r)} \quad , \tag{1}$$

* Work supported by the Federal Ministry for Education and Research (BMBF) under Grant No. 05K13RDA
† kuerzeder@ikp.tu-darmstadt.de

ISBN 978-3-95450-169-4

STATUS AND OPERATION OF THE ALBA LINAC

R. Muñoz Horta, D. Lanaia, F. Pérez, ALBA Synchrotron, Cerdanyola del Vallès, Spain

Abstract

The pre-injector of the ALBA light source is a linac that delivers electrons up to a maximum energy of 125 MeV. It consists of a pre-bunching, a bunching and two accelerating sections feed by two 35 MW klystrons. Since July 2014 ALBA is operating in top-up mode, and the linac is delivering 110 MeV electrons in multibunch mode every 20 minutes. Recently, new injection modes have been implemented and successfully tested. For one side, injection into the ALBA booster is now also available with only one of the two klystrons in operation, and the linac delivering a 67 MeV beam. On the other hand, the linac single bunch mode has been integrated to the top-up operation application. By means of an algorithm, single bunch mode operation provides any kind of filling pattern in the ALBA storage ring, with single bunch shots injected to those buckets with lowest current. The performance of the linac beam operated in these different modes is reported.

INTRODUCTION

The ALBA Synchrotron is a 3 GeV light source in operation for users since May 2012 [1]. Its injector consists of a linac, shown in Fig. 1, typically set at 110 MeV and a full energy booster working at a repetition rate of 3.125 Hz. The injector runs in top-up mode, which requires a high level of operational reliability. For this reason, the ALBA injector has been provided of the 67 MeV injection mode, with which the injection to the storage ring is possible also when the linac is running with only one of its two klystrons. In addition, recent hardware and software upgrades have allowed the ALBA injector to have an accurate control of the amount and of the position of the electrons injected into the storage ring. The new injection capabilities enlarge the scope of research opportunities at ALBA, such as the performance of time-resolved experiments.

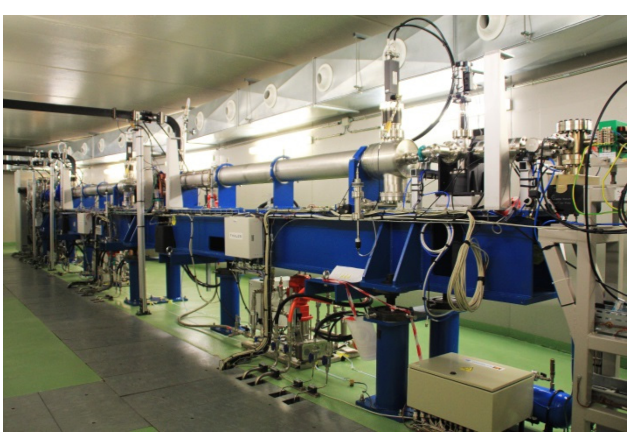

Figure 1: The ALBA linac.

ELECTRON PULSE GENERATION

The beam at the ALBA linac [2] is generated at 90 keV by a thermionic gun. A grid modulates the beam at 500 MHz, creating bunches of 1 ns length which can be extracted in multi or in single bunch modes, see Fig. 2. In multibunch (MBM), trains of bunches separated by 2 ns are produced. In single bunch (SBM), one or several single bunches can be generated separated by an adjustable time interval. The pattern of bunches delivered by the gun can have a maximum length of 400 ns, which is the width of the pulse from the kicker magnet used to inject the beam into the booster.

The maximum charge per single bunch achievable at linac exit is 0.25 nC while minimum measurable charges are in the range of few pC.

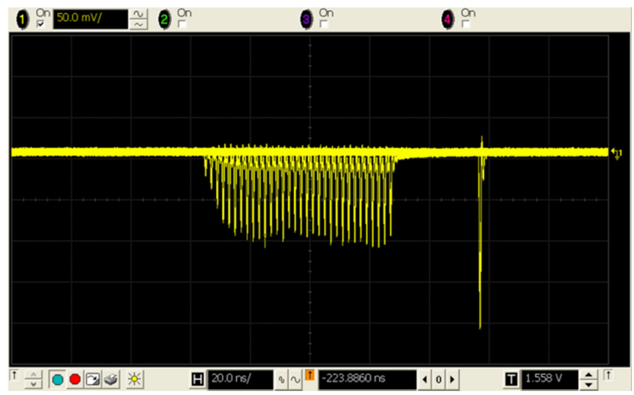

Figure 2: Tain of 32 bunches and one single bunch at FCT right after the electron gun, taken in a two-stage measurement.

After being generated, the electron pulses enter a three stage bunching system consisting of a sub-harmonic prebuncher cavity resonant at 500 MHz (PB1), a 3GHz prebuncher (PB2) and a 22-cell standing wave buncher (BU). At the buncher exit the energy of the beam is of 16 MeV and the bunch length has been reduced by 80%. Two identical travelling wave constant gradient accelerating sections (AS1 and AS2) increase further the energy up to a maximum of 125 MeV. Under normal conditions klystron 1 feeds the bunching section and also the first accelerating structure. Klystron 2 feeds exclusively the second accelerating structure.

LINAC OPERATION

During the first two years of top-up operation the linac performance has been reliable, delivering a stable beam. No failure of the linac system has interrupted the service to users. Most hardware problems use to arise after switching the subsystems off and on. Up to now, the failures that needed a longer reparation time have been related with the electron gun electronics. Besides, fluctuations of the vacuum and instabilities of the high voltage applied

NOVEL SCHEME TO TUNE RF CAVITIES USING REFLECTED POWER*

R. Leewe†, Z. Shahriari, K. Fong, TRIUMF, Vancouver, Canada
M. Moallem, Simon Fraser University, Surrey, Canada

Abstract

Tuning of the natural resonance frequency of an RF cavity is essential for accelerator structures to achieve efficient beam acceleration and to reduce power requirements. Typically, operational cavities are tuned using phase comparison techniques. Phase measurement is subject to temperature drifts and renders this technique labor and time intensive. To eliminate the phase measurement, reduce human oversight and speed up the start-up time for each cavity, this paper presents a control scheme that relies solely on reflected power measurements. A sliding mode extremum seeking algorithm is used to minimize the reflected power. To avoid tuning abrasion, a variable gain minimizes motor movement around the optimum operating point. The system has been tested and is fully commissioned on two drift tube linear accelerator tanks in TRIUMF's ISAC I linear accelerator. Experimental results show that the resonance frequency can be tuned to its optimum operating point while the start-up time of a single cavity and the accompanied human oversight are significantly decreased.

INTRODUCTION

To achieve efficient beam acceleration and to reduce power requirements, the RF cavities need to be tuned such that the excitation frequency is equal to their resonance frequency. The conventional tuning technique at TRIUMF uses a phase comparison of the input coupler and the output antenna of the cavity [1]. A pick-up antenna provides the phase information and a movable tuning plate changes the resonance frequency by changing the capacitance of the cavity.

Phase detectors cannot be located close to the cavity given that it is also a source of x-radiation. The high frequency nature of the phase signal and the necessary long cable length result in a high temperature sensitivity of the phase. Due to thermal effects on amplifier and cables, phase drifts result in inexact cavity frequency adjustment. The temperature sensitivity also leads to phase drifts outside the controllable range necessitating frequent manual phase adjustment. Consequently, starting up a single cavity and tuning its resonance frequency can take up to several minutes.

The phase related difficulties motivated the development of a frequency tuning system based on reflected power or reflected voltage. Room temperature cavities are operated as critically coupled, in which the operating and resonance frequencies of the cavity are equal, the reflected power is zero, and the acceleration field is at its maximum. When the two frequencies diverge, the reflected power increases. A new method to control the cavity's resonance frequency is based on utilizing the reflected power characteristics [2]. The reflected power is a function with minimum. Hence, the frequency tuning using reflected power measurement can be rephrased as an extremum seeking problem.

Extremum seeking control (ESC) or self-optimization approaches can be traced back to the 20th century. It focuses on control problems where a dynamic nonlinear plant is to be regulated to operate at an optimal operating point or to track an optimal trajectory based on a performance criterion. One of the most robust extremum seeking approaches is sliding mode control which does not require the gradient of the performance function.

This paper presents the application of a two time scale sliding mode extremum seeking algorithm to minimize the reflected power. An adaptive gain stops the motor movement in the vicinity of the optimum to eliminate small oscillations around the driving frequency and to reduce motor setup abrasion. Experimental tests were performed on TRIUMF's drift tube linac (DTL) tank 4 and 5.

CAVITY FIELD AND REFLECTED POWER

The cavity behavior can be described by a parallel resonant circuit [3]. The corresponding differential equation in terms of the reflected voltage and under perfect impedance matching condition is stated as [2]

$$\ddot{z} + \gamma\dot{z} + \left(\omega_0^2 + k\theta\right) z = V_f cos\left(\omega_i^2 - \omega_0^2 - k\theta\right). \qquad (1)$$

The relevant variables and parameters are defined as follows:

z reflected voltage;
γ damping coefficient;
ω_0 geometry dependent natural resonance frequency;
V_f forward input voltage amplitude;
ω_i operating frequency;
θ control input;
k tuning sensitivity in terms of $\frac{Hz^2}{mm^2}$

Application of a control input θ to the tuning system of the cavity changes the capacitance of the cavity, which in turn affects the natural resonance frequency of the cavity. The solution to (1) in terms of transient and steady state components as well as the analytical form of reflected signal, $z(t)$, is provided in [2]. The measured reflected power $F(\theta)$ is obtained through the rectified reflected signal, which can be mathematically modeled by a low pass filter as follows

$$F(\theta) + \tau\dot{F}(\theta) = z^2, \qquad (2)$$

where τ denotes the time constant of the low pass filter. The reflected power can then be mathematically expressed as

* Work supported by Natural Science and Research Council NSERC
† Ramona@triumf.ca

ISBN 978-3-95450-169-4

BEAM COMMISSIONING OF THE i-BNCT LINAC*

F. Naito†, S. Anami, Z. Fang, K. Futatsukawa, Y. Honda, Y. Hori
K. Ikegami, M. Kawamura, H. Kobayashi, T. Kurihara, Y. Liu, T. Maruta, T. Miura, T. Miura
T. Miyajima, T. Obina, Y. Sato, T. Shibata, M. Shimamoto, A. Takagi, E. Takasaki
M. Uota, F. Qiu, KEK, Tsukuba, Ibaraki, 305-0801, Japan
H. Kumada, T. Onishi, S. Tanaka, University of Tsukuba, Tsukuba, Ibaraki, 305-8577, Japan
S. Fujikura, University of Tokyo, Bunkyo-ku, Tokyo, 113-0033, Japan
A. Miura, JAEA, Tokai-mura, Ibaraki, 319-1195, Japan
N. Nagura, T. Oba, NAT, Tokai-mura, Ibaraki, 319-1112, Japan
T. Ouchi, ATOX, Tokai-mura, Ibaraki, 319-1112, Japan

Abstract

The beam commissioning of the linac for the boron neutron capture therapy of Ibaraki prefecture (i-BNCT) has been started. The accelerator of i-BNCT consists of the 3-MeV RFQ and 8-MeV DTL. The 8-MeV beam injected on the target made of Beryllium in order to produce a intense neutron beam. The design of RF structure of the linac is based on the J-PARC linac. After the first observation of neutron production on December 2015, significant modifications to the linac were given in order to increase the operation stability and the beam power. The status of the beam commissioning of the i-BNCT is reported.

INTRODUCTION

The boron neutron capture therapy (BNCT) is one of the candidates for the cancer therapy. The principle of the BNCT is as follows:

- Drug which contains Boron ^{10}B is delivered to the cancer affected part.
- Neutrons are irradiated from the outside to the affected part.
- Neutron (<0.1 eV) reacts with Boron ^{10}B. The reaction $^{10}B(\mathrm{n},\alpha)^7Li$ makes α.
- Both of ranges for ^7Li and α in a cell are a few μm. Therefore both particles stop in the cell because those loss the whole kinetic energy.
- The cell affected by cancer is destroyed by the lost energy by particles.

At the beginning of the BNCT development, a nuclear reactor was used as the neutron source. Recently the accelerator based BNCT is being developed in the world because it is possible to install the system in the hospital. The BNCT using neutrons produced by a proton linac has been developed by the collaboration in University of Tsukuba, KEK and the Ibaraki prefectural government [1] . This BNCT system is called i-BNCT. The several private companies are also committed to the i-BNCT. The construction of the system was completed and the beam commissioning has been started. The produced neutron was observed on December 2015 [2]. At that time, the peak beam current from the linac was 20 μA. It was a check to find the serious problem in the accelerator system. After the beam demonstration, a lot of significant modifications to the linac were given in order to increase the operation stability and the beam power.

* Work partially supported by NEDO and Grant-in-Aid for Scientific Research
† fujio.naito@kek.jp

LINAC PARAMETERS

The layout of the i-BNCT accelerator is shown in Fig. 1. The linac of the i-BNCT is composed of the ion source with a multi-cusp magnetic field, 3-MeV RFQ and 8-MeV DTL [1]. Design parameters of cavities are summarized in Table 1. The design of RF structure of the RFQ and the DTL is the same as one of the J-PARC linac. However the cooling water system of i-BNCT is different from that of J-PARC because the beam duty factor of i-BNCT is eight times larger than that of J-PARC as shown in Table 2 .

Figure 1: Perspective of i-BNCT accelerator system.

Table 1: Design Parameters of Cavities

Items	RFQ	DTL
Length	3.1 m	3.0 m
Frequency	324 MHz	324 MHz
Injection energy	50 kV	3 MeV
Ejection energy	3 MeV	8 MeV
Cell number	-	31
Wall loss	340 kW	320 kW

Ion Source and LEBT

The ECR ion source with a pair of solenoid magnet was used for the beam test carried out at last year. However it was not able to keep the design high-voltage of 50 kV because of defects for the high-voltage insulation. Thus

TUNING OF THE CERN 750 MHz RFQ FOR MEDICAL APPLICATIONS

B. Koubek*, A. Grudiev, Y. Cuvet, C. Rossi, M. Timmins, CERN, Geneva, Switzerland

Abstract

CERN has built a compact 750 MHz RFQ as an injector for a hadron therapy linac. This RFQ was designed to accelerate protons to an energy of 5 MeV within only 2 m length. It is divided into four segments and equipped with 32 tuners in total. The RFQ length corresponds to 5λ which is considered to be close to the limit for field adjustment using tuners. Moreover the high frequency results in a sensitive structure and requires careful tuning by means of the alignment of the pumping ports and fixed tuners. This paper gives an overview of the tuning procedure and bead pull measurements of the RFQ.

INTRODUCTION

The HF-RFQ (High Frequency - RFQ) will be used as an injector for the LIGHT project [1], a linac based proton therapy facility. It accelerates protons from 50 keV to 5 MeV within 2 m and is designed to minimize beam losses above 1 MeV [2]. From an RF point of view the very compact 4-vane structure operates at about twice the frequency of existing RFQs [3]. It consists of four modules with a length of about half a meter. The dipolar modes are detuned by means of dipole stabilizer rods at the end plates. The electrode voltage is designed to be constant along the RFQ that requires a constant longitudinal field distribution in terms of tuning. In order to compensate construction errors the structure is equipped with 32 tuners. The 12 pumping ports could be used as additional tuning devices if necessary. The 4 power couplers are placed in the two middle segments of the RFQ, one in each quadrant. Each power coupler will be fed by a 100 kW Inductive Output Tube (IOT) in order to maintain a nominal voltage of 68kV. The Q-factor due to losses in copper is about 6500 according to 3D RF design simulations. The operation frequency is set to 749.48 MHz.

BEAD PULL SYSTEM AND TUNERS

For bead pull measurements on a 4-vane RFQ a bead has to travel through all 4 quadrants consecutively. The bead pull setup is shown in Fig. 1. It is based on the system which was previously used for the measurements of the LINAC4 RFQ at CERN [4] and has been adapted to the dimensions of the HF-RFQ. A wire with 0.3 mm diameter was used and the tension was adjusted with a spring. The wire is set in one closed loop that enables consecutive measurements of all four quadrants while the bead can be pulled around the pulleys to travel between the quadrants. For each quadrant the wire can be adjusted in azimuthal direction using micrometer screws.

The RFQ's length is 5λ which is considered to be a limit for using only tuners to adjust the field [3]. For these tuners a cone-shaped design was chosen in order to minimize RF

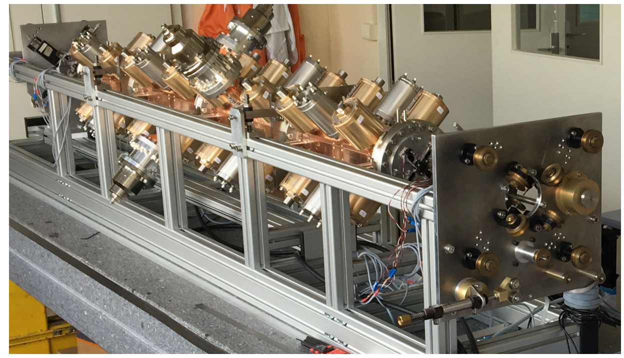

Figure 1: Support with the bead pull system and mounted RFQ.

losses and to be large enough to provide adequate tuning range and sensitivity. All tuners were manufactured with an additional length of 11 mm and a special tool was used in order to adjust the tuner's penetration depth with a 10 µm accuracy. After the tuning process the tuners were cut to their individual length and inserted with the same radial and angular orientation using this tool. Figure 2 shows a cross section of this tool with an inserted tuner.

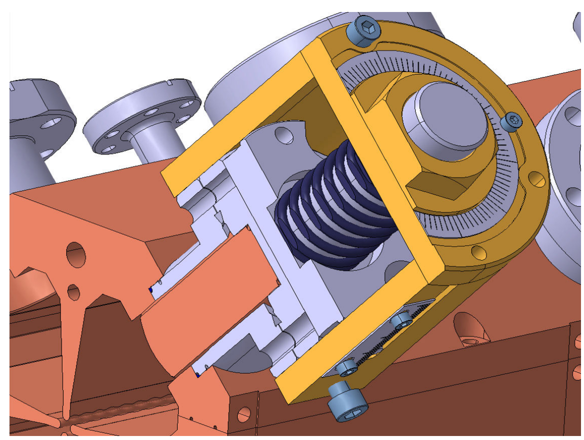

Figure 2: Tuner tooling for precise adjustment for tuning and final assembly after cutting.

RF MEASUREMENTS

The objective of tuning is to provide the proper field distribution according to the beam dynamics requirements and also to adjust the operation frequency. All RF measurements have been done at the defined operating temperature of the RFQ at 24 °C. For precise frequency adjustment the cavity was filled with dry nitrogen to avoid any influence of air humidity. Figure 3 shows a measurement of the mode spectra of the RFQ.

For the field measurements the standard bead pull method was used. The bead was made of aluminum and has a cylindric shape with rounded edges. It has a length of 7 mm

* benjamin.koubek@cern.ch

ISBN 978-3-95450-169-4

DESIGN AND COMMISSIONING OF FRIB MULTIPACTING FREE FUNDAMENTAL POWER COUPLER*

Z. Zheng, S. Stark, K. Saito, J. Popielarski, T. Xu, Y. Yamazaki, FRIB, MSU, MI 48824, USA

Abstract

The original Fundamental Power Coupler (FPC) of Half-Wave Resonator (HWR) for the Facility of Rare Isotope Beams (FRIB) requires multipacting conditioning at operating RF power which is up to 5 kW Continuous Wave (CW). Conditioning takes a lot of time and RF power, and its elimination is highly desirable. To significantly shorten the RF conditioning, we developed a multipacting-free coupler design. This paper reports the latest progress in the optimization and prototype tests of multipacting-free coupler. The choke structure is removed and coupler geometry is further modified to protect the coupler RF window from the electron bombardment. The comparison result of multipacting-free coupler with original coupler was performed on automatic conditioning system, which showed significant time reducing for RF conditioning.

INTRODUCTION

In the Technology Demonstration Cryo-Module (TDCM) test at FRIB, we found heavy multipacting in the FPCs for HWR cavities. It is a phenomenon of secondary electrons' resonance which can breakdown FPC and superconducting RF cavity in the worst case. Even though it can be conditioned by RF power, it always takes a long time and cost consuming. For example, the overall RF conditioning time for power coupler used in FRIB TDCM was more than two weeks.

A suppressing method of the multipacting in FRIB FPC was first introduced in [1]. Subsequently to the optimized method, a multipacting-free coupler design was developed and highly recommended to apply in FRIB by the Accelerator Systems Advisory Committee (ASAC). In this paper, section 2 reports the latest upgrade in the design, section 3 introduces the automatic conditioning system which was developed for RF conditioning of FRIB FPCs, and section 4 reports the comparison tests between original couplers and multipacting-free couplers.

LATEST PROGRESS IN THE DESIGN OF MULTIPACTING-FREE COUPLER

A simple multipacting law for the coaxial couplers was derived in [2].

$$P_n = \frac{A\omega^4 (r_2 - r_1)^4 m^2}{(2n-1)^2 \pi\eta e^2} (\ell n(\frac{r_2}{r_1}))^{-1} \quad (1)$$

P_n is the power where multipacting turned on, r_1 and r_2 are the inner and outer conductor radius respectively, η is the wave impedance in vacuum (377 Ω), A is 1 for traveling wave and 0.25 for standing wave due to superposition theorem, e is electron charge, m is electron mass, ω is RF angular frequency, n is the order of two-point multipacting (for instance n=1 for two-point 1st order multipacting).

Based on Equation (1), we can predict the location and the RF power level where multipacting turns on. A multipacting-free coupler design was proposed according to the law, further upgrade has been applied recently to improve the performance. Figure 1 shows the latest multipacting-free coupler design for prototyping.

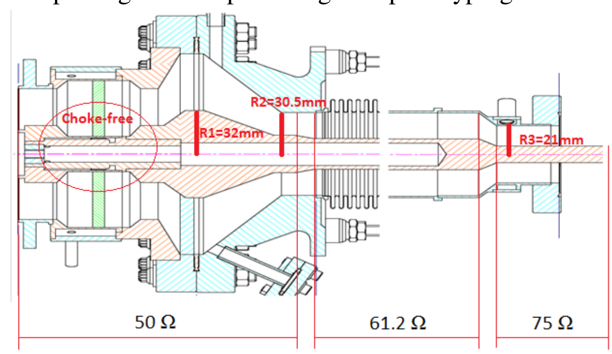

Figure 1: Latest multipacting-free coupler design.

The choke structure near the RF window is a standard techniques for the impedance matching [3], however it is complex and delicate. In order to make the coupler design simple and easy to fabricate, the choke structure was eliminated in the latest multipacting-free coupler design. The inner conductor radius R1 is increased to be larger than R2 in the latest design so that the RF window can be masked from the electrons from beam line.

AUTOMATIC CONDITIONING SYSTEM

The old coupler conditioning system in FRIB used standing wave RF power which can only condition one coupler at time. Due to the characteristic of standing wave, only one local region of coupler is conditioned with old system, thus other parts of coupler remain unconditioned. New conditioning system uses travelling wave RF power which can condition two couplers at the same time and each coupler is fully conditioned. The maximum RF power used for new system is 20kW with 20% duty cycle (limited by heat load of conditioning resonator). The 20 kW is suitable to condition FRIB couplers which have a maximum forward power of 5 kW.

Baking is applied before RF conditioning to initialize the pressure of the whole system below 1e-8 torr. It was operated by PID controller to keep the temperature of system around 120°C. Two protections were used to keep it safe for overnight operation without people onsite. One is fuse wire installed on the controller to keep the current of heat tapes under 5A. The other one is using

*Work supported by the U.S. Department of Energy Office of Science under Cooperative Agreement DE-SC0000661
#zhengw@frib.msu.edu

ULTRA-SHORT BUNCH ELECTRON INJECTOR FOR AWAKE

S. Doebert, CERN, Geneva, Switzerland

Abstract

The proton driven plasma wake field acceleration experiment AWAKE at CERN will start at the end of this year. In 2017 an S-band electron injector producing bunches of a few ps in length will be added to probe the wake fields stimulated by a driving proton beam. In the future this electron injector will have to be upgraded to obtain electron bunches with a length of 100 - 200 fs in order to demonstrate injection into a single bucket of the plasma wave and therefore sustainable acceleration with low energy spread. Target bunch parameters for the study are a bunch charge of 100 pC, 100 fs bunch length, an emittance smaller than 10 mm mrad and a beam energy > 50 MeV. The status of a study to achieve these parameters using X-band accelerator hardware and velocity bunching will be presented.

INTRODCUTION

The proton driven plasma wakefield experiment at CERN called AWAKE [1,2] is about to start operation at the end of 2016. The first phase will use the 400 GeV proton beam from the SPS and a high power laser to trigger a self-modulated instability (SMI) within the roughly 1-2 ns long proton bunch. The modulated proton beam can then drive resonantly plasma wakefields in a rubidium vapour plasma. The layout of the experiment is shown in figure 1. The first phase of the experiment will focus on studying this self-modulated instability and the wakefields by observing their effects on the proton beam.

In a second phase starting at the end of 2017 an electron injector will be added to be able to directly probe the generated wakefields with an electron beam and measure its acceleration. This electron injector consists of a conventional s-band rf gun receiving a fraction of the laser energy used to generate the plasma and the SMI. The energy of the beam is boosted up to 20 MeV by an s-band accelerating structure. Beam charges between 0.1 and 1 nC can be accelerated with an emittance of the order of 2 mm mrad. Initially the bunch length of such beams will be 4 ps sigma initially and might be reduced by a factor of two by compressing the drive laser pulse length. This second phase of AWAKE should demonstrate the principle of electron acceleration with proton driven plasma wakefields. We expect electron beams accelerated up to 1-2 GeV in our 10 m long metal vapour plasma cell. The emphasis is not yet to show acceleration of high quality beams with a reasonable energy spread and emittance preservation.

The longer term goal of the AWAKE experiment however is to investigate if this novel acceleration concepts can be used for high energy physics applications. Therefore the emphasis of the next stage of the experiment named RUN II [3] will be on demonstrating the accelerating of high quality beams and expandability of the plasma cells providing the acceleration. It is clear that the briefly described injector for phase 2 below will not be able to provide the necessary beam parameters for this purpose in particular the bunch length has to be reduced to a fraction of the plasma wavelength in our experiment. Studies are ongoing to determine the optimal parameters for RUN II in terms of bunch length and beam current.

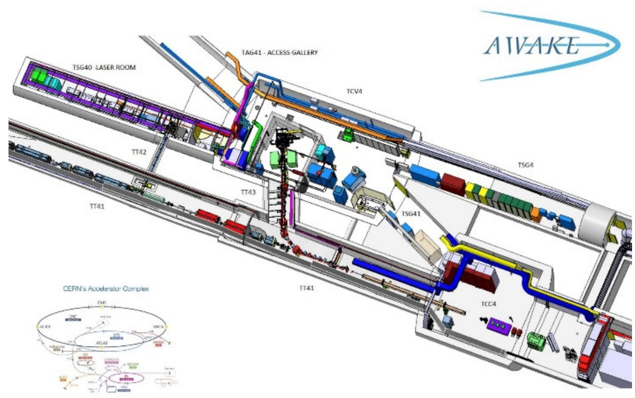

Figure 1: Overview of the AWAKE facility at CERN. A proton beam (lower left) from the SPS is send into a 10 m long plasma cell (lower right) for interaction with a high power laser and an electron beam (central).

BASELINE INJECTOR FOR AWAKE

The electron injector for phase 2 of the AWAKE experiment has been designed taking into account numerous constraints. This part of the experiment was added relatively late to the CERN work package, which led to the choice of recycling partly existing hardware from the CLIC studies. In addition there are serious space restriction in the current setup of AWAKE that uses existing tunnels and caverns. Only about 5 m are available for the electron source, for subsequent acceleration to 20 MeV and for the associated beam line diagnostics. The layout of the injector is shown in figure 2 and is described in detail in [4]. The drive laser pulse for the rf gun is derived from the high power laser enabling the plasma and SMI generation. A custom scheme of quadrupling its frequency and pulse compression in air led naturally to a laser pulse length between 2 and 10 ps FWHM on the cathode. The rf gun is equipped with a load-lock system that allows to use copper cathodes or Cs_2Te cathodes with a higher quantum efficiency. Simulations with the tracking code ASTRA [5] predicts an emittance of 1.8 μm for a bunch charge of 0.2 nC. The gradient used in the rf gun is 100 MV/m and 15 MV/m in the 3 GHz booster

ELECTRON LINAC UPGRADE FOR THOMX PROJECT

L. Garolfi*, C. Bruni, M. El Khaldi, LAL, Orsay, France
N. Faure, A. Perez Delaume, PMB-ALCEN, Peynier, France

Abstract

The injector Linac for Thomx consists of an electron gun and S-band accelerating section. The RF gun is a 2.5 cells photo-injector able to provide electron bunches with 5 MeV energy. During the commissioning phase, a standard S-band accelerating section is able to achieve around 50 MeV corresponding to around 45 keV X-rays energy. Since the maximum targeted X-ray energy is 90 keV, the Linac design will provide a beam energy of 70 MeV. The Linac upgrade of the machine covers many different aspects. The purpose is to increase the compactness of the accelerator complex whereas the beam properties for ring injection are kept. A LAL Orsay-PMB ALCEN collaboration has been established. The program foresees the RF design, prototyping and power tests of a high-gradient compact S-band accelerating structure. To fulfill the technical specifications at the interaction point, the Linac must be carefully designed. Beam dynamics simulations have been performed for optimizing the emittance and the energy spread for the ring entrance. The best set of parameters together with the effect of the accelerating section to the beam dynamics at the end of the Linac are presented.

INTRODUCTION

The Thomx project is taking advantage of the preeminent French technology in accelerator and laser fields. The goal is to design and build a demonstrator with cutting edge performances compared to similar projects either in operation or planned. A flux between $10^{11} - 10^{13}$ ph/s in the hard X-ray range is expected and the photon energy tunability will provide a Compton edge that can be set between 45 and 90 keV [1]. Another goal is to provide a compact, reliable, and tunable source which can operate in a non-laboratory environments such as hospitals or museums. These constraints impose the choice of a high collision rate scheme. The layout of the machine is based on a 50 Hz, normal conducting S-band Linac whose energy is tunable up to 70 MeV, an injection line and a compact electron storage ring. A demonstrator was funded and the components are foreseen to be assembled in the Orsay university campus at the beginning of 2017. The Linac injector is composed of the RF gun, the accelerating section and the beam diagnostic elements. Concerning the accelerating section, the French National Synchrotron Facility (SOLEIL), as a partner of the project is willing to lend a standard S-band accelerating structure that the Linear Accelerator Laboratory (LAL) built for the LEP Injector Linac (LIL) at CERN many years ago.

* garolfi@lal.in2p3.fr

THOMX LINAC SCHEME

A picosecond electron bunch is produced at the photocathode. Then, the accelerating and magnetic fields in the RF gun and solenoids drive the electron beam. After a drift space at the exit of the gun, the electron bunches are boosted up to the ring injection energy by means of the accelerating section. The transfer line ensures the bunch transport from the linac exit to the storage ring. After injection, the electron bunch is recirculated for 20 ms in the ring. The ring optics is designed as such as the beam size is very small in transverse direction, at the interaction point (IP). The project goal is to produce a high flux of 45 keV X-rays energy [2] leading to specifications for the Linac that are summarised in Table 1.

Table 1: Nominal Linac Parameters

Energy	50 MeV
Total Charge per bunch	1 nC
Number of bunches per RF pulse	1 bunch
Normalised rms emittance	< 5 π mm mrad
Energy Spread rms	< 0.3 %
Bunch Length rms	< 5 ps
Average current	50 nA
Repetition rate	50 Hz

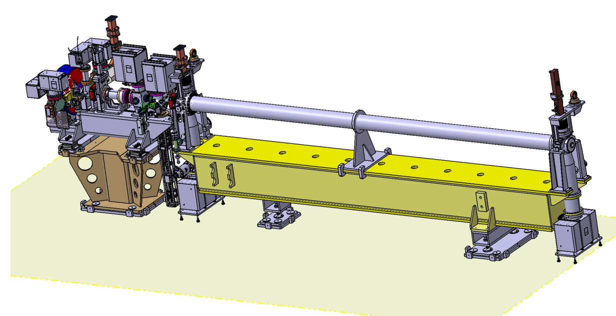

Figure 1: 3D drawing of the Thomx Linac.

RF GUN & SOLENOIDS

The RF gun is 2.5 copper cells with a resonating frequency of 2998.55 MHz. Since low emittance beam together with the possibility of operation with different total charge per bunch are required, the best technical choice is the photo-injector. To minimize risks and taking advantage on the long experience achieved from LAL in the RF gun fabrication, the latter has the same design to that has been constructed for the CLIC Test Facility 3 at CERN (CTF3). This gun has successfully been in operation for four years. To increase the current per bunch with less vacuum constraints, a metallic

ISBN 978-3-95450-169-4

DEVELOPMENT OF 704.4 MHz POWER COUPLER WINDOW FOR MYRRHA PROJECT*

F. Geslin†1 , P. Blache, M. Chabot, J. Lesrel
Institut de Physique Nucléaire d'Orsay (IPNO), CNRS-IN2P3, Orsay, France
S. Sierra, C. Lievin, P. Denis
Thales Electron Devices, Velizy Villacoublay, France
1 also at Thales Electron Devices, Velizy Villacoublay, France

Abstract

Myrrha is an accelerator driven system (ADS) hybrid research reactor designed for spent nuclear fuel burning. The linac controlling the reactor has to be highly reliable (low failure rate). In order to fulfill requirements of ADS projects like Myrrha, IPNO and Thales are involved in a power couplers research and development program. We develop a power coupler window, with "MAX" RF design, for 25 kW CW input power. During the study, we take account of fabrication and cost issues. We present in this paper the result of simulations needed to design this coupler window. The electromagnetic, thermal and thermomechanical simulations were performed with Ansys. The multipacting simulations were performed with Musicc3D, software developed by IPNO. The conditioning and test bench is also described as two prototypes have to be tested this autumn.

INTRODUCTION

Accelerator Driven System projects need high intensity protons linacs. Myrrha [1] require a 4 mA protons beam with a final energy of 600 MeV. The duty cycle of ADS is 100% with failure rate lower than once every ten days for a average power of 2.4 MW. To achieve this reliability the linac is composed by a double-injector, then two sections of superconducting cavities (Fig. 1). The first one is composed of 352 MHz two gap Spoke cavities and the second one by 704 MHz 5 cell elliptical cavities. There is two kind of elliptical cavities : $\beta = 0.47$ and $\beta = 0.65$. Both will be feed with the same type of power coupler.

In this context, IPNO and Thales Electron Devices are leading developement on ceramic windows.

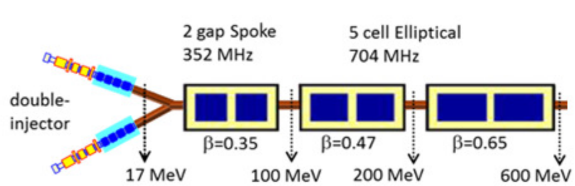

Figure 1: Layout of MYRRHA Linac

* Work supported by Thales Electron Devices
† geslin@ipno.in2p3.fr

DESIGN OF THE 704.4 MHz CERAMIC WINDOW

Figure 2 gives a mechanical view of the 704 MHz power coupler. It is based on "Max RF" design [2] The coupler is basically a coaxial line with a ceramic window to ensure vacuum barrier. Cooling of inner conductor is done with water flow. Part of the outer conductor facing the ceramic is also cooled with water and it is call "waterbox".

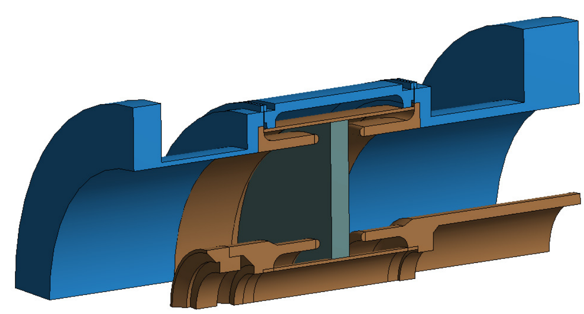

Figure 2: Geometry of the ceramic window

In the front of the ceramic window inside air and vaccum inner conductor is shape in a form call chokes. These particular shape is indeed necesary to lowered the electric field and to prevent sparks. Two important parameters for such design are the characterics of the insulator (mechanical, thermal...) and the geometry of the chokes (thickness and positions). Ceramic used in the design study was a Morgan Braze Alloys AL300 [3]. The dielectric constant of the ceramic given by the manufacturer is 9.

Thermal Simulations

Table 1 gives the power losses in ceramic window for a 25 kW CW full reflected RF incident power. As expected, losses are more important on the inner conductor than on the other part. Dissipation in ceramic is low.

Table 1: Calculated Dynamic Losses of Every Part of Ceramic Window

Losses (W)	incident power 25 kW CW full reflected
outer conductor	10.2 W
inner conductor	28.8 W
ceramic	3.9 W

ISBN 978-3-95450-169-4

DEVELOPMENT OF 352.2 MHz POWER COUPLER WINDOW FOR R&D PURPOSE*

F. Geslin†[1] , D. Reynet, M. Chabot, J. Lesrel
Institut de Physique Nucléaire d'Orsay (IPNO), CNRS-IN2P3,Orsay , France
S. Sierra, C. Lievin
Thales Electron Devices, Velizy Villacoublay, France
[1]also at Thales Electron Devices, Velizy Villacoublay, France

Abstract

IPNO and Thales are conducting power couplers research and development. This paper presents a new window design that fulfills European Spallation Source (ESS) requirements (400 kW RF peak power). The results of electromagnetic, thermal, thermomechanical, multipacting simulations and the consequences of the new ceramic window of power coupler will be reported. The multipacting simulations were performed with Musicc3D, software developed by IPNO. The new design overcome ceramics weakness in tension and allows stronger constraints in the power coupler window.

INTRODUCTION

High-power RF coupler is a keystone of superconducting accelerator. It is the connecting part between the RF transmission line and the RF cavity and provides the electromagnetic power to the cavity and the particle beam. In addition to this RF function it also has to provide the vacuum barrier for the beam vacuum. High-power couplers are one of the most critical parts of the RF superconducting cavity system in an accelerator. RF and mechanical designs are as important as fabrications process, Thales Electrons Devices and IPNO are collaborating in order to improve these aspects and two prototypes are studied.

Multipacting is a parasite phenomenon that is problematic in RF superconducting structure. In power coupler, it could lead to a dramatic failure as ceramic window is delicate component. Developed at IPNO, Musicc3D is a 3D code for modeling Multipacting in RF structures.

DESIGN OF THE CERAMIC WINDOW

The ceramic window developed is a coaxial window with water cooling in the capacitive antenna. A ceramic disc composed of alumina AL300 [1] realise the sealing between the vaccum of the cavity and the air of the coaxial waveguide as shown in Fig. 1. Figure 2 show chokes localised on each conductors and both side of the ceramic disk.

Main specification of the ceramic window are presented Table 1.

Electromagnetic Design

A study of electromagnetic design was performed with HFSS [2]. The last design simulations results are presented

* Work supported by Thales Electron Devices
† geslin@ipno.in2p3.fr

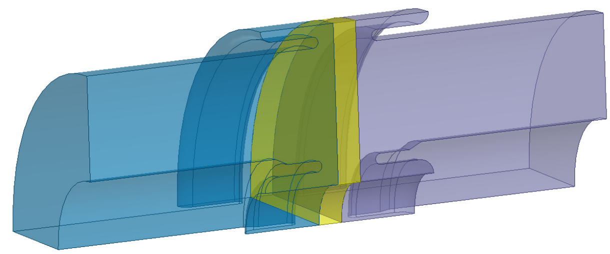

Figure 1: Perceptive view of a quarter of the ceramic window, air is in blue, vacuum in grey and ceramic in yellow.

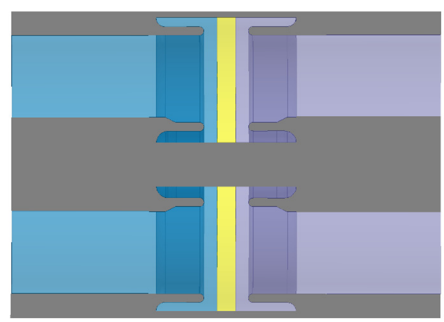

Figure 2: Cross-section of the ceramic window.

here. Figure 3 gives the electric field simulated in the ceramic window for 400 kW CW full reflected power. The highest field (0.74 MV/m) is localise on the chokes tip. The electric field where defaut is suceptible to be problematic for spark as been lowered to 0.3 MV/m by the chokes. It is three times lower than standard electric field maximum requirement [3].

Figure 4 gives the S11 parameter of the window. S11 is −76 dB at a frequency of 352.2 MHz, it show a good adaptation of the ceramic window to the needed frequency.

Table 1: Main Specification of the Ceramic Window

Main requirements	Values
frequency	352.2 Hz
Repetition frequency	14 Hz
Peak power	400 kW
Duty cycle	5 %

ISBN 978-3-95450-169-4

STATUS OF THE DEVELOPMENT AND MANUFACTURING OF LCLS-II FUNDAMENTAL POWER COUPLERS

S. Sierra, C. Lievin, C. Ribaud, Thales, Velizy, France
G. Garcin, G. Vignette, Thales, Thonon Les Bains, France
M. Knaak, M. Pekeler, L. Zweibaeumer, A. Navitski,
RI Research Instruments, Bergisch Gladbach, Germany

Abstract

For the LCLS-II project, Thales and RI Research Instruments are working on the manufacturing and assembly of 132 Fundamental Power Couplers.

The paper describes the production of these Fundamental Power Couplers. The main characteristics are remained at 1.3 GHz.

It describes the main challenges to be overcome principally on the Warm Internal conductor, with a thickness of copper of 150 µm.

We describe the results obtained on the prototype phase and the status of the serial production on the date of the paper.

INTRODUCTION

Fundamental Power couplers for the LCLS-II accelerator are derivate from the TTF3/XFEL fundamental power coupler [1]. They are designed with specific modifications for mounting on the accelerator and some specific design parts for required performances [2].

SLAC (Stanford Linear Accelerator) is in charge of the procurement and contract following, while associated laboratories (JLAb and FermiLab) are in charge of mounting these couplers on cryomodules [3].

The main characteristics of such couplers are:

- RF frequency: 1.3 GHz
- Power up to 7 kW CW
- Tuning : ± 10 mm
- Two ceramics windows

The main metallic sub-assemblies of a coupler are the Warm External Conductor (WEC), Warm Internal Conductor (WIC), The Cold External Conductor (CEC) and the antenna, illustrated in Fig. 1.

The two other critical components are the two cylindrical ceramics.

Main modifications in respect to the XFEL design are:

- Antenna profile in order to be adapted to the cavities performances
- Copper coating thickness of the WIC define at 150 µm thickness in order to avoid too large temperature heating when operating at full power of 7 kW.

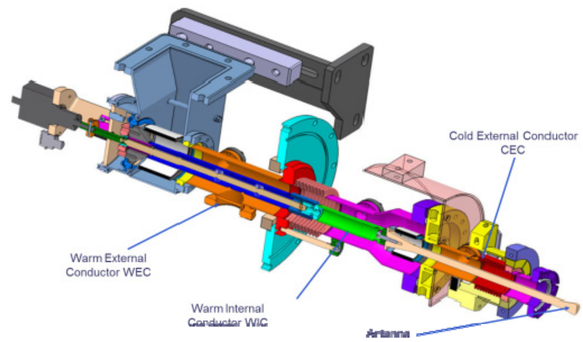

Figure 1: Coupler general layout.

COUPLER MANUFACTURING

Main steps in the coupler manufacturing are exactly the same than the one followed for the XFEL manufacturing [4].

Main steps are: parts assemblies, copper coating of RF surfaces, TiN coating of ceramics windows. Then, EB Welding in order to achieve individual Warm and Cold part of couplers.

Then the coupler parts are clean in an ISO 4 clean room and after drying, they are integrated by pair on a transition waveguide.

After a leak check and a RGA is operated, while the coupler is baked at 150°C they are send to JLab or Fermilab for final integration.

Thales Production Process

The LCLS-II couplers sub-assemblies are based on a brazing technology. This technology allows having a better reproducibility than a welded one, which is more operator dependant and also could be performed by batches, which is useful for a mass production.

All processes used for the manufacturing are derived from the experience earned on the XFEL production in order to minimize risks and optimized production scheduling.

Once the sub-assemblies are brazed and prepared, the three main one (WEC, WIC and CEC) are copper coated, as illustrated in Fig. 2 and Fig. 3.

The copper plating process is the trickiest step for the coupler manufacturing.

IF-MIXTURE PERFORMANCE DURING CAVITY CONDITIONING AT STF-KEK

Sigit Basuki Wibowo*, The Graduate School for Advanced Studies, Kanagawa 240-0193, Japan
Toshihiro Matsumoto, Shinichiro Michizono, Takako Miura, Feng Qiu,
KEK, 1-1 Oho, Tsukuba, Ibaraki 305-0801, Japan

Abstract

The Superconducting rf Test Facility (STF) at High Energy Accelerator Research Organization (KEK) was built for research and development of the International Linear Collider (ILC). In order to satisfy the stability requirement of the accelerating field, a digital low-level RF (LLRF) control system is employed. In this control system, signal from a cavity is down-converted into intermediate frequency (IF) signal before being digitized by analog-to-digital converter (ADC). In order to reduce the required number of ADCs, we proposed a technique that combines several IFs and to be read by a single ADC. Signal reconstruction of each IF is performed by digital signal processing. The performance of this technique, which is named IF-mixture, is reported in this paper.

INTRODUCTION

Superconducting rf Test Facility (STF) at High Energy Accelerator Research Organization (KEK) was built for the purpose of research and development related to International Linear Collider (ILC). The RF is 1.3 GHz with a pulse duration of 1.5 ms and a repetition rate of 5 Hz. An RF stability of 0.07 % (RMS) in amplitude and 0.24° (RMS) in phase are required for the ILC [1]. Because of such a long pulse duration, a digital low-level RF (LLRF) control system may be adopted.

In one RF station of ILC, a single klystron drives 39 cavities. In order to fulfill the accelerating field stability requirements, a digital LLRF control system based on a field programmable gate array (FPGA) board will be installed to control the RF field with vector-sum feedback (FB). Therefore, the amplitude and phase (or I and Q components) of all 39 cavities must be measured to calculate vector-sum. Furthermore, the RF waveform of drive power and reflection power from all the cavities must be monitored to ensure stable operation of the ILC RF station.

In the digital LLRF control system, RF signal from the cavity is down-converted into intermediate frequency (IF) signal by mixing with 1.31 GHz local oscillator (LO). After the down-conversion process, the amplitude and phase information of the signal are still preserved. This signal is then digitized by an analog-to-digital converter (ADC), as shown in Figure 1(a). The I and Q components of the RF signal are determined by digital signal processing (DSP). For a single ILC RF station, the digital LLRF control system requires approximately 120 ADCs.

* sigitbw@post.kek.jp

One possible way to reduce the number of ADCs is to combine several IF signals, to be read by a single ADC, and reconstruct each IF signal by DSP. This technique is named IF-mixture. In our research, we have combined up to four IF signals, thereby reducing the required number of ADCs by a factor of four. Fig. 1(b) shows the example of the technique with two IF signals.

The IF-mixture technique with vector-sum FB control applied to four cavities was successfully developed at STF-KEK [2–4]. Recently, the IF-mixture was developed to accommodate 16 inputs for one board. Vector-sum FB control with eight cavities will be evaluated during STF operation from October to November 2016.

IF-MIXTURE TECHNIQUE

In IF-mixture, several IFs are combined and read by one ADC. Given an input signal containing a number K of IF signals, the combined signal can be written as

$$X(t) = \sum_{i=1}^{K} \left\{ I_i(t) \cdot \cos\left(\omega_{\mathrm{IF}_i} t + \varphi_i\right) \right\} - \sum_{i=1}^{K} \left\{ Q_i(t) \cdot \sin\left(\omega_{\mathrm{IF}_i} t + \varphi_i\right) \right\} \quad (1)$$

where i is the index of the i^{th}-IF signal, $X(t)$ is the combined signal, $I_i(t)$ is the I-component of the i^{th}-IF, $Q_i(t)$ is the Q-component of the i^{th}-IF, φ_i is the phase offset of the i^{th}-IF, and $\omega_{\mathrm{IF}_i} = 2\pi \cdot \mathrm{IF}_i$. In IF-mixture technique, the sampling rate (SR) of the ADC and the frequency of i^{th}-IF must satisfy the condition $L \cdot \mathrm{IF}_i = N_i \cdot \mathrm{SR}$ (L is an integer greater than 3 and N_i is an integer). In IF-mixture, the selection of IF is

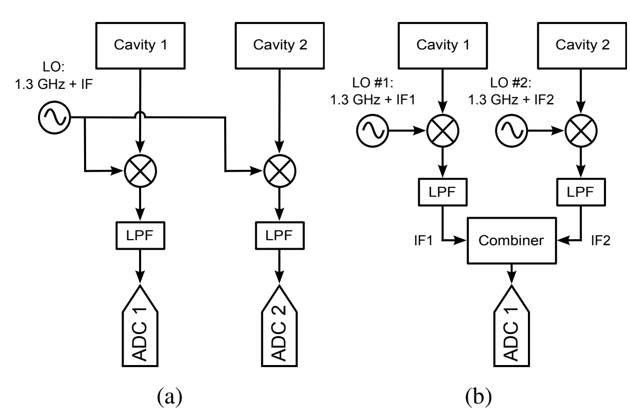

Figure 1: Digital LLRF system schematic: (a) Typical system with single IF and (b) IF-mixture with two IF signals.

ISBN 978-3-95450-169-4

SINGLE LLRF FOR MULTI-HARMONIC BUNCHER*

N. Usher†[1], S. Zhao, D. Morris, J. Brandon, D. Alt

Facility for Rare Isotope Beams (FRIB), East Lansing, MI 48824, USA
[1]also at, Ionetix Corporation, Lansing, MI 48911, USA

Abstract

In this paper, a unique low level radio frequency (LLRF) controller designed for a multi-harmonic buncher (MHB) is presented. Different than conventional designs, the single LLRF output contains three RF frequencies (f_1, f_2 = $2*f_1$, f_3 = $3*f_1$) and is fed to a wide-band amplifier driving the MHB. The challenge is while driving f_1, due to the nonlinearity of the amplifier, the f_2 and f_3 terms will also be generated and will couple into the control of these two modes. Hence an active cancellation algorithm is used to suppress the nonlinear effect of the amplifier. It is demonstrated in a test that the designed LLRF is able to control the amplitude and phase of the three modes independently.

INTRODUCTION

The re-accelerator (ReA3) at the National Superconducting Cyclotron Laboratory (NSCL) is mainly running at 80.5 MHz RF. The existing multi-harmonic buncher (MHB) in ReA3 runs at 80.5 MHz, 161 MHz and 241.5 MHz RF (latter not actively used) [1]. To achieve an increased separation of the beam bunches and minimization of bunch lengths desired for many types of experiments that use time of flight measurements, a lower frequency prebuncher (also an MHB) is designed [2]. To be compatible with the existing ReA3, the fundamental frequency (f_1) of the prebuncher is chosen to be 16.1 MHz. The second harmonic (f_2 = 32.2 MHz) and the third harmonic (f_3 = 48.3 MHz) will also be used.

In the rest of the paper, the RF design for the prebuncher including the resonant circuit, RF input sampling and output synthesis, as well as the control algorithm is described. Following, the bench test verification is presented as a proof of concept. Finally, the experimental results are given followed by conclusions.

RF DESIGN

Normally for MHB the control of each frequency component is done with a dedicated low level radio frequency (LLRF) controller, e.g. in the ReA3 MHB and FRIB MHB [3]. Three LLRF controllers and amplifiers will be needed. Since the frequencies are close enough, one wide band power amplifier could be used to amplify all three frequencies. Also with the more powerful field programmable gate array (FPGA) chip, it is possible to accommodate the logics, including digital mixing, filtering and feedback control, for all three harmonics in one LLRF controller. In this paper, such a unique RF system is designed and implemented.

Resonant Circuit

An effective way to achieve high voltage across the buncher electrodes is using resonant coaxial structures [1]. For this application, two resonant structures were used in parallel. A first coaxial cable was resonated at 16.1 MHz (f_1) and 48.3 MHz (f_3), and a second cable was resonated at 32.2 MHz (f_2). Figure 1 shows a schematic of the RF circuit. The lumped elements represent the feedthrough connections and electrode gap capacitance. Note: the resistors in the schematic were used to de-Q the circuit for simulations only, and were not used in the actual circuit. Good isolation was achieved by carefully selecting the lengths of cables A and B.

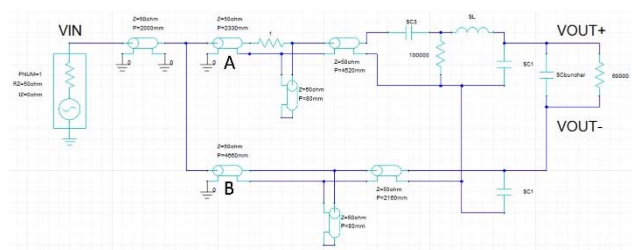

Figure 1: Schematic for RF system.

Each resonant structure includes a roughly quarter wavelength section (or odd multiple thereof) of 7/8” air-dielectric coaxial cable (RFS HCA78-50J) that was coiled to save space. A piece of 3-1/8” rigid transmission line was used as an input-tuning section, which consisted of a sliding short (for setting the resonant frequency) and a slot tuned input port. Figure 2 shows the input-tuning sections in the final installation.

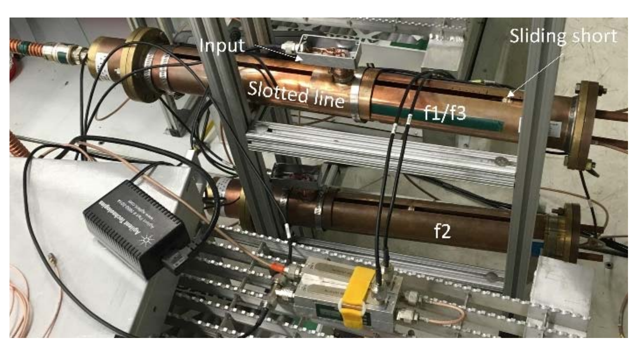

Figure 2: Input-tuning sections of coaxial resonators.

All three frequencies were simultaneously matched with return loss better than -9 dB, as shown in Figure 3.

* Work supported by Michigan State University, National Science Foundation: NSF Award Number PHY-1102511.
† usher@frib.msu.edu

ISBN 978-3-95450-169-4

RESONANCE CONTROL SYSTEM FOR THE CEBAF SEPARATOR UGRADE*

T. Plawski, R. Bachimanchi, B. Bevins, L. Farrish, C. Hovater, G. Lahti, M. Wissmann
Jefferson Lab, Newport News, VA, USA

Abstract

The Continuous Electron Beam Accelerator Facility (CEBAF) energy upgrade from 6 GeV to 12 GeV includes the installation of four new 748.5 MHz normal conducting deflecting cavities in the 5th pass extraction region. The RF system employs two digital LLRF systems controlling four normal conducting cavities in a vector sum configuration. Cavity tune information of the individual cavities is obtained using a multiplexing scheme of the forward and reflected RF signals. Water systems equipped with heaters and valves are used to control resonance. A new FPGA-based hardware and EPICS-based predictive control algorithm has been developed to support reliable operation of the beam extraction process. This paper presents the architecture design of the existing hardware and software as well as a plan to develop a model predictive control system.

INTRODUCTION

The fifth pass CEBAF Separator System consists of four normal conducting, two-cell, deflecting cavities operating at 748.5 MHz as shown in Fig. 1.

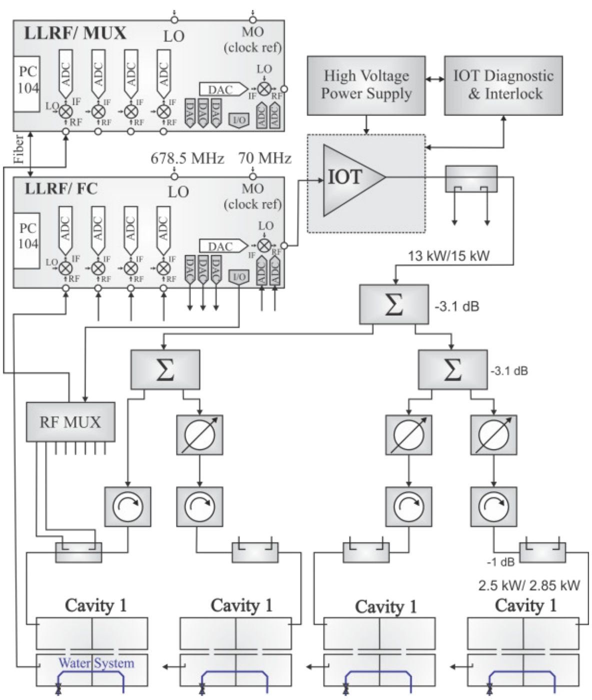

Figure 1: CEBAF 5th pass RF system.

The cavity design parameters and specification can be found in [1] [2]. The cavities are water-cooled and the average resonance frequency shift is around 12 kHz per °C. One high power amplifier (IOT) powers all four cavities; therefore the system employs a vector sum configuration. To minimize the cost of the control system, an FPGA based digital LLRF system developed previously for a one cavity/one amplifier configuration has been adapted to perform vector sum control. The LLRF module has only four receivers available thus it was necessary to adopt an RF multiplexer for signals other than cavity probe. A detailed description of the CEBAF Separator LLRF can be found in [3].

THE RESONANCE CONTROL WATER SYSTEM

Figure 2 shows a simplified diagram of the water system designed to keep the cavity at resonance as well as prevent the resonator from overheating.

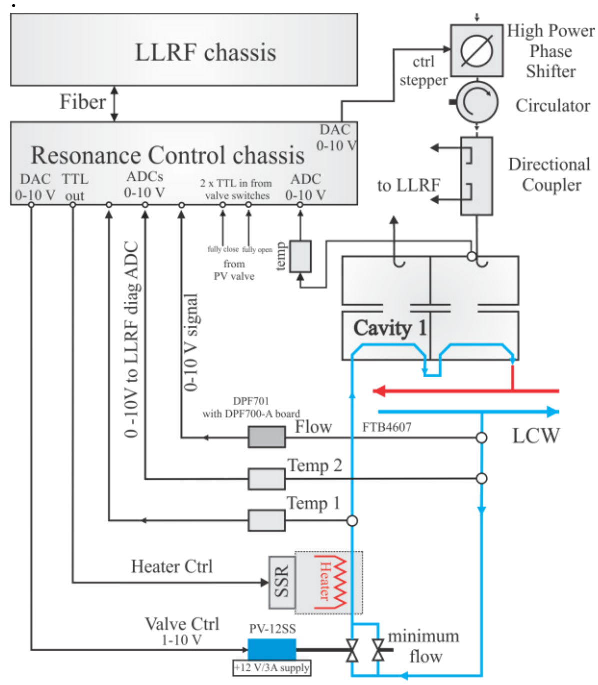

Figure 2: Separator Water System.

As one can see the Low Conductivity Water (LCW), due to construction constraints, runs in an open-loop configuration rather than closed-loop, making the system more vulnerable to fluctuations of the supply LCW temperature and reducing the control loop dynamics. Temperature sensors installed in the system

*Notice: Authored by Jefferson Science Associates, LLC under U.S. DOE Contract No. DE-AC05-06OR23177. The U.S. Government retains a non-exclusive, paid-up, irrevocable, world-wide license to publish or reproduce this manuscript for U.S. Government purposes

DESIGN OF A FRIB HALF-WAVE PRE-PRODUCTION CRYOMODULE*

S. Miller#, H. Ao, B. Bird, G. Bryant, B. Bullock, N. Bultman, F. Casagrande, C. Compton, A. Facco[1], W. Hartung, J. Hulbert, D. Morris, P. Ostroumov, J. Popielarski, L. Popielarski, M. Reaume, K. Saito, M. Shuptar, J. Simon, S. Stark, B. Tousignant, J. Wei, J. Wenstrom, K. Witgen, T. Xu, Z. Zheng
Facility for Rare Isotope Beams, Michigan State University, East Lansing, MI 48824 USA
M. Kelly
ANL- Argonne National Laboratory, Lemont, IL 60439 USA
[1] also at INFN - Laboratori Nazionali di Legnaro, Legnaro (Padova), Italy

Abstract

The driver linac for the Facility for Rare Isotope Beams (FRIB) will require the production of 48 cryomodules (CMs). In addition to the β=0.085 quarter-wave CM, FRIB has completed the design of a β=0.53 half-wave CM as a pre-production prototype. This CM will qualify the performance of the resonators, fundamental power couplers, tuners, and cryogenic systems of the β=0.53 half-wave design. In addition to the successful systems qualification; the β=0.53 CM build will also verify the FRIB bottom up assembly and alignment method on a half-wave CM type. The lessons learned from the β=0.085 pre-production CM build including valuable fabrication, sourcing, and assembly experience have been applied to the design of β=0.53 half-wave CM. This paper will report the design of the β=0.53 half-wave CM as well as the CM interfaces within the linac tunnel.

INTRODUCTION

FRIB is a high-power heavy ion accelerator facility now under construction at Michigan State University under a cooperative agreement with the US DOE [1]. Its driver linac operates in continuous wave mode and accelerates stable ions to energies above 200 MeV/u with the beam power on target up to 400 kW. The linac has a folded layout as shown in Figure 1, which consists of a front-end, three linac segments connected with two folding segments, and a beam delivery system to deliver the accelerated beam to target [2].

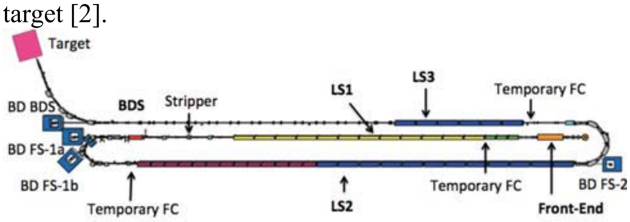

Figure 1: Schematic layout for FRIB driver linac.

The FRIB driver linac utilizes four different low-beta SRF resonator designs in CMs as described in Table 1. For high-beta applications, SRF has become an established technology with a history of industrial optimization efforts; however, for low-beta structures, FRIB will be the first facility utilizing industrially produced resonators on a larger scale [3].

Table 1: Required CM configurations for FRIB. Resonator and solenoid quantities per CM are shown in parenthesis. The β=0.041 CM will utilize a L_{eff}=0.25 m solenoid and all other CMs will utilize a L_{eff}=0.50 m solenoid.

Type	Cryomodule Qty.	Resonator Qty.	Solenoid Qty.
β=0.041	3	12 (4)	6 (2)
β=0.085	11	88 (8)	33 (3)
β=0.29	12	72 (6)	12 (1)
β=0.53	18	144 (8)	18 (1)
Matching Modules	3 (β=0.085) 1 (β=0.53)	12 (4) 4 (4)	N/A
Total	**48**	**332**	**69**

Each CM will be equipped with niobium resonators operating at 2 K with focusing solenoids, which include x-y steering, operating at 4.5 K. Due to the large number of CMs, the FRIB project lends itself to a manufacturing mind-set that incorporates large scale production into the design of individual module types. As a part of this manufacturing mind-set, FRIB has designed a pre-production CM that utilizes eight β=0.53 superconducting half-wave resonators (HWR) and one superconducting solenoid, as seen in Figure 2 [4].

CRYOMODULE DESIGN

The FRIB CMs are based on a modular bottom-supported design which is optimized for mass-production and efficient precision-assembly. Figure 3 displays the subsystem break down of the CM. Four types of superconducting resonators (β=0.041, β=0.085, β=0.29, β=0.53) and two solenoid lengths (Leff = 0.25 m and 0.50 m) are used in multiple configurations for the FRIB linac driver as described Table 1. FRIB CMs have been designed with a focus on

* This material is based upon work supported by the U.S. Department of Energy Office of Science under Cooperative Agreement DE-SC0000661. Michigan State University designs and establishes FRIB as a DOE Office of Science National User Facility in support of the mission of the Office of Nuclear Physics.

millers@frib.msu.edu

ISBN 978-3-95450-169-4

RF LOSSES IN 1.3 GHz CRYOMODULE OF THE LCLS-II SUPERCONDUCTING CW LINAC*

A. Saini†, A. Lunin, N. Solyak, A. Sukhanov, V. Yakovlev, Fermilab, Batavia, USA

Abstract

The Linac Coherent Light Source (LCLS) is an x-ray free electron laser facility. The proposed upgrade of the LCLS facility is based on construction of a new 4 GeV superconducting (SC) linac that will operate in continuous wave (CW) mode. The major infrastructure investments and the operating cost of a SC CW linac are outlined by its cryogenic requirements. Thus, a detail understanding of RF losses in the cryogenic environment is critical for the entire project. In this paper we review RF losses in a 1.3 GHz accelerating cryomodule of the LCLS-II linac. RF losses due to various sources such untrapped higher order modes (HOMs), resonant losses etc. are addressed and presented here.

INTRODUCTION

The Linac Coherent Light Source -II (LCLS–II) [1] is a proposed fourth generation x-ray light source facility under construction at SLAC, California. The LCLS-II is primarily based on construction of a new 4 GeV SC RF linear accelerator (linac) that would operate in the CW regime (see Fig. 1).

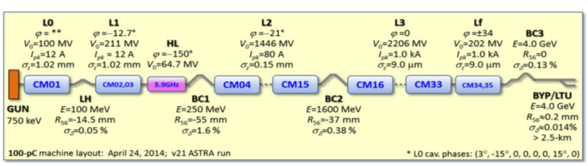

Figure 1: Layout of the LCLS-II SC linac.

The LCLS-II SC linac is segment into several sections which are named as L0, L1, HL, L2, L3 and Lf. All the sections except L1 and HL are separated to each other by intermediate warm sections which are designed for the specific purposes such as laser heating, diagnostic and bunch compressions. Excluding HL, all sections are composed of 9-cell 1.3 GHz SC TESLA like cavities [2]. HL section consists of 9-cell, 3.9 GHz SC cavities [3]. Number of elements and their nominal operational RF parameters in each section are summarized in Table 1 and a detailed description of the LCLS-II SC linac is presented elsewhere [4]. The cryogenic efficiency is significantly lower at operating temperature of 2 K [5]. Thus, operation of the SC linac in CW mode keeps a stringent tolerance on the cryogenic load of the machine. As, one can observe from Table 1 that major portion of the LCLS-II SC linac is comprised of the 1.3 GHz cryomodules and therefore, cryogenic budget of the facility is largely outlined by the cryogenic loads in a 1.3 GHz cryomodule. In this paper, we discuss and present contribution of different sources that result in the dynamic RF losses at the operating temperature of 2 K in a 1.3 GHz cryomodule in the LCLS-II SC linac.

Table 1: Configuration of Each Section in LCLS-II Linac

	Phase (deg)	Gradient (MV/m)	No. of CM's	Avail. cavities
L0	~0	16.3	1	8
L1	-12.7	13.6	2	16
HL	-150	12.5	2	16
L2	-21	15.5	12	96
L3	0	15.7	18	144
Lf	+/-34	15.7	2	18

1.3 GHZ CRYOMDOULE

Figure 2 shows a schematic of 1.3 GHz cryomodule. It accommodates eight cavities, a magnet package that includes a quadrupole magnet, a beam position monitor (BPM) and a dipole corrector and, a beam line absorber at the end.

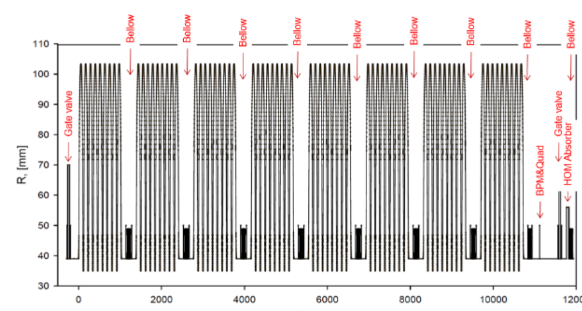

Figure 2: 2D view of a 1.3 GHz cryomodule for the LCLS-II SC linac.

Operating Mode RF Loss in Cavity

The major contribution to the dynamic RF losses in a cryomodule comes from dissipation of the operating mode fields on surface of the SC cavity. Power dissipated (P_d) on surface of a SC cavity is estimated as:

$$P_d = \frac{(E_{acc} L_{ef})^2}{\left(\frac{R}{Q}\right) Q_0}; \qquad (1)$$

where E_{acc} is accelerating gradient, L_{ef} is cavity effective length and Q_0 is unloaded quality factor. For the 1.3 GHz,

* Work supported in part by Fermi Research Alliance, LLC under USA DOE Contract No. DE-AC02-07CH11359, DOE Contract No. DE-AC02-76SF00515 and the LCLS-II Project.
† asaini@fnal.gov

COOL-DOWN PERFORMANCE OF THE CORNELL ERL CRYOMODULES

R. Eichhorn†, M. Ge, F. Furuta, G.H. Hoffstaetter, M. Liepe, S. Markham, T. O'Connell,
P. Quigley, D. Sabol, J. Sears, E. Smith, V. Veshcherevich, D. Widger
CLASSE, Cornell University, Ithaca, NY, USA

Abstract

In the framework of the ERL prototyping, Cornell University has built two cryomodules, one injector module and one prototype Main Linac Cryomodule (MLC). In 2015, the MLC was successfully cooled down for the first time. We will report details on the cool-down as well as cycle tests we did in order to achieve slow and fast cool-down of the cavities. We will also report on the improvement we made on the injector cryomodule which also included a modification of the heat exchanger can that allows now a more controlled cool-down, too.

INTRODUCTION

During an NSF funded R&D phase for an Energy Recovery Linac (ERL), Cornell University has built two cryomodules. The injector cryomodule (ICM) completed in summer 2007 was designed and built to demonstrate high current generation and achieving low emittances.

The second cryomodule built was the main linac cryomodule (MLC) which is supposed to demonstrate highly efficient cw operation. This module was completed by the end of 2014 and cool-down for the first time in fall 2015.

INJECTOR CRYOMODULE

Rebuilt of the Module

While the emittance goal for the injector has been reached [1], the current achieved so far is 75 mA. As of today this is a world record performance [2]. However, the goal set for the ERL was 100 mA. In ramping up beam current, RF power transmitted by the coupler increases. Every cavity is fed by 2 couplers, being designed for a cw power of 60 kW. As we learned, pushing for higher currents we realized that heating of the 80 K thermal intercept of the power couplers became a limitation. We were able to track down to insufficient cooling of the 80 K intercepts to a lack of cryogenic flow [3]. These intercepts are cooled by a stream of parallel cryogenic flows which we found to be unbalanced.

In preparation for building an FFAG based ERL, the injector cryomodule had to be moved, giving us the chance to modify the piping as described. While the actual modification of the piping was only two days of work, disassembling and reassembling the module required 6 month of labour as we almost had to strip down the cold-mass.

In fall 2015, we added a flow restrictor to the HOM cooling channels that previously has stolen all the flow from the couplers. The restrictor consisted of an additional pipe with an adjusted the length of up to 87 cm. A particular difficulty was that available piping is usually specified by its outer diameter, while the inner diameter (being relevant for the cryogenic flow) fluctuates significantly. Eventually we bubble-tested all pipes to be assured the all have the same flow impedance[4].

Improvement in the HX can

Prior to re-cool the ICM we decided to modify the heat exchanger can (HXC), to incorporate the experience we had gained during the past years of operation. The can (in a 3-D design and as a photo) is shown in Fig. 1.

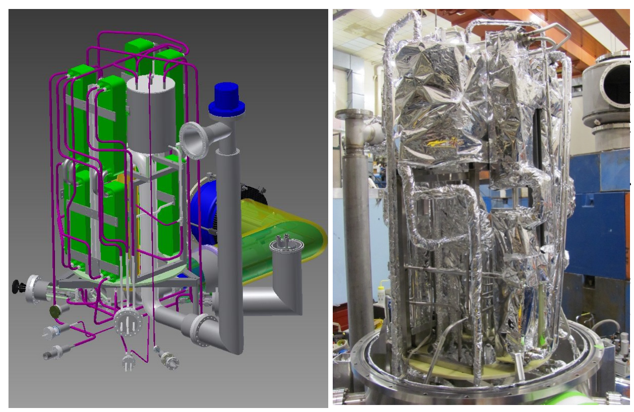

Figure 1: heat exchanger can for the injector cryomodule, sketched and in picture.

Our first HXC in this style used a pair of inlet and outlet valves, rather than pressure regulators to establish flow rate, and a common flow stream for cooling both the 5 K and 80 K loads, using two separate 80 K cooling loops in series to get adequate mass flow. It required both the 5 K and 80 K coolant streams to be near the same pressure, and was harder to cool down from room temperature in a smooth fashion. The JT valve was contained in the HXC, rather than in the cryomodule.

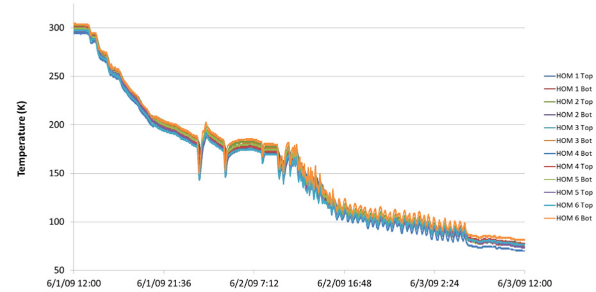

Figure 2: Typical cool-down profile of the ICM using the initial heat exchanger can. Rather huge transients can be seen as well as oscillations on the cooldown from nitrogen to helium temperatures.

† r.eichhorn@cornell.edu

ASSEMBLING EXPERIENCE OF THE FIRST TWO HIE-ISOLDE CRYO-MODULES

M. Therasse, G. Barlow, S. Bizzaglia, O. Capatina, A. Chrul, P. Demarest, J-B. Deschamps, M. Garlache, J-C. Gayde, M. Gourragne, A. Harrison, G. Kautzmann, Y. Leclercq, D. Mergelkuhl, T.P. Mikkola, A. Miyazaki, V. Parma, J. Somoza, M. Struik, S. Teixeira, W. Venturini Delsolaro, L. Williams, P. Zhang,
CERN, Geneva, Switzerland,
J. Dequaire, Intitek, Lyon, France

Abstract

The assembly of the first two cryo-modules (CM1 and CM2) of the new superconducting linear accelerator HIE-ISOLDE (High Intensity and Energy ISOLDE), located downstream of the REX-ISOLDE normal conducting accelerator, started one year and a half ago. After a delicate assembly phase in the cleanroom which lasted nine months, the first cryo-module was transported to the ISOLDE hall on 2 May 2015 and connected to the existing REX-ISOLDE accelerator, increasing the energy of the radioactive ion beams from 2.8 to 4.3 MeV per nucleon. The superconducting linac supplied the CERN-ISOLDE facility with radioactive zinc ions until the end of the proton run in November 2015. At the beginning of 2016, the second cryo-module was installed in the machine, increasing the energy to 5.5 MeV per nucleon.

During commissioning of the first cryo-module in summer 2015, it was found that the performance of the RF superconductive cavities was limited by the over-heating of their RF couplers. The decision was taken to refurbish CM1 and reinstall it at the end of April.

In this paper, we present the challenges faced and the experience gained with the cleanroom assembly of the first two cryo-modules, especially the construction of the SC RF cavities and their RF ancillaries.

INTRODUCTION

The HIE-ISOLDE project involves a major upgrade of the present REX-ISOLDE linac. To increase the beam energy from 3 MeV/u to 10 MeV/u, it is planned to install 4 cryo-modules based on high β superconducting Quarter Wave Resonators (QWR), made of Nb coated on copper cavities [1]. Each cryo-module is composed of five cavities and one superconducting solenoid operating in a common vacuum at 4.5 K [2]. This constraint imposes to take extreme care of the cleanliness during the preparation and the assembly of all the cryo-module parts.

The first cryo-module (CM1) was mounted in 27weeks and was successfully installed last year. It demonstrated that the assembly process in place is effective [3]. The beam vacuum reached 10^{-11} mbar and all cavities were conditioned without difficulties (weak multipacting and no field emission) until 6 MV/m.

During the commissioning of CM1, a performance limitation was observed due to an over-heating of the RF power coupler [3]. After studies and testing an upgraded [4] version was designed to improve the heat dissipation. The new couplers were installed on CM1 during the first shutdown (beginning of 2016) and implemented for the other cryo-modules.

In parallel, due to the difficulties encountered with the cavity production and in order to face a performance degradation, a new cavity design study aimed to simplify the manufacturing of the substrates has been launched.

This paper will present the HIE-ISOLDE cryo-module assembly, the cavity production for CM1 and CM2 and give a brief status of the new cavity design.

HIE-ISOLDE CRYOMODULE ASSEMBLY

The choice of a common vacuum design (insulation and beam vacuum are the same) implied the need to perform the whole cryo-module mounting in a controlled area, to reduce the contamination risk (dust, metallic particles…). All preparations and the assembly proper are done in soft wall cleanrooms ISO 5. The main clean room is equipped with a horizontal laminar air flow and a dedicated assembly tower capable to precisely handle the heavy equipment [2].

All pieces are degreased and cleaned with alcohol, blown off with filtered N_2 gas, and double packed with plastic bags before entering the cleanroom. The standard cleanroom preparation process could not always be applied due to the size and the weight (few tonnes) of some pieces. Anti-dust rinsing with ultrapure water was only done on the cavities at a pressure of 6 bars before final installation.

Figure 1: Cavities installed on the cryo-module frame in the cleanroom ISO 5.

The assembly sequence is divided in 14 main steps described in detail in assembly procedures and in [2]. The superconducting cavities are installed at the end, in order to minimize the risk of contamination and to make it easier to

ISBN 978-3-95450-169-4

PERFORMANCE OF SRF CAVITY TUNERS AT LCLS II PROTOTYPE CRYOMODULE AT FNAL

J. Holzbauer#, Y. Pischalnikov, W. Schappert, J.C. Yun, FNAL, Batavia, IL 60510, USA

Abstract

A compact tuner was designed at Fermilab for the LCLS-II project. The focus of this design with high reliability, including robust active components (electromechanical actuators and piezo actuators) as well as the ability to replace these components without cryomodule disassembly. These tuners have been prototyped and tested in detail on test cavities [1]. Performance of the slow/fast tuners mounted on the eight SRF cavities of the first LCLS-II prototype cryomodule (pCM) assembled at FNAL will be presented.

TUNER DESIGN

Schematics of the tuner design are shown in Figure 1. Coarse tuner is a double lever tuner (with 20:1 ratio) similar to design of the SACLAY I tuner. The tuner is designed to work in the compression regime. The piezo-stack is installed on the cavity end flange, so its force is directly applied to the cavity, not translated through a lever arm or bearing. This configuration will deliver better piezo-tuner resolution and decrease group delay of the fast tuner. This tuner must protect the cavity from deformation in many different configurations of cavity pressure, helium pressure, and insulating pressure. To ensure protection in all scenarios, safety rods between the cavity end flange and main lever of the tuner were added. These safety rods protect cavity from non-elastic deformation during cavity/helium vessel system leak check.

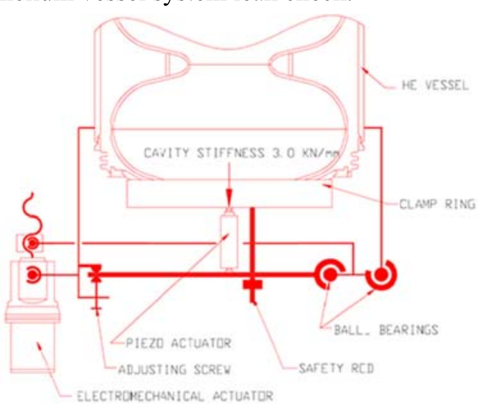

Figure 1: Schematic of the Tuner.

A split ring is attached to the conical flange welded to the cavity beam-pipe (Purple in Figures 2&3). All forces/stroke from tuner to the cavity are translated through this split ring. The tuner is anchored to the helium vessel with two strong horizontal arms (Yellow in Figure 2). The electromechanical actuator connects the left arm and lever system attached through bearings to right arm.

A special adjustment screw (Figure 1) to hold the left side of the lever system to the left arm was introduced into design. This addition allows the release of forces between the cavity and tuner system when either the electromechanical actuator or piezo-stack needs to be replaced through the designated port in cryomodule.

Balls connections were chosen for the connections between encapsulated piezo-stacks and main lever (see Figure 3). This prevents the build-up of shearing forces on the piezo-stack during tuner operation which are detrimental to piezo lifetime. Two adjustment screws (one in each main arm) help to uniformly preload piezo-stacks during assembly.

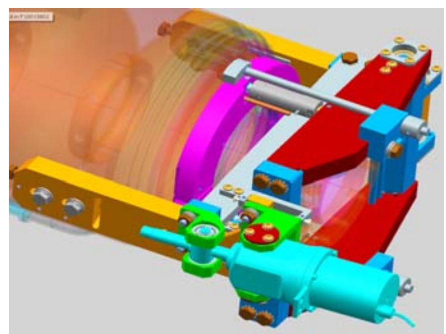

Figure 2: 3-D model of the Tuner, assembled on the cavity/helium vessel system.

PREVIOUS TESTING

Electromechanical actuator is the active element of the slow/coarse tuner. Electromechanical actuator translates rotation of a stepper motor to linear motion of the tuner arms.

Technical requirements call for a tuning sensitivity of 1-2 Hz/step. The selected electromechanical actuator has 200 steps per shaft rotation, gear ratio of 1:50, and spindle pitch of 1 mm. 1 motor step will shift tuner 1mm/200*50=1e-4 mm. With tuner ration of 1:20, this step will compress cavity 5e-6 mm. Given a cavity sensitivity of 300 kHz/mm, this gives a tuning of ΔF=1.5Hz.

Cold testing in the Horizontal Test Stand [2] at Fermilab give a tuning sensitivity of 1.4 Hz/Step and a lash of 30 steps. Short and long range scans (Figures 4 and 5) gave consistent results, down to the limit of the frequency measurement.

*This manuscript has been authorized by Fermi Research Alliance, LLC under Contract N. DE-AC02-07CH11359 with U.S. Department of Energy.
#jeremiah@fnal.gov

STATUS OF BETA=0.53 PRE-PRODUCTION*

H. Ao†, B. Bird, G. Bryant, B. Bullock, N. Bultman, C. Compton, J. Hulbert, S. Miller, J. Popielarski, L. Popielarski, M. Reaume, K. Saito, M. Shuptar, J. Simon, S. Stark, B. Tousignant, J. Wenstrom, K. Witgen, T. Xu, Z. Zheng
Facility for Rare Isotope Beams, Michigan State University, East Lansing, USA
A. Facco, INFN - Laboratori Nazionali di Legnaro, Legnaro (Padova), Italy

Abstract
The Facility for Rare Isotope Beams (FRIB) project is now in the production phase of β=0.041 and 0.085 cryomodule (CM) fabrication and assembly. In addition to these CMs, the assembly of the pre-production β=0.53 CM started in May 2016. The basic mechanical design concept of the β=0.53 CM is similar to the β=0.085, however the β=0.53 CM includes a different type of cavity, some new components, and design features. This paper will describe the recent progress and the lessons learned of the pre-production β=0.53 CM assembly.

INTRODUCTION

FRIB is a new joint project for nuclear science facility funded by the DOE Office of Science and Michigan State University [1, 2]. The FRIB driver accelerator is a superconducting heavy ion linac with a beam power of 400 kW at the target and a beam energy over 200 MeV/u. This driver linac consists of 48 CMs with six types of CM including matching CMs. Figure 1 shows four types of superconducting cavity (β=0.041, 0.085, 0.29, and 0.53) used in these CMs. Quarter-wave resonators (QWRs) at 80.5 MHz are used for low velocities: β=0.041 and 0.085, and half-wave resonators (HWRs) at 322 MHz are for medium velocities: β=0.29 and 0.53.

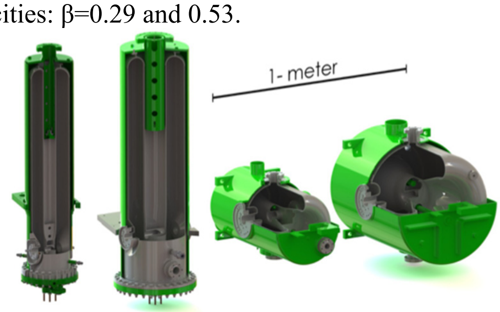

Figure 1: FRIB cavities, from left: β=0.041QWR, β=0.085QWR, β=0.29HWR, and β=0.53HWR.

Figure 2 shows the CM development executed at FRIB. The FRIB CMs adopt the modular bottom-up assembly design for assembly friendly and more tight alignment tolerances. This design was successfully validated by an engineering test cryomodule (ETCM) [3]. As for the QWR CMs, ReA6 and the pre-production β=0.085 CMs successfully demonstrated the FRIB performance. Now the QWR CMs are in the production phase [2].

*Work supported by the U.S. Department of Energy Office of Science under Cooperative Agreement DE-SC0000661
† ao@frib.msu.edu

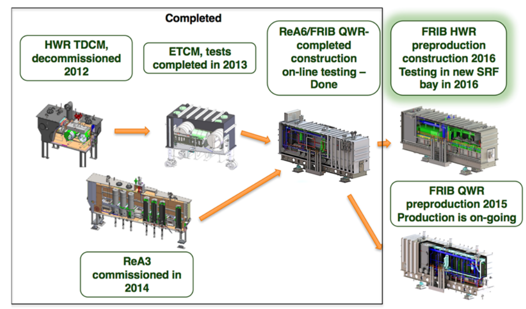

Figure 2: Cyomodule development at FRIB.

In addition to the QWR CMs, the assembly of the pre-production β=0.53 CM started in May 2016 (Fig. 3). The basic design concept is the similar to the β=0.085 CMs, however several differences are introduced, especially fundamental power couplers (FPCs) and mechanical frequency tuners [4]. The magnetic shield design was also changed from a cylinder-like shape to a rectangular box, which is assembled from small plates.

This paper will present the overview and the recent progress of the pre-production β=0.53 CM, particularly focusing on the lessons learned from the build of the CM.

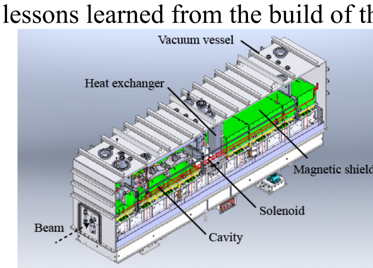

Figure 3: FRIB β=0.53 cryomodule.

PROGRESS, ISSUE AND MITIGATION OF CM ASSEMBLY

Cleanroom Assembly

The coldmass assembly began in the SRF Highbay production cleanroom from the end of March 2016, and then it was moved to the CM assembly area in the East Highbay on 1 May, it took approximately one month. The net throughput was approximately two weeks. Many of the time was spent for waiting the cavity vertical test, the FPC conditioning, and other components, for instance solenoid packages.

All the delivered cavities were visually and dimensionally inspected, processed (heat treatment, buffered chemical polish, high-pressure rinse), RF (cold vertical) tested, and assembled into the coldmass [5]. Figure 4 shows the

THE CRYOGENIC PERFORMANCE OF THE ARIEL E-LINAC CRYOMODULES

Yanyun Ma†, K. Fong, P. Harmer, T. Junginger, D. Kishi, A. Koveshnikov, R.E. Laxdal, N. Muller, E. Thoeng, Z.Y. Yao,V. Zvyagintsev
TRIUMF, 4004 Wesbrook Mall, Vancouver, BC, Canada V6T2A3

Abstract

The Advanced Rare Isotope Laboratory (ARIEL) project at TRIUMF requires a 50 MeV superconducting electron Linac consisting of five nine cell 1.3 GHz cavities divided into three cryomodules with one, two and two cavities in each module respectively. The cryomodule design utilizes an unique box cryomodule with a top-loading cold mass. LHe is distributed in parallel to each cryomodule at 4 K and at ~1.2 bar. Each cryomodule has a cryogenic insert on board that receives the 4 K liquid and produces 2 K liquid into a cavity phase separator. In the cryomodules the natural two-phase convection loops, i.e. siphon loop, are installed which supply 4 K liquid to thermal intercepts and return the vaporized liquid to the 4 K reservoir as a refrigerator load. The design of the cryomodule, the simulation results with Ansys Fluent and the results of the cold tests will be presented.

INTRODUCTION

The ARIEL [1] is an on-going project at TRIUMF which will triple TRIUMF's capability of rare isotope production over the next ten years for the needs of the international scientific community. ARIEL uses a 50 MeV, 10 mA continuous-wave (CW) electron linear accelerator (e-Linac) as a driver accelerator utilizing superconducting bulk niobium technology at 1.3 GHz. The accelerator is divided into three cryomodules [2] including a single cavity injector cryomodule (ICM) and two accelerating cryomodules (ACM) with two cavities each as shown in Fig. 1.

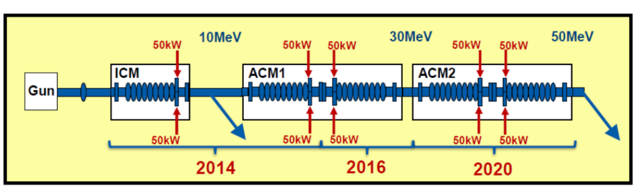

Figure 1: A schematic of the e-linac showing the installation stages.

A first phase consisting of an ICM, and an accelerating cryomodule with just one accelerating cavity on board plus a `dummy' cavity that occupies the second cavity space in the cryomodule (ACMuno) was installed for initial technical and beam tests to 23 MeV in 2014 [3]. The ACMuno configuration allows a full cryo-engineering characterization of the cryomodule. An upgrade that will add a second 1.3 GHz nine-cell cavity to ACM1 is in progress. A 2nd ICM as part of a collaborative agreement with the ANURIB project at VECC [4] is under testing. The 2nd phase will add ACM2 module and a ramp up in beam intensity to the full 50 MeV, 0.5 MW capability.

CRYOMODULE DESIGN

The ARIEL cryomodule design [5], shown in Fig. 2, borrows significantly from the ISAC-II cryomodules. The modular and staged testing/installation sequence of the e-linac suggests that each cryomodule be self-reliant to convert 4 K atmospheric LHe into 2 K He-II. To this end the box cryomodule design has sufficient head room that makes possible the addition of a dedicated 4 K/2 K cryo-insert on each module. Incorporating features of the ISAC-II design reduced the engineering design load within TRIUMF and takes best advantage of the existing infrastructure. This finds important savings in both the cryomodule design, fabrication and testing but also in the cryogenic system design.

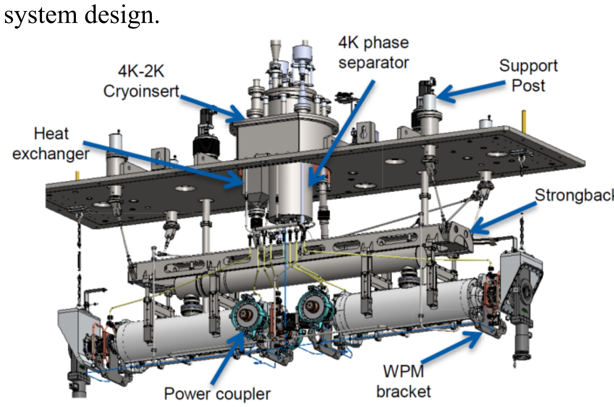

(a) The ACM top assembly.

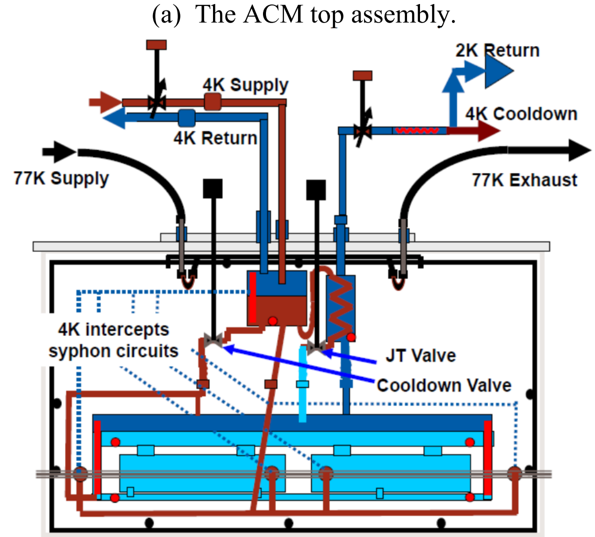

(b) The ACM cryogenic piping schematic.

Figure 2: ACM top assembly and piping schematic.

† mayanyun@triumf.ca

ISBN 978-3-95450-169-4

COST REDUCTION FOR FRIB MAGNETIC SHIELDING*

Z. Zheng#, J. Popielarski, K. Saito, T. Xu, FRIB, MSU, MI 48824, USA

Abstract

Cryogenic magnetic shielding is generally used in SRF cryomodules which is much more expensive than Mu-metal used in room temperature. In order to reduce the cost, FRIB QWR and HWR magnetic shields were redesign to improve the shielding performance so that Mu-metal can be implemented as an alternative shielding material. The magnetic shielding of first FRIB beta=0.085 cryomodule was made up of 50% by cryogenic magnetic shielding and 50 % by mu-metal. Cavities were tested in 4 K and 2 K, the results showed that the Q_O of cavities were similar for both shielding materials, which is a success as a validation test for Mu-metal magnetic shielding.

INTRODUCTION

For superconducting RF cavity, trapped external magnetic field on cavity surface will increase residual surface resistance and reduce cavity Q (unloaded quality factor). In order to lower the residual surface resistance and get a high Q for SRF cavity, magnetic shielding is implemented in the cryomodule. The requirement for FRIB magnetic shielding is to reduce external magnetic field on cavity surface to make $H_{ext\_average}$ smaller than 15 mG. Under this requirement, there are two efforts made for cryomodule magnetic shielding: (1) Reduction of fabrication cost; we simplify FRIB QWR cryomodules' magnetic shielding assemble by eliminating the hats: (2) Reduction of material cost; we optimized shielding structure for implementing Mu-metal as an alternative shielding material. A prototype of new magnetic shielding design with Mu-metal was made and installed in the first FRIB production cryomodule. It is the FRIB QWR085 cryomodule whose magnetic shielding is composed half by cryogenic magnetic shielding and other half by Mu-metal. Cryomodule tested in 2 K showed no difference in cavity Q for both magnetic shielding materials, which is a success as a validation test for new design with Mu-metal. The second section discusses the reduction of fabrication cost by simplify QWR magnetic shielding. The third section introduces the structure optimized for both QWR and HWR magnetic shielding according to EM simulation. The fourth section compares the performance of cryogenic magnetic shielding and Mumetal in FRIB cryomodule test at 2 K.

REDUCTION OF FABRICATION COST

The original magnetic shielding design for FRIB QWR cryomodule is complex, which has six hats around the holes on magnetic shielding to reduce leaking earth magnetic field. Those hats increases fabrication cost and assembling time, also induces a risk of magnetic shielding degradation during assembly. Thus, the elimination of hats is highly desirable. Figure 1 compares the QWR085 original single cavity magnetic shielding design and the hats eliminated new design.

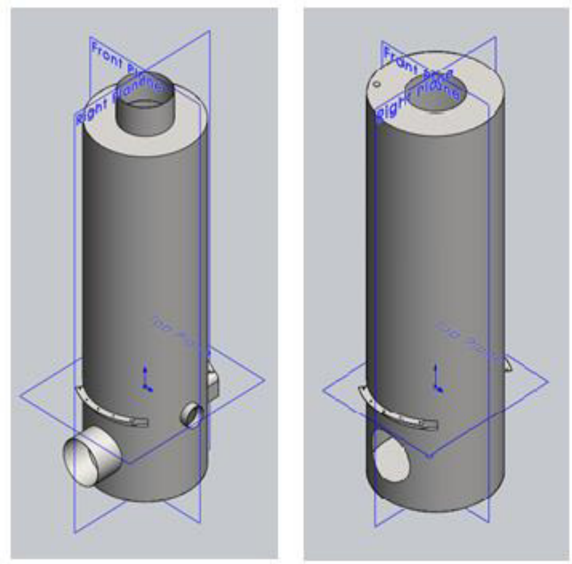

Figure 1: Magnetic shielding with and without hats.

Simulation was done to estimate the Q degradation by earth magnetic field due to elimination of hats. For magnetic shielding with hats, magnetic field on cavity surface are all below 15 mG, while for one without hats, the location near FPC (fundamental power coupler) and Pick-up ports will exceed 15 mG (maximum ≈90 mG, see Fig. 2).

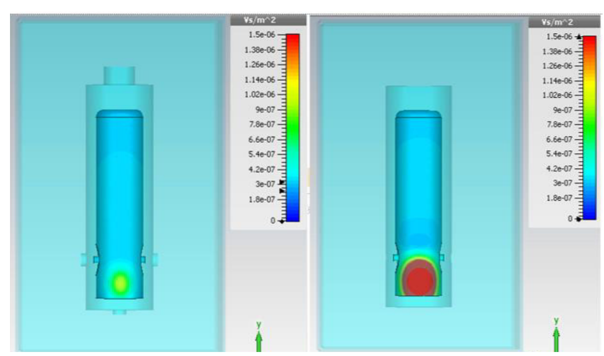

Figure 2: Simulations for shielding with and without hats.

To compare the difference of cavity surface resistance for magnetic shielding with and without hats, we took account the RF H-field distribution inside QWR cavity at nominal gradient. Then, we calculated the additional cavity dissipated power due to earth magnetic field for both magnetic shields by the following equations:

$$R_{res\_mag} = 0.3\ (n\Omega) H_{ext}(mG)\sqrt{f(GHz)} \quad (1)$$

$$P_{loss\_mag} = \frac{1}{2}\int R_{res\_mag}\, H_2 ds \quad (2)$$

*Work supported by the U.S. Department of Energy Office of Science under Cooperative Agreement DE-SC0000661
#zhengw@frib.msu.edu

POLARITY CHECK OF THE FRIB CRYOMODULE SOLENOIDS BY MEASURING LEAKAGE MAGNETIC FIELD*

H. Ao†, D. Luo, F. Marti, K. Saito, S. Shanab
Facility for Rare Isotope Beams, Michigan State University, East Lansing, MI, USA

Abstract

The leakage magnetic field of a 50-cm length 8 T solenoid outside a FRIB cryomodule was observed. The investigation took place to check the polarity of superconducting solenoid using the leakage fields. The maximum leakage field was 1.5 G on the outer surface of the vacuum vessel, and this value agrees very well with calculations. The leakage residual magnetic fields observed thorough the degaussing process of the solenoid can use to establish a basic degaussing procedure. This polarity check procedure has been accepted in FRIB checking lists and to be performed before an integration test and commissioning of the FRIB linac.

INTRODUCTION

A FRIB cryomodule includes superconducting solenoid packages for beam focussing and steering (Fig. 1). These solenoid packages consist of three components: a main 8 T solenoid coil for beam focussing, one pair of bucking coils to cancel the fringe field from the solenoid, which is connected to the main solenoid in series, and one pair of dipole coil for beam steering. All of the magnet polarities have to be confirmed after the installation before the start of the beam commissioning. Normal conducting magnets are easily accessed and checked with a hall probe, but the superconducting solenoids installed in the cryomodule are not straightforward.

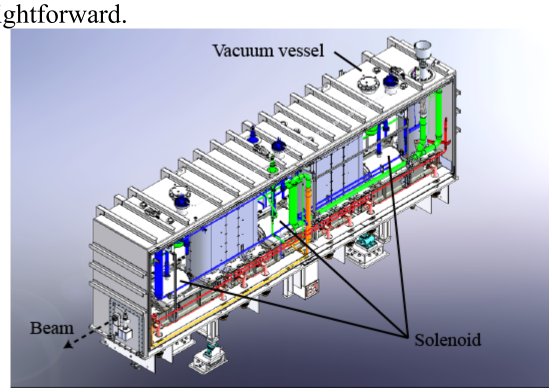

Figure 1: FRIB β=0.085 cryomodule.

The leakage magnetic fields from these magnets was observed outside the FRIB cryomodule [1, 2] to check the polarity of these magnets. The leakage field from the 50-cm superconducting solenoid equipped in the FRIB-1 cryomodule (Fig. 1) was roughly estimated and found to be detectable. The peak field of the main solenoid is 8 T at 92 A and the dipoles vertically and horizontally beam bending are 0.06 Tm at 20 A. After that the rough estimation, the leakage field was calculated more precisely using a 3D model and compered with measurement results. The following section will describe each of these parts in more detail.

ESTIMATION OF LEAKAGE FIELD

First, the strength of magnetic field leakage outside the cryomodule was roughly estimated with POISSON. The solenoid coil dimensions used a FRIB initial design. Assuming a cylindrically symmetric vacuum vessel made of iron with μ=1000 and a thickness of 0.75”, and an operating current of 86 A for the solenoid, a leakage magnetic field of 0.8 G was estimated (Fig. 2), which is fully detectable by using a milli-gauss range magnetometer.

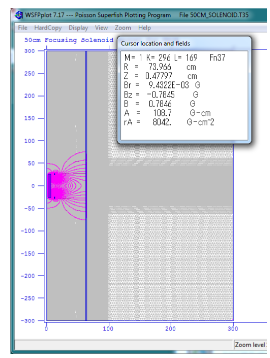

Figure 2: POISSON calculation.

As a next step, the 3D leakage field from the solenoid calculated with ANSYS Maxwell in more detail. The 3D model (Fig. 3) includes the exactly same dimensions as the solenoid of the FRIB-1 cryomodule. This calculation used the B-H curve of steel 1010.

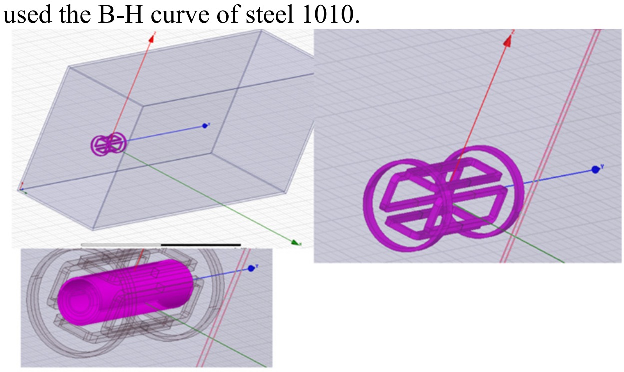

Figure 3: (Upper left) Cryostat with solenoid inside, (Upper right) Dipole coils and background coils, (Lower left) Nested solenoids.

*Work supported by the U.S. Department of Energy Office of Science under Cooperative Agreement DE-SC0000661
†ao@frib.msu.edu

ISBN 978-3-95450-169-4

SOLID-STATE PULSED POWER SYSTEM FOR A STRIPLINE KICKER

Dr. Neal Butler, Fred Niell, Dr. Marcel Gaudreau, Michael Kempkes, Matthew Munderville, Diversified Technologies, Inc., Bedford, MA, USA

Abstract

Diversified Technologies, Inc. (DTI) has designed, built, and demonstrated a prototype pulse amplifier for stripline kicker service capable of less than 5 ns rise and fall times, 5 to 90 ns pulse lengths, peak power greater than 13.7 MW at pulse repetition rates exceeding 100 kHz, and measured jitter under 100 ps. The resulting pulse is precise and repeatable, and will be of great interest to accelerator facilities requiring electromagnetic kickers. The pulse generator is based on the original specifications for the NGLS fast deflector. DTI's planar inductive adder configuration uses compensated-silicon power transistors in low inductance leadless packages with a novel charge-pump gate drive to achieve unmatched performance. The prototyping efforts guided the design of the full unit, however the magnetics and transmission line effects of the system were not revealed until the entire unit was assembled. The unit was brought to LBNL, compared with other researcher's efforts, and was judged very favorably. A number of development prototypes have been constructed and tested, including a successful 18.7 kV, 749 A unit. The modularity of this design will enable configuration of systems to a wide range of potential applications in both kickers and other high speed requirements, including high performance radars, directed energy systems, and excimer lasers.

INTRODUCTION

Diversified Technologies, Inc. (DTI) recently completed an SBIR effort under a grant from the US Department of Energy to research kicker drivers for the Next Generation Light Source (NGLS) injectors. The NGLS specification required a 10 kV, 200 Ampere pulse into 50 Ω, with a 2 ns rise time (10-90%), a highly repeatable flattop with a pulsewidth from 5-40 ns, and a fall time less than 1 µs (defined as down to 10^{-4} of the peak value). DTI chose a novel derivative of the classic inductive adder circuit which has demonstrated not only the required pulse rise times required by NGLS, but also the pulses required by the Advanced Light Source (ALS) upgrade at Lawrence Berkeley National Lab (LBNL), and a number of other commercial, medical, and other non-accelerator-based applications.

DESIGN

Inductive adders have been used for decades in the accelerator physics community to create ultra-high voltage, short rise time deflection pulses in beams. The inductive adder approach can be thought of as a number of pulse transformers with the primary windings in parallel and the secondary windings in series. Such approaches are not typically used in high-PRF applications, and have not shown the fast rise times required for the NGLS kicker. DTI's improvements to the classic inductive adder design include:

- Multiple cores on a single circuit board
- Secondary return current path on the circuit board
- State-of-the-art 650 V rated compensated MOSFETs
- Low inductance leadless flat packages
- Push-pull double voltage drive
- Low inductance backswing clamp
- High performance low delay charge pump gate drives

Re-arranging the circuitry of the classic inductive adder by placing several cores and drive circuits on a single circuit board allows the secondary return current to flow through the ground plane on the circuit board, which minizes the secondary stray inductance (Figure 1).

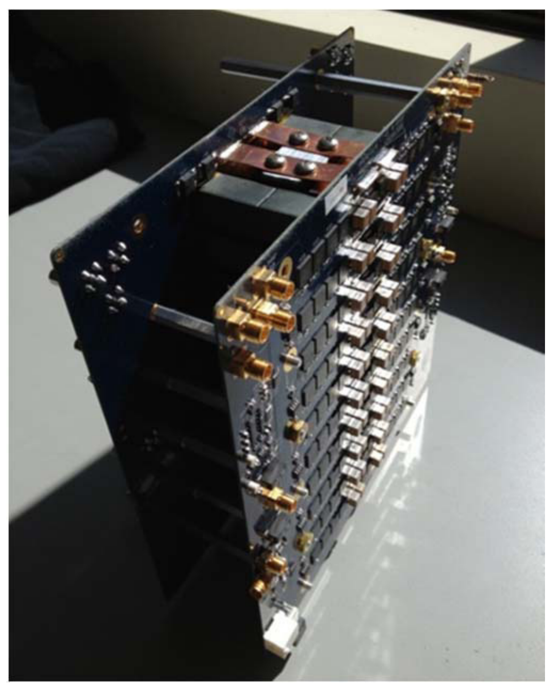

Figure 1: Dual PCB high speed pulser kicker driver system developed by DTI for the NGLS program. This kicker uses commodity 650 V transistors to switch nearly 17 MW, 700 A in 5 ns.

The best figure of merit power transistors are 650 V rated compensated silicon MOSFETs. These are available

OPTICAL DESIGN OF THE PI-TEST MEBT BEAM SCRAPING SYSTEM*

A. Saini†, A. Shemyakin, Fermi National Accelerator Laboratory, Batavia, USA

Abstract

PI-Test [1] is an accelerator facility under construction at Fermilab that will provide a platform to demonstrate critical technologies and concept of front-end of the PIP-II superconducting radio frequency (SRF) linac. It will be capable to accelerate an H^- ion beam with average current of 2 mA up to 25 MeV in continuous wave (CW) regime. To protect the SRF components from beam irradiation, the Medium Energy Beam Transport (MEBT) section of PI-Test includes an elaborated beam scraping system. It consists of four assemblies spread along the MEBT, with each assembly composed of four radiation-cooled, electrically isolated plates that can be moved into the beam in horizontal and vertical direction. The primary objectives of scraping system are to intercept particles with large transverse action and to protect the beamline elements and SRF linac in case of errors with beam focusing or steering. In this paper we formulate requirements for the scraping system and discuss factors affecting its efficiency. An optical design compatible with PI-Test MEBT is also presented.

INTRODUCTION

The uncontrolled beam loss in a linac may result in beam interruptions, radio-activation, and hazard to environment. As discussed elsewhere [2], continuous beam loss on the surface of SRF cavity causes a degradation in its performance. One of the means to decrease the beam loss in the SRF accelerating section of a linac is to install a scraping system at its low energy normal conducting section. Scrapers installed at optimum locations limit the phase space of particles that can enter the SRF and therefore, it allows not only to remove halo particles but also to intercept the beam core in case of errors with focusing or steering of the beam. In this paper we first discuss formulation of the efficiency of a scraping system and then present a realization of the concept at the PI-Test MEBT.

FORMALISM

One-plane (e.g. x) particle motion in the phase space in presence of uncoupled linear fields is characterized by its action (J):

$$J = \frac{1}{2}\left(\gamma x^2 + 2\alpha x x' + \beta x'^2\right); \qquad (1)$$

where α, β, γ are Twiss parameters and x, x' are coordinates of the particle. Particles with large actions outline the beam boundary and, in practice, potential beam loss either due to the beam halo formation or focusing errors. A set of two scrapers inserted symmetrically at a particular location remove particles with large spatial offsets but do not limit the maximum action in the beam (Fig. 1). For the latter, second set of scraper needs to be placed downstream to remove particles that had large angles but small offsets at location of the first set. The efficiency of such scraping system is described by the maximum action left after scraping of a fraction ΔN of the particle distribution.

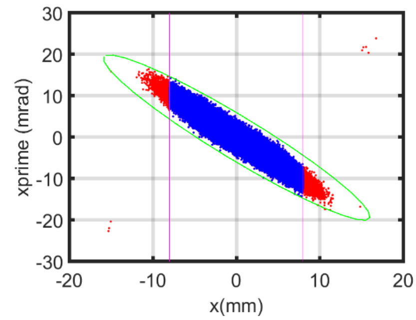

Figure 1: Horizontal beam phase space distribution before (red) and after (blue) a scraper assembly (magenta lines). The particle exhibiting maximum action in the phase space after a beam scraping moves along green ellipse.

Let us consider a beam with an initial Gaussian distribution:

$$g(x,x') = \frac{1}{2\pi\sigma_x\sigma_{x'}} e^{-\left(\frac{(x-\bar{x})^2}{2\sigma_x^2} + \frac{(x'-\bar{x}')^2}{2\sigma_{x'}^2}\right)} = \frac{e^{\frac{-J}{\varepsilon_0}}}{\varepsilon_0}; \qquad (2)$$

where ε_0 is the rms emittance and σ_x, $\sigma_{x'}$ are rms beam size and angle respectively. The scraping system is described by edge to edge separation $2d_i$ between two scrapers facing each other in an assembly i and the betatron phase advance $\Delta\phi$ between two successive scraper assemblies. Normalization of the the scraper insertion w.r.t rms beam size is expressed as:

$$a_i = \frac{d_i}{\sqrt{\beta\varepsilon_0}} \qquad (3)$$

A fraction N_i of the beam intercepted at each set can be expressed as:

$$N_1(a_1) = 1 - erf(a1);$$

$$N_2(a_1, a_2, \Delta\varphi) = \frac{1}{\sqrt{\pi}} \int_{-a_1}^{a_1} e^{-u^2}\left(1 - erf\left(\frac{a_2 - u\cos(\Delta\varphi)}{\sin(\Delta\varphi)}\right)\right) du \qquad (4)$$

Maximum action normalized to rms beam emittance after the second scraper assembly is calculated using following equation:

$$J_{\max} = \frac{a_1^2 + 2a_1a_2\left|\cos(\Delta\varphi)\right| + a_2^2}{\sin(\Delta\varphi)^2} \qquad (5)$$

If fraction of the beam scraped at each location is limited due to constraints such as scraper design specification, outgassing issues, etc., it is reasonable to consider the case when same portion of beam is scraped at both scraper assemblies that implies $N_1=N_2=\Delta N/2$. For known values of ΔN and, $\Delta\phi$ equation (4) can be solved numerically to determine corresponding insertion of scrapers. Then, using equation (5) one can express normalized action as a function of ΔN and, $\Delta\phi$ i.e. $J_{max}(\Delta N, \Delta\phi)$. An estimation has

* Work supported by Fermi Research Alliance, LLC under Contracts No. De-Ac02-07CH11359 with the DOE, USA.
† asaini@fnal.gov

ISBN 978-3-95450-169-4

DEFLECTOR DESIGN FOR SPIN ROTATOR IN MUON LINEAR ACCELERATOR

S. Artikova*, Y. Kondo, Japan Atomic Energy Agency (JAEA), Tokai-mura, Japan
T. Mibe, M. Otani, High Energy Accelerator Research Organization (KEK), Tsukuba, Japan

Abstract

A muon g-2/EDM experiment based on muon linear accelerator was proposed for the J-PARC muon facility [1]. In this experiment, the ultra-slow muons created in muonium target region will be accelerated to 210 MeV kinetic energy then will be injected into the muon storage magnet to measure the decay products depending on the muon spin. Therefore, a spin rotator (device) is a key component of the muon linac. Spin rotator consists of a pair of combined electrostatic and magnetic deflectors and a pair of solenoids which will be placed in between these two deflectors. In this paper, we report the design of these two dispersionless deflectors and the simulation results of the device performance will be discussed.

INTRODUCTION

A new experiment to measure the muon's anomalous magnetic moment $a_\mu=(g-2)/2$ is one of the ongoing research along the construction of the muon linear accelerator at J-PARC(Japan Proton Accelerator Research Complex) [2]. In this experiment, the ultra-slow muons created in muonium target region [3] will be accelerated to 210 MeV kinetic energy. To measure $(g-2)$, longitudinally polarized muons will be injected into 3 T MRI(Magnetic Resonance Imaging)-type solenoid magnet [4] and the decay products depending on the muon spin will be detected. Parity violation in the weak decay of the muon then serves as the spin analyzer. The higher-energy positrons in the muon decay chain $\mu^+ \rightarrow e^+ + \nu_e + \bar{\nu_\mu}$ will be emitted preferentially in the direction of the muon spin at the time of decay. Muons are spin polarized opposite to their momenta or spin and momentum are aligned. In both cases, muons are longitudinally polarized but in an opposite direction. Motivation of developing the spin rotation technique for $(g-2)$ experiment is to provide 180 degrees spin rotation during the transport of muon beam in a linear accelerator. An advantage of using the spin rotator is: muons can be injected into storage magnet either spin and momenta aligned or spin polarized opposite to their momenta. The quoted result for $(g-2)$ is determined by measuring the difference between the angular frequencies of spin precession the magnetic field and orbital cyclotron motion. The characteristic anomalous precession frequency is clearly visible in a wiggle plot of positron counting rate from the previous experiments [5]. If muons are spin rotated by 180 degrees, as a result, this wiggle will be shifted in time by a half period. Spin rotator is designed to be installed after the RFQ where muons will be accelerated up to 0.34 MeV.

Structure and Working Principle of the Spin Rotator

The schematic view of the spin rotator is shown in Fig. 1. It composed of a pair of deflectors and a pair of identical solenoid magnets situated in between the deflectors. Each deflector is designed to combine the magnetic and the electrostatic fields at the same position simultaneously in order to satisfy the requirements of device. An electrostatic deflector

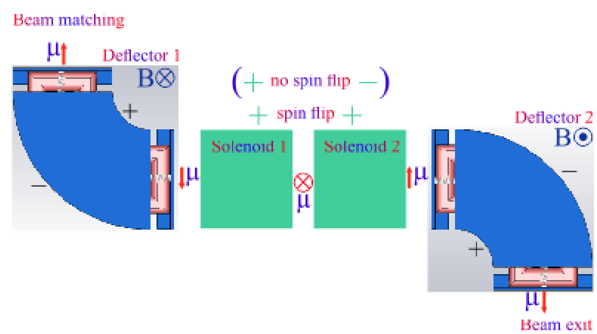

Figure 1: Schematic view of spin rotator. Dipole fields are transverse and the direction of electric fields are radially outward. The red arrows of μ^+ represents the muon spin orientation during the beam transport through the device. Plus signs on solenoids show that the magnetic fields of solenoids oriented in the same direction. Opposite signs show the magnetic field directions are opposite.

consists of two cylindrical electrodes is designed to bend the muon beam by 90° without changing the spin direction. To rotate the spin in a magnetic field generated by a cylindrical dipole an angle between the muon spin and the magnetic field should not be 0 or 180 degrees. After deflection in a normal dipole magnet, the muon spin has the same direction as the muon velocity because g factor is very close to 2. It is also possible to to make 90° deflection with double of the normal dipole magnetic field value, thus the muon spin will rotate 180°. We can use this advantage, then muons are transverse polarized after 90° deflection and perpendicular to the velocity. When beam enters the solenoid the magnetic momentum is perpendicular to the magnetic field. If solenoids' magnetic fields are in the same direction the muon spin rotates by 180°. If magnetic fields are opposite muon spin orientation will not change. Second deflector is an identical but has an opposite field direction regarding to the first one. At the exit of the second deflector muon beam polarization is still longitudinal but an opposite to its initial polarization. B_y using a pair of solenoids (depend on their field directions), the spin rotator can operate in two modes: either spin flip(rotation) or no spin flip.

* sayyora@post.j-parc.jp

COMMISSIONING RESULTS FOR A SUBHARMONIC BUNCHER AT REA*

D. Alt†, J. Brandon, S. Krause, A. Lapierre, D. Morris, S. Nash, N. Usher, A. Villari,
S. Williams, S. Zhao, FRIB, East Lansing, MI, USA
M. Syphers, Northern Illinois University, DeKalb, IL, USA

Abstract

The ReAccelerator facility (ReA) at the National Superconducting Cyclotron Laboratory (NSCL) at Michigan State University (MSU) offers a unique capability to study reactions with low-energy beams of rare isotopes. A beam from the coupled cyclotron facility is stopped in a gas stopping system, charge bred in an Electron Beam Ion Trap (EBIT), and then reaccelerated in a compact superconducting LINAC. The original beam repetition rate at the ReA targets was the same as the LINAC RF frequency of 80.5 MHz. In order to add the capability to bunch at a lower frequency (desirable for many types of experiments using time of flight methods) a 16.1 MHz buncher has been designed, constructed, and commissioned. This paper reports the results of the commissioning of the device, and outlines some future avenues for further improvement of the properties of the bunched beam.

INTRODUCTION

Figure 1 shows the layout of the ReA facility. After charge breeding in the EBIT, the beam is transported to the accelerating section, which consists of a room temperature RFQ and a superconducting LINAC. The 80.5 MHz frequency of the ReA RFQ and LINAC has a period of 12.4 ns. This means that the time-of-flight (tof) measured at a detector is ambiguous by an integer multiple of that period. In order to reduce that ambiguity, a longer period between bunches is desired for tof experiments. One approach to increasing the period without simply discarding large numbers of particles is to bunch the particles before the accelerator at an integer divisor n of the accelerator frequency [1]. With this method, only every nth "bucket" of the accelerator is filled, and the period between bunches increases to n times the original period. The design and construction of this device was the doctoral thesis topic of D. Alt.

DEVICE OVERVIEW

This section presents a brief overview of the design of the device. For more detailed explanations of the rationale behind the design parameters, please see [2].

The basic principle of low β bunching is that for each group of particles to be bunched, a voltage is applied in the longitudinal direction which ramps linearly from strongly decelerating at the head of the bunch to strongly accelerating at the tail. The height of the ramp is chosen so that all the particles in the bunch will arrive at a focal point at the same time. In practice, a perfect linear ramp is not achievable, and an approximation is synthesized from a few Fourier components. As such, some particles will see an incorrect voltage between the end of one ramp and the start of the next one, and will not be bunched correctly.

The frequency chosen for the subharmonic buncher was 16.1 MHz, the 5th subharmonic of the LINAC frequency. This results in a final bunch separation of 62.1 ns. The amount by which the bunch can be compressed in time is determined by the voltage applied to the beam, which in turn is determined by the focal length of the device. The best compromise between efficient bunching, reasonable voltage requirements, and available space on the beamline was determined to be a focal length of 2 m upstream of the focal point at the entrance of the RFQ. The corresponding maximum voltage depends on the rigidity of the species to be accelerated - for the highest rigidity beam which can be accelerated at ReA (Q/A = 1/5) this corresponds to a peak voltage on the first mode of approximately 1700 V.

The bunching waveform is generated by a truncated Fourier series, consisting of the first three sinusoidal components of the Fourier decomposition of the repeated linear ramp. These sine waves are excited in a pair of resonant coaxial structures. The first structure is excited in the $\lambda/4$ and $3\lambda/4$ modes to generate the 16.1 MHz and 48.3 MHz components, and the second is excited in only the $\lambda/4$ mode to produce the 32.2 MHz component. While the relative amplitudes of these components in the infinite Fourier series are 1, -1/2, and 1/3, when the series is truncated these amplitudes must be modified to account for the elimination of the remainder of the series. In order to maintain amplitude and phase stability, these structures are driven by a closed loop Low Level Radio Frequency (LLRF) controller with active feedback. The voltage is applied to the beam by a pair of conical electrodes.

TESTING METHODOLOGY

To observe the time structure of the beam, a timing wire detector was used [3]. This detector consists of a rigid wire centered coaxially within a metal cylinder. A voltage difference between the wire and the cylinder maintains a radial electric field between the two. When the beam enters a hole in the cylinder and strikes the timing wire, secondary electrons are emitted by the wire and carried away by the radial field. Some of these electrons impinge on a multi-channel plate (MCP) detector which in turn sends a signal to the data acquisition setup.

* Supported by Michigan State University, National Science Foundation: NSF Award Number PHY-1102511
† danalt@msu.edu

ISBN 978-3-95450-169-4

PLASMA WINDOW AS CHARGE STRIPPER COMPLEMENT*

A. L. LaJoie†, National Superconducting Cyclotron Laboratory, East Lansing, USA
F. Marti, Facility for Rare Isotope Beams, East Lansing, USA
A. Hershcovitch, P. Thieberger, Brookhaven National Laboratory, Upton, USA

Abstract

Modern ion accelerators, particularly heavy ion accelerators, almost universally make use of charge stripping. A challenge facing facilities, as the demand for higher intensity beams rises, is a stripping media that's highly resistant to degradation, such as a recirculating He gas stripper [1]. A method of keeping the He gas localized in a segment along the beamline by means of a Plasma Window (PW) positioned on both sides of the gas stripper has been proposed and the initial design set forth by Ady Hershcovitch [2]. With a cascaded plasma arc being the interface between high pressure stripper and low pressure beamline, the goal is to minimize gas flowrate from the stripper to the beamline in order to maintain sufficient isolation of the He gas. We present the initial results from the test stand developed at Michigan State University and the planned experimental program that will follow.

INTRODUCTION

Pushing the frontier of intensity and energy of Heavy Ion Beams requires facilities to employ some form of charge stripping. Solid thin carbon foils, while relatively easy to prepare and employ, suffer from often impractically short lifetimes when used with a high intensity heavy ion beam [1]. Alternatively, gaseous stripping media must be maintained at pressures much greater than those of the beamline to present a reasonably high degree of beam-gas interaction. In the case of the Facility for Rare Isotope Beams (FRIB) for example, the pressure of such a stripping gas would be on the order of 300 torr, and beamline pressure would be on the order of 10^{-8} torr. Inclusion of some structure to support such a large pressure differential while maintaining a flowrate low enough to not excessively load the vacuum system, presents a significant challenge with the Plasma Window being one possible solution.

During the R&D for FRIB a helium stripper and a liquid lithium stripper were considered. The first phase of development of the helium stripper contained by plasma windows was performed at Brookhaven National Laboratory (BNL) by Hershcovitch, Thieberger, and collaborators. The liquid lithium stripper was finally selected as the preferred choice because of the expected higher charge states obtained. As the potential applications in other accelerators as strippers or targets were interesting we pursued the development of a test stand at MSU to improve the performance and study the scaling laws of the different design parameters.

The Plasma Window is a wall stabilized DC arc discharge [3] that greatly inhibits the flow of gas between high (~300 torr) and low (~1 torr) pressure regions that the window connects, so provides an interface between high and low pressure without the need for solid material. This is the primary application for the PW under consideration in this work, with the high pressure gas representing a He gas charge stripping media, for example, ideal for use in a heavy ion accelerator. Hershcovitch has mentioned a great deal of other possible applications all stemming from the function of the PW being a pressures interface, such as electron beam welding, non-vacuum material modifications, transmission of high energy synchrotron radiation, and to isolate gas targets for use in fast (fusion) neutron generation or nuclear physics experiments. These will not be further mentioned in this work [2, 4].

Currently, the scaling laws for the PW's operation are not wholly understood. Different mechanisms have been proposed and obtaining some general relationship between flowrate and geometric, plasma, and fluid properties. Minimization of the PW's flowrate in terms of geometry and current supplied relies critically on a thorough understanding of the plasma and fluid processes within. Relevant plasma parameters can vary substantially with respect to initial conditions [5].

PREVIOUS EXPERIMENTS

The functionality of the window as separator of vacuum and atmospheric pressures is attributed primarily to the high temperature of the plasma relative to the inlet gas. Assuming the pressure within the channel is on the order of that in the high pressure inlet gas cell, the density of the gas in the arc must be significantly lower than that at atmosphere, by the ideal gas law. Additionally, viscosity of ions, electrons, and gas exhibit strong (through different mathematical expressions) dependence on temperature [2].

$$\eta_i = 2 * 10^5 \mu^{1/2} \frac{k}{\lambda_i} T_i^{5/2}$$

$$\eta_e = 2.5 * 10^7 \frac{k}{\lambda_e} T_e^{5/2}$$

$$\eta_g = a T_g^x$$

In the above equations, η_i, η_e, and η_g are ion, electron, and gas viscosities respectively, similarly for T_i, T_e, and T_g for temperatures. The respective Coulomb logarithms are

* Work supported by NSF Award No. PHY-1102511
† lajoie@nscl.msu.edu

MANUFACTURING OF MEBT COMBINED QUADRUPOLE & STEERER MAGNETS FOR THE LINEAR IFMIF PROTOTYPE ACCELERATOR LIPAC*

J. Castellanos†, B. Brañas, J. Mollá, C. Oliver, I. Podadera & F. Toral, CIEMAT, Madrid, Spain
R. Iturbe & B. López, Antec SA, Portugalete, Spain
O. Nomen, IREC, Barcelona, Spain

Abstract

The Medium Energy Beam Transport line MEBT [1, 2] is currently being installed on the LIPAC accelerator [3] and has among its components, five quadrupole and steerer magnets which were recently manufactured and tested.

Given the compactness of the MEBT line, each magnet combines, in a common yoke, a strong quadrupole field with a minor horizontal and vertical steering. In this way, each yoke integrates four water-cooled coils (quadrupole coils) and eight air-cooled coils (steerer coils) made of copper wires.

The magnetic design of the five combined magnets was done by CIEMAT [4] and the manufacturing and testing (excluding magnetic measurements) were carried out by the Spanish company Antec SA. With respect to the engineering design, it was mainly done by Antec SA but reviewed and agreed with CIEMAT.

This paper focuses on the technical aspects considered during the manufacturing and assembly of the MEBT magnets. Some details about the factory acceptance tests that were carried out before the magnetic measurements are also described.

INTRODUCTION

The Medium Energy Beam Transport line [1, 2] of the LIPAc accelerator [3] is placed between the RFQ system and the SRF Linac. Figure 1 shows the MEBT line where its five magnets are indicated as MMA01 to MMA05.

One important characteristic of the MEBT magnets is that, due to the short length available, it was decided to use combined magnets, according to the scheme represented in Fig. 2. Basically, each of the four poles of a magnet includes one quadrupole and two steerer coils which are centered on the iron pole. Steerers are located under the quadrupole coils in order to use the available space close to the pole tip [4].

The MEBT magnets should fulfill some strict magnetic quality requirements in order to have the desired control of the beam [4], and their performance should not be affected by ionizing radiations with an integrated dose up to 10^5 Gy. The fundamental MEBT magnets parameters are showed in Table 1.

All the considerations stated above, that is: 1) the compact design, 2) the strict magnetic requirements and 3) the ionizing radiations have a strong impact in the manufacturing techniques that should be followed during the construction and assembly of the magnets. For instance, the compact design complicates the positioning of the coils and the routing of their terminals as well as the design of the electrical and hydraulic connections; the strict magnetic requirements lead to specific manufacturing techniques for the machining of the pole tips and finally, the consideration of ionizing radiations requires a careful selection of the materials and the manufacturing methods, especially those related to the insulation of the conductors and the coils.

This paper summarizes the manufacturing techniques that were followed during the construction of the MEBT magnets in order to fulfill the requirements previously described. In addition, some details of the factory acceptance tests are also presented.

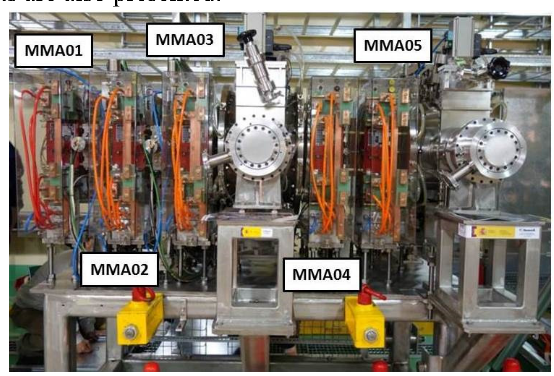

Figure 1: The MEBT line with the magnets installed. The five magnets are indicated as MMA01 to MMA05.

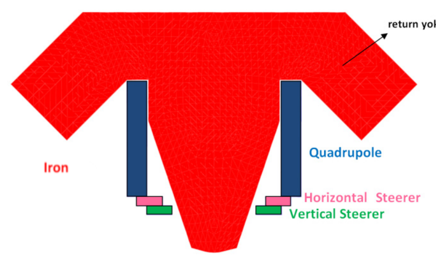

Figure 2: Schematic section of one of the four poles of a MEBT combined magnet. The quadrupole coils and the horizontal and vertical steerer coils are indicated.

Table 1: Main Magnet Parameters. Extract from [4]

Yoke length, height & width, mm	108–500–500
Total mass (including support), kg	220
Water flow, l/min & pressure drop, bar	3 // 5
Design gradient, T/m	25
Aperture diameter, mm	56
Integrated magnetic field (at 75% of aperture), T·m	0.0683
Steerer integrated field, G·m	25

* Work included in BA Agreement activities supported by the Spanish Ministry of Economy and Competitiveness.
† jesus.castellanos@ciemat.es

TOWARDS USER-DEFINED WEB APPLICATIONS IN ACCELERATOR LABS*

D. Liu†, Facility for Rare Isotope Beam, East Lansing, USA

Abstract

Most scientists and engineers in accelerator labs understand the basics of data types and data structures. They have in-depth knowledge about accelerator physics and other engineering domains. Some even develop software applications by themselves. However, they are not web application developers, and very few of them can implement web applications that support multiple users and data storage. In the approach of user-defined web applications, a user defines her/his own web application, test and use it first before sharing it to other users. It saves the communication efforts between developers and users, reduces the time from application design to production. Most importantly, users become the owner of the application and naturally the owner of the data that the application collects and produces. This will largely improve an application's quality and user experience.

SCIENTISTS ARE NOT DEVELOPERS

Most scientists and engineers in large scientific research labs are advanced computer users. They use general office software every day, and they need to use specific applications for their research and work. Some of them even develop software by themselves because available commercial software sometime does not satisfy their special needs.

Some applications developed by scientists are well known and used by the community. Some of such applications were released with an open-source licence, while some were provided with just the binaries. The application authors have to spend their own time to provide limited support. Reusing such software as libraries or services in a new development often is difficult due to intellectual property issues and source-availability issues. For the sake of the research community, there should be a platform to the scientists to easily **share** and manage their applications. The platform should lower the burden of software authors for managing and supporting users.

While some scientists have successfully delivered single-user desktop applications, very few have the technical skills to develop multi-user web applications. It is because this requires the software author to use multiple programming languages, develop both client- and service-side software, and know how to deal with aspects like security, data storage, and application protocols like HTTP.

USER-DEFINED WEB APPLICATIONS

In Section 1, we discussed the two problems in scientific application lifecycle:

1. difficulties to share and manage applications, and
2. difficulties to develop multi-user web applications.

In order to address these problems, we propose the approach of user-defined web application (UDWA).

What is a User-defined Web Application?

A web application has the following advantages compared to a traditional desktop application:

- Supporting multiple concurrent users
- Easy to release and update on diverse operating systems
- Easy to share to other users across organizational and geographical boundaries

Obviously, web applications help to address the first problem.

A user-defined web application is a data-centric web application generated by a web platform from high-level user defined specifications, and provides basic graphical user interface (GUI) and application program interface (API). Ideally, the platform provides an environment for users to compose and test the application specifications including:

1. the structure and types of data that application users will read and write, and
2. the data resources the application will consume.

The Epics process variable and other available UDWA data API's should be supported by the UDWA platform.

Minimal Requirements for Users

In order to use UDWA platform, and be able to define the application specifications, a user needs to understand

- basic data types like string and number;
- basic data structure concepts, like an object with properties and values, and an array of basic types, arrays, and objects;
- get and set the value of a Epics process variable; and
- read and update a resource via the HTTP protocol.

Technical Challenges

The first technical challenge to develop the UDWA platform is to have a data storage service that is able to save

1. the application specifications and their change histories; and
2. data instances saved by an application.

Note that the data instances of an application can be collected according to different data types and structures in the changing application specification. This makes it extremely difficult to store the data instances in a relational database, because the instances may require different data schemas. The same difficult is for the changing application specification if we want to save it in a database.

The second challenge is that the generated user interfaces of a piece of data can be rendered equivalently on

* This material is based upon work supported by the U.S. Department of Energy Office of Science under Cooperative Agreement DESC0000661, the State of Michigan and Michigan State University.

† liud@frib.msu.edu

ISBN 978-3-95450-169-4

FABRICATION AND HIGH-GRADIENT TESTING OF AN ACCELERATING STRUCTURE MADE FROM MILLED HALVES

W. Wuensch, N. Catalan Lasheras, A. Grudiev, G. Mcmonagle, I. Syrachev, B. Woolley, H. Zha, CERN, Geneva, Switzerland
G. Bowden, V. Dolgashev, A. Haase, SLAC, Menlo Park, CA 94025, USA
T. Argyropoulos[1], J. Giner Navarro[1], D. Esperante Pereira[1], IFIC (CSIC-UV), Valencia, Spain
R. Rajamaki, Aalto University, Espoo, Finland
X. Stragier[1], Eindhoven Technical University, Eindhoven, Netherlands
P. J. Giansiracusa, T. G. Lucas, M. Volpi[1], University of Melbourne, Melbourne, Australia
[1]also at CERN, Geneva, Switzerland

Abstract

Accelerating structures made from parts which follow symmetry planes offer many potential advantages over traditional disk-based structures: more options for joining (from bonding to welding), following this more options for material state (heat treated or not) and potentially lower cost since structures can be made from fewer parts. An X-band structure made from milled halves, and with a standard benchmarked CLIC test structure design has been fabricated and high-gradient tested above 95 MV/m.

INTRODUCTION

The development of the high-gradient normal conducting accelerating structures has a strong influence on both performance and cost of the Compact Linear Collider (CLIC). As a consequence, significant effort has been invested in the optimization of the structures, while maintaining the CLIC performance requirements. The latter are defined by a loaded accelerating gradient of 100 MV/m, pulse length of around 200 ns and breakdown rate (BDR) of 10^{-7} 1/pulse/m [1].

The CLIC accelerating structures operate at 11.994 GHz and are made from copper. They are usually manufactured by precision turning and milling of individual cells, and combined with precision milling for complex parts such as RF power couplers. These multiple parts and auxiliary components such as cooling pipes, tuning pins and flanges are bonded into a complete structure [2]. An alternative approach is the use of precision milling to cut cells into metal blocks that comprise halves of the complete structure [3]. This novel accelerating structure design and assembly gives a number of advantages compared to traditional structures. In particular, reduction of the number of precision pieces per structure to two, free choice of joining since there are no RF currents flowing through the metal-to-metal joint and an overall reduction of the total fabrication and handling cost.

In this paper we describe the RF design, fabrication, tuning and high-power testing of a prototype accelerating structure, T24-open, milled out of two halves and brazed together (Fig. 1). It is a full tapered structure which includes 24 regular traveling wave cells and 2 matching cells and works at a $2\pi/3$ phase advance per cell. Each regular cell uses the same iris dimensions as the CLIC-G structure [4]. One of the main motivations for this work is to study the high gradient performance of accelerating structures made with novel manufacturing methods.

RF DESIGN

The RF design and optimization of the structure is described in [3]. The geometry is optimized to simplify the machining process, as well as to reduce the maximum surface electric and magnetic fields and the local modified Poynting vector (S_c) [5]. Therefore, a racetrack profile with 1 mm gap and an elliptical rounding of the irises is selected for the geometry of single cells. The commercial finite element code HFSS [6] was used for the simulations.

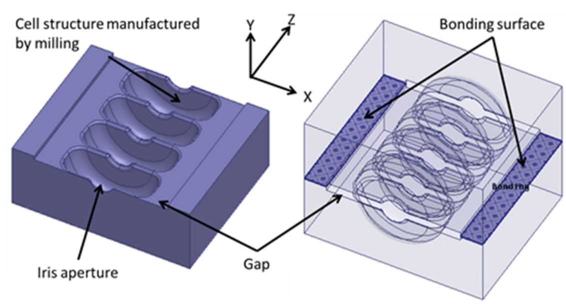

Figure 1: Manufacturing accelerating structure by milling on two halves of copper plate (HFSS model [6]).

The full tapered structure (Fig. 2) uses a so called waveguide coupler, with matching transitions to standard WR-90 waveguides. These are on-axis double-feed and can be manufactured by milling. The matching cell uses same geometry parameters as its neighbor regular cell except for the matching iris aperture. Dimensions are well tuned to minimize the reflection among the cells. The RF parameters of the full tapered structure are listed in Table 1 together with those of the CLIC-G undamped T24 structure.

STRUCTURE FABRICATION AND TUNING

The prototype T24-open structure, shown in Fig. 3, was machined at SLAC.

ISBN 978-3-95450-169-4

DEVELOPMENT OF 1.3 GHz SINGLE-CELL SUPERCONDUCTING CAVITIES WITH NIOBIUM MATERIAL DEVELOPED BY ULBA METALLURGICAL PLANT

T. Ota†, M. Takasaki, M. Yamada, N. Kuroiwa, S. Nomura, T. Tosaka, Y. Otani,
Toshiba Corporation, Yokohama, Japan
Y. Shirota, BE International Corporation, Tokyo, Japan
A. Tsorayev, Y. Krygin, V. Kuznetsov, ULBA Metallurgical Plant, Ust-Kamenogorsk, Kazakhstan,
T. Saeki, H. Hayano, High Energy Accelerator Research Organization, Tsukuba, Japan

Abstract

TOSHIBA has been developing high purity niobium (Nb) material for superconducting cavities with ULBA Metallurgical Plant (UMP) since 2008. Recently, we have produced the high purity Nb plates. Two 1.3 GHz single-cell superconducting cavities using UMP's Nb plates have been fabricated by TOSHIBA and RF tested at High Energy Accelerator Research Organization (KEK). One of the cavities has achieved the accelerating gradient of E_{acc}=31.8 MV/m. The development of high purity Nb plates, details of the fabrication of the cavities and the RF test results are presented in this article.

INTRODUCTION

TOSHIBA has been continuing R&D on the fabrication of superconducting cavities for accelerators in collaboration with KEK since 2009. In order to ensure the quality of the superconducting cavities, the cooperation of the supplier of Nb material and the cavity fabricator is very important. In this sense, we are developing high purity Nb material of superconducting cavities for International Linear Collider (ILC) with UMP. Recently, UMP has produced the high purity Nb ingot in which Residual Resistance Ratio (RRR) value is higher than 300.

HIGH PURITY NB

UMP produces Nb ingots from Nb ore mined at a certain mine where is not Brazil. The impurities of Nb ingot are decreased by multi-melting. We have measured RRR of some samples of Nb ingots. Figure 1 shows RRR values depending on the number of multiple EB melting. RRR value is increasing with the number of melting. Multiple melting is effective for increase in RRR. RRR becomes higher than 300 by repeating of smelting Nb ingot more than six times. The chemical composition of UMP's Nb ingots and the mechanical properties of UMP's plates are shown in Table 1 and Table 2, respectively. UMP's Nb plates have reached to the performance equivalent to Nb plates of superconducting cavities for ILC.

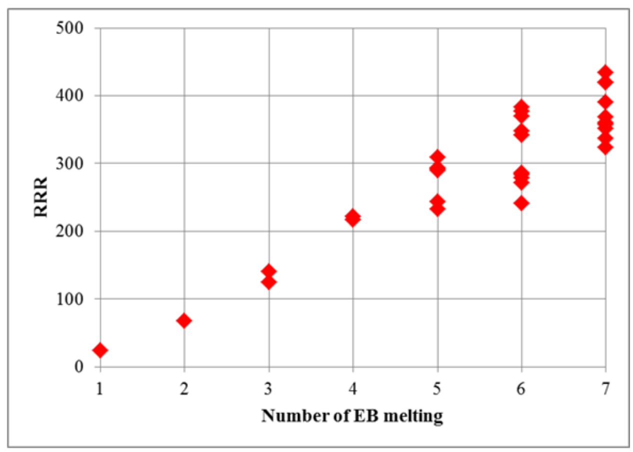

Figure 1: RRR values of multiple EB melting.

Table 1: Chemical Composition of Nb Ingot

	Element (< Wt.ppm)										
	Ta	W	Mo	Ti	Fe	Ni	Si	H_2	N_2	O_2	C
ILC specs	500	70	50	50	30	30	30	2	10	10	10
UMP's Nb	300	25	25	10	10	-	17	2	37	25	20

Table 2: Mechanical Properties Measurement of Nb Plates

	Tensile Strength (MPa)		Yield Strength (MPa)		Elongation (%)		Average Grain Size (μm)
	Longitudinal	Transverse	Longitudinal	Transverse	Longitudinal	Transverse	
ILC specs	140	140	39	39	> 30	> 30	40
UMP's Nb	167	167-172	53-56	55-56	53-56	59-60	23

† tomoko.ota@toshiba.co.jp

ISBN 978-3-95450-169-4

DESIGN STUDY OF A TEST CAVITY FOR EVALUATING RF CRITICAL-MAGNETIC FIELD OF THIN-FILM SUPERCONDUCTOR*

H. Oikawa†, Utsunomiya University, Utsunomiya Tochigi, Japan
T. Higashiguchi, Center for Optical Research and Education, Utsunomiya University, Utsunomiya Tochigi, Japan
Y. Iwashita, Kyoto ICR, Kyoto University, Uji Kyoto , Japan
M. Hino, Kyoto University, Kumadori Osaka, Japan
H. Hayano, S. Kato, T. Kubo, T. Saeki, KEK, Tsukuba Ibaraki, Japan

Abstract

In the second stage of ILC, a superconducting cavity with high gradient of more than 45MV/m is required. To obtain such a high gradient, there has been proposed a method of increasing an RF critical magnetic field of the cavity inner surface by coating multi-layer thin-film superconductor, which their thickness is close to the London penetration depth. By producing a multi-layer thin-film structure in cavity inner surface, it is thought to improve the RF critical magnetic field, and to connect directly to high gradient.

In order to demonstrate an RF critical magnetic field of a thin-film on a surface of Nb, an RF cavity with thin-film coated Nb sample is necessary to measure an RF critical magnetic field below critical temperature of a sample. Also it is necessary to design such a cavity producing strong RF magnetic field parallel to the sample thin-film surface. We have designed a mushroom-shaped cavity for that purpose and fabricated an aluminum model cavity.

In parallel, RRR measurement system was developed to evaluate thin-films.

MULTI-LAYER THIN-FILM SUPECONDUCTOR

A superconducting thin-film for a high electric field of an accelerator cavity application was proposed by Gurevitch 2006 [1]. The study of multi-layer thin-film superconductor is being on a way in many laboratories [2, 3, 4]. In order to achieve high acceleration gradients for the superconducting cavity of the second stage ILC accelerator, we started the study to evaluate a critical magnetic field of superconducting thin-films such as Nb_3Sn and NbN and MgB_2 deposited on the Nb samples. We chose an atomic layer deposition (ALD) method of film formation, which has an advantage of uniform and nm controllablity for thickness on a complex inner-surface structure of cavity. In order to develop application method of ALD on Nb surface, we need to measure lower critical field at a frequency of several kHz using a small coil, a superheating critical magnetic field of RF frequency using RF cavity respectively, as well as RRR for thin-film on a sample. There is theoretical study to evaluate a thickness of each layer for the best performance of multi-layer thin-film superconductor. We have shown that there is an optimum thickness of formed thin layer to get maximum superheating critical magnetic field [5]. Those are the target structure in this study.

†oikawah@post.kek.jp

DESIGN AND MANUFACTURE OF THE ALUMINUM MUSHROOM-SHAPED CAVITY

Calculation of Electromagnetic Field in the Cavity

A mushroom-shaped cavity has a shape of half hemisphere with flat bottom plate. It has an advantage to make strong magnetic field closing well inside of the cavity and facing to the sample surface of the bottom plate, on the other hand, a magnetic field on the hemisphere surface can be reduced compare to the bottom surface. The resonant frequency of the cavity was selected to 3.9 GHz to make it compact as possible. It corresponds to a triple harmonics of 1.3 GHz which is the resonant frequency of the superconducting accelerating cavity of ILC. The shape of the cavity was based on the mushroom-shaped cavity of the SLAC study [6]. The stored RF power is limited by thermal superconductivity destruction of Nb of the cavity. We have designed a cavity so that the magnetic field of the sample surface to the magnetic field of the inner hemisphere wall holds a value twice or more. The electric field in the cavity inner wall has been designed to have minimum, in order not to generate field emission. A cylinder shape port at the top of the mushroom-shaped cavity is a coupled waveguide to put RF power into the cavity. The port is also used for a vacuum pumping port installation. CST MW STUDIO was used to design the cavity. By starting from the shape of SLAC cavity, a model dimensions were optimized to have 3.9 GHz with similar electric field and magnetic field inside. Then a shape of a bottom plate was modified to have strong magnetic field on the sample surface with weak magnetic field on the hemisphere surface. The bottom plate was extruded into the cavity, finally. Figure 1 shows final cavity shape and calculated electromagnetic field of inner surface in the cavity.

From the calculation, maximum excited magnetic field on the bottom sample surface is 51460 A/m, on the other hand, along the inner surface of hemisphere, the maximum excited magnetic field is 20409 A/m. As a result, the

DARK CURRENT STUDIES IN ILC MAIN LINAC

A. Sukhanov*, I. Rakhno, N. Solyak, I. Tropin, Fermilab†, Batavia, IL 60510, USA

Abstract

Studies and optimization of design of the International Linear Collider (ILC) based on the TESLA-type 9-cell 1.3 GHz superconducting RF (SRF) cavities are currently underway. Dark current (DC) electron generated by field emission in SRF cavities can be captured and accelerated in the main ILC linac up to very high energy before they are removed by focusing and steering magnets. DC electrons, interacting with the materials surrounding SRF cavities, produce electromagnetic showers and contribute to the radiation in the main ILC tunnel. In this paper present preliminary results of the simulation study of dark current in the ILC linac.

INTRODUCTION

Design of SRF linacs requires extensive investigation of dark current radiation in order to protect accelerator components from radiation damage and optimize thickness and cost of the radiation shields.

In paper [1] we describe a model of dark current in SRF linac. Our model combine tracking of electrons in RF field of cavities and magnetic field of focusing magnets with MARS simulation of interactions of lost particles with the materials of the accelerator components. In the current paper we apply this model to a study of DC in ILC main linac. Our assumption is that all cavities of the linac contribute equally 50 nA into DC. We perform tracking of DC electrons in sections of linac consisting of up to 40 basic RF units[1]. We consider a "normal" mode of operation of the linac, when both RF power to the cavities and focusing magnets turned on. We also study few "commissioning" modes of operation when only cavities RF power is ON, but focusing magnets are turned OFF.

RESULTS

Normal Mode of Operation

In the normal mode of linac operation, when focusing magnets are turned on, most of the DC electrons are lost in the magnets or in the cavity down stream of the magnet. The maximum energy of the lost DC electrons may reach up to 800 MeV. In this case the equilibrium state, when losses of DC particles along the linac are compensated by newly generated DC electrons, is reached already at the 2nd RF unit. Table 1 summarizes losses in the equilibrium (steady) state at the varius point along the linac. As one can see, the largest losses in normal operation are at the end of the linac and concentrated at the locations of focusing magnets.

Table 1: Equilibrium Losses

Beam Energy, GeV	5	10	15	125	250
Quad, W	0.07	0.15	0.22	1.35	1.7
Cavity, W	0.36	0.36	0.45	0.45	0.2
RF Unit, W	4.1	3.5	3.2	2.7	2.6

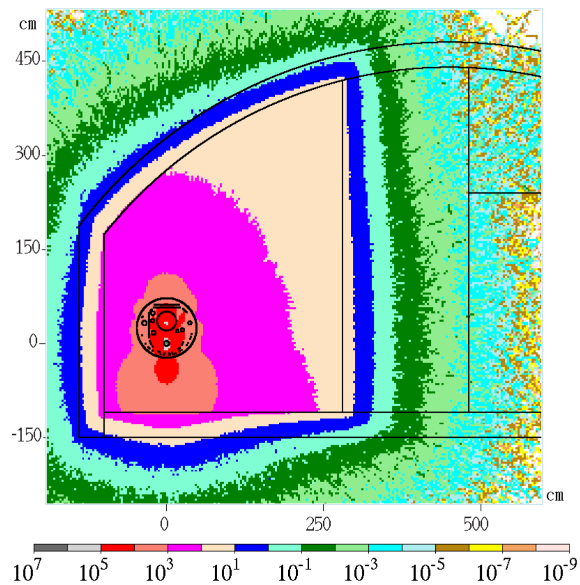

Figure 1: Total prompt dose (mSv/hr, color scale) at the tunnel cross section at the end of ILC linac during normal operation. Focusing magnet strength corresponds to 250 GeV beam.

Figure 1 shows distribution of the total propt dose in the tunnel cross section at the focusing magnet location at the end of the linac. Total dose is about 100 mSv/hr at the tunnel wall. It drops to the safe level of 25 uSv/hr 1.2 m into the wall. In the current design of the ILC main linac 3.5 m concrete wall between main and service tunnels provides very large safety margin for radiation protection.

Operation of Linac with Focusing Magnets Off

Turning off focusing magnets while still having RF power in cavities may potentially present worse conditions for DC radiation than the normal operation of the linac. We consider four distinct scenarios: 1) straight section of the linac (bunch compressor) with steering/correcting magnets turned off ; 2) curved section of linac, which follows Earth curvature, with steering/correcting magnets turned off; 3) curved section with steering magnets on, but no correction for mis-

* ais@fnal.gov

† Operated by Fermi Research Alliance, LLC under Contract No. De-AC02-07CH11359 with the United States Department of Energy.

1 In ILC such unit contains 3 cryo-modules, 26 cavities and a focusing magnet.

ISBN 978-3-95450-169-4

3-CELL SUPERCONDUCTING TRAVELING WAVE CAVITY TUNING AT ROOM TEMPERATURE*

R. Kostin[1,3†], P. Avrakhov[1], A. Kanareykin[1,3], V. Yakovlev[2], N. Solyak[2], T. Khabiboulline[2], P. Berutti[2]
[1]Euclid Techlabs, Bolingbrook, IL
[2]Fermilab, Batavia, IL
[3]St. Petersburg Electrotechnical University LETI, St.Petersburg, Russia

Abstract

A superconducting traveling wave (SCTW) cavity with a feedback waveguide will support a higher average acceleration gradient compared to conventional SRF standing wave cavities [1]. Euclid Techlabs, in collaboration with Fermilab, previously demonstrated a high accelerating gradient in a single cell cavity with a feedback waveguide [2], and the new waveguide design did not limit the cavity performance. The next step is high gradient traveling wave SRF cavity test. A 3-Cell SCTW cavity was designed and developed [3] to demonstrate the SRF traveling wave regime. Two Nb SCTW cavities were built, characterized and cold tested in 2016. This paper presents the results of cavity inspection, field flatness analysis, along with a discussion of the tuning procedure.

INTRODUCTION

The accelerating gradient in RF cavities plays a key role in high energy accelerators [4], since the cost of the project is highly dependent on its length. The current design of an SRF based linear collider uses superconducting Tesla type [5] accelerating cavities with accelerating gradients of 31 MV/m. The Tesla cavity length is restricted to 1 meter because of field flatness degradation and consists of only 9 cells. There is an unavoidable gap between cavities which decreases the average accelerating gradient.

A superconducting traveling wave cavity was proposed to increase the accelerating gradient [1]. However, it requires a feedback waveguide to transfer RF power from the output of the cavity back to its input section. Traveling wave (TW) cavities have lower field flatness sensitivity to the cavity length and, thus can be much longer. Our investigations showed [2] that a 10 meter long TW cavity would have a better field flatness than even a 1 meter standing wave (SW) cavity if it can be fabricated and cleaned with the required tolerances. Thus, if the technology allows building such a long cavity it might increase the accelerating gradient by 22% eliminating beam pipes empty of RF power between cavities. A TW cavity can operate at any phase advance, and, as is well known, a smaller phase advance provides a higher transit time factor. We investigated the phase advance dependence on the accelerating gradient of the SCTW cavity and it was found that 105 degrees gives an optimal accelerating gradient gain of 24% [2]. Overall, a TW cavity may increase the gradient by up to 46% compared to a conventional SW cavity.

The first approach to a TW cavity was a single cell cavity. It was manufactured to prove the feasibility of cleaning the feedback waveguide. The cavity was cleaned at Argonne National Lab and tested at Fermilab at the vertical test stand in liquid helium. A 26 MV/m accelerating gradient was reached [2], which is comparable to Tesla single cell cavities with the same treatment. This opened the way to build a next generation TW cavity – a 3-Cell SCTW cavity [3] to demonstrate operation in the TW regime in a superconducting cavity with a high gradient. Two cavities were manufactured. Their resonant frequencies and Q factors were measured and the results are presented in this paper. Bead-pull measurements were done and are also presented here.

Tuning properties of the 3-Cell TW cavity were investigated [6, 7] and it was found that suppression of microphonics, caused by external pressure variation is possible by power redistribution in the power couplers. Also, a special 2D tuner required for Lorentz force compensation was designed, manufactured and tested [8]. Tuning studies were accomplished by a special analytic model involving S-matrix formalism which is thoroughly described in [9]. These studies provided some insight to the powering scheme which was used for cavity tuning and is presented in this paper.

CAVITY INSPECTION

Two niobium cavities were manufactured by the Spring of 2016. One of these cavities will be tested in liquid helium at Fermilab. This cavity requires additional waveguide reinforcements because of the small bandwidth during the test which will be finished by Fall 2016. The cavity with no stiffening ribs and with some of them installed is depicted in Fig. 1.

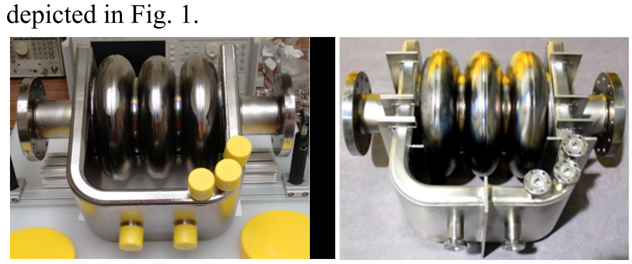

Figure 1: 3-Cell traveling wave cavity with (right) and without (left) stiffening ribs on the waveguide.

The full sized traveling wave cavity was designed to use two TTF-3 couplers with loaded $Q=10^6$ and does not need such reinforcement [3]. Bead-pull measurements were made for both cavities and are depicted in Figure 2. Also

* Work supported by US DOE SBIR # DE-SC0006300
† r.kostin@euclidtechlabs.com

A COMPACT MUON ACCELERATOR FOR TOMOGRAPHY AND ACTIVE INTERROGATION*

R.W. Garnett†, S.S. Kurennoy, L.J. Rybarcyk, LANL, Los Alamos, NM, USA
S. Portillo, E. Schamiloglu, University of New Mexico, Albuquerque, NM, USA
N. Saito, J-PARC, Ibaraki-ken, Japan
K. Hasegawa, JAEA, Ibaraki-ken, Japan

Abstract

Muons have been demonstrated to be great probes for imaging large and dense objects due to their excellent penetrating ability. At present there are no muon accelerators. Development of a compact system that can produce an intense beam of accelerated muons would provide unique imaging options for stockpile stewardship while delivering minimal radiation dose, as well as various homeland-security and industrial applications. Our novel compact accelerator approach allows a single linac to be used to first accelerate an electron beam to 800 MeV to generate muons by interacting with a production target in a high-field solenoid magnet and then to collect and accelerate these low-energy muons to 1 GeV to be used for imaging or active interrogation. The key enabling technology is a high-gradient accelerator with large energy and angular acceptances. Our proposed solution for efficient acceleration of low-energy muons is a 0-mode linac coupled with conventional electron RF accelerating structures to provide a compact system that could deliver a controllable high-flux beam of muons with well-defined energy to allow precise radiographic inspections of complicated objects. The details of the conceptual design will be discussed.

INTRODUCTION

Muons are elementary particles that make great probes for imaging large dense objects due to their excellent penetrating ability. While electrons are easily stopped in dense matter, muons have much higher penetrating ability due to their larger mass. As leptons, they do not experience strong interactions that are typical for protons or neutrons. This makes muons unique probes for large and dense objects. Muon radiography using cosmic muons has been demonstrated [1], but is limited by the relatively low rate and the large energy range of muons produced in cosmic ray showers. Availability of intense beams of mono-energetic muons would enable radiography for large-scale imaging, stockpile stewardship or industry applications, and valuable new tools for improved materials diagnostics (e.g., advanced muon spin relaxation / resonance / rotation). Applied to Homeland Security, beams of negative muons can provide unique elemental analysis of materials via muonic X-rays even under heavily-shielded conditions [2, 3].

The problem is how to make and accelerate enough muons. Muons are unstable particles, with a mean lifetime of 2.2 μs at rest. Nevertheless, this is long enough to accelerate them, increasing their lifetime in the lab frame due to relativistic effects. Muons are the most numerous energetic charged particles at sea level. Produced mainly by proton collisions in the upper atmosphere, muons arrive at sea level at an average flux of about $1/\text{cm}^2/\text{minute}$, comprising roughly half of the total natural radiation background. The atmospheric muon flux depends on the muon incidence angle φ from the vertical direction (φ = 0) as $\sim\cos^2\varphi$ and also on incident muon energy. In the 1-GeV energy range, it decreases by 5 orders of magnitude between the vertical and horizontal directions [4]. In the lab, muons are produced by decays of pions, which are created when a high-energy particle beam hits a target. Most of the created muons have low energies (< 50 MeV) and are spread in all directions. Conventional muon experiments utilize such target-produced muons. Usually only a tiny fraction of all produced muons, those with highest energies and traveling in the forward direction, are captured and used; the resulting muon flux is therefore very low.

An accelerator-based system producing a higher muon flux, at least of order 10^3/s, with energies ~1 GeV or above in a well-directed beam would provide a game-changing advancement for several applications including muon tomography. A moderate-resolution reactor image (±10 cm) achieved by a month-long exposure to cosmic muons would be obtained within minutes. Much higher muon fluxes, up to 10^9/s, are required for active stand-off interrogation to identify nuclear materials in large targets such as a container ship [2, 3].

PRELIMINARY STUDIES

From 2009-2011, the Defense Threat Reduction Agency (DTRA) supported studies at Los Alamos to develop an active stand-off muon interrogation system for identifying special nuclear materials in cargo. Our concept was based on collecting and accelerating low-energy pions and muons to achieve the required very-high muon flux [5]. The key enabling element is a high-gradient muon accelerator with large energy and angular acceptances based on a 0-mode linac operating in a 5-T solenoidal magnetic field to keep particles with large transverse momenta within the linac aperture. The 0-mode linac accelerates low-energy

* Work supported by the United States Department of Energy, National Nuclear Security Agency, under contract DE-AC52-06NA25396.
† rgarnett@lanl.gov

ISBN 978-3-95450-169-4

TRAVELING WAVE ACCELERATING STRUCTURE POWER INPUT CALCULATION WITH EQUIVALENT CIRCUIT METHOD *

S.V. Matsievskiy†, V.I. Kaminskiy NRNU MEPhI, Moscow, Russian Federation

Abstract

Nowadays linac accelerating RF systems design is usually done by the finite difference method. It provides high accuracy of calculations and freedom in topology choosing, but may draw considerable amounts of computer resources with long calculation times. Alternative to this method, equivalent circuit method exists. The basic idea of this method is to build a lumped element circuit, which with certain approximation acts as an original accelerating cell. It drastically reduces the number of equations to solve. This method is long known but usually only used for the particular accelerating structures when speed of calculation is a key-factor. This paper describes an attempt to create more universal and user-friendly software application for calculating electrical field distribution in accelerating structures, provides mathematical equations this software is based on. The resulting application may be used for preliminary calculations of acceleration structures and help to determine cells electrodynamic parameters reducing overall design time.

INTRODUCTION

At present time finite differences method programs are the main tool for the accelerating structure calculations. Its advantages are relative universality and simplicity. These programs are applicable for all types of accelerating structures; same model can be used for different operation mode calculations; for the most part, these programs have friendly user interfaces. However, programs require large amount of time and machine resources. In contrast to finite differences method, the equivalent circuit method may be used for quick calculations of the sections with a large number of cells [1, 2]. There are some downsides to this method also. Firstly, the result of the structure optimization - optimal coupling coefficients and cells frequencies - does not provide information about the geometrical parameters of the structure: either finite difference method calculation or correspondence table are needed. Secondly, for two different cell type or even for a single cell operating in different modes equivalent circuits are needed. In this light it is obvious that the equivalent circuit method can not replace the finite difference method, but can be used to obtain reference parameters for the subsequent accelerating structure optimization, thus reducing calculation time. Particularly useful this program seem to be in application to calculation of the long structures or structures with a constant field gradient.

* This work was supported by a grant from the Ministry of Education of the Russian Federation number 3.2458.2014/K

† MatsievskiySV@gmail.com

EQUATIONS FOR ACCELERATING CELLS

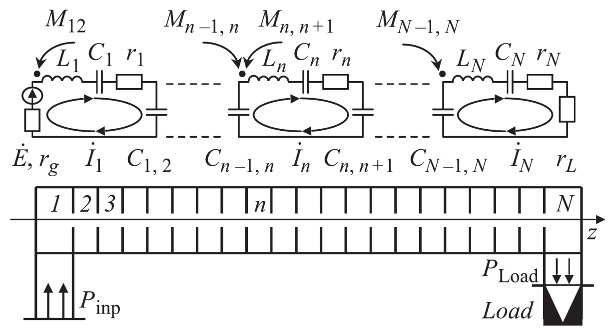

Figure 1: The equivalent circuit of the accelerating structure.

In Fig. 1 the equivalent circuit of the accelerating structure is shown. The equations describing this circuit can be represented in matrix form:

$$|A| \cdot |X| = |B|$$

Here, X is normalized cell field amplitude vector; right side of the equation represents particle current load and the input generator power. Matrix A is cell connection matrix: elements $a_{i,j},\ i \neq j$ characterize connections between the cells i and j. This equation may be solved analytically with some simplifications but it would restrict application of the code to a very specific accelerating structure schemes. Alternatively, relying on the numerical methods, one may obtain solutions for various accelerating structure schemes incorporating different cell types. For example, addition of the waveguide connection between cells i and j would require only the replacement of the rows i and j in the matrix A. Previously obtained analytical solution would not be applicable in this case. Numerical solution allows characteristics calculation of the sections with variable geometry (with a constant gradient), for which analytical solution is very complicated, as well as carrying out calculations of cells tolerances ensuring efficient operation of the structure. Additionally, method of equivalent circuits is applicable for characteristics calculation of biperiodic accelerating structures.

Cells with Waveguide Connection

In Fig. 2 the equivalent circuit of the cell with electric and magnetic coupling and dumping load is shown. This circuit could be used for pure electric coupling cells if magnetic coupling coefficient is set to zero and vice versa. Kirchhoff equations and the input impedance equations for these cells are well known and described in [3].

This scheme can be made even more versatile by adding input generator power and transmission line connections

ISBN 978-3-95450-169-4

BEAM-LOADING COMPENSATION OF A MULTI-BUNCH ELECTRON BEAM BY USING RF AMPLITUDE MODULATION IN LASER UNDULATOR COMPACT X-RAY SOURCE(LUCX)*

M. Fukuda†1, S. Araki, Y. Honda[1], N. Terunuma[1], J. Urakawa, KEK, Ibaraki, Japan
[1]also at SOKENDAI, Ibaraki, Japan
K. Sakaue, WIAS, Waseda University, Tokyo, Japan
M. Washio, RISE, Waseda University, Tokyo, Japan

Abstract

We have been developing a compact X-ray source via laser Compton scattering(LCS) at Laser Undulator Compact X-ray source(LUCX) accelerator in KEK. In here, a multi-bunch electron beam is generated by a 3.6cell photocathode RF-gun and accelerated to 18-24MeV by a 12cell accelerating tube. And then 6-10 keV X-rays are generated by LCS between the beam and a laser pulse stored in a 4-mirror planar optical cavity. Presently, we have achieved the generation of 24MeV beam with total charge of 600nC in 1000bunches. The energy difference is within 1.3% peak to peak. The beam-loading is compensated by ΔT method and amplitude modulation of the RF pulse. However, there is the energy difference at the RF-gun. It is assumed that this causes the reduction of the X-ray flux due to change of the focused beam size. To reduce the energy difference, RF amplitude modulation is also applied to the RF pulse for the gun. The results of this beam-loading compensation will be reported.

INTRODUCTION

X-rays are used in a wide range of applications, for medical examination, biological science, material science and so on. High-flux and high-brightness X-ray is specially generated by synchrotron radiation storage rings with an order of GeV although they are generally large and expensive. On the other hand, an X-ray source via LCS is possible to generate X-rays with a similar energy by using a compact accelerator because the electron-beam energy is an order of tens of MeV. For example, 10keV X-rays can be generated by LCS with 24 MeV electron beam and a laser which wavelength is 1064 nm.

We have constructed a small electron accelerator called LUCX accelerator[1] at KEK in order to develop a compact X-ray source based on LCS. At here, 6-10 keV X-rays are generated by LCS of a multi-bunch electron-beam with the energy of 18-24 MeV and a laser pulse with the wavelength of 1064nm.

LUCX ACCELERATOR

The LUCX accelerator is an S-band normal conducting accelerator which consists of a 3.6cell photo-cathode RF-gun[2], a 12cell standing-wave accelerating tube[2] and a 4-mirror planar optical cavity[3]. The layout is shown in Fig. 1.

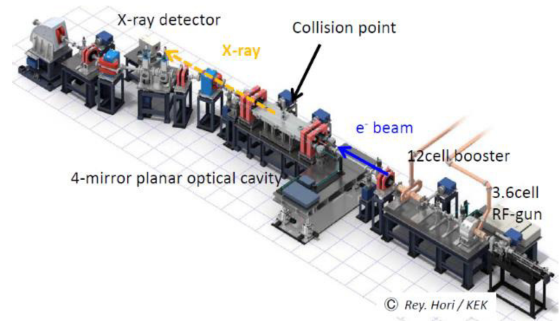

Figure 1: The beamline of the LUCX accelerator.

The RF-gun generates a 7.6MeV multi-bunch electron-beam with total charge of 600nC in 1000 bunches. The beam is accelerated from 7.6MeV to 24MeV by the accelerating tube. After that, the beam collides with a laser pulse stored in the optical cavity and then X-rays are generated by LCS. The beam is separated from the X-rays by the first bending dipole. X-rays are extracted to the air through a beryllium window with the thickness of 300μm.

Figure 2 shows the diagram of the RF system. The master clock of 357MHz for synchronization is generated from the signal of laser pulses injected to the optical cavity in this accelerator. We call this method the laser master system. The frequency of the RF signal delivered to klystrons is converted from 357MHz to 2856MHz. And then the RF signal cut out as a rectangular wave. The pulse is injected to a klystron after amplified.

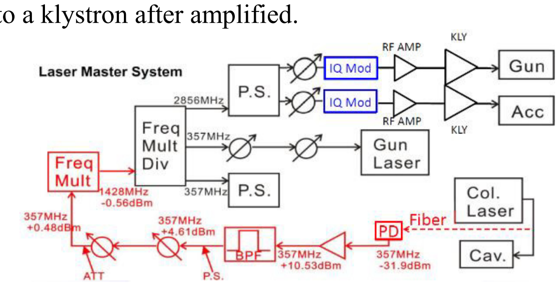

Figure 2: The diagram of the laser master system.

The amplitude of the pulse is modulated by an Inphase-Quadrature (IQ) modulator before the RF amplifier in order to compensate the beam loading effect which causes the energy reduction in a train on the acceleration of a multi-bunch beam. By modulating the amplitude of an RF pulse, the electric field for accelerating can be modified so that the energy reduction is cancelled out.

Two klystrons provide a 4.3μs RF pulse into the RF-gun and the accelerating tube respectively. The injected peak

† mfukuda@post.kek.jp

ISBN 978-3-95450-169-4

LEETCHI: THE HIGH CURRENT ELECTRON SOURCE FOR THE CLIC DRIVE BEAM INJECTOR

K. Pepitone*, S. Doebert, CERN, Geneva, Switzerland
B. Cadilhon, B. Cassany, J. Gardelle, CEA/CESTA, Bordeaux, France

Abstract

LEETCHI is a source which will produce 140 keV, 5 A, 140 µs electron beams at a repetition rate of 50 Hz. The shot to shot and flat top current stability of this drive beam injector for CLIC has to be better than 0.1 % and a geometrical rms-emittance of 14 mm.mrad is expected. The development of a high voltage modulator, to achieve those requirements, is ongoing. A small test stand has been built which allows to diagnose and dump the beam produced by the thermionic cathode. The thermionic cathode is equipped with a grid which will allow us to control the current and eventually to have a feedback on the flattop shape. The beam dump, made of graphite, has been designed using two different codes, the Monte Carlo code GEANT4 to simulate the energy deposition and ANSYS used to simulate the thermal resistance of the graphite due to the long pulse duration. The geometry has been optimized with the ray tracing code EGUN and the 2D PIC-code MAGIC. All these simulations allowed us to optimize the geometry of the gun and to develop diagnostics which must survive to the heat deposition. Finally, the first electrical measurements of the beam will be presented.

INTRODUCTION

In the two beam acceleration scheme of the Compact Linear Collider (CLIC) the drive beam serves as the power source for the main linac [1]. This drive beam is a low energy, high current beam where the beam power is extracted locally by deceleration and directly fed into the main linac. The beam stability of the main beam is critical to obtain the desired luminosity and thereby determined by the stability of the drive beam. This dependence puts severe stability requirements on the drive beam injector. In CLIC the drive beam is generated from a 140 µs long DC electron beam, bunched at a sub-harmonic frequency of 500 MHz and then accelerated with an rf frequency of 1 GHz. The sub-harmonic bunching is used to phase code the beam to enable beam combination using rf deflectors and a series of combiner rings. In the end the long bunch train gets combined to 24 sub-trains which are each 240 ns long and have a 12 GHz bunch repetition rate. The average beam current gets increased from 4.2 A to 100 A during this process (see [1] for more details).

The drive beam injector consists of a thermionic gun, three sub-harmonic buncher cavities, a pre-buncher, a travelling wave buncher and fully loaded accelerating structures [2–4]. A sketch of the electron source is shown in Figure 1. The DC current needed from the gun to obtain 4.2 A average current or a bunch charge of 8.4 nC after bunching is about

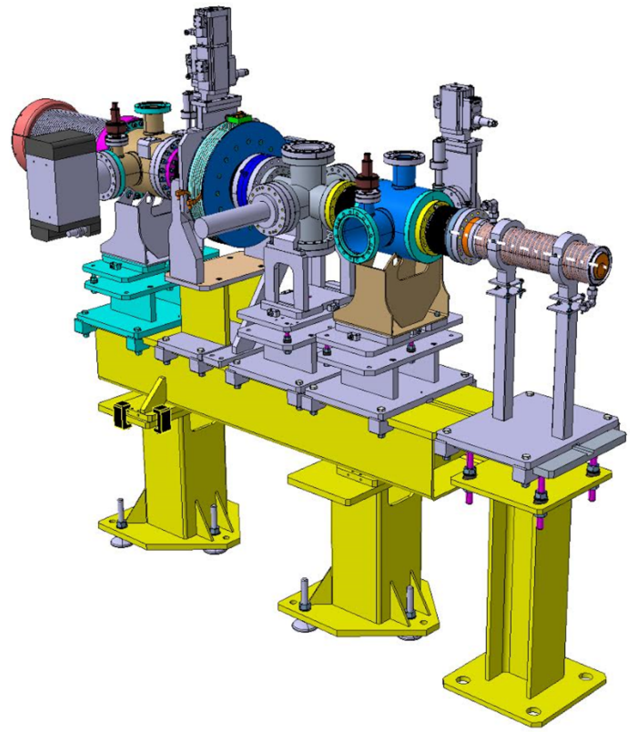

Figure 1: Mechanical layout of LEETCHI including the high voltage ceramic (left), a current transformer, an optical diagnostic and a beam dump.

5 A according to injector simulations [1]. The high average current and long pulse length is a major challenge for the cathode-grid assembly while the required current stability puts severe constraints on the high voltage power supply. Electron source parameters are given in Table 1. The high voltage will be supplied by a solid state modulator currently under development.

Table 1: Electron Source Parameters

Parameters	Values
Gun voltage	140 kV
Beam current	5 to 7 A
Pulse length	140 µs
Repetition rate	50 Hz
Emittance (rms)	< 20 mm.mrad
Shot to shot charge variation	0.1 %
Flat top charge variation	0.1% after correction
Average power	4.9 kW

* kevin.pepitone@cern.ch

LASER-DRIVEN DIELECTRIC NANO-BEAM ACCELERATOR FOR RADIATION BIOLOGY RESEARCHES*

K. Koyama[1†], KEK,Tsukuba, Japan
Z. Chen, H. Okamoto, The Univ. of Tokyo, Tokyo, Japan
M. Uesaka, The Univ. of Tokyo, Tokai, Japan
M. Yoshida, KEK,Tsukuba, Japan
[1]also at The Univ. of Tokyo, Tokai, Japan

Abstract

A dielectric laser accelerator (DLA) consists of single or a pair of binary blazed transmission grating. In case of normal incidence, a normalized grating constant L_G/λ_0 should be equal to a normalized velocity $\beta = v/c$ to synchronize with the electron and an acceleration field; $L_g/\lambda_0 = N\beta$, where N is the harmonic order of the spatial distribution of the acceleration field. We performed simulation at various conditions with the aid of CST-code as well as meep-code before designing a practical system. Bothe results of acceleration gradients calculated by the field simulation and PIC simulation had the same values as $E_x/E_0 = 0.021$ and $E_x/E_0 = 0.147$ for the grating constants of $L_g = 850$ nm and $L_g = 425$ nm, which correspond with acceleration by lower order spatial mode of $N = 2$ and $N = 1$, respectively. Besides analytical works, we fabricated gratings and developed an Yb-doped fiber laser for the acceleration experiment. Gratings of two different materials, a glass silica and crystal silica, were fabricated by the electron beam lithography technique.

INTRODUCTION

In order to estimate the health risk associated with a low radiation dose, basic radiobiological processes must be clarified by irradiating a cell with a well-defined microbeam of ionization radiation at a precisely defined location under an optical microscope. The use of microbeams of X-rays, electrons, and light and heavy ions for radiobiological applications and microfabrications has substantially increased since the early 1990s. A simple and low-cost device called a tapered capillary made of glass can delivers submicron ion beams. The majority of ion accelerators used at microbeam facilities are Van de Graaf accelerators or cyclotrons. X-ray and electron microbeams have also been developed in order to provide useful tools for quantitative analysis in radiation biology research that is complimentary to the ion microbeam. Electron microbeams are easily obtained by using electron microscopes. However, the low-energy electron beam has a troublesome scattering problem. ,

The dimensions of beam sources such as MeV-class ion accelerators, synchrotrons for hard X-ray radiation and MeV-class electron microscopes are extremely large such that only a limited number of facilities can install them. If the size of an accelerators is reduced to be an order of magnitude smaller than that of present accelerators, many radiobiological studies will be performed at small laboratories. Since the DLA has the potential to realize an on-chip accelerator, the research and development of DLAs have been conducted at various institutes.

A combination of a high-frequency electric field and a material with a high dielectric breakdown voltage are indispensable to overcome the limitation of the acceleration gradient. An intense laser pulse and the periodic structure of a dielectric such as silica is capable of increasing the acceleration gradient by an order of magnitude compared to that of a conventional radio-frequency (rf) accelerator. A phase-modulation-type laser accelerator made of a dielectric grating was proposed by Plettner [2], which is much simpler than the two-dimensional [3] and three-dimensional waveguide structures [4]. A typical shapes of a single grating DLA is shown in Fig. 1.

We are studying a structure of the laser field in a proximity of the transmission gratings with the help of numerical simulation codes, meep and CST for designing gratings for the acceleration experiments. In order to avoid the difficulty of an ultra-precision assembling of a dual grating structure, we concentrate on a single grating structure for the present.

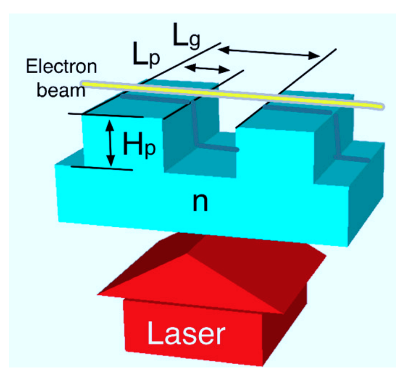

Figure 1: Schematic drawing of DLA.

REQUIRED SPECIFICATIONS

The DLA system for the radiobiology research is schematically drawn as Fig.2 The specifications of the beam for the radiobiological research are listed below [1] .

1. A beam size is as small as a resolving power of an optical microscope of submicron.

* This work was supported by JSPS KAKENHI Grant Number 15H03595
† koyamakz@post.kek.jp

ISBN 978-3-95450-169-4

FIFTH-ORDER MOMENT CORRECTION FOR BEAM POSITION AND SECOND-ORDER MOMENT MEASUREMENT

K. Yanagida*, S. Suzuki, and H. Hanaki, JASRI, Sayo, Hyogo, Japan

Abstract

For the precise measurement of beam positions and second-order moments, we adopted a recursive correction with up to fifth-order moments for a measurement using a six-electrode BPM at SPring-8 linac. The higher-order correction terms are provided by considering an effect from higher-order moments on the output voltages of BPM. We found huge calculation error in a simulated correlation plot between set and calculated vertical positions without correction. This error is also found in a similar correlation plot between the measured vertical positions with fifth-order moment correction and without it.

INTRODUCTION

For measurements of beam position and second-order relative moments [1], six-electrode BPMs with circular cross-section have been installed at SPring-8 linac [2].

To obtain the relative attenuation factors between the BPM electrodes, we developed a beam-based calibration method, i.e., entire calibration. During the entire calibration, beams must be located at a position more than 4 mm from the BPM center.

We also developed a recursive correction scheme with up to fifth-order moments to improve the accuracy of the entire calibration when a beam was located far from the BPM center [3].

Previously, correction terms were usually expressed by the higher-order polynomials of the beam positions for obtaining (calculating) precise beam positions [4]. Because the correction terms came from higher-order moments that appeared on the output voltages of BPM, we constructed a new correction scheme whose correction terms were expressed by higher-order moments.

This paper describes the theoretical features of the correction scheme, the simulation (calculation) by an image charge method, and the experiment results using electron beams at SPring-8 linac.

THEORETICAL FEATURES

Electric Field Calculation

Figure 1 shows the structure of a six-electrode BPM with a circular cross-section that is used at SPring-8 linac. Inner radius R is 16 mm, and the shared radius of each electrode is $6/\pi$.

Suppose an M-particle system where b_N and β_N are the distance from the BPM center and an argument from the x-axis for Nth-charged particles (Fig. 1).

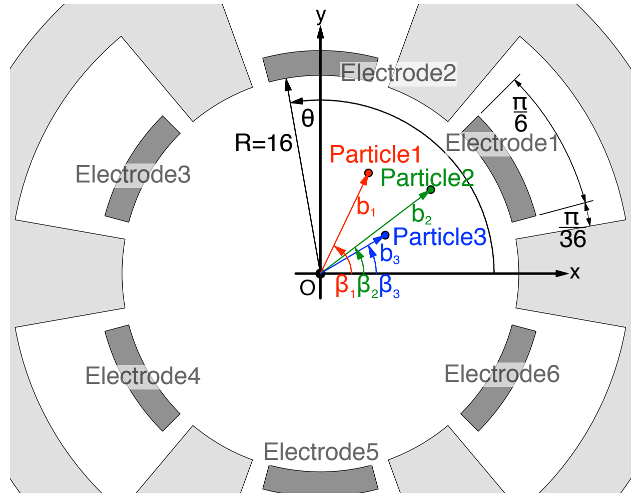

Figure 1: Structure of six-electrode BPM with a typical three-particle system.

Because the electric field on inner surface $E(\theta)$ is a superposition of the electric field generated by all the charged particles, i.e., a beam, $E(\theta)$ is written as follows in Eq. (1) [1]:

$$
\begin{aligned}
E(\theta) &\propto M + 2\sum_{n=1}^{\infty}\sum_{N=1}^{M}\frac{p_{Nn}\cos n\theta + q_{Nn}\sin n\theta}{R^n},\\
&\propto 1 + 2\sum_{n=1}^{\infty}\frac{P_n\cos n\theta + Q_n\sin n\theta}{R^n},\\
p_{Nn} &= b_N^n\cos n\beta_N,\ q_{Nn} = b_N^n\sin n\beta_N,\\
P_n &= \frac{1}{M}\sum_{N=1}^{M}p_{Nn},\ Q_n = \frac{1}{M}\sum_{N=1}^{M}q_{Nn}.
\end{aligned} \tag{1}
$$

In Eq. (1), p_{Nn} and q_{Nn} are the nth-order moments of the Nth-charged particle, and P_n and Q_n are the nth-order absolute moments [1] of the beam.

Output Voltages from Electrode

The output voltage from the dth electrode ($1 \leqq d \leqq 6$) is written as Eq. (2) using geometrical factors c_{dn}, s_{dn}:

$$
\begin{aligned}
V_d &\propto R\int_{(4d-3)\pi/12}^{(4d-1)\pi/12}E(\theta)d\theta = \frac{\pi}{12} + \sum_{n=1}^{\infty}\frac{c_{dn}P_n + s_{dn}Q_n}{R^n},\\
c_{dn} &= \int_{(4d-3)\pi/12}^{(4d-1)\pi/12}\cos n\theta d\theta,\ s_{dn} = \int_{(4d-3)\pi/12}^{(4d-1)\pi/12}\sin n\theta d\theta.
\end{aligned} \tag{2}
$$

If we treat moments up to the fifth-order, all of the geometrical factors can be summarized as f_n, h_n ($1 \leqq n \leqq 5$) in

* ken@spring8.or.jp

HOM SUPPRESSION IMPROVEMENT FOR MASS PRODUCTION OF EXFEL CAVITIES AT RI

A. Sulimov, J.-H. Thie, DESY, Hamburg, Germany
M. Pekeler, D. Trompetter, RI Research Instruments GmbH, Bergisch Gladbach, Germany

Abstract

During cold RF tests of the European XFEL (EXFEL) cavities at DESY it was observed that the damping of the second monopole mode (TM011) showed the largest variation, which was sometimes up to 2-3 times lower than the originally allowed limit. It was concluded that this TM011-damping degradation was caused by cavity geometry deviation within the specified mechanical tolerances. The particular influence of different mechanical parameters was analyzed and additional RF measurements were carried out to find the most critical geometry parameters. Stability of the equator welding and regularity of chemical treatment were investigated for different cavity cells. In spite of the high fabrication rate during EXFEL cavity mass production the TM011 suppression was improved to an acceptable level.

STATISTICS

Some of the EXFEL cavity production engineering data can now be presented as well as final measurements results (see Fig. 1) for Q-factor of the highest frequency (9th peak) in the spectra of TM011 (TM011_9).

The problem with the Higher Order Modes (HOM) suppression efficiency for EXFEL linac [1] made us analyze the whole sequence of cavity production in deeper detail.

To estimate the influence of different factors on TM011 damping efficiency (Q_{load}), we concentrated on the dimensions of the most critical components and inner cavity shape.

The efficiency of HOM extraction depends on the coupling with electromagnetic field through the HOM coupler. It is foreseen to get an asymmetrical field for the TM011 mode with a maximum in cell #1 (managed by the shape of the two end cells). Thus the short end group (EGS) dimensions and the position of its HOM coupler (Fig. 2) are important for investigations.

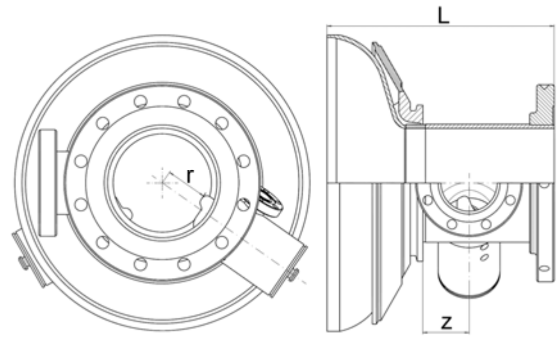

Figure 2: Position of the HOM coupler #1 in EGS: L – length; z – distance between coupler and connecting flange, r – distance between cavity axis and F-part.

The results of statistics analysis and calculations of Q-factor sensitivity (dQ/dM) to these parameters (M = L, z and r) are presented on Figure 3 and summarized in Table 1. One can see that TM011 damping is very sensitive to EGS length and to distance between coupler and connecting flange, but the fluctuation of these values causes the deviation of Q_{load} to less than 20 000. Nevertheless this factor cannot explain the complete range of Q_{load} variation during production (Fig. 1).

The second major parameter is the inner shape accuracy. It was a guess that improvement of subcomponents fabrication accuracy could decrease the average value and deviation of Q_{load}. The shape (Fig. 4) of the end groups for a long side (EGL) and short side [2], as well as the shape of both half-cells of all dumb-bells (DB) were controlled during the serial production (Fig. 5).

The analysis of the 3D shape was done quantitatively. Only the number of points were counted, whose deviation from the ideal shape was between 0.2 mm and 0.3 mm. Their positions were not in consideration, as this would require analyzing all points individually (200 points per half-cell, roughly 1.5e6 points).

No correlation between shape accuracy and HOM suppression efficiency was found.

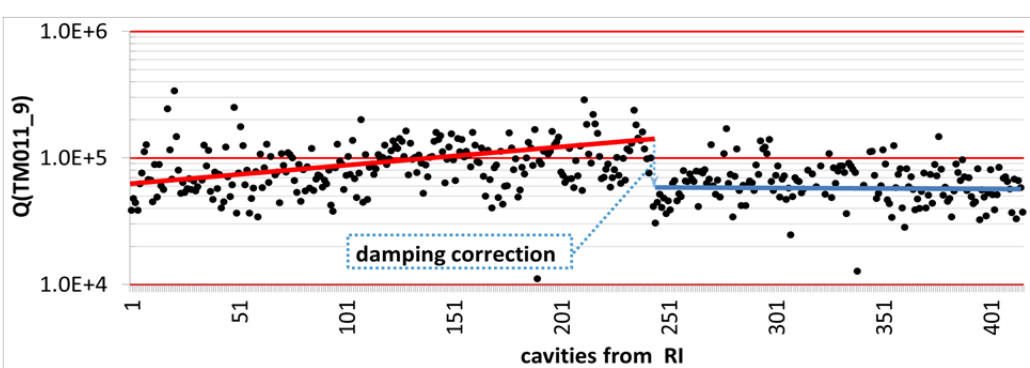

Figure 1: Measurement results of the Q_{load} for the TM011 (zero-mode) at 2K.

ISBN 978-3-95450-169-4

A LASER PULSE CONTROLLER FOR THE INJECTOR LASER AT FLASH AND EUROPEAN XFEL

C. Gruen*, S. Schreiber, T. Schulz, DESY, Hamburg, Germany

Abstract

FLASH is a multi-beamline free-electron laser user facility which provides femtosecond long high brilliant photon pulses in the extreme-UV and soft-X ray wavelength range. One pulsed superconducting linac accelerates electron bunches for two undulator beamlines, while a third beamline is under construction. Within each RF-pulse, trains of hundreds of electron bunches are produced in a photocathode RF gun, accelerated in the linac and distributed by fast kickers into the undulator beamlines. In order to fulfill the parameter ranges of the multiple user experiments each bunch train can be tuned individually in bunch number from 0 - 800, spacing from 1 µs - 25 µs and intensity from 0.1 nC - 1 nC. To make this possible, three injector laser systems are used and this allows FLASH to vary independently the laser settings for the designated undulator beamlines. A laser controller has been developed to make a multi-users operation mode possible. The controller uses a Field Programmable Gate Array (FPGA) to control the time structure of the laser pulses and it provides the interface for the timing and the machine protection system. The controller has been implemented using the MicroTCA.4 technology. The controller was ported to the injector laser system at the European XFEL facility and is in operation since end 2015.

INTRODUCTION

The Free-Electron Laser in Hamburg FLASH [1, 2] at DESY delivers high brilliance XUV and soft X-ray photon pulses to two simultaneous operating photon experiments. The photoinjector, consisting of a normal conducting RF photo cathode gun (RF-gun) and a system of three UV injector lasers, is capable of producing 800 µs long bursts of electron bunches at a repetition rate of 10 Hz. The bursts, called macropulses, are accelerated by a superconducting linac which is equipped with seven 1.3 GHz TESLA-type accelerator modules. The maximum beam energy is 1250 MeV. The complete burst consists of two subtrains of electron bunches. One sub-train is injected into the FLASH1 undulator beamline and the other one is deflected by a system of a flat top kicker and a DC septum magnet into the FLASH2 undulator beamline. This allows FLASH to serve simultaneously various FEL user experiments with bursts of hundreds of photon pulses with the same repetition rate of 10 Hz. In the near future there will be an upgrade of a third beamline which will be operated in a similar way.

For a multi-user FEL operation like at FLASH it is a basic requirement to ensure that it is possible to change the beam parameters individually for the various undulator beamlines. Therefore each of the sub-bunch trains is produced by a different injector laser and each laser has got a different set of parameters. The pattern and the charge can be changed individually for each laser. In addition it is also possible to adjust other beam parameters like energy or bunch compression for each beamline to ensure the highest flexibility of beam parameters for the various user experiments. The repetition rate of the bunches within the sub-bunch trains can be varied between 40 kHz and 1 MHz. A gap of 50 µs between the sub-bunch trains is needed to adapt the RF settings (amplitude and phase of the accelerating field) and for the transition time of the kicker system. A schematic diagram of the bunch patterns for the two FLASH beamlines is shown in Fig. 1.

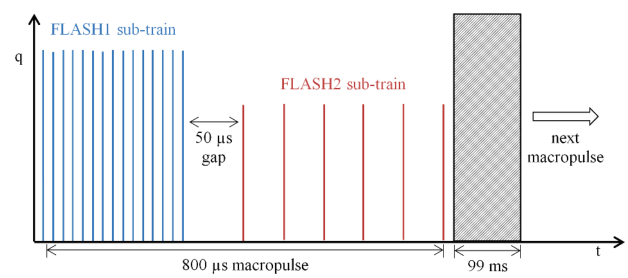

Figure 1: Example of bunch patterns for two FLASH beamlines FLASH1 and FLASH2 with different settings of the injector lasers.

The European XFEL facility [3] is being constructed at DESY and the operating mode will be similar to FLASH. A 17.5 GeV superconducting linac will drive three undulator beamlines that can be operated simultaneously. The XFEL injector is equipped with a UV injector laser, a 1.3 GHz RF-gun, a TESLA-type 1.3 GHz accelerator module, a third harmonic RF system, a laser heater, and diagnostic section. The injector is capable of producing 600 µs long bunch trains with 10 Hz and each burst consists of 2700 bunches. The commissioning of the Injector started in 2015 and the first long bunch train operation has been demonstrated in 2016 [4].

LASER PULSE CONTROLLER

System Overview and Connected Systems

To fulfill the requirements of a multi-beamline operation each injector laser is controlled by a laser pulse controller based on the MicroTCA.4 technology [5]. The timing system [6] distributes the desired bunch pattern information to the laser controller. Each bunch is defined by a 32 bit long data vector called bunch pattern word which specifies the intended undulator beamline and the injector laser responsible for each bunch. The bunch pattern table is an array consisting of 7222 bunch pattern words. Each element of this table

* christian.gruen@desy.de

STATUS AND PROGRESS OF FRIB HIGH LEVEL CONTROLS*

G. Shen†, E. Berryman, D. Chabot, M. Davidsaver, K. Fukushima, Z. He, M. Ikegami, M. Konrad, D. Liu, D. Maxwell, V. Vuppala
FRIB, Michigan State University, East Lansing, USA

Abstract

The Facility for Rare Isotope Beams (FRIB) is a new heavy ion accelerator facility to provide intense beams of rare isotopes currently under construction at Michigan State University. Its driver linac accelerates all stable ions up to uranium, and targets to provide a CW beam with the energy of 200 MeV/u and the beam power of 400 kW. We are actively preparing for the beam commissioning of FRIB fron end. The high level control for incoming commissioning is under active development and deployment. The latest status progress will be presented in this paper.

INTRODUCTION

FRIB [1] is a new project under cooperative agreement between US Department of Energy and Michigan State University (MSU). It is under construction on the campus of MSU and will be a new national user facility for nuclear science. Its driver accelerator is designed to accelerate all stable ions to energies > 200 MeV/u with beam power on the target up to 400 kW [2].

The layout of FRIB is as shown in Fig. 1, which consists of two ECR (Electron Cyclotron Resonance) ion sources, a low energy beam transport with a pre-buncher and a chopper, a RFQ (Radio Frequency Quadrupole) linac, LS1 (Linac segment 1) to accelerate the beam up to > 15 MeV/u, LS2 and LS3 to accelerates the beam > 200 MeV/u, two folding segments to confine the footprint and facilitate beam collimation, and a beam delivery system to transport to the target. The beam is stripped to higher charge states after LS1 section.

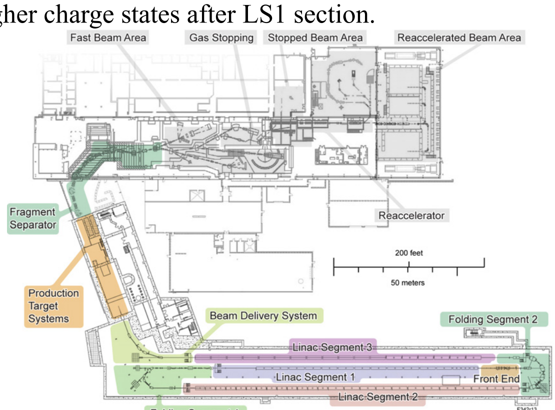

Figure 1: Layout of the FRIB driver accelerator, target and fragment separator.

* This material is based upon work supported by the U.S. Department of Energy Office of Science under Cooperative Agreement DESC0000661, the State of Michigan and Michigan State University.
† shen@frib.msu.edu

ARCHITECTURE

A service-oriented architecture (SOA) has been chosen for FRIB high level controls as shown in Fig 2.

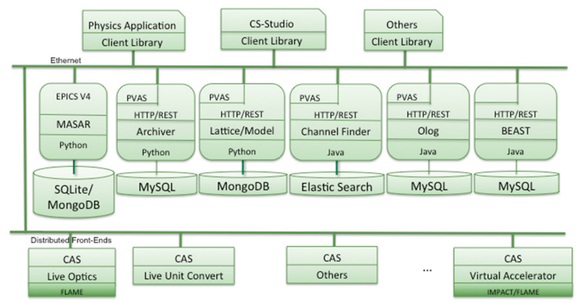

Figure 2: FRIB High Level Controls Architecture.

As shown in Fig. 2, the FRIB high level controls consists of

- Upper level, which includes physics application, software framework for user interface like CS-Studio, and so on;
- Middle layer service, which includes Archive Appliance for data archiving, Olog for operation logbook, MASAR for machine snapshot, BEAST for alarm handler, and so on;
- Low level software EPICS IOC to support the machine operation and commissioning.

More specifically, the development activities covers

- Database based web applications [3], which includes eTraveler, Cable database, Central Configuration Database (CCDB), and so on;
- Control room applications, which includes CS-Studio (Control System Studio), and middle layer services, client CS-Studio applications;
- Physics application, which includes online model, applications for commissioning and operation [4][5], and Python infrastructure.

DATABASE APPLICATIONS

There are three major database-based web applications to support FRIB construction and commissioning, which are eTraveler, Cable, and CCDB respectively.

eTraveler

A traveler is a document or a document collection to capture the history of certification or processes associated with a device.

At FRIB, an eTraveler (Electronic Traveler), as illustrated in Fig. 3, has been implemented as a database web application to create, manage the document online to track predefined processes associated with physical entities for FRIB and capture data accompanying to each step

ISBN 978-3-95450-169-4

IDENTIFICATION OF EMITTING SOURCES OF DARK CURRENTS FROM GRIDDED THERMIONIC ELECTRON GUN AND MEASURES TO SUPPRESS DARK CURRENTS FROM ELECTRON GUN IN SPRING-8 LINEAR ACCELERATOR

Tamotsu Magome*, Tsutomu Taniuchi, Toshiaki Kobayashi, Shinsuke Suzuki, Hirofumi Hanaki, Japan Synchrotron Radiation Research Institute, Sayo, Japan

Abstract

Dark current emitted from the gridded thermionic electron gun of the SPring-8 linear accelerator has been investigated by means of our offline electron-gun test equipment applying DC acceleration voltage to its electron gun. The investigations revealed that the dark current was generated from the wehnelt electrode, the grid electrode, and the cathode surface. Based on this identification of the emitting sources, the electron gun of the test equipment was improved. The anode and wehnelt electrodes were replaced with new electro-polished ones. A cathode assembly was replaced with a newly-developed cathode assembly with a grid electrode smoothed by electro-polishing. The improved electron gun of the test equipment emitted dark current below 4×10^{-12}A during an initial heating time of ten days under the same operating condition as the real accelerator. This dark current was smaller by three orders of magnitude than that of the existing electron gun.

INTRODUCTION

The SPring-8 linear accelerator injected electrons into the SPring-8 electron storage ring via a booster synchrotron. Electrons were emitted from a gridded thermionic electron gun of the linear accelerator. Although bias voltage for the cathode with respect to the grid electrode was large enough to suppress the cathode emission current, dark current was emitted and injected to the downstream electron storage ring. This dark current caused satellite bunches unignorable for precise experiments in the downstream electron storage ring.

To remove this dark current on beam transport, RF kickers and a deflector were installed in the booster synchrotron and in the linear accelerator, respectively. For higher reliability to suppress this dark current, dark current from the electron gun was reduced. Emitting sources of dark current from the electron gun were investigated using our offline electron-gun test equipment applying DC acceleration voltage to the electron gun. Based on results of this investigation, the electron gun of the test equipment was improved.

ELECTRON-GUN TEST EQUIPMENT

The offline electron-gun test equipment was the ultra-high-vacuum chamber with an electron gun and a faraday cup. The electron gun was the same as that of the real accelerator using a cathode assembly (CPI, Y-845) except for the anode electrode. Although acceleration voltage was pulsed (180kV in pulse height, 1ns in pulse width (HMFW)) in the real accelerator, acceleration voltage was DC 85kV in the test equipment. The anode electrode of the test equipment, therefore, was different in shape from that of the real accelerator in order to apply the same electric field on the cathode surface as that in the real accelerator.

The faraday cup was installed on the beam axis at 2.27 cm downstream to the ejection port of the electron gun. An opening of the faraday cup was 4 cm in diameter. This installation position and the opening diameter was designed to capture all of the diverging electrons emitted from the cathode surface even at an emission current of 20A. The faraday cup was 6 cm in depth. The faraday cup was made from fine carbon. The depth and the material of the faraday cup was determined to reduce electron loss from the faraday cup due to electron back scattering lower than one percent. The faraday cup had a suppressor electrode in shape of a ring around the opening of the faraday cup to prevent secondary electrons to escape from the faraday cup. The potential of the faraday cup body and of the suppressor electrode was set to be 0V and -700V, respectively.

Current flowing into the suppressor electrode and the faraday cup body were measured with two ultra-high resistance meters (ADC, 5450), respectively. A bias voltage of -700V was applied to the suppressor electrode with the resistance meter. Measured current values by the resistance meters were stored in a personal computer every three seconds.

The test equipment operated at an acceleration voltage of 85kV, at a cathode heater voltage of 6.0V, at a bias voltage for the cathode of 61.0V, and under pressures lower than 1×10^{-6}Pa, made it possible to measure dark current (expressed in magnitude) as faraday cup current under the same operating condition as the real accelerator.

EMITTING SOURCES OF DARK CURRENT

Wehnelt Electrode

Faraday cup current and suppressor electrode current from the existing electron gun using a new Y-845 cathode assembly was measured to be -4.3×10^{-9}A and -2.5×10^{-10}A, respectively under the same operating condition as the real accelerator. Since the faraday cup was designed to capture all of the electrons emitted from the cathode, this suppressor electrode current was presumed to result from flow of electrons generated at the wehnelt.

* magomago@spring8.or.jp

ISBN 978-3-95450-169-4

THE ARIEL RADIOACTIVE ION BEAM TRANSPORT SYSTEM*†

M. Marchetto‡, T. Alderson, F. Ames, R. Baartman, J. Chak, P. Dirksen, T. Emmens, G. Hodgson, T. Hruskovec, M. Ilagan, R. Laxdal, N. Muller, D. Preddy, D. Rowbotham, S. Saminathan, Q. Temmel, V. Verzilov, D. Yosifov , TRIUMF, Vancouver, CANADA

Abstract

The Advanced Rare IsotopE Laboratory (ARIEL) is going to triple the radioactive ion beam (RIB) production at TRIUMF. The facility will enable multi-user capability in the Isotope Separation and ACceleration (ISAC) facility by delivering three RIBs simultaneously. Two new independent target stations will generate RIBs using a proton driver beam up to 50 kW from the 500 MeV cyclotron and an electron driver beam for photo-fission from the new superconducting e-linac in addition to the existing ISAC RIB production. The multi-user capability is enabled by a complex radioactive ion beam transport switchyard consisting entirely of electrostatic optics. This system includes two separation stages at medium and high resolution with the latter achieved by a mass separator designed for an operational resolving power of 20000 for a 3 μm transmitted emittance. Part of the system also includes an Electron Beam Ion Source (EBIS) charge breeder fed by a radio frequency cooler that allows the post-acceleration of heavy masses. Beam selection downstream of the EBIS is achieved by means of a Nier type separator. The facility is in a detailed design stage and some tests, procurements and partial installation are foreseen by the end of 2016.

INTRODUCTION

The ARIEL project [1] at TRIUMF is an extension of the current ISAC facility [2] with two additional independent target stations meant to produce RIB using the isotope separation on line (ISOL) method [3].

One target station is going to receive 500 MeV proton beam up to 100 μA from a fourth extraction line of the TRIUMF cyclotron [4] while the second is going to produce RIB via photofission [5] using the new electron linac [6] designed to deliver 50 MeV electrons up to 10 mA for a maximum beam power on target of 0.5 MW.

The two combined facilities, illustrated in Fig. 1, are going to produce three simultaneous radioactive ion beams to be delivered to the existing fifteen ISAC experimental stations.

The single-charge beam produced and extracted from the ARIEL targets is going to be delivered through the RIB transport system. This is a complex of electrostatic beam lines where the beam can be selected with various degree of separation. A charge breeding option for post acceleration of heavy elements is part of the system . An analyzing station is also present at ground level to measure yield production.

* Funded under a contribution agreement with NRC (National Research Council Canada)

† Capital funding from CFI (Canada Foundation for Innovation)

‡ marco@triumf.ca

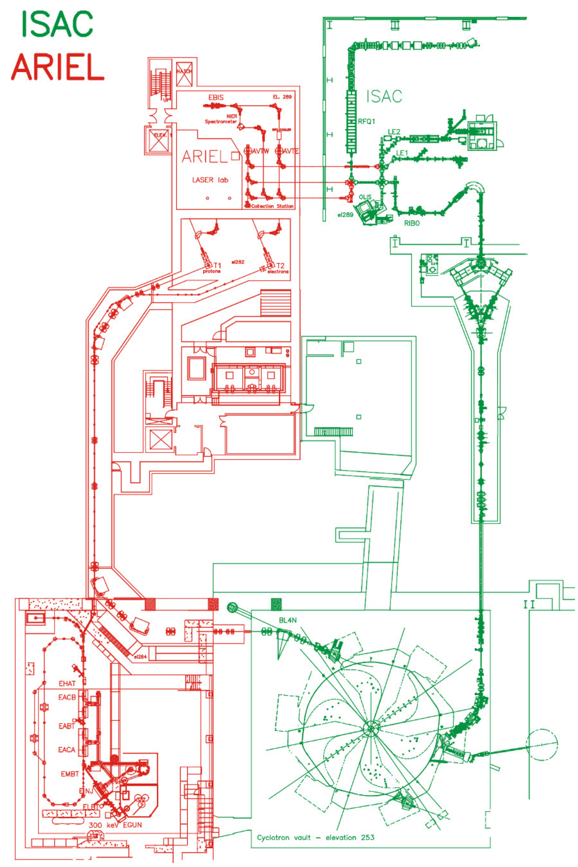

Figure 1: ARIEL (red) and ISAC (green) facilities at TRIUMF.

RIB TRANSPORT SYSTEM

The RIB transport system extends over three levels on the far north side of the new ARIEL building. The beam line design is based on the proven and well understood ISAC electrostatic optics [8] that consists of few optical sections with matched input and output parameters. These sections are based on a 1 m long period with 90° phase advance. The basic ones are: straight periodic, straight crossing, 90° achromatic bending and order reversing necessary to match two consecutive bending sections in the same plane. Some sections have unique lengths in order for the ARIEL beam lines to properly align to the existing ISAC installation.

The beam lines start in the the target hall just downstream of the target stations as represented in Fig. 2. Each target station has a dedicated pre-separator system for isobaric separation of the produced RIB species The mass resolving power of the pre-separator magnetic stage is 300. The dipole magnet is coupled with a 90° toroidal electrostatic bender to compensate dispersion due to energy spread. This selection

ISBN 978-3-95450-169-4

SPIRAL2 PROJECT: INTEGRATION OF THE ACCELERATOR PROCESSES, CONSTRUCTION OF THE BUILDINGS AND PROCESS CONNECTIONS

P. Anger, P. Bisson, O. Danna, X. Hulin, JM. Lagniel, S. Montaigne, F. Perocheau, E. Petit, L. Roupsard, GANIL Laboratory, Caen, France

Abstract

The GANIL SPIRAL 2 Project is based on the construction of a superconducting ion CW LINAC (up to 5 mA - 40 MeV deuteron and 33 MeV proton beams, up to 1 mA - 14.5 MeV/u heavy ion beams) with two experimental areas named S3 (“Super Separator Spectrometer” for very heavy and super heavy element production) and NFS (“Neutron For Science”),

The building studies as well as the accelerator and experimental equipment integration started in 2009. The ground breaking started at the end of 2010. The integration task of the different equipments into the buildings is managed by a trade-oriented integration unit gathering the accelerator integration team, the building prime contractor and a dedicated contracting assistant. All work packages are synthesized at the same time using 3D models. 3D tools are used to carry out integration, synthesis, process connections and the preparation of the future assembly.

Since 2014, the buildings and process connections are received and the accelerator installation is well advanced.

This contribution will describe these 3D tools, the building construction, the process connection status and our experience feedback.

INTRODUCTION

Officially approved in May 2005, the GANIL SPIRAL2 radioactive ion beam facility (Figure 1) was launched in July 2005, with the participation of many French laboratories (CEA, CNRS) and international partners. In 2008, the decision was taken to build the SPIRAL2 complex in two phases: A first one including the accelerator, the Neutron-based research area (NFS) and the Super Separator Spectrometer (S3), and a second one including the RIB production process and building, and the low energy RIB experimental hall called DESIR [1-3].

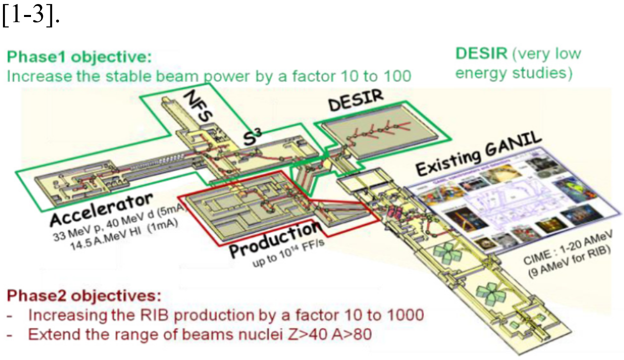

Figure 1: SPIRAL2 project layout, with experimental areas and connexion to the existing GANIL.

In October 2013, due to budget restrictions, the RIB production part was postponed, and DESIR was planned as a continuation of the first phase.

The first phase SPIRAL2 facility is now built, the accelerator installation and connecting tasks are almost done, with the aim of obtaining the first beam for physics (NFS) in 2017 [2][4].

DEFINITION OF THE NEEDS AND PRELIMINARY DESIGN

After the implementation of the Product Breakdown Structure (PBS), a global detailed specification was carried out to define the needs for each room of the building in terms of surface, mechanical stress for the floor, general servitudes to accommodate the accelerator and the experimental processes as well as for all the technical rooms receiving cryogenic, command control, RF power, vacuum systems.... The infrastructure needs (electricity, water cooling, nuclear ventilation, air conditioning, handling systems…) were also defined at that time.

These detailed specifications were used by the building prime contractor to make the building drafts and, in a second time, the preliminary design then the detailed design, with a cost estimate and control at each step.

The SPIRAL2 team took the decision to design the entire project with 3D tools due to the high degree of complexity of the processes and the very high level of the integration including connecting pipes and cables trays. We also wanted to be able to guarantee our ability to install, set up and maintain the equipments. For this 3D work the challenge comes from the fact that the same level of study is required for the building and conventional facilities, processes (ion sources, beam lines, RFQ, SC Linac and associated equipments) and for the process connections. A contracting assistant fully dedicated to these missions of 3D synthesis and 3D integration joined the SPIRAL 2 team in 2009.

The first difficulty was to define whole large reservations (floor or wall opening >1 m^2) for the infrastructure and process distributions in the concrete during the preliminary design phase. This request was due to obtain the authorization to build the facility taking into account the earthquake holding and the depth of the wall for the biological constraints.

The distribution principle was confirmed taking into account the position of electrical cabinets, the cable trays, fluid and RF distributions. The integration of all equipments (processes and infrastructure) was finally

MODERNISATION OF THE 108 MHz RF SYSTEMS AT THE GSI UNILAC

B. Schlitt, G. Eichler, S. Hermann, M. Hoerr, M. Mueh, S. Petit, A. Schnase, G. Schreiber, W. Vinzenz, and J. Zappai, GSI, Darmstadt, Germany

Abstract

A substantial modernisation of the RF systems at the 108 MHz Alvarez type post-stripper section of the GSI heavy ion linac UNILAC was launched in 2014 to prepare the existing facility for future FAIR operation. A new 1.8 MW RF cavity amplifier prototype for low duty-cycle operation (2 ms RF pulse length at 10 Hz repetition rate) based on the widely-used tetrode TH 558 SC was built by THALES. The procurement of a 150 kW solid state driver amplifier is in preparation. An RF test bench for the amplifier prototypes is built at GSI including new control racks, commercial grid power supplies, and a modern PLC system for amplifier control. The existing powerful 1 MVA anode power supplies will be re-used and are also equipped with new PLC systems. The development of a digital low-level RF system based on the MTCA.4 standard and commercial vector modulator and FPGA boards was started. Status and details of the modernisation as well as first commissioning results of the new high power amplifier prototype are reported.

INTRODUCTION

The 40 years old UNIversal Linear ACcelerator UNILAC at GSI and the synchrotron SIS18 will provide high current high brilliance heavy ion beams for the new Facility for Antiproton and Ion Research FAIR. To assure reliable operation as well as the required beam quality, a replacement of the existing Alvarez type post-stripper linac is planned [1] and a substantial modernisation of the corresponding 108 MHz RF systems was launched in 2014 [2, 3].

MODERNISATION OF THE EXISTING POST-STRIPPER RF SYSTEMS

In a first step, the existing Alvarez RF systems are modernised and modularised in a way that the old 1.6 MW high power amplifiers (HPA) and the 160 kW drivers can be replaced by new amplifiers later [2]. Separate control racks are being installed comprising modern PLC systems, new fast interlock and monitoring units, and commercial grid power supplies. These control racks will be used with the existing amplifiers first and with new ones later. For the time being, the HPA stage of the Alvarez tank 3 (A3) was modernised in that way as a prototype. A PLC test system based on Siemens S7-1500 was built and programmed including a human machine interface [4]. The system handles monitoring and interlocks of all cooling circuits and power supplies including turn-on and turn-off sequences of the supply voltages, system access interlocks, control of the motorized tuning circuits of the HPA, basic switch-on and switch-off commands of the driver amplifier and LLRF, etc. The CPU, HMI, and the major part of the PLC system will be installed in the control rack, whereas a subunit will be located in a separate crate in the HPA comprising the I/O modules for all signals provided there. The subunit and the complete PLC system are designed for use with both amplifiers – the existing HPA as well as the new 1.8 MW Thales amplifier. Integration and full tests of the new PLC system in the rebuilt A3 HPA is planned until the end of this year.

The powerful 1 MVA, 24 kV anode power supplies will be re-used in future. The old relay based local control of the A3 supply was substituted by a second Siemens S7-1500 PLC system [3]. First tests of the complete A3 system comprising the upgraded anode power supply and the rebuilt HPA stage (using a manual test control unit instead of the HPA PLC) were successfully performed. The same modernisation is planned for the remaining four Alvarez RF systems within 2016 – 2017.

For long-term substitution of the old driver amplifiers, the procurement of a 150 kW solid state RF amplifier prototype is in preparation.

NEW 1.8 MW AMPLIFIER PROTOTYPE

A new 1.8 MW cavity amplifier prototype for short pulse operation (2 ms pulse length at 10 Hz repetition rate) based on the widely-used tetrode TH 558 SC was developed and built by Thales [5] (Fig. 1) and was delivered to GSI recently.

Figure 1: New 1.8 MW cavity amplifier prototype after factory acceptance tests at THALES.

RADIO FREQUENCY SURFACE PLASMA SOURCE WITH SOLENOIDAL MAGNETIC FIELD *

V. Dudnikov#, R. Johnson, Muons, Inc., Batavia, IL 60510, USA; B. Han, S. Murrey, T. Pinnisi , C. Piller, M. Santana, C. Stinson, M. Stockli, R. Welton, ORNL, Oak Ridge, TN 37831, USA, G. Dudnikova, UMD CP, MD-32611, USA; ICT SBRAS, Novosibirsk, Russia

Abstract

Operation of Radio Frequency Surface Plasma Sources (RF SPS) with a solenoidal magnetic field are described. RF SPS with solenoidal and saddle antennas are discussed. Dependences of beam current and extraction current on RF power, gas flow, solenoidal magnetic field and filter magnetic field are presented.

INTRODUCTION

Efficiency of plasma generation in Radio Frequency (RF) ion source can be increased by application of a solenoidal magnetic field [1-9]. A specific efficiency of positive ion generation was improved by the solenoidal magnetic field from 5 mA/cm^2 kW to 200 mA/cm^2 kW [8, 9]. Chen [10] present explanation for concentration of a plasma density near the axis by magnetic field through a short circuit in a plasma plate. Additional concentration factor can be a secondary ion-electron emission initiated by high positive potential of plasma relative the plasma plate. The secondary emission can be increased by cesiation-injection of cesium for increase of the secondary negative ion emission [11-14], increasing a secondary electron and photo emission.

RF ION SOURCE IN SNS TEST STAND

RF ion source was installed in Spallation Neutron Source (SNS) test stand. A design of ion source and Low Energy Transportation channel (LEBT) is shown in Fig. 1. The RF ion source consist of AlN ceramic chamber with a cooling jacket from keep. At a left side is attached an RF assisted Triggering Plasma Gun (TPG). At a right side is attached a plasma electrode with an extraction system. The discharge chamber is surrounded by a saddle (or solenoidal) antenna. The LEBT at right side consist of accelerator electrode and two electrostatic lenses focusing a beam into a hole of 7.5 mm diameter in a chopper target. The second lens consists of four electrically insulated quadrants, which allow for chopping the beam to form an extraction gap inside the accumulator ring. In addition, the voltages on the quadrants can be varied individually to steer the beam for improving the transmission through the RFQ [15]. In more detail extraction system is presented in Fig. 2. The plasma plate (1) have a collar (2) with a conical converter surface. Cs oven (3) for decomposition of Cs_2CrO_4 cartridges is attached to the collar. The extractor electrode (5) is attached to the plasma plate through ceramic insulator (4). Permanent magnet bars (6) is inserted into the water cooled plasma electrode (5). A ferromagnetic insert (8) can be used for shaping the magnetic field. Accelerating electrode (7) is used for accelerating of extracted ions up to 65 keV.

A plasma is generated by a current in antenna. Solenoidal magnetic field is concentrate the plasma on the axis. A transverse magnetic field generated by permanent magnet (6) located inside the water cooled extractor (5), bend the plasma flux, preventing electrons to escape the plasma. A configuration of the transverse magnetic field is shown in Fig. 1 (below). The plasma outside a 6 mm diameter impacts on the conical surface of a Mo converter, where H- ions are formed. The H- production is enhanced by lowering the Mo work function by adding a partial monolayer of Cs. Negative ions that drift into the source outlet are extracted by its potential of the extractor-electron dump. The extractor, which has a 6 mm aperture, is have a potential up to 8 kV. The 1 kG dipole field integrated into the extractor drives the co-extracted electrons sideways. Most of them are intercepted by the electron dump, which is kept near -57 kV with a +8 kV supply located on the -65 kV platform. The -65 keV H- beam emerges from the extractor and is focused by two electrostatic lenses into the hole of diameter 7.5 mm in a chopper target.

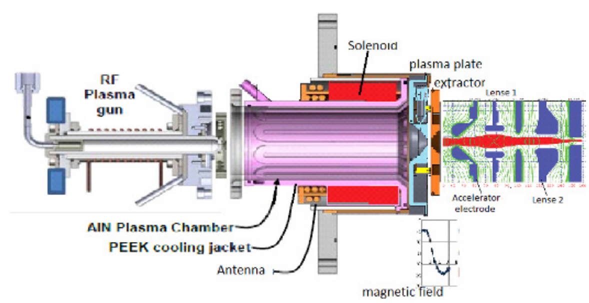

Figure 1: Design of RF Ion Source and LEBT.

EXPERIMENTAL RESULTS

Typically, 200 W from a 600 W, 13 MHz amplifier generates a TPG continuous low-power plasma. Cathode TPG is biased at 310 V with a current ~10 mA. The high current beam pulses 1 ms, up to 60 Hz are generated by up to 50 kW from a pulsed 80 kW, 2 Mz amplifier, connected to the antenna through insulating transformer and matching network. A discharge is triggered at pulsed power Prf= 3.8 kW, antenna current Iant=120 A, antenna voltage Uant=6.5 kV (at 13.56 MHz discharge start from Prf=0.5 kW, Iant=14 A, Uant=1.2kV).

* Work supported in part by US DOE Contract DE-AC05-00OR22725 and by STTR grant, DE-SC0011323.
# email address: Vadim@muonsinc.com

PROGRESS TOWARDS A 2.0 K HALF-WAVE RESONATOR CRYOMODULE FOR FERMILAB'S PIP-II PROJECT*

Z.A. Conway†, A. Barcikowski, G.L. Cherry, R.L. Fischer, B.M. Guilfoyle, C.S. Hopper, M.J. Kedzie, M.P. Kelly, S-h. Kim, S.W.T. MacDonald, P.N. Ostroumov and T.C. Reid, Argonne National Laboratory, Argonne, IL 60439, U.S.A.
V.A. Lebedev, A. Lunin, Fermi National Accelerator Laboratory, Batavia, IL 60510, U.S.A.

Abstract

In support of Fermilab's Proton Improvement Plan-II project Argonne National Laboratory is constructing a superconducting half-wave resonator cryomodule. This cryomodule is designed to operate at 2.0 K, a first for low-velocity ion accelerators, and will accelerate ≥1 mA proton/H^- beams from 2.1 to 10.3 MeV. Since 2014 the construction of 9 162.5 MHz $\beta = 0.112$ superconducting half-wave resonators, the vacuum vessel and the majority of the cryomodule subsystems have been finished. Here we will update on the status of this work and report on preliminary cavity test results. This will include cavity performance measurements where we found residual resistances of < 3 nΩ at low fields and peak voltage gains of 5.9 MV, which corresponds to peak surface fields of 134 MV/m and 144 mT electric and magnetic respectively.

INTRODUCTION

Fermi National Accelerator Laboratory (FNAL) is upgrading its existing accelerator complex to achieve beam power on the Long-Baseline Neutrino Facility (LBNF) target of > 1 MW [1, 2]. FNAL's current injector consisting of the Linac and the Booster accelerators is limited to ~4.4×10^{12} protons per Booster pulse by beam loss. It is the major bottleneck in the string of accelerators limiting the LBNF power. To address this increase of the 300 MeV Booster injection energy is required [2].

The next-generation facility chosen by FNAL to supply the LBFN target calls for an increase in the Booster injection energy with the replacement of the existing 400 MeV Linac by a new 800 MeV superconducting (SC) linac [3, 4]. The first SC cryomodule in the new 800 MeV linac contains 8 half-wave resonators (HWRs) and 8 SC solenoids for the acceleration of an H^- beam from 2.1 to 10.3 MeV. This cryomodule, supplied by Argonne National Laboratory (ANL), will be commissioned as part of the injector accelerator demonstration experiment referred to as the Proton Improvement Plan-II Injector Test (PIP2IT) [5]. The aim of the work presented here is to document the progress toward operating the HWRs in PIP2IT by presenting the cryomodule assembly progress and results for the HWR 2.0 K testing.

* This material is based upon work supported by the U.S. Department of Energy, Office of Science, Office of Nuclear Physics and High-Energy Physics, under Contract No. DE-AC02-76-CH03000 and DE-AC02-06CH11357. This research used resources of ANL's ATLAS facility which is a DOE Office of Science User Facility.
† zconway@anl.gov

CRYOMODULE

The HWR cryomodule design is an evolution of the top-loaded box cryomodule design used successfully at ANL for two separate successful upgrades of the Argonne Tandem Linear Accelerator System [6, 7, 8]. Argonne box cryomodules rely upon the implementation of several techniques to achieve their high-performance levels, such as: electro-polishing in the ANL low-beta EP tool [9], high-pressure high-purity water rinsing with clean-room handling [10] and separate cavity/insulating vacuum systems enabling a cryomodule design which allows the clean assembly to be hermetically sealed prior to installing the "dirty" subsystems of the cryomodule [11]. Compared to other ANL cryomodules the technology has been extended to 2.0 K operation with the addition of a 2/5 K heat exchanger and a J-T expansion valve. The total 2.0 K thermal load is expected to be 50 W, of which 25 W are from the 48 conduction-cooled magnet leads feeding the 8 SC solenoids and the x-y steering coils integrated into each solenoid.

The remainder of this section highlights selected aspects of the design and fabrication status for the HWR cryomodule: (1) the mechanical design of the cavities and cryomodule developed to comply with the DOE Vacuum Vessel Consensus guidelines [12], FNAL Safety [13] and the American Society of Mechanical Engineers (ASME) Boiler and Pressure Vessel Code (BPVC) Section VIII [14] and (2) a brief update of the future fabrication plans leading to the operation of this cryomodule at 2.0 K.

Cryomodule Design

The half-wave cavity cryomodule vacuum vessel design balances the need to house a 6 meter long accelerator string with all of its support systems inside the limited space available for assembly while maintaining compliance with FNAL's safety standards. Figure 1 shows a cross section view of the assembly. Figure 2 shows a picture of the cryomodule vacuum vessel prior to a test of the 70 K coolant systems.

The vacuum vessel has two cryogenic input streams: (1) 5 K 3 bar and (2) 70 K 20 bar gaseous helium. The 70 K helium stream cools the radiation shielding and is used for thermally intercepting penetrations running from room temperature. The 5 K helium coolant stream is split for two separate purposes. One 5 K branch is used for thermal intercepting while the second branch is used for the production of 2.0 K helium. Cooling to 2.0 K is achieved by heat exchanging the input 5 K helium

SIMULATION OF MECHANICAL OSCILLATIONS IN PIP-II CRYOMODULE USING ACE3P*

Liling Xiao, Oleksiy Kononenko, Cho-Kuen Ng
SLAC National Accelerator Laboratory, Menlo Park, CA 94025, USA

Abstract

The linac in PIP-II project at Fermilab consists of different sections of superconducting RF (SRF) cavities that can accelerate the proton beams to 800 MeV. At the end of the linac is a section containing four high β (β = 0.92) cavity cryomodules (CM) operating at 650 MHz, with each one having six SRF cavities. The mechanical modes in a single high beta 650 MHz dressed cavity have been calculated previously. In this paper, the parallel code suite ACE3P is used to simulate the mechanical modes in a string of the high beta 650 MHz multi cavities. The effects of multi cavities on the mechanical mode frequencies and any possible coupling between cavities will be investigated.

INTRODUCTION

Proton Improvement Plan-II (PIP-II) will provide powerful, high-intensity proton beams to the neutrino program at Fermilab. The central construction of PIP-II is an 800 MeV superconducting linac (SCL) injecting into the existing Booster [1]. SCL consists of five types of SRF cavities required for the beam acceleration from low velocity to speed of light [2]. The main parameters of SCL cavities are listed in Table 1.

Table 1: Main Parameters of SCL Cavities

Cavity	β	F (MHz)	E (MV)	CM	Cavity/CM
HWR	0.11	162.5	2.1-11	1	8
SSR1	0.22	325	11-38	2	8
SSR2	0.47	325	38-177	7	5
LB650	0.61	650	177-480	10	3
HB650	0.92	650	480-800	4	6

PIP-II SCL SRF cavities will work in pulsed mode but are compatible with future CW operation. Low beam current with a peak current of 2 mA in combination with high Q_0 results in narrow cavity bandwidth of ~ 60 Hz, and thus the RF field stability is very sensitive to Lorentz Force Detuning (LFD) and microphonics. Therefore, simulating mechanical modes and studying cavity response to various external vibrations for each type of the cavities are essential.

Previous mechanic calculations have been carried out using COMSOL to determine LFD, df/dP (the sensitivity of the cavity resonant frequency to He bath pressure), and the mechanical modes in a single dressed cavity for each type of SCL cavities [3]. The mechanical mode frequencies in a single cavity depend on the boundary conditions imposed on the cavity, which may differ from those in a CM.

The parallel code suite ACE3P developed at SLAC has multi-physics capabilities in integrated electromagnetic, thermal and mechanical simulation [4]. Implemented on massively parallel computers for increased memory, ACE3P makes the mechanical mode simulations for a string of SRF cavities possible. In this paper, the mechanical modes in the high beta 650 MHz CM, as shown in Figure 1, are evaluated using ACE3P.

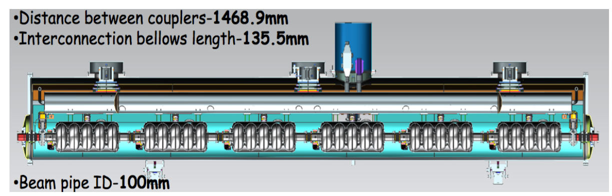

Figure 1: PIP-II high beta 650 MHz CM concept design.

A SINGLE DRESSED CAVITY

FNAL has finished the PIP-II high beta 650 MHz cavity mechanical design as shown in Figure 2. The original blade tuner design has been replaced by a scissor side tuner, which can achieve low df/dP, and be better tunable and less expensive [3,5,6].

First the mechanical modes in a single dressed cavity with and without tuner are analyzed in the following.

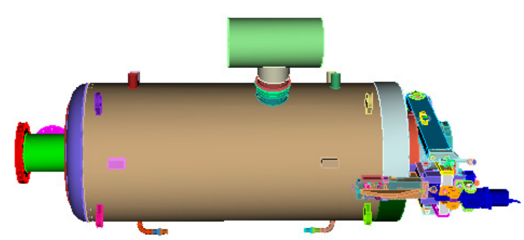

Figure 2: PIP-II high beta 650 MHz dressed cavity

Dressed Cavity without Tuner

A half of the geometry, as shown in Figure 3, is meshed with curved quadratic elements for the mechanical mode simulations. The cavity and stiffening rings are made of Nb (green), the two end transition plates as well as the beampipe and power coupler flanges NbTi (yellow), and the support tabs on the Helium tank stainless steel (blue), respectively, and the Helium tank is made of Ti (grey).

* Work supported by the US DOE under contract DE-AC02-76SF00515

UPDATE ON THE SC 325 MHz CH-CAVITY AND POWER COUPLER PROCESSING*

M. Busch†, M. Amberg, M. Basten, F. Dziuba, P. Mundine, H. Podlech, U. Ratzinger
Institute for Applied Physics, Frankfurt am Main, Germany

Abstract

The 325 MHz CH-cavity which has been developed and successfully vertically tested at the Institute for Applied Physics, Frankfurt, has reached the final production stage. The helium vessel has been welded to the frontal joints of the cavity and further tests in a horizontal environment are in preparation. The corresponding 325 MHz power couplers have been conditioned and tested at a dedicated test stand up to the power level of 40 kW (pulsed) for the targeted beam operation. The final step of the whole prototype development is a beam test with a 11.4 AMeV, 10 mA ion beam at GSI, Darmstadt. Furthermore a new developed test stand for the 217 MHz power couplers is in preparation for the cavities of the sc cw-LINAC project at GSI.

STATUS UPDATE ON THE 325 MHz CH-CAVITY

After successful tests with gradients up to 14.1 MV/m at 2 K [1] the 325 MHz CH-cavity was sent back to Research Instruments for final weldings of the helium vessel and surface treatment. However the final leak tests discovered a small leak inside the membrane bellow within the port for the power coupler (s. Fig. 1). Due to the complex and sensitive position of the leak it was decided to cut out a race track profile around the coupler ports comprising the membrane bellows. A replacement structure is now being produced and will be installed within the next weeks (s. Fig. 2).

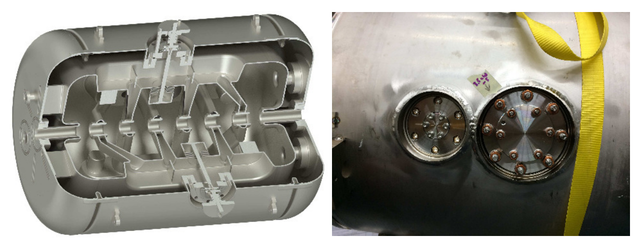

Figure 1: Left: Cross section of the 325 MHz CH-Cavity. Right: Position of the leak (power coupler port).

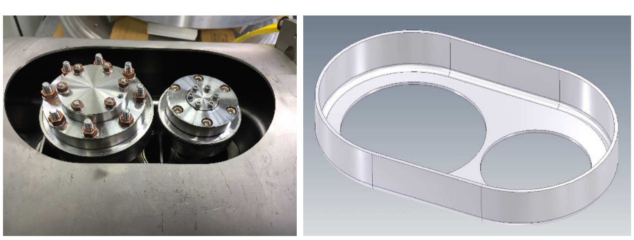

Figure 2: Left: Separated helium vessel comprising membrane bellows. Right: Replacement component.

325 MHz POWER COUPLER TEST SETUP

For the tests of the 325 MHz power couplers a dedicated test stand has been arranged [2]. This setup consists of a tuneable pillbox cavity and enables two power couplers to be conditioned up to 40 kW pulsed power (s. Fig. 3). The couplers were equipped with two Langmuir probes each which were biased with 50 V, four Peltier elements for temperature measurement and a vacuum port. Besides the measurement of P_f and P_r the current of the Langmuir probes (only the current at the warm end of the input coupler is displayed) as well as the pressure between the alumina windows has been recorded to detect Multipacting events (Fig. 4 to 6).

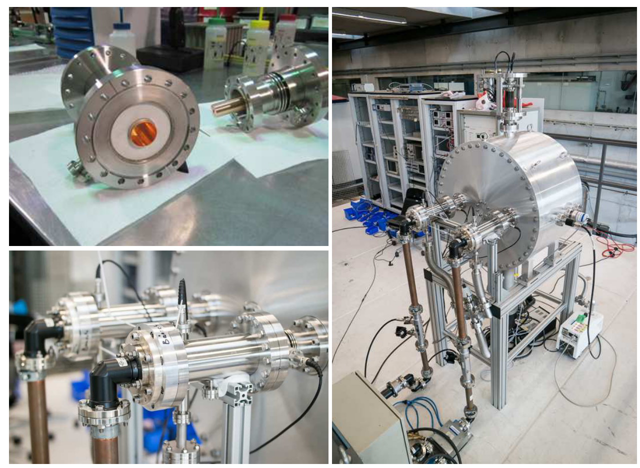

Figure 3: Pictures of the coupler's cold and warm parts (top left) and the assembly with the pill box cavity.

CONDITIONING PHASE

In a first step the couplers were preconditioned with 200 W cw power until the pressure reached a sufficient level (10^{-6} mbar). Then 5 Hz, 1 ms pulses were applied with progressive power from 200 W to 40 kW. The conditioning steps are presented in three parts. In the range from 200 W to 2200 W small pressure variations occured at 1.1 kW to 1.5 kW without any rise in current (s. Fig. 4). This effect is due to degassing and cleaning of the surface. Then several multipacting barriers emerged up to 2.2 kW. The conditioning time for this part was 10 h. The range from 5 kW to 11 kW took 80 min and showed only few and single barriers (s. Fig. 5). The final part from 30 kW to 40 kW took 180 min.

* Work supported by GSI, BMBF Contr. No. 05P15RFRBA
† busch@iap.uni-frankfurt.de

ISBN 978-3-95450-169-4

PERFORMANCES OF THE TWO FIRST SINGLE SPOKE PROTOTYPES FOR THE MYRRHA PROJECT

David Longuevergne, Jean-Luc Biarrotte, Sébastien Blivet, Patricia Duchesne, Guillaume Olry, Hervé Saugnac, IPNO, CNRS-IN2P3 Université Paris Sud, Orsay, France
Yolanda Gómez-Martínez, LPSC, IN2P3 (CNRS), Université, Grenoble Alpes, Grenoble, France
Diana Bachiller-Perea, ACS, Orsay, France

Abstract

The MYRRHA project aims at the construction of an accelerator driven system (ADS) at MOL (Belgium) for irradiation and transmutation experiment purposes [1]. The facility will feature a superconducting LINAC able to produce a proton flux of 2.4 MW (600 MeV - 4 mA). The first section of the superconducting LINAC will be composed of 352 MHz (beta = 0.37) Single Spoke Resonators (SSR) housed in short cryomodules operating at 2K.

After a brief presentation of the cryomodule design, this paper will aim at presenting the RF performances of the SSR tested in vertical cryostat in the framework of European MYRTE project (MYRRHA Research and Transmutation Endeavour) [2] and at comparing experimental results (Lorentz forces, pressure sensitivity, multipacting barriers …) to simulated values.

INTRODUCTION

In the continuation of MAX project (MYRRHA Accelerator eXperiment) [3], MYRTE project is aiming at pursuing the R&D on the MYRRHA research facility. In both projects, a task is dedicated to the R&D of a Spoke cryomodule: a detailed engineering design of the full cryogenic module has been performed and two prototypes of the Single Spoke Resonator (SSR) have been built within MAX project [4]. MYRTE project aims now at assessing the RF performances of the two prototypes at the operating temperature (2K) to validate the mechanical and RF design. In addition, dedicated R&D is being done to improve the intrinsic quality factor (Q_0) by applying heat treatments (low temperature baking, hydrogen degassing ...) on cavities already equipped with their helium jacket (Titanium). This paper will present the baseline results of the two prototypes that have been tested in vertical cryostat. The first heat treatments have not been yet performed, but are foreseen for the end of this year.

SPOKE CRYOMODULE DESIGN

The Cryomodule and Ancillaries

As depicted in Fig. 1, the cryomodule is housing two superconducting SSR made of bulk Niobium with a beta of 0.37 and an operating frequency of 352 MHz. Because of very high reliability requirements, that makes MYRRHA project so specific [5], the cavities could be operated at two different regimes. The first one, the nominal regime, is requiring an accelerating gradient of 6.4 MV/m. The second one, called the fault-recovery regime, activated in case of failure of a neighbour cavity, is requiring an accelerating gradient of 8.4 MV/m. In both regimes, the cavity power dissipations have to be kept below 10W.

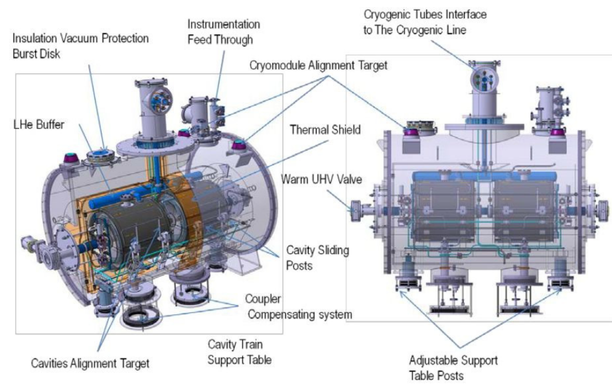

Figure 1: SSR cryomodule for MYRRHA.

The cavities will be powered by a power coupler with a single warm window designed to transfer 20 kW RF power in CW. A prototype has been developed and successfully tested within the EURISOL project [6].

The frequency regulation will be achieved with a cold tuning system by deformation very similar to the ESS design [7]. Some modifications will be done to implement a fast detuning capability to fulfil the fault-recovery requirements.

The magnetic shield is for instance designed to be actively cooled with 4.2K liquid helium. It will be composed of two 1-mm-thick layers of Cryoperm® directly installed around the helium tank to ensure an optimal shielding of the residual magnetic field as it was done for Spiral2 type-B cryomodules [8].

The Single Spoke Cavity

The RF design was achieved following the experience feedback from previous Spoke developments [9][10]. RF parameters are optimized to operate the cavity at very conservative electromagnetic field (E_{peak}<40 MV/m and B_{peak}<80 mT) and to decrease manufacturing difficulties. Table 1 below summarizes the RF parameters of the cavity.

The mechanical designs of the cavity and its helium tank (see Fig. 2), made of titanium, were optimized to limit frequency shifts due to microphonics, pressure variations and Lorentz forces without compromising reliability and manufacturing simplicity (see Table 1). Main parameters can be found in [4].

UPDATE ON SSR2 CAVITY EM DESIGN FOR PIP-II*

P. Berrutti†, T. N. Khabiboulline, V. Yakovlev, Fermilab, Batavia, IL 60510, USA

Abstract

Proton Improvement Plan II (PIP-II) is the future plan for upgrading the Fermilab proton accelerator complex to a beam power capability of at least 1 MW delivered to the neutrino production target. A room temperature section accelerates H- ions to 2.1 MeV and creates the desired bunch structure for injection into the superconducting (SC) linac. SC linac using five cavity types. One 162.5 MHz half wave resonator, two 325 MHz spoke resonators and two 650 MHz elliptical 5-cell cavities, provide acceleration to 800 MeV. The EM design of the second family of spoke resonator is presented in this paper. The work reported is a thorough electromagnetic study including: the RF parameters, multipacting mitigation and transverse field asymmetry. The cavity is now ready for structural design analysis.

INTRODUCTION

PIP-II stands for Proton Improvement Plan-II [1]: it is Fermilab plan for future improvements to the accelerator complex, aimed at providing LBNE (Long Base Neutrino Experiment) operations with a beam power of at least 1 MW on target. The central element of the PIP-II is a new superconducting linac, injecting into the existing Booster. The PIP-II 800 MeV linac derives from Project X Stage 1 design. The room temperature (RT) section includes a Low Energy Beam Transport (LEBT), RFQ and Medium Energy Beam Transport (MEBT), accelerating H- ions to 2.1 MeV and it creates the desired bunch structure for injection into the superconducting (SC) linac. PIP-II will use five SC cavity types: one 162.5 MHz half wave resonator (HWR), two single spoke resonator sections at 325 MHz (SSR1 and SSR2), lastly two families of 650 MHz elliptical cavities low beta (LB) and high beta (HB). The technology map of the PIP-II linac, Fig. 1, shows the transition energies between accelerating structures, and the transition in frequency. This article

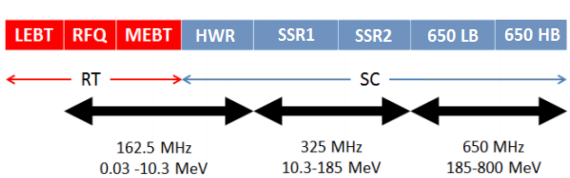

Figure 1: PIP-II linac technology map.

will discuss the electromagnetic (EM) design of the second type of spoke resonators (SSR2): the design has been updated mainly to mitigate multipacting, trying to preserve the cavity performance. The phenomenon of multipacting (MP) consists in electron multiplication at surfaces exposed to an oscillating electromagnetic field, which can represent a serious obstacle for operation of particle accelerator and their RF components. Multipacting, in the previous design of SSR2, has been studied in [2]: the results showed higher intensity and wider power range than for SSR1 cavities, already built and tested at FNAL [3] [4]. The new design lowers the MP intensity and reduces the gradient range in which MP occurs, without compromising the EM cavity parameters. This article summarizes all the studies on SSR2 design for PIP-II: EM parameters, quadrupole field asymmetry and multipacting simulations are presented.

GEOMETRY AND RF PARAMETERS

SSR2 is a single spoke resonator operating at 325 MHz, it will be used in PIP-II linac, for particle acceleration from 35 MeV to 185 MeV. Figure 2 shows the new SSR2 RF design (version 2.6) Y-Z cross-section where Z represents the beam axis, all the main geometry parameters are shown in the picture, their values are reported in Table 1. Electric and magnetic 3D fields have been simulated with COMSOL multiphysics and are plotted in Fig. 3.

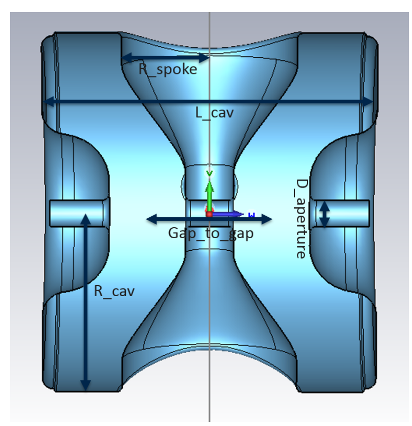

Figure 2: SSR2 v. 2.6 cavity Y-Z cross-section.

Table 1: Main Geometric Parameters

Parameter	Length [mm]
L_cav	500
R_cav	271.6
R_spoke	130.7
D_aperture	40
Gap_to_gap	185.9

The value of β_{opt} = 0.47 has been chosen after optimization of the SSR2 section of PIP-II in [5]. SSR2 design v1.0 and v2.6 EM parameters are reported in Table 2. One can see how the two designs are capable of delivering the same

* Work supported by D.O.E. Contract No. DE-AC02-07CH11359
† berrutti@fnal.gov

R&D STATUS OF THE NEW SUPERCONDUCTING CW HEAVY ION LINAC@GSI*

M. Basten[1,†], M. Amberg[1], W. Barth[2,3], M. Busch[1], F. Dziuba[1], V. Gettmann[3], M. Heilmann[2], S. Mickat[2,3], M. Miski-Oglu[3], H. Podlech[1], M. Schwarz[1], S. Yaramyshev[2]

[1]IAP Goethe University Frankfurt, 60438 Frankfurt am Main, Germany
[2]GSI Helmholtz Centre, 64291 Darmstadt, Germany
[3]HIM Helmholtz-Institute Mainz, 55099 Mainz, Germany

Abstract

For future research in the field of Super Heavy Elements (SHE) a superconducting (sc) continuous wave (cw) ion LINAC with high intensity is highly desirable. Presently a multi-stage R&D program conducted by GSI, HIM and IAP [1] is in progress. The fundamental linac design composes a high performance ion source, a new low energy beam transport line, the High Charge State Injector (HLI) upgraded for cw, and a matching line (1.4 MeV/ u) followed by the new sc-DTL LINAC for acceleration up to 7.3 MeV/ u. The successful commissioning of the first Crossbar-H-mode (CH) cavity (Demonstrator), in a vertical cryo module, was a major milestone in 2015 [2]. The next stage of the new sc cw heavy ion LINAC is the advanced demonstrator comprising a string of cavities and focusing elements build from several short constant-beta sc CH-cavities operated at 217 MHz. Currently the first two sc 8 gap CH-cavities are under construction at Research Instruments (RI), Bergisch Gladbach, Germany. The new design without girders and with stiffening brackets at the front and end cap potentially reduces the overall technical risks during the construction phase and the pressure sensitivity of the cavity. The recent status of the construction phase as well as an outlook for further cavity development of the new cw heavy ion LINAC will be presented.

INTRODUCTION

The construction of cavity 1 and 2 of the advanced demonstrator is the next milestone realizing a new sc heavy ion cw-LINAC at GSI. The first milestone will be the successful beam test of the demonstrator at GSI-HLI. The demonstrator cavity has been successfully rf tested at cryo conditions at Frankfurt University [2]. The recent design of the sc cw-LINAC comprises the demonstrator as first cryomodule and several additional cryomodules each equipped with two short CH-cavities [1, 3]. The overall design of this standard cryomodule will be used for all following cavities. The short cavity with 8 accelerating cells is designed for high power applications at a design gradient of 5 MV/m. Its resonant frequency is the second harmonic of that of the High Charge Injector (HLI) at GSI, Darmstadt. In table 1 the main parameters of the first two 217 MHz CH-cavities are depicted. Figure 1 shows the layout of these cavities.

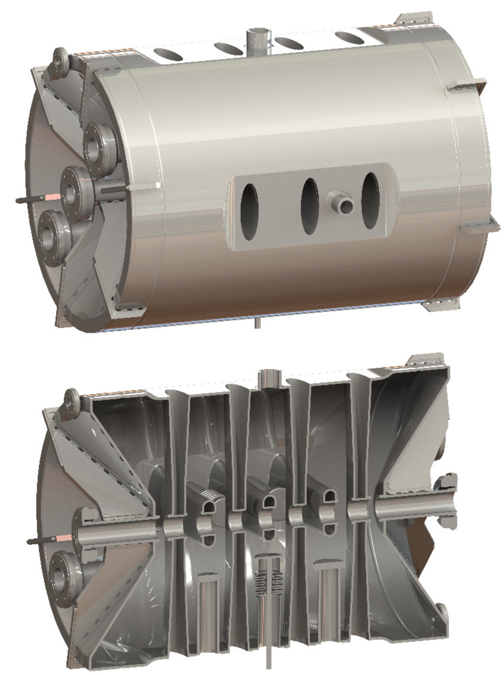

Figure 1: Layout of the sc 217 MHz CH-cavity 2 and 3.

Table 1: Main Parameters of CH-cavity 2 and 3

Parameter	Unit	
β		0.069
Frequency	MHz	216,816
Accelerating cells		8
Length ($\beta\lambda$-definition)	mm	381.6
Cavity diameter (inner)	mm	400
Cell length	mm	47.7
Aperture diameter	mm	30
Static tuner		3
Dynamic bellow tuner		2
Wall thickness	mm	3-4
Accelerating gradient	MV/m	5
E_p/E_a		5.2
B_p/E_a	mT/(MV/m)	<10
G	Ω	50
R_a/Q_0	Ω	1070

* Work supported by HIM, GSI, BMBF Contr. No. 05P15RFRBA
† Basten@iap.uni-frankfurt.de

ISBN 978-3-95450-169-4

FZJ SRF TSR WITH INTEGRATED LHE VESSEL

E. Zaplatin, Forschungszentrum Juelich, Germany

Abstract

Single- or Multi-Spoke SRF cavities are one of the basic accelerating structures for the low and intermediate energy part of many accelerators. Different types of external loads on the resonator walls predetermine the main working conditions of the SC cavities. The most important of them are very high electromagnetic fields that result in strong Lorentz forces acting on cavity walls and the pressure on cavity walls from the helium tank that also deforms the cavity shape. For the accelerators operating in pulsed regime the Lorentz forces are the dominant factor. The liquid helium vessel pressure instability even for 2K operations is the source of large microphonics and dominates for cw operation. Here we propose an innovative integrated helium vessel-cavity and stiffener design that will provide an effective passive damping minimizing df/dp ratio. Minimizing df/dp may be accomplished without an enhancement of the structure rigidity, which in turn minimizes the load on the cavity tuner. A separate stiffening scheme reducing Lorentz force cavity detuning to be added without violation of df/dp optimization.

The developed at the Research Center in Juelich, Germany (FZJ) the 352 MHz, β=v/c=0.48 Triple-Spoke Resonator (Fig. 1) was used as an example to demonstrate the proposed conceptual integrated helium vessel-cavity design.

NAKED CAVITY DESIGN

During SC cavity RF design fabrication technology and structural parameters have to be taken into account. The whole RF design has to be greatly adapted to two main goals - the simplest technology of cavity manufacture and to achieve the best possible mechanical parameters (Lorenz force frequency shift, frequency pressure dependence, resonator tuning scheme and microphonics mitigation).

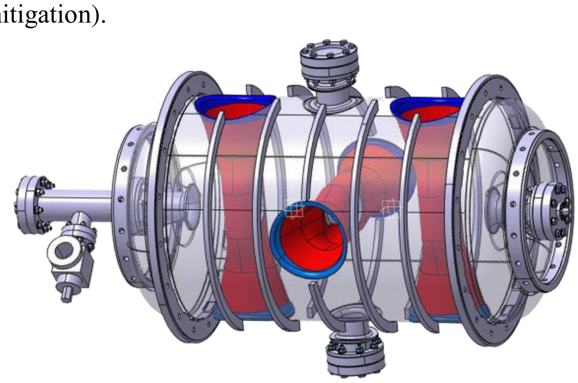

Figure 1: 3D view of FZJ triple-spoke cavity.

The most effective way for the frequency pressure dependence (df/dp) minimization is to find the resonator stiffening scheme that would balance frequency shifts from magnetic and electric stored energy changes caused by the cavity shape deformations. Such self-compensation frequency shift design for multiple-cell resonators was first investigated for the low-beta triple-spoke cavities (see for instance [1-3]). The summary of FZJ TSR structural behaviour can be accurately generalized to the case of arbitrary boundary conditions, characterized by its longitudinal stiffness K_{ext}, (Fig.2).

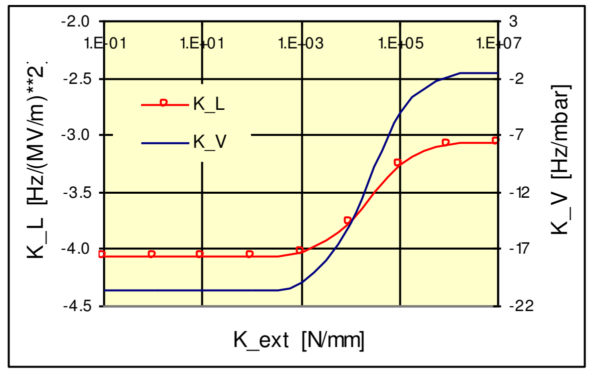

Figure 2: TSR structural analyses results.

MULTI-CELL CAVITY STIFFENING

Based on investigations within HIPPI [3] the new detailed developments of the integrated cavity-helium vessel design to fulfil the main requirements on resonator mechanical parameters were provided. The simulation model (Fig. 3) consists of the resonator surrounded by the cylindrical helium vessel (HV) with rounded end cups. HV connected to the cavity via four rings with two direct joints with beam pipes. The model of both HV end cup rings has possibility of disconnecting HV with the cavity (left/right end cup ring joints). There are possibilities simulating of the slots (left/right end cup slots) in the model of the both HV end cups. The radius of slots R_{slot} can be varied during calculations.

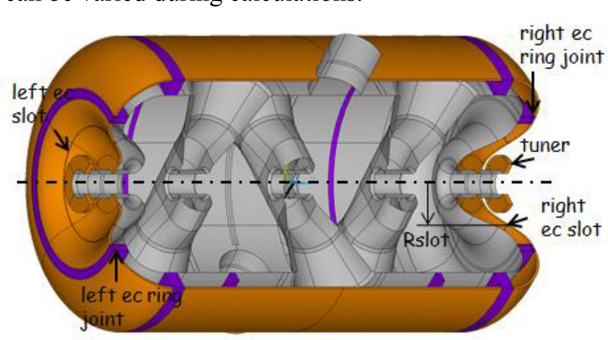

Figure 3: TSR simulation model with helium vessel.

HV constraints consist of the fully fixed right ring connecting cavity with HV. A left beam pipe is supposed

SRF LOW-BETA ELLIPTICAL RESONATOR TWO-RING STIFFENING

E. Zaplatin, Forschungszentrum Juelich, Germany
I. Gonin, T. Khabiboulline, V. Yakovlev, FNAL, Geneva, IL, U.S.A

Abstract

Elliptical SRF cavities are the basic accelerating structures for the high energy part of many accelerators. Since a series of external loads on the resonator walls predetermine the main working conditions of the SC cavities the detailed investigation of their mechanical properties should be conducted in parallel with the main RF design. The effects of very high electromagnetic fields that result in strong Lorentz forces and the pressure on cavity walls from the helium tank that also deforms the cavity shape, the tuning scheme resulting in the change of accelerating field profile and mechanical eigen resonances of cavities which are the main source of the microphonics must be taken into account during integrated design of the resonator and its liquid helium vessel.

SRF elliptical cavities for the medium energies (β=v/c is around 0.6) inherently have more flexible shape and their ultimate stiffening with a "standard" stiffening rings installed between resonator cells becomes problematic. The second set of the rings should enhance the overall cavity rigidity.

In the paper we report the basic investigations of the cavity two-set ring stiffening using FNAL 650 MHz β=0.61 as an example [1]. The single-cell investigation results were used as the reference to develop the ultimate scheme of the helium vessel structure to ensure the best resonator stability.

PRESSURE RESPONSE OF MID-CELL

The response of the cavity to a pressure differential is calculated with vacuum inside the resonator and ambient pressure outside. Differing from the pressure differential case the Lorentz forces at the dome region are directed outward the cavity volume (Fig. 1). So, the choice of the ring position is the trade-off between these two effects.

The procedure of a middle cell stiffening investigations using two-set rings was similar as used for the single-set rings [2]. The main goal was to find the stiffening condition to balance resonator frequency shifts caused by the change of the magnetic and electric stored energies. Hence, the strategy of cavity design should include the integrated simulations of RF and mechanical properties. The simulations are made with the cell-to-cell junction constrained by symmetry.

The second ring installation provides the cavity cell rigidity where LFD is nearly independent on the second ring position since it is defined mainly by the first ring set. Changing the second ring position results in the change in the wall deformations and as a result in df/dp value. There are two places for the second ring where the frequency shift df/dp reaches zero. The summary of simulations is presented on (Fig. 2).

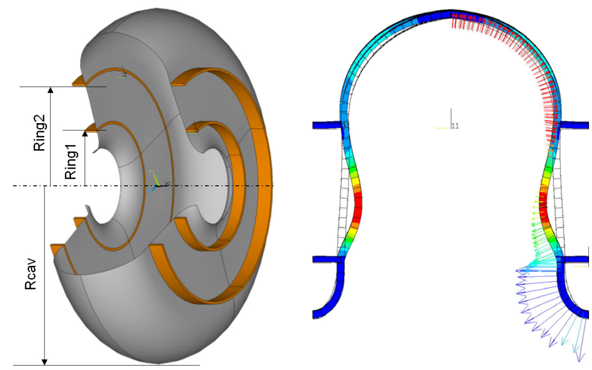

Figure 1: FNAL 650 MHz, β=0.61 mid-cell geometry and Lorentz force deformations with two-set stiffening rings.

The best ring-2 position is R_{ing2}/R_{cav}=0.75 with R_{ing1}/R_{cav}=0.35 that corresponds to the minimum of LFD (K_L=-0.27 Hz/(MV/m)^2) and df/dp=0.

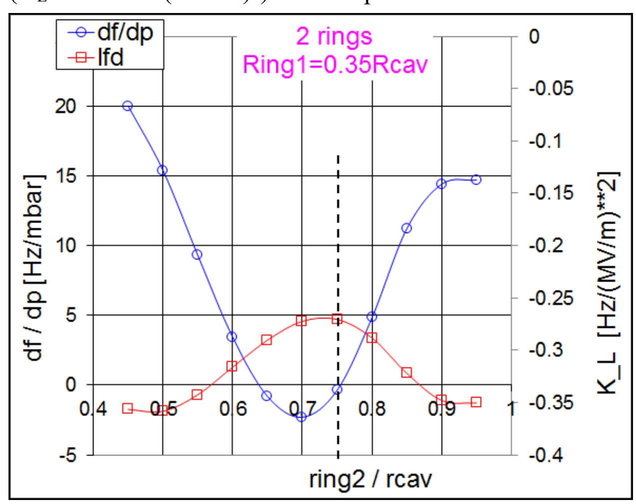

Figure 2: FNAL 650 MHz, β=0.61 mid-cell simulation summary.

MULTI-CELL CAVITY STIFFENING

The simulation model of FNAL PIP-II multi-cell elliptical cavities (650 MHz, β = 0.61, Fig. 3) consists of 5-cell cavity surrounded by the cylindrical helium vessel. A whole helium vessel (HV) except HV end dishes will be made from titanium (Ti). One side of the helium vessel end flanges (right on Fig. 3) is firmly attached to the cavity beam pipes through Nb-Ti end dishes. On the tuning side of the HV (left on Fig. 3) there is a slot in the Nb-Ti end dishes imitating the connection of the tuner. Such slot is bridged by the bellow for vacuum sealing. Bellows are included in the helium vessel to accommodate the motion produced by the tuner. The

ISBN 978-3-95450-169-4

DEVELOPMENT OF A SUPERCONDUCTING TWIN AXIS CAVITY*

H. Park†[1], F. Marhauser, A. Hutton, S. U. De Silva[1], J. R. Delayen[1]
Thomas Jefferson National Accelerator Facility, Newport News, VA 23606, USA
[1]also at Center for Accelerator Science, Old Dominion University, Norfolk, VA 23529, USA

Abstract

Superconducting cavities with two separate accelerating axes have been proposed in the past for energy recovery linac applications [1, 2]. While the study showed the advantages of such cavity, the designs present serious fabrication challenges. Hence the proposed cavities have never been built. The new design, twin axis cavity, proposed by Jefferson Lab and optimized by Center for Accelerator Science at Old Dominion University, allows similar level of engineering and fabrication techniques of a typical elliptical cavity. This paper describes the preliminary results of LOM and HOM spectrum, engineering and fabrication processes of a single cell prototype of the twin axis cavity.

ELECTROMAGNETIC DESIGN

Optimization

The ultimate design goal of the twin axis cavity is a fully optimized 'multicell' cavity. A single cell cavity has more flexibility than a multicell cavity as far as optimizing the rf properties. However our single cell prototype was designed under the same constraints of multicell cavity most notably limiting the cavity length to a half wave length. Therefore, the single cell cavity with beam pipes has a frequency 1484 MHz. The intended frequency of multicell cavity is 1497 MHz which is Jefferson Lab's CEBAF operating frequency. Figure 1 is showing the dumbbell design of twin axis cavity [3].

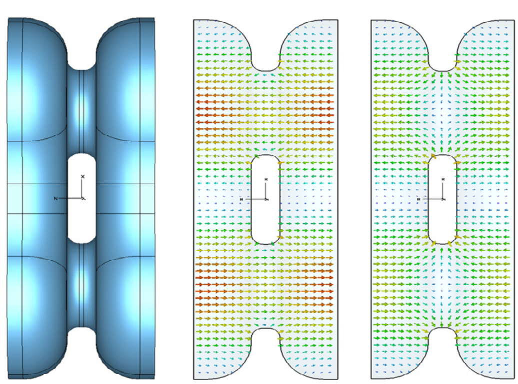

Figure 1: Dumbbell design and its 0 mode and π mode electric field distribution.

As a new design, optimization focused not only on the cavity performance parameters but also on manufacturability and minimizing multipacting. The property of the optimized cavity is shown in the Table 1 and the single cell cavity with beam pipes is shown in Fig. 2.

Table 1: RF Properties of Twin Axis Cavity [2]

Property	Value	Unit
Frequency	1484	MHz
E_p/E_{acc}	2.5	-
B_p/E_{acc}	5.34	mT/(MV/m)
R/Q	63	Ω
G	315	Ω
LOM	1146	MHz
HOM	1872	MHz

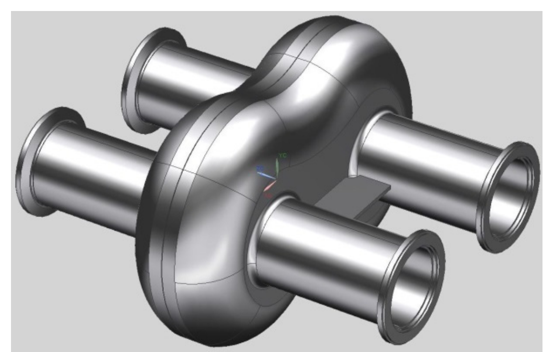

Figure 2: Single cell twin axis cavity.

LOM and HOM Spectrum

The EM design provides the closest LOM and HOM well separated from the operating frequency. For each mode, R/Q was calculated to see its effect on the beam. Depending on the field components on the beam axis, there are longitudinal R/Q and transverse R/Q on X or Y plane.

The accelerating mode's R/Q is

$$\frac{R}{Q}=\frac{\left[\int_{-\infty}^{+\infty}E_z\left(z,x=b,y=0\right)\mathrm{e}^{-j\omega z/c}\mathrm{d}z\right]^2}{\omega U}$$

where E_z is a z component of electric field, b is a beam axis location, ω is the mode's frequency and U is the stored energy in the cavity. In case of deflecting modes, E_z is replaced by E_x or E_y. Also the magnetic field contribution is added as shown below.

$$\frac{R}{Q}=\frac{\left[\int_{-\infty}^{+\infty}\left(E_x+jcB_y\right)\mathrm{e}^{-j\omega z/c}\mathrm{d}z\right]^2}{\omega U}$$

where electric and magnetic fields are still evaluated on the beam axis.

* Work supported by accelerator stewardship test facility pilot program, office of science DOE.
† hkpark@jlab.org

RESONANCE CONTROL FOR NARROW BANDWIDTH PIP-II CAVITIES

J. Holzbauer[#], Y. Pischalnikov, W. Schappert. - FNAL, Batavia, IL 60510, USA

Abstract

The PIP-II project at FNAL calls for a SRF pulsed proton driver linac to support the expanding neutrino physics program including DUNE/LBNF. The relatively low beam current and high quality factors called for in the design means that these cavities will be operated with small RF bandwidths, meaning that they will be sensitive to microphonics. Combined with a 20 Hz pulsed operational structure and the use of four different, complex cavity geometries means that resonance control will be extremely challenging. Work is ongoing at FNAL to develop active resonance stabilization techniques using fast piezoelectric tuners in support of PIP-II. These techniques as well as testing and development results using a prototype, dressed low-beta single-spoke cavity will be presented along with an outlook for future efforts.

PIP-II PROTOTYPE CAVITY

An extensive design and prototyping effort at Fermilab has been focused on a 325 MHz single spoke resonator for the PIP-II project. The cavity has been optimized for performance, multipacting minimization, and pressure sensitivity. Integrated tests have demonstrated functionality of the dressed cavity with tuner and high-power coupler.

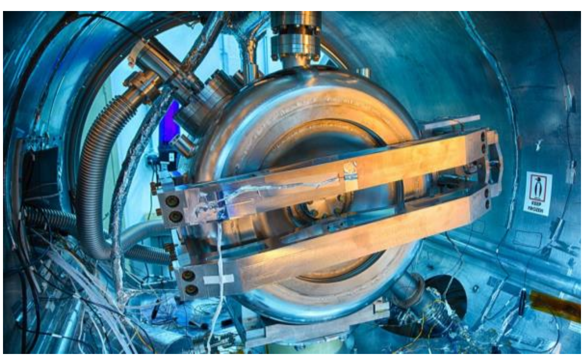

Figure 1: Dressed Single Spoke Resonator with tuner and high-power coupler installed in the Spoke Test Cryostat at Fermilab.

This resonator is designed to operate at 2 K. PIP-II calls for a pulse structure with a 0.5 ms flattop at 12.5 MV/m, 20 Hz repetition rate, and 15% duty cycle. The coupler is designed for operation over several kW with a half bandwidth of 30 Hz. Tuning is accomplished via a single lever tuner attached to the helium vessel, acting on one beam pipe [1]. The motor is actuated via a slow motor for course tuning over large range and two piezo tuners encapsulated in such a way to act together, but still remain functional is one piezo fails. After installation in the Spoke Test Cryostat (STC) seen in Figure 1 and cooldown, the tuner is designed and set to remain barely out of contact with the cavity. The slow motor moved the tuner into contact with the cavity and preload the piezo and tuner. For the following testing, the tuner was loaded and left at the low loading end of the operating tuning range.

The prototype coupler gave an initial half bandwidth of 142 Hz (Loaded Q of 1.15e6). An RF reflector was installed to narrow the cavity bandwidth, giving a final Loaded Q of 5.24e6 (31 Hz half bandwidth).

RF DEVELOPMENT CIRCUIT

Development was done on an FPGA based digital RF system (seen in Figure 2). Direct RF signals are downconverted to 13 MHz via narrowband, analog downconverter. These signals are then digitized at the eighth harmonic, 104 MHz, by 14-bit ADCs.

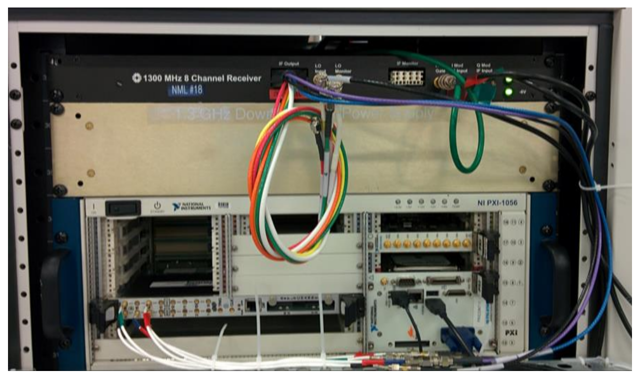

Figure 2: Analog downconverter, RF transceiver, and FPGA-based RF controller.

IF I/Q signals and piezo drive are calculated in the FPGA and generated by 14-bit DACs. IF signals are analog upconverted to RF frequency and sent to the high power amplifier. Monitoring, logging, and setting of registers is done via on-board PC controller. Piezo signal was amplified by a low-noise PiezoJena amplifier up to 150 Volts.

$$\frac{dP}{dt} = -(\omega_{1/2} + i\delta)P + 2\omega_{1/2}F$$

$$\omega_{1/2} = -\frac{\left\langle \mathrm{Re}\left(P^*\left(\frac{dP}{dt}\right)\right)\right\rangle}{\left\langle \mathrm{Re}\left(P^*(P-2F)\right)\right\rangle}$$

$$\delta = -\frac{\mathrm{Im}\left(P^*\left(\frac{dP}{dt} - 2\omega_{1/2}F\right)\right)}{P^*P}$$

Equation 1: Separation of the baseband envelope into real and imaginary parts which allows direct calculation of the cavity half bandwidth and detuning.

FIRST VERTICAL TEST OF SUPERCONDUCTING QWR PROTOTYPE AT RIKEN

K. Yamada*, O. Kamigaito, K. Ozeki, N. Sakamoto, K. Suda, Y. Watanabe,
RIKEN Nishina Center, Wako, Saitama, Japan
E. Kako, H. Nakai, K. Umemori, KEK, Tsukuba, Ibaraki, Japan
A. Miyamoto, K. Sennyu, T. Yanagisawa,
Mitsubishi Heavy Industries Mechatronics Systems, Ltd. (MHS-MS), Kobe, Hyogo, Japan

Abstract

The assembly of a prototype of the RIKEN superconducting quarter-wavelength resonator was completed in June 2016, and the first vertical test of the prototype has been performed at KEK. As a result, acceptably high values of Q_0 and E_{acc} have been achieved. This paper presents the results of the first vertical test as well as the preparation and test procedures.

INTRODUCTION

A CW high-intensity ion accelerator is one of the candidates for a system aimed at reducing the amount of long-lived fission products (LLFP) in high-level radioactive waste by converting LLFP nuclides into short-lived or stable nuclides through nuclear transmutation. For such a transmutation system, efficient acceleration of the ion beam with an intensity greater than 100 mA is required. A superconducting linear accelerator is one of the most promising candidates for realizing such high-intensity ion acceleration. As described in Ref. [1], fabrication of the first prototype of a superconducting quarter-wavelength resonator (SC-QWR) was started at RIKEN Nishina Center last year, in order to develop elemental technologies required for the low-velocity part of the CW high-intensity ion linear accelerator.

FABRICATION OF SC-QWR PROTOTYPE

Figure 1 shows cross-sectional views of the SC-QWR prototype. The design parameters of the prototype SC-QWR are summarized in Table 1. The SC-QWR prototype was made from a bulk Nb sheet with a residual resistance ratio (RRR) of 250. A half-cell comprising the drift tube and stem was formed by stamping them into one piece, as described in Ref. [2]. After the production of its partial components, i.e. the outer cylinder, stem, upper torus, and bottom dome, the resonant frequency of their assembly was measured and careful adjustments were made to the straight section of the top part of the outer cylinder as well as the stem and bottom side of the outer cylinder. The final assembly of the SC-QWR prototype by electron beam welding was completed in June 2016. Photographs of the part and the completed SC-QWR prototype are shown in Fig. 2.

The first cool-down test of the SC-QWR prototype along with the startup of a newly constructed vertical test stand was performed after a test of the buffered chemical polishing (BCP) and high-pressure rinsing (HPR) system [3]. Subsequently, surface treatments of BCP1 (100 μm), annealing, BCP2 (20 μm), ultrasonic cleaning, HPR, and baking were performed sequentially from July through August in 2016. After overcoming several problems with the vertical test stand, the first vertical test was successfully carried out in September 2016.

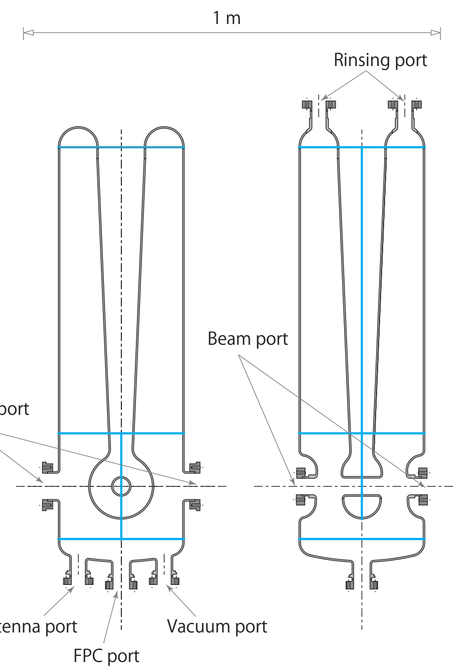

Figure 1: Designed schematics of the SC-QWR prototype.

Table 1: Design Parameters of the SC-QWR Prototype. Surface Resistance was Assumed to be 25 nΩ in the Calculation

Frequency [MHz] at 4.5 K	75.5
Duty [%]	100
β_{opt}	0.08
G [Ω]	23.5
R_{sh}/Q_0 [Ω]	578
Q_0	9.4×10^8
P_0 [W]	3.8
V_{acc} [MV] at E_{acc} = 4.5 MV/m, β = 0.08	1.44
E_{acc} [MV/m]	4.5
E_{peak}/E_{acc}	6.2
B_{peak}/E_{acc} [mT/(MV/m)]	9.7

* nari-yamada@riken.jp

ISBN 978-3-95450-169-4

650 MHz ELLIPTICAL SUPERCONDUCTING RF CAVITIES FOR PIP-II PROJECT*

I.V. Gonin†, E. Borissov, V.K. Jain, C. Grimm, A. Grasselino, S.Kazakov, V. Lebedev, A. Lunin, C. S. Mishra, N. Sharma, N. Solyak, Y. Pischalnikov, A. Rowe, D. Mitchel, T. Nicol, V. P. Yakovlev
Fermi National Accelerator Laboratory, Batavia, IL, USA

Abstract

The PIP-II 800 MeV linac employs 650 MHz elliptical 5-cell CW-capable cavities to accelerate up to 2 mA peak beam current of H^- in the energy range 185 – 800 MeV. The low beta (LB650) $\beta_G = 0.61$ portion should accelerate from 185 MeV to 500 MeV using 33 LB650 dressed cavities in 11 cryomodules. The high beta (HB650) $\beta_G = 0.92$ portion of the linac should accelerate from 500 to 800 MeV using 24 HB650 dressed cavities in 4 cryomodules [1]. The development of both type cavities is going on under IIFC collaboration. This paper presents design methodology. The discussion proceeds from RF design resulting in mechanical dimensions of RF cells to mechanical design and cavity dressing for both low- and high-beta cavities. Further the tuner design and its integration to the dressed cavity is discussed. The paper also explains the salient design features of these dressed cavities.

INTRODUCTION

Proton Improvement Plan II (PIP-II) is Fermilab's plan for future improvements to the accelerator complex, aimed at providing LBNF (Long Base Neutrino Facility) operations with a beam power of at least 1MW on the target. The central element of PIP-II is a new superconducting 800 MeV linac, injecting beam into the 8 GeV Booster.

The room temperature (RT) section includes a Low Energy Beam Transport (LEBT), RFQ and Medium Energy Beam Transport (MEBT). The RT section accelerates H^- to 2.1 MeV and creates the desired bunch structure for injection into the superconducting (SC) linac. The SC linac includes 162.5 MHz Half Wave Resonators, two types of 325 MHz Single Spoke Resonators and two types of 650 MHz 5-cell elliptical cavities [2]. In this article the status of development for last two cavity types (LB650 and HB650) is presented.

RF DESIGN

As mentioned above the PIP-II project employs 2 types of 650 MHz elliptical cavities. In the process of project development the serial iteration of RF design has been done. The shape of both cavities was modified to allow both pulsed and CW operation. Detailed RF optimization of HB650 cavity and RF design for LB650 cavity were presented at IPAC12 [3].

Below we summarize the main parameters of both LB650 and HB650 cavities in Table 1, where we assume that the effective length is equal to 5*βG λ/2.

Table 1: Main Parameters of 650 MHz Cavities

Cavity Parameters	LB650	HB650
β_G	0.61	0.92
β_{opt}	0.65	0.97
$R/Q(\beta_G)$, Ohms	327.4	576
$R/Q(\beta_{opt})$, Ohms	356.3	610
$E_{surf}/E(\beta_G)$	2.43	2.10
$E_{surf}/E(\beta_{opt})$	2.33	2.07
$B_{surf}/E(\beta_G)$, mT/MeV/m	4.6	3.94
$B_{surf}/E(\beta_{opt})$, mT/MeV/m	4.41	3.89
G, Ohms	187	260

DRESSING OF THE CAVITY AND MECHANICAL DESIGN

The LB650 & HB650 cavities consist of five elliptic cells. Although the cavity lengths are different for these cavities, it was decided to have similar mechanical designs of end-groups, helium vessel and tuner. This unification allows to reduce complexity and risk, as well as the cost of development and production. Stiffening rings between the cells and between the end-cell and end-group are important part of the design for both cavities. Optimization of stiffening ring's location and end group design controls the deformation of the cavity and is important part of mechanical design. It has to minimize LFD and *df/dp* without sacrificing the cavity tunability [4, 5]. The final designs of HB650 and LB650 cavities stiffness of 4 and 3 kN/mm, respectively. Based on HOM studies a beam tube diameter of 118 mm is chosen for both cavities [6]. The beam tube at the main coupler (MC) end has a port for the RF power coupler, and the beam pipe at tuner end has a port for RF field probe (FP) antenna. The helium vessel is welded to the end groups. The vessel has two ports for helium filling at the bottom and the two-phase helium return line is provided at 30° from the top of the vessel. At the sides of the helium vessel, four blocks are welded for supporting in the HTS cryostat or cryomodule. Lifting lugs are provided on the helium vessel for assembly and transport of the cavity. A bellows is provided at the tuner end between the helium vessel and the end group in order to provide frequency tuning. Figure 1 shows the various components on the cavity.

* Operated by Fermi Research Alliance, LLC under Contract No. DE-AC02-07CH11359 with the United States Department of Energy.
† gonin@fnal.gov

ISBN 978-3-95450-169-4

BEAM DYNAMICS STUDIES FOR A COMPACT CARBON ION LINAC FOR THERAPY*

A.S. Plastun†, B. Mustapha, A. Nassiri, P.N. Ostroumov
Argonne National Laboratory, Lemont, IL, USA,
L. Faillace, S.V. Kutsaev, E.A. Savin[1], RadiaBeam Technologies, Santa Monica, CA, USA
[1]also at National Research Nuclear University - Moscow Engineering Physics Institute, Moscow, Russia

Abstract

Feasibility of an Advanced Compact Carbon Ion Linac (ACCIL) for hadron therapy is being studied at Argonne National Laboratory in collaboration with RadiaBeam Technologies. The 45-meter long linac is designed to deliver 10^9 carbon ions per second with variable energy from 45 MeV/u to 450 MeV/u. S-band structure provides the acceleration in this range. The carbon beam energy can be adjusted from pulse to pulse, making 3D tumor scanning straightforward and fast. Front end accelerating structures such as RFQ, DTL and coupled DTL are designed to operate at lower frequencies. The design of the linac was accompanied with extensive end-to-end beam dynamics studies which are presented in this paper.

INTRODUCTION

There is strong worldwide interest in carbon ion beam therapy [1, 2], but no such facility exists or under construction in the U.S. A variable energy carbon beam with a maximum energy of 450 MeV/u is required for the most advanced treatment. We propose a high-gradient linear accelerator, the Advanced Compact Carbon Ion Linac (ACCIL). It includes the following main sections: a radiofrequency quadrupole (RFQ) accelerator, drift-tube linac (DTL) section and several coupled DTL tanks, operating at a sub-harmonic of the S-band frequency, and followed by an S-band either traveling wave or standing wave accelerating structure for the energy range from 45 MeV/u to 450 MeV/u. ACCIL is designed to accelerate the proton beam as well.

ADVANCED COMPACT CARBON ION LINAC

In order to satisfy the requirements of compactness, reliability and efficiency we examined S-band accelerating structures and structures operating at the sub-harmonics. The following criteria have defined the set of accelerating structures and their operating frequencies: high real-estate average accelerating gradient of 20 MV/m, reasonable heat load (pulsed and average), breakdown rate below 10^{-6} breakdowns per pulse per meter, the repetition rate of 120 Hz and beam pulse width of 0.5 µs.

* This work was supported by the U.S. Department of Energy, Office of High Energy Physics, under Accelerator Stewardship Grant, Proposal No. 0000219678

† on leave from Institute for Theoretical and Experimental Physics
email: asplastun88@gmail.com

Ion Source

The typical radiation dose for hadron therapy is delivered at the rate of $(3\text{-}10)\cdot 10^8$ carbon ions/sec and 10^{10} protons/sec [3]. Modern electron cyclotron resonance (ECR) ion sources are capable of providing DC carbon beam with an electric current up to 25 µA at (5+) charge state [4]. Fig. 1 shows the plot for the $^{12}C^{5+}$ pulse beam current required to provide 10^9 ions/sec. One can see that this rate can be achieved at 120 Hz repetition rate, pulse width below 0.5 µs, and an electric current of 13.3 µA. The charge state (5+) is preferred to avoid mixture with other ion species (for example, oxygen) from the ion source plasma into the beam. To get the required particle rate for protons at the same duty cycle, the pulse current should be about 27 µA, which can be easily achieved with an ECR source at DC mode.

The DC beam from the ion source should be chopped into 0.5 µs pulses. For the beam dynamics simulation, we assumed transverse normalized 90%-emittance of 0.35 π·mm·mrad, which is similar to the value from commercially available ECR ion sources [4].

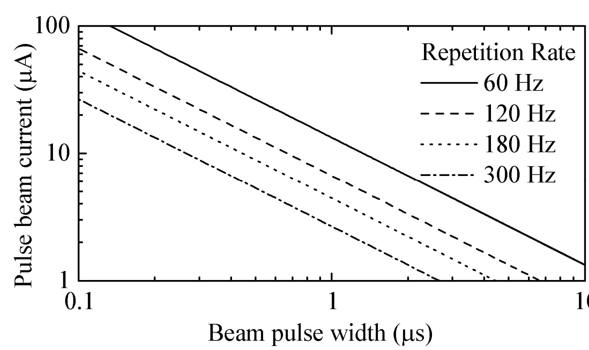

Figure 1: Pulse beam electric current required to provide 10^9 carbon $^{12}C^{5+}$ ions per second.

RFQ

In the front-end, we propose to develop an RFQ based on the brazed technology [5-7] to meet the alignment specifications. The RFQ accelerates the carbon $^{12}C^{5+}$ ion beam to 3 MeV/u on the length L = 4 m. The operating frequency f = 476 MHz provides a reliable accelerating gradient, moderate field sensitivity to local random errors of resonator geometry, which scales as $(f\cdot L)^2$ [8], and effective beam acceptance into the sections of higher frequencies. The foil following the RFQ is used to provide fully stripped carbon $^{12}C^{6+}$ ions from $^{12}C^{5+}$.

EPICS IOC PROTOTYPE OF FRIB MACHINE PROTECTION SYSTEM*

L. Wang†, M. Davis, Z.Y. Li, S. Zhao, G.B. Shen, M. Ikegami, FRIB, East Lansing 48823, USA

Abstract

The FRIB Machine Protection System (MPS) is designed to protect accelerator components from damage by the beam in case of operating failure. MPS includes master and slave nodes, which are controlled by MPS IOC. In this paper, we present design of MPS IOC and status of its prototyping.

INTRODUCTION

The FRIB MPS includes one master and fifty-six slave nodes, and it is to be aware of the machine mode/beam mode/ion type and constantly monitors critical signals. Once the condition to stop beam under the selected machine mode/beam mode/ion type is detected, it issues command to evoke the mitigation devices to switch off beam. MPS interfaces with all devices that require to stop beam quickly. It interfaces with Run Permit System (RPS), Global Timing System (GTS) and MPS IOC as well [1]. MPS IOC communicates with MPS nodes via a customized UDP-based protocol, which is shared by a couple of FRIB UDP-based subsystems and includes the definition of register access, waveform upload, flash memory access and DDR raw data upload. The function of MPS IOC includes register control, remote update of FPGA firmware and DDR raw data transfer. MPS IOC is developed based on asynPortDriver module and the GUI is developed with CS-Studio BOY.

SYSTEM OVERVIEW

There are three virtual machines used for MPS IOC: master IOC, slave IOC and CS-Studio OPI. Master IOC communicates with master node and slave IOC communicates with all the fifty-six slave nodes. MPS network architecture is shown in Fig. 1. Each node has a static IP address, and each IOC can be configured which node to communicate with.

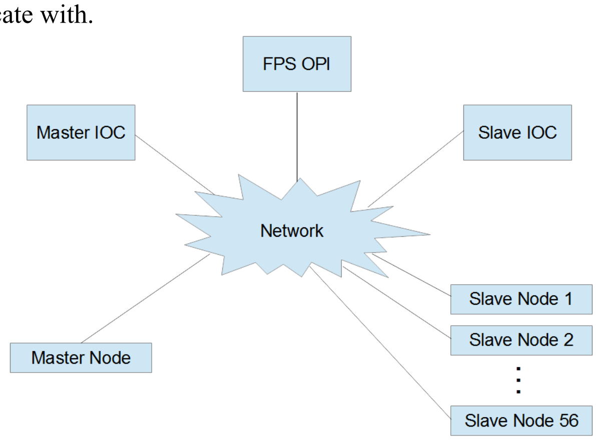

Figure 1: MPS Network Architecture

* Work supported by the U.S. Department of Energy Office of Science under Cooperative Agreement DE-SC0000661
† wanglin@frib.msu.edu

MPS master and slave nodes are separate hardware controllers and provide UDP control interface, so MPS IOC is required to control MPS controllers via UDP packets. The required functions for MPS IOC are as follows:

- Set/read status and parameters in MPS controllers.
- Remotely update the FPGA firmware in MPS controllers.
- Transfer up to 256MB of DDR raw data from each MPS controller to MPS IOC in an acceptable time period.

LCP PROTOCOL

LCP (LLRF Control Protocol) is a UDP-based application layer protocol originally defined by FRIB LLRF (Low-Level Radio Frequency) and is so far also used for FRIB MPS and Prebuncher systems.

Command Definition

It defines register read/write, waveform upload, persistent memory erase/read/write and DDR raw data upload UDP commands for communication between driver and controllers. Each command has request and response packets, which have defined format.

Register Definition

LCP defines three groups of registers: read-only, write-anytime and write-once. All of them are read from controllers periodically, write-anytime register is written to controllers periodically and write-once register is written to controllers only if its value is changed and the writing command is sent only once.

Two threads are responsible for reading or writing data from or to controllers. Sync thread is used in request/response mode and async thread is used in streaming mode. In request/response mode, the sent and received packet are in pair, whereas in streaming mode, one packet that specifies response interval is sent, after which the response packet is received periodically. LCP infrastructure is shown in Fig. 2, the communication between LCP driver and controller and the one between LCP driver and EPICS record are asynchronous.

Implementation

The source code of LCP is divided into two parts:

- LCP protocol layer: a C++ base class, which is derived from asynPortDriver class and is responsible for UDP communication with controllers. Different LCP-based drivers share this part.
- Application layer: a C++ derived class, which handles application-specific issues like register definitions and data process. Different LCP-based drivers build their own copies of this part.

ISBN 978-3-95450-169-4

FIRST PERFORMANCE TEST ON THE SUPERCONDUCTING 217 MHz CH CAVITY AT 4.2 K*

F. Dziuba[†,1], M. Amberg[1,3], W. Barth[2,3], M. Basten[1], M. Busch[1], H. Podlech[1], M. Miski-Oglu[2,3]

[1]IAP University of Frankfurt, 60438 Frankfurt am Main, Germany
[2]GSI Helmholtzzentrum, 64291 Darmstadt, Germany
[3]Helmholtz Institute Mainz (HIM), 55099 Mainz, Germany

Abstract

At the Institute for Applied Physics (IAP) of Frankfurt University a superconducting (sc) 217 MHz Crossbar-H-mode (CH) cavity [1] with 15 accelerating cells and a gradient of 5.5 MV/m has been designed. The cavity is the key component of the demonstrator project at GSI which is the first stage to a new sc continuous wave (cw) linac for the production of Super Heavy Elements (SHE) in the future. A successful and reliable beam operation of this first prototype will be a milestone on the way to the proposed linac. After fabrication at Research Instruments (RI) GmbH, Germany, the cavity without helium vessel has been commissioned at the new cryogenic test facility of the IAP with low level rf power at 4.2 K. The results of this first cold test will be presented in this contribution.

INTRODUCTION

Since in future the existing UNILAC (Universal Linear Accelerator) will be used as an injector for the FAIR (Facility for Antiproton and Ion Research) project, a new dedicated sc cw linac at GSI is proposed to keep the SHE program at an international high level. In this context, a sc 217 MHz CH cavity [2] (see Fig. 1) consisting of 15 accelerating cells, with $\beta = 0.059$ and an effective length of 612 mm (see Tab. 1) has been designed which serves as a first prototype to demonstrate its reliable operability under a realistic accelerator environment. Additionally, the cavity is equipped with nine static and three dynamic tuners to compensate frequency changes caused by manufacturing accuracy during the production phase or to adjust the frequency accordingly during operation [4]. Several flanges in each quadrant of the cavity allow an adequate surface processing. For future beam tests, the cavity will be fed with a 5 kW cw power coupler which is currently ready for rf conditioning. The beam dynamics layout of the cavity is based on the special EQUUS (EQUidistant mUlti-gap Structure) [3] concept. Nevertheless, after latest surface preparation steps the new cavity has been extensivley tested with low level rf power at 4.2 K. Afterwards, a helium vessel made from titanium was welded to the cavity to provide a closed helium circulation.

* Work supported by GSI, HIM, BMBF Contr. No. 05P15RFRBA, EU Project MYRTE

† dziuba@iap.uni-frankfurt.de

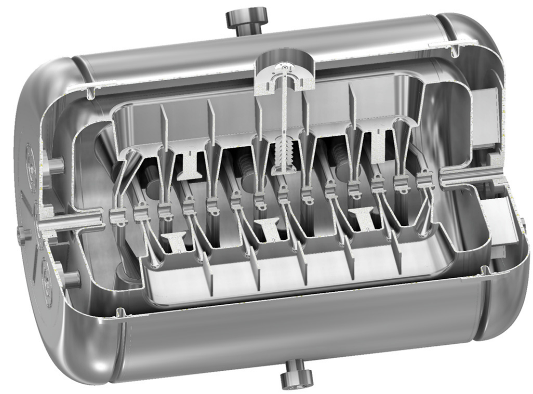

Figure 1: 3D model of the sc 217 MHz CH cavity.

Table 1: Main Parameters of the Cavity

β		0.059
Frequency	MHz	216.816
Accelerating cells		15
Effective length ($\beta\lambda$)	mm	612
Diameter	mm	409
Tube aperture	mm	18 / 20
G	Ω	52
R_a/Q_0		3240
$R_a R_S$	kΩ^2	168
E_a (design)	MV/m	5.5
E_p/E_a		6.3
B_p/E_a	mT/(MV/m)	5.7

EXPERIMENTAL SETUP

At the experimental hall of the IAP a new cryogenic laboratory has been installed for various test purposes of different sc CH cavities allowing performance measurements with low level rf power at 4.2 K and 2.1 K, respectively. The sc 217 MHz cavity was tested at 4.2 K in a vertical cryostat which is surrounded by a radiation cave (see Fig. 2). During the cold test the helium gas was collected by a recovery system. A 50 W broadband amplifier delivered the forward power to the cavity. Further equipment like the rf generator, the rf control system, scopes, power meter, a network analyzer, a piezo amplifier and a spectrum analyzer was arranged in four racks on top of the radiation cave. As shown by Figure 3, the cavity has been provided with seven temperature probes and 60 Thermo-Luminescence-Dosimeter

ISBN 978-3-95450-169-4

OPERATION MODE AND MACHINE STATE CONTROL FOR FRIB DRIVER LINAC OPERATION *

M. Ikegami†, D. Dudley, M. Konrad, Z. Li, G. Shen, V. Vuppala
Facility for Rare Isotope Beams, Michigan State University, MI 48824, USA

Abstract

FRIB (Facility for Rare Isotope Beams) is a heavy ion linac facility to accelerate all stable ions to the energy of 200 MeV/u with the beam power of 400 kW, which is under construction at Michigan State University in USA. It is one of major challenges in FRIB to clearly define operation modes and machine state and to develop a controls system to realize safe and high beam availability operation with various operation modes required from physics experiments. To this end, it is indispensable to have clear definition of operation modes and machine states with appropriate management of transition of those. RPS (Run Permit System) is one of major application software to play a pivotal role to meet the requirement, which helps operators to follow adequate procedures depending on operation mode and machine state. In this paper, we overview main features of RPS for FRIB together with operation modes and machine states to define operation procedures.

INTRODUCTION

The Facility for Rare Isotope Beams (FRIB) is a high-power heavy ion accelerator facility now under construction at Michigan State University under a cooperative agreement with the US DOE [1]. Its driver linac operates in CW (Continuous Wave) mode and accelerates all stable ions to kinetic energies above 200 MeV/u with the beam power on target up to 400 kW. It aims to realize the world highest beam power as a heavy ion linac facility and it is one of major challenges to develop a controls system to support its safe operation with high beam availability. Figure 1 shows a schematic layout of FRIB driver linac.

As a heavy ion accelerator facility, various operation modes are expected with different ion species, beam energy, and so on to meet requirements from physics experiments. At the same time, as a high power accelerator, mitigation of hazards and risks of component damage are major challenges. To meet this requirement, we define operation modes and machine states with their transition procedures, which is basis for establishing safe operation. We also designed Run Permit System (RPS) to help operators to follow the established procedures mitigating risks of operational errors. In this paper, we present operation modes and machine states transitions together with main design features of RPS.

* Work supported by the U.S. Department of Energy Office of Science under Cooperative Agreement DE-SC0000661
† ikegami@frib.msu.edu

MACHINE MODES AND BEAM MODES

In nominal operation, the primary beam is delivered to the target and the secondary beam generated at the target is delivered to an experimental beam line. However, the beams can be delivered to other destinations such as linac beam dumps during beam tuning. We introduce two basic modes of operation, namely, Machine Modes and Beam Modes, to define basic operation envelope. Machine Modes define the area with beam as summarized in Table 1. In each Machine Mode, critical devices define the area with beam. Beam Modes define beam time structure and the maximum peak intensity or beam power. An extracted list of major Beam Modes is shown in Table 2. In nominal operation, CW beam is accelerated. However, we use different beam time structure, such as 50 μs pulse with 1 Hz repetition rate, for tuning purposes. Machine Modes and Beam Modes define a basic set of operation parameters which are sufficient to ensure that the operation is within safe envelope. However, more detailed information is required to adequately configure Machine Protection System (MPS) to protect machine such as information on which of four beam dumps in linac tunnel is in use in Machine Mode M2. It should be noted that Personnel Protection System (PPS) controls Machine Mode as it is closely related to access control.

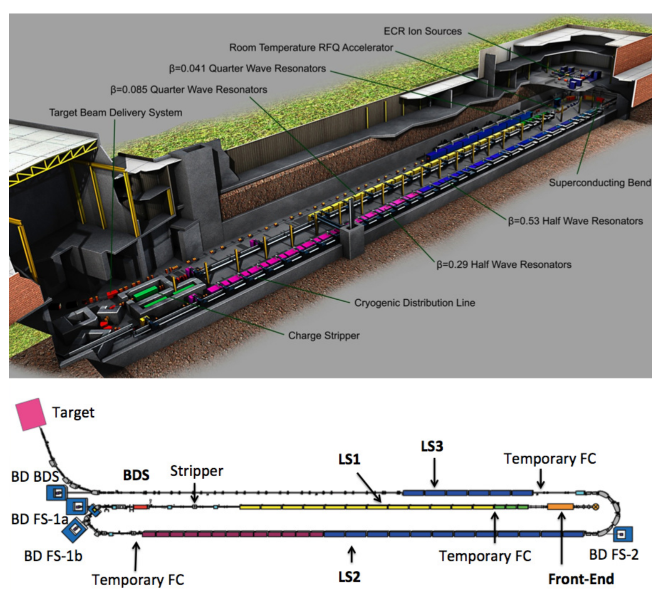

Figure 1: Layout of FRIB driver linac. Top: Cut view of FRIB driver linac building. Bottom: Schematic layout for the FRIB driver linac (top view).

FRIB FAST MACHINE PROTECTION SYSTEM: ENGINEERING FOR DISTRIBUTED FAULT MONITORING SYSTEM AND LIGHT SPEED RESPONSE *

Z.Y. Li †, B. Dalesio, L. Wang, M. Ikegami, S.M. Lidia, S. Zhao, Facility for Rare Isotope Beams, East Lansing, Michigan, USA

Abstract

The Facility for Rare Isotope Beams (FRIB), a high-power, heavy ion facility, can accelerate beam up to 400 kW power with kinetic energy ≥ 200 MeV/u. Its fast protection system is required to detect failure and remove beam within 35 µs to prevent damage to equipment. The fast protection system collects OK/NOK inputs from hundreds of devices, which are distributed over 200 m. The engineering challenge here is to design a distributed control system to collect status from these devices and send out the mitigation signals within 10 µs timing budget and also rearm for the next pulse for 100 Hz beam (10 ms). This paper describes an engineering solution with a master-slave structure adopted in FRIB. Details will be covered from system architecture to FPGA hardware platform design and from communication protocols to physical interface definition. The response time of ~8µs from OK/NOK inputs to mitigation outputs is reached when query method is used to poll the status. A new approach is outlined to use bi-direction loop structure for the slave chain and use streaming mode for data collection from slave to master, ~3µs response time are expected from this engineering optimization.

INTRODUCTION

The Facility for Rare Isotope Beams (FRIB), a high-power, heavy ion facility, can accelerate beam up to 400 kW power with kinetic energy ≥ 200 MeV/u [1][2][3]. A Machine Protection System (MPS) minimizes component damage and operational interruption caused by both acute (fast) and chronic (slow) beam losses [1]. The fast protection system collects OK/NOK inputs from hundreds of devices, such as low level RF controllers, beam loss monitors, and beam current monitors, which are distributed over 200 m. The engineering challenge here is to design a distributed control system to collect status from these devices and send out the mitigation signals within timing budget, also quickly rearm for the next pulse for 100 Hz beam. This paper describes an engineering solution with a master-slave structure adopted in FRIB. Details will be covered from system architecture to FPGA hardware platform design and from communication protocols to physical interface definition, from system prototype to its function verification test results.

SYSTEM ARCHITECTURE

FRIB MPS [3] displayed in Fig. 1 consists of the FPS network, MPS sensors, MPS mitigation devices, and MPS Input Output Controllers (IOCs) [4]. Run Permit System function is needed to start the beam but is separated from MPS system. Time-critical sensors and mitigation devices are connected directly to MPS network. Non-time-critical sensors are connected to MPS network via aggregation PLCs.

For 100% beam loss at full power, or faults other than beam loss, MPS must turn off the beam in a maximum of 35 µS in order to avoid any severe damage to the machine. Response time of 35 µs is based on Analysis of Beam Damage to FRIB Driver Linac. The allocation of response times for FPS will be determined during commissioning. Design goals are:

- 10 µs for device to detect a failure and to inform MPS network about it (including cable delay)
- 10 µs for MPS network to identify the right mitigation action(s) and to distribute the signal to appropriate output(s)
- 5 µs for mitigation device to receive signal and to execute mitigation action (including cable delay)
- 10 µs for beam mitigation time (residual beam in the accelerator)

FPS consists of FPS master, FPS slaves and fiber patch panels. FPS master is linked with each FPS slave chain with one string of fiber from fiber trunk routed between fiber patch panels. FPS shares the fiber trunks and patch panels with Global Timing System (GTS) and network system.

The FRIB machine offers the following mitigation actions which must be controllable from MPS:

A) Remove high voltage from both front end vertical electrostatic dipoles (E-bends). This mitigation action shall take less than 1 µs.

B) Trip Chopper control system to apply deflector voltage to the chopper in the Low Energy Beam Transport system (LEBT) to stop the beam. This mitigation action shall take less than 1 µs.

C) Disable the ECR ion source extraction high voltage via fiber link. This mitigation action shall take less than 50 ms.

FRIB MPS is designed with four operation states:

- Disabled: Status of MPS sensors is not monitored. Mitigations A and B are activated regardless of the sensor inputs.
- Monitor-only: Status of MPS sensors is monitored. Mitigations A and B are activated regardless of the sensor inputs.

* Work supported by Work supported by the U.S. Department of Energy Office of Science under Cooperative Agreement DE-SC0000661.

† liz@frib.msu.edu

THE BEAM ENERGY FEEDBACK SYSTEM IN BEIJING ELECTRON POSITRON COLLIDER II LINEAR ACCELERATOR

S. Wang†[1], X. Huang[1], Y. Chi, Key Laboratory of Particle Acceleration Physics and Technology, IHEP, CAS, Beijing 100049, China
[1]also at University of Chinese Academy of Sciences, Beijing 100049, China

Abstract

The beam energy feedback system in Beijing electron positron collider II (BEPCII) linear accelerator consists of three parts. They are the beam energy measurement Input/Output Controller (BEM IOC), the Graphical User Interface (GUI) based on Qt platform and the phasing system. This article describes the implementation of this system and the online testing which has been passed on March 16th, 2016. By using this feedback system, the injection rate and the energy fluctuation of the injection beam has been improved a lot. Now this system is steady running in the control room of BEPCII linear accelerator.

INTRODUCTION

Beijing electron positron collider has been upgraded into Beijing electron positron collider II. Its storage ring has the higher demand on the quality of the beam at the exit of the linear accelerator [1]. While in the long time operation of the linear accelerator, the drift of the centre energy cannot be avoided. When the beam energy is out of the range, the injection rate will drop rapidly. To suppress the fluctuation of the beam energy at the exit of the linear accelerator and make the whole accelerator run stably, a beam energy feedback system has been developed. This system compensates the drift of the beam energy by making a local adjustment of the energy gain.

To realize the function of beam energy feedback, we first set up a kind of online beam energy measurement mechanism at the exit of the linear accelerator [2]. Then the measurement results together with the target values are sent to calculate the controlled quantity. By using the controlled quantity as the input of the actuator, the beam energy can then be adjusted. Because the klystron is working on the saturation condition, its variation of output power resulted from the variation of driving voltage is very small. To change the energy gain, the only thing we should do is to adjust the accelerating phase of klystron. Therefore, we choose the accelerating phase of klystron K16, the last klystron at the end of the linear accelerator, as the controlled quantity.

COMPOSITION

The schematic diagram of the beam energy feedback system in BEPCII is shown in Fig. 1. This system consists of three parts. They are the IOC controller for beam energy measurement (BEM), the GUI application and the phasing system.

† wangsz@ihep.ac.cn

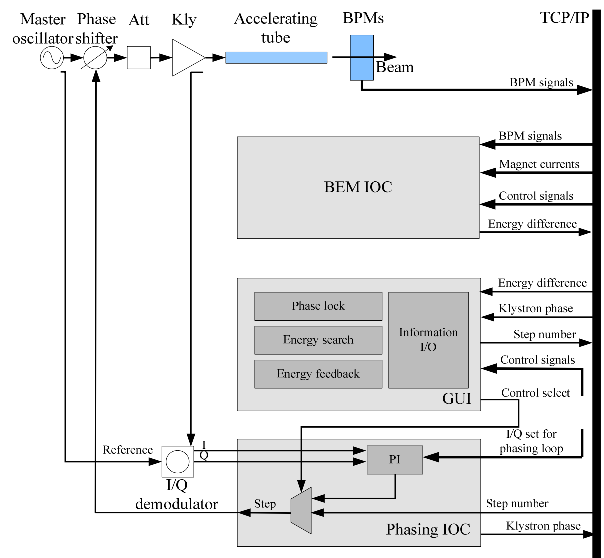

Figure 1: The schematic diagram of the beam energy feedback system in BEPCII LINAC.

The BEM IOC

The BEM IOC uses a kind of online beam energy measurement method. During the injection, the IOC acquires the data from the relevant channels of the EPICS [3], calculates the difference between the actual energy and the nominal energy by using certain programs, and sends the difference to the Ethernet via EPICS channels. The GUI application can then utilize the data come from the local area network.

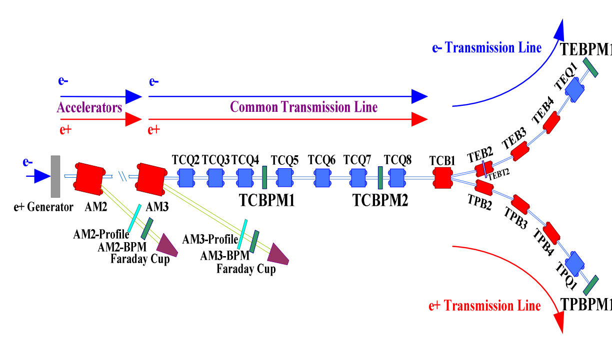

Figure 2: The layout diagram of the BPMs and the magnets at the end of BEPCII LINAC.

The data acquired by the BEM IOC are mainly the beam positions measured by TCBPM1, TCBPM2, TE/PBPM1 and the magnet currents between them (the positions of the BPMs and the magnets are shown in

DEVELOPMENT OF A DIGITAL LLRF CONTROL SYSTEM AT LNL

S. Pavinato*, M. Betti, D. Bortolato, F. Gelain, D. Marcato,
D. Pedretti, INFN, Laboratori Nazionali di Legnaro, 35020 Legnaro,Italy
M. Bellato, R. Isocrate, INFN, Sezione di Padova, 35031 Padova, Italy
M. Bertocco, Department of Information Engineering, University of Padova, 35031 Padova, Italy

Abstract

The new Low-Level Radio Frequency (LLRF) control system for linear accelerator at Legnaro National Laboratories (LNL) of INFN is presently being commissioned. A digital Radio Frequency (RF) controller was implemented. Its goal is to stabilize the amplitude, the phase and the frequency of the superconducting cavities of the Linac. The resonance frequency of the low beta cavities is 80 MHz, while medium and high beta cavities resonate at 160 MHz. Each RF controller controls at the same time eight different cavities. The hardware complexity of the RF controller (RF IOC) is reduced by adopting direct RF sampling and the RF to baseband conversion method. The main hardware components are RF ADCs for the direct undersampling of the signals picked up from cavities, a Xilinx Kintek 7 FPGA for the signal processing and DACs for driving the power amplifiers and hence the cavities. In the RF IOC the serial communication between FPGA and ADCs and between FPGA and DACs is based on JESD204b standard. An RF front-end board (RFFE) is placed between cavities and the RF IOC. This is used to adapt the power level of the RF signal from the cavities to the ADCs and from the DACs to the power amplifiers. This paper addresses the LLRF control system focusing on the hardware design of the RF IOC and RFFE boards and on the first test results carried out with the new controller.

INTRODUCTION

The superconducting linear accelerator ALPI [1] requires a significant RF field stability in phase, amplitude and frequency to ensure the best energy gain of the accelerated beam. The resonance frequency of a first group of ALPI cavities is 80 MHz, while that of a second group is 160 MHz. The cavities act as filters, with an high quality factor. In order to keep the RF field stable in the cavities, amplitude and phase have to be controlled to compensate the impact of microphonic perturbations.

RF CONTROLLER

In order to improve the stability of the RF field in the cavities a new RF control system has been developed [2]. The new digital RF controller system has been designed exploiting the performances of commercial components like RF ADCs, FPGA and DACs. It is based on direct sampling of RF signal and digital signal processing with FPGA. This allows a greater flexibility in programming and diagnostic capabilities, since it is possible to monitor many signals during the processing of the data inside the FPGA, like amplitude and phase of the RF fields in cavities.

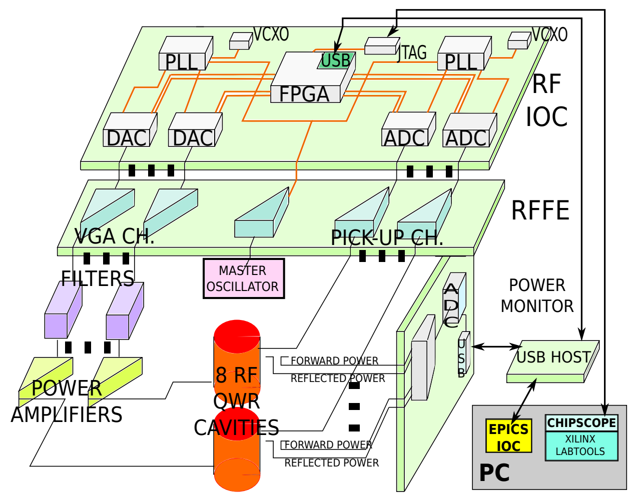

Figure 1: Block diagram of the LLRF system.

A block diagram of the LLRF control for the cavities is represented in Fig. 1. It is based essentially on three boards: the RF input-output controller (RF IOC), the RF front end (RFFE) and the power monitor that measures the reflected and forward powers of the eight controlled cavities. These boards are housed in a single box as shown in Fig. 2. In the RF IOC the signals coming from the cavities are amplified through the RFFE board and then undersampled and digitized. These signals are digitized using the IQ method. As reported in [2] the sampling rate of the ADCs has been chosen so that $f_s = D \times 4 f_{RF}/(4 \times k + 1) = 121.9$ MHz, with D the decimation factor, f_{RF} the resonance frequency and $k = 5$. After processing in the FPGA, the signals are reconverted in analog form, filtered by Helical Resonator filters, amplified via the RFFE and sent to the power amplifiers. To simplify PCB design the communication between FPGA and converters is based on JESD204b serial interface. The control algorithms described in [2] are implemented in the FPGA and written in VHDL code. Fixed-point arithmetic has been preferred over floating-point arithmetic because of its convenience in FPGA implementation.

RF IOC

The RF IOC, Fig. 3, is essentially composed of four high linearity dual channel 16-bit, 250 MSPS analog-to-digital converters ADS42JB69, a Xilinx Kintek 7 FPGA in which the LLRF logic is implemented using VHDL code and four

* stefano.pavinato@lnl.infn.it

TUNING THE IFMIF 5 MEV RFQ ACCELERATOR

Antonio Palmieri, Francesco Grespan, Andrea Pisent, INFN-LNL, Legnaro (PD), Italy

Abstract

In order to allow proper operation of the IFMIF RFQ, it is necessary to perform a campaign of RF measurements on the cavity aimed, on one hand, at determining the basic RF parameters (frequency, Q_0, etc.), on the other hand at verifying the fulfilment of the voltage law within the specified admitted range (±2% target value, ±4% acceptance value) of any of the perturbative components upon successive tuner settings as predicted by the tuner algorithm. These measurements also involve the determination of the proper depth of the end plates and the positioning and length of the Dipole Stabilizers (if any). In this contribution the tuning procedure and the results of such measurements will be presented for the case of the IFMIF RFQ will be described.

INTRODUCTION

The tuning of the whole 9.9 m, 175 MHz IFMIF RFQ [1] was completed at the IFMIF-BA Rokkasho site (Japan) and all the 108 slug tuners were machined to length and installed. The diameter of each tuner and RF port is equal to 90 mm and the diameter of each tuner is equal to 89 mm. The tuner depths inside the RFQ volume were determined by iterative application of the tuning algorithm [2]. The RF measurements were performed with the bead pulling perturbation technique, by making use of aluminum ogive-shaped beads 16 mm diameter and 60 mm length placed on each quadrant bisector at 170 mm height from the beam axis, 50 mm clear from RFQ upper walls. In this way it is possible to measure the quantity

$$v_{sl}=\sqrt{\left(\frac{\mu_0}{2}\right)|\mathbf{H}|^2-\varepsilon_0\ |\mathbf{E}|^2}$$

Then the vane voltages in each quadrant $V_1(z)$, $V_2(z)$, $V_3(z)$ and V_4 (z) are inferred from this quantity by comparison to SUPERFISH calculations. Finally, the three modal components $V_q=(V_1+V_2+V_3+V_4)/2$, $\delta V_{qd1}=(1/\sqrt{2})*(V_1-V_3)$ and $\delta V_{qd2}=(1/\sqrt{2})(V_2-V_4)$ can be determined. The beads are moved along the RFQ with the usage of a set of four motors in dc that are computer controlled with LABVIEW. Such motors move through a system of pulleys four dielectric threads of 0.8 mm diameter. All the bead-pull measurements were performed with an Agilent E5071C Vector Network Analyzer by measuring the phase shift of the S_{21} parameters at the resonant frequency.

Before assembly of the whole RFQ [3], all the 18 mechanical modules (550 mm each) were separately RF and mechanically tested along their production phases [4]. It is worth noticing that the RFQ consists of 1 e.m. segment, therefore no coupling cells are foreseen.

TUNING STEPS

In the initial setup the RFQ was equipped with dummy aluminum tuners and with dummy end plates. Each end plate can be inserted in the RFQ volume in the range 0-25 mm (with the exception of 180 mm diameter around beam axis), in order to allow boundary condition tuning as well. Measurement Step 0 consisted of the determination of mode Spectra and field profile with tuner flush and dummy end plates at nominal insertion of $h_{EC1}=h_{EC2}=12$ mm on both sides of the RFQ. The TE_{210} Quadrupole mode frequency fq_0 was equal to 174.250 MHz. This result has to be compared with the theoretical value of 174 MHz and is in good agreement with the estimation of 174.33 MHz obtained by considering the outcomes of the RF and mechanical measurements of all the 18 modules [3]. Moreover, the dipole-free region is quasi-symmetric, since the frequencies of the neighbouring D modes fd_2 and fd_3 are equal to fq_0-1.9 MHz and fq_0+1.5 MHz respectively. The results of this measurement are shown in Fig. 1.

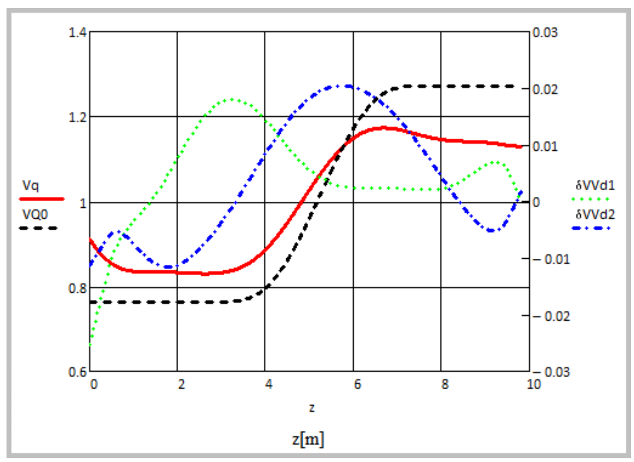

Figure 1: The modal voltage component (A.U.) vs z[m] measured with flush tuners and end plates at nominal settings. Vq and Vq0 are the measured and the nominal voltage, respectively. The components are normalized to 1. The dipole components are in the secondary scale for ease of reading.

From this measurement it is possible to notice that the quadrupole perturbation $\delta V_q=V_q-V_{q0}$ is within ±0.2 V_{q0} and that dipole perturbations are already within the specs; this is a confirmation of the dipole-free region symmetry. Therefore the installation of dipole stabilizing rods was skipped and none of such devices was put in place.

In the following Step 1 the depths of the end plates were changed in order to get the proper boundary conditions and to make the curve Vq(z) get closer to Vq0(z). In this phase

ISBN 978-3-95450-169-4

IFMIF RFQ MODULE CHARACTERIZATION VIA MECHANICAL AND RF MEASUREMENTS

Luigi Ferrari, Antonio Palmieri, Andrea Pisent, INFN-LNL, Legnaro (PD), Italy
Razvan Dima, Adriano Pepato, Alessandro Prevedello, Emil Udup INFN- Sez. di Padova, Padova, Italy

Abstract

The RFQ of the IFMIF/EVEDA [1] project is a 9.9 m long cavity able to accelerate a 130 mA deuteron beam from the input energy of 100 keV to the output energy of 5 MeV. Such RFQ operates at the frequency of 175 MHz and is composed of 18 mechanical modules approximately 0.55 m long each [2]. The RFQ realization involves the INFN. Sections of Padova, Torino and Bologna, as well as the Legnaro National Laboratories (L.N.L.). The metrological measurements via CMM (Coordinate Measuring Machine) provided to be a very effective tool both for quality controls along the RFQ production phases and in the reconstruction of the cavity geometric profile for each RFQ module. The scans in the most sensitive regions with respect to RF frequency, such as modulation, tips, base-vane width and vessel height provided the values of the cavity deviations from nominal geometry to be compared with design physic-driven tolerances and with RF measurements. Moreover, the comparison between mechanical and RF measurements suggests a methodology for the geometric reconstruction of the cavity axis and determines the final machining of the end surfaces of each module in view of the coupling with the adjacent ones. In this paper a description of the meteorological procedures and tests and of the RFQ along its production and assembly phases will be described.

IFMIF RFQ DESCRIPTION

One of the fundamental components of the IFMIF-EVEDA facility, being installed at the site of Rokkasho in Japan is the RFQ (radio Frequency Quadrupole) composed of 18 mechainical modules divided in 3 Supermodules, of 6 modules each. The main RFQ parameters are listed in Table 1. Due to the extremely high current value, the attainment of beam loss control is of paramount importance in such structure. Now, beam loss is determined basically by geometrical tolerances, in three different ways: vane modulation machining (± 0.02 mm), beam axis accuracy along the accelerator, and voltage law accuracy along the structure. In the following this last aspect will be taken into account. The attainment of voltage accuracy within the specified values is determined by the local cross section shape and local cut off frequency mainly depending on pole tip positioning (capacitance between electrodes) [3]. This aspect needs to be checked along both the machining and the brazing phase is the last process that can permanently affect the cross section.

Table 1: IFMIF RFQ Main Parameters

Frequency [MHz]	175
Length [m]	9.8
R_0[mm]	4.13-7.1
ρ/R_0	0.75
Beam Current [mA] (CW)	125
Beam Transmission (Gaussian)	93.7%
Beam Losses [W]	1291
V [kV]	79-132
W [MeV/u]	2.5
$\Delta V/V$ range	± 2% (target value),
Q_0	12000 (25% margin)
RF power [kW] (CW)	1250 (25% margin)

The main construction steps of each RFQ module are organized in the following phases (Fig.1):1: Deep drilling, 2: Electro Discharge Cutting3: Rough Milling 4: Finish Milling 5 Electrode brazing 6 : Corner TIG welding 7: Front face and external references final milling for module alignment.

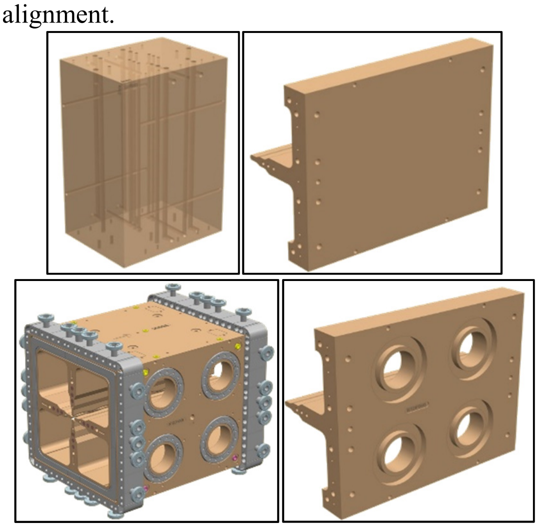

Figure 1: Component geometries along the production phases: 1 ,2, 3,7 (clockwise, from top left).

HIGH-POWER RF TEST OF IFMIF-EVEDA RFQ AT INFN-LNL

Enrico Fagotti, Loris Antoniazzi, Mauro Giacchini, Francesco Grespan†, Maurizio Montis, Antonio Palmieri, INFN/LNL, Legnaro, Italy

Abstract

A partial test at full power and CW duty cycle was performed at INFN-LNL on the last elements of the IFMIF RFQ, approximately two meters of structure, using a specific electromagnetic boundary element on the low energy end. The aim is to reach, in the RFQ coupled with its power coupler system, after an adequate period of conditioning, CW operation at nominal field level (132 kV between electrodes) for at least two hours without breakdown. The description of the experimental setup and procedure, as well as the main results of the conditioning procedure are reported in this paper.

INTRODUCTION

The main goals of the IFMIF RFQ high power test are summarized in the machine state diagram in Figure 1:

1. The RF CONDITIONING of the cavity, performed in Frequency Follower Mode (FF), to prove the RFQ operation at full power regime;
2. The setting up of nominal parameters of the system (temperatures, valve opening, frequency) which identifies the START-UP condition for the cavity;
3. The demonstration of stable operation of the system in RESONANT FREQUENCY CONTROLLED (RFC) mode.

EXPERIMENTAL SETUP

The RFQ was transported from LNL-LAE building to the LNL 3rd experimental hall in November 2014 and it was placed in the test tunnel by crane (Figure 2). This transfer gave the opportunity to verify the maintenance of the field flatness after transport. Figure 3 shows a difference of 0.5% between the two, which is within the measurement accuracy.

In the tunnel the RFQ was baked out, by using a dedicated equipment composed of insulation panels and blower. After 8 days at 100°C, the cavity showed a final vacuum level of 8 x 10^{-9} mbar.

The test was performed between December 2014 and February 2015. The systems involved in the test are:

- The RFQ cavity, composed of the last 3 modules of the IFMIF RFQ (module 16-17-18) and Prototype 2 as boundary element on the low energy end. The Cavity Length was 2.021m (Figure 2).
- The RF power system [1], composed of 175 MHz – 220 kW CW amplifier based on the TH781 tetrode, coaxial wave-guide line, AFT circulator from CIEMAT;
- The Vacuum system, which includes a rough dry pump and turbo pump as pre-vacuum stadium, a cryogenic pump as main pump and an ionic pump as back-up in case of cryo-pump failure or purge.;
- The Cooling system, consisting of a water skid with 2 independent cooling circuits (warm circuit and cold circuit), to finely tune the resonant frequency by temperature regulation.

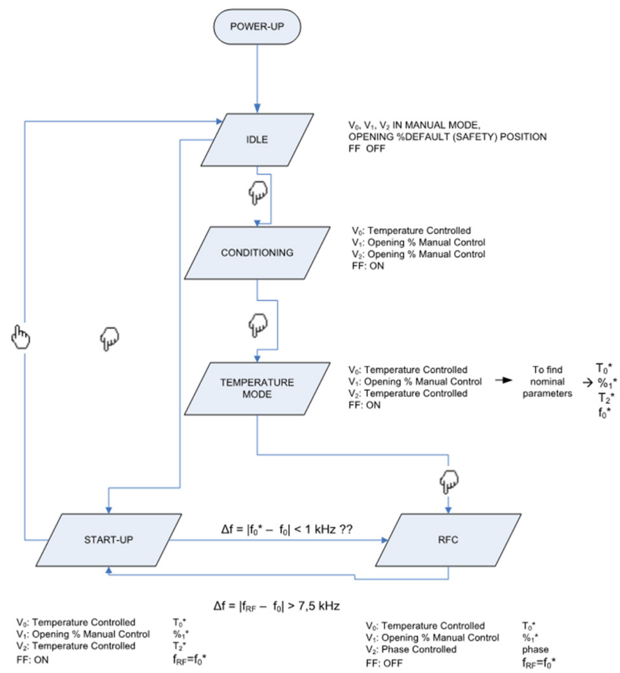

Figure 1: machine state diagram for the IFMIF RFQ high power test. V_0=input valve, V_1=cold circuit valve, V_2=warm circuit valve, FF=RF frequency follower, FLC=field level control, RFC=Resonant frequency control, f_{RF}=RF generator frequency, f_0=cavity resonant frequency.

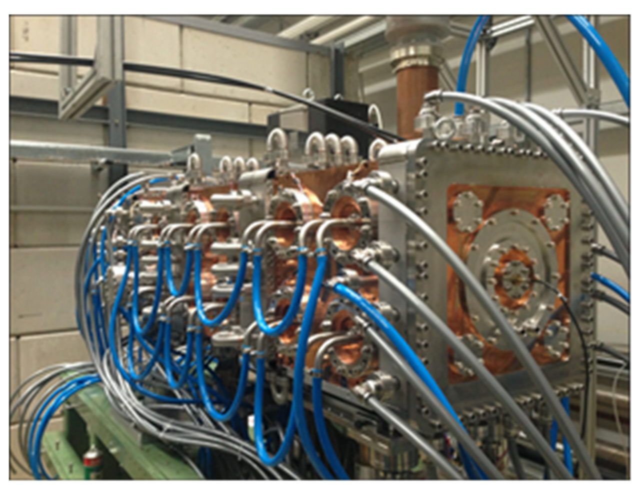

Figure 2: A view of IFMIF RFQ test-bench in the IFMIF tunnel at INFN-LNL.

ISBN 978-3-95450-169-4

RECENT RF AND MECHANICAL DEVELOPMENTS FOR THE ESS RFQ

N. Misiara, A. Albéri, A.-C. Chauveau, D. Chirpaz-Cerbat, G. Bourdelle, M. Desmons, A. France, M. Lacroix, J. Neyret, P.-A. Leroy, G. Perreu, O. Piquet, B. Pottin, H. Przybilski, N. Sellami
CEA/DRF/IRFU/SACM-SIS, Gif-sur-Yvette, France

Abstract

The ESS Radio-Frequency Quadrupole (RFQ) is a 4-vane resonant cavity designed at the frequency of 352.21 MHz frequency. It must accelerate and bunch a 70 mA proton beams from 75 keV to 3.62 Mev of energy with a 4% duty cycle. The current 3D design evolved and is currently divided in 5 segments for a total length of 4.54 m. This paper presents a complete radiofrequency (RF) analysis using the ANSYS Multiphysics 3D RF simulating code HFSS and a RFQ 4-wire transmission line model (TLM). It describes the integrated cooling strategy based on a coupling between the RF power losses and the thermo-mechanical physics in order to allow a proper RFQ tuning once under operation.

INTRODUCTION

Today's final ESS 4-vanes RFQ design is a 4.54m long, 5-sections resonant cavity including 60 adjustable slugs dedicated to the cavity tuning along with 2 power couplers and 40 ports for pumping and couplers. A review of the ESS-RFQ design status and the scheduled fabrication and testing procedures is presented in [1]. ESS being the latest of the RFQ generation designed and to be commissioned by the CEA-IRFU and delivered at ESS in Lund, Sweden, the 4 steps development strategy detailed in [2] was applied. In this paper, only the steps related to the 2D and 3D RF design and thermal structural optimization of the cavity are presented. The focus is given on the multiphysics workflow established between the RF study in both 2D and 3D models and the thermal mechanical analyses with COMSOL (v3.5) and ANSYS (v14.5) workbench platform.

RF & THERMO-MECHANICAL STUDIES OF THE RFQ CAVITY

RF Optimization and Thermal Management

2D RF calculations were mainly used to optimize the RFQ cross section along the beam axis. Early on, the design targeted a constant vane radius with non-constant ramped voltage and consequently, a non-constant modulation mean value and cavity height (Figure 1). The 3D RF results led to the optimization of the vane end-circuits, tuning slugs, end plate rod lengths and the RF power coupler in order to reach the ESS operation specifications. Finally, a TLM was constructed based on those RF calculations in order to specify the tuning range capabilities of the slugs in correlation with the manufacturing tolerances imposed for the final design. Further details on this optimization are compiled in the final RF design review report [3].

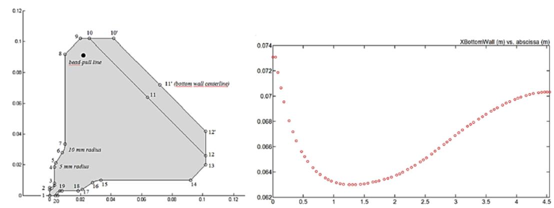

Figure 1: Representation of the ESS-RFQ section with variable cavity back plane height along the beam axis.

The RF power induces a heat deposit in the copper bulk of the RFQ cavity that must be removed through a strategic positioning of cooling channels. The main goal for such cooling system is to limit the cavity deformation and maintain the RFQ frequency and the voltage profile during operation. Although, the cooling strategy for the ESS-RFQ, which is operating under a pulsed-RF mode (nominal duty cycle around 4%; 5% considered in the design phase), is a lesser challenge than continuous wave RFQs such as SPIRAL2, it represents nonetheless an opportunity to verify the workflow between the different numerical tools available for such optimization. Indeed, both COMSOL and ANSYS software provide multiphysics platforms dedicated to studying the coupled effect of RF power dissipation on the structure and reversely the cavity shift in resonance frequency due to the cavity deformation.

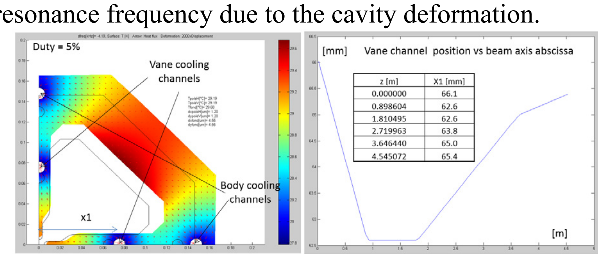

Figure 2: Representation of the 2D deformed section with both channels locations (x1=variable position of vane channel).

COMSOL is appropriate for fast 2D RF, thermal and structural coupled calculations. The 2D study allowed the sizing and the positioning of the cooling channels: two separate circuits (both Ø=10mm) are implemented per section; one for the vane and one for the body, so that the temperature control is possible on each circuit independently. The design criteria is to get the same frequency with and without RF power. One way to satisfy this criteria is to have the same temperature rise along both channels in order to ensure the same transverse deformation for the vane and the cavity back along the RFQ (Figure 2). Those conditions are achieved with a variable position of the inner channels along the beam axis. It is to be noted that the velocity in those channels is limited to 3.2 m/s and they are located so that a minimum of 5 mm

STATUS OF A 325 MHz HIGH GRADIENT CH – CAVITY*

A. M. Almomani† and U. Ratzinger, IAP, Frankfurt University, Germany

Abstract

The reported linac developments aim on compact ion accelerators and on an increase of the effective accelerating field (voltage gain per meter). Within a funded project, a high gradient Crossbar H-type CH – cavity operated at 325 MHz was developed and successfully built at IAP – Frankfurt. The effective accelerating field for this cavity is expected to reach about 13.3 MV/m at a beam energy of 12.5 AMeV, corresponding to β=0.164. The results from this cavity might influence the later energy upgrade of the Unilac at GSI Darmstadt. The aim is a compact pulsed high current ion accelerator for significantly higher energies up to 200 AMeV. Detailed investigations for two different types of copper plating (high lustre and lustre less) with respect to the high spark limit will be performed on this cavity. The 325 MHz GSI 3 MW klystron test stand is best suited for these investigations. Additionally, operating of normal conducting cavities for the case of very short RF pulses will be discussed at cryogenic temperature.

INTRODUCTION

The maximum electric field gain for conventional DTL's is limited by thick walled drift tubes which are housing the focusing elements. Thus, high multipacting risks are expected on the plate capacitor like surfaces around the gaps. The stored energies as well as the risk of spark damages on the cavity surfaces are high. Consequently, quite modest operable field levels have to be chosen.

On the other hand, the slim drift tube geometries in H-mode cavities allow for high effective voltage gains beyond 10 MV/m. This has been demonstrated successfully at CERN linac 3, where the average effective voltage gain reached 10.7 MV/m at 1 ms pulse length [1].

The electric field in H-mode cavities like CH is concentrated on the drift tube structure by the slim drift tube design (Fig. 1). The development of CH – cavities was shown in detail in Ref. [2]. The development of a 70 MeV 70 mA proton linac based on CH – Cavities is currently performed at IAP – Frankfurt together with GSI and is designed with an average effective voltage gain of 3.5 MV/m

The main topic of this paper is focusing on the development of a high field gradient CH – structure [3-5]. These developments will be important in case of a compact linac for low duty factor applications. Moreover, for high current operation the high field gradient acceleration provides the needed longitudinal focusing forces.

Our motivation in this work is to prepare for a later upgrade of the high energy section of the GSI – Unilac. Another motivation is the development of an efficient and compact ion accelerator for medical hospitals where available space is quite limited and proton energies up to around 230 MeV are requested.

CAVITY DEVELOPMENT

To test the field gradient limits of a CH - cavity, a 325 MHz 7 gap prototype (Fig. 1) has been developed and successfully built at IAP – Frankfurt and was fabricated at NTG, Gelnhausen, Germany [3-6]. The structure geometry was optimized for an average effective field gradient reaching up to 13.3 MV/m at β = 0.164. The surface electric field levels are expected to reach about 95 MV/m at very small spots on the 1 mm^2 – levels [6]. The main cavity parameters are given in Table 1.

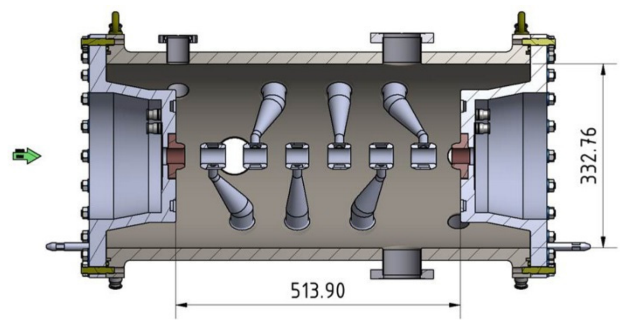

Figure 1: A 3D model for the high field prototype cavity.

Table 1: Main Parameters of the High Field CH – Cavity

Number of Gaps	7
Frequency (MHz)	325.224
Voltage Gain (MV)	6
Eff. Accel. Length (mm)	513.9
Average Eff. Accel. Field (MV/m)	13.3
Power Loss (MW)	1.76
Q_0 – value	12500
Effective Shunt Impedance (MΩ/m)	52.15
Aperture Diameter (mm)	27

The CH – cavity was built from stainless steel and was galvanically copper plated at its inner surface. Two processes with different bath ingredients (high lustre and less lustre copper plating) will be tested against each other at high rf power levels. The main aspect in our case is the sparking limit, besides quality factor, vacuum and rest gas aspects. The first round of copper plating (high lustre) was done at Galvano – T GmbH, Windeck, Germany (Fig. 2).

The drift tube structure was welded into a massive cylindrical tank. The stems with drift tubes are directly water cooled, the cylindrical tank has eight cooling channels in longitudinal direction. The electric and magnetic field distributions are shown in Fig. 3.

* Work supported by BMBF contract No. 05P12RFRB9.
† a.almomani@iap.uni-frankfurt.de

EXPERIENCE WITH THE CONDITIONING OF LINAC4 RF CAVITIES

S. Papadopoulos*, J. M. Balula, F. Gerigk, J-M. Giguet,
J. Hansen, A. Michet, S. Ramberger, N. Thaus, R. Wegner
CERN, Geneva, Switzerland

Abstract

Linac4, the future H^- injector of the PS complex at CERN has reached the hardware and beam commissioning phase. This paper summarizes the experience gained in RF conditioning of the DTL, CCDTL and PIMS cavities. The behaviour in conditioning of these cavities strongly depends on the cavity type and assembly conditions. Examples of conditioning history and vacuum measurements before, during and after conditioning are discussed.

INTRODUCTION

The main accelerating section of Linac4 consists of 3 Drift Tube Linac (DTL), 7 Cell Coupled Drift Tube Linac (CCDTL) and 12 Pi-Mode Structure (PIMS) cavities. The Linac4 cavities operate at 352.2 MHz and the beam duty cycle is 0.08%.

GENERAL CHARACTERISTICS OF THE LINAC4 RF CAVITIES

Conditioning time and efficiency strongly depends on the cavity type, material and its history of surface treatment. These characteristics are therefore outlined in the following before evaluating the conditioning process.

DTL

The DTL cavities have been designed and assembled at CERN with parts manufactured in Spanish industry. The stainless steel DTL tanks were copper-plated at CERN. Drift tubes are made from machined 3d forged OFE copper pieces that are joined by electron beam welding. The drift tubes contain focusing magnets (PMQs) in vacuum made from stainless steel holders with inserts of permanent magnetic SmCo material. The mechanical complexity of the PMQs with a considerable surface area (7489 cm^2 for 45 mm length PMQ) and positioning screws leads to elevated outgassing ($7.4 \cdot 10^{-6}$mbar · l/s for 45 mm length PMQ). Outgassing takes place through the beam apertures of the drift tubes and passes through high field areas between drift tubes. The presence of outgassing products in that area increase the probability of breakdowns. The permanent magnets of the DTL cavities come in two species of 45 mm and 80 mm length that have been made by two different manufacturers. The cavities have been vacuum sealed with all-metal spring loaded seals in order to keep outgassing rates low and to guarantee a good RF contact. The peak electric field in the first cells of tank 1 have been reduced by design in order to reduce the probability for breakdowns [1].

CCDTL

The CCDTL cavities have been constructed at VNIITF, Snezhinsk, while the drift tubes and supports were made at BINP, Novosibirsk. All structures were then assembled and tuned at BINP before shipment to CERN [2]. The cavities are copper plated and contrary to the DTL cavities the drift tubes are joined by vacuum brazing and then electron beam welded to the stem. As the copper pieces are heated during the process of brazing, they become soft. In general soft copper enhances the probability of breakdowns due to an increased amount of crystal dislocations [3]. Considering the RF design, the CCDTL cavities consist of accelerating cells and coupling cells. The coupling cells couple the RF power from the centre cavity to the side cavities. As the structure operates in the pi/2 mode the coupling cells are nominally field free during the pulse flat top. Between the accelerating cells the phase difference is $\Delta\phi = \pi$. The coupling cells are positioned off-center to allow the positioning of external magnets on the beam trajectory. The excitation of multipacting in the coupling cells prolongs the conditioning of the accelerating cells. As long as multipacting persists, accelerating cells fed through coupling cells do not condition efficiently as they do not receive the full power that corresponds to nominal field levels. The conditioning of the CCDTL cavities thus progresses consecutively from the central accelerating cells to coupling cells and finally to the outer accelerating cells.

PIMS

The PIMS cavities were designed and assembled at CERN with parts manufactured in Poland. They are machined from 3d forged OFE copper rings and disks and joined by electron-beam welding. Only the central copper ring sees a brazing operation for the assembly of ring and RF input port [4]. The material and assembly techniques of the cavities provide a good basis for a rapid and effective conditioning.

During RF operation the forward and reflected power to the cavities is measured through directional couplers on the feeding waveguides and the power inside of the cavities is monitored with field probes. The vacuum pressure is also monitored and used as an interlock signal to stop the RF at a certain maximum pressure.

CONDITIONING PROCESS

During the conditioning process breakdowns and multipacting limit the power that can be accepted by the cavity. Outgassing and sparking significantly affects the vacuum

* sotirios.papadopoulos@cern.ch

ISBN 978-3-95450-169-4

RESEARCH ON A TWO-BEAM TYPE DRIFT TUBE LINAC*

L. Lu†1, T. He2, L. Yang 2, W. Ma2, L.P. Sun1, X.B. Xu1. L.B. Shi1, C.X. Li1, Y. He1, H.W. Zhao1
1 Institute of Moden Physcis (IMP), CAS, Lanzhou 730000, China
2 University of Chinese Academy of Sciences, Beijing 100049, China

Abstract

The very high intense heavy-ion beam is a high attraction for heavy ion researches and heavy-ion applications, but it is limited by heavy-ion production of ion source and space-charge-effect in acceleration. There is one way, accelerating several heavy-ion beams in one cavity at same time and funneling them, which could achieve the acceleration of very high intense heavy-ion beam with existing ion source and accelerating technology. The research purpose is to design a two-beam type drift tube linac (DTL), which could be used as high intense heavy ion injector, such as a driver of heavy ion inertial fusion. In this paper, we will introduce our designs, calculations and simulations.

INTRODUCTION

In the last decades, three breakthroughs were invented and developed for high intense heavy ion acceleration [1]: the 1st one is the invention of radio frequency quadrupole (RFQ) type accelerator, which could accelerate more than one dozens of milliampere ion beam [2-3], the 2nd invention is the direct plasma injection scheme (DPIS), which provide a way to produce a very high intense heavy ion beam [4-6], and the 3rd invention is multi-beam IH-RFQ type accelerating structure, which accelerated 108 mA carbon ions successfully in 2010 by using DPIS [7].

These inventions, especially, the invention of multi-beam RFQ, which is suitable for accelerating heavy ions in the very low energy region, make the production and the acceleration of very high intensity heavy ion beam possible such as an injector of heavy ion inertial fusion. In this paper, we propose a 2-beam type DTL for accelerating very high intense heavy ion beam in low-middle energy region. This 2-beam DTL can double the existing beam current and can be used as a post-accelerator to accelerate two high intense heavy ion beams which could be funnelled from four accelerated heavy ion beams after a 4-beam type RFQ [8]. Our proposed 2-beam type DTL is a totally normal interdigital-H (IH) DT structure, using TE_{111} resonated mode and the acceleration will be occurred between drift tubes. The two beam tunnels are off-set from the center of the DT, and both are located in the vertical direction of cavity axis. The image of a proposed 2-beam type DTL is shown in Fig. 1.

Our goal is to design and fabricate a proof of principle (PoP) 2-beam type DTL which could accelerate ions from 50 keV/u up to 1.5 MeV/u in one meter. The focusing method we adopted is the alternative phase focusing (APF) method, which had already accelerated 1.5 MeV P^{2+} CW beam and 7.4 MeV (1.5 MeV – RFQ + 5.9 MeV - DTL) 10 mA-proton beam in 2009 and 2010 [9].

STRUCTURE SIMULATIONS

The beam orbit calculation is used Pi Mode Orbit Calculation (PiMLOC) [10] to calculate the profiles of the DTs and gaps. And the Microwave Studio （MWS） [11] was utilized to perform electromagnetic simulations of the cavity.

In this researcher, the structure, especially the DT structure and location of beam channel were firstly studiedby using MWS. The structure shown in the Fig. 1 is not the first idea, the first thing of our design is to check

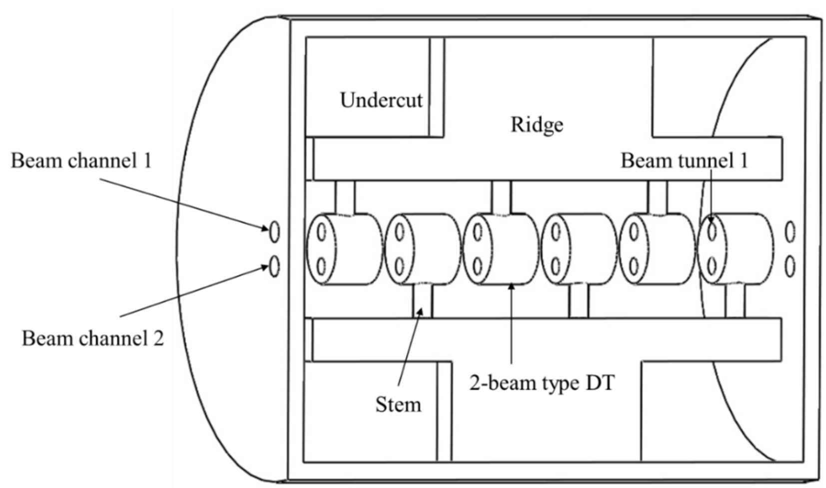

Figure 1: An image of the designed 2-beam type IH-DTL.

* Work supported by NSFS and Youth Innovation Promotion Association of CAS
† luliang@impcas.ac.cn

ISBN 978-3-95450-169-4

MUON ACCELERATION USING AN RFQ

Y. Kondo*, K. Hasegawa, JAEA, Tokai, Naka, Ibaraki, 319-1195, Japan
M. Otani, T. Mibe, Y. Fukao, N. Kawamura, Y. Miyake, K. Shimomura,
KEK, Oho, Tsukuba, Ibaraki, 305-0801, Japan
R. Kitamura, Univ. of Tokyo, Hongo, Tokyo, 113-8654, Japan
K. Ishida, Riken, Wako, Saitama, 351-0198, Japan
N. Saito, J-PARC Center, Tokai, Naka, Ibaraki, 319-1195, Japan

Abstract

A muon linac development for a new muon g-2 experiment is now going on at J-PARC muon science facility. In this experiment, room temperature muons (ultra-slow muons: USMs) are generated and accelerated to 212 MeV using a muon linac. As the first accelerating structure, a spare radio frequency quadruple (RFQ) linac of the J-PARC linac will be used. Prior to constructing the muon linac, we are planning to conduct the first acceleration experiment using this RFQ. For this experiment, a degraded muon beam will be used (slow-muon source), instead of the USM source. In this paper, the beam test of this slow-muon source and simulation studies of the muon acceleration using the RFQ are presented.

INTRODUCTION

The muon anomalous magnetic moment $(g-2)_\mu$ is one of the most promising prove to explore the elementary particle physics beyond the standard model (SM). Currently, the most precise $(g-2)_\mu$ experiment is E821 of Brookhaven national laboratory [1]. The precision is 0.54 ppm and the measured value indicates approximately three standard deviations from the SM prediction. The J-PARC E34 experiment aims to measure the $(g-2)_\mu$ with a precision of 0.1 ppm. In addition, the electric dipole moment (EDM) also can be measured with a precision of $1 \times 10^{-21} e{\cdot}$cm [2]. The experimental method of E34 is completely different from that of the previous experiments. The previous experiments directory used decay muons from the secondary pions generated on the production target. The emittance of such muon beam is very large (typically, 1000 π mm mrad); this is a source of uncertainty of the measurement. On the other hand, E34 will use a low emittance muon beam to improve the precision. The required transverse momentum spread $\Delta p_t/p$ is less than 10^{-5}, and assumed transverse emittance is 1.5 π mm mrad. To satisfy this requirement, we are planning to use ultra-slow muons (USMs) generated by laser-dissociation of thermal muoniums (Mu: μ^+e^-) form a silica-aerogel target [3]. The room temperature USMs (25 meV) should be accelerated to 212 MeV to obtain the required $\Delta p_t/p$. A linac realizes rapid acceleration required to accelerate muons, whose lifetime is very short (2.2 μs). In Figure 1, the configuration of the muon linac [4] is shown.

* yasuhiro.kondo@j-parc.jp

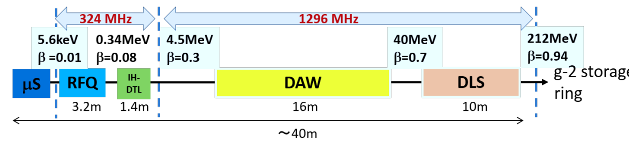

Figure 1: Configuration of the muon linac.

The muon linac will be constructed at the H line [5] of the J-PARC muon science facility (MUSE). The USMs are bunched and accelerated to 340 MeV by a radio frequency quadrupole linac (RFQ). Following the RFQ, an interdigital H-mode drift tube linac [6] is used to accelerate to 4.5 MeV. Then, muons are accelerated to 40 MeV through disk and washer coupled cavity linac section, and finally accelerated to 212 MeV by using disk loaded structure traveling-wave linac. As the first step, a spare RFQ of J-PARC linac (RFQ II [7]) will be used as a front-end accelerator. This RFQ is originally designed to accelerate negative hydrogens. However, by scaling the intervane voltage by the masses, it can be used for muon acceleration [8].

In this paper, present status of muon-acceleration experiment using this RFQ is described.

MUON-ACCELERATION EXPERIMENT USING THE RFQ

Prior to constructing the muon linac, we are planning to conduct a muon-acceleration experiment using RFQ II at the H line. Figure 2 shows the experimental setup.

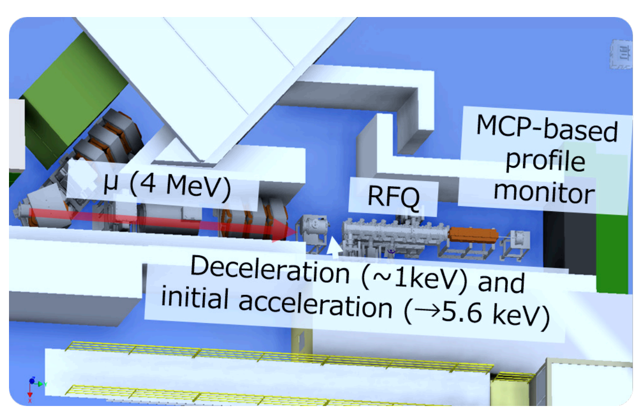

Figure 2: Experimental setup of the muon-acceleration experiment using the RFQ.

RF DESIGN OF A DEUTERON BEAM RFQ

C.X. Li#, Y. He, X.B. Xu, F.F. Wang, Z.L. Zhang, W.P. Dou, Z.J. Wang,
Institute of Modern Physics, CAS, Lanzhou, China

Abstract

In a material irradiation facility in IMP, a RFQ is required for accelerating deuteron beam from 20 keV/u to 1.52 MeV/u. The structure design of the RFQ is drawing on the experience of the RFQ of Injector II of China ADS LINAC. Four-vane structure is adopted and the operation frequency is 162.5 MHz. Inter vane voltage is 65 kV and the Kilpatrick factor is 1.4. Π-mode stabilizing loops are used to move the dipole modes away from the working mode. Slug tuners are used to compensate for capacitance errors induced by machining. Cutbacks and end plate are modified to reach reasonable field flatness. After the structure design and optimization, the simulation results of the cavity frequency is 162.459 MHz, the power loss is 109 kW. The multiphysics simulations are also performed to determine the frequency shift caused by the shift of the cooling water temperature.

INTRODUCTION

A project aimed to construct a fusion reactor material qualification facility has been launched in Institute of Modern Physics, Chinese Academy of Science. The facility, which named CMIF (China Material Irradiation Facility), is an accelerator based neutron source. As shown in Fig. 1, the facility will consisted of ion source, LEBT, RFQ, MEBT, superconducting accelerating section and target system. The accelerator will accelerate 10 mA CW deuteron beam up to 50 MeV. When deuteron beam collide with the granular beryllium alloy particle target, the neutron fluxes with the energy up to 14 MeV will be generated. The neutron fluxes will cause 20-50 dpa per year on specimens. In this paper, the RF structure design with the aid of the CST MWS [1] of the RFQ for CMIF will be introduced.

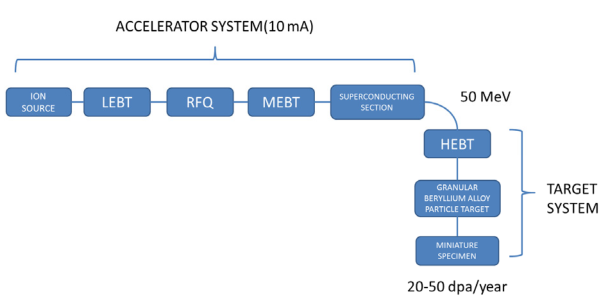

Figure 1: The diagram of CMIF.

MAIN PARAMETER OF CMIF RFQ

For the structure of the RFQ, four-vane type structure for the outstanding stability in CW operation. Based on beam dynamics design, some feature parameters and the vane tip modulation of the RFQ can be obtained, which are necessary for RF Design. The parameters are listed in Table 1. The RFQ will work at the frequency of 162.5 MHz in CW mode. The inter-vane voltage is selected to 65 kV and the Kilpatrick factor is optimized to 1.4.

Table 1: The Main Parameters of CMIF RFQ

Particle	D+ (q/A=1/2)
Operation	CW/pulsed
Vane type	Four vane
Frequency (MHz)	162.50
Kp	1.4
Inter-vane voltage (kV)	65
Vane length (mm)	5250.00
Mean aperture (mm)	4.807

RF STRUCTURE DESIGN

2D Cross Section Design

Before the RF simulation of the RFQ, the profile of the cavity's cross section should be determined. The cross section profile share a common profile with PXIE RFQ [2]. For the symmetry of RFQ, the cross section can be determined by a quadrant. The profile is shown in Fig. 2. And this profile can be determined by the parameters listed in Table 2.

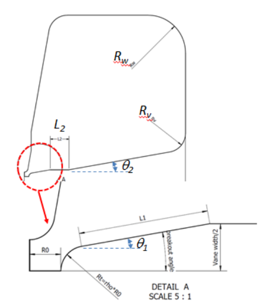

Figure 2: Profile and the parameters of cross section.

Table 2: Parameters to Generate 2D Cross Section Profile

Variables	Value	Unit
R_0	4.807	mm
ρ	0.8	
L_1	27.82	mm
L_2	11.89	mm
θ_1	7.1	Deg.
θ_2	10	Deg.
R_V	20	mm
R_W	40	mm
H	169.3	mm
$R_t = \rho R_0$	3.85	mm

PISL Period Model

The Pi mode stabilized loops are introduced to separate the nearest dipole mode from the working quadrupole

#lichenxing@impcas.ac.cn

DESIGN AND SIMULATION OF A HIGH INTENSITY HEAVY ION RFQ ACCELERATOR INJECTOR*

W. Ma[1,†], L. Lu, X. Xu, L. Sun, Z. Zhang, C. Li, L. Shi, Y. He, H. Zhao
Institute of Modern Physics, Chinese Academy of Science, Lanzhou 730000, China
[1]also at University of Chinese Academy of Sciences, Beijing 100049, China

Abstract

An 81.25 MHz continuous wave (CW) radio frequency quadrupole (RFQ) accelerator has been developed for Low Energy Accelerator Facility (LEAF) at the Institute of Modern Physics (IMP), the Chinese Academy of Science (CAS). In the CW operating mode, the proposed RFQ design adopted the conventional four-vane structure. The main design goals are providing the high shunt impendence with low power losses. In the electromagnetic (EM) design, the π-mode stabilizing loops (PISLs) were optimized to produce a good mode separation. The tuners were also designed and optimized to tune frequency and field flatness of the operating mode. The vane undercuts were optimized to provide a flat field along the RFQ cavity. Additionally, a full length model with modulations was set up for the final EM simulations. In this paper, detailed EM design of the LEAF-RFQ will be presented and discussed. Meanwhile, structure error analysis is also studied.

INTRODUCTION

LEAF project was launched as a pre-research facility for high intensity Heavy Ion Accelerator Facility (HIAF) project [1, 2] at IMP. The LEAF will consist of a 2 mA U^{34+} electron cyclotron resonance ion source, a low energy beam transport line [3], a CW 81.25MHz RFQ accelerator, a medium energy beam transport and an experimental platform for nuclear physics. The layout of the LEAF project is shown in Fig. 1. The LEAF-RFQ will be adopted and used in the HIAF project.

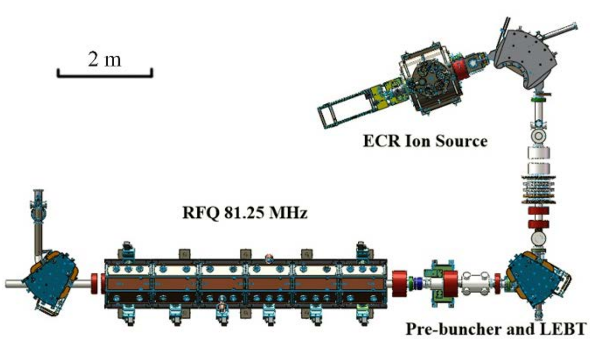

Figure 1: Layout of LEAF project.

The design goal is to design a compact type cavity with lower power loss and high operation stability. Considering that LEAF-RFQ will operate at CW mode, four-vane structure is a better choice than four-rod type [4], which is a more stable structure and has better water cooling. Dipole mode can be excited if the dipole frequency is very close to operating frequency. Therefore, a good frequency separation is always a basic task to diminish the dipole mode effect. There are several methods proposed fighting against the dipole effect, such as, the vane coupling ring [5], PISL [6] and dipole stabilizer rod [7]. PISL is a good choice because it is easy to be cooled. Meanwhile, tuners and undercuts [8] are also used for frequency tuning and field flatness.

In this paper, we focus on EM design and report detailed RF simulations using CST Microwave Studio (MWS) [9]. All parts of the resonator such as PISLs, tuners, and undercuts have been taken into account. Additionally, a complete RFQ model with vane modulations has been built and simulated.

PARAMETERS AND STRUCTURE

According to the requirements of the LEAF project, parameters of LEAF-RFQ are summarized in Table 1.

Table 1: LEAF-RFQ Main Parameters

Parameters	Value
Particle charge state	U^{34+}
Operation	CW/pulsed
Vane type	Four vane
Frequency (MHz)	81.25
Input energy (keV/u)	14
Output energy (MeV/u)	0.5
Inter-vane voltage (kV)	70
Kilpatrick factor	1.55
Peak current (emA)	2
Transmission efficiency (%)	97.2
Length of vane (mm)	5946.92
Average radius of aperture (mm)	5.805

ELECTROMAGNETIC SIMULATIONS

The LEAF-RFQ cross-section has been optimized with the CST MWS. As a result, the cross-section geometry is shown in Fig. 2. The cross-section profile is defined with nine independent variables. Their final optimized values are indicated in the Table 2. In all subsequent 3D simulations, these parameters of cross-section are fixed except H.

* Work supported by NSFC of China under Grant No. 11427904.
† email address: w_ma@impcas.ac.cn

ISBN 978-3-95450-169-4

BEAM COMMISSIONING STATUS AND RESULTS OF THE FNAL PIP2IT LINEAR ACCELERATOR RFQ*

J. M. Steimel, C. Baffes, P. Berutti, J.-P. Carneiro, A. Edelen, J. Edelen, T. Khabiboulline, L. Prost, V. Scarpine, A. Shemyakin, Fermilab, Batavia, IL, USA
M. Hoff, A. Lambert, D. Li, T. Luo, J. Staples, S. Virostek, Berkeley Lab, Berkeley, CA, USA
V. L. S. Sista, Bhabha Atomic Research Centre, Mumbai, India

Abstract

An H- beam was accelerated through a continuous wave (CW) capable, 4-vane, radio frequency quadrupole (RFQ) at Fermilab that was designed and constructed at Berkeley Lab. This RFQ is designed to accelerate up to 10 mA H- beam from 30 keV to 2.1 MeV in a test accelerator (PIP2IT). This paper presents results of specification verification and commissioning.

INTRODUCTION

Fermilab has begun to optimize its injector chain for high proton flux neutrino experiments in a program called the Proton Improvement Plan (PIP) [1]. This program was designed to satisfy the requirements for experiments that are going on-line in the current decade. It will not satisfy intensity requirements for the longer baseline detector, Deep Underground Neutrino Experiment (DUNE) [2], and a new program, Proton Improvement Plan II (PIP-II) [3], is being developed to satisfy those requirements.

The PIP-II design team has proposed building a CW beam capable, Superconducting Radio Frequency (SRF) linac, to replace the current Fermilab linac, bringing the injection energy into the Booster from 400 MeV to 800 MeV, among other improvements to be made to the rest of the accelerator complex. This will satisfy the proton flux requirement needed for DUNE's baseline experimental goal and provide enough beam for other, future proton-based experiments. To alleviate technical risks in the linac design a sub-program called the PIP-II Injector Test (PIP2IT) [4] will prototype the first 25 MeV of the accelerator chain.

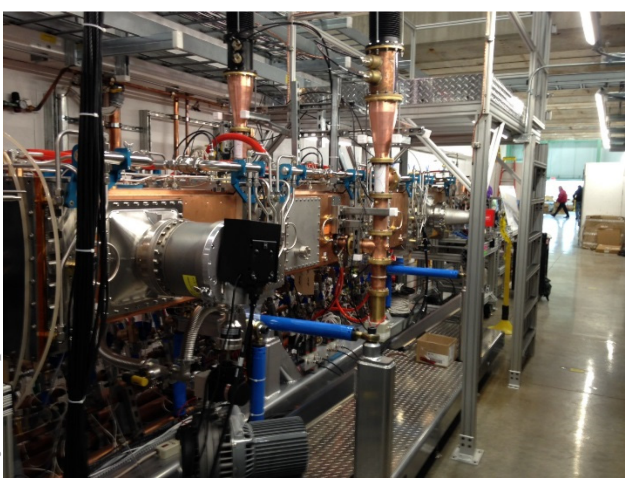

Figure 1: PIP2IT RFQ installed in beam line with support stand, water cooling manifold, and RF distribution connected to input couplers.

The PIP2IT RFQ was designed and constructed at Berkeley Lab [5]. Specifications are listed in Table 1 [6]. Two power input ports on the RFQ divide the 100kW CW load between two input couplers. Figure 1 shows the RFQ with its input couplers connected to the RF power distribution. RF power from the coupler antennas is AC coupled to ground, which allows applying a DC bias on the antennas to inhibit multipacting [7].

Table 1: RFQ Specifications

Parameter	Value	Range
Input Energy	30 keV	+/- 0.5%
Output Energy	2.1 MeV	+/- 1%
Frequency	162.5 MHz	Nominal
Beam Current	1-10 mA	Range
Vane Voltage	60 kV (peak)	Nominal
RF Power	130 kW	Max
Duty Factor	100%	
Transmission	95%	Min
Transverse Emittance	0.25 mm-mrad	Max
Longitudinal Emittance	0.8–1.0 eV-μs	Range

Cooling water temperature adjustment is the sole means of controlling the resonant frequency. Cooling channels and water manifolds were designed to separate the cooling system for the outer walls of the RFQ from the cooling system for the internal vanes [8]. While the resonant frequency response to variations of the overall temperature is weak (~2.5 kHz/°C), the response to a differential temperature between the wall and vanes is much stronger (~30 kHz/°C). Thus, the water cooling infrastructure was designed to allow separate control over the wall and vane water temperatures.

COMMISSIONING PREPARATION

Just prior to shipping to Fermilab, the RFQ was tuned for field flatness and resonant frequency at Berkeley Lab. This involved the design, construction, and testing of a 4.4-meter long bead-pull apparatus and processing system [9]. Eighty copper slug tuners and the two end-plates were adjusted and machined to give a field flatness of ~1% peak-

* Operated by Fermi Research Alliance, LLC under Contract No. DE-AC02-07CH11359 with the United States Department of Energy.

PREPARATION AND INSTALLATION OF IFMIF-EVEDA RFQ AT ROKKASHO SITE

Enrico Fagotti, Loris Antoniazzi, Andrea Baldo, Alex Battistello, Paolo Bottin, Luigi Ferrari, Mauro Giacchini, Francesco Grespan, Maurizio Montis, Andrea Pisent, Francesco Scantamburlo, Daniele Scarpa, INFN/LNL, Legnaro, Italy. David Agguiaro, Andrea Giorgio Colombo, Adriano Pepato, Loris Ramina, INFN/Sez. Di Padova, Padova, Italy. Fabio Borotto Dalla Vecchia, Giovanni Dughera, Giuseppe Giraudo, Alberto Emanuele Macrì, Paolo Mereu, Riccardo Panero, INFN/Sez. Di Torino, Torino, Italy. Takahiro Shinya, Keitaro Kondo, QST, Rokkasho, Japan.

Abstract

The IFMIF-EVEDA RFQ is composed of 18 modules for a total length of 9.8 m and is designed to accelerate the 125 mA D+ beam up to 5 MeV at the frequency of 175 MHz [1]. The RFQ is subdivided into three Super-Modules of six modules each. The Super-Modules were pre-assembled, aligned and vacuum tested at INFN-LNL and then shipped to Rokkasho (Japan). At Rokkasho site a series of test were performed in order to verify the effect of the shipment on the cavity. The assembly debug, shipment equipment and the sequence of operations are described in this paper.

INTRODUCTION

IFMIF-EVEDA RFQ is divided into three SuperModules (SMs), each one composed of six modules. Two over three SMs were produced by two external companies and one was produced in house at INFN [2]. This subdivision was set to reduce production risks and revealed to be very effective. SM1 was produced by RI Research Instruments GmbH, SM3 was produced by CINEL Scientific Instruments S.r.l. and SM2, as just mentioned, was produced in house. SM3 and SM2 modules were produced compliant to the RF constrains while SM1 production was stopped due to frequency unconformities emerged after brazing of four over six modules. Measured nominal frequencies were, on average, 850 kHz higher than design frequencies. One possibility was to recover out of frequency using tuners range but, in this way, tuners range devoted to field errors compensation would reduce too much. For these reasons a mechanical recovery solution was studied for the four modules. The implementation was done by INFN and Cinel Company. Solution consisted in the machining of eight rectangular apertures on the external surface of each module to reduce its frequency (Figure 1). Vacuum closure was guaranteed by copper plugs sealed with Indium wires. Indium sealing was tested at high temperature in order to validate that this solution is compatible with baking process. Tests showed that no problem is encountered up to 100 °C that will be the maximum temperature reachable during RFQ bake-out.

Recovery actions were successfully concluded in September 2015. Moreover, the remaining two modules, whose production was stopped before brazing, were successfully brazed at INFN Legnaro in the same period.

SUPERMODULES ASSEMBLY AT LNL

SMs assembly started with SM2. Alignment of the modules was done under laser tracker supervision. A total of seven 8 mm in diameter cylindrical holes were machined on each module for alignment purpose. Each module can be adjusted in transversal position respect to the beam axis, using three main screws for vertical positioning and four small screws for horizontal one. After modules axes reach collinearity, modules can be moved close together sliding on two couples of rails linked to each module and previously aligned with module axis. Approaching process is followed by laser tracker. At the beginning a Garlock metallic C-seal helicoflex was used for modules coupling. The sealing helicoflex had to be squeezed by two stainless steel frames brazed on the modules copper surfaces. This had to guarantee vacuum tightness and RF joint.

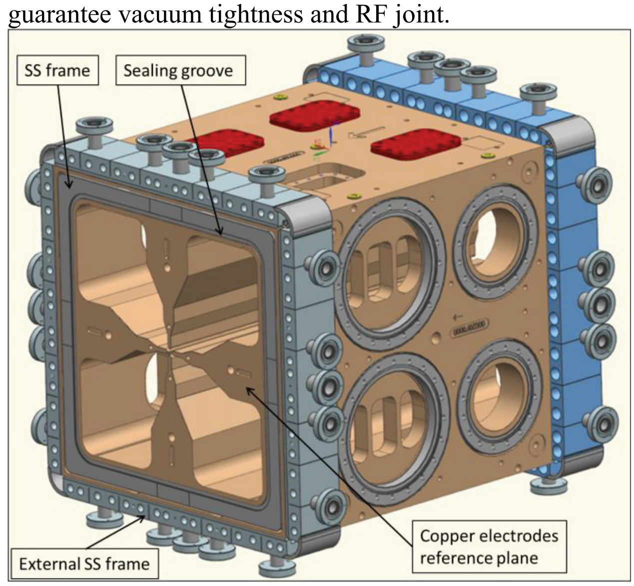

Figure 1: Module M2 layout. Rectangular apertures for frequency recovery are visible.

The first coupling operations revealed some weak points in the procedure. First of all, Garlock C-seal model required too much pressure (higher than that written into specifications) to be squeezed at nominal dimension and this pressure was enough to deform the brazed copper surfaces under stainless steel frame. Moreover in some cases, modules axes and modules main flanges had perpendicularity tolerances exceeding optimum range. As a consequence helicoflex compression was not uniform and this

ISBN 978-3-95450-169-4

SERIES PRODUCTION OF THE RF POWER DISTRIBUTION FOR THE EUROPEAN XFEL

S. Choroba, V. Katalev, DESY, Hamburg, Germany
E. Apostolov, Technical University of Sofia, Sofia, Bulgaria

Abstract

The RF power distribution for the European XFEL allows for individual RF power for the 808 superconducting cavities of the European XFEL. It consists of a number of elements, not only waveguide components, but also girders, cables or cooling systems. The production of the RF distribution consists of several tasks. In order to deal with the schedule of the entire project a detailed planning, organization and monitoring of the series production of the RF power distribution was required. This paper describes the RF power distribution layout and the series production process.

RF SYSTEM LAYOUT

Figure 1 shows the RF waveguide distribution of one RF station for 4 cryogenic accelerator modules. The klystron has two output waveguides (blue) and generates up to 10MW RF power, 2 times 5MW, at 1.4ms and 10Hz repetition rate. The output power can be absorbed in RF loads (red) during test of the RF station or can be transmitted by waveguides (orange) to the accelerator modules (yellow) during accelerator operation. The output power of each arm is split again to 2 module waveguide distributions (grey).

The module waveguide distribution is shown magnified. In the linear part RF power is branched off by asymmetric shunt tees for a pair of cavities and then split again. In front of each cavity an isolator is installed, which protects the klystron from reflected power. Within the module waveguide distribution the phase is adjusted by fixed phase shifters and controlled for each individual cavity by adjustable phase shifters. The phase between the modules can be adjusted by additional adjustable phase shifters if required. In the first layout the shunt tees between modules and for a pair of cavities were assumed to be 3 dB shunt tees, whereas the asymmetric shunt tees in the linear part of the distribution are 3 dB, 4.77 dB and 6 dB. With this design all cavities would be supplied by the same RF power. The advantage of this layout is that uses the same type of components for all waveguide distributions and allows for preproduction independent of the accelerator module production status. The disadvantage is that the weakest cavity with lowest achievable gradient determines the input power for all cavities connected to this power station and thus limits even stronger and better cavities.

Therefore it was assumed that during production of the cavities pre-sorting with respect to maximum achievable gradient and grouping them appropriately in modules will be possible. It was assumed that 2 cavities with the same maximum achievable gradient could be grouped into a pair [1, 2]. By changing the coupling ratios of the asymmetric

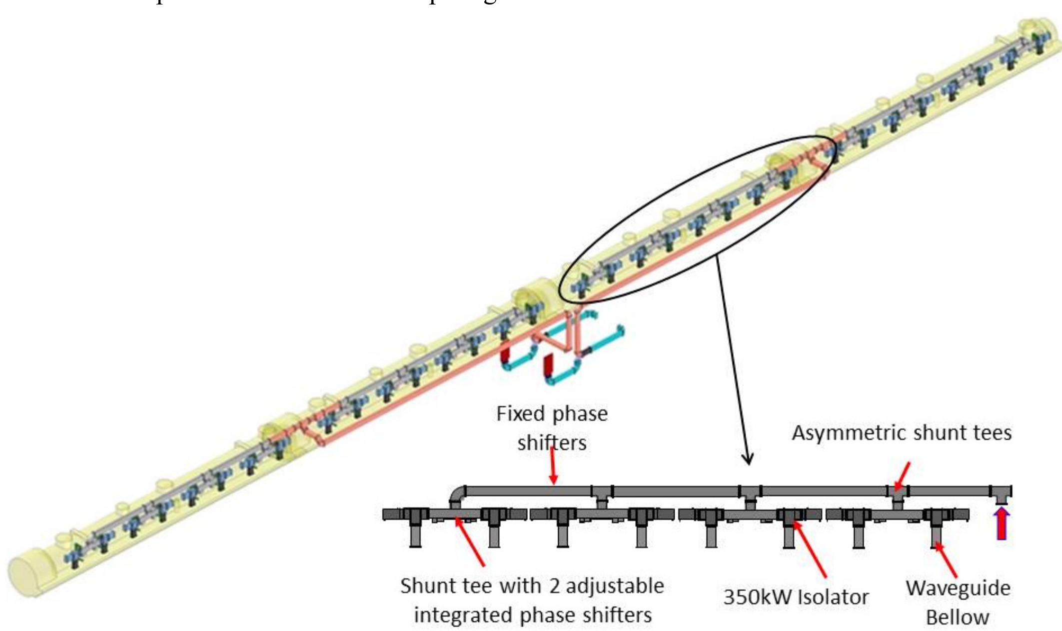

Figure 1: RF waveguide distribution layout for one RF station.

QUALITY FACTOR MEASUREMENT METHOD USING MULTI DECAY TIME CONSTANTS ON CAVITY*

Juwan Kim, Heetae Kim†

Rare Isotope Science Project, Institute for Basic Science, Daejeon 34047, Republic of Korea

Abstract

Quality factor measurement method using multi decay time constants on superconducting cavity is suggested. In most cases of vertical test, one decay time constant is measured around critical coupling and coupling constants are measured using forward and reflected rf power to get intrinsic quality factor. We use multi decay time constants method to measure the quality factor, which uses three decay time constants. Two more switches before and after the cavity are added to the measurement system. Decay time constants are measured by switching off the rf power switch in front of rf source, the forward power switch in front of input power coupler, and then the pickup power switch behind the pickup coupler, respectively, at the same power of steady state.

INTRODUCTION

Nb superconducting cavity can be operated below the critical temperature of superfluid, 2.172 K. Superfluid helium shows negligible viscosity and extremely high thermal conductivity. Properties of superfluid helium fog generated from the liquid helium surface were studied [1-3]. RAON superconducting radio frequency (SRF) test facility was designed [4] and constructed. The RAON SRF test facility consists of cavity test, cryomodule test cryogenic system, and cleanroom. The cleanroom is used for cavity processes and assembles. Residual resistivity ratio test of niobium was performed and the conditions of electron-beam welding were studied [5]. A half-wave resonator cryomodule was test in low temperature [6]. RF system and useful information such as gradient quality factor, RF-heat loads and loaded Q's were shown to test superconducting cavity [7]. Measurement of quality factor is important to test superconducting cavity.

In this research, we show how to measure quality factors from multi decay time constants measurement.

MULTI DECAY TIME CONSTANTS

The width of the resonance for a cavity in frequency spectrum is measured by either a network analyzer or a spectrum analyzer. The quality factor of the cavity can be expressed as $\omega/\Delta\omega$ where $\Delta\omega$ is half the resonance width. In normal conducting cavities, $\Delta\omega$ can be measured since it is order of kHz. It is very hard to measure the quality factor of a typical niobium superconducting cavity with a network analyzer since the value of the quality factor is very big and $\Delta\omega$ is too small.

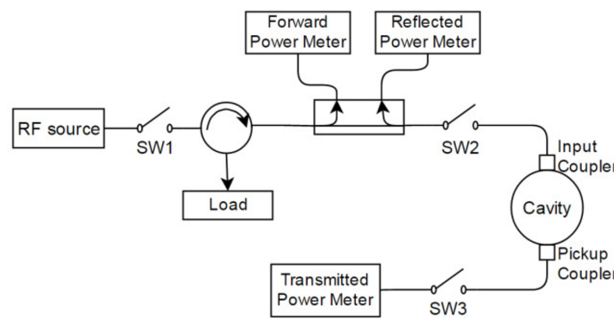

Figure 1: Schematic diagram of a cavity for quality factor measurement using multi decay time constants.

Figure 1 shows the schematic diagram of a cavity for quality factor measurement using multi decay time constants. RF source, circulator, bidirectional coupler, cavity, input coupler, pickup coupler, transmitted power meter, and three switches are shown in Fig. 1. Three switches are useful to measure the decay time constants.

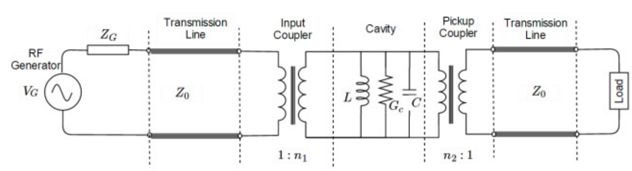

Figure 2: Equivalent circuit for a cavity with two couplers such as input coupler and pickup coupler. The input coupler is being driven by an rf generator and the pickup coupler helps to measure transmitted power.

The schematic diagram of the quality factor measurement of Fig. 1 corresponds to the equivalent circuit of Fig. 2 which does not include switches. Figure 2 shows the equivalent circuit for a cavity with two couplers. The input coupler is being driven by an rf generator and transmitted power is measured with the pickup coupler. After the rf generator is turned off, the total dissipated power is the sum of the power dissipated in the cavity and the power which leaks out the couplers [8].

$$P_{tot} = P_c + P_e + P_t, \tag{1}$$

* This work was supported by the Rare Isotope Science Project of Institute for Basic Science funded by the Ministry of Science, ICT and Future Planning (MSIP) and the National Research Foundation (NRF) of the Republic of Korea under Contract 2013M7A1A1075764.
† kim_ht7@yahoo.com

ISBN 978-3-95450-169-4

N-DOPED NIOBIUM ACCELERATING CAVITIES: ANALYZING MODEL APPLICABILITY

W. Weingarten†, retiree from CERN, Geneva, Switzerland
R. Eichhorn, N. Stillin, Cornell Laboratory for Accelerator-Based Sciences and Education, Ithaca, NY, USA

Abstract

The goal of this research was to analyse data from multiple cavities in order to test the viability of a model for surface resistance proposed previously. The model intends to describe the behaviour of the quality factor with respect to the RF field strength, while exploring the physical cause of this phenomenon; the model is pretty general, but will be checked here specifically for N-doped niobium cavities. The data were obtained from two single-cell 1.3 GHz cavities manufactured and tested at Jefferson Lab in Newport News, VA, USA.

INTRODUCTION

The slope of the quality factor Q of superconducting (sc) cavities in dependence of the accelerating gradient E, Q(E), is still a subject of debate. Several models were presented, thereof most based on a homogeneous surface and field dependent parameters.

Instead, here a model is further investigated that involves a composite surface of a homogeneous superconductor with embedded tiny weak sc defects of size comparable to the coherence length, from now on simply called "defects".

IMPURITY BASED MODEL

Our model which we will apply to the data has been partially published before [1,2]. It is based on the following assumptions, derived from many experimental data:

i. The RF losses of a sc niobium cavity are generated by a composite from at least two origins, a pure niobium host surface with embedded defects. Their number depends on the temperature and the RF magnetic field.
ii. These defects are themselves compounds of various purity of niobium and its alloys.
iii. The transition to the normal conducting (nc) state of the defects occurs, by the proximity effect, at relatively low RF magnetic fields and relatively low critical temperatures, as compared to the critical field and critical temperature of pure niobium.
iv. A distinction is made for defects at the surface and those in the bulk. When a defect at the surface becomes nc, the RF field shifts deeper into the bulk. When a defect in the bulk becomes nc, the RF field does not penetrate deeper.
v. With growing magnetic field, the defects become nc; this increases the RF losses at the surface and reduces the RF losses in the bulk.
   a. The increase of RF losses at the surface originates from entry of magnetic flux enlarging the number of nc electrons.
   b. The decrease of RF losses in the bulk arises from the lowering of the mean free path of the nc electrons, when the cutting edge of defects having already passed to the nc state penetrates deeper into the bulk. Their number increases logarithmically with the magnetic field (exactly valid only for a defect density constant with depth).
vi. Above a distinct temperature (~2K), the defects, when they become nc, show enlarged RF losses. The physical reason is still unclear. Possible explanations proposed are percolation [1,2] and larger thermal impedance from the transition of the liquid helium from the superfluid to the normal fluid state [3].

To analyse the new data we use the plain ansatz as suggested by [1,2] describing a temperature independent defect density without percolation.

The significance of the different terms in relation to the preceding statements (i) – (vi) is indicated in (1). The function f(B) gives the fraction of defects already undergone nc and is chosen to unity for B=B' (at the maximum Q-value), because all defects are supposed to be nc there. The variables as used in (1) are explained in Tab. 1.

$$R_s = \left(\overbrace{A\cdot\frac{e^{-(\Delta/T)}}{T}+R_{res}}^{\substack{BCS\ and\ residual\\ surface\ resistance}}\right) - \overbrace{\left(\underbrace{A\cdot\frac{e^{-(\Delta/T)}}{T}+R_{res}}_{temperature\ dependent\ factor}\right)\cdot\underbrace{[f(B)-L_2/L_1\cdot f(B)]}_{field\ dependent\ factor}}^{\substack{contribution\ to\ surface\ resistance\\ from\ defects\ in\ bulk}} + \overbrace{R_{s1}\cdot(-\kappa^{-2})\left\{1+\frac{\ln\left[1-\left(\frac{\kappa B}{B_C}\right)^2\right]}{\left(\frac{\kappa B}{B_C}\right)^2}\right\}}^{\substack{contribution\ to\ surface\ resistance\\ from\ defects\ on\ surface}} \quad (1)$$

$$f(B) = \begin{cases} \dfrac{\ln(B/B_C^*)}{\ln(B'/B_C^*)}, B \geq B_C^* \\ 0, B < B_C^* \end{cases}$$

By fitting the data, it turned out that χ^2 could be reduced by supplementing these relations by a temperature dependence of the critical field B_c^* of the defect in the bulk:

$$B_C^*(T, T'^*, B_{C0}^*) = B_{C0}^*\cdot[1-(T/T'^*)^2]\cdot\Theta(T'^*-T) \quad (2)$$

† wolfgangweingarten@cern.ch

FAST ENVELOPE TRACKING FOR SPACE CHARGE DOMINATED INJECTORS*

R. Baartman†, TRIUMF, Vancouver, Canada

Abstract

High brightness injectors are increasingly pushing against space charge effects. Usually, particle tracking codes such as ASTRA, GPT, or PARMELA are used to model these systems however these can be slow to use for detailed optimization. It becomes increasingly challenging in future projects such as LCLS-II where space charge effects are still significant after BC1 and BC2 at 250 and 1600 MeV respectively. This talk will describe an envelope tracking approach that compares well against the particle tracking codes and could facilitate much faster optimization.

INTRODUCTION

Commonly, particle tracking simulation codes are used to design and then commission and finally have operators tune accelerators. Only a few particles would be needed if they act individually, but if space charge fields are significant, this rises to 10^5 to 10^6 or even more. A known, simpler technique is to track rms sizes and correlations (second moments), since then space charge can be included at little cost.

In this note, we expand this technique to more complex cases, beyond the usual integrable ones such as drifts, solenoids, quadrupoles and dipoles. In particular, we apply it to time-varying fields such as in linear accelerators.

SACHERER ENVELOPE THEORY REVIEW

Instead of multiparticle simulations, we look at the "envelope", i.e. treat the beam statistically. [1]

If there is a distribution of particles, one would like to calculate the final distribution from the initial. The behaviour of the beam centroid

$$\langle \mathbf{X} \rangle = \sum_{i=1}^{N} \mathbf{X}/N \tag{1}$$

(where N is the number of particles, and $\mathbf{X}$ is the column vector $(x, P_x, y, P_y, z, P_z)^T$ as in eqn. 6) is determined by the same transfer matrix $\mathbf{M}$ as for an individual particle. This is the equation of 'first moments'. At the next level, one would like to calculate the evolution of the beam widths, or, 'second moments' given by

$$\boldsymbol{\sigma} \equiv \frac{1}{N}\sum_{i=1}^{N} \mathbf{X}\mathbf{X}^T \tag{2}$$

For example, $\sigma_{11} = \langle x^2 \rangle$, $\sigma_{12} = \langle xP_x \rangle$, $\sigma_{13} = \langle xy \rangle$, ... For a distribution of particles so dense that we do not see graininess on any scale of our diagnostics, the sums go over into integrals.

Here, s is the independent variable, so coordinates 5 and 6 are rsp. time and energy: $z = \beta_0 c\Delta t$, $P_z = (\beta_0 c)^{-1}\Delta E$. (This is further explained below.)

By direct substitution into the definition of $\boldsymbol{\sigma}$, we find

$$\boldsymbol{\sigma}_\mathrm{f} = \mathbf{M}\boldsymbol{\sigma}_\mathrm{i}\mathbf{M}^T \tag{3}$$

As well, we can define an *infinitesimal transfer matrix* $\mathbf{F}$ where $\mathbf{X}' = \mathbf{F}\mathbf{X}$ and the transfer matrix of an infinitesimal length ds is $\mathbf{M} = \mathbf{I} + \mathbf{F}ds$, we find directly

$$\boldsymbol{\sigma}' = \mathbf{F}\boldsymbol{\sigma} + \boldsymbol{\sigma}\mathbf{F}^T. \tag{4}$$

This is the **envelope equation**. For the full 6D case, it represents 21 equations. (Because σ is symmetric.)

Infinitesimal Transfer Matrix

The general Hamiltonian can be Taylor-expanded by orders in the 6 dependent variables[1],

$$H(\mathbf{x}; s) = \sum_i \left.\frac{\partial H}{\partial x_i}\right|_0 x_i + \frac{1}{2}\sum_{i,j}\left.\frac{\partial^2 H}{\partial x_i \partial x_j}\right|_0 x_i x_j + \ldots \tag{5}$$

The subscript 0 means that the derivatives are evaluated on the reference trajectory $\forall i,\ x_i = 0$. Terms of first order are eliminated by transforming to a coordinate system measured with respect to the reference trajectory. The remaining terms are second order and higher, and for linear motion, we simply truncate at the second order.

Then the Hamiltonian looks like $H = Ax^2 + BxP_x + Cxy + \ldots + UP_z^2$: there are 21 independent terms. $A = \frac{1}{2}\frac{\partial^2 H}{\partial x^2}$, and so on; all derivatives are evaluated on the reference trajectory, and may be a function of the independent variable. We know the equations of motion from the Hamiltonian to be: $x' = \partial H/\partial P_x$, $P_x' = -\partial H/\partial x$, etc., where primes denote derivatives w.r.t. the independent variable. Therefore the equations of motion:

$$\begin{pmatrix} x' \\ P_x' \\ y' \\ P_y' \\ z' \\ P_z' \end{pmatrix} = \begin{pmatrix} \frac{\partial^2 H}{\partial P_x \partial x} & \frac{\partial^2 H}{\partial P_x^2} & \cdots & \frac{\partial^2 H}{\partial P_x \partial P_z} \\ -\frac{\partial^2 H}{\partial x^2} & -\frac{\partial^2 H}{\partial x \partial P_x} & \cdots & -\frac{\partial^2 H}{\partial x \partial P_z} \\ \frac{\partial^2 H}{\partial P_y \partial x} & \frac{\partial^2 H}{\partial P_y \partial P_x} & \cdots & \frac{\partial^2 H}{\partial P_y \partial P_z} \\ -\frac{\partial^2 H}{\partial y \partial x} & -\frac{\partial^2 H}{\partial y \partial P_x} & \cdots & -\frac{\partial^2 H}{\partial y \partial P_z} \\ \frac{\partial^2 H}{\partial P_z \partial x} & \frac{\partial^2 H}{\partial P_z \partial P_x} & \cdots & \frac{\partial^2 H}{\partial P_z^2} \\ -\frac{\partial^2 H}{\partial z \partial x} & -\frac{\partial^2 H}{\partial z \partial P_x} & \cdots & -\frac{\partial^2 H}{\partial z \partial P_z} \end{pmatrix} \begin{pmatrix} x \\ P_x \\ y \\ P_y \\ z \\ P_z \end{pmatrix} \tag{6}$$

* This work has been supported by the Natural Sciences and Engineering Research Council of Canada. TRIUMF also receives federal funding via a contribution agreement through the National Research Council of Canada.

† baartman@triumf.ca

[1] In this shorthand, $x_1 = x$, $x_2 = P_x$, $x_3 = y$, ...

ISBN 978-3-95450-169-4

INSTALLATION AND ON-LINE COMMISSIONING OF EBIS AT ATLAS*

P.N. Ostroumov†1, A. Barcikowski, J. Clark, C.A. Dickerson, M. Hendricks, Y. Luo, R.C. Pardo, C. Peters, M. Power, G. Savard, S.I. Sharamentov, R.C. Vondrasek, G. Zinkann,
Argonne National Laboratory, Argonne, 9700 S. Cass Av, IL 60439, USA
[1]also at FRIB, Michigan State University, 640 S. Shaw Lane, East Lansing, MI 48824, USA

Abstract

An Electron Beam Ion Source Charge Breeder (EBIS-CB) has been developed at Argonne to breed radioactive beams from the CAlifornium Rare Ion Breeder Upgrade (CARIBU) facility at ATLAS. The CARIBU EBIS-CB has been successfully commissioned offline with an external singly-charged cesium ion source [1]. The EBIS performance meets the breeding requirements to deliver CARIBU beams to ATLAS. EBIS can provide charge-to-mass ratios ≥ 1/7 for all CARIBU beams with breeding times in the range of 6 ms to 30 ms. A record high breeding efficiency of up to 28% into a single charge state of Cs^{28+} has been demonstrated. Following the offline testing EBIS was moved to the front end of ATLAS where the alignment of EBIS was substantially improved and additional beam diagnostic tools both for electron and ion beams were installed. This paper will discuss EBIS improvements and present the results of on-line commissioning.

INTRODUCTION

The major features of the CARIBU EBIS are: ultra-high vacuum, high electron beam current with relatively low energy in the trap, optimized linear focusing and steering fields in the injection and extraction region, good alignment of the electron and ion beam transport system components and availability of 8 pairs of steering dipole coils for the transport of the electron beam. A typical charge state distribution of the EBIS charge-bred cesium beam downstream of a 70-degree analyzing magnet measured in off-line tests is shown in Fig. 1. The energy spread of the extracted ions has been determined by using a beam tracking code and fitting the simulated ion beam distribution to the measured data. This preliminary data indicates that for a typical beam with a mass-to-charge ratio of 4.75, the total relative energy spread at 5σ level will be ~0.18% in the ATLAS Low Energy Beam Transport (LEBT). Operation at higher repetition rates, up to 30 Hz, is dictated by the space charge limit in the radio-frequency quadrupole cooler-buncher (RFQ-CB), which precedes the EBIS-CB in the final installation, in order to maintain a high bunching efficiency. Recently, it was decided to include a multi-reflection time-of-flight (MR-TOF) mass-spectrometer between the RFQ-CB and EBIS-CB. The MR-TOF can provide isobar purification with mass resolution down to 1/50,000. This paper describes the design of the new beam transport systems and the overall integration of the EBIS-CB into ATLAS including the first experiment with breeding and acceleration of radioactive ion beam.

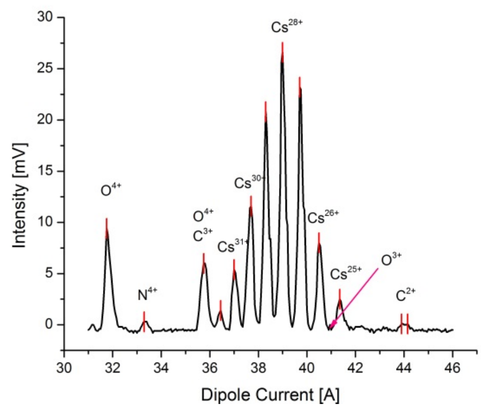

Figure 1: Typical spectrum of the EBIS beam with Cs^{1+} injection.

EBIS INTEGRATION

The 3D layout of the EBIS High-Voltage (HV) platform with respect to CARIBU and ATLAS is shown in Fig. 2. The EBIS injection and extraction beamline components and power supplies are installed on a HV platform biased to the same potential as the CARIBU platform. In addition, the electron gun, the SC solenoid and the electron collector of the EBIS are biased with respect to the HV platform. The total accelerating voltage will be adjusted to provide a 30.5 keV/u injection energy into the ATLAS-RFQ. The details of the EBIS integration into CARIBU and ATLAS including a thorough beam optics design are given in ref. [2].

A new frame for the EBIS HV platform was constructed. Major EBIS subsystems were disassembled to move from the off-line test area to ATLAS and install on the new platform as shown in Fig. 3.

CARIBU TO EBIS BEAMLINE

The CARIBU facility can deliver radioactive beams of singly charged ions in the mass range from 80 to 160 AMU, formed from the fission fragments of a 1 Curie ^{252}Cf source. Mass separation of the beams is performed using two 60° dipole magnets. The mass separator is followed by the RFQ-CB which provides cooling and bunching of the beam [3]. Recently, a Multi-Reflection Time of Flight (MR-TOF) spectrometer and mass separator has been installed downstream of the RFQ-CB. The mass resolving power of the MR-TOF can reach up to

* This work was supported by the U.S. Department of Energy, Office of Nuclear Physics, under Contract DE-AC02-06CH11357. This research used resources of ANL's ATLAS facility, which is a DOE Office of Science User Facility.
† Ostroumov@frib.msu.edu

INTENSE BEAM PRODUCTION OF HIGHLY CHARGED IONS BY THE SUPERCONDUCTING ECR ION SOURCE SECRAL FOR HEAVY ION LINACS*

L. Sun#, H. W. Zhao, W. Lu, J. W. Guo, Y .C. Feng, W. H. Zhang, X. Z. Zhang, Y. Yang, C. Qian, X. Fang, Z. Shen, W. Wu, L. Zhu, L. Z. Ma
IMP/CAS, Lanzhou, 730000, China

Abstract

Superconducting ECR ion source (SC-ECRIS) represents the state of the art technologies of ECR ion sources. Existing SC-ECRISs developed in different labs have contributed significantly for ECRIS technology advancement in the last 15 years. Recently the superconducting ECR ion source SECRAL operated at 24 GHz at IMP has produced many new world recorded beam intensities of highly charged ions due to new technologies applied, such as a new microwave coupling scheme. At the meantime, the world first 4th generation ECR ion source operated at 45 GHz is being developed at IMP. All these developments on intense beam production of highly charged ions with superconducting ECR ion source may play significant roles for the next generation heavy ion linacs such as FRIB and iLinac of HIAF project. This paper will report the recent developments of intense highly charged heavy ion beams at IMP and the discussion on perspectives of next generation ECRIS for the future heavy ion liancs.

INTRODUCTION

Highly charged ion sources have been widely used as preinjectors of highly stripped heavy ion beams for accelerators. EBIS (Electron Beam Ion Source) and ECRIS (ECR Ion Source) are the two types of highly recognized high charge state ion sources used in worldwide heavy ion accelerator labs. EBIS is capable of producing low duty factor very high charge state high peak current ion beams, for instance the powerful RHIC-EBIS at BNL, for the RHIC heavy ion program, 1.7 emA Au^{32+} with the pulse length of ~10 μs is required from the ion source in order to deliver 3×10^9 ions/pulse to the Booster at a repetition rate of 5 Hz [1]. As for the production of high repetition rate or CW highly charged ion beams of high intensity, ECRIS is an indispensable machine. Yves Jongen firstly put ECRIS in accelerator injection more than 35 years ago [2]. With this success, ECRISs have been widely used in worldwide laboratories as HCI (Highly Charged Ion) injectors. They have firstly proven the success in the field of cyclotrons, and later on in the field of linear accelerators. Nowadays, high power and high energy Linacs could not be possible without the contribution of high performance HCI ECRISs, such as FRIB at MSU, ROAN in South Korea, SPIRAL 2 project in GANIL, and etc. And the increasing needs from accelerator community, especially the recent fast advancement of high current high power Linacs has greatly stimulated the development of HCI ECRISs.

ECR ion sources have been used in IMP as the heavy ion injectors for over 20 years. Absolutely, the incorporation of ECR ion source to the heavy ion accelerator complex has already improved the machines' performance. The existing facility HIRFL (Heavy Ion Research Facility in Lanzhou), is mainly composed of one K69 cyclotron SFC, one K450 cyclotron SSC, RIBLL1 for radioactive beam production, cooler storage rings CSRm and CSRe, and the radioactive beam line RIBLL2 to connect the two rings [3, 4]. Linac injector systems have also been designed and under construction at IMP, as an upgrade program to boost the performance of the SSC cyclotron and also the storage ring. In phase 1 of the upgrade program, a project proposal has been issued to build a dedicated injection linac injector for SSC with ~ 1 MeV/u U^{34+} beam (Fig.1). The most interested ion beam for the design is several puA of U^{34+}, however the more preferred one is U^{37+}. Fundamentally, only with a SECRAL type 3rd generation ECR ion source, the goal could be achieved. Therefore, it is essential to use the existing SECRAL ion source to produce intense HCI beams to demonstrate the performance desired, and at the meantime, a high performance ECRIS for SSC-linac is under development.

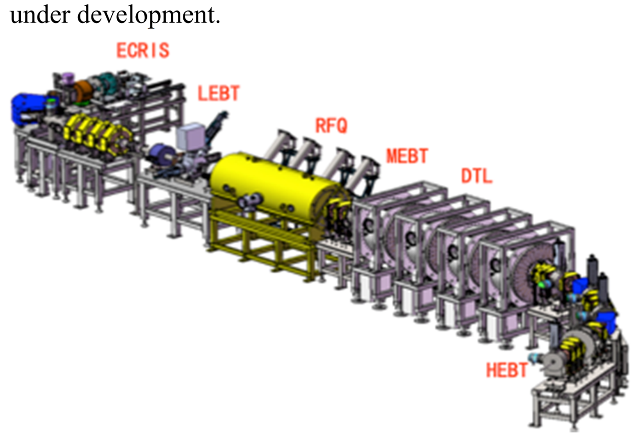

Figure 1: Layout of SSC-Linac.

SECRAL was connected to the injection line of HIRFL complex in 2007 and as of early 2016, more than 25,000 hours' beam time has been accomplished. It has been proved to be a very reliable and high performance ECR ion source. Especially, the recent progress with high intensity Ar and Xe beams, such as 1.42 emA Ar^{12+}, 1.1 emA Xe^{26+}, 0.67 emA Ca^{12+}, 0.68 emA Bi^{31+} and etc., has demonstrated its performance and capacity [5].

*Work supported by NSF (contract No. 11375244), NSF (contract No. 11427904) and MOST (contract No. 2014CB845500).
#sunlt@impcas.ac.cn

ION EFFECTS IN HIGH BRIGHTNESS ELECTRON LINAC BEAMS

S. Full*, A. Bartnik, I.V. Bazarov, J. Dobbins, B. Dunham, G.H. Hoffstaetter, K. Smith
CLASSE, Cornell University, Ithaca, New York 14853, USA

Abstract

Electron beams ionize rest gas particles which then accumulate around them, disturbing beam dynamics and causing background radiation. While this effect has been predicted in the past, linacs have hitherto not suffered from it because of their rather small beam current. The effect of ions increases with larger currents and smaller cross sections of the beam, and it has clearly been observed in Cornell's high-brightness ERL injector for the first time. This paper will show experimental evidence for ions, demonstrate strategies for their elimination, and will compare the experimental data to theories of beam-ion interactions.

INTRODUCTION

In an accelerator's vacuum chamber, any residual gas is rapidly ionized by collisions with the electron beam. At high beam currents, the resulting positive ions become trapped inside of the negatively charged beam and can cause a variety of effects including charge neutralization, coherent and incoherent tune shifts, optical errors, beam halo, beam losses, or even beam instabilities [1, 2]. Even with improvements in vacuum technology, ions can fully neutralize a beam within seconds for vacuum pressures as low as 1 nTorr. Therefore one must directly remove the trapped ions to avoid or mitigate these potential effects.

The Cornell DC photoinjector was built to serve as the injector for Cornell's proposed Energy Recovery linac (ERL). It is designed to operate with a beam energy of 5–15 MeV and beam currents up to 100 mA, corresponding to a bunch charge of 77 pC at a repetition rate of 1.3 GHz. Unlike previous linacs, the photoinjector reaches a new regime of beam parameters where ion trapping becomes a concern. Although problematic ion accumulation in linacs has been predicted in the past [1], it has rarely been observed due to low repetition rates that allow ions to drift out of the center of the beam pipe between bunches. In this paper we present some of the first observations of actual ion trapping in a high current linac. We also share the results of recent experiments in the photoinjector [3] that have validated the effectiveness of three different clearing methods: ion clearing electrodes, bunch gaps, and beam shaking.

EVIDENCE OF ION TRAPPING

Once trapped inside of the beam, the ions oscillate back and forth inside of the beam's potential with a characteristic frequency that depends on beam current, transverse beam size, and the ion's mass [3]. In general, trapping occurs when the ion oscillation frequency is significantly less than the bunch repetition rate. This makes the ion oscillation frequency a good estimate for determining whether or not ion trapping will occur within an accelerator. For the photoinjector, we both predicted and measured an ion oscillation frequency on the order of kHz [3] for millimeter beam sizes, which is significantly less than the 325 MHz or 1.3 GHz bunch repetition rates used here. Therefore, we expect there to be ion trapping in the photoinjector.

During reliability test runs at 20 mA and 350 keV, we have observed beam trips that limit stable machine operation to approximately 10-15 minutes. The beam trips were the direct result of the gun's high voltage power supply tripping off. Employing ion clearing techniques, primarily clearing electrodes and/or bunch gaps, allowed stable beam operation for at least 24 hours, leading us to conclude that ions are the cause of the trips. Note that no testing was done for more than 24 hours.

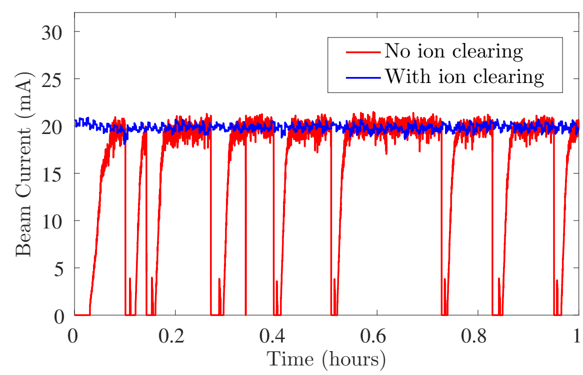

Figure 1: During certain running conditions, the photoinjector suffers from intermittent beam trips every 10–15 minutes. While employing ion clearing methods, we can obtain a stable beam current for at least 24 hours.

Although we have yet to determine the exact mechanism of these trips, we currently have two theories. The first is that trapped ions drift backwards and strike the cathode, ejecting particles that then cause arcing. This would ultimately trip off the high voltage power supply. The process of the ions striking and destroying the center of the cathode (known as ion back bombardment) is expected and dealt with during normal operation. However, in the past ion back bombardment in the photoinjector has not always been linked to these type of trips. The second theory is that dust particles become trapped inside of the beam and drift longitudinally towards the DC gun, where they eventually cause arcing that trips off the power supply. In both cases, the fact that the beam is low energy and the absence of a Superconducting RF cavity (which can impede the longitudinal motion of ions) between sections A1 and A3 (shown in Fig. 2) during these runs are likely important factors in explaining this phenomenon.

* sf345@cornell.edu

DEVELOPMENT OF A MUON LINAC FOR THE G-2/EDM EXPERIMENT AT J-PARC

M. Otani, N. Kawamura, T. Mibe, F. Naito, M. Yoshida, KEK, Oho, Tsukuba, 305-0801, Japan
K. Hasegawa, T. Ito, Y. Kondo, JAEA, Tokai, Naka, Ibaraki, 319-1195, Japan
N. Hayashizaki, Tokyo Institute of Technology, Tokyo, 152-8550, Japan
Y. Iwashita, Kyoto University, Kyoto, 611-0011, Japan
Y. Iwata, NIRS, Chiba, 263-8555, Japan
R. Kitamura, University of Tokyo, Hongo, 113-8654, Japan
N. Saito, J-PARC Center, Tokai, Naka, Ibaraki, 319-1195, Japan

Abstract

We are developing a linac dedicated to the muon acceleration for muon g-2/EDM experiment at J-PARC. The muon linac consists of a radio-frequency-quadrupole (RFQ), an inter-digital H-mode (IH) drift tube linac (DTL), a disk-and-washer (DAW) -type coupled cell linac (CCL), and a disk-loaded structure. This paper describes the design of each structure and current progress towards muon acceleration with the RFQ, which is expected to be the first practical realization of muon acceleration in the world.

INTRODUCTION

Though the discovery of the Higgs boson at LHC completed the discovery of all particles predicted by the Standard Model (SM) of elementary particle physics, some observations such as the existence of dark matter indicate new physics beyond SM at some energy scale or interaction scale. One of the clues for such new physics is the anomaly of the muon anomalous magnetic moment of $(g-2)_\mu$: a difference of approximately three standard deviations exists between the SM prediction and the measured value (with a precision of 0.54 ppm) of $(g-2)_\mu$ [1]. However, measurement with higher precision is necessary to confirm this anomaly. Low-emittance muon beams will facilitate more precise measurements, as the dominant systematic uncertainties in the previous experimental results are due to the muon beam dynamics in the muon storage ring.

At present, we are developing a muon linac for the $(g-2)_\mu$ experiment at the Japan Proton Accelerator Research Complex (J-PARC) [2] in order to realize a low-emittance muon beam. In the experiment, ultra slow muons with an extremely small transverse momentum of 3 keV/c (kinetic energy W = 25 meV) are generated via thermal muonium production [3] followed by laser dissociation [4]. The generated ultra slow muons are electro-statically accelerated to $\beta = v/c = 0.01$ (5.6 keV) and injected into the muon linac.

Figure 1 shows the muon linac configuration. In order to obtain a longitudinally bunched beam, a RFQ accelerator is employed for the first-stage acceleration. The operational frequency is chosen to be 324 MHz, in order to optimize the experiences at the J-PARC H^- RFQ. Although conventional linacs adopt Alvarez DTLs after RFQs, an IH-DTL is employed during the stage of particle velocity $\beta = 0.08$ to 0.28 (4.5 MeV) to yield a higher acceleration efficiency. After the muon is accelerated to $\beta = 0.28$, a DAW-type CCL is employed for effective acceleration. The operational frequency is chosen as 1.3 GHz because a 30 MW klystron, which was originally developed as the RF source for the KEKB linac [5], is applied for our project. Because the β variation is modest in the high-β region, the design emphasis has been shifted for achieving a high accelerating gradient, in order to realize a sufficiently short distance. Therefore, a disk-loaded structure is used for β greater than 0.7 (42 MeV).

The muon beam current is very small ($\sim 10^6$ muon paer second with 25 pulses per second). The pulse width is approximately 10 nsec, and the duty is also small.

In this paper, we describe the designs of each accelerator structure and the current progress towards muon acceleration.

LINAC DESIGN

RFQ

An RFQ is employed for initial acceleration ($\beta = 0.01 \sim 0.08$). In order to demonstrate the muon acceleration in a timely manner at a low cost, the existing RFQ that was originally developed as a J-PARC linac spare [6] is utilized. The RFQ was designed to accelerate H^-. In order to accelerate muons with the RFQ, the power is reduced to 1/80 of the design power. Figure 2 shows the beam evolution calculated by PERMTEQM [7] with the deduced power setting. The evolution shows good transmission (95%) for muons. The current progress towards actual muon acceleration with this RFQ is described in the next section. In addition, an RFQ dedicated to the acceleration of muons is being developed, the details of which can be found elsewhere [8]

IH-DTL

Inter-digital H-mode DTL [9, 10] is used for $\beta = 0.08$–0.28. In order to achieve high-efficiency acceleration, the alternative phase focusing (APF) scheme is employed [11–13]; in this scheme, transverse and longitudinal focusing are achieved with only the RF field, and no additional focusing element is necessary.

The APF IH-DTL for muons was designed [14] by LINACSapf [15], CST MW Studio [16], and GPT [17]. First, the synchronous phase array is optimized for an idealized APF.

STATUS OF THE PAL-XFEL*

H.-S. Kang†, D. E. Kim, K.-W Kim, I. S. Ko, T.-Y. Koo, H.-S. Lee, K.-H. Park,
PAL, Pohang, Kyungbuk, Korea

Abstract

The construction of the PAL-XFEL was completed at the end of 2015 and the FEL commissioning started from the beginning of 2016. The commissioning aims for the lasing of 0.5 nm FEL in the first campaign by July 2016, and for the lasing of 0.1 nm hard X-ray FEL in the second campaign by December 2016. The commissioning results of the 0.5 nm FEL lasing will be presented.

INTRODUCTION

The Pohang Accelerator Laboratory (PAL), Pohang, South Korea, is developing a 0.1 nm SASE based FEL, named PAL-XFEL, for high power, short pulse X-ray coherent photon sources. It is adjacent to the existing 3-rd generation light source, PLS-II, which was upgraded to a 3-GeV/400-mA/6-nm facility in 2010 (see Fig. 1). The PAL-XFEL project was started from 2011 with the five-year total budget of 400 MUSD, its building construction completed by the end of 2014, and successively the installation of linac, undulator, and beam line followed and was completed in January 2016. The FEL commissioning started in April 2016.

The PAL-XFEL includes a 10-GeV S-band normal conducting linac, which is 700 m long and consists of a photocathode RF gun, 174 S-band accelerating structures with 50 klystron/modulators, one X-band RF system for linearization [1], and three bunch compressors (see Table 1 and Fig. 2). Beyond the 10-GeV linac, a 250-m long hard x-ray undulator hall follows. An experimental hall, which is 60-meters long and 16-meters wide, is located at the end of the facility. The total length of the building is 1,110 meters.

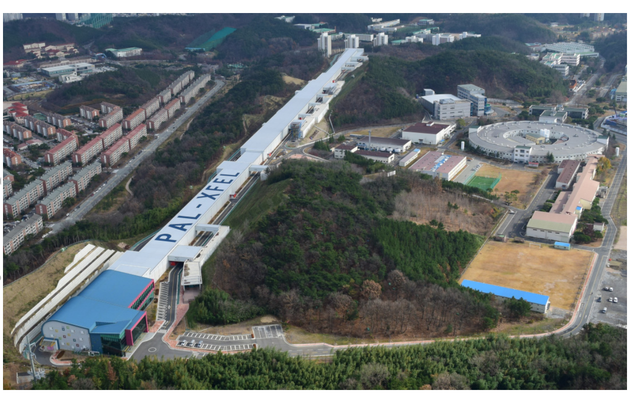

Figure 1: Picture of PAL-XFEL building.

The PAL-XFEL linac is divided into four acceleration sections (L1, L2, L3, and L4), three bunch compressors (BC1, BC2, BC3), and a dogleg transport line to undulators as shown in Fig. 2 [2]. A laser heater to mitigate micro-bunching instability is placed right after the 135 MeV injector, and an X-band cavity is placed right before BC1. A soft X-ray FEL branch line is located at 3 GeV point of the 10-GeV linac.

Originally, 0.3 nm FEL lasing was planned in the first campaign. But, the cavity BPM electronics essential for the undulator line were not fully functional, only 14 out of the minimum number of 22 for 20 undulators. We had to use only 12 undulators, therefore, decided to get lasing of 0.5 nm FEL instead of 0.3 nm.

Table 1: Parameters of PAL-XFEL

Linac	
FEL radiation wavelength	0.1 nm
Electron energy	10 GeV
Slice emittance	0.5 mm-mrad
Beam charge	0.2 nC
Peak current at undulator	3.0 kA
Pulse repetition rate	60 Hz
Electron source	Photo-cathode RF-gun
Linac structure	S-band normal conducting
Undulator	
Type	out-vacuum, variable gap
Length	5 m
Undulator period	2.6 cm
Undulator min. gap	8.3 mm
Vacuum chamber dimension	13.4 x 6.7 mm

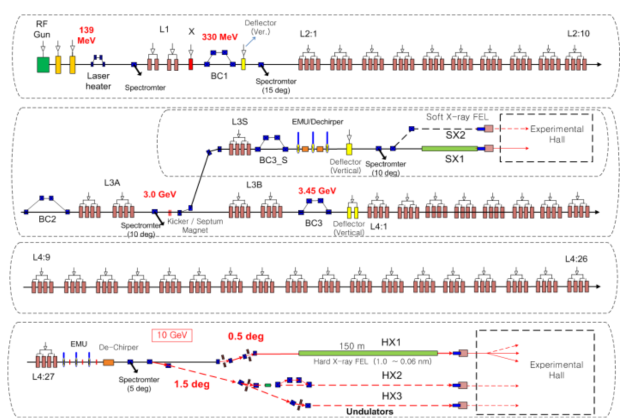

Figure 2: Schematic layout of PAL-XFEL.

LINAC COMMISSIONING

The installation of accelerating structures, magnets, vacuum chambers, and klystron modulators for the 10-

* Work supported by Ministry of Science and Technology of Korea
† hskang@postech.ac.kr